

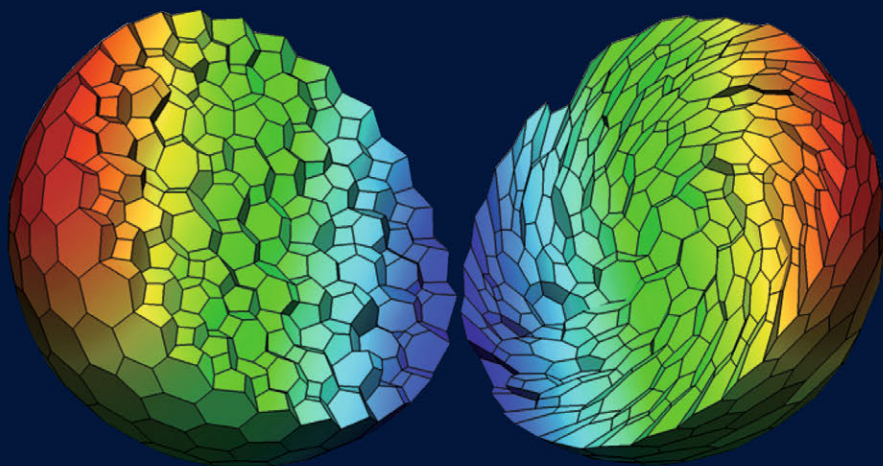
Volume 11

The Mimetic Finite Difference Method for Elliptic Problems

Lourenço Beirão da Veiga • Konstantin Lipnikov
Gianmarco Manzini

MS&A

Modeling, Simulation & Applications



MS&A

Volume 11

Editor-in-Chief

A. Quarteroni

Series Editors

T. Hou

C. Le Bris

A.T. Patera

E. Zuazua

For further volumes:
<http://www.springer.com/series/8377>

Lourenço Beirão da Veiga
Konstantin Lipnikov
Gianmarco Manzini

The Mimetic Finite Difference Method for Elliptic Problems

 Springer

Lourenço Beirão da Veiga
Dipartimento di Matematica “Federico Enriques”
Università degli Studi di Milano
Italy

Konstantin Lipnikov
Theoretical Division
Los Alamos National Laboratory
USA

Gianmarco Manzini
Theoretical Division
Los Alamos National Laboratory
USA

ISSN: 2037-5255 ISSN: 2037-5263 (electronic)
MS&A – Modeling, Simulation & Applications
ISBN 978-3-319-02662-6 ISBN 978-3-319-02663-3 (eBook)
DOI 10.1007/978-3-319-02663-3
Springer Cham Heidelberg New York Dordrecht London

Library of Congress Control Number: 2013951789

© Springer International Publishing Switzerland 2014

This work is subject to copyright. All rights are reserved by the Publisher, whether the whole or part of the material is concerned, specifically the rights of translation, reprinting, reuse of illustrations, recitation, broadcasting, reproduction on microfilms or in any other physical way, and transmission or information storage and retrieval, electronic adaptation, computer software, or by similar or dissimilar methodology now known or hereafter developed. Exempted from this legal reservation are brief excerpts in connection with reviews or scholarly analysis or material supplied specifically for the purpose of being entered and executed on a computer system, for exclusive use by the purchaser of the work. Duplication of this publication or parts thereof is permitted only under the provisions of the Copyright Law of the Publisher’s location, in its current version, and permission for use must always be obtained from Springer. Permissions for use may be obtained through RightsLink at the Copyright Clearance Center. Violations are liable to prosecution under the respective Copyright Law.

The use of general descriptive names, registered names, trademarks, service marks, etc. in this publication does not imply, even in the absence of a specific statement, that such names are exempt from the relevant protective laws and regulations and therefore free for general use.

While the advice and information in this book are believed to be true and accurate at the date of publication, neither the authors nor the editors nor the publisher can accept any legal responsibility for any errors or omissions that may be made. The publisher makes no warranty, express or implied, with respect to the material contained herein.

Cover Design: Beatrice F, Milano
Typesetting with L^AT_EX: PTP-Berlin, Protago T_EX-Production GmbH, Germany (www.ptp-berlin.de)

Springer is a part of Springer Science+Business Media (www.springer.com)

Preface

This book offers a systematic and thorough examination of theoretical and computational aspects of the modern *mimetic finite difference* (MFD) method. The MFD method preserves or mimics underlying properties of physical and mathematical models, thereby improving the fidelity and predictive capability of computer simulations. We focus here on the numerical solution of elliptic partial differential equation (PDEs) on unstructured polygonal and polyhedral meshes for which the MFD method has proven to be very successful in the last five decades.

The book covers advanced research topics and issues. Most of the presented material is the result of our research work that has been published in the last decade. Our intention is to offer a deep introduction to the major aspects of the MFD method such as the design principles for the development of new schemes, tools for the convergence analysis, and matrix formulas ready for a code implementation, to the widest possible audience. Nonetheless, to appreciate our effort a minimum background is required in the linear algebra, functional analysis, and numerical analysis of PDEs. It will be helpful for the reader to have some familiarity with the classical lowest-order finite element schemes, such as the primal linear and mixed Raviart-Thomas methods, the classical finite volume and finite difference schemes.

The book is structured in three parts with four chapters each.

The MFD method has a strong theoretical foundation, which is reviewed in Part I, entitled *Foundation*. In Chap. 1, after a short motivation for using the MFD method in applications, we give an historical introduction to the development of the mimetic technology and an overview of all mathematical models considered in the book. We present their strong and weak formulations and summarize results concerning the existence and regularity of weak solutions. We also introduce the notion of shape-regular polyhedral and polygonal meshes that are extensively used throughout the book. In Sect. 1.3 we illustrate a few basic design principles of the mimetic discretization method on the simplest one-dimensional Poisson equation. This section is particularly suitable for readers not familiar with the mimetic technology.

The theoretical foundation of the existing compatible discretization methods dates back to the fundamental work of Whitney on geometric integration. No surprise that the MFD method is related to some of the most basic concepts of discrete differential

forms such as the chain-cochain duality and discrete Stokes theorems. The mimetic schemes are derived in part by mimicking the Stokes theorems in a discrete setting. The further development of this concept is in Chap. 2, where a discrete vector and tensor calculus (DVTC), the core of the MFD method that separates it from finite volume methods, is introduced. Using fundamental physical principles, we formulate natural discrete analogues of the first-order differential operators *divergence*, *gradient*, and *curl*. Compatible adjoint discrete operators are defined via duality relationships, more precisely, via discrete integration by parts formulas. The derivation of these operators uses the notion of mimetic inner products that approximate L^2 products of scalar or vector functions.

The practical construction of accurate inner products on unstructured polygonal and polyhedral meshes requires a set of new theoretical tools that are introduced in Chap. 3. We introduce the stability and consistency conditions that play the fundamental role in proving well-posedness and accuracy of the mimetic discretizations. We also connect the mimetic inner products with reconstruction operators that make a useful theoretical tool but are never built in practice. This chapter highlights a unique feature of the MFD method. On polyhedral (including hexahedral and sometimes simplicial) meshes, it produces a family of schemes with equivalent properties such as the stencil size and convergence rate.

In Chap. 4 we extend the mimetic discretization technology to general bilinear forms, which allows us to apply the MFD method to a wider range of problems. We moreover present a different approach to mimetic discretizations that takes the steps from the weak formulation of the problem, rather than the strong one. Although this approach turns out to be often equivalent to the construction presented in the previous chapters, this is not always the case and it is very useful to have a clear picture of both methodologies. Furthermore, in Chap. 4 we focus on the detailed analysis of the stability and consistency conditions. We show again that the MFD method provides a family of schemes that share some important properties, e.g., accuracy and stability, so that the convergence analysis can be carried out simultaneously for the entire family.

Part II is entitled *Mimetic Discretization of Basic PDEs*. It explains how the MFD method can be applied for solving the steady-state diffusion equation in the primal and mixed formulations, Maxwell's equations, and the steady Stokes equations. We extended the construction of mimetic inner products (in three discrete spaces) to the case of tensorial coefficients. We also provide theoretical construction of various reconstruction operators, prove stability results, and derive a priori and a posteriori error estimates in mesh-dependent norms.

A useful but also limited viewpoint is to consider the MFD method as an extension of some classical discretization methods to polygonal and polyhedral meshes. Indeed, the family of low-order mimetic schemes contains many well-known finite volume, finite difference and finite elements schemes. On special regular grids (orthogonal Cartesian grids or logically rectangular grids), we recover such schemes as the particular members of the mimetic family. However, the mimetic schemes work perfectly on unstructured polygonal and polyhedral meshes, with arbitrarily-shaped cells that may be even non-convex and degenerate.

In Chap. 5, we apply the MFD method for solving the steady-state diffusion equation in a *mixed* form and show how this method generalizes the lowest-order Raviart-Thomas and BDM finite element methods on simplicial meshes to unstructured polygonal and polyhedral meshes in two and three spatial dimensions. We also investigate additional important issues such as the super convergence, solution post-processing, a-posteriori error estimation and adaptivity.

In Chap. 6, we apply the MFD method for solving the steady-state diffusion equation in a *primal* form and show how this method generalizes the linear Galerkin method on simplicial meshes to unstructured polygonal and polyhedral meshes in two and three spatial dimensions. On meshes of simplices, the nodal mimetic formulation coincides with the linear Galerkin finite element method. On rectangular meshes, particular members of the mimetic family coincide with a number of classical finite difference schemes (5-point Laplacian, 9-point Laplacian, Q_1 finite element method). For two-dimensional problems, we also describe and analyze arbitrary-order mimetic schemes. Finally, we consider the a-posteriori error estimation and adaptivity for the low order mimetic schemes.

In Chap. 7, we apply the MFD for two time-dependent problems governed by Maxwell's equations and the magnetostatic problem. We discuss the conservation of energy in the mimetic discretizations and provide formulas ready for the code implementation. The convergence analysis of the MFD method for the magnetostatic problem is a work in progress and therefore is incomplete.

In Chap. 8, we derive and analyze mimetic schemes for the steady-state Stokes equations. Analysis of the inf-sup stability condition imposes constraints on the discrete spaces for the velocity and pressure. We first develop a mimetic method that takes inspiration from classical finite elements and show the good behavior of such scheme. Afterwards, we use the flexibility of the mimetic technology to build a more computationally efficient method, that makes use of much less degrees of freedom and still satisfies the constraints above.

We were asked frequently by our colleagues about the applicability of the MFD method to a wider class of problem. The Part III entitled *Further Developments* describes how the mimetic technology contributes to solving challenging problems emerging in modeling complex physical processes. This includes solution of non-linear PDEs, preservation of maximum principles, and stability and accuracy of discretizations on deforming (e.g., Lagrangian) meshes.

Chapter 9 is devoted to the problems of structural mechanics. We first present an MFD method for the linear elasticity problem, considering both the displacement-pressure and stress-displacement formulations. Afterwards, we present a mimetic scheme for the Reissner-Mindlin plate bending problem, which uses deflection and rotation as unknown variables. Our additional interest of these problems is related to the fact that, in order to derive and analyze the numerical schemes, a large number of mimetic operators and discrete spaces must be considered at once.

In Chap. 10, we present the MFD method for the convection-diffusion equation, and the obstacle problem. We also consider the case of high Peclet numbers characterizing a convection-dominated regime where the continuum solution may display strong parabolic and exponential boundary layers.

In Chap. 11, we consider a new emerging research direction dubbed *m-adaptation*, which stands for *mimetic adaptation*. The m-adaptation allows us to select an optimal scheme from the family of mimetic schemes in accordance with some problem-dependent criteria that may include a discrete maximum principle (DMP), reduction of a numerical dispersion, and boosting performance of algebraic solvers. Even if the m-adaptation is still under development, a few interesting results are already available for the derivation of positive schemes or schemes satisfying a DMP. In this chapter, we analyze the family of the lowest-order mimetic schemes for the diffusion equation in the mixed and primal forms. We formulate the constructive sufficient conditions for the existence of a subfamily of mimetic scheme that satisfy the DMP.

In Chap. 12, we extend the MFD method to generalized polyhedral meshes with cells featuring non-planar faces. Such cells appear in Lagrangian simulations where the computational mesh is moved and deformed with the fluid. We use again the flexibility of the mimetic construction to add velocity unknowns only on strongly curved mesh faces in order to recover the optimal convergence rate.

Our final note is about the *computational aspects* of the mimetic technology. In each of the Chaps. 5–12, one or more sections are dedicated to the implementation details. The reader will find explicit formulas for the local mass and stiffness matrices. Additional interesting implementation details can be found in Chap. 4. Once the local matrices are coded, building the global mass or stiffness matrix can be done using the conventional assembly process, like in the finite element method.

Los Alamos, New Mexico and Milano-Pavia, Italy
September, 2013

Lourenço Beirão da Veiga
Konstantin Lipnikov
Gianmarco Manzini

Acknowledgements

We express our sincere gratitude to Dr. Mikhail Shashkov and Prof. Franco Brezzi. Both of them have given invaluable contributions to the development of the mimetic finite difference method and taught us how to develop and theoretically analyze new mimetic schemes. We also thank them for creating a very stimulating and challenging scientific atmosphere for our research in Los Alamos and Pavia and for the many useful comments and discussions.

We express our deepest gratitude to Prof. Valeria Simoncini, who helped us enormously to develop the first algebraic analysis of the modern mimetic discretizations. It is our great pleasure to thank our colleagues, friends and collaborators that worked with us over the years on the development of mimetic discretizations, their analysis and extension to various applications. The essential part of this book is based on joint papers with Paola Antonietti, Annalisa Buffa, Andrea Cangiani, Jerome Droniou, Francesca Gardini, Vitaly Gyrya, Carlo Lovadina, David Mora, Alessandro Russo, Daniil Svyatskiy, and Marco Verani.

For many stimulating discussions and constructive comments that influenced our research directions on mimetic methods and, more in general, enriched our scientific perspective, we thank I. Aavatsmark, M. Arioli, D. Arnold, F. Auricchio, F. Bassi, L. Bergamaschi, L. Berlyand, M. Berndt, E. Bertolazzi, N. Bigoni, J. Bishop, V. Bokil, P. Bochev, D. Boffi, L. Bonaventura, D. Burton, A. Cangiani, J. Castillo, C. Chinosi, E. Coon, D. Chapelle, Y. Coudière, L. Demkowicz, D. Di Pietro, I. Duff, V. Dyadechko, M. Edwards, A. Ern, R. Eymard, M. Floater, L. Formaggia, T. Gallouët, V. Ganzha, R. Garimella, L. Gastaldi, E. Georgoulis, M. Gerritsma, A. Gillette, T. Gianakon, N. Gibson, G. Srinivasan, J. Fung, R. Herbin, A. Hirani, K. Hormann, F. Hubert, M. Hyman, A. Iollo, M. Kenamond, R. Klöfkor, T. Kolev, Y. Kuznetsov, R. Liska, R. Loubere, L. D. Marini, P.-H. Maire, S. Mantica, J. Morel, D. Moulton, E. Nelson, R. Nicolaidis, J. Niiranen, G. Paulino, L.F. Pavarino, I. Perugia, J. Perot, C. Pierre, J. Pitkaranta, M. Putti, A. Reali, S. Rebay, J. Reynolds, R. Rieben, S. Runnels, G. Sangalli, S. Scacchi, G. Scovazzi, P. Smolarkiewicz, S. Steinberg, R. Stenberg, N. Sukumar, C. Talischi, F. Teixeira, K. Trapp, P. Vachal,

D. Vassilev, Yu. Vassilevski, A. Veneziani, M. Vohralík, E. Wachspress, A. Weiser, M. Wheeler, and I. Yotov.

The work on this book took three long years and was often done using personal time. We are in a great debt to our families for their continuous support and encouragement during this difficult period.

For kindly providing us with the opportunity of publishing this book in the Springer Series, we are greatly indebted to Prof. Alfio Quarteroni and Dr. Francesca Bonadei, who manifested a cyclopean patience towards us and our efforts in the last years. We thank anonymous reviewers for valuable comments that helped us to improve this book. We owe a great many thanks to the T-5 Group Leaders P. Swart and K. Rasmussen for their continuous support of this book.

Part of this work was performed under the auspices of the National Nuclear Security Administration of the US Department of Energy at Los Alamos National Laboratory under Contract No. DE-AC52-06NA25396. The authors gratefully acknowledge the partial support of the US Department of Energy Office of Science Advanced Scientific Computing Research (ASCR) Program in Applied Mathematics Research; the Istituto di Matematica Applicata e Tecnologie Informatiche del Consiglio Nazionale delle Ricerche (IMATI-CNR) di Pavia, Italy; the Istituto Universitario di Studi Superiori (IUSS) di Pavia, Italy; the Dipartimento di Matematica “F. Enriques”, Università Statale degli Studi di Milano, Italy.

Contents

Part I Foundation

1	Model elliptic problems	3
1.1	A brief history of the mimetic finite difference method	6
1.2	Other compatible discretization methods	14
1.3	Principles of mimetic discretizations	18
1.4	Scalar elliptic problems	24
1.4.1	Diffusion equation in primal form	24
1.4.2	Diffusion equation in mixed form	25
1.4.3	Advection-diffusion equation in mixed form	26
1.5	Vector elliptic problems	27
1.5.1	Stokes problem	27
1.5.2	Linear elasticity problem	28
1.5.3	Reissner-Mindlin plate bending problem	31
1.5.4	Magnetostatics problem	32
1.6	Polyhedral meshes	33
1.6.1	Mesh shape regularity	34
1.6.2	Consequences of the mesh regularity assumptions	36
1.7	Polygonal meshes	39
2	Foundations of mimetic finite difference method	41
2.1	Degrees of freedom and discrete fields	43
2.2	Discrete spaces and projection operators	45
2.3	Primary mimetic operators	47
2.3.1	The discrete gradient operator $\nabla_h : \mathcal{V}_h \rightarrow \mathcal{E}_h$	47
2.3.2	The discrete curl operator $\text{curl}_h : \mathcal{E}_h \rightarrow \mathcal{F}_h$	48
2.3.3	The discrete divergence operator $\text{div}_h : \mathcal{F}_h \rightarrow \mathcal{P}_h$	48
2.3.4	Discrete versions of the Stokes theorem	49
2.3.5	Basic properties of the primary operators	50
2.3.6	Matrix representation of the primary operators	52

2.4	Derived mimetic operators	53
2.5	Second-order discrete operators	55
2.6	Exact identities	57
2.6.1	The kernel of the primary operators	58
2.6.2	The kernel of the derived operators	59
2.6.3	The kernel of the second-order mimetic operators	61
2.7	Discrete Helmholtz decomposition theorems	64
3	Mimetic inner products and reconstruction operators	67
3.1	Mimetic inner product	67
3.2	Properties of the reconstruction operators	71
3.3	Minimal reconstruction operators	73
3.3.1	The reconstruction operators $R_v^\mathcal{V}$, $R_e^\mathcal{E}$, $R_f^\mathcal{F}$ and $R_p^\mathcal{P}$	74
3.3.2	The reconstruction operators $R_e^\mathcal{V}$, $R_f^\mathcal{E}$ and $R_p^\mathcal{F}$	74
3.3.3	The reconstruction operators $R_f^\mathcal{V}$ and $R_p^\mathcal{E}$	79
3.3.4	The reconstruction operator $R_p^\mathcal{V}$	83
3.4	Mimetic inner products for a single cell	84
3.4.1	Mimetic inner product in $\mathcal{V}_{h,P}$	86
3.4.2	Mimetic inner product in $\mathcal{E}_{h,P}$	86
3.4.3	Mimetic inner product in $\mathcal{F}_{h,P}$	88
3.4.4	Mimetic inner product in $\mathcal{D}_{h,P}$	88
3.4.5	Formula for the inner product matrix	88
4	Mimetic discretization of bilinear forms	91
4.1	Discrete bilinear forms	92
4.1.1	Consistency condition	94
4.1.2	Stability condition	96
4.2	Algebraic form of the consistency condition	97
4.3	Formula for matrix M_P	99
4.4	Stability analysis	103
4.4.1	Stability result in the natural norm	103
4.4.2	Stability result in the mesh-dependent norm	108
4.5	Construction of stabilization matrix M_P^1	111
4.6	The inverse of matrix M_P	113
Part II Mimetic Discretization of Basic PDEs		
5	The diffusion problem in mixed form	117
5.1	Mimetic discretization	118
5.1.1	Degrees of freedom and projection operators	118
5.1.2	Strong and weak forms of the discrete equations	119
5.1.3	Stability and consistency conditions	121
5.1.4	A family of mimetic schemes	123
5.2	Convergence analysis and error estimates	128
5.2.1	Preliminary lemmas	129

5.2.2	Stability analysis	130
5.2.3	Convergence of the vector variable	132
5.2.4	Convergence of the scalar variable	133
5.3	Exact reconstruction operators	136
5.3.1	Existence of exact reconstruction operators	138
5.3.2	Superconvergence of the scalar variable	140
5.4	A posteriori estimates	142
5.4.1	Post-processing of the scalar variable	143
5.4.2	A residual-based a posteriori estimator	143
5.5	Second-order approximation of the flux	146
5.5.1	Derivation of the mimetic scheme	147
5.5.2	Convergence analysis	151
5.5.3	Solution post-processing	154
6	The diffusion problem in primal form	155
6.1	Overview of the method	155
6.1.1	Discretization of the strong form of the equations	156
6.1.2	Discretization of the weak formulation	158
6.2	Low-order mimetic method	159
6.2.1	Degrees of freedom	159
6.2.2	The consistency and stability conditions	160
6.2.3	Discretization of linear functional \mathcal{L}_h	162
6.2.4	Convergence theorem	163
6.2.5	Derivation of bilinear form \mathcal{A}_h	163
6.2.6	A family of mimetic schemes	166
6.3	Arbitrary-order mimetic method	170
6.3.1	Degrees of freedom	172
6.3.2	The consistency and stability conditions	174
6.3.3	Discretization of linear functional \mathcal{L}_h	176
6.3.4	Derivation of bilinear form \mathcal{A}_h	177
6.4	Convergence analysis	179
6.4.1	Reconstruction operator	179
6.4.2	Stability of the projection operator	183
6.4.3	Proof of the convergence theorem	185
6.4.4	L^2 -estimate of the approximation error	188
6.5	A posteriori estimates	189
6.5.1	Mesh refinement and related results	189
6.5.2	A consistent coarse-grid problem	192
6.5.3	A posteriori error analysis	192
6.5.4	An inexpensive error indicator	194
7	Maxwell's equations	197
7.1	Maxwell's equations	197
7.2	Mimetic discretizations	198
7.2.1	Degrees of freedom and projection operators	198

7.2.2	Strong form of discrete equations	200
7.2.3	Divergence constraints and energy conservation	202
7.2.4	Stability and consistency conditions	204
7.2.5	A family of mimetic schemes	208
7.3	Magnetostatics equations	210
7.3.1	Strong and weak forms of discrete equations	211
7.3.2	Stability and consistency conditions	214
7.3.3	Convergence analysis	215
8	The Stokes problem	221
8.1	The mimetic formulation	222
8.1.1	Degrees of freedom and projection operators	222
8.1.2	Mimetic operators, inner products and bilinear forms	225
8.1.3	Discrete strong and weak formulations	226
8.1.4	Stability and consistency conditions	228
8.1.5	Formula for the stiffness matrix	230
8.2	Convergence analysis and error estimates	233
8.2.1	Preliminaries and technical lemmas	233
8.2.2	Stability analysis	234
8.2.3	Error estimates	241
8.3	Reduced edge bubbles formulation	247
8.3.1	The modified mimetic discretization	248
8.3.2	Stability of the modified scheme	249
8.3.3	A macroelement technique	250
8.3.4	Sufficient conditions for the stability	252
8.4	Existence of the reconstruction operator	256
8.4.1	Construction of the scalar reconstruction operator	256
8.4.2	Construction of the vector reconstruction operator	258
 Part III Further Developments		
9	Elasticity and plates	263
9.1	Displacement-pressure formulation of linear elasticity	263
9.2	Stress-displacement formulation of linear elasticity	265
9.2.1	Assumptions on mesh and data	266
9.2.2	Degrees of freedom and projection operators	267
9.2.3	Discrete mimetic operators	268
9.2.4	Weak form of discrete equations	270
9.2.5	Practical construction of the scalar product	272
9.2.6	Stability and convergence analysis	274
9.3	Reissner-Mindlin plates	276
9.3.1	Assumptions on mesh and data	277
9.3.2	Degrees of freedom and projection operators	277
9.3.3	Discrete operators and norms	279
9.3.4	Mimetic inner products and bilinear forms	280

9.3.5	Weak form of discrete equations	283
9.3.6	A priori error estimates	283
9.4	Implementation of the method	284
9.4.1	Stiffness matrix for the bilinear form $a_{h,P}$	285
9.4.2	Stiffness matrix for the shear energy term	286
10	Other linear and nonlinear mimetic schemes	289
10.1	Advection-diffusion equation	289
10.1.1	Discretization of the advective term	290
10.1.2	An alternative hybrid discretization of the advection term	295
10.1.3	Convergence analysis	296
10.1.4	Shock-capturing behavior	298
10.2	Obstacle problem	302
10.2.1	The problem formulation	302
10.2.2	A mimetic discretization	302
10.2.3	Convergence of the method	304
10.2.4	Numerical test	309
11	Analysis of parameters and maximum principles	311
11.1	Hybridization techniques	312
11.1.1	The mixed-hybrid mimetic formulation	313
11.1.2	Convergence analysis for Lagrange multipliers	314
11.2	Monotonicity conditions for the mixed-hybrid formulation	317
11.2.1	Triangular and tetrahedral cells	320
11.2.2	Parallelograms	320
11.2.3	Oblique parallelepipeds	324
11.2.4	AMR cells	328
11.3	Monotonicity conditions for the nodal formulation	331
11.3.1	Geometric notation for a quadrilateral cell	331
11.3.2	Sufficient monotonicity conditions on quadrilaterals cells	332
11.4	Non-linear optimization	334
12	Diffusion problem on generalized polyhedral meshes	339
12.1	Diffusion problem in mixed form	340
12.2	Polyhedral meshes with curved faces	341
12.3	Mimetic discretization	346
12.3.1	Degrees of freedom and projection operators	346
12.3.2	Strong and weak forms of discrete equations	349
12.3.3	Stability and consistency conditions	350
12.3.4	Derivation of mimetic inner product	352
12.4	Convergence analysis and error estimates	358
12.4.1	Stability analysis	358
12.4.2	Convergence of the vector variable	361
12.4.3	Convergence of the scalar variable	364
12.5	Exact reconstruction operators	365

12.5.1 Existence of the exact reconstruction operator	365
12.5.2 Superlinear convergence of the scalar variable	367
References	371
Index	391

Part I
Foundation

Model elliptic problems

*“Late Latin mimeticus,
from Greek mimētikos,
from mimeisthai to imitate,
from mimos mime”
(Merriam-Webster’s dictionary
on the origin of word mimetic)*

The mathematical models used to describe our understanding of physical processes become more sophisticated every decade. Thanks to the enormous growth of computational capabilities, modern computer simulations include dozens of coupled physical phenomena. This imposes new requirements on the underlying numerical models. In addition to be accurate approximations of the mathematical models, the best discrete models try to preserve or mimic other important properties of PDEs such as the conservation laws, symmetries, maximum principles, and asymptotic limits. The mimetic finite difference (MFD) method is one of the existing tools used by numerical analysts to design such discrete models.

The MFD method combines the best properties of advanced discretization methods. Like the finite volume method, it works on general polygonal and polyhedral meshes. Like the finite element method, it has a fast growing convergence theory. This book is focused on what is perhaps the most important aspect of the mimetic discretization technology – the derivation of numerical schemes on unstructured polygonal and polyhedral meshes for elliptic PDEs.

It is nowadays recognized that the polyhedral meshes propose a number of advantages for practical applications. When coupled with a robust discretization method such as the MFD, they are more robust to mesh distortion and anisotropy. Meshes with skewed and non-convex cells can still satisfy shape-regularity conditions (see Sect. 1.6) to guarantee high quality of numerical results, a feature that is useful not only for a mesh generation of complex domains, but also for capturing solution features and using dynamically changing meshes. Regular polyhedral and polygonal elements have more rotational symmetries with respect to tetrahedra and hexahedra. This turns out to be very useful in applications such as the topology optimization where a bias to certain mesh directions has to be avoided as most as possible.

The modern simulators of geophysical flows use polyhedral meshes due their flexibility to represent geometric objects varying by many orders in size: tilted geological layers, sharp pinch-outs, faults, and small wells [362]. The applications include anal-

ysis of fresh water subsurface reservoirs, geothermal energy extraction, and control of the fate of hazardous waste buried under the surface. A computational mesh is often built by starting with a two-dimensional polygonal mesh and extruding it in the vertical direction, which leads to a prismatic polyhedral mesh. The MFD method allows us to approximate almost any PDEs on a mesh with arbitrarily shaped cells which makes it well suited for subsurface applications.

Locally refined meshes used in simulation to improve the accuracy of the numerical solution belong to the class of polygonal and polyhedral meshes. In the modern MFD technology the “hanging nodes” are treated as regular mesh nodes thus ensuring automatically full conformity of the discrete solution. The use of polygonal meshes simplifies and makes more efficient the practical implementation of mesh adaptation algorithms and may have a large impact in a numerical solution of dynamic contact problems, such as the problems with sliding domains.

These advantages of polygonal and polyhedral meshes have been recognized by practitioners and implemented in a number of commercial codes, see for example, [152, 298], and publicly available subsurface simulators [274, 362]. The useful features of polygonal and polyhedral meshes stimulated recent development of mimetic schemes for other fundamental classes of problems such as magnetostatics (Chap. 7), fluid mechanics (Chap. 8) and structural mechanics (Chap. 9).

In addition to relatively simple treatment of polyhedral meshes, the MFD method has a number of other interesting properties that stem from the flexibility of its construction and allows it to tackle challenging problems. For example, accurate modeling of geological flows and dispersive transport on polyhedral meshes requires numerical schemes to preserve maximum principles to avoid underestimation and overestimation of concentration of transported chemicals which may be amplified significantly by a nonlinearity of chemical reactions. The MFD method provides a family of schemes that share important properties, such as accuracy and stability. The richness of this family leads to a new research direction called *m-adaptation*, which stands for the mimetic adaptation. The m-adaptation allows us to select an optimal scheme (when possible) in accordance with a problem-dependent criterion, e.g. the maximum principle. Even if the m-adaptation is still under development, some promising results are available and discussed in Chap. 11.

The flexibility of mimetic framework allows us to build stable discretizations with the minimum number of stabilizing degrees of freedom. In Chap. 8, we introduce a stable low-order mimetic scheme for the Stokes problem that uses only vertex-based degrees of freedom for fluid velocity and cell-centered degrees of freedom for pressure.

To model elastic and plastic deformation of solids or geological reservoirs (e.g. due to an extensive pumping out of water or oil), large number of engineering codes use hexahedral and polyhedral meshes. The deformation even of a shape-regular mesh leads to mesh cells with strongly curved faces which require special treatment in almost any discretization method. A similar issue arises in modeling compressible and visco-elastic flows using Lagrangian schemes where the mesh is moving with fluid. The MFD method again has an elegant solution to this problem. Additional degrees of freedom are introduced to capture curvature of mesh faces (Chap. 12); however,

the whole construction of the scheme is not changed. The discretization framework uses local consistency and stability conditions that can accommodate almost any definition of degrees of freedom.

The family of mimetic schemes contains many well-known finite volume (FV) and finite element (FE) methods as particular members. In Chap. 5, we show that the MFD method contains the two-point flux approximation method on orthogonal meshes and the Raviart-Thomas FE method on simplicial meshes. In Chap. 6, we establish a similar result for a nodal mimetic discretization. The MFD method coincides with the Galerkin FE method on simplicial meshes. In the case of quadrilateral meshes, a family of nodal mimetic schemes contains the classical finite difference schemes (5-point and 9-point Laplacians) and the Q_1 FE method. Thus, the MFD method preserves all properties of these methods on a class of simple meshes and extends them to very general polygonal and polyhedral meshes.

The theoretical analysis of the MFD method uses many tools introduced originally in the finite element community such as the Agmon's inequality and a priori error estimates on polyhedral domains. In addition to that, new tools were developed during the last decade using the notion of the reconstruction operator. On a simplex, the reconstruction operator is often (but not always!) a finite element shape function. On a general polyhedron, it is just a theoretical tool that is never needed in practice but is useful to prove error estimates.

The theoretical foundation of the mimetic and compatible discretization methods dates back to the fundamental work of Whitney on geometric integration. The MFD method is related to some of the most basic concepts of discrete differential forms (chain-cochain duality, discrete Stokes theorems). Similar ideas were applied, sometimes naively, many times in the past, as we describe in the historical introductory section. Thus, it is no surprise that the core of the MFD method is a discrete vector and tensor calculus (DVTC). It helps us to prove discrete energy conservation for Maxwell's equations (Chap. 7), symmetry and positive of discrete systems (Chap. 5) and in general to build methods that preserve the underlying structure of the continuum problem for more involved cases such as the Reissner-Mindlin plate bending (Chap. 9).

Modern research topics on the MFD method includes developments of a high-order DVTC and related mimetic schemes, mimetic schemes using non-standard degrees of freedom (solution derivatives), and a posteriori error analysis. Some of these topics are discussed in Chaps. 5 and 6. A similar research is going on for the polygonal and polyhedral FE method, although the available results are much more limited so far.

In the first part of the present chapter we will briefly describe the history of the mimetic finite difference method. Afterwards, we will present the main model problems considered in this book together with minimal results such as the well-posedness and the regularity of the solution. Finally, we will introduce the notation of shape-regular polyhedral and polygonal meshes, together with a set of results useful in the rest of the book.

1.1 A brief history of the mimetic finite difference method

The early history of the mimetic finite difference (MFD) method includes the work carried out in the Soviet Union and for various reasons not well known in the West. The subsequent historic notes and references are representative and by no means pretend to be complete. They represent Authors' involvement in the development and learning of mimetic, and compatible in general, discretization methods.

The development of the MFD method can be divided into four periods. The **first period** begins in the mid-fifties and its main characteristics are:

- the development of numerical methods using discrete operators that preserve important properties of continuum operators;
- the use of orthogonal meshes, where the construction of such mimetic operators is relatively simple;
- the use of the compatibility property of mimetic operators to prove stability and convergence results.

It is pertinent to note that the discrete mimetic operators are build independently, and only then it is proved that they satisfy some duality relationships. The seminal paper [345] (English translation [315]) is one of the earliest work, known to us, based on the concept that discrete analogs of differential operators satisfy discrete analogs of integral identities. These compatible discrete operators are used to derive finite difference schemes and their mimetic properties can be used to prove the stability and convergence of such schemes. The most comprehensive presentation of this theory is in [313, 314, 317, 318].

The importance of compatible discretizations of differential operators has been also recognized and clearly articulated in the series of papers [244–246]. There, the author introduces finite difference analogs of the first-order differential operators ∇ , curl, and div on uniform orthogonal meshes and proves discrete versions of some fundamental identities of calculus, including the orthogonal decomposition theorem. The author proves stability and convergence of the resulting finite difference discretizations for the Laplace equation and elliptic equations with discontinuous coefficients. Similar ideas are used in [237] to discretize the Navier-Stokes equations in a stream function formulation. The discrete model satisfies a law of energy dissipation similar to the one in the continuum case.

In [238] we find a different approach to building compatible discretizations based on the algebraic topology. The differential equations are written using exterior differential forms and discrete analogs of an exterior derivative and the Hodge $*$ operator are constructed. This approach is applied to the Laplace equation, the biharmonic equation, Lamé's equations for isotropic linear elasticity, and steady-state Maxwell's equations. A detailed treatment of Lamé's equations is also given in [236].

In a distinct series of papers [134–137] the concepts of the algebraic topology are used to discretize partial differential equations (PDEs) on orthogonal meshes. In this work, the square mesh on a plane is interpreted as a topological complex. The co-boundary and boundary operators, acting on functions of the complex and defined by the combinatorial structure, generate the difference analogs of the classical differen-

tial operators of mathematical physics, such as ∇ , div , curl , and Laplacian. Furthermore, a discrete model for the steady Euler equations is proposed in [135]. Due to quasi-linearity of these equations, it becomes necessary to introduce a suitable product between discrete differential forms; to this purpose, the Whitney product [361] is chosen. Detailed description of this approach to the construction of discrete models is in the book [138].

In this period, we find a few important papers in the West that introduce elements of the mimetic methodology. In [349], strong relationships between some quantities of physical theories and basic geometric and chronometric objects are investigated. This study leads to a classification of physical theories, where the equations of physics can be described by a single mathematical process, the co-boundary process, which is the exterior differential on co-chains. In [140], a finite difference method on simplicial meshes based on the Whitney forms and a discrete Hodge theory is developed. In [364] a numerical scheme is proposed for solving time-dependent Maxwell's equations on rectangular meshes using a staggered discretization: edge unknowns for the electric field and face unknowns for the magnetic field. This work is the foundation of an entire class of numerical schemes for computational electromagnetics, cf. [341], the *finite difference time domain (FDTD) method*. In [23, 24, 311] mimetic methods for shallow water equations and climate modeling that preserve mass, potential enstrophy and vorticity on logically rectangular meshes are proposed.

Mimetic methods with similar properties are also found for triangular meshes in [299] and [70]. In [183] a finite difference scheme is proposed for second-order elliptic Dirichlet boundary value problems on irregular networks with the topological structure of a logically rectangular mesh. This scheme uses discrete divergence and gradient operators that can be shown are dual to each other. The optimal rate of convergence in a discrete energy-like norm is proved. We also mention the numerical approach proposed in [307] which preserves mass, potential enstrophy, and energy on hexagonal geodesic meshes, and approach in [5] which proposes a mimetic finite difference discretization for the incompressible Navier-Stokes equations. It turns out that these properties are fundamental requirements for a long-term numerical integration of the equations of incompressible fluid motion.

The **second period** in the development of the MFD method begins in the mid-seventies. The new research is motivated by the necessity to solve PDEs with discontinuous coefficients on non-orthogonal meshes. These issues arise naturally in modeling physical problems like the Inertial Confinement Fusion [292, 354], Tokamak [222], high velocity impact dynamics [365], and shape charges [358], which involve domains with complex shapes, several coupled physical processes including gas dynamics, heat conduction, and electromagnetism, and Lagrangian meshes that move with fluid flow. The main characteristics of this period are:

- the derivation of compatible discrete operators is based on variational principles and discrete integral identities; hence, it is not carried out independently for each operator as in the first period;
- components of vector variables (tangential and normal with respect to mesh edges and faces) are used as the degrees of freedom for vector fields;

- a conservative staggered discretization (using cell and nodal grid functions) of the equations of the Lagrangian hydrodynamics is developed.

At the beginning of this period, the variational principle is used to construct different mimetic operators. One operator is identified as the *primary operator* and discretized directly. The other operator is constructed through a discrete version of a variational principle and called the *derived operator*. This technology is summarized in books [316, 348]. The developed schemes are successfully applied to the heat conduction equation [168, 347] and the magnetic diffusion equations [167, 172, 235].

In these works, only selected components of vector variables are used as the degrees of freedom. For example, the heat flux and the magnetic flux density \mathbf{B} are represented by their normal components on mesh faces because these components are continuous across material interfaces. Likewise, the electric field intensity \mathbf{E} is represented by its tangential components on the mesh edges because these components are also continuous. For such a selection of the degrees of freedom, a discretization of integrals in a variational principle becomes a non-trivial task and leads to the development of *mimetic inner products*. These inner products use discrete representations (for example, vectors \mathbf{E}_h and $\tilde{\mathbf{E}}_h$) of continuum vector functions (resp, \mathbf{E} and $\tilde{\mathbf{E}}$) and provide accurate approximations of integrals, e.g:

$$[\mathbf{E}_h, \tilde{\mathbf{E}}_h]_{\mathcal{E}} = \int_{\Omega} \mathbf{E} \cdot \tilde{\mathbf{E}} dV + O(h^p) \quad \forall \mathbf{E}_h, \tilde{\mathbf{E}}_h \in \mathcal{E}_h,$$

where \mathcal{E}_h is a discrete space of edge-based grid functions, the brackets represent its mimetic inner product, h is the characteristic mesh size and p the order of approximation. In the same years, similar ideas appear in the finite element community and lead to the development of mixed finite elements for elliptic and Maxwell's equations, cf. [282, 305].

Another approach to the discretization of Maxwell's equations, the *finite integration technique* (FIT) in introduced in [359]. It uses the primary mesh for the discretization of Faraday's induction law and a dual mesh for the discretization of Maxwell-Ampère's law. An interpolation of the electric field \mathbf{E} and the magnetic field \mathbf{H} between the meshes is needed to discretize the constitutive relations $\mathbf{D} = \varepsilon \mathbf{E}$ and $\mathbf{B} = \mu \mathbf{H}$, where ε is the electric permittivity and μ is the magnetic permeability of the medium. Only later, it was recognized that the interpolation must satisfy special properties for the method to be stable [118]. It is pertinent to note that the mimetic schemes developed in [167, 168, 172, 235, 347] do not require a dual mesh. We refer the reader to [211] where connections between mimetic, mixed finite element and other methods are also discussed.

As we mentioned before, algebraic topology provides natural framework for describing discrete structures. Applying it to the electromagnetism (see, for example, book [75] and references therein) formal mathematical structures associated with edges and faces can be introduced. These structures correspond to the mimetic discretizations of the electric and magnetic fields. Construction of consistent adjoint operators leads to a major problem: the discretization of the Hodge $*$ operator (compare with the interpolation issue in the FIT method). Some contributions to the topic

are made in [170]. Discretization of the Hodge $*$ operator on general grids requires a complex set of mathematical tools. Moreover, these tools are natural for particular discretizations of vector fields and cannot be extended easily to many popular discretizations such as that using nodal values.

The variational principles are also actively used to construct conservative finite difference methods on staggered grids for gas dynamics, magneto-hydrodynamics and dynamics of deformable media, see [171, 187–189, 346] for more details.

The use of the variational principle in the construction of derived operators can be marked as the true beginning of a systematic development of the MFD method. The design principles for the MFD method described in Chap. 2 are clearly formulated in several papers including [169, 230, 312, 319, 320]. There, we find basic tools of the mimetic construction: discrete spaces equipped with inner products, primary discrete operators, discrete derived operators built from discrete duality relationships, and the connection of the duality principle with the desired properties for a discrete model.

In this period, the method is not yet called mimetic. The closest translation from Russian is “*support operator method*”, which does not make much sense besides the fact that the discrete operators support the derivation of numerical schemes for PDEs. Because of this, publishers used a few different translations in English such as “basic operators” and “reference operators”.

Subsequent publications, listed in almost chronological order, show a wide use of the mimetic approach. Axisymmetric difference operators in orthogonal coordinate systems are derived in [232, 233]. Mimetic discrete operators for Voronoi meshes are constructed in [327, 329]. The approach is also extended to equations of gas dynamics in the framework of free-Lagrangian methods [273, 327, 328]. Mimetic discretizations for elliptic equations on non-matching grids are developed in [153]. Mimetic schemes for Maxwell’s equations in the cylindrical geometry on an orthogonal grid are proposed in [139]. The biharmonic equation is treated in [331]. Arbitrary quadrilateral meshes for solving elliptic problems are considered in [324].

During this period, various publications are focused on the analysis of stability and convergence properties of the mimetic discretizations [25–27, 131, 186, 310]. In most of these papers, the stability and convergence results are proved in energy norms induced by the mimetic inner products.

Mimetic discretizations are also used to solve problems of practical interest. We mention a few representative papers: solving Navier-Stokes equations on the Voronoi meshes [22]; solving static problems of elasticity [231]; modeling of the Rayleigh-Taylor instability [181]; modeling compression of a toroidal plasma by the quasi-spherical liner [179, 180]; modeling of a controlled laser fusion [356]; computer simulations of an over-compressed detonation wave in a conic canal [227]; simulation of a magnetic field in a spiral band reel [36, 98]; calculation of viscous incompressible fluid flow with a free surface on two-dimensional Lagrangian meshes [130]; modeling of a microwave plasma generator [260]; and simulation of the collapse of a quasi-spherical target in a hard cone [342].

The design principles for the development of mimetic discretizations are summarized in book [323]. The author applies the support operator method to construct mimetic methods for elliptic and parabolic equations as well as for the equations of

Lagrangian gas dynamics. Only nodal and cell-centered discretizations of vector and scalar functions are considered in this book. The book contains a computer disk with examples of codes implementing various mimetic schemes.

Several papers published in the second period develop a different approach to mimetic discretizations; namely, compatible discretizations for the Lagrangian hydrodynamics [100, 101, 216]. There, the differential operators are not approximated directly, but rather the momentum and internal energy equations are discretized through a balance of the kinetic and internal energy that conserves the total energy. This approach, although specific to the hydrodynamics equations, is quite general. It can be applied to the case where forces of arbitrary nature (e.g., artificial numerical viscosity) are present and/or added to the momentum equation.

Finally, we mention other numerical methods developed during this period that contain mimetic ideas: [284, 285, 287, 288, 309] and [267, 268]. In particular, [267] emphasizes the fact that a discretization of the divergence operator has to be consistent with the change of volume of the computational cell. The same idea is used to construct a mimetic discretization in [188].

The **third period** in the development of the mimetic discretizations begins approximately in the mid-nineties. The main characteristics of this period are:

- the systematic development of the mathematical foundation for the mimetic discretizations and a discrete vector and tensor calculus (DVTC);
- the extension of the mimetic approach to more general meshes including polygonal, polyhedral, locally refined and non-matching meshes;
- an extensive and careful testing of the mimetic discretizations for many different PDEs.

The systematic development of the mathematical foundation for the DVTC begins with three seminal papers [206, 210, 215]. In [215], natural discrete analogs (primary mimetic operators) for ∇ , div , and curl on logically rectangular grids are constructed. Discrete analogs of several important theorems of the continuum calculus are also proved such as $\text{div } \mathbf{A} = 0$ if and only if $\mathbf{A} = \text{curl } \mathbf{B}$. The internal structure of the primary mimetic operators is described in terms of primitive difference and metric operators. In this paper, the terminology “mimetic difference operators” and “mimetic discretizations” is used for the first time, although the word “mimetic” has been already used in the unpublished report [209].

The derived mimetic operators (the discrete dual operators) corresponding to the primary operators are constructed in [210]. The construction of the derived operators is based on the duality principle, e.g.

$$[\mathbf{u}_h, \tilde{\nabla}_h p_h]_{\mathcal{F}_h} = -[\text{div}_h \mathbf{u}_h, p_h]_{\mathcal{P}_h}, \quad \forall \mathbf{u}_h \in \mathcal{F}_h, p_h \in \mathcal{P}_h,$$

where \mathcal{F}_h and \mathcal{P}_h are discrete spaces for face-based and cell-based grid functions, respectively. In other words, the derived gradient operator $\tilde{\nabla}_h$ is negatively adjoint to the primary mimetic operator div_h with respect to the inner products in spaces \mathcal{F}_h and \mathcal{P}_h . The internal structure of the derived operators in terms of primitive difference operators and the inner product matrices is described there. The discrete analogs of

major theorems of the vector calculus are also presented. The set of primary and derived mimetic operators allows one to construct discrete analogs of second-order operators like $\operatorname{div} \nabla$, $\nabla \operatorname{div}$, $\operatorname{curl} \operatorname{curl}$, and the vector Laplace operator $\Delta = \nabla \operatorname{div} - \operatorname{curl} \operatorname{curl}$, which are needed to discretize various PDEs.

The discrete Helmholtz orthogonal decomposition theorems for logically rectangular meshes, for both face-based and edge-based representations of vector fields, are developed in [212]. The DVTC is used in [68] to transfer divergence-free fields represented by their normal components on mesh faces between two different meshes. In [102], the mimetic technology is used to discretize the divergence of a tensor and the gradient of a vector using two different representations of the tensor field via their projections on face normal and edge tangent vectors.

A DVTC calculus is not unique. This fact is exploited in [206] to extend the discrete operators to a domain boundary. The boundary conditions are incorporated into the definition of new mimetic operators. For example, on the boundary, the discrete divergence operator is equal to the normal component of its vector argument. The discrete duality principle includes boundary terms. This fact leads to a new definition of inner products; however, the design principle remains the same – the derived gradient operator is still the negatively adjoint of the (extended) primary divergence operator. This strategy allows us to discretize Neumann and Robin boundary conditions in a natural way using the framework of mimetic discretizations.

The mimetic inner product is usually not unique. In [213], two inner products, which correspond to different reconstructions of a vector field inside a mesh cell, are compared. It is shown that the absolute error is two-three times smaller when the reconstruction uses the Piola transformation compared to the piecewise constant reconstruction. This work is the first analysis of optimal reconstruction operators, see the next period. The non-uniqueness of the mimetic inner product is also analyzed in [286, 352] to develop a unified formulation for the covolume and support operator methods in two dimensions.

Another important paper of this period is [257]. There, equations for the mimetic inner product matrix are derived from accuracy considerations, in particular, from the requirement that the discrete gradient must be exact for linear functions. A solution to this problem is proposed for triangular meshes.

The mimetic inner products for vector functions developed so far are not suitable for degenerate cells (cells with 180° angle between two edges or cells having edges with zero length) and non-convex cells. In [239], a new approach to the construction of inner products for general polygonal cells is proposed. Each cell is subdivided into triangles and new temporary unknowns are introduced on internal edges. Then, the standard mimetic inner product is defined for each triangle and, finally, the temporary unknowns are eliminated using two conditions: the discrete divergence is constant in the cell and the inner product satisfies a stability condition (see Chap. 2). This approach works for arbitrarily-shaped polygons. Moreover, the inner product depends continuously on the shape of the cell, for example, this is the case when a quadrilateral degenerates to a triangle. The same construction is used in [254] for arbitrary polyhedral meshes.

A conceptually new development of the mimetic discretizations is the introduction of the *local support operator method* for diffusion problems [277], where both cell and face unknowns are used to represent the scalar variable. This approach allows one to reduce the discrete problem to a system of algebraic equations with a symmetric positive definite (SPD) matrix and use efficient algebraic solvers. The new technology is developed for triangular meshes [178], meshes with local refinement [251], and non-matching meshes [62].

High-order mimetic discretizations, which use a wider stencil, are developed in [111, 112]. A more extensive research on higher-order schemes is performed in the next period.

Convergence analysis of the mimetic discretizations starts to use more tools from the functional analysis and related discretization methods. For diffusion problems, the convergence results are obtained in [61–63, 214]. The second-order convergence (superconvergence) of the vector variable on smooth meshes is proved in [63]. A mortar technique for the mimetic discretizations on non-matching meshes is developed and analyzed in [62].

In this period, the mimetic discretizations are applied to a wide range of problems: diffusion equations with strongly discontinuous anisotropic coefficients [205, 208, 325]; Maxwell's equations and equations of a magnetic diffusion [207, 211]; equations of the Lagrangian hydrodynamics on general polygonal meshes [104], including an artificial viscosity [103]; equations of a solid dynamics and shallow water equations [266]; and the Lagrangian hydrodynamics on curvilinear logically rectangular meshes preserving spatial symmetries [265].

The foundation for a systematic development of conservative compatible discretizations based on the balance of the kinetic and internal energy is built in [108–110]. Readers may also be interested in the review paper [229] where some other mimetic properties of numerical algorithms are discussed, as well as in paper [299] where conservation properties of unstructured staggered discretizations are discussed.

The **fourth period** in the development of the mimetic discretizations begins after the IMA meeting in 2004 [142]. It is based on the collaboration between the Los Alamos National Laboratory, USA, and a research group in Milano-Pavia, Italy. The main characteristics of this period are:

- the development of novel mathematical tools for design of mimetic discretizations of various PDEs and their convergence analysis;
- the development of a rich parametric family of mimetic discretizations that includes many other discretization methods as particular members;
- the development of arbitrary-order discretizations for elliptic problems, the analysis of the stability and discrete maximum principles.

A set of new mathematical tools introduced in [90] forms the foundation for a rigorous convergence theory for the mimetic discretizations. The subsequent papers [92, 93] develop a new approach to the construction of an accurate mimetic inner product. This inner product is built algebraically to satisfy the consistency and stability conditions that enforce the optimal convergence rate and lead to independent

cell-based problems. Such construction is easy to implement in a computer code. A strategy for a systematic development of mimetic inner products for cochain spaces is discussed in [83, 85].

The consistency and stability conditions have already appeared in a different form in [257], but the new approach results in a number of important developments that are more transformational than incremental. First, the new consistency condition can be formulated for non-convex polygonal and polyhedral cells, including cells with non-planar faces [91]. Second, the consistency and stability conditions do not determine a single scheme but an entire family of mimetic schemes. All members of this family share common properties such as accuracy and convergence rate and have the same stencil size for the derived operators. Third, such family of schemes contains many well-known finite volume and finite element methods.

In [91, 92], the new technology is used to develop and analyze a mimetic discretization for generalized polyhedral meshes having strongly non-flat mesh faces. In [253], it is applied to build a mimetic discretization for equations of the magnetic diffusion in the axisymmetric cylindrical geometry. This scheme remains accurate near the axis of symmetry $r = 0$ and, most important, leads to a consistent calculation of the Joule heating on strongly distorted meshes.

It has been soon discovered that, due to the generality in the allowed meshes, the MFD method constitutes a very appealing ground for the application of adaptive refinement techniques, that, in turn, need some tools in order to estimate the local errors. A residual-based a posteriori estimator for mimetic discretizations has been developed in [41] for the diffusion problem in mixed form, and combined with an adaptive strategy in [54]. The estimator makes use also of a post-processing technique introduced in [106].

The families of mimetic schemes are analyzed in [193, 249, 250] and sub-families of schemes with additional properties are found. The schemes satisfying a discrete maximum principle for diffusion problems are described in [249, 250] for a class of two-dimensional and three-dimensional meshes. In [193], a new mimetic scheme for a well-studied acoustics equation is developed. This scheme has complexity of roughly two second-order schemes but shows the fourth-order numerical dispersion and the sixth-order numerical anisotropy. The last property has never been reported for other state-of-the-art fourth-order schemes.

In [84], the mathematical tools for building accurate mimetic inner products have been extended to semi-inner products representing an energy norm. This allowed us to build new mimetic discretizations for primary formulations of second-order PDEs. A nodal mimetic discretization on polygonal and polyhedral meshes for elliptic problems is developed in [84]. Optimal convergence estimate in the energy norm is proved there. Later, this technology has been extended to more complicated equations, such as the linear elasticity equation [42], the Stokes equations [46, 49] and Reissner-Mindlin plate equations [52, 57]. In [47] the advantage of having polygonal grids is used in order to develop more efficient inf-sup stable elements for the Stokes problem. A hybrid error estimator for the method in [84] has been developed in [16].

It turns out that higher-order mimetic discretizations can be built using the same framework: adding more degrees of freedom and enforcing stronger consistency con-

ditions. The arbitrary-order mimetic discretizations of diffusion problems are developed and analyzed in [50]. In [43], this approach has been recasted as the *virtual element method* (VEM). The VEM is a finite element method where the discrete spaces are virtual in the sense that they are not build explicitly and instead are characterized through properties. Other contributions to the VEM are found in [14, 44, 55, 56, 94]. The practical implementation of the VEM can be based on the mimetic inner products.

The new mimetic discretizations have demonstrated their efficiency in solving convection-diffusion problems in both diffusive [107] and convection-dominated regimes [45], eigenvalue problems in mixed form [105], mixed formulation of a linear elasticity [42], modeling of biological suspensions [194], and modeling of flows in porous media [252].

Finally, the mimetic finite difference method has been developed and analyzed also for nonlinear equations, such as the obstacle problem [17], elliptic quasilinear problems [20] and control problems [19]. A study of dedicated solvers for the MFD method has been initiated in [21].

In this period, development, analysis, and application of the mimetic discretizations have been done by various research groups in Europe and USA including sub-surface flows on corner-point meshes [1]; development of mimetic discretizations based on a discrete calculus for fluid dynamics [300, 301], geophysical flows [5, 70, 307, 344]; oil reservoir simulations [10, 191, 326]; seismic wave propagation on multi-GPU system [330]; viscoelastic wave modeling and rupture dynamics [158, 159]; poroelasticity problems [280]; electromagnetics [35, 258, 259]; plasma physics [297]; astrophysics [279]; pharmaceutical science [119]; general relativity [39]; and image processing [40]. Furthermore, a systematic comparison with other numerical methods for solving 2-D and 3-D elliptic problems with strongly anisotropic diffusion tensors was carried out and presented in the conference benchmarks [165, 195].

1.2 Other compatible discretization methods

The idea of incorporating properties of the continuum calculus in the design of numerical schemes appears in various methods. In a series of articles published in the seventies (see, e.g., [349, 350] and the references therein), it was observed that many physical theories have a very similar formal structure from the geometrical, algebraic and analytic standpoints. This principle has led to Tonti's diagram, a classification scheme of the physical quantities and the physical theories in which they are involved. For example, balance equations, continuity equations, equations of motion, and circuit equations state that one physical quantity defined on a d -dimensional manifold is equal to another physical quantity defined on its boundary. The equations can be reformulated in a finite framework using basic concepts from the algebraic topology such as fully discrete functions (cochains) defined on combination of grid objects (chains) rather than functions in the continuum. Going further along this direction, it is possible to establish a set of direct algebraic relations among geometrically-based

physical variables that is suitable to numerical applications, e.g., the *cell method* (CM) [269, 351]. Although the CM is derived directly from the experimental laws, thus avoiding a discretization of differential equations, its mimetic nature is evident per se. The CM is consistent by design; however, it may result in a non-symmetric discretization for a symmetric problem. Moreover, since the stability condition is not one of the design principles, the CM may lead to an unstable discretization on a strongly distorted mesh.

A unified computational model is proposed in [114, 295, 296] to make a bridge between the geometry and the physical behavior of engineering systems. This model uses differential k -forms and their discrete representation through k -cochains over a cell complex, a finite approximation to a manifold which abstracts only its topological properties, and the co-boundary operator acting on cochains to represent a geometry-based differentiation process. It turns out that only a small set of the usual combinatorial operators, e.g., boundary, co-boundary, and dualization, are sufficient to represent a variety of physical laws and invariants. Cochains as a numerical discretization mechanism and connection with a finite element analysis are also investigated in [295].

The *covolume method* [285] is another example of a compatible discretization method. This method was originally developed for the planar $\text{div} - \text{curl}$ system and was extended later to three-dimensional systems [288], the Navier-Stokes equations, and Maxwell's equations [287]. It can be viewed as a significant generalization of Yee's method to simplicial meshes, and thus can be applied to complex geometries. Like the FDTD, the covolume method requires two orthogonal meshes to approximate the electric and magnetic fields. This is one of its major features but also its major limitation. To this purpose, the Delaunay triangulation and the corresponding Voronoi diagram are the natural choice. Every edge of the Voronoi mesh is orthogonal to the corresponding face of the Delaunay triangulation, and viceversa. The covolume and MFD methods use the same primary operators. However, the construction of the dual operators in the covolume method relies strongly on the orthogonality property of the Delaunay and Voronoi meshes.

Mimetic ideas are also found in [293, 294], where finite difference approximations of differential operators on logically rectangular grids and weighted inner products are designed so that a summation by parts formula mimicking the integration by parts holds. The analogy between the discrete and continuum calculus is rather strong, even stability estimates for these finite difference schemes are obtained following the argument used for continuum problems, including hyperbolic, parabolic, and mixed hyperbolic-parabolic systems. Further developments are found in [271, 338], where the Euler equations are solved using an energy-stable scheme based on the fifth-order summation-by-parts operators, and in [272], where fourth-, sixth- and eighth-order accurate finite difference operators are derived for second-order derivatives.

The *finite volume (FV) method*, introduced originally in [150, 151] for the heat equation and dubbed as the *integrated finite difference method*, leads to the largest class of schemes that can handle unstructured polygonal and polyhedral meshes, non-linear problems, and problems with anisotropic coefficients (see discussion in [160, 161, 164]). These schemes are mimetic in the sense that they enforce balance equa-

tions for mass, momentum, and energy on each mesh cell. The discrete operators in the balance equations coincide with the primary mimetic operators; e.g., the balance of fluxes corresponds to the primary divergence operator acting on face grid functions. The essential difference between the FV and MFD methods is in the approximation of constitutive laws.

In the pioneering works on the integrated finite difference method [151, 281] for the heat equation, Fourier's law is approximated using a two-point flux formula. A diffusive flux across a mesh interface involves temperature unknowns only in the two adjacent cells. Thus, the total number of unknowns equals to the number of mesh cells. This scheme offers the advantage of a very compact computational stencil, but a consistent formulation requires meshes satisfying a rather restrictive orthogonality constraint, e.g., the Voronoi meshes. Combined with a first order-convection flux, this approach is applied to the numerical discretization of non-coercive convection-diffusion equations in [145].

To overcome the disadvantages of the two-point flux formula, an alternative strategy was proposed in [120], namely, the *diamond scheme*. This scheme uses a piecewise constant approximation of the full solution gradient inside auxiliary diamond-shaped subcells. In two-dimensions, the diamond-subcell is formed by a mesh edge and centers of two neighboring cells. The formula for the gradient requires to know auxiliary solution values at end points of each edge. They can be expressed by a linear interpolation of the primary unknowns at neighboring cells. The resulting FV scheme is consistent provided that the interpolation is exact for piecewise linear solutions. Interpolation algorithms based on least squares are known to be quite accurate [64, 66, 123, 124, 262, 263] and used for the discretization of more complex problems [261]. Linearity preserving algorithms are used in more recent papers [363]. Non-linear averages are also investigated in the literature, usually to provide discrete maximum and minimum principles [65, 242, 243, 255].

A breakthrough in the diamond scheme methodology comes from [196, 197], where it is proposed to treat the vertex values as independent unknowns. The resulting scheme combines two distinct FV schemes on two overlapping meshes, the mesh of the primal cells where the original diamond scheme is formulated, and the mesh of the dual control volumes built around the vertices of the primal mesh. The method can be also reformulated in the framework of mimetic discretizations by introducing discrete divergence and gradient operators which are in a duality relationship, i.e. a discrete integration by parts formula holds. This fact motivates the name of the method: the *discrete duality finite volume (DDFV) method*. Such analog requires an inner product for the discrete scalar unknowns that is defined by using simultaneously the overlapping primal and dual meshes and an inner product for the discrete vector unknowns that is defined on the diamond mesh, an auxiliary mesh whose cells are related to the edges of the primal cells. The DDFV method was applied to the Laplace equation in [141] and has shown to provide a very accurate approximation of the solution gradient on distorted meshes [195]. A generalization to nonlinear elliptic equations is found in [13], and to the div-curl problems in [129].

The DDFV method has been also generalized to three-dimensional problems. However, it is subtle to preserve the discrete duality property, which is the basis

for proving well-posedness of the method as well as for deriving optimal estimates of the discretization error. To this purpose, several strategies have been proposed in the literature, mainly in [198, 199], in [122, 302], in [12] and in [121].

Another class of FV methods, consistent by design, is constructed by introducing additional unknowns on mesh faces. Examples of such methods include the *hybrid finite volume method* [162, 163], and the *mixed finite volume method* [146]. These FV methods introduce stabilization terms that can be connected with the stability condition of the mimetic finite difference method, see [148].

Another approach to overcome the limitations induced by the two-point flux formula comes from the multi-point flux approximation (MPFA) method [3, 4] and similar, but developed independently, the control-volume distributed (CVD) method [154, 155]. In the MPFA and CVD methods, fluxes on mesh interfaces having a common point are defined simultaneously from local consistency and continuity conditions. On general meshes, these methods produce non-symmetric schemes for symmetric problems. A lack of a stability condition may result in numerical instabilities on strongly distorted meshes. The MPFA method can be reformulated using the mixed finite element framework as in [360] or the mimetic framework with inner products induced by non-symmetric matrices as in [256]. The latter approach is also used to analyze convergence of the MPFA method in [228].

The *mixed finite element (MFE) method* is, perhaps, the most developed compatible discretization framework, mainly on simplicial meshes. An overview of this method is well beyond the scope of this paper, and for this reason we just refer to the fundamental book [88], the most recent overview provided in the book [69], and the references therein.

Although not related directly to the mimetic concepts, a wide literature has been developed in the last decade to generalize the finite element method to polygonal meshes, namely, the *polygonal finite element method (PFEM)*. We mention the pioneering book [357] and the most recent papers [58, 127, 177, 278, 336, 337, 340].

Although the reformulation of the mimetic discretizations in the framework of differential forms is beyond the scope of this book, it is worth mentioning some important works in this direction. Using topological concepts, strong similarities between numerical methods of very different nature, such as finite volumes, finite differences, and finite elements are outlined in [270]. The connection between the Whitney forms and the MFEs (Nedelec elements) and its application to computational electromagnetics are explored in a series of papers published in the nineties, cf. [72–74] and the references therein, and summarized in the book [75]. A review of basic concepts of the mimetic discretizations and their relations with notions from the algebraic topology is found in [67]. Finite element techniques have been recently recasted in the framework of the Whitney forms and formalized in the finite element exterior calculus, cf. [33, 34]. In this respect, we also mention the work in [200, 201] and the extensions proposed in [96, 97]. The discrete exterior calculus [132, 202] makes it possible to reproduce some well-established finite difference and finite volume methods using unifying notation of the differential forms. Extensions of the FDTD and *finite element time domain* (FETD) methods for solving transient Maxwell's equations in complex media are reviewed in [343].

1.3 Principles of mimetic discretizations

In this section, we highlight the basic principles of the mimetic discretizations using the simple one-dimensional Poisson equation:

$$\begin{aligned} -\frac{d^2 p}{dx^2} &= b, \quad x \in (0, 1), \\ p(0) &= p(1) = 0, \end{aligned} \quad (1.1)$$

where $b(x)$ is a sufficiently smooth given source term. We write this second-order equation as a system of two first-order equations:

$$u = -\frac{dp}{dx}, \quad \frac{du}{dx} = b. \quad (1.2)$$

Let us consider a uniform mesh with $(n + 1)$ nodes $x_i = (i - 1)\Delta x$, where $\Delta x = 1/n$, see Fig. 1.1. We select the following degrees of freedom. The discrete function $u_h \in \mathbb{R}^{n+1}$ approximates the continuum function u at mesh nodes, i.e. $u_h = (u_i)_{i=1}^{n+1}$ and $u_i \approx u(x_i)$. The discrete function $p_h \in \mathbb{R}^n$ is approximated at centers of mesh intervals, i.e. $p_h = (p_{i+1/2})_{i=1}^n$ and $p_{i+1/2} \approx p(x_{i+1/2})$. The well-know finite difference discretization of (1.2) reads:

$$\begin{aligned} u_i &= -\frac{p_{i+1/2} - p_{i-1/2}}{\Delta x}, \quad i = 1, \dots, n + 1, \\ \frac{u_{i+1} - u_i}{\Delta x} &= b(x_{i+1/2}), \quad i = 1, \dots, n, \end{aligned} \quad (1.3)$$

where $p_{1/2} = p_{n+3/2} = 0$. The original mimetic schemes were developed using finite-difference operators, which explains the words “finite difference” in the name of the method. We can formally re-write these equations introducing symbols $\tilde{\nabla}_h$ and div_h (used frequently in this book) for the gradient and divergence operators, respectively:

$$u_h = -\tilde{\nabla}_h p_h, \quad \text{div}_h u_h = b_h,$$

where $b_h = (b_{i+1/2})_{i=1}^n$, and, clearly,

$$(\tilde{\nabla}_h p_h)_i = \frac{p_{i+1/2} - p_{i-1/2}}{\Delta x}, \quad (\text{div}_h u_h)_{i+1/2} = \frac{u_{i+1} - u_i}{\Delta x}. \quad (1.4)$$

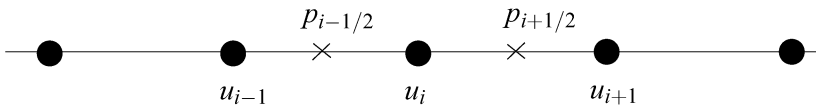


Fig. 1.1. Degrees of freedom in the mixed discretization. Mesh nodes are mark with solid disks

Let us multiply the first equation in (1.3) by u_i and the second one by $p_{i+1/2}$. It is not difficult to verify that

$$\Delta x \sum_{i=1}^{n+1} \frac{p_{i+1/2} - p_{i-1/2}}{\Delta x} u_i = -\Delta x \sum_{i=1}^n \frac{u_{i+1} - u_i}{\Delta x} p_{i+1/2}. \quad (1.5)$$

Using the definitions introduced in (1.4), we have the equivalent expression

$$\Delta x \sum_{i=1}^{n+1} (\tilde{\nabla}_h p_h)_i u_i = -\Delta x \sum_{i=1}^n (\operatorname{div}_h u_h)_{i+1/2} p_{i+1/2}. \quad (1.6)$$

Formula (1.5), and its equivalent expression (1.6), is a discrete integration by parts formula, i.e., a discrete analog of the continuum Green formula

$$\int_0^1 \frac{dp}{dx} u dx = - \int_0^1 p \frac{du}{dx} dx \quad \forall u \in H^1(0,1), p \in H_0^1(0,1).$$

The duality between the discrete gradient and the discrete divergence operators seems like the natural property of the finite difference scheme (1.3). It has many useful consequences; for instance, the elimination of unknowns u_i leads to a system of equations with a symmetric and positive definite matrix. This in turn implies the existence and uniqueness of the solution p_h .

The first mimetic principle is to preserve this discrete duality property in two and three-dimensions on arbitrary polygonal and polyhedral meshes. Apparently this is not possible if we discretize the gradient and divergence operators independently of each other. Let us elaborate this point using the formal presentation of the discrete duality (1.5):

$$[\tilde{\nabla}_h p_h, u_h]_{\mathcal{F}_h} = -[p_h, \operatorname{div}_h u_h]_{\mathcal{P}_h} \quad \forall p_h \in \mathcal{P}_h, \forall u_h \in \mathcal{F}_h. \quad (1.7)$$

Here $\mathcal{P}_h = \mathbb{R}^n$ and $\mathcal{F}_h = \mathbb{R}^{n+1}$ are spaces for p_h and u_h , respectively, and brackets mean the inner products in these spaces:

$$[v_h, u_h]_{\mathcal{F}_h} = \sum_{i=1}^{n+1} \Delta x v_i u_i \quad \forall v_h, u_h \in \mathcal{F}_h$$

and

$$[q_h, p_h]_{\mathcal{P}_h} = \sum_{i=1}^n \Delta x q_{i+1/2} p_{i+1/2} \quad \forall q_h, p_h \in \mathcal{P}_h.$$

The other equivalent way to represent the inner products is to use mass matrices:

$$[v_h, u_h]_{\mathcal{F}_h} = v_h^T M_{\mathcal{F}_h} u_h, \quad [q_h, p_h]_{\mathcal{P}_h} = q_h^T M_{\mathcal{P}_h} p_h.$$

In the considered one-dimensional example, the mass matrices $M_{\mathcal{F}_h}$ and $M_{\mathcal{P}_h}$ are scalar matrices, more precisely, the identity matrices multiplied by Δx . Using these matrices in (1.7), we obtain

$$\tilde{\nabla}_h = -M_{\mathcal{F}_h}^{-1} \operatorname{div}_h^T M_{\mathcal{P}_h}. \quad (1.8)$$

Thus, the discrete divergence operator and the inner product matrices define the unique discrete gradient operator. If we change one of them, we obtain a new scheme where these operators remain negatively adjoint to each other. On an unstructured mesh, only the discrete gradient operator defined via the duality property (1.7) leads to a system of algebraic equations for p_h (after elimination of u_h) with a symmetric and positive definite matrix. For a general PDE, certain discrete operators (called *primal*) will be defined directly as in (1.3), while others (called *dual*) will be defined by discrete duality as in (1.8).

Unfortunately, on unstructured meshes, the construction of the mass matrices is a non-trivial task. This book explains, in particular, how such matrices can be build for polygonal and polyhedral meshes and a great variety of PDEs. The construction uses two additional principles leading to the consistency and stability conditions. We illustrate these principles using the matrix $M_{\mathcal{F}_h}$ and the one-dimensional example.

To simplify the construction of the mass matrix, we typically break it into pieces M_i associated with mesh intervals $[x_i, x_{i+1}]$:

$$M_{\mathcal{F}_h} = \sum_{i=1}^n \mathcal{N}_i^T M_i \mathcal{N}_i, \quad (1.9)$$

where \mathcal{N}_i are the assembling matrices identical to that used in the finite element method. They contains only ones and zeros that indicate in which rows and columns of the global matrix the entries of the local matrix M_i should be inserted.

The local matrices M_i are 2×2 matrices and have the same interpretation as the global mass matrix, more precisely:

$$(v_i, v_{i+1}) M_i \begin{pmatrix} u_i \\ u_{i+1} \end{pmatrix} \approx \int_{x_i}^{x_{i+1}} v u dx.$$

In the one-dimensional case, the global mass matrix is a scalar matrix; hence, it is easy to verify that the following matrices satisfy (1.9):

$$M_i^{FD} = \frac{\Delta x}{2} \begin{pmatrix} 1 & 0 \\ 0 & 1 \end{pmatrix}.$$

A direct calculation shows

$$(v_i, v_{i+1}) M_i^{FD} \begin{pmatrix} u_i \\ u_{i+1} \end{pmatrix} = \Delta x (v_i u_i + v_{i+1} u_{i+1}) = \int_{x_i}^{x_{i+1}} v u dx + O((\Delta x)^3).$$

Thus, the local mass matrices play the role of a quadrature rule for integrals. The accuracy of this quadrature is sufficient to prove that the finite difference scheme is second-order accurate for both p and u . This observation is true for a general polygonal or polyhedral mesh. The quality of a local approximation of cell integrals affects the accuracy of the resulting mimetic scheme. Let us show how the local matrix can be derived from two conditions that can be generalized to arbitrary dimension.

Let us replace the function v by a constant v^0 and the function u by a linear function u^1 . We assume that v^0 equals the average value of v on the $[x_i, x_{i+1}]$ and u^1 takes values

u_i and u_{i+1} at the end points of this interval. Then,

$$\int_{x_i}^{x_{i+1}} v^0 u^1 dx = \int_{x_i}^{x_{i+1}} v u dx + O((\Delta x)^2).$$

This reduced accuracy requirement still leads to the second-order scheme, but most important, it allows us to connect the integrals with the local inner products. We have the following identity:

$$\int_{x_i}^{x_{i+1}} v^0 u^1 dx = \frac{\Delta x}{2} v^0 (u_i + u_{i+1}) = (v^0, v^0) M_i^{FD} \begin{pmatrix} u_i \\ u_{i+1} \end{pmatrix}$$

that holds for any v^0 , u_i , and u_{i+1} . The mimetic consistency condition states: find a 2×2 symmetric positive definite matrix M_i such that

$$(v^0, v^0) M_i \begin{pmatrix} u_i \\ u_{i+1} \end{pmatrix} = \int_{x_i}^{x_{i+1}} v^0 u^1 dx \quad \forall v^0, \forall (u_i, u_{i+1}). \quad (1.10)$$

We already know one solution given by M_i^{FD} . It is not difficult to verify that the matrix M_i^{RT} appearing the lowest-order Raviart-Thomas finite element method also satisfies Eq. (1.10):

$$M_i^{RT} = \frac{\Delta x}{6} \begin{pmatrix} 2 & 1 \\ 1 & 2 \end{pmatrix}.$$

Apparently, there exist a one-parameter family of solutions M_i that includes both positive definite and indefinite matrices. Most of SPD matrices will lead to a well behaved numerical scheme, which obviously leave some room for an optimization (see Chap. 11). To eliminate indefinite matrices from the analysis, we need the stability condition that states: There exists two positive constants σ_* and σ^* independent of Δx such that

$$\sigma_* \Delta x (u_i^2 + u_{i+1}^2) \leq (u_i, u_{i+1}) M_i \begin{pmatrix} u_i \\ u_{i+1} \end{pmatrix} \leq \sigma^* \Delta x (u_i^2 + u_{i+1}^2) \quad \forall (u_i, u_{i+1}).$$

For the finite difference matrix this condition holds with $\sigma_* = \sigma^* = 1$. For the Raviart-Thomas matrix, we have $\sigma_* = 1$ and $\sigma^* = 3$. Multiple examples of the application of the consistency and stability conditions will be considered in the subsequent chapters.

Remark 1.1. In the engineering community, the consistency condition is closely related to the patch test.

For general polygonal and polyhedral meshes, the concept of the consistency and stability conditions allows us to derive accurate approximations of the L^2 integrals of scalar and vector functions presented by various degrees of freedom, including point values, normal and tangential components, and face and cell moments. This concept can be extended to derive high-order schemes on such meshes (see Chaps. 5 and 6).

The consistency and stability conditions can be used to derive discrete representations of more general bilinear forms, such as that representing H^1 -type semi-inner

products of scalar and vector functions. Moreover, by making use of this construction one can develop a different approach to mimetic discretizations, based on the variational form of the problem (rather than the strong form). Although the two methodologies are often equivalent, this second one turns out to be more flexible; it is therefore convenient to have a clear picture of both approaches. Let us illustrate this second choice through a simple application on the one-dimensional Poisson equation. Its weak formulation reads:

Find $p \in H_0^1(0, 1)$ such that

$$\int_0^1 \frac{dp}{dx} \frac{dq}{dx} dx = \int_0^1 b q dx \quad \forall q \in H_0^1(0, 1).$$

Let us select the following degrees of freedom. The discrete vector $p_h \in \mathbb{R}^{n-1}$ approximates the continuum function p at mesh nodes, i.e. $p_h = (p_i)_{i=1}^{n-1}$ and $p_i \approx p(x_{i+1})$. Similarly, let $q_h \in \mathbb{R}^{n-1}$ be the approximation of q .

There are a few admissible approximations of the right-hand side integral in the weak formulation, e.g.

$$\Delta x \sum_{i=1}^n b(x_i) q_i = \int_0^1 b q dx + O((\Delta x)^2).$$

For the left-hand we formally introduce a global stiffness matrix M such that

$$p_h^T M q_h \approx \int_0^1 \frac{dp}{dx} \frac{dq}{dx} dx + O(\Delta x),$$

i.e. we are looking for a numerical scheme that will be the first-order accurate in the energy norm. The global stiffness matrix is assembled from elemental matrices M_i , where $i = 1, \dots, n-1$. The consistency and stability conditions are now used to find local stiffness matrices that represent accurate (at least, first-order) approximations of the local bilinear forms.

We consider the interval $[x_i, x_{i+1}]$ and make the following observation. Let $p = p^1 + O((\Delta x)^2)$ on this interval, where p^1 is a linear function with values p_i and p_{i+1} at the end points of the interval. Then, for all sufficiently regular functions q

$$\begin{aligned} \int_{x_i}^{x_{i+1}} \frac{dp}{dx} \frac{dq}{dx} dx &= \int_{x_i}^{x_{i+1}} \frac{dp^1}{dx} \frac{dq}{dx} dx + O((\Delta x)^2) \\ &= \frac{dp^1}{dx} (q(x_{i+1}) - q(x_i)) + O((\Delta x)^2). \end{aligned} \tag{1.11}$$

The mimetic consistency condition states: Find a local stiffness matrix M_i such that

$$(p^1(x_i), p^1(x_{i+1})) M_i \begin{pmatrix} q_i \\ q_{i+1} \end{pmatrix} = \int_{x_i}^{x_{i+1}} \frac{dp^1}{dx} \frac{dq}{dx} dx \quad \forall p^1, q. \tag{1.12}$$

Therefore, each solution to (1.12) satisfies:

$$(p^1(x_i), p^1(x_{i+1})) M_i \begin{pmatrix} q_i \\ q_{i+1} \end{pmatrix} = \int_{x_i}^{x_{i+1}} \frac{dp}{dx} \frac{dq}{dx} dx + O((\Delta x)^2) \quad \forall p, q,$$

which is sufficient to prove linear convergence to the solution in an energy-type norm.

Note that the right hand side in (1.12) is computable due to the second identity in (1.11), stating that

$$\int_{x_i}^{x_{i+1}} \frac{dp^1}{dx} \frac{dq}{dx} dx = \frac{dp^1}{dx} (q(x_{i+1}) - q(x_i))$$

for all linear p^1 and regular q . The consistency condition (1.12) can be simplified by noting that q_h is an arbitrary vector:

$$M_i \begin{pmatrix} p^1(x_i) \\ p^1(x_{i+1}) \end{pmatrix} = \frac{dp^1}{dx} \begin{pmatrix} -1 \\ +1 \end{pmatrix} \quad \forall p^1.$$

There is no need to consider all possible linear function p^1 . It is sufficient to take two linearly independent functions, e.g. $p^1 = 1$ and $p^1 = x - x_{i+1/2}$ that give two matrix equations. We write these equation in a compact form:

$$M_i \begin{pmatrix} 1 & -\Delta x/2 \\ 1 & +\Delta x/2 \end{pmatrix} = \begin{pmatrix} 0 & -1 \\ 0 & +1 \end{pmatrix}.$$

The solution is now obvious (and unique):

$$M_i = \frac{1}{\Delta x} \begin{pmatrix} +1 & -1 \\ -1 & +1 \end{pmatrix}.$$

The same matrix appears in the Galerkin finite element method. A similar result holds in higher dimensions for triangular and tetrahedral cells. However, for more general polygonal and polyhedral cells, the number of independent equations generated by the consistency condition is smaller than the size of the stiffness matrix. In such a case, the solution of the matrix equation is not unique. To avoid spurious solutions, the elemental stiffness matrix is required to satisfy the stability condition (see Chap. 4).

Various bilinear forms are considered in the subsequent chapters. But the discretization strategy remains the same: select a proper polynomial approximation space for p and the proper degrees of freedom, so that the right-hand side of the consistency condition can be simplified and written in terms of the degrees of freedom. The matrix form of the consistency condition is always looks like $M_i N_i = R_i$ where N_i and R_i are computed using the cell geometry and problem coefficients. The generic formula from Chap. 4 gives a solution M_i to this matrix equation that satisfies the stability condition.

The development of higher-order mimetic schemes uses the same strategy; the set of degrees of freedom typically may include point-values and moments of functions associated to vertexes, edges, faces and elements.

1.4 Scalar elliptic problems

Throughout this book we use a regular font for scalar functions (e.g., p , u , or c) and a bold font for vector functions and tensors (e.g., \mathbf{u} and $\boldsymbol{\sigma}$). Also, we assume that the computational domain Ω is a Lipschitz domain, i.e. its boundary $\Gamma = \partial\Omega$ can be described locally by a Lipschitz continuous function. Moreover we will assume that the boundary of Ω is divided into two parts

$$\Gamma = \Gamma_D \cup \Gamma_N,$$

each being a (possibly void) finite sum of connected components of Γ .

1.4.1 Diffusion equation in primal form

The steady-state diffusion problem for scalar field p is given by the Poisson equation [303]:

$$\begin{aligned} -\operatorname{div}(\mathbf{K}\nabla p) &= b & \text{in } \Omega, \\ p &= g^D & \text{on } \Gamma_D, \\ (\mathbf{K}\nabla p) \cdot \mathbf{n} &= g^N & \text{on } \Gamma_N, \end{aligned} \quad (1.13)$$

where \mathbf{K} is the diffusion tensor describing the material properties, b is the forcing term, g^D and g^N are the boundary functions defining the Dirichlet and Neumann boundary conditions, respectively. We assume for simplicity that $\operatorname{meas}(\Gamma_D) > 0$ to avoid a non-trivial kernel. In addition to that, we make the following standard assumptions.

(H1) The diffusion tensor $\mathbf{K} : \Omega \rightarrow \mathbb{R}^{2 \times 2}$ is a $d \times d$ bounded, measurable, and symmetric tensor. Moreover, \mathbf{K} is *strongly elliptic*, i.e., there exist two positive constants κ_* and κ^* such that for every $\mathbf{x} \in \Omega$ it holds

$$\kappa_* \|\mathbf{v}\|^2 \leq \mathbf{v} \cdot \mathbf{K}(\mathbf{x})\mathbf{v} \leq \kappa^* \|\mathbf{v}\|^2 \quad \forall \mathbf{v} \in \mathbb{R}^d, \quad (1.14)$$

where $\|\mathbf{v}\| = (\mathbf{v} \cdot \mathbf{v})^{1/2}$ is the Euclidean norm of vector \mathbf{v} .

(H2) The boundary data functions g^D , g^N belong to $H^{1/2}(\Gamma_D)$ and the dual of $H_{00}^{1/2}(\Gamma_N)$, respectively. The load function b belongs to the dual of $H_{0,D}^1(\Omega)$ that is introduced below. Moreover, we assume that Γ_D is of positive measure.

Remark 1.2. From the assumption of strong ellipticity it follows that the matrix $\mathbf{K}(\mathbf{x})$ is positive definite for every $\mathbf{x} \in \Omega$. Hence, the inverse matrix $\mathbf{K}(\mathbf{x})^{-1}$ is also symmetric and positive definite, and satisfies analogous lower and upper bounds involving, respectively, $(\kappa^*)^{-1}$ and κ_*^{-1} .

Let us consider the functional space

$$H_g^1(\Omega) = \{w \in H^1(\Omega) : w = g \text{ on } \Gamma_D\}$$

for the function g in $H^{1/2}(\Gamma_D)$. Let $H_{0,D}^1(\Omega)$ denote the space $H_g^1(\Omega)$ in the case $g = 0$. Problem (1.13) can be restated in the variational form: *Find $p \in H_{g^D}^1(\Omega)$ such that*

$$\int_{\Omega} \mathbb{K} \nabla p \cdot \nabla w \, dV = \langle b, w \rangle_{\Omega} + \langle g^N, w \rangle_{\Gamma_N} \quad \forall w \in H_{0,D}^1(\Omega). \quad (1.15)$$

The terms in the right-hand side represent duality products that can be written as regular integrals in case of smooth boundary data.

Under assumptions **(H1)**–**(H2)**, problem (1.13) is well-posed [190]. The existence and uniqueness of the weak solution of the variational formulation follows by the coerciveness and boundedness of the bilinear form in the left-hand side of (1.15). The following regularity result holds.

Theorem 1.1. *There exist two constants $1/2 < \sigma \leq 1$ and $C = C(\Omega, \sigma, \mathbb{K}) > 0$ such that the following holds. If the load $b \in L^2(\Omega)$, the tensor $\mathbb{K} \in W^{1,\infty}(\Omega)$ and the boundary data functions $g^N \in H^{\sigma-1/2}(\Gamma_N)$ and $g^D \in H^{\sigma+1/2}(\Gamma_D)$, then the solution to the Poisson equation $p \in H^{1+\sigma}(\Omega)$ with the bound*

$$\|p\|_{H^{1+\sigma}(\Omega)} \leq C \left(\|b\|_{L^2(\Omega)} + \|g^D\|_{H^{\sigma+1/2}(\Omega)} + \|g^N\|_{H^{\sigma-1/2}(\Omega)} \right). \quad (1.16)$$

Moreover, if Ω is convex, then $\sigma = 1$.

1.4.2 Diffusion equation in mixed form

We formulate the Darcy problem by rewriting problem (1.13) in the equivalent mixed form for the scalar solution field p and the vector flux field \mathbf{u} as

$$\begin{aligned} \mathbf{u} + \mathbb{K} \nabla p &= 0 & \text{in } \Omega, \\ \operatorname{div} \mathbf{u} &= b & \text{in } \Omega, \\ p &= g^D & \text{on } \Gamma^D, \\ \mathbf{u} \cdot \mathbf{n} &= -g^N & \text{on } \Gamma^N. \end{aligned} \quad (1.17)$$

We consider again assumption **(H1)** from the previous section and modify assumption **(H2)** as follows.

(H2a) The boundary data functions g^D, g^N belong to $H^{1/2}(\Gamma_D)$ and the dual of $H_{00}^{1/2}(\Gamma_N)$, respectively. The load function b belongs to $L^2(\Omega)$. Moreover, we assume that Γ_D has positive measure.

Let us introduce the space

$$X_g = \{\mathbf{v} \in H(\operatorname{div}, \Omega) : \mathbf{v} \cdot \mathbf{n} = -g \text{ on } \Gamma_N\}.$$

The variational formulation of problem (1.17) is as follows: *Find* $\mathbf{u} \in X_{g^N}$ *and* $p \in L^2(\Omega)$ *such that*

$$\int_{\Omega} \mathbb{K}^{-1} \mathbf{u} \cdot \mathbf{v} dV - \int_{\Omega} p \operatorname{div} \mathbf{v} dV = -\langle g^D, \mathbf{v} \cdot \mathbf{n} \rangle_{\Gamma_D} \quad \forall \mathbf{v} \in X_0, \quad (1.18)$$

$$\int_{\Omega} q \operatorname{div} \mathbf{u} dV = \int_{\Omega} b q dV \quad \forall q \in L^2(\Omega). \quad (1.19)$$

Under assumptions **(H1)** and **(H2a)** it is possible to show that problem (1.17) is well-posed [190]. Moreover, the same regularity result stated in Theorem 1.1 holds again.

1.4.3 Advection-diffusion equation in mixed form

Many biological and geophysical problems involve transport of the scalar field c (species concentration for mass transfer in porous media or temperature for heat transfer) with the vector field β . This process is described by the advection-diffusion equation:

$$\begin{aligned} \operatorname{div}(\beta c - \mathbb{K} \nabla c) &= b & \text{in } \Omega, \\ c &= g^D & \text{on } \Gamma. \end{aligned} \quad (1.20)$$

Let us introduce the diffusive flux $\mathbf{u} = -\mathbb{K} \nabla c$ and the total flux $\tilde{\mathbf{u}} = \mathbf{u} + \beta c$. Then, the advection-diffusion problem can be reformulated as follows:

$$\begin{aligned} \tilde{\mathbf{u}} + \mathbb{K} \nabla c - \beta c &= 0 & \text{in } \Omega, \\ \operatorname{div} \tilde{\mathbf{u}} &= b & \text{in } \Omega, \\ c &= g^D & \text{on } \Gamma. \end{aligned} \quad (1.21)$$

We consider assumptions **(H1)**–**(H2a)** and make an additional assumption on the velocity field:

(H3) $\beta \in C^1(\overline{\Omega})^d$ and is such that $\operatorname{div} \beta \geq 0$.

The variational formulation of problem (1.21) is as follows: *Find* $\tilde{\mathbf{u}} \in H(\operatorname{div}, \Omega)$ *and* $p \in L^2(\Omega)$ *such that*

$$\begin{aligned} \int_{\Omega} \mathbb{K}^{-1} \tilde{\mathbf{u}} \cdot \mathbf{v} dV - \int_{\Omega} c \operatorname{div} \mathbf{v} dV - \int_{\Omega} \mathbb{K}^{-1} \beta c \cdot \mathbf{v} dV &= \langle g^D, \mathbf{v} \cdot \mathbf{n} \rangle_{\Gamma}, \\ \int_{\Omega} q \operatorname{div} \tilde{\mathbf{u}} dV &= \int_{\Omega} b q dV, \end{aligned} \quad (1.22)$$

hold for all $\mathbf{v} \in H(\operatorname{div}, \Omega)$ and $q \in L^2(\Omega)$.

Under assumptions **(H1)**, **(H2a)** and **(H3)**, problem (1.22) is well-posed. Under such hypotheses, a regularity result analogous to Theorem 1.1 holds also for the present problem.

1.5 Vector elliptic problems

We consider examples of vector elliptic problems that can be solved numerically using mimetic discretizations.

1.5.1 Stokes problem

The incompressible Stokes problem for the vector field \mathbf{u} and the scalar pressure field p is given by

$$-\operatorname{div}(v\varepsilon(\mathbf{u})) + \nabla p = \mathbf{b} \quad \text{in } \Omega, \quad (1.23)$$

$$\operatorname{div} \mathbf{u} = 0 \quad \text{in } \Omega, \quad (1.24)$$

$$\mathbf{u} = \mathbf{g}^D \quad \text{on } \Gamma^D, \quad (1.25)$$

$$v\varepsilon(\mathbf{u}) \cdot \mathbf{n} = \mathbf{g}^N \quad \text{on } \Gamma^N, \quad (1.26)$$

where \mathbf{b} is the forcing term, $v > 0$ is the fluid viscosity, \mathbf{g}^D and \mathbf{g}^N are boundary data, and $\varepsilon(\mathbf{u})$ is the symmetric strain tensor,

$$\varepsilon(\mathbf{u}) = \frac{1}{2}(\nabla \mathbf{u} + (\nabla \mathbf{u})^T).$$

Let us consider the functional space $V = (H^1(\Omega))^d$, space

$$V_{\mathbf{g}^D} = \{ \mathbf{u} \in V \text{ such that } \mathbf{u} = \mathbf{g}^D \text{ on } \Gamma^D \}, \quad (1.27)$$

and the subspace $V_0 \subset V$ obtained by setting $\mathbf{g} = 0$ in the definition above. We assume minimal regularity of input data.

(H4) The vector-valued function \mathbf{b} belongs to the dual of V_0 , the vector-valued function \mathbf{g}^N belongs to the dual of $(H_{00}^{1/2}(\Gamma^N))^d$, and $\mathbf{g}^D \in (H^{1/2}(\Gamma^D))^d$. For a pure Dirichlet problem ($\Gamma^N = \emptyset$), \mathbf{g}^D must also satisfy the compatibility condition

$$\int_{\Gamma} \mathbf{g}^D \cdot \mathbf{n} \, dS = 0.$$

The space Q of admissible pressures depends on the Neumann boundary condition:

$$Q = \begin{cases} L^2(\Omega) & \text{if } \Gamma^N \neq \emptyset, \\ L^2(\Omega)/\mathbb{R} & \text{if } \Gamma^N = \emptyset, \end{cases} \quad (1.28)$$

where we denote

$$L^2(\Omega)/\mathbb{R} = \left\{ q \in L^2(\Omega) : \int_{\Omega} q \, dV = 0 \right\}.$$

Multiplying equations (1.23)–(1.24) by the test functions $\mathbf{v} \in V_0$ and $q \in Q$, respectively, and integrating by parts yields the variational formulation:

Find $\mathbf{u} \in V_{\mathbf{g}^D}$ and $p \in Q$ such that

$$\int_{\Omega} \mathbf{v} \boldsymbol{\varepsilon}(\mathbf{u}) : \boldsymbol{\varepsilon}(\mathbf{v}) dV - \int_{\Omega} p \operatorname{div} \mathbf{v} dV = \langle \mathbf{b}, \mathbf{v} \rangle_{Q_{\Omega}} + \langle \mathbf{g}^N, \mathbf{v} \rangle_{\Gamma^N} \quad \forall \mathbf{v} \in V_0, \quad (1.29)$$

$$\int_{\Omega} q \operatorname{div} \mathbf{u} dV = 0 \quad \forall q \in Q, \quad (1.30)$$

where the double dot “:” stands for the standard contraction operator between tensors. The Dirichlet condition (1.25) is taken into account as the essential boundary condition by seeking the velocity in space $V_{\mathbf{g}^D}$. The terms on the right hand side represent duality products, but in the case $\mathbf{b} \in (L^2(\Omega))^d$ and $\mathbf{g}^N \in (L^2(\Gamma^N))^d$ their can be written as regular integrals.

Let us assume that $\operatorname{meas}(\Gamma^D) > 0$ and \mathbf{v} is bounded from below by a positive constant. Then, due to Korn’s inequality, see for instance [116], we have the coercivity of the bilinear form above over the space V_0 :

$$\int_{\Omega} \mathbf{v} \boldsymbol{\varepsilon}(\mathbf{v}) : \boldsymbol{\varepsilon}(\mathbf{v}) dV \geq \alpha \|\mathbf{v}\|_{H^1(\Omega)}^2 \quad \forall \mathbf{v} \in V_0, \quad (1.31)$$

where α is a positive constant. Moreover, the following inf-sup condition holds, see [184]. There exists a positive constant β such that for every $q \in Q$ it is possible to find $\mathbf{v} \in V_0$ that satisfies

$$\int_{\Omega} q \operatorname{div} \mathbf{v} dV \geq \beta \int_{\Omega} q dV \quad \text{and} \quad \|\mathbf{v}\|_{H^1(\Omega)} \leq 1. \quad (1.32)$$

The above coercivity and inf-sup conditions are sufficient for proving the existence and uniqueness of the solution of (1.29)–(1.30). Moreover, we have the following regularity result, see [224].

Theorem 1.2. *Let Ω be a convex domain. Furthermore, let $\mathbf{b} \in (L^2(\Omega))^d$ and the boundary data $\mathbf{g}^N \in (H^{1/2}(\Gamma^N))^d$, $\mathbf{g}^D \in (H^{3/2}(\Gamma^D))^d$. Then, solution $\mathbf{u} \in (H^2(\Omega))^d$, $p \in H^1(\Omega)$, and there exists a positive constant $C = C(\Omega)$ such that*

$$\|\mathbf{u}\|_{H^2(\Omega)} + \|p\|_{H^1(\Omega)} \leq C \left(\|\mathbf{b}\|_{L^2(\Omega)} + \|\mathbf{g}^D\|_{H^{3/2}(\Omega)} + \|\mathbf{g}^N\|_{H^{1/2}(\Omega)} \right).$$

The Stokes problem is very similar to the displacement-pressure formulation of the incompressible linear elasticity problem, which is considered in the next section.

1.5.2 Linear elasticity problem

Let domain Ω represent an elastic body that is blocked on a part of the boundary $\Gamma^D \subset \partial\Omega$ and is free on the remaining part Γ^N . We assume that $\operatorname{meas}(\Gamma^D) > 0$ in order to eliminate the rigid body motions. Then, following the classical theory of

linear elasticity (see, e.g., [115]), the deformation of Ω is governed by

$$\boldsymbol{\sigma} = \mathbb{C}\boldsymbol{\varepsilon}(\mathbf{u}) \quad \text{in } \Omega, \quad (1.33)$$

$$-\mathbf{div} \boldsymbol{\sigma} = \mathbf{b} \quad \text{in } \Omega, \quad (1.34)$$

$$\mathbf{u} = \mathbf{g}^D \quad \text{on } \Gamma^D, \quad (1.35)$$

$$\boldsymbol{\sigma} \cdot \mathbf{n} = \mathbf{g}^N \quad \text{on } \Gamma^N, \quad (1.36)$$

where $\boldsymbol{\sigma}$ is the stress tensor, \mathbf{b} the external loading term, \mathbf{u} the displacement vector, \mathbb{C} the tensor of elastic moduli, \mathbf{g}^D the boundary displacement, and \mathbf{g}^N the boundary force.

In general, \mathbb{C} can be a full fourth-order tensor; however, many materials are described by the two Lamè parameters μ and λ . In this case,

$$\mathbb{C}\boldsymbol{\varepsilon}(\mathbf{u}) = 2\mu\boldsymbol{\varepsilon}(\mathbf{u}) + \lambda \operatorname{tr}(\boldsymbol{\varepsilon}(\mathbf{u}))\mathbb{I}$$

where \mathbb{I} is the second-order identity tensor, and tr is the trace operator.

We make the following assumptions.

(H5) The material functions $\mu(x)$ and $\lambda(x)$ belong to $L^\infty(\Omega)$ and there exist two positive constants μ_* , μ^* such that $\mu_* \leq \mu(x) \leq \mu^*$ on Ω .

(H6) The boundary functions \mathbf{g}^D and \mathbf{g}^N belong, respectively, to $(H^{1/2}(\Gamma^D))^d$ and the dual of $(H_{00}^{1/2}(\Gamma^N))^d$. The load function \mathbf{b} belongs to $(L^2(\Omega))^d$.

Let us define the following space of stress tensor fields:

$$H_{\mathbf{div}}(\Omega; \mathbf{g}) = \{ \boldsymbol{\tau} \in (L^2(\Omega))^{d \times d} : \operatorname{div} \boldsymbol{\tau} \in (L^2(\Omega))^d, \boldsymbol{\tau} \cdot \mathbf{n} = \mathbf{g} \text{ on } \Gamma^N \}.$$

The space $H_{\mathbf{div}}(\Omega; 0)$ is derived from the previous definition by setting $\mathbf{g} = 0$. A mixed weakly symmetric formulation of problem (1.33)-(1.36) reads:

Find $(\boldsymbol{\sigma}, \mathbf{u}, \mathbf{s}) \in H_{\mathbf{div}}(\Omega; \mathbf{g}^N) \times (L^2(\Omega))^d \times (L^2(\Omega))^d$ such that:

$$\int_{\Omega} \mathbb{C}^{-1} \boldsymbol{\sigma} : \boldsymbol{\tau} dV + \int_{\Omega} \mathbf{u} \cdot \mathbf{div} \boldsymbol{\tau} dV + \int_{\Omega} \mathbf{s} \cdot \mathbf{as}(\boldsymbol{\tau}) dV = \langle \mathbf{g}^D, \boldsymbol{\tau} \cdot \mathbf{n} \rangle_{\Gamma^D} \quad \forall \boldsymbol{\tau} \in H_{\mathbf{div}}(\Omega; 0), \quad (1.37)$$

$$\int_{\Omega} \mathbf{div} \boldsymbol{\sigma} \cdot \mathbf{v} dV = \langle \mathbf{b}, \mathbf{v} \rangle_{\mathcal{Q}_{\Omega}} \quad \forall \mathbf{v} \in (L^2(\Omega))^d, \quad (1.38)$$

$$\int_{\Omega} \mathbf{as}(\boldsymbol{\sigma}) \cdot \mathbf{q} dV = 0 \quad \forall \mathbf{q} \in L^2(\Omega). \quad (1.39)$$

In three dimensions, the anti-symmetry operator $\mathbf{as} : \mathbb{R}^{3 \times 3} \rightarrow \mathbb{R}^3$ is defined by

$$\mathbf{as}(\boldsymbol{\tau}) = \begin{pmatrix} \boldsymbol{\tau}_{12} - \boldsymbol{\tau}_{21} \\ \boldsymbol{\tau}_{13} - \boldsymbol{\tau}_{31} \\ \boldsymbol{\tau}_{23} - \boldsymbol{\tau}_{32} \end{pmatrix}, \quad (1.40)$$

where the subindices indicate components of the tensor. In two dimensions, \mathbf{as} becomes a scalar operator, $\mathbf{as}(\boldsymbol{\tau}) = \boldsymbol{\tau}_{12} - \boldsymbol{\tau}_{21}$.

The bilinear form $\int_{\Omega} \mathbb{C}^{-1} \boldsymbol{\sigma} : \boldsymbol{\tau} dV$ is symmetric and L^2 -positive definite since

$$\mathbb{C}^{-1} \boldsymbol{\tau} = \frac{1}{2\mu} \boldsymbol{\tau} - \frac{\lambda}{2\mu(2\mu + d\lambda)} \text{tr}(\boldsymbol{\tau}) \mathbb{I}. \quad (1.41)$$

In the limiting case of an incompressible material, when $\lambda \rightarrow +\infty$, the coercivity on the whole space of tensors is lost and holds only on the subspace of traceless tensors. Under assumptions **(H4)**–**(H5)**, problem (1.37)–(1.39) is stable; thus, its solution exists and is unique (see, for instance, [30, Theorem 2.1]). Moreover, the following regularity result holds [116].

Theorem 1.3. *Let domain Ω be convex and the material data $\mu, \lambda \in W^{1,\infty}(\Omega)$. Furthermore, let the load $\mathbf{b} \in (L^2(\Omega))^d$ and the boundary data $\mathbf{g}^N \in (H^{1/2}(\Gamma_N))^d$, $\mathbf{g}^D \in (H^{3/2}(\Gamma_D))^d$. Then, for the solution of problem (1.37)–(1.39) we have $\boldsymbol{\sigma} \in (H^1(\Omega))^{d \times d}$, $\mathbf{u} \in (H^2(\Omega))^d$, and $\mathbf{s} \in (H^1(\Omega))^d$. Moreover, there exists a positive constant $C = C(\Omega, \mu, \lambda)$ such that*

$$\|\boldsymbol{\sigma}\|_{H^1(\Omega)} + \|\mathbf{u}\|_{H^2(\Omega)} + \|\mathbf{s}\|_{H^1(\Omega)} \leq C(\|\mathbf{b}\|_{L^2(\Omega)} + \|\mathbf{g}^D\|_{H^{3/2}(\Omega)} + \|\mathbf{g}^N\|_{H^{1/2}(\Omega)}).$$

Note that there exists a different variational formulation of continuum equations (1.33)–(1.36) that shows strong connection with the Stokes problem. Let assumption **(H4)** of Sect. 1.5.1, and assumption **(H5)** of this section hold. Let the spaces $V_{\mathbf{g}^D}$, V_0 , and Q be defined as in Sect. 1.5.1. Substituting (1.33) into (1.34), introducing the pressure

$$p = \lambda \text{tr}(\boldsymbol{\varepsilon}(\mathbf{u})) = \lambda \text{div} \mathbf{u}, \quad (1.42)$$

and then following the same steps as for the Stokes problem, we obtain a displacement-pressure variational problem:

Find $\mathbf{u} \in V_{\mathbf{g}^D}$ and $p \in Q$ such that

$$\int_{\Omega} 2\mu \boldsymbol{\varepsilon}(\mathbf{u}) : \boldsymbol{\varepsilon}(\mathbf{v}) dV - \int_{\Omega} p \text{div} \mathbf{v} dV = \langle \mathbf{b}, \mathbf{v} \rangle_{Q_0} + \langle \mathbf{g}^N, \mathbf{v} \rangle_{\Gamma^N} \quad \forall \mathbf{v} \in V_0, \quad (1.43)$$

$$\int_{\Omega} q \text{div} \mathbf{u} dV - \lambda^{-1} \int_{\Omega} pq dV = 0 \quad \forall q \in Q. \quad (1.44)$$

The above problem resembles to the variational formulation of the Stokes problem. Indeed, in the case of incompressible elasticity, $\lambda = +\infty$, the corresponding integral disappears and the two problems become essentially identical. The stability and regularity results for the Stokes problem hold also for problem (1.43)–(1.44).

Although formulation (1.43)–(1.44) is equivalent to (1.37)–(1.39), their discretizations will lead to different schemes.

1.5.3 Reissner-Mindlin plate bending problem

Consider an elastic plate $\Omega \times (-\frac{t}{2}, \frac{t}{2})$ of thickness t such that $0 < t \leq \text{diam}(\Omega)$. The two-dimensional domain Ω represents the midsection of the plate. The deformation of this plate is described by the Reissner-Mindlin model [275, 306] using three unknowns: the rotations $\boldsymbol{\beta} = (\beta_1, \beta_2)$ of fibers that are initially normal to plate's mid-surface, the scaled shear stresses $\boldsymbol{\gamma} = (\gamma_1, \gamma_2)$, and the transverse displacement w . Assuming for simplicity that the plate is clamped on its whole boundary $\partial\Omega$, we have the following equations:

$$-\text{div } \mathbb{C}\boldsymbol{\varepsilon}(\boldsymbol{\beta}) - \boldsymbol{\gamma} = \mathbf{0} \quad \text{in } \Omega, \quad (1.45)$$

$$-\text{div}(\boldsymbol{\gamma}) = b \quad \text{in } \Omega, \quad (1.46)$$

$$\boldsymbol{\gamma} = \kappa t^{-2}(\nabla w - \boldsymbol{\beta}) \quad \text{in } \Omega, \quad (1.47)$$

$$\boldsymbol{\beta} = \mathbf{0} \quad \text{on } \partial\Omega, \quad (1.48)$$

$$w = 0 \quad \text{on } \partial\Omega, \quad (1.49)$$

where \mathbb{C} is the tensor of bending moduli,

$$\mathbb{C}\boldsymbol{\tau} := \frac{E}{12(1-\nu^2)}((1-\nu)\boldsymbol{\tau} + \nu \text{tr}(\boldsymbol{\tau})\mathbb{I}),$$

with $E > 0$ being the Young modulus and $0 < \nu < 1/2$ being the Poisson ratio for the material.

To write a variational formulation of this problem, we first introduce an elliptic bilinear form

$$\begin{aligned} a(\boldsymbol{\beta}, \boldsymbol{\eta}) &:= \int_{\Omega} \mathbb{C}\boldsymbol{\varepsilon}(\boldsymbol{\beta}) : \boldsymbol{\varepsilon}(\boldsymbol{\eta}) \, dV \\ &= \frac{E}{12(1-\nu^2)} \int_{\Omega} ((1-\nu)\boldsymbol{\varepsilon}(\boldsymbol{\beta}) : \boldsymbol{\varepsilon}(\boldsymbol{\eta}) + \nu \text{div}\boldsymbol{\beta} \text{div}\boldsymbol{\eta}) \, dV, \end{aligned}$$

where $\boldsymbol{\varepsilon}$ is the two-dimensional strain tensor defined by

$$\varepsilon_{ij}(\boldsymbol{\beta}) = \frac{1}{2} \left(\frac{\partial \beta_j}{\partial x_i} + \frac{\partial \beta_i}{\partial x_j} \right), \quad 1 \leq i, j \leq 2.$$

We make the following assumption.

(H7) The load b is in $H^{-1}(\Omega)$, the dual of $H_0^1(\Omega)$.

For notation's convenience, we introduce a tensor-product space $\mathcal{H} = (H_0^1(\Omega))^2 \times H_0^1(\Omega)$. Then, a variational formulation of problem (1.45)–(1.49) reads:

Find $(\boldsymbol{\beta}, w) \in \mathcal{H}$ and $\boldsymbol{\gamma} \in (L^2(\Omega))^2$ such that

$$a(\boldsymbol{\beta}, \boldsymbol{\eta}) + \int_{\Omega} \boldsymbol{\gamma} \cdot (\nabla v - \boldsymbol{\eta}) dV = \langle b, v \rangle_{\mathcal{Q}} \quad \forall (\boldsymbol{\eta}, v) \in \mathcal{H}, \quad (1.50)$$

$$\int_{\Omega} (\nabla w - \boldsymbol{\beta}) \cdot \boldsymbol{\delta} dV - \kappa^{-1} t^2 \int_{\Omega} \boldsymbol{\gamma} \cdot \boldsymbol{\delta} dV = 0 \quad \forall \boldsymbol{\delta} \in (L^2(\Omega))^2, \quad (1.51)$$

where $\kappa = \alpha E / 2(1 + \nu)$ is the shear modulus using the correction factor α , which equals to 5/6 for clamped plates. There exists a unique solution to the above problem and the following regularity result holds [117, 133].

Theorem 1.4. *Let Ω be a convex polygon. Then, for any $t \in (0, \text{diam}(\Omega))$ and $b \in L^2(\Omega)$, the components of the solution $(\boldsymbol{\beta}, w)$ to (1.50)–(1.51) are in $H^2(\Omega)$ while the components of $\boldsymbol{\gamma}$ are in $H^1(\Omega)$. Moreover it holds*

$$\|\boldsymbol{\beta}\|_{H^2(\Omega)} + \|w\|_{H^2(\Omega)} + t\|\boldsymbol{\gamma}\|_{H^1(\Omega)} + \|\boldsymbol{\gamma}\|_{H_{\text{div}}(\Omega)} \leq C\|b\|_{L^2(\Omega)}, \quad (1.52)$$

where C is independent of t .

We must observe that the clamped boundary conditions play an important role in the regularity result above. Indeed, there are different sets of homogeneous boundary conditions which generate layers in the rotation variable such that the solution $\boldsymbol{\beta}$ is not guaranteed to lay in $H^2(\Omega)$ even for regular problem data. For example, this happens when a part of the boundary is set free (see, for instance, [32]).

1.5.4 Magnetostatics problem

Magnetostatics studies magnetic fields in systems where the currents are either constant in time or do not alternate rapidly. Magnetostatics is widely used in micromagnetics to model magnetic recording devices.

Let \mathbf{H} be the magnetic field intensity and \mathbf{J} the divergence-free current density. The mathematical formulation of magnetostatics has a form of a *div-curl* problem:

$$\text{curl} \mathbf{H} = \mathbf{J} \quad \text{in } \Omega, \quad (1.53)$$

$$\text{div}(\mu \mathbf{H}) = 0 \quad \text{in } \Omega, \quad (1.54)$$

$$\mathbf{H} \times \mathbf{n} = \mathbf{g}' \quad \text{on } \Gamma, \quad (1.55)$$

where μ is the magnetic permeability tensor and \mathbf{g}' is a vector-valued boundary function. The tensor coefficient μ may be discontinuous. However, the tangential component of \mathbf{H} and the normal component of $\mu \mathbf{H}$ are continuous across discontinuity interfaces of μ .

From a physical standpoint, the domain Ω should be the whole three-dimensional space, and the magnetic field should satisfy a radiation condition such as $\mathbf{H} \rightarrow 0$ at infinity. In practice, we assume that Ω is a bounded, simply connected, polyhedral domain with a Lipschitz boundary Γ , and replace the radiation condition by the Dirichlet boundary condition (1.55).

Condition (1.54) allows us to introduce the vector potential \mathbf{u} such that $\operatorname{curl} \mathbf{u} = \mu \mathbf{H}$. The choice of \mathbf{u} is not unique as we can always add the gradient of any scalar function without changing \mathbf{H} . Thus, to obtain a weak formulation that admits a unique solution, we consider the *Coulomb gauge*, which leads to a divergence-free vector potential. More precisely, we require that the vector field \mathbf{u} be the solution of the following set of equations:

$$\operatorname{curl}(\mu^{-1} \operatorname{curl} \mathbf{u}) = \mathbf{J} \quad \text{in } \Omega, \quad (1.56)$$

$$\operatorname{div} \mathbf{u} = 0 \quad \text{in } \Omega, \quad (1.57)$$

$$\mathbf{u} \times \mathbf{n} = \mathbf{g} \quad \text{in } \Gamma. \quad (1.58)$$

We derive the variational formulation for this problem in the following steps. First, we introduce a Sobolev space

$$H(\operatorname{curl}, \Omega) = \{ \mathbf{v} \in (L^2(\Omega))^d : \operatorname{curl} \mathbf{v} \in (L^2(\Omega))^d \} \quad (1.59)$$

and an affine space of admissible weak solutions

$$H_{\mathbf{g}}(\operatorname{curl}, \Omega) = \{ \mathbf{v} \in H(\operatorname{curl}, \Omega) : \mathbf{v} \times \mathbf{n} = \mathbf{g} \text{ on } \Gamma \}. \quad (1.60)$$

We do not explicitly require that the vector fields in $H_{\mathbf{g}}(\operatorname{curl}, \Omega)$ be divergence-free. Instead, we will take into account the solenoidal constraint (1.57) through the introduction of the Lagrangian multiplier p , which belongs to the Sobolev space $H_0^1(\Omega)$. We make the following assumptions.

(H8) The magnetic density tensor μ is a bounded, measurable, and symmetric tensor. Moreover, μ is strongly elliptic, see **(H1)** for more detail.

(H9) The external current field \mathbf{J} is in the dual of $H_0(\operatorname{curl}, \Omega)$. The boundary function $\mathbf{g} \in (H^{-1/2}(\operatorname{div}, \Gamma))$.

The variational formulation of problem (1.56)–(1.58) reads: *Find $\mathbf{u} \in H_{\mathbf{g}}(\operatorname{curl}, \Omega)$ and $p \in H_0^1(\Omega)$ such that*

$$\int_{\Omega} \mu^{-1} \operatorname{curl} \mathbf{u} \cdot \operatorname{curl} \mathbf{v} dV + \int_{\Omega} \mathbf{v} \cdot \nabla p dV = \langle \mathbf{J}, \mathbf{v} \rangle_{\mathcal{Q}} \quad \forall \mathbf{v} \in H_0(\operatorname{curl}, \Omega), \quad (1.61)$$

$$\int_{\Omega} \mathbf{u} \cdot \nabla q dV = 0 \quad \forall q \in H_0^1(\Omega). \quad (1.62)$$

Under assumptions **(H8)**–**(H9)**, the well-posedness of (1.61)–(1.62) can be proved in the framework of Brezzi-Babuska theory for saddle-point problems. A regularity results for the present problem can be found for instance in [11].

1.6 Polyhedral meshes

Large part of this book is devoted to solving elliptic PDEs in three dimensions using polyhedral meshes; however, developed schemes can be readily applied in two di-

mensions using polygonal meshes. Note that tetrahedral and hexahedral meshes are just subsets of polyhedral meshes.

1.6.1 Mesh shape regularity

Convergence analysis of mimetic discretizations is performed on a sequence of *shape regular* polyhedral meshes $\{\Omega_h\}_h$ where h is the diameter of the largest element in Ω_h and $h \rightarrow 0$. A polyhedron P is a closed domain in three dimensions with flat faces and straight edges. A shape-regular mesh satisfies the following minimal assumptions introduced originally in [84]:

(MR) [*Shape-regularity*] There exist two positive real numbers \mathcal{N}^s and ρ_s such that every mesh Ω_h admits a conforming sub-partition T_h into shape-regular tetrahedra such that

- **(MR1)** every polyhedron $P \in \Omega_h$ admits a decomposition $T_h|_P$ made of less than \mathcal{N}^s tetrahedra that includes all vertices of P ;
- **(MR2)** each tetrahedron $T \in T_h$ is shape-regular: the ratio of radius r_T of the inscribed sphere to diameter h_T is bounded from below:

$$\frac{r_T}{h_T} \geq \rho_s > 0. \quad (1.63)$$

Remark 1.3. We point out that only existence of a tetrahedral partition T_h is required, a fact that can be easily verified in most cases.

Assumptions **(MR1)**–**(MR2)** impose weak restrictions on the shape of admissible elements in order to avoid various pathological situations such as slivers and needles. Nonetheless, the meshes of $\{\Omega_h\}_h$ may contain very generally shaped elements, for instance, non-convex or degenerate elements. Two examples of shape-regular polyhedra are shown in Fig. 1.2.

We denote the faces of polyhedron P by f , its edges by e , and its vertices (also called nodes) by v . Let $|P|$, $|f|$ and $|e|$ denote the volume of P , area of f , and length of e , respectively. We indicate with h_e, h_f, h_P the diameter of edge e , face f and polyhedron P , respectively.

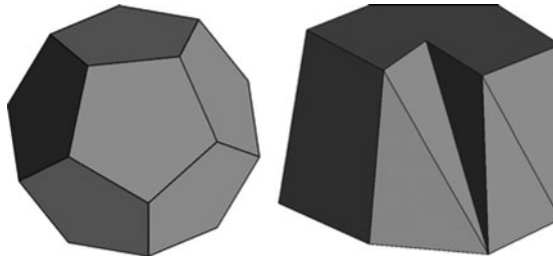


Fig. 1.2. Shape-regular convex (left) and degenerate non-convex (right) polyhedra

Let \mathbf{n}_f be a unit normal vector to face f fixed once and for all, and $\boldsymbol{\tau}_e$ be a unit tangent edge vector with *a priori* fixed orientation. Let \mathbf{x}_P be the centroid of polyhedron P . Similarly, we define centroids \mathbf{x}_f and \mathbf{x}_e for face f and edge e , respectively. Finally, \mathbf{x}_v is the coordinate vector of node v .

We denote the sets of mesh nodes v , edges e , faces f , and polyhedra P by \mathcal{V} , \mathcal{E} , \mathcal{F} , and \mathcal{P} , respectively. Let \mathcal{Q} be one of these sets. We define the subsets $\mathcal{Q}(P)$, $\mathcal{Q}(f)$, and $\mathcal{Q}(e)$, which are formed by the mesh objects of \mathcal{Q} that are related, respectively, to polyhedron P , face f , and edge e . When the argument has a higher topological dimension, the resulting set $\mathcal{Q}(P)$, $\mathcal{Q}(f)$, or $\mathcal{Q}(e)$ is the collection of mesh objects that belong to the boundary of P , f , and e , respectively. For example, $\mathcal{E}(P)$ denotes all the edges forming the boundary of polyhedron P . When the argument has a lower topological dimension, the resulting set $\mathcal{Q}(f)$, $\mathcal{Q}(e)$, or $\mathcal{Q}(v)$ is the collection of mesh objects sharing face f , edge e , or node v , respectively. For example, $\mathcal{P}(e)$ denotes all polyhedra sharing edge e . When the topological degrees are the same, we consider the subset of items that are connected in some sense to the argument. For example, $\mathcal{E}(e)$ is the set of edges sharing at least a node with e . In the following we will also make use of the more intuitive boundary symbol in order to indicate sub-sets of vertexes, edges or faces. For instance $\{v\}_{v \in \partial P}$ indicates the set of vertexes of polygon P , the symbol $\{e\}_{e \in \partial f}$ denotes the set of edges pertaining to face f , and so on. Finally, the symbol $\#\mathcal{Q}(\sigma)$ where σ may be v , e , f and P is the cardinality of set $\mathcal{Q}(\sigma)$, i.e., the number of objects that are in this set. For example, $\#\mathcal{E}(P)$ is the number of edges of polyhedron P .

Assume for a moment that each polyhedron P is star-shaped with respect to a point $\bar{\mathbf{x}}_P \in P$, and each face f is star-shaped with respect to a point $\bar{\mathbf{x}}_f \in f$. These points may or may not coincide with the corresponding centroids. Then, we say that the sub-partition T_h is *simple* if it is built in the following way. First, each face f is subdivided into triangles by connecting each vertex $v \in \mathcal{V}(f)$ with the point $\bar{\mathbf{x}}_f$. Second, each element P is decomposed into tetrahedra by connecting each vertex v of P and each point $\bar{\mathbf{x}}_f$, $f \in \mathcal{F}_P$, with the point $\bar{\mathbf{x}}_P$.

In certain cases, assumption **(MR)** can be made stronger by adding the following condition:

(MR3) each polyhedron P is star-shaped with respect to a point $\bar{\mathbf{x}}_P \in P$, and each face f is star-shaped with respect to a point $\bar{\mathbf{x}}_f \in f$. Moreover, the tetrahedral sub-partition T_h is simple.

This assumption imposes additional constraints on the shape of mesh elements with respect to assumptions **(MR1)**–**(MR2)**. Still, the family of admissible meshes remains significantly large to meet demands of engineering applications. Later, in analysis of mimetic discretizations, we will use either the minimal assumptions **(MR1)**–**(MR2)** or the expanded assumptions **(MR1)**–**(MR3)**.

Remark 1.4. Another set of mesh assumptions can be found in the literature on mimetic discretizations, for example, in [90]. Although these assumptions seem more complicated, it is possible to prove that they are equivalent to assumptions **(MR1)**–**(MR3)**, see, e.g., [41]. Therefore, we do not list them here.

1.6.2 Consequences of the mesh regularity assumptions

The regularity assumptions **(MR1)**–**(MR2)** lead to a few useful consequences. These consequences are not necessary for understanding the mimetic method, but will be extensively used in the theoretical derivations of the subsequent chapters.

(M1) There exist two positive integers $\mathcal{N}^{\mathcal{F}}$ and $\mathcal{N}^{\mathcal{E}}$ depending only on \mathcal{N}^s such that every element P has at most $\mathcal{N}^{\mathcal{F}}$ faces, and every face f has at most $\mathcal{N}^{\mathcal{E}}$ edges.

(M2) For every element $P \in \Omega_h$, all the related geometrical quantities scale in a uniform way. More precisely, there exists a constant a_\star depending only on \mathcal{N}^s and ρ_s such that for all faces $f \in \partial P$ and all edges $e \in \partial P$ it holds

$$a_\star h_P^3 \leq |P| \leq h_P^3, \quad a_\star h_P^2 \leq |f| \leq h_P^2,$$

and

$$h_P \leq a_\star^{-1} h_f, \quad h_P \leq a_\star^{-1} h_e.$$

(M3) There exists a constant b_\star depending only on \mathcal{N}^s and ρ_s such that for all $P \in \Omega_h$ and all $T \in \mathbb{T}_h|_P$ it holds

$$h_P \leq b_\star h_T.$$

(M4) [Agmon inequality] There exists a constant C^{Agm} independent of h_P and such that:

$$\sum_{f \in \partial P} \|\phi\|_{L^2(f)}^2 \leq C^{Agm} \left(h_P^{-1} \|\phi\|_{L^2(P)}^2 + h_P \|\phi\|_{H^1(P)}^2 \right) \quad (1.64)$$

for any function $\phi \in H^1(P)$.

(M5) [Approximation estimates] Let $m \in \mathbb{N}$. Then, there exists a constant C^{Int} independent of h_P such that for any function $q \in H^{s+1}(P)$ with $s \in \mathbb{R}$ and $0 \leq s \leq m$ there exists an approximating polynomial $q_P^{(m)} \in \mathbb{P}_m(P)$ such that

$$\|q - q_P^{(m)}\|_{L^2(P)} + \sum_{k=1}^{\lfloor s \rfloor} h_P^k |q - q_P^{(m)}|_{H^k(P)} \leq C^{Int} h_P^{s+1} |q|_{H^{s+1}(P)}, \quad (1.65)$$

where $\lfloor s \rfloor$ is the integer part of s .

Property **(M1)** follows immediately from assumption **(MR1)** by observing that each edge (respectively, face) of P is the union of edges (respectively, faces) of at most \mathcal{N}^s tetrahedra.

The upper bounds on area and volume in property **(M2)** follow from the definition of h_P . Since the sub-partition \mathbb{T}_h is shape regular (assumption **(MR1)**) and the number of tetrahedra in $\mathbb{T}_h|_P$ is bounded by \mathcal{N}^s , there exists a constant C_\star depending only on \mathcal{N}^s and ρ_s such that

$$\min_{T \in \mathbb{T}_h|_P} h_T \geq C_\star \max_{T \in \mathbb{T}_h|_P} h_T.$$

Since

$$h_P \leq \sum_{T \in \mathbb{T}_h|_P} h_T \leq \mathcal{N}^s \max_{T \in \mathbb{T}_h|_P} h_T,$$

property **(M3)** follows immediately with $b_* = C_*^{-1} \mathcal{N}^s$. After that, the remaining inequalities in **(M2)** follow from **(M3)**. For instance,

$$|P| \geq \mathcal{N}^s \min_{T \in \mathbb{T}_h|_P} |T| \geq \frac{4\pi \mathcal{N}^s}{3} r_{T'}^3 \geq \frac{4\pi \mathcal{N}^s \rho_s^3}{3} h_{T'}^3 \geq \frac{4\pi \rho_s^3 C_*^3}{3(\mathcal{N}^s)^2} h_P^3,$$

where T' denotes the tetrahedron with the smallest diameter. A similar set of inequalities is obtained for f . Finally, the constant a_* is defined as the smallest one in all inequalities.

Property **(M4)** is a scaled trace inequality, and is well known to hold for shape regular meshes made of tetrahedra, see for instance [7, 28, 78]. Since \mathbb{T}_h is shape regular, we have that, for all $T \in \mathbb{T}_h$,

$$\|\phi\|_{L^2(\partial T)}^2 \leq C \left(h_T^{-1} \|\phi\|_{L^2(T)}^2 + h_T \phi^2_{H^1(T)} \right)$$

with C independent of the particular T . Due to **(M3)**, the above bound can be written as

$$\|\phi\|_{L^2(\partial T)}^2 \leq C \left(h_P^{-1} \|\phi\|_{L^2(T)}^2 + h_P \phi^2_{H^1(T)} \right) \quad (1.66)$$

with a different C , still independent of T . Therefore, property **(M4)** follows from (1.66) by simply observing that the union of all faces f in ∂P is a union of faces of tetrahedra in \mathbb{T}_h , and thus

$$\sum_{f \in \partial P} \|\phi\|_{L^2(f)}^2 \leq C \sum_{T \in \mathbb{T}_h|_P} \left(h_P^{-1} \|\phi\|_{L^2(T)}^2 + h_P \phi^2_{H^1(T)} \right),$$

which immediately gives the desired result.

The proof of property **(M5)** is more involved. Indeed, the approximation result (1.65) is well known for star-shaped elements, see for instance [78, Lemma 4.3.8]. Since, accordingly to **(MR)**, the polyhedron P may be not star shaped, the approximation bound must rely on more general results in [149]. We derive them here in the version of [17] which better adapts to our situation. In order to keep the notation simpler in the following developments, we will use symbol H^0 for the L^2 space. We start with the following result.

Lemma 1.1. *Let ω_h be a connected conforming mesh of N shape regular tetrahedra satisfying the regularity condition (1.63) and $\omega = \cup_{T \in \omega_h} T$. Furthermore, let k and m be non-negative integer numbers. Then, there exists a constant $C' = C'(\rho_s, N, m, k)$ such that*

$$|q^{(m)}|_{H^k(\omega)} \leq C' |q^{(m)}|_{H^k(T)} \quad \forall T \in \omega_h, \quad \forall q^{(m)} \in \mathbb{P}_m(\omega). \quad (1.67)$$

Proof. We only sketch the proof. Given N , there exist a finite number of possible connectivity configurations of the tetrahedra in ω_h . Therefore, there exist a finite number

of reference meshes $\widehat{\omega}_h$ such that each admissible mesh ω_h can be mapped into a reference mesh. Since both norms in (1.67) have the same kernel and the space \mathbb{P}_m is finite dimensional, there exists a constant $C'' = C''(N, m, k)$ such that the lemma is true on all reference meshes. Then, the lemma follows easily from a scaling argument since all the maps have bounded norms due to the mesh regularity of ω_h . \square

Consider an element $P \in \Omega_h$. Let $k, m \in \mathbb{N}$ be non-negative integers and $s \in \mathbb{R}$, $0 \leq s \leq m$. We prove property **(M5)** by induction on the number N of tetrahedra in $T_h|_P$. Recall that N is bounded by \mathcal{N}^s of Assumption **(MR1)**. We start observing that, if T_1 and T_2 are two tetrahedrons (of a shape regular family of meshes) which share one face, then the union $U = T_1 \cup T_2$ is star shaped with respect to a ball. Moreover the ratio of the radius of such ball divided by the diameter of U is uniformly bounded from below. Such result is easy to check and we do not prove it here. As a consequence, for any $U = T_1 \cup T_2$ we can apply the well known interpolation bound on star shaped domains, see for instance [115]. For all $q \in H^{s+1}(U)$, there exists $q^{(m)} \in \mathbb{P}_m(U)$, such that

$$h_U^k |q - q^{(m)}|_{H^k(U)} \leq C_U h_U^{s+1} |q|_{H^{s+1}(U)}, \quad (1.68)$$

with $C_U = C_U(k, m, s, \rho_s)$ and where ρ_s is the shape regularity constant appearing in **(MR2)**. Furthermore, the same result obviously applies if U is a single tetrahedron. Thus we obtained that, if $N = 1$ or 2 the bound in (1.65) is proved with $C^{int} = ([s] + 1)C_U$. We now assume that (1.65) holds for meshes of up to N tetrahedra (with a constant C depending only on k, m, s, ρ_s , and N). Let $T_h|_P$ be composed of $N + 1$ tetrahedra. Let T_1 be any tetrahedron from $T_h|_P$ and let T_2 be any other tetrahedron from $T_h|_P$ which has a common face with T_1 . Then, we consider the following two subsets of P

$$A = T_1 \cup T_2 \quad \text{and} \quad B = \{\cup T : T \in T_h|_P, T \neq T_1\}.$$

It is clear that $A \cup B = P$ and $A \cap B = T_2$. By the induction hypothesis, the interpolation result (1.65) is true for both A and B . Given any $q \in H^{s+1}(P)$, let $q_A^{(m)}$ and $q_B^{(m)}$ in $\mathbb{P}_m(T)$ be the interpolation polynomials for q on subsets A and B , respectively:

$$h_A^k |q - q_A^{(m)}|_{H^k(A)} \leq C h_A^{s+1} |q|_{H^{s+1}(A)}, \quad h_B^k |q - q_B^{(m)}|_{H^k(B)} \leq C h_B^{s+1} |q|_{H^{s+1}(B)}.$$

Using property **(M3)**, we obtain

$$h_P^k |q - q_A^{(m)}|_{H^k(A)} \leq C h_P^{s+1} |q|_{H^{s+1}(A)}, \quad h_P^k |q - q_B^{(m)}|_{H^k(B)} \leq C h_P^{s+1} |q|_{H^{s+1}(B)} \quad (1.69)$$

with another constant C depending only on k, m, s, ρ_s , and \mathcal{N}^s . By the triangle inequality, one easily gets

$$|q - q_A^{(m)}|_{H^k(P)} \leq |q - q_A^{(m)}|_{H^k(A)} + |q - q_B^{(m)}|_{H^k(B)} + |q_A^{(m)} - q_B^{(m)}|_{H^k(B)}. \quad (1.70)$$

For the last term above, we apply Lemma 1.1 (with $\omega = B$ and $T = T_2$) and then the

triangle inequality to obtain

$$\begin{aligned}
 |q_A^{(m)} - q_B^{(m)}|_{H^k(B)} &\leq C' |q_A^{(m)} - q_B^{(m)}|_{H^k(T_2)} \\
 &\leq C' (|q_A^{(m)} - q|_{H^k(T_2)} + |q - q_B^{(m)}|_{H^k(T_2)}) \\
 &\leq C' (|q_A^{(m)} - q|_{H^k(A)} + |q - q_B^{(m)}|_{H^k(B)}).
 \end{aligned}
 \tag{1.71}$$

Combining (1.70), (1.71) and the interpolation bounds (1.69) yields

$$h_P^k |q - q_A^{(m)}|_{H^k(P)} \leq \sqrt{2}(1 + C') C h_P^{s+1} |q|_{H^{s+1}(P)},$$

which implies property **(M5)**.

1.7 Polygonal meshes

A two-dimensional *polygonal mesh* is a collection of polygons. The notation for the polygonal meshes is essentially equivalent to that for polyhedral meshes. Therefore, we stress only important differences.

The sets $\mathcal{P}, \mathcal{E}, \mathcal{V}$ represent the sets of mesh polygons (also called elements), edges and vertices, respectively. Throughout the book we will use both terms, face and edge, to denote an edge of a polygon; however, the selected term will remain consistent across each chapter. Therefore, the set \mathcal{F} is the same as the set \mathcal{E} .

Assumptions **(MR1)**–**(MR3)** are easily adjusted to polygonal meshes. A sub-partition T_h into tetrahedra becomes a sub-partition into triangles. In the case of **(MR3)**, a simple sub-partition T_h is obtained in one step by connecting each vertex $v \in \mathcal{V}_P$ to the point \bar{x}_P , see Fig. 1.3. Hereafter, we will refer to Assumptions **(MR1)**–**(MR3)** for analysis of both polygonal and polyhedral meshes.

Among properties **(M1)**–**(M5)**, only the second one has to be modified slightly. Introducing the space dimension constant d ($d = 2$ in 2-D and $d = 3$ in 3-D), we reformulate this property as follows.

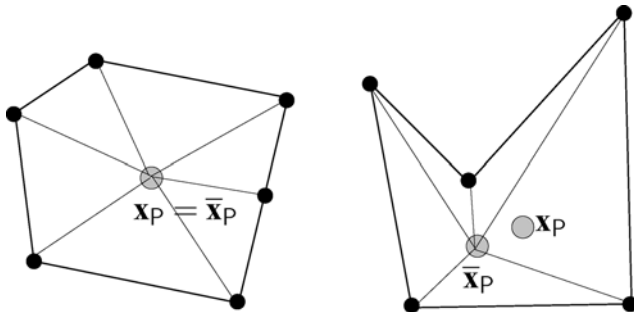


Fig. 1.3. Examples for simple partitions of shape-regular polygons

(M2) For every element $P \in \Omega_h$, the related geometrical quantities are uniformly bounded from above and below. More precisely, there exists a constant a_* depending only on \mathcal{N}^s and ρ_s such that, for all faces $f \in \partial P$ and all edges $e \in \partial P$, it holds

$$a_* h_P^d \leq |P| \leq h_P^d, \quad a_* h_P^{d-1} \leq |f| \leq h_P^{d-1},$$

and

$$h_P \leq a_*^{-1} h_f, \quad h_P \leq a_*^{-1} h_e.$$

Hereafter, we will refer to properties **(M1)**, modified **(M2)** and **(M3)**–**(M5)** for analysis of both polygonal and polyhedral meshes.

Foundations of mimetic finite difference method

*“The higher your structure is to be,
the deeper must be its foundation.”*

(Saint Augustine)

The mimetic discretization technology relies on a discrete vector and tensor calculus (DVTC) that deals with discrete fields and discrete operators. The DVTC makes it possible to reproduce (or mimic) fundamental identities of continuum calculus, such as kernels of operators (see Sect. 2.6) and the Helmholtz decomposition theorems (see Sect. 2.7), in the discrete framework. It also guarantees symmetry and positivity of discrete operators when these properties hold for the corresponding differential operators.

The DVTC can be built in an abstract form by exploiting duality relationships between pairs of differential operators. In such construction, we first derive one discrete operator, called *the primary operator*, from first principles and then built the other one, called *the derived operator*, through a discrete analog of the integration by parts formula.

To define the primary operators, i.e., gradient, divergence and curl, we consider their coordinate invariant formulations:

$$\int_{\mathbf{x}_a}^{\mathbf{x}_b} \nabla p \cdot \boldsymbol{\tau} dL = p(\mathbf{x}_a) - p(\mathbf{x}_b), \quad (2.1)$$

$$\int_S (\text{curl } \mathbf{u}) \cdot \mathbf{n} dS = \int_{\partial S} \mathbf{u} \cdot \boldsymbol{\tau} dL, \quad (2.2)$$

$$\int_V \text{div } \mathbf{u} dV = \int_{\partial V} \mathbf{u} \cdot \mathbf{n} dS, \quad (2.3)$$

where $\boldsymbol{\tau}$ is the unit vector tangent to either a curve connecting points \mathbf{x}_a and \mathbf{x}_b or a polygonal boundary ∂S , $\nabla p \cdot \boldsymbol{\tau}$ is the directional derivative of the scalar field p along such curves, and \mathbf{n} is the unit normal vector to the surface S or ∂V (see Fig. 2.1).

Equations (2.1)–(2.3) are different forms of the Stokes theorem. They suggest a naturally choice for degrees of freedom and their relations with various mesh objects such as vertices, edges, faces and cells. Note also that (2.2) requires a proper orientation of the normal and tangent vectors.

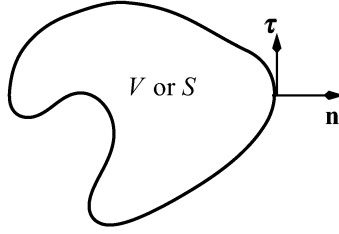


Fig. 2.1. Domain with a smooth boundary

The duality relations for the first-order differential operators are given by Green's formulas:

$$\int_{\Omega} p \operatorname{div} \mathbf{u} dV = - \int_{\Omega} \nabla p \cdot \mathbf{u} dV + \int_{\partial\Omega} p (\mathbf{u} \cdot \mathbf{n}) dS, \quad (2.4)$$

$$\int_{\Omega} \mathbf{u} \cdot \operatorname{div} \boldsymbol{\sigma} dV = - \int_{\Omega} \nabla \mathbf{u} \cdot \boldsymbol{\sigma} dV + \int_{\partial\Omega} \mathbf{u} \cdot (\boldsymbol{\sigma} \cdot \mathbf{n}) dS, \quad (2.5)$$

$$\int_{\Omega} \mathbf{u} \cdot \operatorname{curl} \mathbf{v} dV = \int_{\Omega} (\operatorname{curl} \mathbf{u}) \cdot \mathbf{v} dV + \int_{\partial\Omega} (\mathbf{u} \times \mathbf{v}) \cdot \mathbf{n} dS. \quad (2.6)$$

To ease the presentation, we assume that the boundary integrals in (2.4)–(2.6) are zero, i.e. the functions satisfy proper boundary conditions. This assumption is quite natural when we deal with partial differential equations with (essential) homogeneous boundary conditions. For example, if $p \in H_0^1(\Omega)$ in the first formula, $\mathbf{u} \in (H_0^1(\Omega))^d$ in the second formula, and $\mathbf{u} \in H_0(\operatorname{curl}, \Omega)$ in the third formula, we obtain:

$$\int_{\Omega} p \operatorname{div} \mathbf{u} dV = - \int_{\Omega} \nabla p \cdot \mathbf{u} dV, \quad (2.7)$$

$$\int_{\Omega} \mathbf{u} \cdot \operatorname{div} \boldsymbol{\sigma} dV = - \int_{\Omega} \nabla \mathbf{u} \cdot \boldsymbol{\sigma} dV, \quad (2.8)$$

$$\int_{\Omega} \mathbf{u} \cdot \operatorname{curl} \mathbf{v} dV = \int_{\Omega} (\operatorname{curl} \mathbf{u}) \cdot \mathbf{v} dV. \quad (2.9)$$

Remark 2.1. Inhomogeneous boundary conditions can be treated by extending the first-order operators to the boundary, see, for instance, [206]. The DVTC that results from this approach is different.

In the mimetic approach, a problem coefficient is combined with a differential operator and the two are discretized simultaneously. For example, let \mathbf{K} be a positive definite tensor. Formula (2.7) is obviously equivalent to

$$\int_{\Omega} p \operatorname{div} \mathbf{u} dV = - \int_{\Omega} \mathbf{K}^{-1} (\mathbf{K} \nabla p) \cdot \mathbf{u} dV. \quad (2.10)$$

Relation (2.10) is a duality relation between the two first-order operators div and $\text{K}\nabla$ if we interpret the volume integral in the right-hand side as a weighted inner product for vector fields with K^{-1} as the weight. The discrete analogs of such operators will satisfy a similar duality relation with respect to the discrete analog of this weighted inner product.

Let $\mathcal{D}: S \rightarrow S^*$ represent the operator in the left-hand side of formulas (2.7)–(2.9). Then, the operator in the right-hand side is its dual $\mathcal{D}^*: S^* \rightarrow S$, and the formulas can be written in the abstract form

$$[\mathcal{D}u, v]_{S^*} = [u, \mathcal{D}^*v]_S, \quad \forall u \in S, \quad v \in S^*, \quad (2.11)$$

where brackets indicate inner products in the corresponding spaces. These inner product may be occasionally weighted by the problem coefficients.

Let \mathcal{D}_h be the discrete analog of \mathcal{D} acting from the discrete space S_h into the discrete space S_h^* . We assume that the spaces S_h and S_h^* are equipped with the inner products $[\cdot, \cdot]_{S_h}$ and $[\cdot, \cdot]_{S_h^*}$. Then, the duality relationship

$$[\mathcal{D}_h u_h, v_h]_{S_h^*} = [u_h, \mathcal{D}_h^* v_h]_{S_h}, \quad \forall u_h \in S_h, \quad v_h \in S_h^* \quad (2.12)$$

defines the unique operator \mathcal{D}_h^* . This discrete dual operator has a number of important properties. By taking $v_h = \mathcal{D}_h u_h$ we obtain the following inequality:

$$[\mathcal{D}_h^*(\mathcal{D}_h u_h), u_h]_{S_h} = [\mathcal{D}_h u_h, \mathcal{D}_h u_h]_{S_h^*} \geq 0, \quad \forall u_h \in S_h. \quad (2.13)$$

If one enriches the discrete spaces S_h and S_h^* by adding more degrees of freedom and modifies accordingly the primary operator \mathcal{D}_h , implicit definition (2.12) gives a new dual operator \mathcal{D}_h^* , the derived operator, for which inequality (2.13) holds. If one chooses different inner products, definition (2.12) gives again a consistent dual operator. For this reason, the arising discrete systems always preserve symmetry and positivity properties of continuum problems.

2.1 Degrees of freedom and discrete fields

We define a discrete field as a collection of degrees of freedom. We consider four different types of discrete fields defined by the degrees of freedom associated with four different mesh objects: vertices, edges, faces, and elements. A natural enumeration of mesh objects allows one to write a discrete field as an algebraic vector of degrees of freedom.

- A vertex-based discrete field p_h is defined by attaching one number $p_{h,v}$ (we shall write simply p_v) to each mesh vertex v . The discrete field p_h can be often interpreted as an approximation of a continuous scalar function $p(\mathbf{x})$ at mesh vertices, e.g. $p_v = p(\mathbf{x}_v)$.
- An edge-based discrete field \mathbf{u}_h is defined by attaching one number $u_{h,e}$ (we shall write simply u_e) to each mesh edge e . The discrete field \mathbf{u}_h can be often interpreted

as an approximation of the tangential component of a vector function $\mathbf{u}(\mathbf{x})$ on mesh edges.

- A face-based discrete field \mathbf{u}_h is defined by attaching one number $u_{h,f}$ (we shall write simply u_f) to each mesh face f . The discrete field \mathbf{u}_h can be often interpreted as an approximation of the normal component of a vector function $\mathbf{u}(\mathbf{x})$ on mesh faces.
- An element-based discrete field p_h (also called a cell-based discrete field) is defined by attaching one number $p_{h,P}$ (we shall write simply p_P) to each mesh element P . The mesh element function p_h can be often interpreted as an approximation of a continuous scalar function $p(\mathbf{x})$ at centers of mesh elements, e.g. $p_P = p(\mathbf{x}_P)$.

Hereafter, we denote continuous and discrete scalar fields by letters in a normal font (e.g. pressure $p(\mathbf{x})$ and p_h), and continuous and discrete vector and tensor fields by letters in a bold font (e.g. velocity $\mathbf{u}(\mathbf{x})$ and \mathbf{u}_h).

Let \mathcal{V}_h , \mathcal{E}_h , \mathcal{F}_h , and \mathcal{P}_h denote the sets of vertex-based, edge-based, face-based, and element-based discrete fields, respectively. The isomorphism between discrete fields and algebraic vectors can be used to define the linear operations on a set of discrete fields. For instance, the sum of two discrete fields $p_h, q_h \in \mathcal{P}_h$ is defined via the sum of the two corresponding vectors. In this way, every set of discrete fields is given the algebraic structure of a linear space. Later, we will refer to \mathcal{V}_h , \mathcal{E}_h , \mathcal{F}_h , and \mathcal{P}_h as linear vector spaces.

Let \mathcal{S}_h denote anyone of the spaces \mathcal{V}_h , \mathcal{E}_h , \mathcal{F}_h , or \mathcal{P}_h . We will write $\dim(\mathcal{S}_h)$ for the dimension of space \mathcal{S}_h .

The discrete fields are illustrated in Fig. 2.2 for a single prismatic mesh element. Restriction of a vertex-based function to this element is marked with dots. Restrictions of an edge-based and a face-based functions are marked with arrows.

Remark 2.2. Additional properties will be assigned later to discrete fields, so that various mathematical operations will be well defined. For instance, an element-based function p_h can be defined to be constant inside each element, so that its point-wise value will be well defined for every interior point of every mesh element. Similarly a face-based function can be defined to be constant over each mesh face. This is one of the reasons why we prefer to work with discrete fields rather than with algebraic vectors of degrees of freedom.

Throughout the book we will use restrictions of discrete fields to a submesh or a single element. A restriction of a generic discrete field $s_h \in \mathcal{S}_h$ to a geometric object Q is denoted by $s_h|_Q$ (or simply by s_Q). A few examples are given below.

- Let $\mathbf{v}_h \in \mathcal{E}_h$. Then, $\mathbf{v}_h|_f = (v_e)_{e \in \partial f}$ denotes the subset of degrees of freedom v_e attached to the edges e that form the boundary of face f . Let $\mathcal{E}_{h,f}$ denote the set of restrictions $\mathbf{v}_h|_f$ for all edge-based discrete fields.
- Let $\mathbf{v}_h \in \mathcal{E}_h$. Then, $\mathbf{v}_h|_P = (v_e)_{e \in \partial P}$ denotes the subset of degrees of freedom v_e attached to the edges e that form the boundary of element P . Let $\mathcal{E}_{h,P}$ denote the set of restrictions $\mathbf{v}_h|_P$ for all edge-based discrete fields.

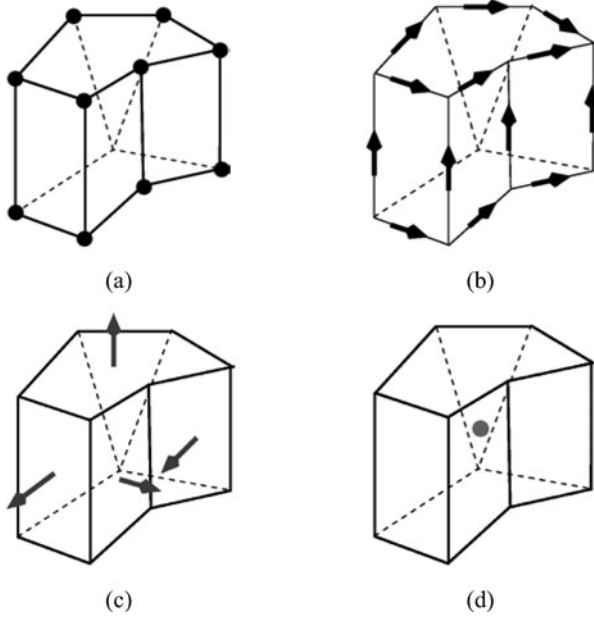


Fig. 2.2. Plot (a) shows a node-based discrete field; plot (b) shows an edge-based discrete field, the arrows indicate the local orientation of the edges; plot (c) shows a face-based discrete field, the arrows indicate the local orientation of the faces; plot (d) shows a cell-based discrete field

- Let $\mathbf{v}_h \in \mathcal{F}_h$. Then, $\mathbf{v}_h|_P = (v_f)_{f \in \partial P}$ denotes the subset of degrees of freedom v_f attached to the faces f that form the boundary of element P . Let $\mathcal{F}_{h,P}$ denote the set of restrictions $\mathbf{v}_h|_P$ for all face-based discrete fields.

Using the isomorphism with a space of algebraic vectors, each space ($\mathcal{E}_{h,f}$, $\mathcal{E}_{h,P}$, and $\mathcal{F}_{h,P}$) may be given the algebraic structure of a linear space. Later, we will refer to $\mathcal{E}_{h,f}$, $\mathcal{E}_{h,P}$, and $\mathcal{F}_{h,P}$ as linear vector spaces.

Remark 2.3. Up to a suitable rescaling of the quantities defined above, it is possible to re-interpret the entire setting in terms of *co-chains* [33], i.e., 3-D discrete k -forms, where $k = 0$ corresponds to \mathcal{V}_h , $k = 1$ to \mathcal{E}_h , $k = 2$ to \mathcal{F}_h , and $k = 3$ to \mathcal{P}_h . Although the algebraic topology is a very powerful framework, we do not pursue anymore such topic.

2.2 Discrete spaces and projection operators

The projection operators translate the spaces of sufficiently smooth scalar or vector-valued functions into the discrete spaces \mathcal{V}_h , \mathcal{E}_h , \mathcal{F}_h , and \mathcal{P}_h . In other words, they return discrete approximations of continuum scalar and vector fields. In the language

of differential forms, the projection operators correspond to the De Rham projection operators.

We denote the projection operators by the generic symbol $\Pi^{\mathcal{S}}$. The restriction of $\Pi^{\mathcal{S}}$ to a specific mesh object Q is denoted by $\Pi_Q^{\mathcal{S}}$, where Q can be a single mesh element. The projection operators satisfy the commuting diagram property of Lemma 2.2 that involve the differentiation operators ∇ , curl , div and their discrete counterparts ∇_h , curl_h , div_h .

The vertex projection operator

Let $p(\mathbf{x})$ be a sufficiently regular scalar function so that we can take its pointwise values, for example $p \in H^1(\Omega) \cap C^0(\bar{\Omega})$. Its approximation $p_h \in \mathcal{V}_h$ is obtained by applying the vertex projection operator $\Pi^{\mathcal{V}}$:

$$p_h = \Pi^{\mathcal{V}}(p) = (p_v)_{v \in \mathcal{V}}, \quad p_v = p(\mathbf{x}_v), \quad (2.14)$$

where \mathcal{V} is the set of mesh vertices. Obviously, the dimension of space \mathcal{V}_h is equal to the number of mesh vertices. The local projection operators $\Pi_Q^{\mathcal{V}}(p)$ for $Q \in \{v, e, f, P\}$ are defined similarly:

$$\Pi_Q^{\mathcal{V}}(p) = (p_v)_{v \in Q}.$$

For example, $\Pi_P^{\mathcal{V}}(p)$ is a discrete field in $\mathcal{V}_{h,P}$ defined at vertices of element P . For a cubic cell, the dimension of $\mathcal{V}_{h,P}$ is eight.

The edge projection operator

Let $\mathbf{u}(\mathbf{x})$ be a sufficiently regular vector-valued function, so that the integrals of its tangential component are well defined along the mesh edges. Its approximation $\mathbf{u}_h \in \mathcal{E}_h$ is obtained by applying the edge projection operator $\Pi^{\mathcal{E}}$:

$$\mathbf{u}_h = \Pi^{\mathcal{E}}(\mathbf{u}) = (u_e)_{e \in \mathcal{E}}, \quad u_e = \frac{1}{|e|} \int_e \mathbf{u} \cdot \boldsymbol{\tau}_e dL, \quad (2.15)$$

where \mathcal{E} is the set of mesh edges. Obviously, the projector is surjective and the dimension of space \mathcal{E}_h is equal to the number of mesh edges. We recall that $\boldsymbol{\tau}_e$ denotes the unit vector parallel to edge e . The orientation of $\boldsymbol{\tau}_e$ is fixed once and for all. The local edge projection operators $\Pi_Q^{\mathcal{E}}(q)$ for $Q \in \{v, e, f, P\}$ are defined similarly:

$$\Pi_Q^{\mathcal{E}}(\mathbf{u}) = (u_e)_{e \in Q}.$$

For example, $\Pi_P^{\mathcal{E}}(\mathbf{u})$ is a discrete field in $\mathcal{E}_{h,P}$ defined on the edges of element P . For a cubic cell, the dimension of $\mathcal{E}_{h,P}$ is 12.

The face projection operator

Let $\mathbf{u}(\mathbf{x})$ be a sufficiently regular vector-valued function, so that the integrals of its normal component are well defined on the mesh faces. For example, \mathbf{u} can be taken in the Sobolev space $(L^s(\Omega))^d$, $s > 2$, with divergence in $L^2(\Omega)$. Its approximation

$\mathbf{u}_h \in \mathcal{F}_h$ is obtained by applying the face projection operator $\Pi^{\mathcal{F}}$:

$$\mathbf{u}_h = \Pi^{\mathcal{F}}(\mathbf{u}) = (u_f)_{f \in \mathcal{F}}, \quad u_f = \frac{1}{|f|} \int_f \mathbf{u} \cdot \mathbf{n}_f dS, \quad (2.16)$$

where \mathcal{F} is the set of mesh faces. Obviously, the projector is surjective and the dimension of space \mathcal{F}_h is equal to the number of mesh edges. We recall that \mathbf{n}_f is the unit vector orthogonal to face f . The orientation of \mathbf{n}_f is fixed once and for all. The local face projection operators $\Pi_Q^{\mathcal{E}}(\mathbf{u})$ for $Q \in \{e, f, P\}$ are defined similarly:

$$\Pi_Q^{\mathcal{E}}(\mathbf{u}) = (u_f)_{f \in Q}.$$

For example, $\Pi_P^{\mathcal{F}}(\mathbf{u})$ is a discrete field in $\mathcal{F}_{h,P}$ defined on the faces of element P . For a cubic cell, the dimension of $\mathcal{F}_{h,P}$ is six.

The cell projection operator

Let $p(\mathbf{x})$ be a sufficiently regular scalar function, so that its integrals on compact subsets of Ω exist, for example $p \in L^1(\Omega)$. Its approximation $p_h \in \mathcal{P}_h$ is obtained by applying the cell projection operator $\Pi^{\mathcal{P}}$:

$$p_h = \Pi^{\mathcal{P}}(p) = (p_P)_{P \in \mathcal{P}}, \quad p_P = \frac{1}{|P|} \int_P p dV, \quad (2.17)$$

where \mathcal{P} is the set of mesh elements. The dimension of \mathcal{P}_h is equal to the number of the mesh cells.

2.3 Primary mimetic operators

The primary mimetic operators are the discrete gradient operator, ∇_h , the discrete curl operator, curl_h , and the discrete divergence operator, div_h . These three operators are derived naturally from the Stokes theorem in one, two and three spatial dimensions.

2.3.1 The discrete gradient operator $\nabla_h : \mathcal{V}_h \rightarrow \mathcal{E}_h$

The Stokes theorem (2.1) on the one-dimensional edge e connecting the vertices v_1 and v_2 (and oriented from the former to the latter) becomes:

$$\int_e \frac{\partial p}{\partial \boldsymbol{\tau}_e} dL = \int_e \nabla p \cdot \boldsymbol{\tau}_e dL = p(\mathbf{x}_{v_2}) - p(\mathbf{x}_{v_1}). \quad (2.18)$$

In view of Eq. (2.18), it is straightforward to define the discrete gradient operator ∇_h applied to a vertex-based discrete field p_h on edge e as follows:

$$(\nabla_h p_h)_e = \frac{p_{v_2} - p_{v_1}}{|e|}. \quad (2.19)$$

In accordance with (2.12), the discrete gradient operator ∇_h acts from \mathcal{V}_h to \mathcal{V}_h^* . The linear space \mathcal{V}_h^* is related to the mesh edges and coincides with \mathcal{E}_h .

Let $p_h = \Pi^{\mathcal{V}}(p)$. If $p \in C^2(\Omega)$, the Taylor expansion shows that ∇_h is the first-order accurate approximation of the continuous gradient operator in the sense that

$$(\nabla_h p_h)_e = (\nabla p)(\mathbf{x}_e) + O(h_e).$$

The discrete gradient operator is exact for linear functions p .

2.3.2 The discrete curl operator $\text{curl}_h : \mathcal{E}_h \rightarrow \mathcal{F}_h$

The Stokes theorem (2.2) applied to the two-dimensional face f gives:

$$\int_f (\text{curl } \mathbf{u}) \cdot \mathbf{n}_f dS = \int_{\partial f} \mathbf{u} \cdot \boldsymbol{\tau}_{f,e} dL, \quad (2.20)$$

where the tangential vector $\boldsymbol{\tau}_{f,e}$ is oriented counter-clockwise along ∂f when looking from the tip of the normal vector \mathbf{n}_f . In view of Eq. (2.20), it is straightforward to define the discrete operator curl_h applied to an edge-based mesh \mathbf{u}_h on face f as follows:

$$(\text{curl}_h \mathbf{u}_h)_f = \frac{1}{|f|} \sum_{e \in \mathcal{E}_f} \alpha_{f,e} |e| u_e. \quad (2.21)$$

The factor $\alpha_{f,e} = \pm 1$ is determined by the mutual orientation of the tangential vectors $\boldsymbol{\tau}_e$, $\boldsymbol{\tau}_{f,e}$ and the normal vector \mathbf{n}_f . In accordance with (2.12), the discrete curl operator acts from \mathcal{E}_h to \mathcal{E}_h^* . The linear space \mathcal{E}_h^* is related to the mesh faces and coincides with \mathcal{F}_h .

Let $\mathbf{u}_h = \Pi^{\mathcal{E}}(\mathbf{u})$. If $\mathbf{u} \in (C^2(\Omega))^d$, the mid-point quadrature gives that curl_h is the first-order accurate approximation of the continuous curl operator in the sense that

$$(\text{curl}_h \mathbf{u}_h)_f = \frac{1}{|f|} \int_f (\text{curl } \mathbf{u}) \cdot \mathbf{n}_f dS = (\text{curl } \mathbf{u})(\mathbf{x}_f) + O(h_f).$$

The discrete curl operator is exact for linear vector-valued functions \mathbf{u} .

2.3.3 The discrete divergence operator $\text{div}_h : \mathcal{F}_h \rightarrow \mathcal{P}_h$

The Stokes theorem (2.3) on the three-dimensional cell P becomes:

$$\int_P \text{div } \mathbf{u} dV = \int_{\partial P} \mathbf{u} \cdot \mathbf{n}_P dS, \quad (2.22)$$

where \mathbf{n}_P is the outward unit normal vector. In view of Eq. (2.22), it is straightforward to define the discrete operator div_h applied to a face-based discrete field \mathbf{u}_h on cell P as follows:

$$(\text{div}_h \mathbf{u}_h)_P = \frac{1}{|P|} \sum_{f \in \mathcal{F}_P} \alpha_{P,f} |f| u_f. \quad (2.23)$$

The factor $\alpha_{P,f} = \mathbf{n}_f \cdot \mathbf{n}_{P,f} = \pm 1$ is determined by the mutual orientation of the normal vectors $\mathbf{n}_{P,f}$ and \mathbf{n}_f . In accordance with (2.12), the discrete divergence operator acts

from \mathcal{F}_h to \mathcal{F}_h^* . The linear space \mathcal{F}_h^* is related to the mesh cells and coincides with \mathcal{P}_h .

Let $\mathbf{u}_h = \Pi^{\mathcal{F}}(\mathbf{u})$. If $\mathbf{u} \in (C^2(\Omega))^d$, the mid-point quadrature gives that div_h is the first-order accurate approximation of the continuous divergence operator in the sense that

$$(\text{div}_h \mathbf{u}_h)_P = \frac{1}{|P|} \int_P \text{div} \mathbf{u} dV = (\text{div} \mathbf{u})(\mathbf{x}_P) + O(h_P).$$

The discrete divergence operator is exact for linear vector-valued functions \mathbf{u} .

2.3.4 Discrete versions of the Stokes theorem

The definition of the primary mimetic operators is based on the Stokes theorem applied to a single mesh object. Let us show that a discrete version of the Stokes theorem holds for a collection of mesh objects.

Example 2.1. Formula (2.1) states that the line integral between two points \mathbf{x}_a and \mathbf{x}_b , corresponding to two vertices v_0 and v_n does not depend on the path connecting them. Let us consider the mesh path L_h joining v_0 and v_n through the sequence of mesh vertices $v_0, v_1, \dots, v_{n-1}, v_n$, where each pair of consecutive vertices (v_{i-1}, v_i) is connected by a mesh edge e_i , for $i = 1, \dots, n$. By assuming that the discrete gradient of $p_h \in \mathcal{V}_h$ is constant on each mesh edge and integrating along this path, we obtain:

$$\int_{L_h} \nabla_h p_h dL = \sum_{i=1}^n |e_i| (\nabla_h p_h)_{e_i} = \sum_{i=1}^n (p_{v_i} - p_{v_{i-1}}) = p_{v_n} - p_{v_0}.$$

The results does not depend on the mesh path connecting v_0 and v_n , see Fig. 2.3. This is the discrete analog of the 1-D Stokes theorem.

Example 2.2. Let S be a surface embedded in the three-dimensional space and bounded by a closed curve L . Formula (2.2) states that the total flux of the vorticity of a field \mathbf{u} through the surface S depends only on the curve L . Let us consider a set of mesh faces f forming a discrete surface S_h (approximating S) which is bounded by a set of mesh edges e forming a closed mesh path L_h . In addition, we assume that

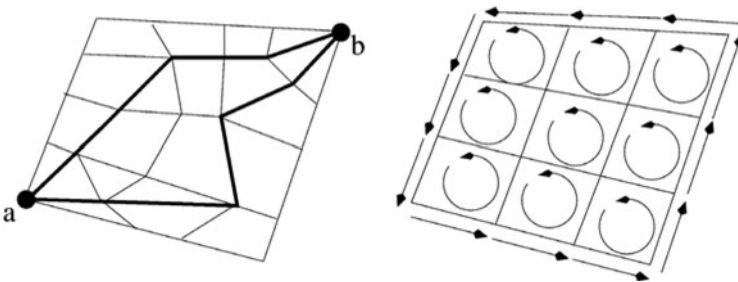


Fig. 2.3. Two-dimensional illustrations for Examples 2.1 (left) and 2.2 (right)

the orientations of \mathbf{n}_f , $f \in S_h$, and $\boldsymbol{\tau}_e$, $e \in L_h$, are consistent with the orientations of the normal and tangential vectors in the Stokes theorem (2.2). By assuming that the discrete curl of $\mathbf{u}_h \in \mathcal{E}_h$ is constant on each mesh face and integrating it over S_h , we obtain:

$$\int_{S_h} \text{curl}_h \mathbf{u}_h dS = \sum_{f \in S_h} |f| (\text{curl}_h \mathbf{u}_h)_f = \sum_{e \in L_h} |e| u_e.$$

For a fixed mesh path L_h , the results does not depend on the surface S_h , see Fig. 2.3. This is the discrete analog of the 2-D Stokes theorem.

Example 2.3. Let V be a simply-connected domain bounded by a surface S . Formula (2.3) states that the integral of the divergence over V is equal to the outward flux of a vector field through the surface S . Let us consider a set of mesh cells P forming a simply-connected domain V_h (approximating V) which is bounded by a set of mesh faces f forming a closed discrete surface S_h . In addition, let the normals \mathbf{n}_f , $f \in S_h$, point out of V_h . By assuming that the discrete divergence of $\mathbf{u}_h \in \mathcal{F}_h$ is constant inside each cell and integrating it over V_h , we obtain:

$$\int_{V_h} \text{div}_h \mathbf{u}_h dV = \sum_{P \in V_h} |P| (\text{div}_h \mathbf{u}_h)_P = \sum_{f \in S_h} |f| u_f.$$

This is the discrete analog of the 3-D Stokes theorem also known as Gauss's theorem or Ostrogradsky's theorem.

2.3.5 Basic properties of the primary operators

Discrete analogs of the fundamental calculus relationships such as $\text{curl} \circ \nabla = 0$ and $\text{div} \circ \text{curl} = 0$ hold also for the primary mimetic operators. These properties are discussed in detail in Sect. 2.6. Here, we establish a result related to the stability of mimetic discretizations for the diffusion problem and prove a commuting diagram property that involves the differential operators ∇ , curl and div , their discrete analogs ∇_h , curl_h and div_h , and the projection operators of Sect. 2.2.

To avoid unnecessary complications, we consider a polyhedral domain Ω , which it is fully covered by the mesh.

Lemma 2.1. *Let Ω have a Lipschitz continuous boundary. Then, the primary divergence operator div_h is surjective, i.e., $\text{img}(\text{div}_h) = \mathcal{P}_h$.*

Proof. We need to prove that for any discrete field q_h in \mathcal{P}_h there exists a discrete field \mathbf{v}_h in \mathcal{F}_h such that $q_h = (q_P)_{P \in \mathcal{P}} = \text{div}_h \mathbf{v}_h$. A constructive proof of this statement allows us to build \mathbf{v}_h in a systematic way once the field q_h in \mathcal{P}_h is given. The field \mathbf{v}_h is obtained in three steps.

1. We define the piecewise-constant function $q \in L^2(\Omega)$ such that $q|_P = q_P$. Note that $q_h = \Pi^{\mathcal{P}}(q)$.

2. We define a function ϕ as the solution of the Laplace equation:

$$\begin{aligned}\Delta \phi &= q & \text{in } \Omega, \\ \phi &= 0 & \text{on } \partial\Omega.\end{aligned}$$

Since Ω_h has a Lipschitz continuous boundary, there exist $s > 2$ such that $\phi \in W^{1,s}(\Omega)$.

3. We take $\mathbf{v} = \nabla \phi$, so that $\operatorname{div} \mathbf{v} = q$. Finally, we define $\mathbf{v}_h \in \mathcal{F}_h$ as the face projection of \mathbf{v} , i.e., $\mathbf{v}_h = \Pi^{\mathcal{F}}(\mathbf{v})$.

To complete the proof, let us show that $q_h = \operatorname{div}_h \mathbf{v}_h$. Due to the regularity of ϕ , the face integrals of \mathbf{v} do exist. Starting from definition (2.23), we make the following developments:

$$\begin{aligned}(\operatorname{div}_h \mathbf{v}_h)_P &= \frac{1}{|P|} \sum_{f \in \partial P} \alpha_{P,f} |f| v_f && \text{[use (2.16)]} \\ &= \frac{1}{|P|} \sum_{f \in \partial P} \alpha_{P,f} \int_f \mathbf{v} \cdot \mathbf{n}_f dS && \text{[collect the face integrals]} \\ &= \frac{1}{|P|} \int_{\partial P} \mathbf{v} \cdot \mathbf{n}_P dS && \text{[use the divergence theorem]} \\ &= \frac{1}{|P|} \int_P \operatorname{div} \mathbf{v} dV && \text{[use } \operatorname{div} \mathbf{v} = q\text{]} \\ &= \frac{1}{|P|} \int_P q dV = q_P.\end{aligned}$$

This proves the assertion of the lemma. □

Lemma 2.2. *The following commuting diagram holds:*

$$\begin{array}{ccccccc} H^1(\Omega) & \xrightarrow{\nabla} & H(\operatorname{curl}, \Omega) & \xrightarrow{\operatorname{curl}} & H(\operatorname{div}, \Omega) & \xrightarrow{\operatorname{div}} & L^2(\Omega) \\ \Pi^{\mathcal{V}} \downarrow & & \Pi^{\mathcal{E}} \downarrow & & \Pi^{\mathcal{F}} \downarrow & & \Pi^{\mathcal{P}} \downarrow \\ \mathcal{V}_h & \xrightarrow{\nabla_h} & \mathcal{E}_h & \xrightarrow{\operatorname{curl}_h} & \mathcal{F}_h & \xrightarrow{\operatorname{div}_h} & \mathcal{P}_h \end{array}$$

Proof. To prove the left part of the commuting diagram, let q be a sufficiently regular scalar function on Ω . Using the definitions of $\Pi^{\mathcal{E}}$ and $\Pi^{\mathcal{V}}$, applying the fundamental theorem of calculus, and recalling the definition of the discrete gradient operator in (2.19) yield

$$\Pi_e^{\mathcal{E}}(\nabla q)|_e = \frac{1}{|e|} \int_e (\nabla q) \cdot \boldsymbol{\tau}_e dL = \frac{q(\mathbf{x}_{v_2}) - q(\mathbf{x}_{v_1})}{|e|} = (\nabla_h \Pi^{\mathcal{V}}(q))_e,$$

which holds for any oriented edge $\mathbf{e} \in \mathcal{E}$ with vertices \mathbf{v}_1 and \mathbf{v}_2 .

To prove the middle part of the commuting diagram, let \mathbf{v} be a sufficiently regular vector function on Ω . Using the definitions of $\Pi^{\mathcal{F}}$ and $\Pi^{\mathcal{V}}$, applying the circulation theorem, and recalling the definition of the discrete curl operator in (2.21) yield

$$\begin{aligned} \Pi^{\mathcal{F}}(\operatorname{curl}(\mathbf{v}))|_f &= \frac{1}{|f|} \int_f \operatorname{curl} \mathbf{v} \cdot \mathbf{n}_f dS = \frac{1}{|f|} \sum_{\mathbf{e} \in \partial f} \int_{\mathbf{e}} \mathbf{v} \cdot \boldsymbol{\tau}_{f,\mathbf{e}} dL \\ &= \frac{1}{|f|} \sum_{\mathbf{e} \in \partial f} |\mathbf{e}| \alpha_{f,\mathbf{e}} v_{\mathbf{e}} = (\operatorname{curl}_h \Pi^{\mathcal{E}}(\mathbf{v}))_f. \end{aligned}$$

To prove the right part of the commuting diagram, let \mathbf{v} be a sufficiently regular vector function on Ω . Using the definitions of $\Pi^{\mathcal{P}}$ and $\Pi^{\mathcal{F}}$, applying the divergence theorem, and recalling the definition of the discrete divergence operator in (2.23) yield

$$\Pi^{\mathcal{P}}(\operatorname{div} \mathbf{v})|_P = \frac{1}{|P|} \int_P \operatorname{div} \mathbf{v} dV = \frac{1}{|P|} \sum_{f \in \partial P} \int_f \mathbf{v} \cdot \mathbf{n}_{P,f} dS \quad (2.24)$$

$$= \frac{1}{|P|} \sum_{f \in \partial P} |f| \alpha_{P,f} v_f = (\operatorname{div}_h \Pi^{\mathcal{F}}(\mathbf{v}))_P. \quad (2.25)$$

This proves the assertion of the lemma. \square

2.3.6 Matrix representation of the primary operators

Recall that a discrete field can be interpreted via an algebraic vector. Similarly, the three primary operators ∇_h , curl_h and div_h can be interpreted via matrices. There is a strong connection between such matrices and the topological structure of the mesh. In fact, the matrices representing ∇_h , curl_h and div_h are the adjacency matrices of the mesh up to a diagonal rescaling of their rows and columns.

The matrix associated with ∇_h and rescaled with the edge lengths represents vertex-edge connections. The matrix associated with curl_h and rescaled with edge and face measures represents edge-face connections. The matrix associated with div_h and rescaled with face and cell measures represents face-cell connections. With a small abuse of notation, these matrices are denoted using the same symbol of the corresponding discrete operators.

The matrix representation is extremely useful as it allows us to reinterpret the action of a discrete operator as a matrix-vector product. For example, if $N^{\mathcal{V}}$ and $N^{\mathcal{E}}$ are, respectively, the number of nodes and edges in the mesh, the discrete gradient operator ∇_h is a rectangular $N^{\mathcal{E}} \times N^{\mathcal{V}}$ matrix. Then, the expression $\mathbf{v}_h = \nabla_h p_h$, can be evaluated by multiplying the matrix ∇_h by the $N^{\mathcal{V}}$ -sized vector $(p_P)_{P \in \mathcal{P}_h}$. The result is $N^{\mathcal{E}}$ -sized vector $(v_{\mathbf{e}})_{\mathbf{e} \in \mathcal{E}_h}$. A similar interpretation holds for curl_h and div_h .

It will be always clear from the context whether ∇_h should be interpreted as an operator or a matrix. For example, the expression $\mathbf{u}_h^T \nabla_h p_h$ means a vector-matrix-vector product.

2.4 Derived mimetic operators

The duality relationship (2.12) leads to three new mimetic operators, denoted by $\widetilde{\nabla}_h$, $\widetilde{\text{curl}}_h$, and $\widetilde{\text{div}}_h$, that are adjoint to the primary operators div_h , curl_h , and ∇_h , respectively. More precisely, formula (2.12) defines uniquely an adjoint operator \mathcal{D}_h^* for each primary operator d_h . Using this formula, we define the adjoint operators ∇_h^* , curl_h^* , and div_h^* for the primary operators ∇_h , curl_h , and div_h , respectively. To reflect the nature of the adjoint operators better, we identify $\widetilde{\nabla}_h \equiv -\text{div}_h^*$, $\widetilde{\text{curl}}_h \equiv \text{curl}_h^*$, and $\widetilde{\text{div}}_h \equiv -\nabla_h^*$. Since the new operators are derived from the primary operators, we refer to them as the *derived mimetic operators*.

A formal definition of the derived operators leaves freedom in selecting inner products in the discrete spaces. The results proved in this chapter do not limit this selection. In the subsequent chapters, we will show that the accuracy of mimetic discretizations does depend on this selection. The derivation of accurate inner products is in the heart of the mimetic technology.

Let the spaces \mathcal{V}_h , \mathcal{E}_h , \mathcal{F}_h , or \mathcal{P}_h be equipped with inner products and a matrix representation be available for each of them. We recall that an inner product $[\cdot, \cdot]_{\mathcal{S}_h}$, where \mathcal{S}_h is one of the spaces \mathcal{V}_h , \mathcal{E}_h , \mathcal{F}_h , or \mathcal{P}_h , can be represented by a symmetric positive definite matrix $M_{\mathcal{S}}$. For the moment, we simply assume that there exists a matrix $M_{\mathcal{S}}$ such that

$$[\mathbf{u}_h, \mathbf{v}_h]_{\mathcal{S}_h} = (\mathbf{u}_h)^T M_{\mathcal{S}} \mathbf{v}_h, \quad \forall \mathbf{u}_h, \mathbf{v}_h \in \mathcal{S}_h. \quad (2.26)$$

Let us insert the primary and adjoint operators div_h and div_h^* into formula (2.12) and recall the renaming of the adjoint operators:

$$[\text{div}_h \mathbf{v}_h, p_h]_{\mathcal{P}_h} = [\mathbf{v}_h, \text{div}_h^* p_h]_{\mathcal{F}_h} \equiv -[\mathbf{v}_h, \widetilde{\nabla}_h p_h]_{\mathcal{F}_h}, \quad (2.27)$$

which holds for every $\mathbf{v}_h \in \mathcal{F}_h$ and every $p_h \in \mathcal{P}_h$. Applying formula (2.26) to the inner products in spaces \mathcal{P}_h and \mathcal{F}_h , we obtain the following algebraic expression:

$$\mathbf{v}_h^T \text{div}_h^T M_{\mathcal{P}} p_h = -\mathbf{v}_h^T M_{\mathcal{F}} \widetilde{\nabla}_h p_h,$$

where div_h^T is the transpose of matrix div_h . Since vectors \mathbf{v}_h and p_h are arbitrary, we have the matrix relation

$$M_{\mathcal{F}} \widetilde{\nabla}_h = -\text{div}_h^T M_{\mathcal{P}},$$

from which it follows that

$$\widetilde{\nabla}_h \equiv -\text{div}_h^* = -M_{\mathcal{F}}^{-1} \text{div}_h^T M_{\mathcal{P}}. \quad (2.28)$$

In other words, the derived gradient operator is negatively adjoint to the primary divergence operator. Now, it becomes clear that the properties (e.g., accuracy) of the derived gradient operator depend on the properties of two inner product matrices.

The duality relation between the discrete curl operator curl_h and its adjoint $\text{curl}_h^* \equiv \widetilde{\text{curl}}_h$ implies that

$$[\text{curl}_h \mathbf{v}_h, \mathbf{w}_h]_{\mathcal{F}_h} = [\mathbf{v}_h, \text{curl}_h^* \mathbf{w}_h]_{\mathcal{E}_h} \equiv [\mathbf{v}_h, \widetilde{\text{curl}}_h \mathbf{w}_h]_{\mathcal{E}_h} \quad (2.29)$$

holds for every $\mathbf{w}_h \in \mathcal{F}_h$ and every $\mathbf{v}_h \in \mathcal{E}_h$. Applying formula (2.26) to the inner products, we obtain its algebraic form:

$$\mathbf{v}_h^T \text{curl}_h^T M_{\mathcal{F}} \mathbf{w}_h = \mathbf{v}_h^T M_{\mathcal{E}} \widetilde{\text{curl}}_h \mathbf{w}_h,$$

where curl_h^T is the transpose of matrix curl_h . Since vectors \mathbf{v}_h and p_h are arbitrary, we have the matrix relation

$$M_{\mathcal{E}} \widetilde{\text{curl}}_h = \text{curl}_h^T M_{\mathcal{F}}$$

from which we obtain that

$$\widetilde{\text{curl}}_h = M_{\mathcal{E}}^{-1} \text{curl}_h^T M_{\mathcal{F}}. \quad (2.30)$$

In the continuum setting, the curl operator is a self-adjoint operator. In the discrete setting, we have two distinct curl operators, the primary and the derived curl operator, and the derived curl operator is adjoint to the primary curl operator.

Finally, the duality relation between the discrete gradient operator ∇ and its adjoint $\nabla_h^* \equiv -\widetilde{\text{div}}_h$ implies that the relation

$$[\nabla_h q_h, \mathbf{w}_h]_{\mathcal{E}_h} \equiv [q_h, \nabla_h^* \mathbf{w}_h]_{\mathcal{V}_h} = -[q_h, \widetilde{\text{div}}_h \mathbf{w}_h]_{\mathcal{V}_h} \quad (2.31)$$

holds for every $q_h \in \mathcal{V}_h$ and $\mathbf{w}_h \in \mathcal{E}_h$. By applying formula (2.26) to the inner products, we reformulate (2.31) as follows:

$$q_h^T \nabla_h^T M_{\mathcal{E}} \mathbf{w}_h = -q_h^T M_{\mathcal{V}} \widetilde{\text{div}}_h \mathbf{w}_h,$$

where ∇_h^T is the transpose of matrix ∇_h . Since vectors q_h and \mathbf{w}_h are arbitrary, we have the matrix relation

$$M_{\mathcal{V}} \widetilde{\text{div}}_h = -\nabla_h^T M_{\mathcal{E}},$$

from which we obtain that

$$\widetilde{\text{div}}_h = -M_{\mathcal{V}}^{-1} \nabla_h^T M_{\mathcal{E}}. \quad (2.32)$$

In other words, the derived divergence operator is negatively adjoint to the primary gradient operator.

Remark 2.4. With a few exceptions, the inner product matrices are often irreducible matrices for unstructured meshes. Thus, their inverse matrices are dense and the stencil of the derived operators is non-local. A similar statement can be made for other compatible discretization methods such as the mixed finite element method.

Remark 2.5. The derived operators also contains information about the coefficients of the partial differential equation. For example, let the functions q and \mathbf{v} be zero on the boundary of Ω . In view of the relation

$$\int_{\Omega} K \nabla q \cdot \mathbf{v} dV = - \int_{\Omega} q \text{div} K \mathbf{v} dV, \quad (2.33)$$

if we define a primary operator $\nabla_h \approx \nabla$, it follows that $\widetilde{\text{div}}_h \approx \text{div}(\mathbb{K} \cdot)$. This property is implicit in the definition of the mimetic inner product that approximates the integral in the right-hand side of (2.33).

2.5 Second-order discrete operators

We can combine the first-order primary and derived operators to form the second-order operators $\text{div}_h \widetilde{\nabla}_h$, $\widetilde{\text{div}}_h \nabla_h$, $\widetilde{\text{curl}}_h \text{curl}_h$, and $\text{curl}_h \widetilde{\text{curl}}_h$, which are discrete analogs of the continuum operators $\Delta = \text{div} \nabla$ and $\text{curl} \text{curl}$. These discrete operators preserve various properties of the continuum operators. For example, the operator $\widetilde{\text{curl}}_h \text{curl}_h: \mathcal{E}_h \rightarrow \mathcal{E}_h$ is self-adjoint with respect to the inner product in space \mathcal{E}_h . It can be used to design a mimetic scheme for the electric field in Maxwell's equations. The operator $\text{curl}_h \widetilde{\text{curl}}_h: \mathcal{F}_h \rightarrow \mathcal{F}_h$ is self-adjoint with respect to the inner product in space \mathcal{F}_h . It can be used to design a mimetic scheme for solving the equations of magnetic diffusion.

We also have two discrete analogs of the vector Laplace operator $\Delta = \nabla \text{div} - \text{curl} \text{curl}$, which are given by

$$\Delta_{\mathcal{E}_h} = \nabla_h \widetilde{\text{div}}_h - \widetilde{\text{curl}}_h \text{curl}_h: \mathcal{E}_h \rightarrow \mathcal{E}_h$$

and

$$\Delta_{\mathcal{F}_h} = \widetilde{\nabla}_h \text{div}_h - \text{curl}_h \widetilde{\text{curl}}_h: \mathcal{F}_h \rightarrow \mathcal{F}_h.$$

The discrete operators $\Delta_{\mathcal{E}_h}$ and $\Delta_{\mathcal{F}_h}$ are symmetric and semi-negative definite with respect to the inner products in spaces \mathcal{E}_h and \mathcal{F}_h , respectively. Such combined operators provide a quick and elegant way to design mimetic discretizations of PDEs, which we illustrate with a few examples. For simplicity of exposition, we assume that the coefficients describing material properties are equal to 1.

Example 2.4. Let us consider the diffusion problem in mixed form:

$$\mathbf{u} = -\nabla p \quad \text{in } \Omega, \quad (2.34)$$

$$\text{div } \mathbf{u} = b \quad \text{in } \Omega, \quad (2.35)$$

subject to homogeneous Dirichlet boundary conditions. We assume that b is a sufficiently smooth function.

A mimetic discretization of this problem is given by introducing two discrete fields $p_h \in \mathcal{P}_h$ and $\mathbf{u}_h \in \mathcal{F}_h$ that satisfy the discrete analog of (2.34)–(2.35):

$$\mathbf{u}_h = -\widetilde{\nabla}_h p_h, \quad (2.36)$$

$$\text{div}_h \mathbf{u}_h = b_h, \quad (2.37)$$

where $b_h \in \mathcal{P}_h$ is the cell-based discrete field approximating b , i.e. $b_h = \Pi^{\mathcal{P}}(b)$. From (2.36)–(2.37) we immediately obtain the *cell-centered* mimetic scheme for p_h :

$$-\text{div}_h \widetilde{\nabla}_h p_h = b_h. \quad (2.38)$$

This scheme is well-posed since the discrete operator $\operatorname{div}_h \widetilde{\nabla}_h$ is associated with a full rank matrix, as shown in Lemma 2.7. Moreover, the operator $\operatorname{div}_h \widetilde{\nabla}_h$ is self-adjoint with respect to the inner product in space \mathcal{P}_h . Substituting the expression of $\widetilde{\nabla}_h$ given by (2.28), we obtain the following linear system:

$$\operatorname{div}_h M_{\mathcal{F}}^{-1} \operatorname{div}_h^T M_{\mathcal{D}} p_h = b_h.$$

We stress that this cell-centered discretization of the Poisson equation includes already the homogeneous Dirichlet boundary condition. Mimetic discretizations of this type will be the subject of Chap. 5.

Example 2.5. Consider again the diffusion problem (2.34)–(2.35) subject to homogeneous Neumann boundary conditions. An alternative mimetic discretization of this problem is obtained by introducing the two discrete fields $p_h \in \mathcal{V}_h$ and $\mathbf{u}_h \in \mathcal{E}_h$ that satisfy

$$\mathbf{u}_h = -\nabla_h p_h \quad \text{in } \Omega, \quad (2.39)$$

$$\widetilde{\operatorname{div}}_h \mathbf{u}_h = b_h \quad \text{in } \Omega, \quad (2.40)$$

where $b_h \in \mathcal{V}_h$ is the vertex-based discrete field approximating b , i.e., $b_h = \Pi^{\mathcal{V}}(b)$. From (2.39)–(2.40) we immediately obtain the *nodal* mimetic scheme for p_h :

$$-\widetilde{\operatorname{div}}_h \nabla_h p_h = b_h. \quad (2.41)$$

The kernel of the discrete operator $\widetilde{\operatorname{div}}_h \nabla_h$ consists of constant discrete fields in \mathcal{V}_h , as shown in Lemma 2.8. This mimics the similar property of the continuum problem that has a solution defined up to an arbitrary constant. Note that the Dirichlet boundary condition can be imposed by setting prescribed values to the components of p_h at the boundary nodes and eliminating the corresponding equations from the global system.

The operator $\widetilde{\operatorname{div}}_h \nabla_h$ is also self-adjoint with respect to the inner product in space \mathcal{V}_h . Substituting the expression of $\widetilde{\operatorname{div}}_h$ given by (2.28), we obtain the following algebraic system:

$$M_{\mathcal{V}} \nabla_h^T M_{\mathcal{E}}^{-1} \nabla_h p_h = b_h.$$

Mimetic discretizations of this type will be the subject of Chap. 6.

Example 2.6. Let us consider the div-curl problem for a vector potential \mathbf{A} and a scalar function p which reads as

$$\operatorname{curl}(\mu^{-1} \operatorname{curl} \mathbf{A}) + \nabla p = \mathbf{J} \quad \text{in } \Omega, \quad (2.42)$$

$$\operatorname{div} \mathbf{A} = 0 \quad \text{in } \Omega, \quad (2.43)$$

$$\mathbf{A} \times \mathbf{n} = 0 \quad \text{on } \partial\Omega, \quad (2.44)$$

where \mathbf{J} is a given current. For simplicity, we assume that the magnetic permeability is given by $\mu = 1$.

Let \mathcal{V}_h^0 denote a proper subspace of \mathcal{V}_h consisting of vectors whose components are zero for boundary nodes. Similarly, let \mathcal{E}_h^0 denote a proper subspace of \mathcal{E}_h consisting of vectors whose components are zero for boundary edges. We discretize this

problem by introducing the discrete fields $p_h \in \mathcal{V}_h^0$ and $\mathbf{A}_h \in \mathcal{E}_h^0$ that satisfy

$$\widetilde{\text{curl}}_h \text{curl}_h \mathbf{A}_h + \nabla_h p_h = \mathbf{J}_h, \quad (2.45)$$

$$\widetilde{\text{div}}_h \mathbf{A}_h = 0, \quad (2.46)$$

where $\mathbf{J}_h = (J_e)_{E \in \mathcal{E}}$ represents the vector function \mathbf{J} in \mathcal{E}_h and the degrees of freedom J_e are defined by (2.15). The linear algebraic formulation follows immediately by using the definition of primary and derived operators:

$$\mathbf{M}_\mathcal{E}^{-1} \text{curl}_h^T \mathbf{M}_\mathcal{F} \text{curl}_h \mathbf{A}_h + \nabla_h p_h = \mathbf{J}_h, \quad (2.47)$$

$$\mathbf{M}_\mathcal{Y}^{-1} \nabla_h^T \mathbf{M}_\mathcal{E} \mathbf{A}_h = 0. \quad (2.48)$$

Since $\mathbf{M}_\mathcal{E}^{-1}$ can be dense on an unstructured mesh, a computationally tractable system is obtained by multiplying the first equation by $\mathbf{M}_\mathcal{E}$. A symmetric system is obtained by multiplying the second equation by $\mathbf{M}_\mathcal{Y}$. The well-posedness of this mimetic method for the general case with $\mu > 0$ is proved in [248].

2.6 Exact identities

A set of fundamental properties of the continuous calculus are exactly reproduced in the discrete setting by the primary and derived operators. These properties characterize the kernel of the partial differential operators, e.g., $\text{curl} \circ \nabla = 0$ and $\text{div} \circ \text{curl} = 0$, and their preservation in the DVTC is one of the most important aspects of the mimetic methods. Indeed, they play a crucial role for the stability of the numerical approximation of PDEs such as Navier-Stokes and Maxwell's equations. Other discrete analogs of the continuous calculus regard the Helmholtz decomposition theorem that will be discussed in the next section.

For clarity of presentation, we always assume that the computational mesh Ω_h is topologically connected in accordance with the following definition.

Definition 2.1. A polyhedral mesh is called *face-connected* if it cannot be split into two submeshes that have no common faces but may have common vertices and edges.

Definition 2.2. Let χ denote a closed mesh surface formed by a subset of mesh faces without inner loops. A face-connected polyhedral mesh is called *simply connected* if, for any such χ , there exists a subset Ω_χ of mesh elements that form a simply-connected domain with boundary χ .

We will also denote the range (or image) of a primary or derived operator d by $\text{img}(d)$ and its null space by $\ker(d)$; the orthogonal complement of a linear subspace Q by $(Q)^\perp$ and its trivial subspace, which only contains the zero element, by $\{0\}_Q$.

2.6.1 The kernel of the primary operators

Let us first characterize the kernel of the primary gradient operator.

Lemma 2.3. *Let Ω_h be a simply-connected mesh. Then, the kernel of ∇_h is formed by the subset of the constant vectors of \mathcal{P}_h , i.e., those vectors whose entries have the same value.*

Proof. From definition (2.19) we can easily see that $\nabla_h p_h = 0$ if and only if $p_{v_1} = p_{v_2}$ for any edge $e = (v_1, v_2)$. Since the mesh is simply-connected, p_h is a constant vector. Thus, we can identify the subspace of the constant vectors in \mathcal{V}_h with the null space of ∇_h . \square

Let us now characterize the kernel of the primary curl and divergence operators. More precisely, in the following lemma we prove that $\ker(\text{curl}_h) = \text{img}(\nabla_h)$ and $\ker(\text{div}_h) = \text{img}(\text{curl}_h)$. The two conditions are the mimetic analogs of $\text{curl} \circ \nabla = 0$ and $\text{div} \circ \text{curl} = 0$, respectively.

Lemma 2.4. *Let the domain Ω and its mesh partition Ω_h be simply connected. Then,*

$$\text{curl}_h \mathbf{v}_h = 0 \quad \text{if and only if} \quad \mathbf{v}_h = \nabla_h q_h \quad (2.49)$$

for some $q_h \in \mathcal{V}_h$ and

$$\text{div}_h \mathbf{v}_h = 0 \quad \text{if and only if} \quad \mathbf{v}_h = \text{curl}_h \mathbf{u}_h \quad (2.50)$$

for some $\mathbf{u}_h \in \mathcal{E}_h$.

Proof. The “if” part of the lemma’s assertion can be readily verified since from a straightforward calculation it follows that $\text{curl}_h \nabla_h = 0$ and $\text{div}_h \text{curl}_h = 0$.

To prove the “only if” part of assertion (2.49) we consider a discrete field $\mathbf{v}_h \in \mathcal{E}_h$ such that $\text{curl}_h \mathbf{v}_h = 0$. We need to find a discrete field $q_h \in \mathcal{V}_h$ such that $\mathbf{v}_h = \nabla_h q_h$. Let us choose a vertex v_1 of the mesh. As the mesh is simply connected, any other vertex v_i can be reached from v_1 through a mesh path of consecutive edges $\{e_k\}_{k=2}^i$ that begins at v_1 and ends at v_i . Let us now introduce the discrete field $q_h \in \mathcal{V}_h$ that takes the value

$$q_{v_i} = q_{v_1} + \sum_{k=2}^i \alpha_{i,k} |e_k| v_{e_k} \quad (2.51)$$

at v_i , where $\alpha_{i,k}$ in (2.51) is the sign ± 1 that depends on the orientation of the k -th edge e_k with respect to the mesh path. Now, since $\text{curl}_h \mathbf{v}_h = 0$ and the mesh is simply connected q_{v_i} is independent of the mesh path and must only depend on q_{v_1} . This initial value can be left undefined, which is equivalent to say that q_h is defined up to a constant vector. By construction, it immediately holds that $\nabla_h q_h = \mathbf{v}_h$, as the constant vectors are in the kernel of the primary gradient operator, see Lemma 2.3.

To prove the *only if* part of assertion (2.50), let us consider a discrete field $\mathbf{v}_h \in \mathcal{P}_h$ such that $\text{div}_h \mathbf{v}_h = 0$. We need to find a discrete field $\mathbf{u}_h \in \mathcal{E}_h$ such that $\mathbf{v}_h = \text{curl}_h \mathbf{u}_h$. On a logically rectangular mesh this result can be proved by using a simple

constructive argument, see, e.g., [210, 215]. However, its extension to the case of general unstructured meshes is not trivial. Herein, we use a different argument that is based on the properties of the continuum operators. Let $\mathbf{v} \in H(\operatorname{div}, \Omega) \cap (C^0(\bar{\Omega}))^d$ be a vector function whose restriction to each cell P is such that

$$\begin{aligned} \operatorname{div} \mathbf{v} &= 0 && \text{in } P, \\ \mathbf{n}_{P,f} \cdot \mathbf{v} &= \alpha_{P,f} v_f && \text{on } f \in \partial P, \end{aligned}$$

where v_f is the component of the face-based function \mathbf{v}_h associated with the mesh face f of ∂P . Since $\operatorname{div} \mathbf{v} = 0$ in Ω , there exists a vector potential $\mathbf{u} \in (H^1(\Omega))^3$ (a scalar stream function in 2D) such that $\mathbf{v} = \operatorname{curl} \mathbf{u}$. The proof can be found in [184]. Let us introduce the discrete field \mathbf{u}_h , whose component are the mean values of $\mathbf{u} \cdot \boldsymbol{\tau}_e$ along the mesh edges, see, e.g., (2.15).

Now, through a straightforward calculation that starts from the definition of the face degrees of freedom in (2.16), we obtain

$$\begin{aligned} v_f &= \frac{1}{|f|} \int_f \mathbf{v} \cdot \mathbf{n}_f dS && [\text{substitute } \mathbf{v} = \operatorname{curl} \mathbf{u}, \text{ cf. [184]}] \\ &= \frac{1}{|f|} \int_f (\operatorname{curl} \mathbf{u}) \cdot \mathbf{n}_f dS && [\text{apply the Circulation Theorem, see (2.2)}] \\ &= \frac{1}{|f|} \int_{\partial f} \mathbf{u} \cdot \boldsymbol{\tau}_e dS && [\text{split the integral on } \partial f] \\ &= \frac{1}{|f|} \sum_{e \in \mathcal{E}_f} \alpha_{f,e} \int_e \mathbf{u} \cdot \boldsymbol{\tau}_f dL && [\text{use definitions (2.15) and (2.21)}] \\ &= (\operatorname{curl}_h \mathbf{u}_h)_f. \end{aligned}$$

This proves the assertion of the lemma. \square

2.6.2 The kernel of the derived operators

As for the primary operators, also the kernel of the derived operators is similarly characterized. The noteworthy difference is the result of the following lemma, which establishes that the derived gradient operator in this specific DVTC is injective.

Lemma 2.5. *The kernel of the derived operator $\tilde{\nabla}_h$ is the trivial subspace $\{0\}_{\mathcal{P}_h}$.*

Proof. Let p_h be a cell function in \mathcal{P}_h such that $\tilde{\nabla}_h p_h = 0$. From (2.28) it follows that

$$-M_{\mathcal{F}}^{-1} \operatorname{div}_h^T M_{\mathcal{P}} p_h = 0. \quad (2.52)$$

Since $M_{\mathcal{F}}$ is a non-singular inner product matrix, Eq. (2.52) implies that $\operatorname{div}_h^T M_{\mathcal{P}} p_h = 0$, or, equivalently, that

$$M_{\mathcal{P}} p_h \in \ker(\operatorname{div}_h^T).$$

From Lemma 2.1 we know that div_h is a surjective operator, i.e., $\text{img}(\text{div}_h) = \mathcal{P}_h$. Using a standard algebraic relation yields:

$$\ker(\text{div}_h^T) = (\text{img}(\text{div}_h))^\perp = (\mathcal{P}_h)^\perp = \{0\}_{\mathcal{P}_h}.$$

This proves the assertion of the lemma. \square

It is natural to expect that the kernel of a discrete gradient operator contains the constant vectors as is the case of the kernel of the primary operator ∇_h , see Lemma 2.3. Thus, the assertion of Lemma 2.5 may seem strange at a first glance. However, in the construction of the DVTC that we carry out in this chapter we have assumed that the boundary integrals in formulas (2.7)–(2.9) are zero and the result of Lemma 2.5 reflects this fact. Indeed, a comparison between formula (2.7) and (2.27) shows that the operator $\tilde{\nabla}_h$ incorporates also the boundary part in the right hand side of (2.27).

For example, on an orthogonal mesh, it holds that

$$(\tilde{\nabla}_h p_h)_f = \begin{cases} (p_{P_2} - p_{P_1})/d_{12} & \text{if } f = \mathcal{F}_{P_1} \cap \mathcal{F}_{P_2}, \\ -p_{P_1}/d_{1f} & \text{if } f = \mathcal{F}_{P_1} \cap \partial\Omega, \end{cases} \quad (2.53)$$

where d_{12} is the distance between the centroids of P_1 and P_2 , and d_{1f} is the distance between the centroid of P_1 and face f . Now, let $\tilde{\nabla}_h p_h = 0$. From the first relation in (2.53) it follows that all p_P are equal. From the second relation in (2.53) it follows that p_P is zero if a face of ∂P is also a boundary face. Therefore, all the p_P are zero and the kernel of $\tilde{\nabla}_h$ must be the discrete field $p_h = 0$.

Let us now characterize the kernel of the derived curl and divergence operators. More precisely, in the following lemma we prove that $\ker(\widetilde{\text{curl}}_h) = \text{img}(\tilde{\nabla}_h)$ and $\ker(\widetilde{\text{div}}_h) = \text{img}(\widetilde{\text{curl}}_h)$. The two conditions are the mimetic analogs of $\text{curl} \circ \nabla = 0$ and $\text{div} \circ \text{curl} = 0$, respectively.

Lemma 2.6. *Let the domain Ω and its mesh partition Ω_h be simply connected. Then,*

$$\widetilde{\text{curl}}_h \mathbf{v}_h = 0 \quad \text{if and only if} \quad \mathbf{v}_h = \tilde{\nabla}_h p_h \quad (2.54)$$

for some $p_h \in \mathcal{P}_h$ and

$$\widetilde{\text{div}}_h \mathbf{v}_h = 0 \quad \text{if and only if} \quad \mathbf{v}_h = \widetilde{\text{curl}}_h \mathbf{u}_h \quad (2.55)$$

for some $\mathbf{u}_h \in \mathcal{F}_h$.

Proof. By using the matrix definitions of $\tilde{\nabla}_h$, $\widetilde{\text{curl}}_h$, and $\widetilde{\text{div}}_h$ given in (2.28), (2.30), and (2.32), respectively, and the results of Lemma 2.4, a straightforward calculation shows that

$$\widetilde{\text{curl}}_h \tilde{\nabla}_h = -M_{\mathcal{E}}^{-1} \text{curl}_h^T M_{\mathcal{F}} M_{\mathcal{F}}^{-1} \text{div}_h^T M_{\mathcal{D}} = -M_{\mathcal{E}}^{-1} (\text{div}_h \text{curl}_h)^T M_{\mathcal{D}} = 0,$$

and

$$\widetilde{\text{div}}_h \widetilde{\text{curl}}_h = -M_{\mathcal{V}}^{-1} \nabla_h^T M_{\mathcal{E}} M_{\mathcal{E}}^{-1} \text{curl}_h^T M_{\mathcal{F}} = -M_{\mathcal{V}}^{-1} (\text{curl}_h \nabla_h)^T M_{\mathcal{F}} = 0,$$

which proves the “if” part of the Lemma.

To prove the “*only if*” part of assertion (2.54) let us consider a discrete field $\mathbf{v}_h \in \mathcal{F}_h$ such that $\widetilde{\text{curl}}_h \mathbf{v}_h = 0$. We need to find a discrete field $p_h \in \mathcal{P}_h$ such that $\mathbf{v}_h = \nabla_h p_h$. The definition of $\widetilde{\text{curl}}_h$ in (2.30) implies that

$$\widetilde{\text{curl}}_h \mathbf{v}_h = -M_{\mathcal{E}}^{-1} \text{curl}_h^T M_{\mathcal{F}} \mathbf{v}_h = 0.$$

Since $M_{\mathcal{E}}$ is a non-singular inner product matrix, it follows that $\text{curl}_h^T M_{\mathcal{F}} \mathbf{v}_h = 0$, or, equivalently, that

$$M_{\mathcal{F}} \mathbf{v}_h \in \ker(\text{curl}_h^T).$$

Now, we apply the result of Lemma 2.4, see (2.50), and a standard algebraic relation to obtain:

$$\ker(\text{curl}_h^T) = (\text{img}(\text{curl}_h))^\perp = (\ker(\text{div}_h))^\perp = \text{img}(\text{div}_h^T). \quad (2.56)$$

Equation (2.56) implies that there exists a vector $q_h \in \mathcal{P}_h$ such that $M_{\mathcal{F}} \mathbf{v}_h = \text{div}_h^T q_h$. As $M_{\mathcal{P}}$ is also a non-singular matrix, we can introduce the vector $p_h = -M_{\mathcal{P}}^{-1} q_h$, so that $M_{\mathcal{F}} \mathbf{v}_h = -\text{div}_h^T M_{\mathcal{P}} p_h$, and using (2.28) we obtain that

$$\mathbf{v}_h = -M_{\mathcal{F}}^{-1} \text{div}_h^T M_{\mathcal{P}} p_h = \widetilde{\nabla}_h p_h.$$

To prove the “*only if*” part of assertion (2.55), let us consider a discrete field $\mathbf{v}_h \in \mathcal{E}_h$ such that $\widetilde{\text{div}}_h \mathbf{v}_h = 0$. Equation (2.32) implies that

$$\widetilde{\text{div}}_h \mathbf{v}_h = -M_{\mathcal{V}}^{-1} \nabla_h^T M_{\mathcal{E}} \mathbf{v}_h = 0.$$

Since $M_{\mathcal{V}}$ is a non-singular inner product matrix, it follows that $\nabla_h^T M_{\mathcal{E}} \mathbf{v}_h = 0$, or, equivalently, that

$$M_{\mathcal{E}} \mathbf{v}_h \in \ker(\nabla_h^T).$$

Now, we apply the result of Lemma 2.4, see (2.49), and a standard algebraic relation to obtain:

$$\ker(\nabla_h^T) = (\text{img}(\nabla_h))^\perp = (\ker(\text{curl}_h))^\perp = \text{img}(\text{curl}_h^T). \quad (2.57)$$

The definition of $\widetilde{\text{div}}_h$ in (2.57) implies that there exists a vector $\mathbf{w}_h \in \mathcal{F}_h$ such that $M_{\mathcal{E}} \mathbf{v}_h = \text{curl}_h^T \mathbf{w}_h$. As $M_{\mathcal{F}}$ is a non singular matrix, we can introduce the vector $\mathbf{u}_h = M_{\mathcal{F}}^{-1} \mathbf{w}_h$, so that $M_{\mathcal{E}} \mathbf{v}_h = \text{curl}_h^T M_{\mathcal{F}} \mathbf{u}_h$, and using (2.30) we obtain that

$$\mathbf{v}_h = M_{\mathcal{E}}^{-1} \text{curl}_h^T M_{\mathcal{F}} \mathbf{u}_h = \widetilde{\text{curl}}_h \mathbf{u}_h.$$

This proves the assertion of the lemma. \square

2.6.3 The kernel of the second-order mimetic operators

In this section we investigate the properties of the kernels of the combined mimetic operators introduced in Sect. 2.5.

The kernel of the second-order mimetic operator $\text{div}_h \widetilde{\nabla}_h$ is characterized by the following lemma.

Lemma 2.7. *The product $\operatorname{div}_h \widetilde{\nabla}_h$ is a full rank matrix, i.e., $\ker(\operatorname{div}_h \widetilde{\nabla}_h) = \{0\}_{\mathcal{P}_h}$.*

Proof. Let us consider a cell-based discrete field q_h in \mathcal{P}_h such that $\operatorname{div}_h \widetilde{\nabla}_h q_h = 0$. By using the definition of the derived operator $\widetilde{\nabla}_h$ given in (2.27) we obtain

$$0 = \left[\operatorname{div}_h \widetilde{\nabla}_h q_h, q_h \right]_{\mathcal{P}_h} = - \left[\widetilde{\nabla}_h q_h, \widetilde{\nabla}_h q_h \right]_{\mathcal{F}_h},$$

from which it follows that $\widetilde{\nabla}_h q_h = 0$. We apply the result of Lemma 2.5, which implies that $q_h = 0$. \square

The kernel of the second-order mimetic operator $\widetilde{\operatorname{div}}_h \nabla_h$ is characterized by the following lemma.

Lemma 2.8. *Let Ω_h be simply-connected. The kernel of the combined mimetic operator $\widetilde{\operatorname{div}}_h \nabla_h$ is formed by the constant vectors of \mathcal{V}_h .*

Proof. Let us consider a node-based discrete field q_h in \mathcal{V}_h such that $\widetilde{\operatorname{div}}_h \nabla_h q_h = 0$. By using the definition of the derived operator $\widetilde{\operatorname{div}}_h$ given in (2.31) we obtain

$$0 = \left[\widetilde{\operatorname{div}}_h \nabla_h q_h, q_h \right]_{\mathcal{V}_h} = - \left[\nabla_h q_h, \nabla_h q_h \right]_{\mathcal{E}_h},$$

from which it follows that $\nabla_h q_h = 0$. We apply the result of Lemma 2.3, which implies that q_h is a constant vector. \square

The kernels of the operators $\widetilde{\operatorname{curl}}_h \operatorname{curl}_h$ and $\operatorname{curl}_h \widetilde{\operatorname{curl}}_h$ are characterized by the following lemma.

Lemma 2.9. *Let the domain Ω and mesh Ω_h be simply connected. Then,*

$$\widetilde{\operatorname{curl}}_h \operatorname{curl}_h \mathbf{v}_h = 0 \quad \text{if and only if} \quad \mathbf{v}_h = \nabla_h q_h \quad (2.58)$$

for some $q_h \in \mathcal{V}_h$, and

$$\operatorname{curl}_h \widetilde{\operatorname{curl}}_h \mathbf{v}_h = 0 \quad \text{if and only if} \quad \mathbf{v}_h = \widetilde{\nabla}_h q_h \quad (2.59)$$

for some $q_h \in \mathcal{P}_h$.

Proof. The “if” part of (2.58) is a consequence of Lemma 2.4. The “if” part of (2.59) is a consequence of Lemma 2.6.

To prove the “only if” part of assertion (2.58), let us consider a discrete field $\mathbf{v}_h \in \mathcal{E}_h$ such that $\widetilde{\operatorname{curl}}_h \operatorname{curl}_h \mathbf{v}_h = 0$. By using the definition of the derived operator $\widetilde{\operatorname{curl}}_h$ given in (2.29) we obtain

$$0 = \left[\mathbf{v}_h, \widetilde{\operatorname{curl}}_h \operatorname{curl}_h \mathbf{v}_h \right]_{\mathcal{E}_h} = \left[\operatorname{curl}_h \mathbf{v}_h, \operatorname{curl}_h \mathbf{v}_h \right]_{\mathcal{F}_h},$$

from which it follows that $\operatorname{curl}_h \mathbf{v}_h = 0$. Lemma 2.4, see (2.49), implies the existence of a field $q_h \in \mathcal{V}_h$ such that $\mathbf{v}_h = \nabla_h q_h$.

To prove the “only if” part of assertion (2.59), let us consider a discrete field $\mathbf{v}_h \in \mathcal{F}_h$ such that $\text{curl}_h \widetilde{\text{curl}}_h \mathbf{v}_h = 0$. By using again (2.29) we obtain

$$0 = [\mathbf{v}_h, \text{curl}_h \widetilde{\text{curl}}_h \mathbf{v}_h]_{\mathcal{F}_h} = [\widetilde{\text{curl}}_h \mathbf{v}_h, \widetilde{\text{curl}}_h \mathbf{v}_h]_{\mathcal{E}_h},$$

from which it follows that $\widetilde{\text{curl}}_h \mathbf{v}_h = 0$. Lemma 2.6, see (2.54), implies the existence of a field $q_h \in \mathcal{P}_h$ such that $\mathbf{v}_h = \widetilde{\nabla}_h q_h$. This proves the assertion of the lemma. \square

The two mimetic operators $\widetilde{\text{curl}}_h \text{curl}_h$ and $\text{curl}_h \widetilde{\text{curl}}_h$ are also in the definition of the edge-based and face-based vector Laplace operators. The kernel of these latter is characterized by the following lemma.

Lemma 2.10. *The null space of the vector Laplace operators $\Delta_{\mathcal{E}_h}$ and $\Delta_{\mathcal{F}_h}$ are the trivial subspaces $\{0\}_{\mathcal{E}_h}$ and $\{0\}_{\mathcal{F}_h}$, respectively.*

Proof. (i) To prove that $\ker(\Delta_{\mathcal{E}_h}) = \{0\}_{\mathcal{E}_h}$, we consider a discrete field \mathbf{v}_h in \mathcal{E}_h such that $\Delta_{\mathcal{E}_h} \mathbf{v}_h = 0$. It follows that:

$$\begin{aligned} 0 &= [\mathbf{v}_h, \Delta_{\mathcal{E}_h} \mathbf{v}_h]_{\mathcal{E}_h} && \text{(use the definition of } \Delta_{\mathcal{E}_h} \text{)} \\ &= [\mathbf{v}_h, \nabla_h \widetilde{\text{div}}_h \mathbf{v}_h]_{\mathcal{E}_h} - [\mathbf{v}_h, \widetilde{\text{curl}}_h \text{curl}_h \mathbf{v}_h]_{\mathcal{E}_h} && \text{(use (2.31) and (2.29))} \\ &= -[\widetilde{\text{div}}_h \mathbf{v}_h, \widetilde{\text{div}}_h \mathbf{v}_h]_{\mathcal{P}_h} - [\text{curl}_h \mathbf{v}_h, \text{curl}_h \mathbf{v}_h]_{\mathcal{F}_h}, \end{aligned}$$

from which we have

$$\widetilde{\text{div}}_h \mathbf{v}_h = 0 \quad \text{and} \quad \text{curl}_h \mathbf{v}_h = 0. \quad (2.60)$$

These two conditions imply that $\mathbf{v}_h = 0$. In fact, by using the result of Lemma 2.6, from the first equation in (2.60) it follows that there exists a discrete field $\mathbf{u}_h \in \mathcal{F}_h$ such that $\mathbf{v}_h = \text{curl}_h \mathbf{u}_h$. The second equation in (2.60) implies that $\text{curl}_h \widetilde{\text{curl}}_h \mathbf{u}_h = 0$, while Lemma 2.9 (cf. (2.59)) implies that there exists a discrete field $q_h \in \mathcal{P}_h$ such that $\mathbf{u}_h = \widetilde{\nabla}_h q_h$. We substitute back these expressions and apply again Lemma 2.6 to obtain that

$$\mathbf{v}_h = \widetilde{\text{curl}}_h \mathbf{u}_h = \widetilde{\text{curl}}_h \widetilde{\nabla}_h q_h = 0$$

regardless of q_h .

(ii) To prove that $\ker(\Delta_{\mathcal{F}_h}) = \{0\}_{\mathcal{F}_h}$, let us consider a face vector \mathbf{v}_h in \mathcal{F}_h such that $\Delta_{\mathcal{F}_h} \mathbf{v}_h = 0$. It follows that:

$$\begin{aligned} 0 &= [\mathbf{v}_h, \Delta_{\mathcal{F}_h} \mathbf{v}_h]_{\mathcal{F}_h} && \text{(use the definition of } \Delta_{\mathcal{F}_h} \text{)} \\ &= [\mathbf{v}_h, \widetilde{\nabla}_h \text{div}_h \mathbf{v}_h]_{\mathcal{F}_h} - [\mathbf{v}_h, \text{curl}_h \widetilde{\text{curl}}_h \mathbf{v}_h]_{\mathcal{F}_h} && \text{(use (2.27) and (2.29))} \\ &= -[\text{div}_h \mathbf{v}_h, \text{div}_h \mathbf{v}_h]_{\mathcal{P}_h} - [\widetilde{\text{curl}}_h \mathbf{v}_h, \widetilde{\text{curl}}_h \mathbf{v}_h]_{\mathcal{F}_h}, \end{aligned}$$

from which we have:

$$\text{div}_h \mathbf{v}_h = 0 \quad \text{and} \quad \widetilde{\text{curl}}_h \mathbf{v}_h = 0. \quad (2.61)$$

These two conditions imply that $\mathbf{v}_h = 0$. In fact, by using the result of Lemma 2.4, from the first equation in (2.61) it follows that there exists a discrete field $\mathbf{u}_h \in \mathcal{E}_h$ such that $\mathbf{v}_h = \text{curl}_h \mathbf{u}_h$. The second equation in (2.61) implies that $\widetilde{\text{curl}}_h \text{curl}_h \mathbf{u}_h = 0$, while Lemma 2.9 (cf. (2.58)) implies that there exists a discrete field $q_h \in \mathcal{V}_h$ such that $\mathbf{u}_h = \nabla_h q_h$. We substitute back these expressions and apply again Lemma 2.4 to obtain

$$\mathbf{v}_h = \text{curl}_h \mathbf{u}_h = \text{curl}_h \nabla_h q_h = 0$$

regardless of q_h . This proves the assertion of the lemma. \square

2.7 Discrete Helmholtz decomposition theorems

We present two discrete versions of the Helmholtz decomposition theorem.

Theorem 2.1. *Let domain Ω and mesh Ω_h be simply-connected. Then, for any discrete field \mathbf{v}_h in \mathcal{F}_h there exists a unique q_h in \mathcal{P}_h and a unique \mathbf{u}_h in \mathcal{E}_h with $\widetilde{\text{div}}_h \mathbf{u}_h = 0$ such that*

$$\mathbf{v}_h = \widetilde{\nabla}_h q_h + \text{curl}_h \mathbf{u}_h. \quad (2.62)$$

Proof. Let us first show that (2.62) is an orthogonal decomposition in \mathcal{F}_h . In fact, using the definition of the derived operator $\widetilde{\nabla}_h$ and the result of Lemma 2.4, we obtain

$$\left[\text{curl}_h \mathbf{u}_h, \widetilde{\nabla}_h q_h \right]_{\mathcal{F}_h} = - [\text{div}_h \text{curl}_h \mathbf{u}_h, q_h]_{\mathcal{P}_h} = 0.$$

We apply the primary mimetic operator div_h to both sides of (2.62) and obtain the relation:

$$\text{div}_h \mathbf{v}_h = \text{div}_h \widetilde{\nabla}_h q_h. \quad (2.63)$$

The combined mimetic operator $\text{div}_h \widetilde{\nabla}_h$ is a full rank operator, and, thus, it is non-singular, cf. Lemma 2.7. Therefore, a solution $q_h \in \mathcal{P}_h$ to (2.63) exists and is unique for any discrete field \mathbf{v}_h in \mathcal{F}_h .

From (2.63) we immediately have that

$$\text{div}_h (\mathbf{v}_h - \widetilde{\nabla}_h q_h) = 0$$

and thus $(\mathbf{v}_h - \widetilde{\nabla}_h q_h)$ is in the kernel of the operator div_h . Therefore, by applying (2.50), we immediately have the existence of $\mathbf{u}_h \in \mathcal{E}_h$ such that (2.62) is satisfied.

The uniqueness of \mathbf{u}_h follows under the assumption that $\widetilde{\text{div}}_h \mathbf{u}_h = 0$. In fact, let \mathbf{u}'_h be another edge field such that $\text{curl}_h \mathbf{u}'_h = \text{curl}_h \mathbf{u}_h$ and $\widetilde{\text{div}}_h \mathbf{u}'_h = 0$. Clearly, $\text{curl}_h (\mathbf{u}_h - \mathbf{u}'_h) = 0$, and by applying Lemma 2.4 (cf. Eq. (2.49)), we can prove the existence of a discrete field $q_h \in \mathcal{V}_h$ such that $\mathbf{u}_h - \mathbf{u}'_h = \nabla_h q_h$. Now, the following development

$$[\nabla_h q_h, \nabla_h q_h]_{\mathcal{E}_h} = [\mathbf{u}_h - \mathbf{u}'_h, \nabla_h q_h]_{\mathcal{E}_h} = [\widetilde{\text{div}}_h (\mathbf{u}_h - \mathbf{u}'_h), q_h]_{\mathcal{V}_h} = 0,$$

implies that $\nabla_h q_h = 0$, or, equivalently, that $\mathbf{u}_h = \mathbf{u}'_h$. \square

Corollary 2.1. *The four discrete spaces \mathcal{V}_h , \mathcal{E}_h , \mathcal{F}_h and \mathcal{P}_h are such*

$$\dim(\mathcal{F}_h) = \dim(\mathcal{P}_h) + \dim(\mathcal{E}_h) - \dim(\mathcal{V}_h) + 1. \quad (2.64)$$

Proof. The orthogonality of the decomposition requires that the dimension of \mathcal{F}_h must be equal to the dimension of \mathcal{P}_h plus the dimension of \mathcal{E}_h minus the dimensions of the kernels of $\widetilde{\nabla}_h$ and curl_h . The assertion of the corollary follows because the kernel of $\widetilde{\nabla}_h$ has dimension equal to zero and the kernel of curl_h is the image of ∇_h . \square

For a single polyhedron we can substitute $\dim(\mathcal{P}_h) = 1$ in the corollary's assertion and we obtain the famous *Euler's polyhedron formula*.

The second discrete Helmholtz decomposition theorem holds in space \mathcal{E}_h .

Theorem 2.2. *Let domain Ω and mesh Ω_h be simply-connected. Then, for any $\mathbf{v}_h \in \mathcal{E}_h$ there exist a discrete field $q_h \in \mathcal{V}_h$, which is unique up to an additive constant field, and a unique discrete field $\mathbf{u}_h \in \mathcal{F}_h$ with $\text{div}_h \mathbf{u}_h = 0$ such that*

$$\mathbf{v}_h = \nabla_h q_h + \widetilde{\text{curl}}_h \mathbf{u}_h. \quad (2.65)$$

Proof. Let us first show that (2.65) is an orthogonal decomposition. In fact, we use the definition of the derived operator $\widetilde{\text{curl}}_h$ and the result of Lemma 2.6 (see Eq. (2.55)) and we obtain

$$[\widetilde{\text{curl}}_h \mathbf{u}_h, \nabla_h q_h]_{\mathcal{E}_h} = - [\widetilde{\text{div}}_h \widetilde{\text{curl}}_h \mathbf{u}_h, q_h]_{\mathcal{V}_h} = 0.$$

We apply the derived mimetic operator $\widetilde{\text{div}}_h$ to both sides of (2.65) and obtain the following relation:

$$\widetilde{\text{div}}_h \mathbf{v}_h = \widetilde{\text{div}}_h \nabla_h q_h. \quad (2.66)$$

The kernel of $\widetilde{\text{div}}_h \nabla_h$ consists of the constant vectors of \mathcal{V}_h , cf. Lemma 2.8. Therefore, for any discrete field $\mathbf{v}_h \in \mathcal{E}_h$, there exists a solution $q_h \in \mathcal{V}_h$ to (2.66). Moreover, this solution is unique up to an additive constant.

Due to Eq. (2.66) it holds that $(\mathbf{v}_h - \nabla_h q_h)$ is in the kernel of the operator $\widetilde{\text{div}}_h$. Therefore (2.65) simply follows by applying (2.55).

The uniqueness of \mathbf{u}_h follows under the assumption that $\text{div}_h \mathbf{u}_h = 0$. In fact, let \mathbf{u}'_h be another edge field such that $\widetilde{\text{curl}}_h \mathbf{u}'_h = \widetilde{\text{curl}}_h \mathbf{u}_h$ and $\text{div}_h \mathbf{u}'_h = 0$. Clearly, $\widetilde{\text{curl}}_h (\mathbf{u}_h - \mathbf{u}'_h) = 0$, and by applying Lemma 2.6 (cf. Eq. (2.54)), we obtain that $\mathbf{u}_h - \mathbf{u}'_h = \widetilde{\nabla}_h q_h$ for some discrete field $q_h \in \mathcal{P}_h$. Now, the following development is true:

$$[\widetilde{\nabla}_h q_h, \widetilde{\nabla}_h q_h]_{\mathcal{E}_h} = [\mathbf{u}_h - \mathbf{u}'_h, \widetilde{\nabla}_h q_h]_{\mathcal{E}_h} = [\text{div}_h (\mathbf{u}_h - \mathbf{u}'_h), q_h]_{\mathcal{P}_h} = 0,$$

which implies that $\widetilde{\nabla}_h q_h = 0$, or, equivalently, that $\mathbf{u}_h = \mathbf{u}'_h$. \square

Remark 2.6. Using the same argument used for the proof of Corollary 2.1 we obtain again (2.64).

Mimetic inner products and reconstruction operators

*“Whatever good things we build
end up building us.”*
(Jim Rohn)

The first goal of this chapter is to derive explicit formulas for inner product matrices $M_{\mathcal{P}}$, $M_{\mathcal{F}}$, $M_{\mathcal{E}}$, and $M_{\mathcal{D}}$ that were formally introduced in Chap. 2. The second goal is to create foundations for the theoretical analysis of mimetic discretizations.

A reconstruction operator is an important concept in the theoretical analysis of mimetic schemes. It maps a mesh function into a continuum function and allows to describe mimetic discretizations using a finite element language. Such an interpretation exists for a large set of mimetic schemes (but not all of them) which makes it a valuable theoretical tool.

3.1 Mimetic inner product

Let \mathcal{S}_h denote one of the spaces introduced in Chap. 2, e.g., \mathcal{V}_h , \mathcal{E}_h , \mathcal{F}_h , or \mathcal{D}_h , and $\mathcal{S}_{h,P}$ be its restriction to cell P . We consider a projection operator

$$\Pi_P^{\mathcal{S}} : X|_P \rightarrow \mathcal{S}_{h,P}.$$

Various projection operators were introduced in Sect. 2.2.

Let \mathcal{T}_P be the space of trial functions. To build the low-order mimetic schemes, this space is defined as the space of constant scalar or vector functions. The trial space is generalized in Chap. 4 to allow building of higher-order mimetic schemes. Let $S_{h,P}$ be a subspace of $X|_P$ with the following properties.

- (B1) The projection operator $\Pi_P^{\mathcal{S}}$ is surjective from $S_{h,P}$ to $\mathcal{S}_{h,P}$.
- (B2) The space $S_{h,P}$ contains the trial space \mathcal{T}_P .
- (B3) Let $q \in \mathcal{T}_P$ and $v \in S_{h,P}$. Then, the integral $\int_P qv dV$ can be calculated exactly using the degrees of freedom, i.e the components of vector $\Pi_P^{\mathcal{S}}(v)$.

The assumption (B1) states that the space $S_{h,P}$ is rich enough. In all mimetic schemes discussed later in this book, it is defined originally as an infinite dimensional space. The assumption (B2) is connected with the accuracy of a mimetic scheme that

we want to design. In this chapter we consider the low-order schemes; hence, the trial space \mathcal{T}_P contains only constant functions. The assumption **(B3)** is problem-dependent; a more general framework will be introduced in Chap. 4. In general, the space $S_{h,P}$ is selected such that assumption **(B3)** can be easily shown.

Each mimetic inner product is assembled from local inner products:

$$[u_h, v_h]_{\mathcal{S}_h} = \sum_{P \in \Omega_h} [u_{h,P}, v_{h,P}]_{\mathcal{S}_{h,P}} \quad \forall u_h, v_h \in \mathcal{S}_h,$$

where $u_{h,P}$ and $v_{h,P}$ are the restrictions of mesh functions u_h and v_h to element P , respectively.

Definition 3.1 (Consistency condition). The inner product is said to satisfy the consistency condition if

$$[\Pi_P^{\mathcal{S}}(q), \Pi_P^{\mathcal{S}}(v)]_{\mathcal{S}_{h,P}} = \int_P q v dV \quad \forall q \in \mathcal{T}_P, \forall v \in S_{h,P}. \quad (3.1)$$

For a polyhedral cell, the space of all vectors $\Pi_P^{\mathcal{S}}(q)$ can be smaller than the space $\mathcal{S}_{h,P}$. In such a case, the consistency condition does not define the inner product uniquely. To avoid numerical instabilities, we need the *stability condition*.

Definition 3.2 (Stability condition). The inner product is said to satisfy the stability condition if

$$C_* |P| \|v_{h,P}\|^2 \leq [v_{h,P}, v_{h,P}]_{\mathcal{S}_{h,P}} \leq C^* |P| \|v_{h,P}\|^2 \quad \forall v_{h,P} \in \mathcal{S}_{h,P} \quad (3.2)$$

with positive constants C_* and C^* independent of P and $v_{h,P}$.

Remark 3.1. In general, we do not need the infinite dimensional space $S_{h,P}$ to characterize the mimetic inner product in the finite dimensional space $\mathcal{S}_{h,P}$. It is possible to build the mimetic method using a finite dimensional space $S_{h,P}$ isomorphic to $\mathcal{S}_{h,P}$. Hence, in addition to the above conditions, we may require

$$\dim(S_{h,P}) = \dim(\mathcal{S}_{h,P}). \quad (3.3)$$

In such case the projection operator will clearly be an invertible mapping from $S_{h,P}$ into $\mathcal{S}_{h,P}$ and thus the two spaces will be isomorphic. Hereafter, we assume that (3.3) holds true. Finally, note that a finite dimensional space $S_{h,P}$ is not unique. \square

Let us consider a reconstruction operator

$$R_P^{\mathcal{S}} : \mathcal{S}_{h,P} \rightarrow S_{h,P}$$

that is inverse to the projection operator. Due to assumptions **(B1)**–**(B2)** and (3.3), each function in $S_{h,P}$ is the reconstruction of a (unique) discrete field in $\mathcal{S}_{h,P}$, see also the important Remark 3.2.

If the reconstruction operator would be easy to build, the local inner product could be defined explicitly:

$$[u_{h,P}, v_{h,P}]_{\mathcal{S}_{h,P}} = \int_P R_P^{\mathcal{S}}(u_{h,P}) R_P^{\mathcal{S}}(v_{h,P}) dV. \quad (3.4)$$

Unfortunately, this is possible only for cells with simple geometry (e.g. tetrahedron or hexahedron). We will show, that for an arbitrary-shaped cell P , the reconstruction operator can be defined through the solution of a local PDE problem. In this case, its calculation becomes a non-trivial task. For this reason, the MFD method never calculates the reconstruction operator explicitly. Instead, it is defined implicitly, not always uniquely, via properties of space $S_{h,P}$.

In subsequent sections, we study various reconstruction operators. Then, we use their properties to show that the computation of the right-hand side in (3.1) does not depend on the behavior of the reconstructed field $R_P^{\mathcal{S}}(v_{h,P})$ inside cell P . We conclude this introductory part with an important remark and a simple example that serves the purpose to present the idea behind the construction.

Remark 3.2. Selection of a space $S_{h,P}$ that satisfies **(B1)**–**(B3)** and (3.3) yields immediately a definition of the reconstruction operator $R_P^{\mathcal{S}}$ as the inverse of $\Pi_P^{\mathcal{S}}$ restricted to $S_{h,P}$. Viceversa, if one builds first a reconstruction operator $R_P^{\mathcal{S}}$, then a space $S_{h,P}$ will be automatically defined as the image of $R_P^{\mathcal{S}}$. Both approaches are equivalent. Clearly the reconstruction operator needs to satisfy certain properties to ensure that space $S_{h,P}$ can be useful for the derivation of the method. In the main part of the present chapter we will follow the second approach and focus our attention on reconstruction operators and obtain the space $S_{h,P}$ as an implicit consequence. In Chap. 4, we will employ the first approach and focus on the space $S_{h,P}$, thus avoiding the need to build the related reconstruction operator. \square

Example 3.1. Let us consider the case $d = 2$ and the mimetic space \mathcal{F}_h associated to the edges of a polygonal mesh. We want to build a local inner product

$$[\cdot, \cdot]_{\mathcal{F}_{h,P}} : \mathcal{F}_{h,P} \times \mathcal{F}_{h,P} \rightarrow \mathbb{R}$$

that mimics the standard $L^2(P)$ scalar product and satisfies the consistency condition (3.1). For the space of trial functions \mathcal{T}_P we choose the space of constant vectors, $\mathcal{T}_P = [\mathbb{P}_0(P)]^2$. Then,

$$[\Pi_P^{\mathcal{F}}(\mathbf{c}), \mathbf{v}_{h,P}]_{\mathcal{F}_{h,P}} = \int_P \mathbf{c} \cdot \mathbf{v} dV \quad \forall \mathbf{v} \in S_{h,P}, \forall \mathbf{c} \in \mathcal{T}_P, \quad (3.5)$$

where $\mathbf{v}_{h,P} = \Pi_P^{\mathcal{F}}(\mathbf{v})$. We start by defining a finite dimensional space $S_{h,P}$ of vector functions living on P that satisfies **(B1)**–**(B3)** and (3.3). We require that space $S_{h,P}$ satisfies two inclusions:

$$[\mathbb{P}_0(P)]^2 \subseteq S_{h,P} \subseteq \{ \mathbf{w} \in H_{\text{div}}(P) : \mathbf{w}|_f \cdot \mathbf{n}_f \in \mathbb{P}_0(f) \forall f \in \partial P, \text{div} \mathbf{w} \in \mathbb{P}_0(P) \}. \quad (3.6)$$

The first inclusion implies that the space $S_{h,P}$ contains the constant vector functions, that is **(B2)**. The second inclusion will be fundamental for property **(B3)**.

There exists an infinite number of choices for $S_{h,P}$; for instance, one may build $S_{h,P}$ by solving a set of diffusion problems on P associated with basis vectors in $\mathcal{F}_{h,P}$. Since, as it will be shown below, this choice does not change our conclusions, we do not need to elaborate on it. Thus, let the reconstruction operator be any stable operator

$$R_P^{\mathcal{F}} : \mathcal{F}_{h,P} \rightarrow S_{h,P}$$

that is inverse to the projection operator (and thus preserves the degrees of freedom). As already noted in Remark 3.2, defining $S_{h,P}$ yields a definition of $R_P^{\mathcal{F}}$ and, viceversa, defining $R_P^{\mathcal{F}}$ gives a definition of $S_{h,P}$. In the present example, we will focus on the first approach, i.e. on the definition of $S_{h,P}$. It will be convenient to characterize the space of test functions as the space of gradients of linear functions:

$$\mathcal{T}_P = \left\{ \nabla q : q \in \mathbb{P}_1(P), \int_P q dV = 0 \right\}.$$

The consistency condition (3.5) states that the inner product is exact when one of its arguments is a constant vector field and the other is a function from $S_{h,P}$. Using the definition of $S_{h,P}$, we show that the right hand side in (3.5) is computable and does not depend on the particular choice of $R_P^{\mathcal{F}}$. Indeed, replacing $\mathbf{c} = \nabla q$, where $\int_P q dV = 0$, integrating by parts and using (3.6), more precisely that $\operatorname{div}(R_P^{\mathcal{F}}(\mathbf{v}_{h,P})) \in \mathbb{P}_0(P)$, we obtain

$$\begin{aligned} \int_P \nabla q \cdot R_P^{\mathcal{F}}(\mathbf{v}_{h,P}) dV &= - \int_P q \operatorname{div}(R_P^{\mathcal{F}}(\mathbf{v}_{h,P})) dV + \sum_{f \in \partial P} \int_f R_P^{\mathcal{F}}(\mathbf{v}_{h,P}) \cdot \mathbf{n}_{P,f} q dS \\ &= \sum_{f \in \partial P} \int_f R_P^{\mathcal{F}}(\mathbf{v}_{h,P}) \cdot \mathbf{n}_{P,f} q dS. \end{aligned}$$

Note that the functions in $S_{h,P}$ have constant normal component on each face f . Using definition (2.16) and recalling that $\Pi_P^{\mathcal{F}} \circ R_P^{\mathcal{F}}$ is the identity operator, we obtain

$$R_P^{\mathcal{F}}(\mathbf{v}_{h,P})|_f \cdot \mathbf{n}_{P,f} = \frac{1}{|f|} \int_f R_P^{\mathcal{F}}(\mathbf{v}_{h,P}) \cdot \mathbf{n}_{P,f} dS = (\Pi_P^{\mathcal{F}} R_P^{\mathcal{F}}(\mathbf{v}_{h,P}))_f = (\mathbf{v}_{h,P})_f = v_f.$$

Inserting the last two formulas in (3.5) gives a new form of the consistency condition:

$$[\Pi_P^{\mathcal{F}}(\nabla q), \mathbf{v}_{h,P}]_{\mathcal{F}_{h,P}} = \sum_{f \in \partial P} v_f \int_f q dS \quad \forall \mathbf{v}_{h,P} \in \mathcal{F}_{h,P}, \forall q \in \mathbb{P}_1(P)/\mathbb{R}. \quad (3.7)$$

The above condition does not depend on the choice of the reconstruction operator $R_P^{\mathcal{F}}$; hence, it should not be built in practice. \square

The above example will be continued in Sect. 3.4, where the consistency condition (3.7) will be written explicitly in a matrix-vector form. The reader can safely skip the intermediate theoretical sections.

3.2 Properties of the reconstruction operators

Let us list the formal properties that the reconstruction operators must satisfy for the spaces $\mathcal{V}_h, \mathcal{E}_h, \mathcal{F}_h$, and \mathcal{P}_h . The existence and application of the reconstructed operators to building the mimetic inner product will be described in the next sections. By building a (local) reconstruction operator, from $\mathcal{S}_{h,P}$ into a finite dimensional functional space living on P , that satisfies the five properties below, we guarantee that the ensuing image space $\mathcal{S}_{h,P}$ satisfies **(B1)**–**(B3)**. Clearly, such a reconstruction operator is not always unique.

We will use symbol $R_\sigma^\mathcal{J}$ to denote the reconstruction operator in space \mathcal{S}_h of mesh functions restricted to the geometric object σ that can be cell P , face f , edge e , or vertex v . The set of reconstruction operators $\{R_\sigma^\mathcal{J}\}$ is defined for all meaningful combinations of \mathcal{S}_h and σ .

The reconstruction operator $R_\sigma^\mathcal{J}$ is required to satisfy the five formal properties labeled as **(R1)**–**(R5)**. These properties involve the projection operators $\Pi_\sigma^\mathcal{J}$, the differentiation operators ∇ , curl, div and their discrete counterpart ∇_h , curl_h , div_h . For some choices of \mathcal{S}_h and σ , the five properties do not determine a unique operator $R_\sigma^\mathcal{J}$, and we obtain a family of reconstruction operators. A reconstruction operator $R_\sigma^\mathcal{J}$ is called *admissible* if it satisfies the five properties.

We point out that the commuting property **(R3)** and the locality property **(R5)** lead to the inter-dependence between the reconstruction operators. For this reason, the derivation of the reconstruction operators must be done in a precise order. We denote a constant scalar function by c , a constant vector function by \mathbf{c} , the generic identity operator by l , a three-dimensional point by \mathbf{x} , a local two-dimensional point on face f by $\xi \in f$, and a local one-dimensional point on edge e by $\xi \in e$.

(R1) Right inverse property. Each reconstruction operator is a right inverse of the corresponding projection operator:

- on P : $\Pi_P^\mathcal{Y} \circ R_P^\mathcal{Y} = l$, $\Pi_P^\mathcal{E} \circ R_P^\mathcal{E} = l$, $\Pi_P^\mathcal{F} \circ R_P^\mathcal{F} = l$, $\Pi_P^\mathcal{P} \circ R_P^\mathcal{P} = l$;
- on f : $\Pi_f^\mathcal{Y} \circ R_f^\mathcal{Y} = l$, $\Pi_f^\mathcal{E} \circ R_f^\mathcal{E} = l$, $\Pi_f^\mathcal{F} \circ R_f^\mathcal{F} = l$;
- on e : $\Pi_e^\mathcal{Y} \circ R_e^\mathcal{Y} = l$, $\Pi_e^\mathcal{E} \circ R_e^\mathcal{E} = l$;
- on v : $\Pi_v^\mathcal{Y} \circ R_v^\mathcal{Y} = l$.

The last case is trivial and we consider it only for the sake of completeness.

(R2) Accuracy property. Each reconstruction operator is exact on constant functions:

- on P : $R_P^\mathcal{Y} \circ \Pi_P^\mathcal{Y}(c) = c$, $R_P^\mathcal{E} \circ \Pi_P^\mathcal{E}(\mathbf{c}) = \mathbf{c}$, $R_P^\mathcal{F} \circ \Pi_P^\mathcal{F}(\mathbf{c}) = \mathbf{c}$, $R_P^\mathcal{P} \circ \Pi_P^\mathcal{P}(c) = c$;
- on f : $R_f^\mathcal{Y} \circ \Pi_f^\mathcal{Y}(c) = c$, $R_f^\mathcal{E} \circ \Pi_f^\mathcal{E}(\mathbf{c}) = \mathbf{c}$, $R_f^\mathcal{F} \circ \Pi_f^\mathcal{F}(\mathbf{c}) = \mathbf{c}$;
- on e : $R_e^\mathcal{Y} \circ \Pi_e^\mathcal{Y}(c) = c$, $R_e^\mathcal{E} \circ \Pi_e^\mathcal{E}(\mathbf{c}) = \mathbf{c}$;
- on v : $R_v^\mathcal{Y} \circ \Pi_v^\mathcal{Y}(c) = c$.

The last case is again trivial.

(R3) Commuting property. The reconstruction operators commute with the continuum and discrete differentiation operators:

- on P: $R_P^\mathcal{E} \circ \nabla_h = \nabla \circ R_P^\mathcal{V}$, $R_P^\mathcal{F} \circ \text{curl}_h = \text{curl} \circ R_P^\mathcal{E}$, $R_P^\mathcal{D} \circ \text{div}_h = \text{div} \circ R_P^\mathcal{F}$;
- on f: $R_f^\mathcal{E} \circ \nabla_h = \nabla \circ R_f^\mathcal{V}$, $R_f^\mathcal{F} \circ \text{curl}_h = \text{curl} \circ R_f^\mathcal{E}$;
- on e: $R_e^\mathcal{E} \circ \nabla_h = \nabla \circ R_e^\mathcal{V}$.

In the second case, we consider the two-dimensional curl operator $\text{curl } \boldsymbol{\varphi} = \frac{\partial \phi_1}{\partial \xi_1} - \frac{\partial \phi_2}{\partial \xi_2}$ where $\boldsymbol{\varphi} = (\phi_1, \phi_2)$ is a two-dimensional vector field. In the third case, ∇ denotes the derivative $\frac{\partial}{\partial \xi}$ with respect to the local coordinate ξ defined along edge e.

(R4) Orthogonality property. The reconstructed functions are orthogonal to a special subspace of linear polynomials with zero average. Let \mathbf{x}_P be the barycenter of P, $\boldsymbol{\xi}_f$ be the barycenter of f, and ξ_e be the mid-point of e. Then,

- on P:

$$\int_P R_P^\mathcal{E}(\boldsymbol{\varphi}) \cdot \mathbf{p}^1 dV = 0 \quad \forall \boldsymbol{\varphi} \in \mathcal{E}_{h,P}, \forall \mathbf{p}^1 \in \mathcal{O}_P^\mathcal{E} \equiv c(\mathbf{x} - \mathbf{x}_P), \forall c \in \mathbb{R};$$

$$\int_P R_P^\mathcal{F}(\boldsymbol{\varphi}) \cdot \mathbf{p}^1 dV = 0 \quad \forall \boldsymbol{\varphi} \in \mathcal{F}_{h,P}, \forall \mathbf{p}^1 \in \mathcal{O}_P^\mathcal{F} \equiv \mathbf{c} \times (\mathbf{x} - \mathbf{x}_P), \forall \mathbf{c} \in \mathbb{R}^3};$$

$$\int_P R_P^\mathcal{D}(\boldsymbol{\varphi}) p^1 dV = 0 \quad \forall \boldsymbol{\varphi} \in \mathcal{D}_{h,P}, \forall p^1 \in \mathcal{O}_P^\mathcal{D} \equiv \mathbf{c} \cdot (\mathbf{x} - \mathbf{x}_P), \forall \mathbf{c} \in \mathbb{R}^3};$$

- on f:

$$\int_f R_f^\mathcal{E}(\boldsymbol{\varphi}) \cdot \mathbf{p}^1 dS = 0 \quad \forall \boldsymbol{\varphi} \in \mathcal{E}_{h,f}, \forall \mathbf{p}^1 \in \mathcal{O}_f^\mathcal{E} \equiv c(\boldsymbol{\xi} - \boldsymbol{\xi}_f), \forall c \in \mathbb{R};$$

$$\int_f R_f^\mathcal{F}(\boldsymbol{\varphi}) \cdot p^1 dS = 0 \quad \forall \boldsymbol{\varphi} \in \mathcal{F}_{h,f}, \forall p^1 \in \mathcal{O}_f^\mathcal{F} \equiv \mathbf{c} \cdot (\boldsymbol{\xi} - \boldsymbol{\xi}_f), \forall \mathbf{c} \in \mathbb{R}^2};$$

- on e:

$$\int_e R_e^\mathcal{E}(\boldsymbol{\varphi}) \cdot p^1 dL = 0 \quad \forall \boldsymbol{\varphi} \in \mathcal{E}_{h,e}, \forall p^1 \in \mathcal{O}_e^\mathcal{E} \equiv c(\xi - \xi_e), \forall c \in \mathbb{R}.$$

For $R_P^\mathcal{D}$, $R_f^\mathcal{F}$ and $R_e^\mathcal{E}$ the orthogonality property is trivially satisfied as the reconstructed function is a constant. Nonetheless, for $R_f^\mathcal{E}$, $R_P^\mathcal{E}$ and $R_P^\mathcal{F}$ ensuring this property requires a careful design. These issues are discussed in Sect. 3.3.

(R5) Data locality property. The trace of the reconstructed function on a boundary face f of a cell P or on the boundary edge e of a face f only depends on the local degrees of freedom associated with f or e:

- on P, for every $f \in \partial P$:

$$R_P^{\mathcal{V}}(\varphi)|_f = R_f^{\mathcal{V}}(\varphi|_f) \quad \forall \varphi \in \mathcal{V}_{h,P} \text{ and } \varphi|_f \in \mathcal{V}_{h,f},$$

$$R_P^{\mathcal{E}}(\varphi)|_f = R_f^{\mathcal{E}}(\varphi|_f) \quad \forall \varphi \in \mathcal{E}_{h,P} \text{ and } \varphi|_f \in \mathcal{E}_{h,f},$$

$$R_P^{\mathcal{F}}(\varphi) \cdot \mathbf{n}_f = R_f^{\mathcal{F}}(\varphi|_f) = \varphi_f \quad \forall \varphi \in \mathcal{F}_{h,P} \text{ and } \varphi|_f \in \mathcal{F}_{h,f}.$$

- on f, for every $e \in \partial f$:

$$R_f^{\mathcal{V}}(\varphi)|_e = R_e^{\mathcal{V}}(\varphi|_e) \quad \forall \varphi \in \mathcal{V}_{h,f} \text{ and } \varphi|_e \in \mathcal{V}_{h,e},$$

$$R_f^{\mathcal{E}}(\varphi)|_e \cdot \boldsymbol{\tau}_e = R_e^{\mathcal{E}}(\varphi|_e) = \varphi_e \quad \forall \varphi \in \mathcal{E}_{h,f} \text{ and } \varphi|_e \in \mathcal{E}_{h,e}.$$

This property expresses the local dependence of the reconstruction operators and guarantees continuity (in a weak or strong sense) of the reconstructed functions in neighboring cells. For example, consider the scalar function $R_P^{\mathcal{V}}(\varphi)$ defined on cell P that is reconstructed from the vertex-based mesh function $\varphi \in \mathcal{V}_{h,P}$. The restriction of $R_P^{\mathcal{V}}(\varphi)$ to a boundary face f of ∂P , i.e., $R_P^{\mathcal{V}}(\varphi)|_f$, is determined completely by the values of φ at the vertices of f, i.e., $\varphi|_f$. Thus, this trace may be given by any admissible reconstruction operator $R_f^{\mathcal{V}}(\varphi|_f)$ acting on that face.

3.3 Minimal reconstruction operators

We will present a constructive proof of the existence of a unique set of admissible reconstruction operators that satisfy properties **(R1)**–**(R5)**.

About one third of the reconstruction operators is not defined uniquely by the five properties **(R1)**–**(R5)**. The uniqueness is restored by solving a minimization problem. For this reason, we refer to the resulting operator as the *minimal reconstruction operator*. A family of admissible reconstruction operators can be derived from the minimal reconstruction operator.

Figure 3.1 shows the inter-dependence between the reconstruction operators. For example, construction of operator $R_P^{\mathcal{E}}$ requires to know operator $R_P^{\mathcal{F}}$ to satisfy the commuting property **(R3)** and operator $R_f^{\mathcal{E}}$ to satisfy the data locality property **(R4)**. For this reason, we first define the operators $R_v^{\mathcal{V}}$, $R_e^{\mathcal{E}}$, $R_f^{\mathcal{F}}$ and $R_P^{\mathcal{P}}$ located on the main diagonal, which are trivial and unique. Then we define the reconstruction operators $R_e^{\mathcal{V}}$, $R_f^{\mathcal{E}}$, and $R_P^{\mathcal{F}}$ located on the first sub-diagonal as the solutions of partial differential equations that are specifically designed to ensure properties **(R1)**–**(R5)**. As we will see later, the orthogonality property **(R4)** is a crucial condition for the derivation of operators $R_f^{\mathcal{E}}$, $R_P^{\mathcal{E}}$, and $R_P^{\mathcal{F}}$ and deserves a careful treatment. Finally, we derive the remaining reconstruction operators $R_f^{\mathcal{V}}$, $R_P^{\mathcal{E}}$, and $R_P^{\mathcal{V}}$.

For every non-trivial reconstruction operator, we also show that the mean value of the reconstructed function depends only on the input mesh function and a few geometrical quantities. Therefore, if there exists a family of admissible reconstruction operators, all members of this family return the same mean value. This average prop-

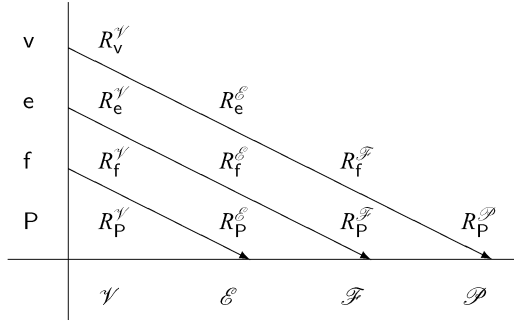


Fig. 3.1. Recursive definition of the reconstruction operators: the operators are defined along diagonals as indicated by arrows starting from the main (the largest) diagonal and moving down

erty plays a crucial role in the derivation of the mimetic inner product. In short, see details below, it shows that this inner product does not depend on a reconstruction operator when one of the arguments in the inner product is the grid projection of a constant scalar or vector field. We will prove this property directly for the operators R_e^V , R_f^E and R_P^F (on the first sub-diagonal in Fig. 3.1) and will derive a recursive relations for the others using properties **(R4)** and **(R5)**.

3.3.1 The reconstruction operators R_v^V , R_e^E , R_f^F and R_P^P

These reconstruction operators, which corresponds to the main diagonal in Fig. 3.1, are the simplest ones as they reconstruct a constant scalar field from the unique data available from the grid function to which they are applied:

$$R_v^V(\varphi) = \varphi_v \quad \forall \varphi = (\varphi_v)_{v \in \mathcal{V}_v} \in \mathcal{V}_{h,v}, \quad (3.8)$$

$$R_e^E(\varphi) = \varphi_e \quad \forall \varphi = (\varphi_e)_{e \in \mathcal{E}_e} \in \mathcal{E}_{h,e}, \quad (3.9)$$

$$R_f^F(\varphi) = \varphi_f \quad \forall \varphi = (\varphi_f)_{f \in \mathcal{F}_f} \in \mathcal{F}_{h,f}, \quad (3.10)$$

$$R_P^P(\varphi) = \varphi_P \quad \forall \varphi = (\varphi_P)_{P \in \mathcal{P}_P} \in \mathcal{P}_{h,P}. \quad (3.11)$$

Properties **(R1)**–**(R3)** for all the operators and property **(R4)** for R_e^E , R_f^F and R_P^P follow immediately as such operators return constant fields.

3.3.2 The reconstruction operators R_e^V , R_f^E and R_P^F

These operators correspond to the second diagonal in Fig. 3.1. The operator R_e^V is defined uniquely, while the other two operators lead to a family of admissible reconstructions. A unique reconstruction is provided by solving a minimization problem.

3.3.2.1 The 1-D reconstruction operator $R_e^{\mathcal{Y}}$

Let ξ be the local coordinate parametrizing the position along the edge $e = (v_1, v_2)$ and such that $\xi = 0$ corresponds to the vertex v_1 and $\xi = 1$ to the vertex v_2 . Let $\varphi = (\varphi_{v_1}, \varphi_{v_2})$ be a vertex-based mesh function from $\mathcal{Y}_{h,e}$. The reconstructed function $R_e^{\mathcal{Y}}(\varphi)$ along the edge e is the unique solution of the following boundary value problem:

$$\begin{aligned} \frac{d}{d\xi} R_e^{\mathcal{Y}}(\varphi) &= \varphi_{v_2} - \varphi_{v_1} \quad \xi \in [0, 1], \\ R_e^{\mathcal{Y}}(\varphi)|_{\xi=0} &= \varphi_{v_1} \quad \text{and} \quad R_e^{\mathcal{Y}}(\varphi)|_{\xi=1} = \varphi_{v_2}. \end{aligned}$$

The solution is the linear polynomial:

$$R_e^{\mathcal{Y}}(\varphi)(\xi) = \varphi_{v_1} + (\varphi_{v_2} - \varphi_{v_1})\xi. \quad (3.12)$$

Property **(R1)** is satisfied because $(\Pi_e^{\mathcal{Y}} \circ R_e^{\mathcal{Y}})(\varphi)$ returns the values of $R_e^{\mathcal{Y}}(\varphi)(\xi)$ at edge end-points $\xi = 0$ and $\xi = 1$, which are φ_{v_1} and φ_{v_2} , respectively. Property **(R2)** is satisfied because, if φ is the projection of a constant function c , then $\varphi_{v_2} = \varphi_{v_1} = c$ and $R_e^{\mathcal{Y}}(\varphi)(\xi) = c$ for every $\xi \in [0, 1]$. Property **(R3)** is satisfied because $(\nabla \circ R_e^{\mathcal{Y}})\varphi = dR_e^{\mathcal{Y}}(\varphi)/d\xi$ and

$$\varphi_{v_2} - \varphi_{v_1} = R_e^{\mathcal{G}}(\varphi_{v_2} - \varphi_{v_1}) = R_e^{\mathcal{G}}(\nabla_h \varphi|_e) = (R_e^{\mathcal{G}} \circ \nabla_h)\varphi.$$

Lemma 3.1. *Let e be the edge connecting vertices v_1 and v_2 . For every vertex-based function $\varphi = (\varphi_v)_{v \in \partial e} \in \mathcal{Y}_{h,e}$ it holds:*

$$\int_e R_e^{\mathcal{Y}}(\varphi) dL = \frac{\varphi_{v_1} + \varphi_{v_2}}{2} |e| \quad \forall e \in \mathcal{E}. \quad (3.13)$$

Proof. Since $R_e^{\mathcal{Y}}(\varphi)$ is a linear function of e , the midpoint quadrature rule gives

$$\int_e R_e^{\mathcal{Y}}(\varphi) dL = R_e^{\mathcal{Y}}(\varphi)(\mathbf{x}_e) |e| = \frac{\varphi_{v_1} + \varphi_{v_2}}{2} |e|, \quad (3.14)$$

where \mathbf{x}_e is the edge midpoint. \square

3.3.2.2 The 2-D reconstruction operator $R_f^{\mathcal{G}}$

Let $\varphi = (\varphi_e)_{e \in \partial f}$ be an edge-based mesh function from $\mathcal{E}_{h,f}$. The two-dimensional vector function reconstructed from φ takes the form $R_f^{\mathcal{G}}(\varphi) = \boldsymbol{\varphi} + \boldsymbol{\varphi}_0$. The first function $\boldsymbol{\varphi} \in H(\text{curl}, f)$ is the solution of following boundary value problem:

$$\text{curl } \boldsymbol{\varphi} = \text{curl}_h \varphi \quad \text{in } f, \quad (3.15)$$

$$\text{div } \boldsymbol{\varphi} = 0 \quad \text{in } f, \quad (3.16)$$

$$\boldsymbol{\varphi} \cdot \boldsymbol{\tau}_e = \varphi_e \quad \text{on } e \in \partial f. \quad (3.17)$$

The second function satisfies two conditions: $\text{curl } \boldsymbol{\varphi}_0 = 0$ in f and $\boldsymbol{\varphi}_0 \cdot \boldsymbol{\tau}_e = 0$ on edges $e \in \partial f$. Since we consider here a single face f , we can assume that unit tangential

vectors $\boldsymbol{\tau}_e$ are oriented counter-clockwise as required by the Stokes theorem; thus, $\alpha_{f,e} = 1$.

Condition (3.16) ensures that problem (3.15)–(3.17) has a unique solution. Conditions (3.15) and (3.17) are necessary to show properties **(R1)**, **(R3)** and **(R5)**. The accuracy property **(R2)** and the orthogonality property **(R4)** follow from a proper choice of function $\boldsymbol{\varphi}_0$.

Let us discuss these properties in details. Property **(R1)** holds because the projection operator $\Pi_f^\mathcal{E}$ uses only boundary values of the reconstructed function:

$$(\Pi_f^\mathcal{E} \circ R_f^\mathcal{E})(\boldsymbol{\varphi})|_e = \frac{1}{|e|} \int_e R_f^\mathcal{E}(\boldsymbol{\varphi}) \cdot \boldsymbol{\tau}_e dS = \frac{1}{|e|} \int_e (\boldsymbol{\varphi} + \boldsymbol{\varphi}_0) \cdot \boldsymbol{\tau}_e dS = \varphi_e.$$

Property **(R3)** is satisfied because $\text{curl}_h \boldsymbol{\varphi} = R_f^\mathcal{F}(\text{curl}_h \boldsymbol{\varphi}) = (R_f^\mathcal{F} \circ \text{curl}_h)(\boldsymbol{\varphi})$, from which it follows that

$$(\text{curl} \circ R_f^\mathcal{E}) \boldsymbol{\varphi} = \text{curl}(R_f^\mathcal{E}(\boldsymbol{\varphi})) = \text{curl}(\boldsymbol{\varphi} + \boldsymbol{\varphi}_0) = \text{curl}_h \boldsymbol{\varphi} = (R_f^\mathcal{F} \circ \text{curl}_h) \boldsymbol{\varphi}.$$

Property **(R5)** is satisfied because $R_f^\mathcal{E}(\boldsymbol{\varphi}) \cdot \boldsymbol{\tau}_e = (\boldsymbol{\varphi} + \boldsymbol{\varphi}_0) \cdot \boldsymbol{\tau}_e = \varphi_e = R_e^\mathcal{E}(\varphi|_e)$ for every edge e of ∂f (note that $R_e^\mathcal{E}$ is unique).

Now, we are left to determine a suitable vector function $\boldsymbol{\varphi}_0$ to ensure properties **(R2)** and **(R4)**. As $\text{curl} \boldsymbol{\varphi}_0 = 0$, we take $\boldsymbol{\varphi}_0 = \nabla q$ for some scalar function q in $H_0^1(f)$. As q has zero trace on ∂f , its tangential derivative along each edge is zero; hence the condition $\boldsymbol{\varphi}_0 \cdot \boldsymbol{\tau}_e = 0$ is preserved. Imposing the orthogonality condition **(R4)** and integrating by parts yield:

$$\int_f \boldsymbol{\varphi} \cdot (\boldsymbol{\xi} - \boldsymbol{\xi}_f) dS = - \int_f \nabla q \cdot (\boldsymbol{\xi} - \boldsymbol{\xi}_f) dS = 2 \int_f q dS. \quad (3.18)$$

Equation (3.18) gives us a necessary condition to choose q as a function of $\boldsymbol{\varphi}$ but the choice is not unique. To fix this, let us define

$$\chi := \frac{1}{2} \int_f \boldsymbol{\varphi} \cdot (\boldsymbol{\xi} - \boldsymbol{\xi}_f) dS \quad \text{and} \quad \mathcal{H}_\chi(f) = \left\{ q \in H_0^1(f) \text{ such that } \int_f q dS = \chi \right\},$$

and take $p \in H_0^1(f)$ as the unique solution of the minimization problem:

$$\min_{q \in \mathcal{H}_\chi(f)} \int_f \nabla q \cdot \nabla q dS.$$

Then, we set $\boldsymbol{\varphi}_0 := \nabla p$. To show that condition **(R2)** is satisfied by $\boldsymbol{\varphi} + \boldsymbol{\varphi}_0$, we consider $\boldsymbol{\varphi} = \Pi_f^\mathcal{E}(\mathbf{c})$ for some constant vector $\mathbf{c} \in \mathbb{R}^2$. The unique solution to (3.15)–(3.17) is $\boldsymbol{\varphi} = \mathbf{c}$, which implies that $\chi = 0$. The minimization process returns $q = 0$ and, hence, $\boldsymbol{\varphi}_0 = 0$. We conclude that $R_f^\mathcal{E}(\boldsymbol{\varphi}) = \boldsymbol{\varphi} + \nabla p$ is the admissible minimal reconstruction operator.

A family of admissible reconstruction operators is obtained by taking $\boldsymbol{\varphi}_0 = \nabla \mathcal{M}(\boldsymbol{\varphi})$ where $\mathcal{M} : \boldsymbol{\varphi} \rightarrow q$ may be any linear operator that respects (3.18) and returns $\mathcal{M}(\mathbf{c}) = 0$ for every constant vector function \mathbf{c} .

Lemma 3.2. *Let \mathbf{e}_i for $i = 1, 2$ be the i -th vector of the canonical basis of \mathbb{R}^2 , and p_i^1 be a linear polynomial of $\mathcal{O}_f^\mathcal{E}$ such that $\mathbf{e}_i = \text{curl} p_i^1$. Then, for every admissible*

reconstruction operator $R_f^{\mathcal{E}}$ and every edge-based mesh function $\varphi = (\varphi_e)_{e \in \partial f} \in \mathcal{E}_{h,f}$ it holds:

$$\int_f R_f^{\mathcal{E}}(\varphi) \cdot \mathbf{e}_i dS = \sum_{e \in \partial f} \varphi_e \int_e p_i^1 dL. \quad (3.19)$$

Proof. Using conditions of the lemma and integrating by parts, we obtain

$$\begin{aligned} \int_f R_f^{\mathcal{E}}(\varphi) \cdot \mathbf{e}_i dS &= \int_f R_f^{\mathcal{E}}(\varphi) \cdot \text{curl} p_i^1 dS \\ &= - \int_f p_i^1 \text{curl} R_f^{\mathcal{E}}(\varphi) dS + \sum_{e \in \partial f} \int_e \boldsymbol{\tau}_e \cdot R_f^{\mathcal{E}}(\varphi) p_i^1 dL. \end{aligned} \quad (3.20)$$

The first integral term in the right-hand side of (3.20) is zero. Indeed, using the commuting property **(R3)**, the fact that $R_f^{\mathcal{F}}$ is constant on f , cf. (3.10), and the definition of space $\mathcal{O}_f^{\mathcal{E}}$, we obtain:

$$\int_f p_i^1 \text{curl} R_f^{\mathcal{E}}(\varphi) dS = \int_f R_f^{\mathcal{F}}(\text{curl}_h \varphi) p_i^1 dS = R_f^{\mathcal{F}}(\text{curl}_h \varphi) \int_f p_i^1 dS = 0.$$

The locality property **(R5)** and the definition of $R_e^{\mathcal{E}}$ given in (3.9) yield

$$\int_e \boldsymbol{\tau}_e \cdot R_f^{\mathcal{E}}(\varphi) p_i^1 dL = \int_e R_e^{\mathcal{E}}(\varphi_e) p_i^1 dL = \varphi_e \int_e p_i^1 dL.$$

This proves the assertion of the lemma. \square

3.3.2.3 The 3-D reconstruction operator $R_P^{\mathcal{F}}$

Let $\varphi = (\varphi_f)_{f \in \partial P}$ be a face-based mesh function from $\mathcal{F}_{h,P}$. The three-dimensional vector function reconstructed from φ inside cell P takes the form $R_P^{\mathcal{F}}(\varphi) = \boldsymbol{\varphi} + \boldsymbol{\varphi}_0$. The first function $\boldsymbol{\varphi} \in H(\text{div}, P)$ is the solution of the following problem:

$$\text{div} \boldsymbol{\varphi} = \text{div}_h \varphi \quad \text{in } P, \quad (3.21)$$

$$\text{curl} \boldsymbol{\varphi} = 0 \quad \text{in } P, \quad (3.22)$$

$$\boldsymbol{\varphi} \cdot \mathbf{n}_f = \varphi_f \quad \forall f \in \partial P. \quad (3.23)$$

The second function must satisfy two conditions: $\text{div} \boldsymbol{\varphi}_0 = 0$ in P and $\boldsymbol{\varphi}_0 \cdot \mathbf{n}_f = 0$ on faces $f \in \partial P$. Since we consider here a single polyhedron P , we can assume that the unit normal vectors \mathbf{n}_f are exterior to P ; hence, $\alpha_{P,f} = 1$.

Condition (3.22) ensures that problem (3.21)–(3.23) has a unique solution $\boldsymbol{\varphi}$. Conditions (3.21) and (3.23) are necessary to show properties **(R1)**, **(R3)**, and **(R5)**. The accuracy property **(R2)** and the orthogonality property **(R4)** follow from a proper choice of function $\boldsymbol{\varphi}_0$.

Let us discuss these issues in details. Property **(R1)** is satisfied because the projection operator $\Pi_P^{\mathcal{F}}$ returns the face degrees of freedom of φ due to (3.23):

$$(\Pi_P^{\mathcal{F}} \circ R_P^{\mathcal{F}})(\varphi)_f = \frac{1}{|f|} \int_f R_P^{\mathcal{F}}(\varphi) \cdot \mathbf{n}_f dS = \frac{1}{|f|} \int_f (\boldsymbol{\varphi} + \boldsymbol{\varphi}_0) \cdot \mathbf{n}_f dS = \frac{\varphi_f}{|f|} \int_f dS = \varphi_f.$$

The commuting property **(R3)** holds because $\operatorname{div}_h \boldsymbol{\varphi} = R_{\mathcal{P}}^{\mathcal{F}}(\operatorname{div}_h \boldsymbol{\varphi}) = (R_{\mathcal{P}}^{\mathcal{F}} \circ \operatorname{div}_h) \boldsymbol{\varphi}$ from which it follows that

$$(\operatorname{div} \circ R_{\mathcal{P}}^{\mathcal{F}}) \boldsymbol{\varphi} = \operatorname{div}(R_{\mathcal{P}}^{\mathcal{F}}(\boldsymbol{\varphi})) = \operatorname{div}(\boldsymbol{\varphi} + \boldsymbol{\varphi}_0) = \operatorname{div}_h \boldsymbol{\varphi} = (R_{\mathcal{P}}^{\mathcal{F}} \circ \operatorname{div}_h) \boldsymbol{\varphi}.$$

The locality property **(R5)** is satisfied because $R_{\mathcal{P}}^{\mathcal{F}}(\boldsymbol{\varphi}) \cdot \mathbf{n}_f = \boldsymbol{\varphi}_f = R_f^{\mathcal{F}}(\boldsymbol{\varphi}_f)$ for every $f \in \partial\mathcal{P}$.

What is left is to determine a suitable function $\boldsymbol{\varphi}_0$ that ensures properties **(R2)** and **(R4)**. Since $\operatorname{div} \boldsymbol{\varphi}_0 = 0$, we can define $\boldsymbol{\varphi}_0 = \operatorname{curl} \mathbf{q}$ for some vector function $\mathbf{q} \in H_0(\operatorname{curl}, \mathcal{P})$. The quantity $\operatorname{curl} \mathbf{q} \cdot \mathbf{n}_f$ depends only on the tangential derivatives of \mathbf{q} on f . Since $\mathbf{q} \times \mathbf{n}_f = 0$ on f , these derivatives are zero and the condition $\boldsymbol{\varphi}_0 \cdot \mathbf{n}_f = \operatorname{curl} \mathbf{q} \cdot \mathbf{n}_f = 0$ is preserved. Imposing the orthogonality condition **(R4)** and integrating by parts yield:

$$-\int_{\mathcal{P}} \boldsymbol{\varphi} \cdot (\mathbf{c} \times (\mathbf{x} - \mathbf{x}_{\mathcal{P}})) dV = \int_{\mathcal{P}} \operatorname{curl} \mathbf{q} \cdot (\mathbf{c} \times (\mathbf{x} - \mathbf{x}_{\mathcal{P}})) dV = 2 \int_{\mathcal{P}} \mathbf{q} \cdot \mathbf{c} dV, \quad (3.24)$$

which holds for every constant vector $\mathbf{c} \in \mathbb{R}^3$. Equation (3.24) gives us a necessary condition to choose \mathbf{q} as a function of $\boldsymbol{\varphi}$ but the choice is not unique. To fix this, let us define

$$\boldsymbol{\chi} := \frac{1}{2} \int_{\mathcal{P}} \boldsymbol{\varphi} \times (\mathbf{x} - \mathbf{x}_{\mathcal{P}}) dV \quad \text{and} \quad \mathbf{H}_{\boldsymbol{\chi}}(\mathcal{P}) = \left\{ \mathbf{q} \in H_0(\operatorname{curl}, \mathcal{P}) : \int_{\mathcal{P}} \mathbf{q} dV = \boldsymbol{\chi} \right\},$$

and take $\mathbf{p} \in H_0(\operatorname{curl}, \mathcal{P})$ as the unique solution of the minimization problem:

$$\min_{\mathbf{q} \in \mathbf{H}_{\boldsymbol{\chi}}(\mathcal{P})} \int_{\mathcal{P}} |\mathbf{q}|^2 dV.$$

Then, we set $\boldsymbol{\varphi}_0 := \operatorname{curl} \mathbf{p}$. To show that condition **(R2)** is satisfied by $\boldsymbol{\varphi} + \boldsymbol{\varphi}_0$, we consider $\boldsymbol{\varphi} = \Pi_{\mathcal{P}}^{\mathcal{F}}(\mathbf{c})$ for some constant vector $\mathbf{c} \in \mathbb{R}^3$. The unique solution to (3.21)–(3.23) is $\boldsymbol{\varphi} = \mathbf{c}$, which implies that $\boldsymbol{\chi} = 0$. The minimization process returns $\mathbf{q} = 0$; hence, $\boldsymbol{\varphi}_0 = 0$. We conclude that $R_{\mathcal{P}}^{\mathcal{F}}(\boldsymbol{\varphi}) = \boldsymbol{\varphi} + \operatorname{curl} \mathbf{p}$ is an admissible minimal reconstruction operator.

A family of admissible reconstruction operator is obtained by taking $\boldsymbol{\varphi}_0 = \operatorname{curl} \mathcal{M}(\boldsymbol{\varphi})$, where $\mathcal{M} : \boldsymbol{\varphi} \rightarrow \mathbf{q}$ can be any vector-valued linear operator that respects (3.24) and returns $\mathcal{M}(\mathbf{c}) = 0$ for every constant vector function \mathbf{c} .

Lemma 3.3. *Let \mathbf{e}_i be the i -th vector of the canonical basis of \mathbb{R}^3 , $i = 1, 2, 3$. Then, for every admissible reconstruction operator $R_{\mathcal{P}}^{\mathcal{F}}$ and every face function $\boldsymbol{\varphi} = (\boldsymbol{\varphi}_f)_{f \in \partial\mathcal{P}} \in \mathcal{F}_{h,\mathcal{P}}$ it holds:*

$$\int_{\mathcal{P}} R_{\mathcal{P}}^{\mathcal{F}}(\boldsymbol{\varphi}) \cdot \mathbf{e}_i dV = \sum_{f \in \partial\mathcal{P}} \boldsymbol{\varphi}_f |f| \mathbf{e}_i \cdot (\mathbf{x}_f - \mathbf{x}_{\mathcal{P}}). \quad (3.25)$$

Proof. Let $\mathbf{e}_i = \nabla p_i^1$ where $p_i^1(\mathbf{x}) := \mathbf{e}_i \cdot (\mathbf{x} - \mathbf{x}_P)$. Using this and integrating the left hand side of (3.25) by parts, we obtain

$$\begin{aligned} \int_P R_P^{\mathcal{F}}(\varphi) \cdot \mathbf{e}_i dV &= \int_P R_P^{\mathcal{F}}(\varphi) \cdot \nabla p_i^1 dV \\ &= - \int_P p_i^1 \operatorname{div} R_P^{\mathcal{F}}(\varphi) dV + \sum_{f \in \partial P} \int_f \mathbf{n}_{P,f} \cdot R_P^{\mathcal{F}}(\varphi) p_i^1 dV. \end{aligned} \quad (3.26)$$

The first integral term in the right-hand side of (3.26) is zero. Indeed, using the commuting property **(R3)** and the fact that $R_P^{\mathcal{F}}$ is constant on P , cf. (3.11), we obtain:

$$\int_P p_i^1 \operatorname{div} R_P^{\mathcal{F}}(\varphi) dV = \int_P R_P^{\mathcal{F}}(\operatorname{div}_h \varphi) p_i^1 dV = R_P^{\mathcal{F}}(\operatorname{div}_h \varphi) \int_P p_i^1 dV = 0.$$

The locality property **(R5)** and the midpoint integration rule give

$$\int_f \mathbf{n}_{P,f} \cdot R_P^{\mathcal{F}}(\varphi) p_i^1 dV = \varphi_f \int_f p_i^1 dV = \varphi_f |f| \mathbf{e}_i \cdot (\mathbf{x}_f - \mathbf{x}_P).$$

This proves the assertion of the lemma. \square

3.3.3 The reconstruction operators $R_f^{\mathcal{Y}}$ and $R_P^{\mathcal{E}}$

These two operators correspond to the third diagonal in Fig. 3.1. Their construction uses the reconstruction operators described above.

3.3.3.1 The 2-D reconstruction operator $R_f^{\mathcal{Y}}$

Let $\varphi = (\varphi_v)_{v \in \partial f}$ be a vertex function from $\mathcal{V}_{h,f}$. A scalar function $R_f^{\mathcal{Y}}(\varphi)$ reconstructed from φ on face f is the unique solution of the following problem:

$$\nabla R_f^{\mathcal{Y}}(\varphi) = R_f^{\mathcal{E}}(\nabla_h \varphi) \quad \text{in } f, \quad (3.27)$$

$$R_f^{\mathcal{Y}}(\varphi) = R_e^{\mathcal{Y}}(\varphi_e) \quad \text{on } e \in \partial f, \quad (3.28)$$

where $R_f^{\mathcal{E}}$ and $R_e^{\mathcal{Y}}$ are the admissible reconstruction operators defined in Sect. 3.3.2.

Property **(R1)** holds because the projection operator $\Pi_f^{\mathcal{Y}}$ evaluates function values at vertices v of f , which are determined uniquely by the boundary conditions (3.28) and the properties of $R_e^{\mathcal{Y}}(\varphi)$. Property **(R5)** is the boundary condition (3.28). To show property **(R2)**, let us take $\varphi = \Pi_f^{\mathcal{Y}}(c)$ for a constant function c . Then $\varphi_v = c$ for every vertex v and $\nabla_h \varphi = 0$. Hence, the right-hand side of (3.27) is zero and the solution to the problem is a constant that must take the same value c . Property **(R3)** is implied directly by (3.27).

The right-hand side in (3.27) is not unique unless we consider the minimal admissible reconstruction operator $R_f^{\mathcal{E}}$, see Sect. 3.3.2. Taking the divergence of both sides of (3.27) yields that $R_f^{\mathcal{Y}}(\varphi)$ is a solution of the boundary value problem:

$$\Delta(R_f^{\mathcal{Y}}(\varphi)) = \operatorname{div}(R_f^{\mathcal{E}}(\nabla_h \varphi)) \quad \text{in } f, \quad (3.29)$$

$$R_f^{\mathcal{Y}}(\varphi) = R_e^{\mathcal{Y}}(\varphi_e) \quad \text{on } e \in \partial f. \quad (3.30)$$

Since the right-hand side of (3.30) is determined uniquely by (3.12), the solution is unique. Obviously, it also the solution to problem (3.27)–(3.28).

Let us show that the accuracy property **(R2)** can be extended to linear functions. Consider $\varphi = \Pi_f^{\mathcal{Y}}(p^1)$ for a linear function p^1 . Note that the right-hand side of (3.29) is zero and the right-hand side of (3.30) is the trace of p^1 on ∂f . Hence, p^1 is the solution of this problem and $R_f^{\mathcal{Y}}(\Pi_f^{\mathcal{Y}}(p^1)) = p^1$.

Lemma 3.4. *Let $\mathbf{n}_{f,e}$ denote the exterior unit vector orthogonal to $e \in \partial f$. Then, for every admissible reconstruction operator $R_f^{\mathcal{Y}}$ and every vertex-based mesh function $\varphi = (\varphi_v)_{v \in \partial f} \in \mathcal{Y}_{h,f}$ it holds that*

$$\int_f R_f^{\mathcal{Y}}(\varphi) dS = \frac{1}{2} \sum_{e \in \partial f} (\boldsymbol{\xi}_e - \boldsymbol{\xi}_f) \cdot \mathbf{n}_{f,e} \int_e R_e^{\mathcal{Y}}(\varphi|_e) dL. \quad (3.31)$$

Proof. We use the identity $2 = \operatorname{div}(\boldsymbol{\xi} - \boldsymbol{\xi}_f)$ and integrate the left-hand side of (3.31) by parts:

$$\begin{aligned} 2 \int_f R_f^{\mathcal{Y}}(\varphi) dS &= \int_f R_f^{\mathcal{Y}}(\varphi) \operatorname{div}(\boldsymbol{\xi} - \boldsymbol{\xi}_f) dS \\ &= - \int_f \nabla R_f^{\mathcal{Y}}(\varphi) \cdot (\boldsymbol{\xi} - \boldsymbol{\xi}_f) dS + \sum_{e \in \partial f} \int_e R_f^{\mathcal{Y}}(\varphi)|_e \mathbf{n}_{f,e} \cdot (\boldsymbol{\xi} - \boldsymbol{\xi}_f) dL. \end{aligned} \quad (3.32)$$

The first integral in the right-hand side is zero. Indeed, using the commuting property **(R3)** and the orthogonality property **(R4)**, we obtain:

$$\int_f \nabla R_f^{\mathcal{Y}}(\varphi) \cdot (\boldsymbol{\xi} - \boldsymbol{\xi}_f) dS = \int_f R_f^{\mathcal{E}}(\nabla_h \varphi) \cdot (\boldsymbol{\xi} - \boldsymbol{\xi}_f) dS = 0.$$

Note that $(\boldsymbol{\xi} - \boldsymbol{\xi}_f) \cdot \mathbf{n}_{f,e}$ is constant along edge e and can be evaluated at the edge mid-point. Applying the locality property **(R5)**, we obtain:

$$\int_e R_f^{\mathcal{Y}}(\varphi)|_e \mathbf{n}_{f,e} \cdot (\boldsymbol{\xi} - \boldsymbol{\xi}_f) dL = \mathbf{n}_{f,e} \cdot (\boldsymbol{\xi}_e - \boldsymbol{\xi}_f) \int_e R_e^{\mathcal{Y}}(\varphi|_e) dL.$$

This proves the assertion of the lemma. \square

Remark 3.3. We can evaluate the integrals in the right-hand side of (3.32) using the result of Lemma 3.1. Thus, the average of $R_f^{\mathcal{Y}}(\varphi)$ on f is the same for all admissible reconstruction operators $R_f^{\mathcal{Y}}$ and depends only on φ and a few geometric quantities.

3.3.3.2 The 3-D reconstruction operator $R_P^{\mathcal{E}}$

Let $\varphi = (\varphi_e)_{e \in \partial P}$ be an edge-based mesh function from $\mathcal{E}_{h,P}$. The three-dimensional vector field reconstructed from φ inside cell P has the form $R_P^{\mathcal{E}}(\varphi) = \boldsymbol{\varphi} + \boldsymbol{\varphi}_0$. The first function $\boldsymbol{\varphi} \in H(\operatorname{curl}, P)$ is the solution of the following problem:

$$\operatorname{curl} \boldsymbol{\varphi} = R_P^{\mathcal{F}}(\operatorname{curl}_h \varphi) \quad \text{in } P, \quad (3.33)$$

$$\operatorname{div} \boldsymbol{\varphi} = 0 \quad \text{in } P, \quad (3.34)$$

$$(\boldsymbol{\varphi})_{\perp, f} = R_f^{\mathcal{E}}(\varphi|_f) \quad \text{on } f \in \partial P, \quad (3.35)$$

where $R_{\mathbb{P}}^{\mathcal{F}}$ is the admissible reconstruction operator defined in Sect. 3.3.2 and $(\boldsymbol{\varphi})_{\perp, \mathbf{f}}$ denotes the orthogonal projection on the plane of \mathbf{f} . In other words, we fix the tangential component of $\boldsymbol{\varphi}$ on $\partial\mathbb{P}$. The second function $\boldsymbol{\varphi}_0$ must satisfy two conditions: $\text{curl } \boldsymbol{\varphi}_0 = 0$ in \mathbb{P} and $\boldsymbol{\varphi}_0 = 0$ on $\partial\mathbb{P}$.

Condition (3.34) is introduced to ensure that the problem (3.33)–(3.35) has a unique solution. Conditions (3.33) and (3.35) are necessary to ensure properties **(R1)**, **(R3)**, and **(R5)**. The accuracy property **(R2)** and the orthogonality property **(R4)** follow from a proper choice of function $\boldsymbol{\varphi}_0$.

Let us discuss these properties in more details. The data locality property **(R5)** holds immediately due to selection of boundary conditions in (3.35). Property **(R1)** holds because the projections operator $\Pi_{\mathbb{P}}^{\mathcal{E}}$ returns values of the reconstructed function averaged over edges. Using this and definition (3.17), we obtain:

$$(\Pi_{\mathbb{P}}^{\mathcal{E}} \circ R_{\mathbb{P}}^{\mathcal{E}})(\boldsymbol{\varphi})|_{\mathbf{e}} = \frac{1}{|\mathbf{e}|} \int_{\mathbf{e}} (\boldsymbol{\varphi} + \boldsymbol{\varphi}_0) \cdot \boldsymbol{\tau}_{\mathbf{e}} dL = \frac{1}{|\mathbf{e}|} \int_{\mathbf{e}} R_{\mathbf{f}}^{\mathcal{E}}(\boldsymbol{\varphi}|_{\mathbf{f}}) \cdot \boldsymbol{\tau}_{\mathbf{e}} dL = \varphi_{\mathbf{e}},$$

where \mathbf{f} is any face to which \mathbf{e} belongs. The commuting property **(R3)** holds because

$$(\text{curl} \circ R_{\mathbb{P}}^{\mathcal{E}}) \boldsymbol{\varphi} = \text{curl} R_{\mathbb{P}}^{\mathcal{E}}(\boldsymbol{\varphi}) = \text{curl}(\boldsymbol{\varphi} + \boldsymbol{\varphi}_0) = R_{\mathbb{P}}^{\mathcal{F}}(\text{curl}_h \boldsymbol{\varphi}) = (R_{\mathbb{P}}^{\mathcal{F}} \circ \text{curl}_h) \boldsymbol{\varphi}.$$

What is left is to determine a suitable function $\boldsymbol{\varphi}_0$ to ensure properties **(R2)** and **(R4)**. Since $\text{curl } \boldsymbol{\varphi}_0 = 0$, we take $\boldsymbol{\varphi}_0 = \nabla q$ for some scalar function q in $H_0^1(\mathbb{P})$. As q has zero trace on $\partial\mathbb{P}$, its tangential derivatives on each face $\mathbf{f} \in \partial\mathbb{P}$ are also zeros, and the condition $\boldsymbol{\varphi}_0 = 0$ on $\partial\mathbb{P}$ is preserved. Imposing the orthogonality condition and integrating by parts yield:

$$\int_{\mathbb{P}} \boldsymbol{\varphi} \cdot (\mathbf{x} - \mathbf{x}_{\mathbb{P}}) dV = - \int_{\mathbb{P}} \nabla q \cdot (\mathbf{x} - \mathbf{x}_{\mathbb{P}}) dV = 3 \int_{\mathbb{P}} q dV. \quad (3.36)$$

Equation (3.36) gives us a necessary condition to choose q as a function of $\boldsymbol{\varphi}$ but the choice is not unique. To fix this, let us define

$$\chi := \frac{1}{3} \int_{\mathbb{P}} \boldsymbol{\varphi} \cdot (\mathbf{x} - \mathbf{x}_{\mathbb{P}}) dV \quad \text{and} \quad \mathcal{H}(\mathbb{P}) = \left\{ q \in H_0^1(\mathbb{P}) : \int_{\mathbb{P}} q dV = \chi \right\},$$

and take $p \in H_0^1(\mathbb{P})$ as the unique solution of the minimization problem:

$$\min_{q \in \mathcal{H}(\mathbb{P})} \int_{\mathbb{P}} \nabla q \cdot \nabla q dV. \quad (3.37)$$

Then, we set $\boldsymbol{\varphi}_0 := \nabla p$. To show that the accuracy property **(R2)** is satisfied by $\boldsymbol{\varphi} + \boldsymbol{\varphi}_0$, we consider $\boldsymbol{\varphi} = \Pi_{\mathbb{P}}^{\mathcal{E}}(\mathbf{c})$ for some constant vector $\mathbf{c} \in \mathbb{R}^3$. The unique solution to (3.33)–(3.35) is $\boldsymbol{\varphi} = \mathbf{c}$, which implies that $\chi = 0$. The minimization process returns $q = 0$ and, hence, $\boldsymbol{\varphi}_0 = 0$. We conclude that $R_{\mathbb{P}}^{\mathcal{E}}(\boldsymbol{\varphi}) = \boldsymbol{\varphi} + \nabla p$ is the minimal admissible reconstruction operator.

A family of admissible reconstruction operators is obtained by taking $\boldsymbol{\varphi}_0 = \nabla \mathcal{M}(\boldsymbol{\varphi})$ where $\mathcal{M} : \boldsymbol{\varphi} \rightarrow q$ that can be any linear operator that respects (3.36) and such that $\mathcal{M}(\mathbf{c}) = 0$ for every constant vector function \mathbf{c} .

Lemma 3.5. *Let \mathbf{e}_i be the i -th vector of the canonical basis of \mathbb{R}^3 , $i = 1, 2, 3$. For every admissible reconstruction operator $R_{\mathbb{P}}^{\mathcal{E}}$ and every edge-based mesh function*

$\boldsymbol{\varphi} = (\varphi_e)_{e \in \partial P} \in \mathcal{E}_{h,P}$ it holds:

$$\int_P R_P^\mathcal{E}(\boldsymbol{\varphi}) \cdot \mathbf{e}_i dV = \frac{1}{2} \sum_{f \in \partial P} \boldsymbol{\alpha}_{f,i} \cdot \int_f R_f^\mathcal{E}(\varphi_f) dS, \quad (3.38)$$

where $R_f^\mathcal{E}$ is any admissible reconstruction operator and

$$\boldsymbol{\alpha}_{f,i} = (\mathbf{n}_{P,f} \cdot (\mathbf{x}_f - \mathbf{x}_P) \mathbf{e}_i + \mathbf{n}_{P,f} \cdot \mathbf{e}_i (\mathbf{x}_P - \mathbf{x}_f))_{\perp, f}. \quad (3.39)$$

Proof. Let us rewrite \mathbf{e}_i using the following identity

$$2\mathbf{e}_i = \text{curl} \mathbf{p}_i^1(\mathbf{x}) \quad \text{with} \quad \mathbf{p}_i^1(\mathbf{x}) = \mathbf{e}_i \times (\mathbf{x} - \mathbf{x}_P). \quad (3.40)$$

Substituting (3.40) in (3.38) and integrating by parts, we obtain

$$\begin{aligned} 2 \int_P R_P^\mathcal{E}(\boldsymbol{\varphi}) \cdot \mathbf{e}_i dV &= \int_P R_P^\mathcal{E}(\boldsymbol{\varphi}) \cdot \text{curl} \mathbf{p}_i^1 dV \\ &= \int_P \text{curl} R_P^\mathcal{E}(\boldsymbol{\varphi}) \cdot \mathbf{p}_i^1 dV + \sum_{f \in \partial P} \int_f R_f^\mathcal{E}(\boldsymbol{\varphi}) \cdot (\mathbf{n}_{P,f} \times \mathbf{p}_i^1) dS. \end{aligned} \quad (3.41)$$

The volume integral in the right-hand side of (3.41) is zero. Indeed, using the commuting property **(R3)** and the orthogonality property **(R4)**, we obtain:

$$\int_P \text{curl} R_P^\mathcal{E}(\boldsymbol{\varphi}) \cdot \mathbf{p}_i^1 dV = \int_P R_P^\mathcal{F}(\text{curl}_h \boldsymbol{\varphi}) \cdot \mathbf{p}_i^1 dV = 0.$$

The locality property **(R5)** gives

$$\int_f R_f^\mathcal{E}(\boldsymbol{\varphi}) \cdot (\mathbf{n}_{P,f} \times \mathbf{p}_i^1) dS = \int_f R_f^\mathcal{E}(\varphi_f) \cdot (\mathbf{n}_{P,f} \times \mathbf{p}_i^1)_{\perp, f} dS. \quad (3.42)$$

Applying vector calculus, we obtain:

$$\mathbf{n}_{P,f} \times \mathbf{p}_i^1 = \mathbf{n}_{P,f} \cdot (\mathbf{x} - \mathbf{x}_P) \mathbf{e}_i - (\mathbf{n}_{P,f} \cdot \mathbf{e}_i) (\mathbf{x} - \mathbf{x}_P). \quad (3.43)$$

Note that $\mathbf{n}_{P,f} \cdot (\mathbf{x} - \mathbf{x}_P)$ is a constant quantity on f . Adding and subtracting \mathbf{x}_f , we rewrite (3.43) as follows:

$$\mathbf{n}_{P,f} \times \mathbf{p}_i^1 = \mathbf{n}_{P,f} \cdot (\mathbf{x}_f - \mathbf{x}_P) \mathbf{e}_i - (\mathbf{n}_{P,f} \cdot \mathbf{e}_i) (\mathbf{x}_f - \mathbf{x}_P) - (\mathbf{n}_{P,f} \cdot \mathbf{e}_i) (\mathbf{x} - \mathbf{x}_f) \quad (3.44)$$

The first two terms in the right-hand side form a vector parallel to the plane of f . The same is true for the third term. Consider a local coordinate system $\boldsymbol{\xi}$ associated with the plane of f . Then, the orthogonal projection is quite simple:

$$(\mathbf{n}_{P,f} \times \mathbf{p}_i^1)_{\perp, f} = \boldsymbol{\alpha}_{f,i} - (\mathbf{n}_{P,f} \cdot \mathbf{e}_i) (\boldsymbol{\xi} - \boldsymbol{\xi}_f). \quad (3.45)$$

Inserting this in (3.42), we obtain:

$$\int_f R_f^\mathcal{E}(\boldsymbol{\varphi}) \cdot (\mathbf{n}_{P,f} \times \mathbf{p}_i^1) dS = \int_f R_f^\mathcal{E}(\varphi_f) \cdot \boldsymbol{\alpha}_{f,i} dS - (\mathbf{n}_{P,f} \cdot \mathbf{e}_i) \int_f R_f^\mathcal{E}(\varphi_f) \cdot (\boldsymbol{\xi} - \boldsymbol{\xi}_f) dS.$$

The assertion of the lemma follows by observing that the last integral is zero due to the orthogonality property **(R4)**. \square

Remark 3.4. The average of the reconstructed function $R_P^\mathcal{E}(\boldsymbol{\varphi})$ on P depends on averages of the reconstructed functions $R_f^\mathcal{E}(\varphi_f)$ on faces f . According to Lemma 3.3, the

later do not depend on the choice of the reconstruction operator. Thus, the average of $R_{\mathbf{P}}^{\mathcal{E}}(\varphi)$ is the same for all admissible reconstruction operators and depends only on φ and a few geometrical quantities.

3.3.4 The reconstruction operator $R_{\mathbf{P}}^{\mathcal{V}}$

Let $\varphi = (\varphi_{\mathbf{v}})_{\mathbf{v} \in \partial \mathbf{P}}$ be a vertex-based mesh function from $\mathcal{V}_{h,\mathbf{P}}$. A scalar function reconstructed from φ inside cell \mathbf{P} is the unique solution of the following problem

$$\nabla R_{\mathbf{P}}^{\mathcal{V}}(\varphi) = R_{\mathbf{P}}^{\mathcal{E}}(\nabla_h \varphi) \quad \text{in } \mathbf{P}, \quad (3.46)$$

$$R_{\mathbf{P}}^{\mathcal{V}}(\varphi)|_{\mathbf{f}} = R_{\mathbf{f}}^{\mathcal{V}}(\varphi) \quad \text{on } \mathbf{f} \in \partial \mathbf{P}, \quad (3.47)$$

where $R_{\mathbf{P}}^{\mathcal{E}}$ and $R_{\mathbf{f}}^{\mathcal{V}}$ are admissible reconstruction operators defined in Sect. 3.3.3.

From Sect. 3.3.3 we know that an admissible reconstruction operator can be written as $R_{\mathbf{P}}^{\mathcal{E}}(\varphi) = \boldsymbol{\varphi} + \nabla \mathcal{M}(\boldsymbol{\varphi})$, where $\boldsymbol{\varphi}$ is a divergence-free field. Taking the divergence of both side of (3.46), we obtain the following necessary condition:

$$\Delta R_{\mathbf{P}}^{\mathcal{V}}(\varphi) = \Delta \mathcal{M}(\boldsymbol{\varphi}).$$

The solution $R_{\mathbf{P}}^{\mathcal{V}}(\varphi)$ is determined uniquely by taking $\mathcal{M}(\boldsymbol{\varphi}) = p$, where p is the solution of the minimization problem (3.37). We refer to such a reconstruction operator as the *minimal reconstruction operator*.

Property **(R1)** holds because the projection operator $\Pi_{\mathbf{P}}^{\mathcal{V}}$ returns values of the reconstructed function at vertices \mathbf{v} of \mathbf{P} and these values are defined uniquely by boundary conditions (3.47). To show that the accuracy property **(R2)** holds, let us consider $\varphi = \Pi_{\mathbf{P}}^{\mathcal{V}}(c)$ for a constant function c . Since $\varphi_{\mathbf{v}} = c$ for every vertex \mathbf{v} of \mathbf{P} , we have $\nabla_h(\varphi) = 0$; hence, the right-hand side of (3.46) is zero. Thus, the solution is constant on \mathbf{P} and must take the same value c due to the boundary conditions. The commuting property **(R3)** follows immediately from (3.46).

The accuracy property can be extended to linear functions. Let $p^1 \in \mathbb{P}_1(\mathbf{P})$ and $\varphi = \Pi_{\mathbf{P}}^{\mathcal{V}}(p^1)$. Since ∇p^1 is a constant vector, we have:

$$\begin{aligned} \nabla R_{\mathbf{P}}^{\mathcal{V}}(\Pi_{\mathbf{P}}^{\mathcal{V}}(p^1)) &= R_{\mathbf{P}}^{\mathcal{E}}(\nabla_h \Pi_{\mathbf{P}}^{\mathcal{V}}(p^1)) \quad [\text{use } \mathbf{(R3)}] \\ &= R_{\mathbf{P}}^{\mathcal{E}}(\Pi_{\mathbf{P}}^{\mathcal{E}}(\nabla p^1)) \quad [\text{use } \mathbf{(R4)}] \\ &= \nabla p^1. \end{aligned}$$

Thus, $R_{\mathbf{P}}^{\mathcal{V}}(\varphi) = p^1$ satisfies (3.46). We have already proved that the reconstruction operator $R_{\mathbf{f}}^{\mathcal{V}}$ is exact for linear functions; hence, $R_{\mathbf{P}}^{\mathcal{V}}(\varphi) = p^1$ satisfies boundary conditions (3.47). We conclude that $(R_{\mathbf{P}}^{\mathcal{V}} \circ \Pi_{\mathbf{P}}^{\mathcal{V}})(p^1) = p^1$.

Lemma 3.6. *Let \mathbf{e}_i for $i = 1, 2, 3$ be the i -th vector of the canonical basis of \mathbb{R}^3 . For every admissible reconstruction operator $R_{\mathbf{P}}^{\mathcal{V}}$ and every vertex-based mesh function $\varphi = (\varphi_{\mathbf{v}})_{\mathbf{v} \in \partial \mathbf{P}} \in \mathcal{V}_{h,\mathbf{P}}$ it holds:*

$$\int_{\mathbf{P}} R_{\mathbf{P}}^{\mathcal{V}}(\varphi) dV = \frac{1}{3} \sum_{\mathbf{f} \in \partial \mathbf{P}} (\mathbf{x}_{\mathbf{f}} - \mathbf{x}_{\mathbf{P}}) \cdot \mathbf{n}_{\mathbf{P},\mathbf{f}} \int_{\mathbf{f}} R_{\mathbf{f}}^{\mathcal{V}}(\varphi|_{\mathbf{f}}) dS, \quad (3.48)$$

where $R_f^{\mathcal{Y}}$ is any admissible reconstruction operator defined in Sect. 3.3.3.

Proof. Let us consider the identity $3 = \operatorname{div}(\mathbf{x} - \mathbf{x}_P)$. Integrating by parts and using the data locality property, we obtain

$$\begin{aligned} 3 \int_P R_P^{\mathcal{Y}}(\varphi) dV &= \int_P R_P^{\mathcal{Y}}(\varphi) \operatorname{div}(\mathbf{x} - \mathbf{x}_P) dV \\ &= - \int_P \nabla R_P^{\mathcal{Y}}(\varphi) \cdot (\mathbf{x} - \mathbf{x}_P) dV + \sum_{f \in \partial P} \int_f R_P^{\mathcal{Y}}(\varphi)|_f (\mathbf{x} - \mathbf{x}_P) \cdot \mathbf{n}_{P,f} dS \\ &= - \int_P \nabla R_P^{\mathcal{Y}}(\varphi) \cdot (\mathbf{x} - \mathbf{x}_P) dV + \sum_{f \in \partial P} \int_f R_f^{\mathcal{Y}}(\varphi|_f) (\mathbf{x} - \mathbf{x}_P) \cdot \mathbf{n}_{P,f} dS. \end{aligned} \quad (3.49)$$

The first integral term in the right-hand side is zero. Indeed, using the commuting property **(R3)** and the orthogonality property **(R4)**, we obtain:

$$\int_P \nabla R_P^{\mathcal{Y}}(\varphi) \cdot (\mathbf{x} - \mathbf{x}_P) dV = \int_P R_P^{\mathcal{E}}(\nabla_h \varphi) \cdot (\mathbf{x} - \mathbf{x}_P) dV = 0. \quad (3.50)$$

Using (3.50) in (3.49), we rewrite it as:

$$\int_P R_P^{\mathcal{Y}}(\varphi) dV = \frac{1}{3} \sum_{f \in \partial P} \int_f R_f^{\mathcal{Y}}(\varphi|_f) (\mathbf{x} - \mathbf{x}_P) \cdot \mathbf{n}_{P,f} dS. \quad (3.51)$$

The assertion of the lemma follows by noting that $(\mathbf{x} - \mathbf{x}_P) \cdot \mathbf{n}_{P,f}$ is constant on face f and can be evaluated at its barycenter \mathbf{x}_f . \square

Remark 3.5. Combining the results of Lemmas 3.6, 3.4, and 3.1, we conclude that the average of $R_P^{\mathcal{Y}}(\varphi)$ over cell P is the same for all admissible reconstruction operators and depends only on φ and a few geometrical quantities.

3.4 Mimetic inner products for a single cell

Let us return back to a generic space \mathcal{S}_h that can represent \mathcal{V}_h , \mathcal{E}_h , \mathcal{F}_h or \mathcal{P}_h . Its restriction to cell P , $\mathcal{S}|_P = \mathcal{S}_{h,P}$, represents $\mathcal{V}_{h,P}$, $\mathcal{E}_{h,P}$, $\mathcal{F}_{h,P}$, or $\mathcal{P}_{h,P}$. Any inner product can be represented by a symmetric positive-definite matrix:

$$[u_{h,P}, v_{h,P}]_{\mathcal{S}_{h,P}} = u_{h,P}^T M_{\mathcal{S},P} v_{h,P}, \quad \forall u_{h,P}, v_{h,P}. \quad (3.52)$$

We define the space \mathcal{T}_P of the test functions (see the consistency condition (3.1)) as the space of constant (scalar or vector) functions, i.e. $\mathcal{T}_P = \mathbb{P}_0(P)$. Let $v_{h,P} = \Pi_P^{\mathcal{S}}(v)$ for $v \in \mathcal{S}_{h,P}$. Using property (3.3), we can rewrite the consistency condition in the equivalent form:

$$[\Pi_P^{\mathcal{S}}(c), v_{h,P}]_{\mathcal{S}_{h,P}} = \int_{\Omega} c R_P^{\mathcal{S}}(v_{h,P}) dV \quad (3.53)$$

for all $v_{h,P} \in \mathcal{S}_{h,P}$ and any constant (scalar or vector) function $c \in \mathbb{P}_0(P)$.

We will systematically use this form of the consistency condition to derive its linear algebra form:

$$M_{\mathcal{S},P} N_{\mathcal{S},P} = R_{\mathcal{S},P}, \quad (3.54)$$

where matrices $N_{\mathcal{F},P}$ and $R_{\mathcal{F},P}$ are computable. This is the matrix equation with respect to the unknown matrix $M_{\mathcal{F},P}$. Hereafter, the construction is limited to a single cell P . Thus, for each particular space, we can safely drop the subscripts from our matrix notations and write $MN = R$.

Remark 3.6. We restrict our attention to the fundamental case of the standard L^2 scalar product. The extension to more a general scalar product, for instance, with a symmetric and strictly positive definite tensorial weight is introduced in Part II.

Before showing the inner products for the spaces $\mathcal{V}_{h,P}, \mathcal{E}_{h,P}, \mathcal{F}_{h,P}, \mathcal{D}_{h,P}$ in three dimensions, we complete the two-dimensional Example 3.1.

Example 3.2. Let us recall the consistency condition (3.7) for the mimetic inner product in space $\mathcal{F}_{h,P}$ in two dimensions

$$[\Pi_P^{\mathcal{F}}(\nabla q), \mathbf{v}_{h,P}]_{\mathcal{F}_{h,P}} = \sum_{f \in \partial P} v_f \int_f q dS \quad \forall \mathbf{v}_{h,P} \in \mathcal{F}_{h,P}, \forall q \in \mathbb{P}_1(P)/\mathbb{R}, \quad (3.55)$$

where $\mathbf{v}_{h,P} = (v_f)_{f \in \partial P}$.

We select a natural basis for the quotient space $\mathbb{P}_1(P)/\mathbb{R} = \text{span}\{x - x_P, y - y_P\}$, where x, y are the Cartesian coordinates and (x_P, y_P) is the barycenter of P . Inserting $q = x - x_P$ in (3.55), we get

$$[\Pi_P^{\mathcal{F}}(\mathbf{e}_1), \mathbf{v}_{h,P}]_{\mathcal{F}_{h,P}} = \sum_{f \in \partial P} v_f \int_f (x - x_P) dS \quad (3.56)$$

where the vector $\mathbf{e}_1 = (1, 0)^T$. By enumerating the faces of P , the right hand side above can be written as a scalar product of the vectors $\mathbf{v}_{h,P}$ and $R_1 = (R_{1,f})_{f \in \partial P}$, with

$$R_{1,f} = \int_f (x - x_P) dS \quad \forall f \in \partial P.$$

Let $N_1 = \Pi_P^{\mathcal{F}}(\mathbf{e}_1)$. Then, (3.56) can be expressed as an algebraic condition on the local inner product matrix:

$$MN_1 = R_1.$$

The same argument applied to $q = y - y_P$ leads to the second algebraic condition $MN_2 = R_2$ where $N_2 = \Pi_P^{\mathcal{F}}(\mathbf{e}_2)$, $R_2 = (R_{2,f})_{f \in \partial P}$, and $R_{2,f} = \int_f (y - y_P) dS$. We can combining the two algebraic conditions in one matrix equation:

$$MN = R, \quad (3.57)$$

where $N = [N_1, N_2]$ and $R = [R_1, R_2]$. Equation (3.57) is the algebraic form of the consistency condition. Solution of this equation is given briefly in Sect. 3.4.5 and in more details in Chap. 4. \square

As a final remark, we note that the construction of other inner product matrices follow the same pattern that starts from a consistency condition, that can be represented as a surface integral as in (3.55) and leads to the typical mimetic equation $MN = R$, but with different matrices N and R .

3.4.1 Mimetic inner product in $\mathcal{Y}_{h,P}$

For every constant function c defined on cell P and any vertex-based mesh function φ from $\mathcal{Y}_{h,P}$, we apply the consistency condition (3.53) to obtain

$$[\varphi, \Pi_P^{\mathcal{Y}}(c)]_{\mathcal{Y}_{h,P}} = \int_P R_P^{\mathcal{Y}}(\varphi) c dV. \quad (3.58)$$

Let us take $c = 1$ as a basis for the space of constant functions. Applying first Lemma 3.6 and then Lemma 3.4, and finally Lemma 3.1, we obtain

$$[\varphi, \Pi_P^{\mathcal{Y}}(1)]_{\mathcal{Y}_{h,P}} = \frac{1}{3} \sum_{f \in \partial P} (\mathbf{x}_f - \mathbf{x}_P) \cdot \mathbf{n}_{P,f} \sum_{e \in \partial f} (\boldsymbol{\xi}_e - \boldsymbol{\xi}_f) \cdot \mathbf{n}_{f,e} \frac{\varphi_{v_1} + \varphi_{v_2}}{2} |e|, \quad (3.59)$$

where we recall that $\boldsymbol{\xi}_e$ is the midpoint of edge $e \in \partial f$, $\boldsymbol{\xi}_f$ and \mathbf{x}_f denote the barycenter of face f in a local and the global coordinate systems, and $\mathbf{n}_{f,e}$ is the unit vector orthogonal to $e \in \partial f$ in the plane containing f . Reordering the above sum yields

$$\begin{aligned} [\varphi, \Pi_P^{\mathcal{Y}}(1)]_{\mathcal{Y}_{h,P}} &= \frac{1}{6} \sum_{v \in \partial P} \sum_{\substack{e \in \partial f \\ e \ni v}} \sum_{\substack{f \in \partial P \\ f \ni e}} (\mathbf{x}_f - \mathbf{x}_P) \cdot \mathbf{n}_{P,f} (\boldsymbol{\xi}_e - \boldsymbol{\xi}_f) \cdot \mathbf{n}_{f,e} \varphi_v |e| \\ &\equiv \sum_{v \in \partial P} R_{1,v} \varphi_v, \end{aligned} \quad (3.60)$$

with the obvious definition of coefficients $R_{v,1}$. Collecting these coefficients, we form a vector $R_1 \in \mathcal{Y}_{h,P}$:

$$R_1 = (R_{1,v})_{v \in \partial P}.$$

Let $N_1 = \Pi_P^{\mathcal{Y}}(1)$. The definition of the projection operator implies that all components of vector N_1 equal to 1. Using the matrix representation of the inner product (see formula (3.52)), we rewrite (3.60) as follows:

$$\varphi^T M N_1 = \varphi^T R_1.$$

Since φ is an arbitrary vector, we obtain the matrix equation

$$M N_1 = R_1.$$

Comparing with (3.54), we conclude that matrices N and R are single-column matrices in the considered case.

Remark 3.7. Recall that the reconstruction operator $R_P^{\mathcal{Y}}$ is also exact for linear functions. Therefore, the above construction can be extended in order to satisfy the consistency condition (3.53) for any test function in $\mathbb{P}_1(P)$.

3.4.2 Mimetic inner product in $\mathcal{E}_{h,P}$

Let $\{\mathbf{e}_1, \mathbf{e}_2, \mathbf{e}_3\}$ denote the canonical basis of \mathbb{R}^3 . Treating \mathbf{e}_i , $i = 1, 2, 3$, as constant vector functions over cell P , $\{\mathbf{e}_1, \mathbf{e}_2, \mathbf{e}_3\}$ form a basis for $[\mathbb{P}_0(P)]^3$. For every $i = 1, 2, 3$ and any edge-based mesh function φ in $\mathcal{E}_{h,P}$, we apply the consistency condi-

tion (3.53) to obtain

$$[\varphi, \Pi_P^\mathcal{E}(\mathbf{e}_i)]_{\mathcal{E}_{h,P}} = \int_P R_P^\mathcal{E}(\varphi) \cdot \mathbf{e}_i \, dV. \quad (3.61)$$

We develop the right-hand side using first Lemma 3.5 and then Lemma 3.2. From the first lemma it follows that

$$[\varphi, \Pi_P^\mathcal{E}(\mathbf{e}_i)]_{\mathcal{E}_{h,P}} = \frac{1}{2} \sum_{f \in \partial P} \boldsymbol{\alpha}_{f,i} \cdot \int_f R_f^\mathcal{E}(\varphi|_f) \, dS, \quad (3.62)$$

where $R_f^\mathcal{E}$ is any admissible reconstruction operator for $f \in \partial P$ and the vector-valued constant $\boldsymbol{\alpha}_{f,j} \in \mathbb{R}^2$ is given by (3.39):

$$\boldsymbol{\alpha}_{f,i} = (\mathbf{n}_{P,f} \cdot (\mathbf{x}_f - \mathbf{x}_P) \mathbf{e}_i + \mathbf{n}_{P,f} \cdot \mathbf{e}_i (\mathbf{x}_P - \mathbf{x}_f))_{\perp, f}, \quad (3.63)$$

where \mathbf{x}_f and \mathbf{x}_P are the barycenters of f and P , respectively. Each vector $\boldsymbol{\alpha}_{f,i}$ lies on the two-dimensional face f and can be expanded in the canonical basis $\{\boldsymbol{\eta}_1, \boldsymbol{\eta}_2\}$ of \mathbb{R}^2 as:

$$\boldsymbol{\alpha}_{f,i} = \sum_{k=1}^2 \alpha_{f,i,k} \boldsymbol{\eta}_k.$$

From Lemma 3.2 it follows that for every admissible reconstruction operator $R_f^\mathcal{E}$ and every edge function $\varphi = (\varphi_e)_{e \in \partial f} \in \mathcal{E}_{h,f}$ it holds that

$$\boldsymbol{\alpha}_{f,i} \cdot \int_f R_f^\mathcal{E}(\varphi|_f) \, dS = \sum_{k=1}^2 \alpha_{f,i,k} \boldsymbol{\eta}_k \cdot \int_f R_f^\mathcal{E}(\varphi|_f) \, dS = - \sum_{k=1}^2 \alpha_{f,i,k} \sum_{e \in \partial f} \alpha_{f,e} \varphi_e \int_e p_k^1 \, dL,$$

where $\boldsymbol{\eta}_k = \text{curl } p_k^1$. The orientation of tangent vectors $\boldsymbol{\tau}_e$ is now important. We no longer can make a simplifying assumption, like in Lemma 3.2 and must carry around the factor $\alpha_{f,e} = \pm 1$. Taking $p_k^1(\boldsymbol{\xi}) = \boldsymbol{\eta}_k \times (\boldsymbol{\xi} - \boldsymbol{\xi}_f)$ and re-ordering summations, we obtain

$$\begin{aligned} [\varphi, \Pi_P^\mathcal{E}(\mathbf{e}_i)]_{\mathcal{E}_{h,P}} &= -\frac{1}{2} \sum_{k=1}^2 \sum_{f \in \partial P} \alpha_{f,i,k} \sum_{e \in \partial f} \alpha_{f,e} \varphi_e |e| (\boldsymbol{\eta}_k \times (\boldsymbol{\xi}_e - \boldsymbol{\xi}_f)) \\ &= \sum_{e \in \mathcal{E}_P} \left(-\frac{1}{2} \sum_{k=1}^2 \sum_{f \in \partial P} \sum_{e \in \partial f} \alpha_{f,i,k} \alpha_{f,e} |e| (\boldsymbol{\eta}_k \times (\boldsymbol{\xi}_e - \boldsymbol{\xi}_f)) \right) \varphi_e \\ &\equiv \sum_e R_{i,e} \varphi_e, \end{aligned} \quad (3.64)$$

with the obvious definition of coefficients $R_{i,e}$. Collecting these coefficients, we form a vector $R_i \in \mathcal{E}_{h,P}$:

$$R_i = (R_{i,e})_{e \in \partial P}.$$

Let $N_i = \Pi_P^\mathcal{E}(\mathbf{e}_i)$. Using the matrix representation of the inner product (see formula (3.52)), we rewrite (3.64) as follows:

$$\boldsymbol{\varphi}^T M N_i = \boldsymbol{\varphi}^T R_i.$$

Since φ is an arbitrary vector, for each i , we obtain the matrix equation

$$MN_i = R_i.$$

Let us form matrices $R = [R_1, R_2, R_3]$ and $N = [N_1, N_2, N_3]$. We conclude that the algebraic form of the generic consistency condition (see formula (3.54)) in the considered case is $MN = R$ with the three-column matrices N and R .

3.4.3 Mimetic inner product in $\mathcal{F}_{h,P}$

For every constant vector \mathbf{e}_i , $i = 1, 2, 3$, as in the previous subsection, and for every face-based mesh function $\varphi \in \mathcal{F}_{h,P}$, we apply the consistency condition (3.53), to obtain

$$[\varphi, \Pi_P^{\mathcal{F}}(\mathbf{e}_i)]_{\mathcal{F}_{h,P}} = \int_P R_P^{\mathcal{F}}(\varphi) \cdot \mathbf{e}_i dV. \quad (3.65)$$

We develop the right-hand side using Lemma 3.3:

$$[\varphi, \Pi_P^{\mathcal{F}}(\mathbf{e}_i)]_{\mathcal{F}_{h,P}} = \sum_{f \in \partial P} \varphi_f \mathbf{e}_i \cdot (\mathbf{x}_f - \mathbf{x}_P) |f| \equiv \sum_{f \in \partial P} \varphi_f R_{i,f}, \quad (3.66)$$

with the obvious definition of coefficients $R_{i,f}$. Collecting these coefficients, we form a vector $R_i \in \mathcal{E}_{h,P}$, $R_i = (R_{i,f})_{f \in \partial P}$. Let $N_i = \Pi_P^{\mathcal{F}}(\mathbf{e}_i)$. Using the matrix representation of the inner product (see formula (3.52)), we rewrite (3.66) as follows:

$$\varphi^T MN_i = \varphi^T R_i.$$

Let us form matrices $R = [R_1, R_2, R_3]$ and $N = [N_1, N_2, N_3]$. We conclude that the algebraic form of the generic consistency condition (see formula (3.54)) in the considered case is $MN = R$ with the three-column matrices N and R .

3.4.4 Mimetic inner product in $\mathcal{P}_{h,P}$

This case is trivial, since $\varphi \in \mathcal{P}_{h,P}$ is just the number φ_P . Let $\psi \in \mathcal{P}_{h,P}$. The consistency condition (3.53) with $c = \psi_P$ gives

$$[\varphi, \Pi_P^{\mathcal{P}}(\psi_P)]_{\mathcal{P}_{h,P}} = \int_P R_P^{\mathcal{P}}(\varphi) \psi_P dV = |P| \varphi_P \psi_P.$$

Hence, $M = |P|$.

3.4.5 Formula for the inner product matrix

Consider the matrix equation $MN = R$ with matrices N and R derived above. Here, we give a quick solution to this equation and leave its detailed analysis to Chap. 4 and Part II.

A simple proof by contradiction can be used to show that matrix N has a full rank. Let us show that matrix R has also a full rank. If we take $u_{h,P}$ and $v_{h,P}$ in definition (3.52) as the columns of matrix N , apply the consistency condition (3.59)

and the accuracy property **(R3)**, we obtain:

$$[u_{h,P}, v_{h,P}]_{\mathcal{S}_{h,P}} = \mathbf{N}_i^T \mathbf{M} \mathbf{N}_j = \mathbf{R}_i^T \mathbf{N}_j = \int_P c_i c_j dV,$$

where c_i and c_j are constant (scalar or vector) functions generating vectors \mathbf{N}_i and \mathbf{N}_j , respectively. Since, functions c_i are orthogonal basis functions, the product $\mathbf{N}^T \mathbf{R}$ is the diagonal positive definite matrix; hence, non-singular. This implies that matrix \mathbf{R} must have a full rank.

A partial solution to the matrix equation is given by

$$\mathbf{M}^0 = \mathbf{R}(\mathbf{R}^T \mathbf{N})^{-1} \mathbf{R}^T,$$

which can be verified by direct substitution. The matrix \mathbf{M}^0 is positive semi-definite, and it is positive definite only when the number of rows in \mathbf{N} is bigger than the number of columns. The problem is rectified by adding to \mathbf{M}^0 another positive semi-definite matrix \mathbf{M}^1 such that $\mathbf{M}^1 \mathbf{N} = 0$, e.g.

$$\mathbf{M}^1 = \gamma(\mathbf{I} - \mathbf{N}(\mathbf{N}^T \mathbf{N})^{-1} \mathbf{N}^T), \quad \gamma > 0.$$

The final solution, recommended for practical calculations is given by

$$\mathbf{M} = \mathbf{M}^0 + \mathbf{M}^1 = \mathbf{R}(\mathbf{R}^T \mathbf{N})^{-1} \mathbf{R}^T + \frac{1}{m} \text{trace}(\mathbf{M}^0) (\mathbf{I} - \mathbf{N}(\mathbf{N}^T \mathbf{N})^{-1} \mathbf{N}^T), \quad (3.67)$$

where m is the size of matrix \mathbf{M} . It is not difficult to show that this matrix is always positive definite, for instance, using a proof by contradiction. A more difficult task is to prove that it satisfies the stability condition (3.2) which is only true for shape-regular cells. Detailed analysis of the stability condition is presented in the next chapter after a generalization of the consistency condition.

Remark 3.8. Formula (3.67) gives only one of the possible solutions to the matrix equation $\mathbf{M} \mathbf{N} = \mathbf{R}$. A complete family of solutions is derived later. This family contains matrices \mathbf{M} for which we can prove existence of reconstruction operators $R_P^{\mathcal{S}}(\cdot)$ such that formula (3.4) holds true. It may also contain matrices for which the existing analysis tools are insufficient to give a definite answer.

Mimetic discretization of bilinear forms

*"Complexity that works is built up
out of modules that work perfectly,
layered one over the other."
(Kevin Kelly)*

In the previous chapter we described the mimetic inner products that are low-order approximations of classical L^2 products of continuum functions u and v :

$$[u_{h,P}, v_{h,P}]_{\mathcal{S}_h, P} = \int_P u v dV + O(h_P) |P|,$$

where $u_{h,P}, v_{h,P}$ are discrete mesh functions from a space \mathcal{S}_h :

$$u_{h,P} = \Pi_{h,P}^{\mathcal{S}}(u), \quad v_{h,P} = \Pi_{h,P}^{\mathcal{S}}(v).$$

In this chapter, we extend the developed discretization tools to more general bilinear forms. More precisely, let us consider an elliptic problem:

Find $u \in X$ such that:

$$\mathcal{B}(u, v) = \langle f, v \rangle \quad \forall v \in X, \tag{4.1}$$

where X is a Hilbert space, $\mathcal{B} : X \times X \rightarrow \mathbb{R}$ is a symmetric, continuous and coercive bilinear form and f is a loading term in the dual space of X . Essential boundary conditions are included in the definition of X . Natural boundary conditions are included in the definition of the loading term. Due to the Lax-Milgram lemma, the problem is well posed [80].

The mimetic discretization of problem (4.1) includes three steps that are typical for all discretization methods; however, each step has features that are unique for the mimetic approach.

1. *Definition of the discrete space \mathcal{S}_h .* We define the space \mathcal{S}_h through the degrees of freedom, which are real numbers associated with a collection of various geometric objects such as cells, faces, edges and/or vertices of a mesh Ω_h . The choice of the degrees of freedom is, obviously, problem dependent. Examples of \mathcal{S}_h include the fundamental spaces $\mathcal{P}_h, \mathcal{F}_h, \mathcal{E}_h, \mathcal{V}_h$ introduced in Chap. 2. The mimetic approach allows us to mix degrees of freedom with different physical meaning (pointwise values, moments, normal and tangential components of tensors) associated with different geometric objects. In contrast with the finite

element method, no shape functions are constructed explicitly; hence, no unisolvency condition is needed.

2. *Construction of the discrete bilinear form $\mathcal{B}_h : \mathcal{S}_h \times \mathcal{S}_h \rightarrow \mathbb{R}$.* Since the MFD method does not use shape functions in its construction, the discrete bilinear forms are built from different principles called the *consistency* and *stability* conditions. The consistency condition is an exactness property stating that the bilinear form \mathcal{B}_h reproduces exactly (up to some reconstruction operator) the continuum form \mathcal{B} when at least one of its two arguments lives in a special subspace of \mathcal{S}_h . The stability condition guarantees that the discrete bilinear form \mathcal{B}_h is uniformly coercive and continuous, which leads to a well-posed scheme.
3. *Construction of the discrete loading term $\langle f, \cdot \rangle_{\mathcal{Q}_h} : \mathcal{S}_h \rightarrow \mathbb{R}$.* The discrete loading term is a continuous linear operator that approximates the right-hand side of (4.1).

Once these steps are completed, the mimetic scheme reads as follows: *Find $u_h \in \mathcal{S}_h$ such that:*

$$\mathcal{B}_h(u_h, v_h) = \langle f, v_h \rangle_{\mathcal{Q}_h} \quad \forall v_h \in \mathcal{S}_h. \quad (4.2)$$

The above construction uses a direct discretization of the variational form of the problem and is different from the approach proposed in Chap. 2 that reformulates the original second-order PDE as a system of two first-order equations. Although the two approaches turn out to be often equivalent (at the level of discrete equations), this second one has a wider range of applications.

In the subsequent sections, we will develop a framework for a proper choice of the discrete space \mathcal{S}_h and the construction of the bilinear form \mathcal{B}_h . We will also discuss the implementation of \mathcal{B}_h in a computer program. The construction of $\langle f, \cdot \rangle_{\mathcal{Q}_h}$ will be discussed in the next chapters for specific PDEs.

Remark 4.1. In the case of simplicial meshes, the MFD method leads often to the same scheme as a finite element method that uses the same degrees of freedom. The proposed framework can be used as an alternative numerical approach to the construction of local stiffness and mass matrices. For instance, a practical implementation of high-order finite element methods (e.g. Argyris element) can be done more efficiently using the MFD framework.

4.1 Discrete bilinear forms

We assume that the bilinear form \mathcal{B} is given in the form of an integral over a computational domain Ω . If Ω_h is a subdivision of Ω into polyhedral cells P (see Sect. 1.6.2), \mathcal{B} can be split into the sum of local terms

$$\mathcal{B}(u, v) = \sum_{P \in \Omega_h} \mathcal{B}_P(u, v) \quad \forall u, v \in X, \quad (4.3)$$

where \mathcal{B}_P is a symmetric and positive semi-definite bilinear form associated with cell P . By analogy with (4.3), we split the bilinear form \mathcal{B}_h into the sum of local

terms

$$\mathcal{B}_h(u_h, v_h) = \sum_{P \in \Omega_h} \mathcal{B}_{h,P}(u_{h,P}, v_{h,P}) \quad \forall u_h, v_h \in \mathcal{S}_h, \quad (4.4)$$

where $\mathcal{B}_{h,P} : \mathcal{S}_{h,P} \times \mathcal{S}_{h,P} \rightarrow \mathbb{R}$ is a symmetric and positive semi-definite bilinear form associated with cell P and $\mathcal{S}_{h,P} = \mathcal{S}_{h|P}$. Let $n_{\mathcal{S}_{h,P}}$ denote the dimension of the local space $\mathcal{S}_{h,P}$.

Let us consider a polyhedral cell P and define the *kernel of the bilinear form* \mathcal{B}_P as follows:

$$\ker(\mathcal{B}_P) = \{v \in X|_P \text{ such that } \mathcal{B}_P(v, v) = 0\}. \quad (4.5)$$

We also define a sufficiently rich finite-dimensional space of *trial functions* \mathcal{T}_P such that the following inclusions hold:

$$\ker(\mathcal{B}_P) \subseteq \mathcal{T}_P \subset X|_P \quad \text{and} \quad \mathbb{P}_k(P) \subseteq \mathcal{T}_P \quad (4.6)$$

for some integer $k \in \mathbb{N}$.

Remark 4.2. Our notation is tailored for spaces of scalar functions. In the case of spaces of vector-valued functions, we replace the second inclusion by $(\mathbb{P}_k(P))^d \subseteq \mathcal{T}_P$ where $d > 1$ is the space dimension.

Let $n_{\mathcal{T}_P}$ denote the dimension of space \mathcal{T}_P and functions q^j form a basis in this space:

$$\mathcal{T}_P = \text{span}\{q^1, q^2, \dots, q^{n_{\mathcal{T}_P}}\}.$$

The requirement that a polynomial space is included in \mathcal{T}_P is necessary to ensure the accuracy of the method. In practice, it often holds that $\mathcal{T}_P = \mathbb{P}_k(P)$ for some integer k . The other requirement, $\ker(\mathcal{B}_P) \subseteq \mathcal{T}_P$, is used in Sect. 4.3 to assure that the local discrete bilinear forms $\mathcal{B}_{h,P}$ reproduces the kernel of the continuum form \mathcal{B}_P .

Like in the previous chapter, we consider a subspace $S_{h,P} \subset X|_P$. Again, this space is never constructed explicitly and only its generic properties are used in the MFD method.

(B1) The projection operator $\Pi_P^S : X|_P \rightarrow \mathcal{S}_{h,P}$ restricted to $S_{h,P}$ is surjective on $\mathcal{S}_{h,P}$, i.e. $\mathcal{S}_{h,P} = \Pi_P^S(S_{h,P})$.

(B2) $S_{h,P}$ contains the trial space \mathcal{T}_P .

(B3) $\mathcal{B}_P(v, q)$ with $v \in S_{h,P}$ and $q \in \mathcal{T}_P$ can be computed *exactly* using only q and the degrees of freedom of v .

Note that the space $S_{h,P}$ can be infinite dimensional and in general it may be convenient (and simpler) to keep it like that avoiding to enforce further conditions on $S_{h,P}$. Nevertheless, one can always choose a space $S_{h,P}$ (possibly by selecting a subspace) such that

$$\dim(S_{h,P}) = \dim(\mathcal{S}_{h,P}). \quad (4.7)$$

In such case the projection operator $\Pi_{\mathcal{P}}^S$ becomes an invertible application from $S_{h,\mathcal{P}}$ into $\mathcal{S}_{h,\mathcal{P}}$ and the discrete fields in $\mathcal{S}_{h,\mathcal{P}}$ are the degrees of freedom of the functions in $S_{h,\mathcal{P}}$. Thus, each function $v \in S_{h,\mathcal{P}}$ is uniquely determined by its degrees of freedom $\Pi_{\mathcal{P}}^S(v)$ and the choice of $S_{h,\mathcal{P}}$ determines a reconstruction operator

$$R_{\mathcal{P}}^{\mathcal{S}} : \mathcal{S}_{h,\mathcal{P}} \rightarrow S_{h,\mathcal{P}}.$$

The reconstruction operator $R_{\mathcal{P}}^{\mathcal{S}}$ must satisfy a different set of conditions compared to the reconstruction operators of Chap. 3. Indeed, properties **(R3)**–**(R4)** depend on the definition of the bilinear form $\mathcal{B}_{\mathcal{P}}$. The right inverse property **(R1)** and the accuracy property **(R2)** are now replaced automatically by the fact that the reconstruction operator is the inverse of the projection operator on space $S_{h,\mathcal{P}}$.

Like in Chap. 3, a family of reconstruction operators may exist. Different reconstruction operators define different spaces $S_{h,\mathcal{P}}$. The properties **(B2)** and **(B3)** are common for all reconstruction operators in the family and are required to ensure the accuracy of the MFD method. Stability of the method is controlled by imposing uniform bounds on the reconstruction operators.

The property **(B3)** is fundamental to establish an algebraic form of the consistency condition that makes the derivation of the method possible. This derivation uses only the degrees of freedom of $v \in S_{h,\mathcal{P}}$ and is independent of the reconstruction operator. In low-order mimetic schemes, the degrees of freedom are often related to the boundary of \mathcal{P} and the space $S_{h,\mathcal{P}}$ is selected to reduce the computation of $\mathcal{B}_{\mathcal{P}}(v, q)$ to $\partial\mathcal{P}$. In high-order mimetic schemes, some degrees of freedom of v may be also related to the interior of \mathcal{P} such as cell moments with respect to the polynomials. In such a case, the computation of $\mathcal{B}_{\mathcal{P}}(v, q)$ is more involved but again feasible with a proper selection of $S_{h,\mathcal{P}}$. We stress again that in a computer program, we do not need to construct the space $S_{h,\mathcal{P}}$ as well as the reconstruction operator.

Remark 4.3. In contrast to the previous chapter, in the present one we will focus more on the space $S_{h,\mathcal{P}}$ rather than on the reconstruction operator. The two approaches are equivalent, as noted in Remark 3.2.

4.1.1 Consistency condition

Definition 4.1 (Consistency condition). We say that the bilinear form $\mathcal{B}_{h,\mathcal{P}}$ satisfies the *consistency condition* if

$$\mathcal{B}_{h,\mathcal{P}}(\Pi_{\mathcal{P}}^S(v), \Pi_{\mathcal{P}}^S(q)) = \mathcal{B}_{\mathcal{P}}(v, q) \quad \forall v \in S_{h,\mathcal{P}}, \forall q \in \mathcal{T}_{\mathcal{P}}. \quad (4.8)$$

Condition (4.8) is compatible with the symmetry of $\mathcal{B}_{\mathcal{P}}$ and $\mathcal{B}_{h,\mathcal{P}}$, and is in fact the *accuracy property*. Whenever $\mathcal{B}_{h,\mathcal{P}}$ is applied to the degrees of freedom of a function in $\mathcal{T}_{\mathcal{P}}$ and of a function in $S_{h,\mathcal{P}}$, it returns the exact value of the bilinear form $\mathcal{B}_{\mathcal{P}}$. If (4.7) holds, we can reformulate the consistency condition using the reconstruction operator as follows.

Definition 4.2 (Consistency condition, alternative definition). We say that the bilinear form $\mathcal{B}_{h,P}$ satisfies the *consistency condition* if

$$\mathcal{B}_{h,P}(\Pi_P^S(q), v_{h,P}) = \mathcal{B}_P(q, R_P^S(v_{h,P})) \quad \forall v_{h,P} \in \mathcal{S}_{h,P}, \forall q \in \mathcal{T}_P. \quad (4.9)$$

Let us illustrate these preliminary developments with an example.

Example 4.1. Let us consider a convex polygon P and take $X_P = H^1(P)$. Let $\mathcal{S}_{h,P} = \mathcal{V}_{h,P}$ and

$$\mathcal{B}_P(u, v) = \int_P K_P \nabla u \cdot \nabla v dV, \quad (4.10)$$

where K_P is a constant tensor. Thus, we are looking for a node-based discretization of the Poisson equation.

Let $\mathcal{T}_P = \mathbb{P}_1(P)$ be the space of linear polynomials, $u = q$ for some $q \in \mathcal{T}_P$, and $v_{h,P} = \Pi_P^V(v)$. Integrating the right-hand side of the consistency condition (4.8) by parts and noting that $K_P \nabla q$ is a constant vector, we obtain:

$$\begin{aligned} \mathcal{B}_P(q, v) &= - \int_P \operatorname{div}(K_P \nabla u) v dV + \int_{\partial P} (\mathbf{n}_P \cdot K_P \nabla q) v dS \\ &= \sum_{e \in \partial P} \mathbf{n}_{P,e} \cdot K_P \nabla q \int_e v dS, \end{aligned} \quad (4.11)$$

where e denotes an edge of ∂P and $\mathbf{n}_{P,e}$ its exterior normal vector. Each edge integral could be calculated exactly using, for example, the trapezoidal rule if v were a linear function along the edge. For the edge e connecting the couple of vertices (v_1, v_2) , we could obtain:

$$\int_e v dS = \frac{|e|}{2} (v(\mathbf{x}_{v_1}) + v(\mathbf{x}_{v_2})) = \frac{|e|}{2} (v_{v_1} + v_{v_2}). \quad (4.12)$$

In general, the linearity assumption is not required. Instead, we can define $S_{h,P}$ as any space of functions that can be integrated exactly on edges $e \in \partial P$ with the trapezoidal rule,

$$S_{h,P} \subset \left\{ v \in H^1(P) \cap C^0(\bar{P}) : \int_e v dS = \frac{|e|}{2} (v(\mathbf{x}_{v_1}) + v(\mathbf{x}_{v_2})) \quad \forall e = (v_1, v_2) \in \partial P \right\},$$

and such that $S_{h,P}$ contains the space $\mathcal{T}_P = \mathbb{P}_1(P)$. Note that the two conditions above are clearly compatible since the restriction of a linear function to an edge is a linear one dimensional function.

One does not really need to define further the space $S_{h,P}$ since the information above is sufficient to implement the consistency condition and build the local bilinear form. Nevertheless, if one prefers to define a finite dimensional space $S_{h,P}$ (isomorphic to $\mathcal{S}_{h,P}$), a possible choice is given by the solutions of the harmonic problems:

$$\begin{aligned} \operatorname{div}(K \nabla v) &= 0 && \text{in } P, \\ v|_e &= \tilde{v}_e && \text{on } e \in \partial P, \end{aligned}$$

where \tilde{v}_e is the linear interpolation of the edge end-point values $v(\mathbf{x}_{v_1}) = v_{v_1}$ and $v(\mathbf{x}_{v_2}) = v_{v_2}$. If polygon P has a non-trivial shape, explicit calculation of the basis functions in $S_{h,P}$ will be an expensive procedure and must be avoided. In any case, the final form of the consistency condition for the present example becomes

$$\mathcal{B}_{h,P}(\Pi_P^S(q), v_{h,P}) = \sum_{e \in \partial P} \frac{|e|}{2} (\mathbf{n}_{P,e} \cdot \mathbf{K}_P \nabla q)(v_{v_1} + v_{v_2})$$

for all $q \in \mathcal{T}_P = \mathbb{P}_1(P)$ and for all $v_{h,P} \in \mathcal{V}_{h,P}$. Note that we have derived the above explicit condition without the complete knowledge of the functions in $S_{h,P}$. \square

4.1.2 Stability condition

The symmetric and positive semi-definite bilinear form $\mathcal{B}_{h,P}$ can be represented by a symmetric and positive semi-definite matrix M_P :

$$\mathcal{B}_{h,P}(u_{h,P}, v_h) = u_{h,P}^T M_P v_{h,P}. \quad (4.13)$$

We show later that if the dimension of the trial space \mathcal{T}_P is less than the size of matrix M_P , the consistency condition does not define a unique matrix M_P . For the bilinear form considered in Example 4.1, matrix M_P has size n , where n is the number of vertices of P . Since the dimension of \mathcal{T}_P is three, we obtain a family of matrices that satisfy the consistency condition whenever $n \geq 4$.

The aforementioned family may include ill-conditioned matrices and a stability condition is required to ensure the well-posedness of the discrete problem. The stability condition can be formulated in various norms. For the moment, we consider a local semi-norm $\|v_{h,P}\|_{\mathcal{S}_{h,P}}$ on $\mathcal{S}_{h,P}$, which is such that $\|v_{h,P}\|_{\mathcal{S}_{h,P}} = 0$ if and only if $v_{h,P} = \Pi_P^S(v)$ for some function $v \in \ker(\mathcal{B}_P)$, and we define the global semi-norm as follows:

$$\|v_h\|_{\mathcal{S}_h}^2 = \sum_{P \in \Omega_h} \|v_{h,P}\|_{\mathcal{S}_{h,P}}^2 \quad \forall v_h \in \mathcal{S}_h.$$

In most practical cases, this operator defines a norm on a subspace of mesh functions that satisfy the essential boundary conditions.

Definition 4.3 (Stability condition). There exist two positive constants C_\star and C^\star , which are independent of h and P , such that

$$C_\star \|v_{h,P}\|_{\mathcal{S}_{h,P}}^2 \leq \mathcal{B}_{h,P}(v_{h,P}, v_{h,P}) \leq C^\star \|v_{h,P}\|_{\mathcal{S}_{h,P}}^2 \quad \forall v_{h,P} \in \mathcal{S}_{h,P}. \quad (4.14)$$

The definition of the discrete semi-norm $\|v_{h,P}\|_{\mathcal{S}_{h,P}}$ is clearly problem dependent but, most importantly, it does not depend on the reconstruction operator. In practice, we often consider a semi-norm that is spectrally equivalent to $\mathcal{B}_P(R_P^{\mathcal{J}}(v_{h,P}), R_P^{\mathcal{J}}(v_{h,P}))$ and is easily computable. Let us illustrate this with the following example.

Example 4.2. Let us consider the bilinear form and the discrete space $\mathcal{V}_{h,P}$ from Example 4.1. Using definition of the primary gradient operator (2.19), we introduce

the mesh-dependent semi-norm

$$\| \| v_{h,P} \| \|_{\mathcal{V}_{h,P}}^2 = |P| \sum_{e \in \partial P} (\nabla_h v_{h,P})_e^2 = |P| \sum_{e=(v_1,v_2) \in \partial P} \frac{v_{v_2} - v_{v_1}}{|e|}^2. \quad (4.15)$$

Clearly, $\| \| v_{h,P} \| \|_{\mathcal{V}_{h,P}} = 0$ if and only if $v_{h,P}$ is a constant vertex-based mesh function. Thus, the kernels of $\| \| \cdot \| \|_{\mathcal{V}_{h,P}}$ and $\mathcal{B}_{h,P}$ coincide. Indeed, let c be a constant function on P and $c_{h,P} = \Pi_P^S(c)$. Since, c belongs to \mathcal{T}_P , definition (4.10) implies that:

$$\mathcal{B}_{h,P}(c_{h,P}, c_{h,P}) = \mathcal{B}_{h,P}(\Pi_P^S(c), c_{h,P}) = \mathcal{B}(c, c) = 0.$$

Finally, it can be easily checked that, under suitable mesh assumptions, the local semi-norms above scale, with respect to the element size h_P , as the $H^1(P)$ semi-norm. \square

4.2 Algebraic form of the consistency condition

Here, we derive the algebraic equations for the matrix M_P in (4.13). In view of splitting (4.4), the global matrix representing \mathcal{B}_h is built by assembling the local matrices M_P . In order to simplify the exposition, let us assume that (4.7) holds. We stress again that such a condition is not restrictive as one can always choose a subspace of the space $S_{h,P}$.

For any $q \in \mathcal{T}_P$, $v \in S_{h,P}$ and $v_{h,P} = \Pi_P^S(v)$, the right-hand side of the consistency condition (4.8) is a linear functional with respect to $v_{h,P}$ and thus (4.2) can be written as

$$\mathcal{B}_{h,P}(\Pi_P^S(q), v_{h,P}) = R_q^T v_{h,P} \quad \forall v_{h,P} \in \mathcal{S}_{h,P}, \quad (4.16)$$

where vector $R_q \in \mathcal{V}_{h,P}$ depends on q and the bilinear form \mathcal{B} . Note that the right hand sides of (4.1) and (4.2), and thus R_q , is computable thanks to assumption **(B3)**. Vector R_q depends linearly on q and so does the projection operator $\Pi_P^S(q)$. Therefore, it is sufficient to enforce the above equality only for functions q^i , $i = 1, \dots, n_{\mathcal{T}_P}$, that form a basis of \mathcal{T}_P . Let us define the following vectors:

$$N_i = \Pi_P^S(q^i) \quad \text{and} \quad R_i = R_{q^i}. \quad (4.17)$$

Remark 4.4. Both matrices N and R depend on the geometry of cell P . However, the analysis presented in the rest of this chapter is done for a single cell P , so we do not need a more complex notation like N_P and R_P .

Using these vectors and representation (4.13), we rewrite (4.16) as follows:

$$N_i^T M_P v_{h,P} = R_i^T v_{h,P}.$$

Since Π_P^S is surjective, $v_{h,P}$ is an arbitrary vector, and we obtain $n_{\mathcal{T}_P}$ algebraic equations

$$M_P N_i = R_i. \quad (4.18)$$

If we introduce two rectangular matrices, $\mathbf{N} = [\mathbf{N}_1, \dots, \mathbf{N}_{n_{\mathcal{T}_P}}]$ and $\mathbf{R} = [\mathbf{R}_1, \dots, \mathbf{R}_{n_{\mathcal{T}_P}}]$, the algebraic equations can be written in the compact form

$$\mathbf{M}_P \mathbf{N} = \mathbf{R}. \quad (4.19)$$

Therefore the bilinear form $\mathcal{B}_{h,P}$ in (4.13) satisfies the consistency condition if and only if the associated matrix \mathbf{M}_P satisfies the following (algebraic) consistency condition.

Definition 4.4 (Algebraic consistency condition). Let columns of matrices \mathbf{N} and \mathbf{R} be defined by (4.17). We say that matrix \mathbf{M}_P satisfies *the algebraic consistency condition* if $\mathbf{M}_P \mathbf{N} = \mathbf{R}$.

The projection operator Π_P^S is defined explicitly and the basis functions q^i are often polynomials. Hence, the vectors \mathbf{N}_i can be easily calculated for any cell P , while for all low-order mimetic schemes the calculation of \mathbf{R}_i is reduced to the evaluation of surface integrals, as shown in the following example.

Example 4.3. Let us consider again the diffusion problem described in Example 4.1. Let n be the number of vertices in cell P . We take $q^1(\mathbf{x}) = 1$, $q^2(\mathbf{x}) = x - x_P$, and $q^3(\mathbf{x}) = y - y_P$ as the basis functions of \mathcal{T}_P . The vertex-based projection operator returns the point values of the basis functions:

$$\Pi_P^{\mathcal{V}}(q^1)|_v = 1, \quad \Pi_P^{\mathcal{V}}(q^2)|_v = x_v - x_P, \quad \Pi_P^{\mathcal{V}}(q^3)|_v = y_v - y_P$$

for any vertex v of P . We enumerate the vertices counterclockwise as in Fig. 4.1 by using the index $i = 1, 2, \dots, n$ and we recall that $\mathbf{x}_{v_i}^T = (x_{v_i}, y_{v_i})$ is the position vector of the i -th vertex. Let $\mathbb{1} = (1, 1, \dots, 1)^T$ be the n -sized vector all of whose components are equal to 1. In view of (4.17), matrix \mathbf{N} is given by

$$\mathbf{N} = (\mathbb{1}, \widehat{\mathbf{N}}) \quad \text{where} \quad \widehat{\mathbf{N}} = \begin{pmatrix} x_{v_1} - x_P & y_{v_1} - y_P \\ x_{v_2} - x_P & y_{v_2} - y_P \\ \vdots & \vdots \\ x_{v_n} - x_P & y_{v_n} - y_P \end{pmatrix}. \quad (4.20)$$

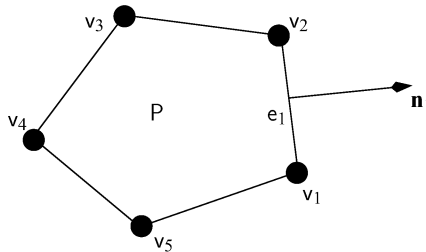


Fig. 4.1. Illustration for Example 4.3

To derive the explicit formula for matrix R , we insert (4.12) in (4.11) and change the summation from edges to vertices:

$$\mathcal{B}_P(v, q) = \sum_{v \in \partial P} \sum_{e \ni v} \mathbf{n}_{P,e} \cdot K_P \nabla q \frac{|e|}{2} \Big|_v. \quad (4.21)$$

Taking $q = q^i$ and comparing (4.21) with (4.16) gives us the formulas for the components of column R_i . The first column, R_1 , corresponds to $q^1 = 1$; thus, this is the zero vector due to $\nabla q^1 = 0$. Let $e_i = (v_i, v_{i+1})$ for $i = 1, 2, \dots, n$ (with $v_{n+1} \equiv v_1$) be the clockwise enumeration of the cell edges and let \mathbf{n}_i be the unit outward normal vector to e_i . It is easy to see that the second sum in (4.21) has exactly two terms. For vertex v_i they correspond to edges e_i and e_{i+1} (with $e_{n+1} \equiv e_1$). In order to calculate the components of columns R_2 and R_3 , we use $\nabla q^2 = (1, 0)^T$ and $\nabla q^3 = (0, 1)^T$ in (4.21). Therefore, the matrix R takes the form

$$R = (0, \widehat{R}) \quad \text{where} \quad \widehat{R} = \frac{1}{2} \begin{pmatrix} |e_n| \mathbf{n}_n^T + |e_1| \mathbf{n}_1^T \\ |e_1| \mathbf{n}_1^T + |e_2| \mathbf{n}_2^T \\ \vdots \\ |e_{n-1}| \mathbf{n}_{n-1}^T + |e_n| \mathbf{n}_n^T \end{pmatrix} K_P. \quad (4.22)$$

In this example we have introduced a block column partitioning of matrices N and R with respect to the kernel of \mathcal{B}_P . We will use a similar block partitioning in the next subsection. \square

4.3 Formula for matrix M_P

At this point we can assume that we know both matrices N and R and solve the algebraic equation $M_P N = R$. We choose the basis functions $q^i \in \mathcal{T}_P$ in such a way that the first \tilde{n} of them spans the kernel of \mathcal{B}_P :

$$\ker(\mathcal{B}_P) = \text{span} \{ q^1, q^2, \dots, q^{\tilde{n}} \}. \quad (4.23)$$

This ordering induces the block partitionings $N = (\widetilde{N}, \widehat{N})$ and $R = (\widetilde{R}, \widehat{R})$, where \widetilde{N} and \widetilde{R} correspond to the first \tilde{n} basis functions q^i . From (4.18) it is obvious that $M_P \widetilde{N} = \widetilde{R}$ and $M_P \widehat{N} = \widehat{R}$. The matrices introduced so far satisfy a few exact identities that follow from the following lemma.

Lemma 4.1. *Matrix $R^T N$ is symmetric and positive semi-definite. Moreover,*

$$N_i^T R_j = \mathcal{B}_P(q^i, q^j), \quad 1 \leq i, j \leq n_{\mathcal{T}_P}. \quad (4.24)$$

Proof. Let us take $q = q^j$ and $v_{h,P} = \Pi_P^S(q^i)$ in (4.16). Then, using the consistency condition (4.8), we obtain

$$R_j^T N_i = \mathcal{B}_{h,P}(\Pi_P^S(q^i), \Pi_P^S(q^j)) = \mathcal{B}_P(q^i, q^j).$$

The assertion of the lemma follows from the symmetry and positive-definiteness of the bilinear form. \square

Corollary 4.1. *Let \tilde{N} , \tilde{R} , and \widehat{R} be the matrices introduced above. Then*

$$\tilde{R} = 0 \quad \text{and} \quad \tilde{N}^T \widehat{R} = 0. \quad (4.25)$$

Proof. Let $i \leq \tilde{n}$, so that $q^i \in \ker(\mathcal{B}_P)$. By applying formula (4.24) with $i = j$ and $R_i = M_P N_i$, we obtain

$$N_i^T M_P N_i = \mathcal{B}_P(q^i, q^i) = 0.$$

As M_P is positive semi-definite, N_i is in the kernel of M_P , i.e., $R_i = M_P N_i = 0$, and we have that $\tilde{R} = 0$.

Let $i \leq \tilde{n} < j$. Due to the symmetry of matrix M_P , we obtain

$$N_i^T R_j = N_i^T M_P N_j = (M_P N_i)^T N_j.$$

The second statement of the lemma follows immediately, since N_i is in the kernel of matrix M_P . \square

The matrix $R^T N$ plays a crucial role in the solution of the matrix equation $M_P N = R$. Let $\hat{n} = n_{\mathcal{F}_P} - \tilde{n}$. To emphasize the block structure of $R^T N$, we introduce a generic zero rectangular matrix O and a zero square matrix O_s of size s . Corollary (4.1) implies that

$$N^T R = \begin{pmatrix} O_{\tilde{n}} & O^T \\ O & \widehat{N}^T \widehat{R} \end{pmatrix}, \quad (4.26)$$

where matrix $\widehat{N}^T \widehat{R}$ has size \hat{n} and is symmetric and positive definite.

Let us comment on the relationship between the kernel of $N^T R$ and the kernel of \mathcal{B}_P . A direct calculation offers an insightful characterization of the matrix kernel. Let us consider a vector $z_h \in \mathbb{R}^{n_{\mathcal{F}_P}}$ and partition it as $z_h^T = (\widehat{z}_h^T, \widehat{z}_h^T)$ in accordance with the block-partitioning (4.26). It holds that

$$z_h^T N^T R z_h = \widehat{z}_h^T \widehat{N}^T \widehat{R} \widehat{z}_h,$$

and the right-hand side is zero if and only if $\widehat{z}_h = 0$. Thus, $z_h \in \ker(N^T R)$ if and only if $\widehat{z}_h = 0$. On the other hand, using Lemma 4.1 and the bilinearity of \mathcal{B}_P , we can write

$$z_h^T N^T R z_h = \mathcal{B}_P \left(\sum_{i=1}^{n_{\mathcal{F}_P}} z_i q^i, \sum_{i=1}^{n_{\mathcal{F}_P}} z_i q^i \right). \quad (4.27)$$

Therefore $z_h \in \ker(N^T R)$ if and only if $\sum_{i=1}^{n_{\mathcal{F}_P}} z_i q^i \in \ker(\mathcal{B}_P)$, i.e., if and only if $z_i = 0$ for all $i > \tilde{n}$ due to (4.23).

Remark 4.5. Let $z_h = \{z_i\}_{i=1}^{n_{\mathcal{F}_P}}$ and $v = \sum_{i=1}^{n_{\mathcal{F}_P}} z_i q^i$. In general, $z_h \neq \Pi_P^S(v)$.

Now, let us introduce the pseudo-inverse of matrix $N^T R$:

$$(N^T R)^\dagger = \begin{pmatrix} O_{\tilde{n}} & O^T \\ O & (\widehat{N}^T \widehat{R})^{-1} \end{pmatrix}. \quad (4.28)$$

When $\tilde{n} = \dim(\ker(\mathcal{B}_P)) > 0$, we recall that the product of matrix $N^T R$ and its pseudo-inverse is not the identity matrix

$$(N^T R)^\dagger N^T R = \begin{pmatrix} O_{\tilde{n}} & O^T \\ O & (\widehat{N}^T \widehat{R})^{-1} \end{pmatrix} \begin{pmatrix} O_{\tilde{n}} & O^T \\ O & \widehat{N}^T \widehat{R} \end{pmatrix} = \begin{pmatrix} O_{\tilde{n}} & O^T \\ O & I_{\tilde{n}} \end{pmatrix} \neq I_{n_{\mathcal{B}_P}}.$$

Example 4.4. By using the matrices R and N built in Example 4.3, one can immediately compute the matrix $N^T R$. An alternative, and a more elegant way, is to apply formula (4.24). Since $\nabla q^1 = (0, 0)^T$, $\nabla q^2 = (1, 0)^T$ and $\nabla q^3 = (0, 1)^T$, we obtain

$$\widehat{N}^T \widehat{R} = |P| K_P.$$

Such a formula is typical for low-order mimetic methods and leads to an efficient calculation of matrix M_P . \square

Lemma 4.2. *The matrix*

$$M_P^0 = R(R^T N)^\dagger R^T = \widehat{R}(\widehat{R}^T \widehat{N})^{-1} \widehat{R}^T \quad (4.29)$$

satisfies the algebraic consistency condition of Definition 4.4.

Proof. Let us first note that

$$R(R^T N)^\dagger R^T = \begin{pmatrix} 0 & \widehat{R} \\ O & (\widehat{R}^T \widehat{N})^{-1} \end{pmatrix} \begin{pmatrix} 0 \\ \widehat{R}^T \end{pmatrix} = \widehat{R}(\widehat{R}^T \widehat{N})^{-1} \widehat{R}^T,$$

which shows the second equality in (4.29). From the second equation in (4.25) we have $\widehat{R}^T \widehat{N} = 0$. A straightforward calculation yields:

$$M_P^0 N = \widehat{R}(\widehat{R}^T \widehat{N})^{-1} \widehat{R}^T (\widehat{N}, \widehat{N}) = (0, \widehat{R}(\widehat{R}^T \widehat{N})^{-1} \widehat{R}^T \widehat{N}) = (0, \widehat{R}) = R,$$

from which the assertion of the lemma follows. \square

Unfortunately, the matrix M_P^0 does not always satisfy the stability condition of Definition 4.3. Indeed, any vector that is orthogonal to the columns of \widehat{R} is in the kernel of M_P^0 , cf. (4.29). The dimension of this kernel is at least $n_{\mathcal{J}_{h,P}} - n_{\mathcal{B}_P} + \tilde{n}$, which could be larger than \tilde{n} , the dimension of the kernel of \mathcal{B}_P . To fix this problem, we introduce a correction matrix M_P^1 and define the final matrix as follows:

$$M_P = M_P^0 + M_P^1. \quad (4.30)$$

This correction should not break the algebraic consistency condition and must guarantee the stability condition. Sufficient conditions for such a correction matrix are given in the next lemma.

Lemma 4.3. *Let M_P^1 be a symmetric and positive semi-definite matrix with the kernel characterization $\ker(M_P^1) = \text{img}(N)$. Then, the matrix M_P given by (4.30) is symmetric, positive semi-definite and satisfies the algebraic consistency condition. Moreover,*

$$\ker(M_P) = \{v_h \in \mathcal{S}_{h,P} : v_h = \Pi_P^S(v) \text{ for } v \in \ker(\mathcal{B}_P)\}. \quad (4.31)$$

Proof. The first assertion of the lemma follows from the definition of matrix M_P^0 and the hypothesis on M_P^1 . Indeed, $M_P N = (M_P^0 + M_P^1) N = M_P^0 N = R$.

To prove the second assertion of the lemma, let us note that $v_h \in \ker(M)$ if and only if

$$0 = v_h^T M_P v_h = v_h^T M_P^0 v_h + v_h^T M_P^1 v_h. \quad (4.32)$$

Since M_P^0 and M_P^1 are positive semi-definite, both terms in the right-hand side are zero. The second zero term, $v_h^T M_P^1 v_h = 0$, implies that v_h is in the kernel of M_P^1 ; hence, by the hypothesis $v_h = N z_h$ for some vector z_h . Writing $z_h^T = (\widehat{z}_h^T, \widetilde{z}_h^T)$, the first zero term gives

$$0 = v_h^T M_P^0 v_h = (\widehat{R}^T \widehat{N} \widehat{z}_h)^T (\widehat{R}^T \widehat{N})^{-1} (\widehat{R}^T \widehat{N} \widehat{z}_h). \quad (4.33)$$

Since $\widehat{R}^T \widehat{N}$ is a positive definite matrix, we have that $\widehat{z}_h = 0$. Thus, each vector in the kernel of M_P^0 is a linear combination of the first \widetilde{n} columns of N . The definition of these columns gives:

$$v_h = \sum_{i=1}^{\widetilde{n}} z_i N_i = \sum_{i=1}^{\widetilde{n}} z_i \Pi_P^S(q^i) = \Pi_P^S\left(\sum_{i=1}^{\widetilde{n}} z_i q^i\right).$$

The linear combination of the first \widetilde{n} functions q^i form the kernel of \mathcal{B}_P . \square

As shown by the previous lemma, the kernel of matrix M_P corresponds bijectively to the kernel of the bilinear form \mathcal{B}_P , so that

$$\ker(M_P) = \text{span} \left\{ \Pi_P^S(q^1), \Pi_P^S(q^2), \dots, \Pi_P^S(q^{\widetilde{n}}) \right\}. \quad (4.34)$$

If q^i is in $\ker(\mathcal{B}_P)$, the definition of M_P in (4.13) and the consistency condition (4.8) yield:

$$\Pi_P^S(q^i)^T M_P \Pi_P^S(q^i) = \mathcal{B}_{h,P}(\Pi_P^S(q^i), \Pi_P^S(q^i)) = \mathcal{B}_P(q^i, q^i) = 0 \quad (4.35)$$

and $\Pi_P^S(q^i)$ is in $\ker(M_P)$ and viceversa. If \mathcal{B}_P is an L^2 scalar product, we have $\widetilde{n} = 0$, which in turn implies that matrix M_P is positive definite as expected. Moreover, since $\ker(R^T N)$ becomes the trivial space $\{0\}$, the pseudo-inverse of this matrix equals to its normal inverse and we get the following formula:

$$M_P = R(R^T N)^{-1} R^T + M_P^1.$$

4.4 Stability analysis

Here, we will show how the stability of the discrete bilinear form $\mathcal{B}_{h,\mathbb{P}}$ defines necessary bounds on the matrix $M_{\mathbb{P}}^{\mathbb{1}}$. The first part of our analysis is based on a suitable projection operator here denoted by $\pi_{\mathbb{P}}$ to describe the structure of matrix $M_{\mathbb{P}}$. A similar operator has been used in the mimetic literature to derive post-processed discrete solutions, but never in such a generality. In the second part, we derive a stability condition in a more practical Euclidean norm.

We will keep the discussion quite general leaving the treatment of applications to the next chapters. However, all major steps in the analysis will be illustrated with a simple bilinear form.

4.4.1 Stability result in the natural norm

Let us assume (4.7) and define, only for the present section, a discrete semi-norm as follows:

$$\|v_{h,\mathbb{P}}\|_{\mathcal{S}_{h,\mathbb{P}}} = \mathcal{B}_{\mathbb{P}}(v, v) \quad \forall v_{h,\mathbb{P}} \in \mathcal{S}_{h,\mathbb{P}}, v \in S_{h,\mathbb{P}} \text{ and } v_{h,\mathbb{P}} = \Pi_{\mathbb{P}}^{\mathcal{S}}(v), \quad (4.36)$$

or, equivalently, by

$$\|v_{h,\mathbb{P}}\|_{\mathcal{S}_{h,\mathbb{P}}} = \mathcal{B}_{\mathbb{P}}(R_{\mathbb{P}}^{\mathcal{S}}(v_{h,\mathbb{P}}), R_{\mathbb{P}}^{\mathcal{S}}(v_{h,\mathbb{P}})).$$

This semi-norm has mainly a theoretical value and it is normally not used in practice. The stability analysis in this subsection relies on the operator $\pi_{\mathbb{P}}$, which represents an orthogonal projection onto the subspace $\mathcal{T}_{\mathbb{P}}/\ker(\mathcal{B}_{\mathbb{P}})$ with respect to the energy bilinear form $\mathcal{B}_{\mathbb{P}}$. Part of this section takes inspiration from ideas introduced in the virtual element method [43].

Definition 4.5. Let us consider the linear operator $\pi_{\mathbb{P}} : \mathcal{S}_{h,\mathbb{P}} \rightarrow \mathcal{T}_{\mathbb{P}}/\ker(\mathcal{B}_{\mathbb{P}})$ such that for any $v_h \in \mathcal{S}_{h,\mathbb{P}}$ the function $\pi_{\mathbb{P}}(v_h)$ is such that

$$\mathcal{B}_{\mathbb{P}}(\pi_{\mathbb{P}}(v_h), q) = \mathcal{B}_{h,\mathbb{P}}(v_h, \Pi_{\mathbb{P}}^{\mathcal{S}}(q)) \quad \forall q \in \mathcal{T}_{\mathbb{P}}/\ker(\mathcal{B}_{\mathbb{P}}). \quad (4.37)$$

Remark 4.6. If the discrete field v_h is the collection of degrees of freedom of a function v of $S_{h,\mathbb{P}}$, i.e., $v_h = \Pi_{\mathbb{P}}^{\mathcal{S}}(v)$, the consistency condition (4.8) implies that

$$\mathcal{B}_{\mathbb{P}}(\pi_{\mathbb{P}}(v_h), q) = \mathcal{B}_{\mathbb{P}}(v, q) \quad \forall q \in \mathcal{T}_{\mathbb{P}}/\ker(\mathcal{B}_{\mathbb{P}}), \quad (4.38)$$

and therefore the operator $\pi_{\mathbb{P}}$ is an energy projection on $\mathcal{T}_{\mathbb{P}}/\ker(\mathcal{B}_{\mathbb{P}})$. Indeed, for any trial function q of $\mathcal{T}_{\mathbb{P}}$ we use (4.37) and we obtain

$$\begin{aligned} \mathcal{B}_{\mathbb{P}}(\pi_{\mathbb{P}}(v_h), q) &= \mathcal{B}_{h,\mathbb{P}}(v_h, \Pi_{\mathbb{P}}^{\mathcal{S}}(q)) && \text{[substitute } v_h = \Pi_{\mathbb{P}}^{\mathcal{S}}(v)\text{]} \\ &= \mathcal{B}_{h,\mathbb{P}}(\Pi_{\mathbb{P}}^{\mathcal{S}}(v), \Pi_{\mathbb{P}}^{\mathcal{S}}(q)) && \text{[use (4.8)]} \\ &= \mathcal{B}_{\mathbb{P}}(v, q), \end{aligned}$$

which implies (4.38). □

Example 4.5. Let us consider again the bilinear form from Example 4.1. In this example $\mathcal{T}_P = \mathbb{P}_1(P)$ with the basis functions $q^1 = 1$, $q^2 = x - x_P$, and $q^3 = y - y_P$. The kernel of $\ker(\mathcal{B}_P)$ consists of constant functions. Let $v_h = \Pi_P^{\mathcal{T}}(v)$ for some function $v \in S_{h,P}$. The scalar function $\pi_P(v_h)$ (defined up to a constant) is a linear polynomial of the form:

$$\pi_P(v_h)(x, y) = c_1(x - x_P) + c_2(y - y_P), \quad c_1, c_2 \in \mathbb{R}. \quad (4.39)$$

The two scalar coefficients c_1 and c_2 , which form $\nabla \pi_P(u_h)$, are determined from (4.37) by taking $q = q^2$ and $q = q^3$, respectively. Since $\nabla q^2 = (1, 0)^T$ and $\nabla \pi_P(u_h)$ is a constant vector on P , we obtain:

$$\mathcal{B}_P(\pi_P(v_h), q^2) = \int_P K_P \nabla \pi_P(v_h) \cdot \nabla q^2 dV = |P| \nabla \pi_P(v_h) \cdot K_P \begin{pmatrix} 1 \\ 0 \end{pmatrix}.$$

On the other hand,

$$\mathcal{B}_P(v, q^2) = \int_P K_P \nabla v \cdot \nabla q^2 dV = \left(\int_P \nabla v dV \right) \cdot K_P \begin{pmatrix} 1 \\ 0 \end{pmatrix}.$$

Similar relations hold for $q = q^3$. As K_P is a non singular matrix, we find:

$$\nabla \pi_P(v_h) = \frac{1}{|P|} \int_P \nabla v dV. \quad (4.40)$$

Thus, $\nabla \pi_P(v_h)$ is the average of the gradient of v , and, in the next example, we will show that it does not depend on the behavior of v inside cell P . In order to build a polynomial approximation of v_h , we need to add to $\pi_P(v_h)$ a constant that represents an average value of v_h over P . A possible choice is to take the arithmetic average of all components of vector v_h . \square

The following lemma summarizes other properties of the operator π_P .

Lemma 4.4. *The linear operator π_P given by (4.37) satisfies the following properties:*

(i) π_P is invariant with respect to the projection operator Π_P^S in the sense that

$$\pi_P \circ \Pi_P^S \circ \pi_P(v_h) = \pi_P(v_h) \quad \forall v_h \in \mathcal{S}_{h,P};$$

(ii) $\pi_P \circ \Pi_P^S$ is self-adjoint with respect to the bilinear form \mathcal{B}_P in the sense that

$$\mathcal{B}_P(\pi_P \circ \Pi_P^S(u), v) = \mathcal{B}_P(u, \pi_P \circ \Pi_P^S(v)) \quad \forall u, v \in S_{h,P};$$

(iii) for any pair of functions u and v of $S_{h,P}$ with degrees of freedom u_h and v_h , the following decomposition holds:

$$\mathcal{B}_P(u, v) = \mathcal{B}_P(\pi_P(u_h), \pi_P(v_h)) + \mathcal{B}_P(u - \pi_P(u_h), v - \pi_P(v_h)). \quad (4.41)$$

Proof. (i) Let q be any function from $\mathcal{T}_P/\ker(\mathcal{B}_P)$. We first apply Definition 4.5 and then the consistency property (4.8) to obtain the relation

$$\mathcal{B}_P(\pi_P \circ \Pi_P^S \circ \pi_P(v_h), q) = \mathcal{B}_{h,P}(\Pi_P^S \circ \pi_P(v_h), \Pi_P^S(q)) = \mathcal{B}_P(\pi_P(v_h), q).$$

The result follows from the positive semi-definiteness of the bilinear form.

(ii) To see that $\pi_P \circ \Pi_P^S$ is symmetric with respect to the bilinear form \mathcal{B}_P , let us note that for any $v_h \in \mathcal{S}_{h,P}$ the function $\pi_P(v_h)$ belongs to $\mathcal{T}_P/\ker(\mathcal{B}_P)$ and can play the role of q in (4.8). Thus, for any couple of functions u and v of $\mathcal{S}_{h,P}$, the consistency relation (4.8) (with $q = \pi_P \circ \Pi_P^S(u)$) and Definition 4.5 (with $v_h = \Pi_P^S(v)$) gives:

$$\begin{aligned} \mathcal{B}_P(\pi_P \circ \Pi_P^S(u), v) &= \mathcal{B}_{h,P}(\Pi_P^S \circ \pi_P \circ \Pi_P^S(u), \Pi_P^S(v)) \\ &= \mathcal{B}_P(\pi_P \circ \Pi_P^S(u), \pi_P \circ \Pi_P^S(v)). \end{aligned} \quad (4.42)$$

Now, we revert this argument by using Definition 4.5 (with $u_h = \Pi_P^S(u)$) and applying the consistency relation (4.8) (with $q = \pi_P \circ \Pi_P^S(v)$):

$$\begin{aligned} \mathcal{B}_P(\pi_P \circ \Pi_P^S(u), \pi_P \circ \Pi_P^S(v)) &= \mathcal{B}_{h,P}(\Pi_P^S(u), \Pi_P^S \circ \pi_P \circ \Pi_P^S(v)) \\ &= \mathcal{B}_P(u, \pi_P \circ \Pi_P^S(v)). \end{aligned} \quad (4.43)$$

Assertion (ii) follows by combining (4.42) and (4.43).

(iii) The isomorphism between $\mathcal{S}_{h,P}$ and $\mathcal{S}_{h,P}$ implies that $u_h = \Pi_P^S(u)$ and $v_h = \Pi_P^S(v)$. The definition (4.37) gives $\mathcal{B}_P(u - \pi_P(u_h), \pi_P(v_h)) = 0$. A similar orthogonality property holds when u and v are swapped. Using the above properties, we make the following developments:

$$\begin{aligned} &\mathcal{B}_P(\pi_P(u_h), \pi_P(v_h)) + \mathcal{B}_P(u - \pi_P(u_h), v - \pi_P(v_h)) \\ &= \mathcal{B}_P(\pi_P(u_h), \pi_P(v_h)) + \mathcal{B}_P(u - \pi_P(u_h), v) \\ &= \mathcal{B}_P(u, v) + \mathcal{B}_P(\pi_P(u_h), \pi_P(v_h) - v) \\ &= \mathcal{B}_P(u, v). \end{aligned}$$

This completes the proof of the lemma. \square

Let us derive an explicit form for the operator $\pi_P(v_h)$ that uses only the degrees of freedom.

Lemma 4.5. *For any $v_h \in \mathcal{S}_{h,P}$, the discrete field $\Pi_P^S \circ \pi_P(v_h)$, is given by*

$$\Pi_P^S \circ \pi_P(v_h) = \widehat{\mathbf{N}}(\widehat{\mathbf{R}}^T \widehat{\mathbf{N}})^{-1} \widehat{\mathbf{R}}^T v_h. \quad (4.44)$$

Proof. Since $\pi_P(v_h)$ belongs to the quotient space $\mathcal{T}_P/\ker(\mathcal{B}_P)$, we can expand it on the set of basis functions $\{q^{\widehat{n}+1}, \dots, q^{\widehat{n}_{\mathcal{T}_P}}\}$. Let $\mathbf{c} = \{c_j\}_{j=1}^{\widehat{n}}$ be the coefficients of

such expansion (recall that $\widehat{n} = n_{\mathcal{F}_P} - \widehat{n}$), so that

$$\pi_P(v_h) = \sum_{j=1}^{\widehat{n}} c_j q^{\widehat{n}+j}. \quad (4.45)$$

Let us use expansion (4.45) as one of the arguments in the bilinear form \mathcal{B}_P and $q^{\widehat{n}+i} \in \mathcal{T}_P$ as the other argument. Then, Lemma 4.1 gives

$$\mathcal{B}_P(\pi_P(v_h), q^{\widehat{n}+i}) = \sum_{j=1}^{\widehat{n}} c_j \mathcal{B}_P(q^{\widehat{n}+j}, q^{\widehat{n}+i}) = \sum_{j=1}^{\widehat{n}} \widehat{R}_i^T \widehat{N}_j c_j = \widehat{R}^T \widehat{N} \mathbf{c}. \quad (4.46)$$

Definition (4.37) of columns of the matrix \mathbf{R} implies that

$$\mathcal{B}_P(\pi_P(v_h), q^{\widehat{n}+i}) = \mathbf{R}_{\widehat{n}+i}^T v_h. \quad (4.47)$$

We combine formulas (4.46) and (4.47) to obtain the relation $\widehat{R}^T \widehat{N} \mathbf{c} = \widehat{R}^T v_h$ from which it follows that

$$\mathbf{c} = (\widehat{R}^T \widehat{N})^{-1} \widehat{R}^T v_h.$$

Applying the projection operator Π_P^S to both sides of (4.45), using its linearity and definition of the column of matrix \mathbf{N} , we obtain:

$$\Pi_P^S \circ \pi_P(v_h) = \sum_{j=1}^{\widehat{n}} c_j \Pi_P^S(q^{\widehat{n}+j}) = \sum_{j=1}^{\widehat{n}} c_j \mathbf{N}_{\widehat{n}+j} = \widehat{N} \mathbf{c} = \widehat{N} (\widehat{R}^T \widehat{N})^{-1} \widehat{R}^T v_h,$$

which is the assertion of the lemma. \square

Example 4.6. We apply Lemma 4.5 to the projection operator (4.39) from Example 4.5. Note that $\nabla \pi_P(v_h) = (c_1, c_2)^T = \mathbf{c}$. Hence,

$$\nabla \pi_P(v_h) = (\widehat{R}^T \widehat{N})^{-1} \widehat{R}^T v_h.$$

This can be verified by a straightforward calculation using formula (4.40) and integration by parts:

$$\nabla \pi_P(v_h) = \frac{1}{|\mathbf{P}|} \int_{\mathbf{P}} \nabla v dV = \frac{1}{|\mathbf{P}|} \sum_{e \in \partial \mathbf{P}} \int_e \mathbf{n}_{\mathbf{P},e} v dS,$$

where $v_h = \Pi_P^S(v)$ and $v \in S_{h,\mathbf{P}}$. As function v belongs to $S_{h,\mathbf{P}}$ its edge integrals are calculated exactly using the trapezoidal quadrature rule, see Example 4.1. Let us consider again the local clockwise enumeration of edges and vertices of polygon \mathbf{P} . Using the formula for matrix $\widehat{\mathbf{R}}$ (see Example 4.3) and the main formula in Example 4.4,

$\widehat{\mathbf{R}}^T \widehat{\mathbf{N}} = \mathbf{K}_P |\mathbf{P}|$, we obtain:

$$\begin{aligned} \nabla \pi_P(v_h) &= \frac{1}{|\mathbf{P}|} \sum_{i=1}^{N_P'} \mathbf{n}_i \frac{|e_i|}{2} (v_{v_i} + v_{v_{i+1}}) = \frac{1}{2|\mathbf{P}|} \sum_{i=1}^{N_P'} v_{v_i} (\mathbf{n}_i |e_i| + \mathbf{n}_{i+1} |e_{i+1}|) \\ &= \frac{1}{|\mathbf{P}|} \mathbf{K}_P^{-1} \widehat{\mathbf{R}}^T v_h = (\widehat{\mathbf{R}}^T \widehat{\mathbf{N}})^{-1} \widehat{\mathbf{R}}^T v_h, \end{aligned} \quad (4.48)$$

which is exactly the value calculated applying Lemma 4.5. \square

With these developments, we can connect the matrix decomposition $\mathbf{M}_P = \mathbf{M}_P^0 + \mathbf{M}_P^1$ with the orthogonal decomposition (4.41). First, the projection operator π_P allows us to connect the matrix \mathbf{M}_P^0 with the bilinear form \mathcal{B}_P restricted to space \mathcal{T}_P .

Lemma 4.6. *Let u, v be functions from \mathcal{T}_P , and u_h, v_h their degrees of freedom. Then,*

$$\mathcal{B}_P(\pi_P(u_h), \pi_P(v_h)) = u_h^T \mathbf{M}_P^0 v_h. \quad (4.49)$$

Proof. As both $\pi_P(u_h)$ and $\pi_P(v_h)$ are functions of $\mathcal{T}_P / \ker(\mathcal{B}_P)$ we can use Lemma 4.5 and the consistency condition to start the following chain of relations:

$$\begin{aligned} \mathcal{B}_P(\pi_P(v_h), \pi_P(u_h)) &= \mathcal{B}_{h,P}(\Pi_P^S(\pi_P(u_h)), v_h) \quad [\text{use (4.13)}] \\ &= \Pi_P^S(\pi_P(u_h))^T \mathbf{M}_P v_h \quad [\text{use (4.44)}] \\ &= u_h^T \widehat{\mathbf{R}} (\widehat{\mathbf{R}}^T \widehat{\mathbf{N}})^{-1} \widehat{\mathbf{N}}^T \mathbf{M}_P v_h \quad [\text{use } \widehat{\mathbf{N}}^T \mathbf{M} = \widehat{\mathbf{R}}^T] \\ &= u_h^T \widehat{\mathbf{R}} (\widehat{\mathbf{R}}^T \widehat{\mathbf{N}})^{-1} \widehat{\mathbf{R}}^T v_h \quad [\text{use (4.29)}] \\ &= u_h^T \mathbf{M}_P^0 v_h, \end{aligned}$$

which is the assertion of the lemma. \square

Example 4.7. Referring to Example 4.1 we find that

$$u_h^T \mathbf{M}_P^0 v_h = \int_P \mathbf{K}_P \nabla \pi_P(u_h) \cdot \nabla \pi_P(v_h) dV. \quad (4.50)$$

Let $u, v \in S_{h,P}$ and $u_h = \Pi_P^S(u)$, $v_h = \Pi_P^S(v)$. Let us insert formula (4.50) into the orthogonal decomposition (4.41):

$$\int_P \mathbf{K}_P \nabla u \cdot \nabla v dV = u_h^T \mathbf{M}_P^0 v_h + \int_P \mathbf{K}_P \nabla(u - \pi_P(u_h)) \cdot \nabla(v - \pi_P(v_h)) dV.$$

In view of this formula, matrix \mathbf{M}_P^1 provides an approximation of the second term:

$$u_h^T \mathbf{M}_P^1 v_h \approx \int_P \mathbf{K}_P \nabla(u - \pi_P(u_h)) \cdot \nabla(v - \pi_P(v_h)) dV.$$

The stability condition with respect to the energy norm must use the matrix \mathbf{M}_P^1 that is spectrally equivalent to this term on the space orthogonal to \mathcal{T}_P . This issue is considered in the stability theorems that follows. \square

Theorem 4.1. *Let matrices M_P^0 and M_P^1 satisfy the hypothesis of Lemma 4.3. Furthermore, let s_* and s^* be positive constants independent of P such that*

$$s_* \mathcal{B}_P(v - \pi_P(v_h), v - \pi_P(v_h)) \leq v_h^T M_P^1 v_h \leq s^* \mathcal{B}_P(v - \pi_P(v_h), v - \pi_P(v_h)) \quad (4.51)$$

for all $v_h \in \mathcal{S}_{h,P}$ and $v = R_P^\mathcal{J}(v_h)$. Then, the local bilinear form $\mathcal{B}_{h,P}$, represented by matrix $M_P = M_P^0 + M_P^1$, satisfies the stability inequalities

$$C_* \| \| v_h \| \|_{\mathcal{S}_{h,P}}^2 \leq v_h^T M_P v_h \leq C^* \| \| v_h \| \|_{\mathcal{S}_{h,P}}^2$$

with constants $C_* = \min(1, s_*)$ and $C^* = \max(1, s^*)$.

Proof. We recall that the $\| \| \cdot \| \|_{\mathcal{S}_{h,P}}$ norm was defined in (4.36). We use (4.13) and (4.30), then (4.49), and finally the right inequality in (4.51) and decomposition (4.41), to obtain:

$$\begin{aligned} v_h^T M_P v_h &= v_h^T M_P^0 v_h + v_h^T M_P^1 v_h \\ &\leq \mathcal{B}_P(\pi_P(v_h), \pi_P(v_h)) + s^* \mathcal{B}_P((v - \pi_P(v_h)), (v - \pi_P(v_h))) \\ &\leq \max(1, s^*) (\mathcal{B}_P(\pi_P(v_h), \pi_P(v_h)) + \mathcal{B}_P((v - \pi_P(v_h)), (v - \pi_P(v_h)))) \\ &= \max(1, s^*) \mathcal{B}_P(v, v) \\ &= C^* \| \| v_h \| \|_{\mathcal{S}_{h,P}}^2. \end{aligned} \quad (4.52)$$

Using the same argument but with the left inequality in (4.51), we obtain

$$\begin{aligned} v_h^T M_P v_h &= v_h^T M_P^0 v_h + v_h^T M_P^1 v_h \\ &\geq \mathcal{B}_P(\pi_P(v_h), \pi_P(v_h)) + s_* \mathcal{B}_P((v - \pi_P(v_h)), (v - \pi_P(v_h))) \\ &\geq \min(1, s_*) (\mathcal{B}_P(\pi_P(v_h), \pi_P(v_h)) + \mathcal{B}_P((v - \pi_P(v_h)), (v - \pi_P(v_h)))) \\ &= C_* \| \| v_h \| \|_{\mathcal{S}_{h,P}}^2. \end{aligned} \quad (4.53)$$

This completes the proof of the theorem. \square

4.4.2 Stability result in the mesh-dependent norm

Let us define a computable discrete semi-norm using the Euclidean norm of mesh function $v_h \in \mathcal{S}_{h,P}$. With a little abuse of notation, we will use the same symbol adopted in (4.36) for the non-computable semi-norm, since the purpose of the two discrete semi-norms is the same. The consistency condition gives us the matrix M_P^0 that is independent of the norm used in the stability analysis. Therefore, spectral properties of this matrix, such as its trace, can be used to define a proper scaling of the Euclidean norm:

$$\| \| v_h \| \|_{\mathcal{S}_{h,P}} = \text{trace}(M_P^0) \min_{q_h \in \ker(\mathcal{B}_{h,P})} \| v_h \| + q_h.$$

This semi-norm is the norm on the quotient space $\mathcal{S}_{h,P}/\ker(\mathcal{B}_{h,P})$. To formulate the stability result, we introduce the effective condition number $\text{cond}(M_P^0)$ as the ratio of the maximum eigenvalue to the smallest positive eigenvalue:

$$\text{cond}(M_P^0) = \lambda_{\max}(M_P^0) / \lambda_{\min}^+(M_P^0).$$

The general idea of the stabilization is to make matrix M_P^1 comparable to matrix M_P^0 in the spectral sense. The mesh shape-regularity assumptions (MR1)–(MR2) play an important role in the analysis below.

Theorem 4.2. *Let matrices M_P^0 and M_P^1 satisfy the hypothesis of Lemma 4.3. Furthermore, let us assume that*

$$s_* \lambda_{\min}^+(M_P^0) v_h^T v_h \leq v_h^T M_P^1 v_h \quad \forall v_h \in \ker(N^T), \quad (4.54)$$

$$v_h^T M_P^1 v_h \leq s^* \lambda_{\max}(M_P^0) v_h^T v_h \quad \forall v_h \in \mathcal{S}_{h,P} \quad (4.55)$$

for some positive constant s_* , s^* independent of P and v_h . Then, the local bilinear form $\mathcal{B}_{h,P}$, represented by matrix $M_P = M_P^0 + M_P^1$, satisfies the stability inequalities

$$C_* (\text{cond}(M_P^0))^{-2} \|v_h\|_{\mathcal{S}_{h,P}}^2 \leq v_h^T M_P v_h \leq C^* \|v_h\|_{\mathcal{S}_{h,P}}^2 \quad (4.56)$$

with C_* and C^* independent of P .

Proof. First, we prove the left inequality in (4.56). Consider the following orthogonal decomposition of vector $v_h \in \mathcal{S}_{h,P}$:

$$v_h = \widehat{v}_h + v_h^c, \quad \widehat{v}_h \in \text{img}(N), \quad v_h^c \in \ker(N^T). \quad (4.57)$$

We note that $M_P^1 \widehat{v}_h = 0$ by the definition of this matrix. Therefore,

$$v_h^T M_P v_h = (\widehat{v}_h + v_h^c)^T M_P^0 (\widehat{v}_h + v_h^c) + (v_h^c)^T M_P^1 v_h^c = T_1 + T_2. \quad (4.58)$$

To estimate the first term, we bound the cross-product $\widehat{v}_h^T M_P^0 v_h^c$ from below using the standard inequality for algebraic vectors \mathbf{a} and \mathbf{b} :

$$2\mathbf{a}^T \mathbf{b} \leq \varepsilon \mathbf{a}^T \mathbf{a} + \frac{1}{\varepsilon} \mathbf{b}^T \mathbf{b},$$

which holds for every $\varepsilon > 0$. Applying this inequality, we obtain:

$$T_1 \geq (1 - \varepsilon) \widehat{v}_h^T M_P^0 \widehat{v}_h + \left(1 - \frac{1}{\varepsilon}\right) (v_h^c)^T M_P^0 v_h^c = T_{11} + T_{12}. \quad (4.59)$$

In the following developments, we assume that $\varepsilon < 1$, so that $T_{11} \geq 0$ and $T_{12} \leq 0$. The term T_{11} is bounded using the minimum positive eigenvalue of matrix M_P^0 :

$$T_{11} \geq (1 - \varepsilon) \lambda_{\min}^+(M_P^0) \widehat{v}_h^T \widehat{v}_h. \quad (4.60)$$

The term \mathbb{T}_{12} is bounded using the maximum positive eigenvalue:

$$\mathbb{T}_{12} \geq \left(1 - \frac{1}{\varepsilon}\right) \lambda_{\max}(\mathbb{M}_{\mathbb{P}}^0) (v_h^c)^T v_h^c. \quad (4.61)$$

Since $\ker(\mathbb{N}^T) = (\text{img}(\mathbb{N}))^\perp$, the second term in the last right-hand side of (4.58) is bounded by our assumption (4.54). Now, we combine inequalities (4.60), (4.61), and (4.54) to obtain the following lower bound:

$$v_h^T \mathbb{M}_{\mathbb{P}} v_h \geq (1 - \varepsilon) \lambda_{\min}^+(\mathbb{M}^0) \widehat{v}_h^T \widehat{v}_h + \left(s_* \lambda_{\min}^+(\mathbb{M}^0) + \left(1 - \frac{1}{\varepsilon}\right) \lambda_{\max}(\mathbb{M}_{\mathbb{P}}^0) \right) (v_h^c)^T v_h^c.$$

Note that the coefficients in front of the vector norms are strictly positive if

$$1 > \varepsilon > (1 + s_*/\text{cond}(\mathbb{M}_{\mathbb{P}}^0))^{-1}.$$

If we set ε to the mid-point of this interval, after some calculations, we obtain

$$v_h^T \mathbb{M}_{\mathbb{P}} v_h \geq \frac{s_*}{2(\text{cond}(\mathbb{M}_{\mathbb{P}}^0))^2 (1 + s_*) n_{\mathcal{T}_{\mathbb{P}}}} \|v_h\|_{\mathcal{T}_{h,\mathbb{P}}}^2 = \frac{C_*}{(\text{cond}(\mathbb{M}_{\mathbb{P}}^0))^2} \|v_h\|_{\mathcal{T}_{h,\mathbb{P}}}^2.$$

The left inequality of (4.56) follows by noting that $(\widehat{v}_h^T \widehat{v}_h + (v_h^c)^T v_h^c) = \|v_h\|^2$ since \widehat{v}_h and v_h^c are orthogonal.

Second, we prove the right inequality in (4.56). Using the upper bound (4.55) yields:

$$v_h^T \mathbb{M}_{\mathbb{P}} v_h = v_h^T (\mathbb{M}_{\mathbb{P}}^0 + \mathbb{M}_{\mathbb{P}}^1) v_h \leq (1 + s^*) \lambda_{\max}(\mathbb{M}_{\mathbb{P}}^0) v_h^T v_h \leq (1 + s^*) \|v_h\|_{\mathcal{T}_{h,\mathbb{P}}}^2.$$

The proof is completed by setting $C^* = (1 + s^*)$. \square

The result of the theorem implies that a better conditioning of matrix $\mathbb{M}_{\mathbb{P}}^0$ improves the spectral bound of matrix $\mathbb{M}_{\mathbb{P}}$. In practice, this can be achieved by scaling correctly the degrees of freedom. In all lower-order mimetic schemes considered in this book, $\text{cond}(\mathbb{M}_{\mathbb{P}}^0)$ depends only on the shape-regularity constants of cell \mathbb{P} . In general, this effective condition number remains the primary quantity to be controlled in the development of mimetic schemes.

Remark 4.7. Inequalities (4.54) and (4.55) allows us to vary the stabilization matrix $\mathbb{M}_{\mathbb{P}}^1$ to build a scheme that has not only the prescribed order of accuracy but also possesses additional properties. In Chap. 11, this freedom will be used to enforce the discrete maximum principle on a family of meshes.

4.5 Construction of stabilization matrix M_P^1

The following lemma provides a general form for the family of stabilization matrices M_P^1 .

Lemma 4.7. *Let M_P^0 be the matrix given in (4.29). Let D and U be any matrices with the following properties:*

- (i) D is a full rank matrix of size $n_{\mathcal{S}_{h,P}} \times (n_{\mathcal{S}_{h,P}} - n_{\mathcal{T}_P})$ such that $\text{img}(D) = \ker(N^T)$ i.e. its columns form a basis for $\ker(N^T)$;
- (ii) U is a symmetric and positive definite matrix of size $(n_{\mathcal{S}_{h,P}} - n_{\mathcal{T}_P})$.

Furthermore, let $M_P^1 = DUD^T$ and

$$M_P = M_P^0 + M_P^1 = R(R^T N)^\dagger R^T + DUD^T.$$

Then, matrix M_P is symmetric, semi-positive definite, and satisfies the algebraic consistency condition. Moreover,

$$\ker(M_P) = \{v_h \in \mathcal{S}_{h,P} : v_h = \Pi_P^S(v) \text{ for } v \in \ker(\mathcal{B}_P)\}.$$

Proof. The assertions of the lemma follow immediately from Lemma 4.3 if we prove that $\ker(M_P^1) = \text{img}(N)$. Let $z_h \in \ker(M_P^1)$. As U is positive definite, the condition

$$0 = z_h^T M_P^1 z_h = (D^T z_h)^T U (D^T z_h)$$

implies that $D^T z_h = 0$, i.e., z_h is orthogonal to the columns of D . Since

$$\text{img}(D) = \ker(N^T) = (\text{img}(N))^\perp,$$

we have $z_h \in \text{img}(N)$. Therefore, $\ker(M_P^1) \subseteq \text{img}(N)$.

Let $z_h \in \text{img}(N)$. Then, there exists a discrete field a_h such that $z_h = Na_h$. From $D^T N = 0$, which is true by the hypothesis, it follows that $M_P^1 z_h = DUD^T z_h = DUD^T N a_h = 0$. Hence, $z_h \in \ker(M_P^1)$ and $\text{img}(N) \subseteq \ker(M_P^1)$.

We conclude that $\ker(M_P^1) = \text{img}(N)$. \square

Remark 4.8. The columns of N and D form a basis for $\mathbb{R}^{n_{\mathcal{S}_{h,P}}}$.

The entries of U can be arbitrary chosen as long as the matrix remains symmetric and positive definite. These entries can be treated as parameters that, together with the positivity constraint, define a family of admissible matrices M_P satisfying the consistency condition. The symmetry reduces the number of parameters to

$$\frac{1}{2}(n_{\mathcal{S}_{h,P}} - n_{\mathcal{T}_P} + 1)(n_{\mathcal{S}_{h,P}} - n_{\mathcal{T}_P}).$$

The stability condition imposes additional constraints on the parameters. Still, in our experience, these parameters may vary several orders in magnitude with a minor to

moderate impact on the accuracy of the mimetic scheme, see, e.g., Example 5.1. The optimal choice of these parameters is problem dependent and is still an open issue. For a computer program, we recommend the simple choice of matrix U that leads to the one-parameter family of well-behaved mimetic schemes of the following corollary.

Corollary 4.2. *A one-parameter family for the matrices M_P that satisfies hypotheses (i) – (ii) in Lemma 4.7 is given by*

$$M_P = R(R^T N)^\dagger R^T + \lambda (I - N(N^T N)^{-1} N^T), \quad (4.62)$$

where λ is real strictly positive parameter. A convenient choice for λ is given by

$$\lambda = \frac{2}{n_{\mathcal{S}_{h,P}}} \text{trace}\left(R(R^T N)^\dagger R^T\right); \quad (4.63)$$

with such choice, the matrix M_P in (4.62) satisfies the hypotheses (4.54)–(4.55) appearing in Theorem 4.2.

Proof. Formula (4.62) is easily derived by choosing

$$U = \lambda(D^T D)^{-1}, \quad (4.64)$$

in Lemma 4.7. Indeed, columns of N and D form a basis in $\mathcal{S}_{h,P}$, the space of the $n_{\mathcal{S}_{h,P}}$ -sized vectors. Moreover, the columns of D are orthogonal to that of N . Thus,

$$D(D^T D)^{-1} D^T + N(N^T N)^{-1} N^T = I. \quad (4.65)$$

Setting λ as in (4.63) takes into account the proper scaling of the matrix M_P^0 . It is not difficult to verify conditions (4.54) and (4.55) of the stability Theorem 4.2. Indeed, one easily has by the definition of D that

$$\|v_h\|^2 = v_h^T (I - N(N^T N)^{-1} N^T) v_h \quad \forall v_h \in \ker(N^T),$$

and, since the involved matrix is a projection,

$$v_h^T (I - N(N^T N)^{-1} N^T) v_h \leq \|v_h\|^2 \quad \forall v_h \in \mathcal{S}_{h,P}.$$

Finally, $\text{trace}(M_P^0)$ is bounded from above by $n_{\mathcal{S}_{h,P}} \lambda_{\max}(M_P^0)$ and from below by $\lambda_{\min}^+(M_P^0)$. \square

Remark 4.9. For the diffusion problem considered in Examples 4.1–4.3 the scaling factor in (4.63) leads to a diagonal matrix M_P when P is a square cell and the diffusion tensor K_P is a scalar matrix (multiple of the identity matrix). Moreover, since $\text{trace}(M_P^0)$ is the sum of the eigenvalues of M_P^0 , we have that λ belongs to the spectrum of M_P^0 . Another typical choice is setting $1/d$ instead of $2/n_{\mathcal{S}_{h,P}}$ in (4.63). \square

4.6 The inverse of matrix M_P

Let us consider the case of $\ker(\mathcal{B}_P) = \emptyset$, e.g. the case of mimetic inner products considered in Chap. 3. Then, the algebraic consistency condition of Definition 4.4 can be formulated with respect to the inverse of matrix M_P and takes the form

$$W_P R = N. \quad (4.66)$$

Matrix W_P is used in the efficient implementation of the mimetic schemes for the diffusion problems in mixed form. As for the mixed finite element method, a hybridization procedure can be employed to reduce a saddle-point algebraic system to the equivalent system with a positive definite matrix. This procedure requires only the inverse matrix M_P^{-1} . Matrix M_P^{-1} can be substituted by matrix W_P .

The general solution of Eq. (4.66) is given by

$$W_P = N (N^T R)^{-1} N^T + \tilde{D} \tilde{U} \tilde{D}^T, \quad (4.67)$$

where the columns of matrix \tilde{D} form a basis for $\ker(R^T)$ and \tilde{U} is a symmetric positive definite matrix of parameters. A formula similar to (4.63) is found by setting

$$\tilde{U} = \tilde{\lambda} (\tilde{D}^T \tilde{D})^{-1} \quad \text{with} \quad \tilde{\lambda} = \frac{2}{n_{\mathcal{S}_{h,P}}} \text{trace} \left(N (N^T R)^{-1} N^T \right). \quad (4.68)$$

After simple algebraic manipulations, we obtain

$$W_P = N (N^T R)^{-1} N^T + \tilde{\lambda} (I - R(R^T R)^{-1} R^T). \quad (4.69)$$

The family of matrices W_P satisfying (4.67) are the inverse of the matrices M_P considered in Lemma 4.7 in the following sense. The inverse of each matrix M_P can be written as in (4.67) through a suitable choice of the matrices \tilde{D} and \tilde{U} . However, for a given couple of matrices R and N , the matrix W_P in (4.69) with $\tilde{\lambda}$ given as in (4.68) is not the inverse of the matrix M_P in (4.62) with λ given by (4.63).

Part II
Mimetic Discretization of Basic PDEs

The diffusion problem in mixed form

The velocity of flow of a liquid through a porous medium due to difference in pressure is proportional to the pressure gradient in the direction of flow.
(Darcy's law)

The diffusion problem in a mixed form is governed by the following set of equations:

$$\mathbf{u} + K\nabla p = 0 \quad \text{in } \Omega, \quad (5.1)$$

$$\operatorname{div} \mathbf{u} = b \quad \text{in } \Omega, \quad (5.2)$$

$$p = g^D \quad \text{on } \Gamma^D, \quad (5.3)$$

$$\mathbf{u} \cdot \mathbf{n} = -g^N \quad \text{on } \Gamma^N, \quad (5.4)$$

where the vector variable \mathbf{u} represents the flux of the scalar unknown p . The unknown p may be a pressure, a temperature, or a flow density depending on the physical interpretation that we give to this mathematical model. The mixed form of the diffusion problem provides an opportunity for a better approximation of the flux and the *exact* satisfaction of balance condition (5.2), e.g., [90, 205, 208].

The lowest-order mimetic discretization uses one degree of freedom per mesh face to approximate \mathbf{u} and one degree of freedom per mesh element to approximate p . It is first-order accurate for \mathbf{u} and second-order accurate for p provided that $p \in H^2(\Omega)$. On meshes of simplices (triangles in 2-D and tetrahedra in 3-D), the resulting mimetic discretization can be interpreted as a generalization of the lowest-order Raviart-Thomas finite element method, e.g. [88, 282, 305]. A posteriori error estimates for the method of [90] were developed and analyzed in [41, 53].

Different generalizations of the lowest-order scheme can be found in the literature. In [48, 54, 192] a more accurate representation of the flux variable, with d degrees of freedom per face, is introduced and analyzed. A larger number of degrees of freedom for the flux is introduced also in [256], in order to obtain a matrix with a special structure so that all flux unknowns can be eliminated explicitly. The resulting scheme can also be considered as a generalization of the multi-point flux approximation (MPFA) methods [2, 154]. Using again additional degrees of freedom for the flux, like in [256], but relaxing the matrix sparsity structure requirements lead to schemes in [48, 54, 192] that are second-order accurate for both p and \mathbf{u} . Finally, a mimetic discretizations for the convection-diffusion problem was developed in [45, 107].

In Sect. 5.1 we present the mimetic discretization of problem (5.1)–(5.4). In Sect. 5.2 we carry out the convergence analysis and derive error estimates in mesh-dependent norms. In Sect. 5.3 we reformulate the method using the exact reconstruction operator and derive a superconvergent estimate for p . In Sect. 5.4 we build a residual-based error indicator that can be used to drive an adaptive mesh refinement and derive the related a posteriori error estimates. In Sect. 5.5 we describe one extension of the scheme that has a better approximation of the flux. Throughout the chapter we assume the mesh regularity conditions (MR1)–(MR3) of Sect. 1.6.2.

5.1 Mimetic discretization

In this section, we first introduce the degrees of freedom and the associated projection operators. Then, we discuss two approaches based on Chaps. 2 and 4 which approximate the strong and weak forms of the equations. For exposition's sake, we will focus on the three-dimensional problem. The two-dimensional problem can be discretized in an analogous way.

5.1.1 Degrees of freedom and projection operators

The mimetic approximation of (5.1)–(5.4) starts with a suitable definition of the degrees of freedom for scalar and vector fields. We use the discrete spaces from Sect. 2.2 illustrated in Fig. 5.1.

- The space of discrete scalar fields \mathcal{P}_h is defined by attaching one degree of freedom to every mesh cell $P \in \Omega_h$. The value associated with cell P is denoted by q_P . The collection of all degrees of freedom form the algebraic vector $q_h \in \mathcal{P}_h$,

$$q_h = (q_P)_{P \in \Omega_h}.$$

- The space of discrete flux fields \mathcal{F}_h is defined by attaching one degree of freedom to each mesh face $f \in \mathcal{F}$. The value associated with face f is denoted by u_f . The

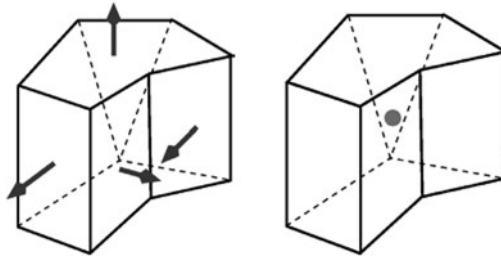


Fig. 5.1. Geometric location of degrees of freedom in the low-order MFD scheme: arrows represent fluxes u_f (on four visible faces), dot represents p_P

collection of all degrees of freedom form the algebraic vector $\mathbf{u}_h \in \mathcal{F}_h$,

$$\mathbf{u}_h = (u_f)_{f \in \mathcal{F}}.$$

The value u_f represents the average normal flux of \mathbf{u} across mesh face f in the direction of \mathbf{n}_f . It will be convenient to introduce the flux $u_{P,f}$ across f in the direction of $\mathbf{n}_{P,f}$. Obviously, it holds that $u_{P,f} = \alpha_{P,f} u_f$ where $\alpha_{P,f} = \mathbf{n}_{P,f} \cdot \mathbf{n}_f$.

The restriction of \mathbf{u}_h to cell $P \in \Omega_h$ is denoted by $\mathbf{u}_P = (u_f)_{f \in \partial P}$ and represents the collection of the normal fluxes in the directions \mathbf{n}_f . The set of these discrete fields form a linear space $\mathcal{F}_{h,P}$ which is the restriction of \mathcal{F}_h to P . In contrast to the previous chapters, we do not use in this chapter the longer notation $\mathbf{u}_{h,P}$ for \mathbf{u}_P .

The face-based projection operator $\Pi^{\mathcal{F}} : X \rightarrow \mathcal{F}_h$ is defined by (2.16) and is stable for vector functions from the following space

$$X(\Omega) = \left\{ \mathbf{v} \in (L^s(\Omega))^d, s > 2, \text{ with } \operatorname{div} \mathbf{v} \in L^2(\Omega) \right\}. \quad (5.5)$$

In the sequel, it will be convenient to use a shorter symbol for the projection operator, $\mathbf{v}^I = \Pi^{\mathcal{F}}(\mathbf{v})$. According to the definition of the projection operator, we have

$$\mathbf{v}^I = (v_f^I)_{f \in \mathcal{F}}, \quad v_f^I = \frac{1}{|f|} \int_f \mathbf{v} \cdot \mathbf{n}_f dS. \quad (5.6)$$

The cell-based projection operator $\Pi^{\mathcal{P}} : L^2(\Omega) \rightarrow \mathcal{P}_h$ is defined by (2.17). To ease the notation, we will also use the new (compact) notation for this projection operator, $q^I = \Pi^{\mathcal{P}}(q)$. According to the definition of the projection operator, we have

$$q^I = (q_P^I)_{P \in \mathcal{P}}, \quad q_P^I = \frac{1}{|P|} \int_P q dV. \quad (5.7)$$

As shown in Lemma 2.2, the projection operators (5.7) and (5.6) commute with the discrete divergence operator defined in (2.23). This fact reflects the consistency of definition (2.23) with the Gauss Theorem. We formally restate this property for future reference in this chapter.

Lemma 5.1. *For all $\mathbf{v} \in X$, it holds*

$$(\operatorname{div} \mathbf{v})^I = \operatorname{div}_h \mathbf{v}^I. \quad (5.8)$$

5.1.2 Strong and weak forms of the discrete equations

We endow the spaces \mathcal{F}_h and \mathcal{P}_h with the mimetic inner products that are constructed in Sect. 3.4 for the case of the conventional $L^2(\Omega)$ inner product. In space \mathcal{P}_h , we consider the inner product

$$[p_h, v_h]_{\mathcal{P}_h} = \sum_{P \in \Omega_h} |P| p_P v_P. \quad (5.9)$$

Note that formula (5.9) is exact for piecewise constant functions defined on mesh Ω_h . On its turn, we endow \mathcal{F}_h with the inner product

$$[\mathbf{u}_h, \mathbf{v}_h]_{\mathcal{F}_h} = \sum_{P \in \Omega_h} [\mathbf{u}_P, \mathbf{v}_P]_P, \quad (5.10)$$

which is assembled from local inner products $[\cdot, \cdot]_P$ in $\mathcal{F}_{h,P}$ introduced in Sect. 3.4. Later in this chapter, we generalize the construction of local inner products described in Chap. 3 to the case of weighted L^2 inner products. For the moment, we only note that the local mimetic inner product satisfies the stability and consistency conditions that lead to a stable and accurate numerical scheme.

Let for a moment $\Gamma^N = \emptyset$ and $g^D = 0$. We approximate the differential operators “div” and “K ∇ ” by using the primary and derived discrete operators introduced in Sects. 2.3 and 2.4:

$$\operatorname{div} \approx \operatorname{div}_h \quad \text{and} \quad \operatorname{K}\nabla \approx \tilde{\nabla}_h = -M_{\mathcal{F}}^{-1} \operatorname{div}_h^T M_{\mathcal{D}}, \quad (5.11)$$

cf. equations (2.23) and (2.28). The matrices $M_{\mathcal{F}}$ and $M_{\mathcal{D}}$ are built by assembling the local mimetic inner product matrices $M_{\mathcal{D},P}$ and $M_{\mathcal{F},P}$ respectively (see Sects. 2.3 and 2.4).

As pointed out in Chap. 2, the discrete operators allow us to write immediately a mimetic approximation of equations (5.1)–(5.2) as

$$\mathbf{u}_h + \tilde{\nabla}_h p_h = 0, \quad (5.12)$$

$$\operatorname{div}_h \mathbf{u}_h = b^I, \quad (5.13)$$

where $b^I = \Pi^{\mathcal{D}}(b)$. The linear system arising from (5.12)–(5.13) reads:

$$\mathbf{u}_h - M_{\mathcal{F}}^{-1} \operatorname{div}_h^T M_{\mathcal{D}} p_h = 0, \quad (5.14)$$

$$\operatorname{div}_h \mathbf{u}_h = b^I, \quad (5.15)$$

Remark 5.1. In general, matrix $M_{\mathcal{F}}^{-1}$ is a dense matrix. We can avoid the calculation of this matrix by multiplying both sides of Eq. (5.14) by $M_{\mathcal{F}}$. The linear system can be also symmetrized by multiplying both sides of Eq. (5.15) by $M_{\mathcal{D}}$.

A numerical treatment of heterogeneous Dirichlet and Neumann boundary conditions is possible but a bit awkward in the classical mimetic schemes due to their finite difference nature. For example, for this purpose, extended discrete operators are introduced in [206]. An alternative approach is based on employing the mimetic discretization technology for an approximation of the weak formulation (1.18)–(1.19).

We now introduce the variational, or weak, mimetic discretization of the problem. Let the boundary data g^D and g^N be integrable on Γ^D and Γ^N , respectively. Then, we introduce the space

$$\mathcal{F}_{h,g} = \left\{ \mathbf{v}_h \in \mathcal{F}_h : v_f = \frac{1}{|f|} \int_f g^N dS \quad \forall f \in \mathcal{F}^N \right\}$$

where $\mathcal{F}^N \subset \mathcal{F}$ is the set of mesh faces in Γ^N . Setting $g^N = 0$ in the previous definition gives the linear space $\mathcal{F}_{h,0}$. For function $g^D \in L^1(\Gamma^D)$, we define a linear functional

$$\langle g^D, \mathbf{v}_h \rangle_h = \sum_{f \in \mathcal{F}^D} v_f \int_f g^D dS, \quad (5.16)$$

where $\mathcal{F}^D \subset \mathcal{F}$ is the set of mesh faces in Γ^D .

Let the loading term b be integrable on Ω . Then, the mimetic discretization of the weak formulation (1.18)–(1.19) reads:

Find $(\mathbf{u}_h, p_h) \in \mathcal{F}_{h,g} \times \mathcal{P}_h$ such that

$$[\mathbf{u}_h, \mathbf{v}_h]_{\mathcal{F}_h} - [p_h, \operatorname{div}_h \mathbf{v}]_{\mathcal{P}_h} = -\langle g^D, \mathbf{v}_h \rangle_h \quad \forall \mathbf{v}_h \in \mathcal{F}_{h,0}, \quad (5.17)$$

$$[\operatorname{div}_h \mathbf{u}_h, q_h]_{\mathcal{P}_h} = [b^I, q_h]_{\mathcal{P}_h} \quad \forall q_h \in \mathcal{P}_h, \quad (5.18)$$

where we use the inner products introduced in (5.9) and (5.10).

Remark 5.2. Formulation (5.17)–(5.18) does not require a discrete gradient operator. However, such an operator can be deduced from the first equation using the duality argument, similar to how it was done in Chap. 2. \square

Remark 5.3. In the case of homogeneous Dirichlet boundary conditions, a linear system arising from (5.17)–(5.18) is equivalent to (5.14)–(5.15) after its symmetrization (see Remark 5.1). In the rest of this chapter, we will use formulation (5.17)–(5.18) since it provides a simpler treatment of the boundary conditions.

5.1.3 Stability and consistency conditions

In this section, we detail the two fundamental conditions of *stability* (coercivity) and *consistency* that must be satisfied by the inner product $[\cdot, \cdot]_{\mathcal{P}}$ in order to obtain a convergent method [93]. Both conditions have been introduced in the general framework of Chap. 4.

Let $K_{\mathcal{P}}$ be the approximation of the diffusion tensor K on cell \mathcal{P} given by

$$K_{\mathcal{P}} = \frac{1}{|\mathcal{P}|} \int_{\mathcal{P}} K dV. \quad (5.19)$$

If K is sufficiently regular, its cell average could also be substituted by its value at the barycenter of \mathcal{P} , i.e., $K_{\mathcal{P}} = K(\mathbf{x}_{\mathcal{P}})$. Using (5.19), we define a discontinuous tensorial field \bar{K} such that $\bar{K}|_{\mathcal{P}} = K_{\mathcal{P}}$.

Since $[\cdot, \cdot]_{\mathcal{P}}$ is the inner product, it induces a norm on $\mathcal{F}_{h,\mathcal{P}}$. This property is stated by the stability condition **(S1)** below.

(S1) (*Stability condition*). There exist two positive constants σ_* and σ^* independent of the mesh size h such that for every \mathcal{P} it holds

$$\sigma_* |\mathcal{P}| \sum_{f \in \partial \mathcal{P}} |v_f|^2 \leq [\mathbf{v}_{\mathcal{P}}, \mathbf{v}_{\mathcal{P}}]_{\mathcal{P}} \leq \sigma^* |\mathcal{P}| \sum_{f \in \partial \mathcal{P}} |v_f|^2 \quad \forall \mathbf{v}_{\mathcal{P}} \in \mathcal{F}_{h,\mathcal{P}}.$$

Condition **(S1)** states that the inner product $[\cdot, \cdot]_{\mathbf{P}}$ is coercive; in other words, $[\mathbf{v}_{\mathbf{P}}, \mathbf{v}_{\mathbf{P}}]_{\mathbf{P}} = 0$ if and only if $\mathbf{v}_{\mathbf{P}} = \mathbf{0}$. Moreover, the lower and upper bounds force the inner product to scale as $|\mathbf{P}|$, which is natural because $[\cdot, \cdot]_{\mathbf{P}}$ approximates a volume integral over \mathbf{P} .

Let us define the following space:

$$S_{h,\mathbf{P}} = \{ \mathbf{v} \in (L^s(\mathbf{P}))^d, s > 2, \text{ with } \operatorname{div} \mathbf{v} = \text{const}, \mathbf{v} \cdot \mathbf{n}_f = \text{const} \quad \forall f \in \partial \mathbf{P} \}.$$

According to the theory developed in Part I of this book, this space must satisfy three assumptions **(B1)**–**(B3)**. We recall the first two assumptions, while the third assumption **(B3)** from Chap. 4 will be addressed below.

(B1) The local projection operator from $S_{h,\mathbf{P}}$ to $\mathcal{F}_{h,\mathbf{P}}$ must be surjective.

(B2) The space $S_{h,\mathbf{P}}$ must contain the trial space of constant vector functions:

$$\mathcal{F}_{\mathbf{P}} = \{ \mathbf{v} : \mathbf{P} \rightarrow \mathbb{R}^d \text{ such that } \mathbf{v} = \mathbf{K}_{\mathbf{P}} \nabla q \text{ with } q \in \mathbb{P}_1(\mathbf{P}) \}.$$

It is immediate to verify that the space $S_{h,\mathbf{P}}$ above satisfies both conditions. The space $S_{h,\mathbf{P}}$ is used in the following condition.

(S2) (*Consistency condition*). For any vector function $\mathbf{v} \in S_{h,\mathbf{P}}$, any linear polynomial q , and every element \mathbf{P} of Ω_h it holds

$$[(\mathbf{K}_{\mathbf{P}} \nabla q)_{\mathbf{P}}^{\mathbf{I}}, \mathbf{v}_{\mathbf{P}}^{\mathbf{I}}]_{\mathbf{P}} = \int_{\mathbf{P}} \mathbf{K}_{\mathbf{P}}^{-1} (\mathbf{K}_{\mathbf{P}} \nabla q) \cdot \mathbf{v} dV. \quad (5.20)$$

We do not simplify $\mathbf{K}_{\mathbf{P}}$ in order to stress the fact that the natural L^2 inner product in the space of fluxes is defined with the tensorial weight $\mathbf{K}_{\mathbf{P}}^{-1}$. As discussed in Chaps. 3 and 4, consistency condition **(S2)** is the accuracy property. To make it useful, the right-hand side of (5.20) must be computable easily and be independent of the values of \mathbf{v} inside \mathbf{P} . Integrating by parts and using the properties of space $S_{h,\mathbf{P}}$, we obtain

$$\begin{aligned} \int_{\mathbf{P}} \mathbf{K}_{\mathbf{P}} (\mathbf{K}_{\mathbf{P}}^{-1} \nabla q) \cdot \mathbf{v} dV &= \int_{\mathbf{P}} \nabla q \cdot \mathbf{v} dV \\ &= - \int_{\mathbf{P}} q \operatorname{div} \mathbf{v} dV + \sum_{f \in \partial \mathbf{P}} \int_f \mathbf{v} \cdot \mathbf{n}_{\mathbf{P},f} q dS \\ &= - \operatorname{div}_{\mathbf{P}} \mathbf{v}_{\mathbf{P}}^{\mathbf{I}} \int_{\mathbf{P}} q dV + \sum_{f \in \partial \mathbf{P}} \alpha_{\mathbf{P},f} \mathbf{v}_f^{\mathbf{I}} \int_f q dS, \end{aligned} \quad (5.21)$$

since $\operatorname{div}_{\mathbf{P}} \mathbf{v}_{\mathbf{P}}^{\mathbf{I}} = (\operatorname{div} \mathbf{v})|_{\mathbf{P}} = \text{const}$ and $\mathbf{v}_f^{\mathbf{I}} = \mathbf{v} \cdot \mathbf{n}_{\mathbf{P},f} = \text{const}$. Thus, average normal components of \mathbf{v} on faces f are all what is needed to calculate the integral. But, they are our degrees of freedom and always available in the numerical scheme. This is the property required by assumption **(B3)** in Chap. 4.

A property similar to **(S2)** has been used for the first time in [257] to build a one-parameter family of inner product matrices for a triangular cell. This family includes the mass matrix appearing in the lowest order Raviart-Thomas finite element method on triangular meshes. In the next section, we show how to build a family of inner product matrices for an arbitrary polyhedral element \mathbf{P} .

Remark 5.4. Note that we do not require the space $S_{h,P}$ to be finite dimensional and isomorphic to $\mathcal{F}_{h,P}$. Nevertheless nothing forbids us to choose it such that, in addition to the above conditions, we have

$$\dim(S_{h,P}) = \dim(\mathcal{F}_{h,P}). \quad (5.22)$$

This is, for instance, what happens when reconstruction operators are introduced in Sect. 5.3. Each reconstruction operator defines a finite-dimensional space $S_{h,P}$ that is isomorphic to $\mathcal{F}_{h,P}$. The general form of the consistency condition **(S2)** shows clearly that one does not need to build the space $S_{h,P}$ explicitly. Indeed, Eq. (5.21) demonstrates that the right hand side of the consistency condition does not depend on the shape of functions in $S_{h,P}$; hence, the explicit knowledge of a reconstruction operator is not needed. \square

5.1.4 A family of mimetic schemes

Any inner product can be represented by a symmetric and positive definite matrix:

$$[\mathbf{u}_P, \mathbf{v}_P]_P = \mathbf{u}_P^T M_P \mathbf{v}_P. \quad (5.23)$$

As discussed in Chap. 3, matrix M_P satisfies equation of type $M_P N_P = R_P$, where N_P and R_P are rectangular matrices. Let us show that a similar formula holds the case of a weighted inner product. More precisely, we use consistency condition **(S2)** to derive the matrices R_P and N_P . Since, only ∇q is used by this condition, its simplification is possible if we restrict the choice of the polynomials q to the quotient space $\mathbb{P}_1(P)/\mathbb{R}$, i.e., the linear space of polynomials of degree one with zero mean value on P . For such a polynomial, the volume integral in the right-hand side of (5.21) is zero and **(S2)** becomes

$$[(K_P \nabla q)^I, \mathbf{v}_P^I]_P = \sum_{f \in \partial P} \alpha_{P,f} \nu_f \int_f q dS, \quad (5.24)$$

showing more explicitly that $[\cdot, \cdot]_P$ depends only on boundary data. Discarding constant functions is not at all restrictive because no new information is incorporated into a scheme by taking $q = 1$. In fact, setting $q = 1$ in (5.21) reproduces the definition of the discrete divergence given in (2.23):

$$0 = -|P| \operatorname{div}_P \mathbf{v}_P^I + \sum_{f \in \partial P} \alpha_{P,f} \nu_f^I |f|.$$

Now, let us consider the three polynomial functions:

$$q^1(x,y,z) = x - x_P, \quad q^2(x,y,z) = y - y_P, \quad \text{and} \quad q^3(x,y,z) = z - z_P,$$

where we recall that $\mathbf{x}_P = (x_P, y_P, z_P)^T$ is the barycenter of P . We define a vector $\mathbf{N}_j = (K_P \nabla q^j)_P^I = \Pi_P^{\mathcal{F}}(K_P \nabla q^j)$. If we enumerate the faces of P by an index running from 1 to $N_P^{\mathcal{F}}$ (the number of faces of P), the explicit formula for the i -th component

of N_j is

$$(N_j)_i = \frac{1}{|f_i|} \int_{f_i} \mathbf{n}_{f_i} \cdot K_P \nabla q^j dS = \mathbf{n}_{f_i}^T K_P \cdot \nabla q^j.$$

Let us define the $N_P^{\mathcal{F}} \times 3$ matrix $N_P = [N_1, N_2, N_3]$. Since ∇q^j is the three-dimensional vector with 1 at the j -th entry and zero elsewhere, the i -th row of this matrix is $\mathbf{n}_{f_i}^T K_P$. Thus,

$$N_P = \begin{pmatrix} \mathbf{n}_{f_1}^T \\ \mathbf{n}_{f_2}^T \\ \vdots \\ \mathbf{n}_{f_{N_P^{\mathcal{F}}}}^T \end{pmatrix} K_P. \quad (5.25)$$

Now we can reformulate (5.24) as follows:

$$[(K_P \nabla q^j)^I, \mathbf{v}_P^I]_P = (\mathbf{v}_P^I)^T M_P N_j = (\mathbf{v}_P^I)^T R_j, \quad (R_j)_i = \alpha_{P,f_i} \int_f q^j dS, \quad (5.26)$$

which must hold for every discrete vector field \mathbf{v}_P^I . The vector R_j depends on q^j and the geometry of cell P . Let $R_P = [R_1, R_2, R_3]$. As \mathbf{v}_P^I is arbitrary, we obtain the three matrix conditions:

$$M_P N_j = R_j, \quad \text{for } j = 1, 2, 3, \quad (5.27)$$

that can be written in the compact form

$$M_P N_P = R_P. \quad (5.28)$$

Finally, we provide the explicit formula for matrix R_P . The face integral (see (5.26)) of a linear function equals to its value at the barycenter \mathbf{x}_f times the face area. Thus,

$$R_P = \begin{pmatrix} \alpha_{P,f_1} |f_1| (\mathbf{x}_{f_1} - \mathbf{x}_P)^T \\ \alpha_{P,f_2} |f_2| (\mathbf{x}_{f_2} - \mathbf{x}_P)^T \\ \vdots \\ \alpha_{P,f_{N_P^{\mathcal{F}}}} |f_{N_P^{\mathcal{F}}}| (\mathbf{x}_{f_{N_P^{\mathcal{F}}}} - \mathbf{x}_P)^T \end{pmatrix}. \quad (5.29)$$

The following result is the particular case of the general statement found in Lemma 4.1.

Lemma 5.2. *For any polyhedral cell P , we have*

$$N_P^T R_P = K_P |P|. \quad (5.30)$$

Proof. Without loss of generality, we place the origin of the coordinate system into the barycenter of P , i.e. $\mathbf{x}_P = (0, 0, 0)^T$. We denote the i -th spatial coordinate by $x^{(i)}$, i.e., $\mathbf{x} = (x^{(1)}, x^{(2)}, x^{(3)})^T$. Let \mathbf{e}_j be the three-dimensional vector whose j -th compo-

ment is 1 and others are 0. We write the j -th columns of $|P|K_P$ as $|P|K_P \mathbf{e}_j$ to start the developments:

$$\begin{aligned} |P|K_P \mathbf{e}_j &= K_P \int_P \mathbf{e}_j dV = K_P \int_P \nabla x^{(j)} dV = K_P \int_{\partial P} \mathbf{n}_P x^{(j)} dS \\ &= K_P \sum_{f \in \partial P} \alpha_{P,f} \mathbf{n}_f \int_f x^{(j)} dS = K_P \sum_{f \in \partial P} \alpha_{P,f} \mathbf{n}_f |f| x_f^{(j)}. \end{aligned}$$

Comparison with (5.25) and (5.29) gives

$$|P|K_P \mathbf{e}_j = N_P^T R_P \mathbf{e}_j \quad j = 1, 2, 3.$$

This proves the assertion of the lemma. \square

It is easy to verify by direct substitution that all the (symmetric and positive semi-definite) matrices of the form below satisfy (5.28):

$$M_P = R_P (R^T N_P)^{-1} R_P^T + M_P^{(1)}, \quad (5.31)$$

where $M_P^{(1)}$ is a symmetric and positive semi-definite matrix such that $\ker(M_P^{(1)}) = \text{img}(N_P)$. As the choice of $M_P^{(1)}$ is not unique, formula (5.31) represents a family of matrices, and, thus, a family of numerical schemes. As discussed in Sect. 4.5, an effective choice of $M_P^{(1)}$ is given by the scaled orthogonal projector:

$$M_P^{(1)} = \gamma_P (I - N_P (N_P^T N_P)^{-1} N_P^T), \quad \gamma_P = \frac{1}{N_P^{\mathcal{F}} |P|} \text{trace}(R_P K_P^{-1} R_P^T). \quad (5.32)$$

Theorem 5.1. *Let the mesh assumptions (MR1)–(MR2) of Sect. 1.6.2 hold. Moreover, let assumption (MR3) of Sect. 1.6.2 be satisfied with $\bar{\mathbf{x}}_P = \mathbf{x}_P$, the barycenter of P , and $\bar{\mathbf{x}}_f = \mathbf{x}_f$, the barycenter of face f , for every face $f \in \partial P$. Then, the inner product matrix M_P given by (5.31) and (5.32) satisfies the stability condition (S1) with constants σ_* and σ^* that depend only on the space dimension d , the mesh regularity constants appearing in (MR1)–(MR2), and the ellipticity constants κ_* , κ^* that bound the spectrum of K_P .*

Proof. The boundness of K_P can be formalized as

$$\kappa_* |\xi|^2 \leq \xi^T K_P \xi \leq \kappa^* \|\xi\|^2 \quad \forall \xi \in \mathbb{R}^d,$$

where $\|\xi\|^2 = \xi^T \xi$. In this proof, we indicate generic positive constants appearing in various inequalities by c_i , $i \geq 1$. These constants may depend only on κ_* , κ^* and on the regularity constants \mathcal{N}^s and ρ_s of assumptions (MR1)–(MR2). Property (M2), see Sect. 1.6.2, implies that all geometric objects of cell P have bounded measures:

$$a_* h_P^3 \leq |P| \leq h_P^3, \quad a_* h_P^2 \leq |f| \leq h_P^2,$$

where we recall that h_P is the diameter of P and a_* depends only on \mathcal{N}^s and ρ_s . Using these results, we show a number of intermediate estimates. From the definition

of matrix N_P in (5.25) it follows

$$\|N_P \mathbf{w}\|^2 = \sum_{f \in \partial P} (\mathbf{n}_f^T K_P \mathbf{w})^2 \leq \mathcal{N}^s(\kappa^*)^2 \|\mathbf{w}\|^2 \quad \forall \mathbf{w} \in \mathbb{R}^d. \quad (5.33)$$

Let now $\bar{\mathbf{x}}_P$ and $\bar{\mathbf{x}}_f$ be the points introduced in **(MR3)** of Chap. 1. By our assumption, these points correspond to barycenters \mathbf{x}_P and \mathbf{x}_f , respectively. From the definitions of γ_P in (5.32) and matrix R_P in (5.29) we have

$$\gamma_P = \frac{1}{N_P^{\mathcal{F}} |P|} \text{trace}(R_P K_P^{-1} R_P^T) = \frac{1}{N_P^{\mathcal{F}} |P|} \sum_{f \in \partial P} |f|^2 (\mathbf{x}_f - \mathbf{x}_P)^T K_P^{-1} (\mathbf{x}_f - \mathbf{x}_P).$$

The argument employed in the proof of **(M2)** can be used again to show that the distance between \mathbf{x}_P and \mathbf{x}_f is bounded (up to positive uniform constants) from below and above by the diameter h_P . Therefore,

$$c_1 |P| \leq \gamma_P \leq c_2 |P|.$$

A similar argument can be used to derive the following upper bound:

$$\|R_P^T \mathbf{v}_P\|^2 = \sum_{i=1}^d |R_i^T \mathbf{v}_P|^2 \leq 3 \|\mathbf{v}_P\|^2 \sum_{f \in \partial P} |f|^2 \|\mathbf{x}_f - \mathbf{x}_P\|^2 \leq c_3 |P|^2 \|\mathbf{v}_P\|^2.$$

Finally, we need a special lower bound for the Euclidean norm of $R_P^T \mathbf{v}_P$. Let us now decompose $\mathbf{v}_P = \mathbf{v}_{P,N} + \mathbf{v}_{P,\perp}$, where $\mathbf{v}_{P,N} \in \text{img}(N_P)$ and $\mathbf{v}_{P,\perp} \in (\text{img}(N_P))^\perp$; hence, $\|\mathbf{v}_P\|^2 = \|\mathbf{v}_{P,N}\|^2 + \|\mathbf{v}_{P,\perp}\|^2$. Using (5.33), we obtain:

$$\|R_P^T \mathbf{v}_{P,N}\| = \|R_P^T N_P \mathbf{w}\| = |P| \|K_P \mathbf{w}\| \geq \frac{|P| \kappa_*}{\sqrt{\mathcal{N}^s \kappa^*}} \|N_P \mathbf{w}\| = \frac{|P| \kappa_*}{\sqrt{\mathcal{N}^s \kappa^*}} \|\mathbf{v}_{P,N}\|.$$

Let us note that

$$\mathbf{v}_P^T M_P \mathbf{v}_P = (R_P^T (\mathbf{v}_{P,N} + \mathbf{v}_{P,\perp})) \frac{K_P^{-1}}{|P|} (R_P^T (\mathbf{v}_{P,N} + \mathbf{v}_{P,\perp})) + \mathbf{v}_{P,\perp}^T M_P^{(1)} \mathbf{v}_{P,\perp}.$$

With the above developments, it is easy to obtain the upper bound in the stability estimate **(S1)** with a mesh-independent constant:

$$\mathbf{v}_P^T M_P \mathbf{v}_P \leq \frac{1}{|P| \kappa_*} \|R_P^T \mathbf{v}_P\|^2 + \gamma_P \|\mathbf{v}_P\|^2 \leq c_4 |P| \|\mathbf{v}_P\|^2.$$

The lower bound requires a little bit more work. We recall the following vector inequality:

$$-2 \mathbf{a} \cdot \mathbf{c} \leq \varepsilon \|\mathbf{a}\|^2 + \frac{1}{\varepsilon} \|\mathbf{c}\|^2 \quad \forall \varepsilon > 0.$$

Using this inequality, we obtain

$$\begin{aligned} \mathbf{v}_P^T M_P \mathbf{v}_P &\geq \frac{\kappa_*}{|P|} \|R_P^T(\mathbf{v}_{P,N} + \mathbf{v}_{P,\perp})\|^2 + \gamma_P \|\mathbf{v}_{P,\perp}\|^2 \\ &\geq \frac{\kappa_*}{|P|} \|R_P^T \mathbf{v}_{P,N}\|^2 (1 - \varepsilon) + \frac{\kappa_*}{|P|} \|R_P^T \mathbf{v}_{P,\perp}\|^2 \left(1 - \frac{1}{\varepsilon}\right) + \gamma_P \|\mathbf{v}_{h,\perp}\|^2. \end{aligned}$$

If we take $\varepsilon < 1$ and apply the above inequalities, we get the following estimate:

$$\mathbf{v}_P^T M_P \mathbf{v}_P \geq c_5 (1 - \varepsilon) |P| \|\mathbf{v}_{P,N}\|^2 + \left(c_6 \left(1 - \frac{1}{\varepsilon}\right) + c_7\right) |P| \|\mathbf{v}_{P,\perp}\|^2.$$

The lower bound is obtained by requiring both terms in the right-hand side to be positive. This gives $\varepsilon = c_6 / (c_6 + \frac{1}{2}c_7)$. This proves the assertion of the theorem. \square

Example 5.1. This example shows how the accuracy of the mimetic discretization depend on the choice of the parameter γ_P other than that in formula (5.32). Let us add a scalar factor $\tilde{\gamma} > 0$ to γ_P , so that the case $\tilde{\gamma} = 1$ gives the scheme described above. Let us consider diffusion problem (5.1)–(5.4) in the unit square Ω with the Dirichlet boundary condition on $\partial\Omega$. We define the diffusion tensor by

$$K = \begin{pmatrix} (1+x)^2 + y^2 & -xy \\ -xy & (1+x)^2 + y^2 \end{pmatrix}.$$

The source term b and the boundary function g^D are defined by the exact solution

$$p(x,y) = x^3 y^2 + x \sin(2\pi xy) \sin(2\pi y).$$

This example has been proposed in [93]. The computational mesh and profile of the exact solution are shown in Fig. 5.2.

Figure 5.3 shows relative approximation errors for p and \mathbf{u} in mesh-dependent norms (see the next section) as functions of $\tilde{\gamma}$. There exists a quite big interval $\tilde{\gamma} \in$

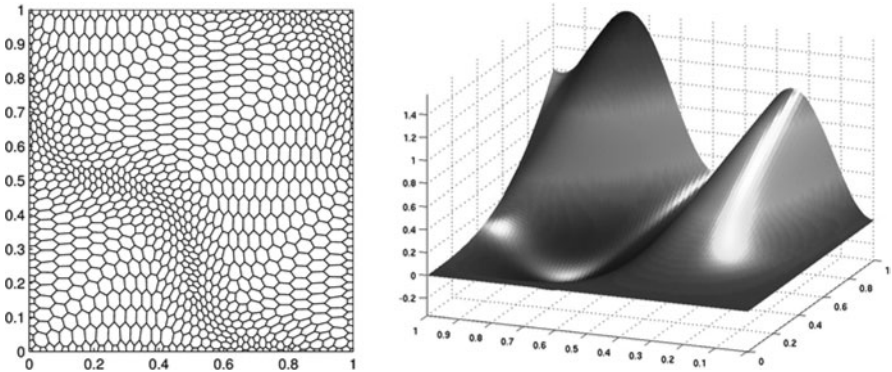


Fig. 5.2. Computational mesh and solution profile in Example 5.1

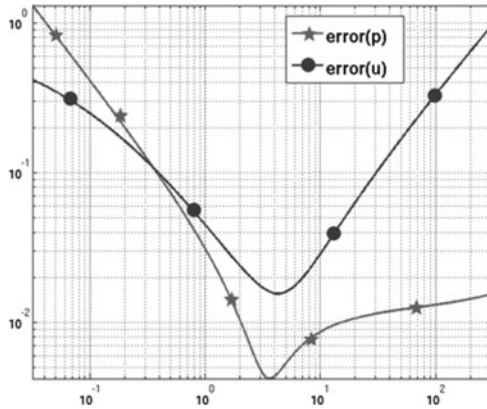


Fig. 5.3. Dependence of the approximation errors on the parameter $\tilde{\gamma}$ (see Example 5.1)

[2, 80] where the errors vary only 3 times. What is remarkable here is that for all values of $\tilde{\gamma}$ we observed the second-order convergence rate for p and 1.5 convergence rate for \mathbf{u} . This example shows that there exists a big room for various optimization strategies like that discussed in Chap. 11. Finally, we note that similar conclusions can be drawn for a large range of numerical tests.

5.2 Convergence analysis and error estimates

In this section we derive error estimates for the mimetic scheme (5.17)–(5.18). Error bounds for the vector variable are proved in Sect. 5.2.3 and for the scalar variable in Sect. 5.2.4. These estimates show the linear convergence of the method and are similar to that for the lowest-order Raviart-Thomas finite element method [88, 282, 305] on simplicial meshes.

Superconvergence is proved in Sect. 5.3 for the scalar variable under a few additional assumptions. For simplicity of exposition, we consider only the Dirichlet boundary condition in the superconvergence analysis.

The errors estimated will be proved in the following discrete norms:

$$\|\mathbf{v}_h\|_{\mathcal{F}_h}^2 := [\mathbf{v}_h, \mathbf{v}_h]_{\mathcal{F}_h} \quad \forall \mathbf{v}_h \in \mathcal{F}_h$$

and

$$\|q_h\|_{\mathcal{D}_h}^2 := [q_h, q_h]_{\mathcal{D}_h} = \sum_{P \in \Omega_h} |P| |q_P|^2 \quad \forall q_h \in \mathcal{D}_h.$$

Due to assumption (S1), the first norm is spectrally equivalent to

$$\|\mathbf{v}_h\|_{\mathcal{F}_h}^2 \preceq \sum_{P \in \Omega_h} |P| \sum_{f \in \partial P} |v_f|^2.$$

These proofs combine the steps in [90] with the ideas from [48].

5.2.1 Preliminary lemmas

In this section, we collect technical results that are used in the convergence analysis. We will use a stronger form of property **(M5)**, see (1.65). The modified property states that for any function $q \in H^{s+1}(\mathbb{P})$ with $s \in \mathbb{R}$ and $-1/2 < s \leq m$ for some given integer m we can find a polynomial $q_{\mathbb{P}}^{(m)}$ of degree m such that

$$\|q - q_{\mathbb{P}}^{(m)}\|_{L^2(\mathbb{P})} + \sum_{k=1}^{\lfloor s \rfloor} h_{\mathbb{P}}^k |q - q_{\mathbb{P}}^{(m)}|_{H^k(\mathbb{P})} \leq C^{Jm} h_{\mathbb{P}}^{s+1} |q|_{H^{s+1}(\mathbb{P})}, \quad (5.34)$$

where $\lfloor s \rfloor$ is the integer part of s , and C^{Jm} is a positive constant independent of $h_{\mathbb{P}}$.

We will also need a stronger form of the trace inequality in assumption **(M4)**, see (1.65). It states [256] that for every $q \in H^s(\mathbb{P})$ with $s > 1/2$, we have

$$\sum_{f \in \partial \mathbb{P}} \|\phi\|_{L^2(f)}^2 \leq C^{Agm} \left(h_{\mathbb{P}}^{-1} \|\phi\|_{L^2(\mathbb{P})}^2 + h_{\mathbb{P}}^{2s-1} \|\phi\|_{H^s(\mathbb{P})}^2 \right). \quad (5.35)$$

In addition to the strong ellipticity condition expressed in **(H1)**, see Sect. 1.4.1, we assume that the diffusion tensor \mathbf{K} is also locally Lipschitz continuous on Ω_h .

(H1b) All entries of tensor \mathbf{K} (and, hence, of \mathbf{K}^{-1}) are in $W^{1,\infty}(\mathbb{P})$ for every $\mathbb{P} \in \Omega_h$. Assumption **(H1b)** implies that

$$\max_{i,j=1,d} \sup_{x \in \mathbb{P}} |(\mathbf{K}_{\mathbb{P}})_{ij} - \mathbf{K}_{ij}(x)| \leq C_{\mathbf{K}}^* h_{\mathbb{P}}, \quad (5.36)$$

where $C_{\mathbf{K}}^*$ is independent of $h_{\mathbb{P}}$ and the polyhedron \mathbb{P} . A similar bound holds for $\mathbf{K}_{\mathbb{P}}^{-1}$ as it is a first-order approximation of \mathbf{K}^{-1} .

Lemma 5.3. *Let us consider $\mathbb{P} \in \Omega_h$ and $\mathbf{v} \in (H^1(\mathbb{P}))^d$. Then, there exists a non-negative constant C independent of h such that*

$$\|\mathbf{v}_{\mathbb{P}}^{\mathbf{I}}\|_{\mathbb{P}}^2 \leq C \left(\|\mathbf{v}\|_{L^2(\mathbb{P})}^2 + h_{\mathbb{P}}^2 \|\mathbf{v}\|_{H^1(\mathbb{P})}^2 \right). \quad (5.37)$$

Proof. This lemma follows from the definition of the face projector, cf. (5.6), and property **(M4)**, see Sect. 1.6.2. \square

The proofs of the following three lemmas can be found in [48].

Lemma 5.4. *Let $q \in H^2(\Omega)$ and $q^{(1)}$ be a piecewise polynomial such that $q^{(1)}|_{\mathbb{P}}$ is the linear approximation of q over \mathbb{P} satisfying (5.34). Then, there exists a positive constant C_2 independent of q and h such that for every $\mathbf{v}_h \in \mathcal{F}_h$ it holds:*

$$\left[(\mathbf{K} \nabla (q - q^{(1)}))^{\mathbf{I}}, \mathbf{v}_h \right]_{\mathcal{F}_h} \leq C_2 h |q|_{H^2(\Omega)} \|\mathbf{v}_h\|_{\mathcal{F}_h}. \quad (5.38)$$

Lemma 5.5. *There exists a positive constant C independent of h such that for every $\mathbf{v}_h \in \mathcal{F}_h$ and every $q \in H^2(\Omega)$ it holds*

$$\left[((K - \bar{K})\nabla q)^{\mathbf{l}}, \mathbf{v}_h \right]_{\mathcal{F}_h} \leq Ch(|q|_{H^1(\Omega)} + h|q|_{H^2(\Omega)}) \|\mathbf{v}_h\|_{\mathcal{F}_h}. \quad (5.39)$$

Lemma 5.6. *Let $q \in H^2(\Omega)$ and $q^{(1)}$ be a piecewise polynomial such that $q^{(1)}|_P$ is the linear approximation of q over P satisfying (5.34). Then, there exists a positive constant C_1 independent of q and h such that for every $\mathbf{v}_h \in \mathcal{F}_h$ it holds:*

$$\sum_{P \in \Omega_h} \sum_{f \in \partial P} \alpha_{P,f} v_f \int_f q_P^{(1)} dS - \langle q|_{\partial\Omega}, \mathbf{v}_h \rangle_h \leq C_1 h \|q\|_{H^2(\Omega)} \|\mathbf{v}_h\|_{\mathcal{F}_h}, \quad (5.40)$$

where $\langle \cdot, \cdot \rangle_{\mathcal{Q}}$ is the bilinear form introduced in (5.16), and $\alpha_{P,f} = \pm 1$ takes into account the orientation of the face f with respect to P .

We conclude this section by noting that the commuting diagram property (5.8) characterizes the numerical solution \mathbf{u}_h and the projection $\mathbf{u}^{\mathbf{l}}$ of the exact solution as follows

$$\operatorname{div}_h(\mathbf{u}_h - \mathbf{u}^{\mathbf{l}}) = 0. \quad (5.41)$$

Indeed, let $\chi^{(P)}$ be the piecewise constant function with value 1 over cell P and zero over the other cells. Taking $q = \chi^{(P)}$ in (5.18), we have that $\operatorname{div}_P \mathbf{u}_P = b_P^{\mathbf{l}}$, from which we conclude that $\operatorname{div}_h \mathbf{u}_h = b^{\mathbf{l}}$. Using (5.2) and (5.8) yield

$$\operatorname{div}_h \mathbf{u}_h = b^{\mathbf{l}} = (\operatorname{div} \mathbf{u})^{\mathbf{l}} = \operatorname{div}_h \mathbf{u}^{\mathbf{l}}.$$

5.2.2 Stability analysis

The lemma below states a stability condition, namely, the *inf-sup* condition [88], that is used in the convergence analysis. We present two different proofs of this lemma. The first proof follows [48] and uses a result from the theory of mixed finite elements when the Raviart-Thomas $\mathbb{RT}_0 - \mathbb{P}_0$ scheme is applied on the submesh \mathcal{T}_h of simplexes introduced in assumption **(MR3)**, see Sect. 1.6.2. This proof is valid for very general domains as no convexity assumption is required. The second proof follows [90] and is based on the solution of an auxiliary problem that requires the domain to be convex to have an H^2 -regular solution. This proof does not use any regularity assumption on the submesh \mathcal{T}_h .

We recall that the lowest-order Raviart-Thomas finite element space on \mathcal{T}_h is defined as follows [88, 305]:

$$\mathbb{RT}_0(\mathcal{T}_h) = \left\{ \mathbf{v} \in H(\operatorname{div}, \Omega) : \mathbf{v}|_T = \mathbf{a}_T + b_T \mathbf{x} \quad \forall T \in \mathcal{T}_h, \quad \mathbf{a}_T \in \mathbb{R}^d, b_T \in \mathbb{R} \right\}$$

and

$$\mathbb{P}_0(\mathcal{T}_h) = \left\{ q \in L^2(\Omega) : q|_T = \text{const} \quad \forall T \in \mathcal{T}_h \right\}.$$

Lemma 5.7 (Inf-sup condition). *There exists a positive constant β independent of h such that for every cell-based mesh field $q_h \in \mathcal{P}_h$ there exists a face-based mesh field $\mathbf{v}_h \in \mathcal{F}_h$ such that*

$$\operatorname{div}_h \mathbf{v}_h = q_h, \quad (5.42)$$

$$\|\|\mathbf{v}_h\|\|_{\mathcal{F}_h} \leq \beta \|q_h\|_{\mathcal{P}_h}. \quad (5.43)$$

First proof. Let us consider the submesh \mathbb{T}_h introduced in assumption **(MR)**. The submesh \mathbb{T}_h is a conforming partition of Ω_h into shape-regular simplexes \mathbb{T} . Let us identify q_h with the discontinuous piecewise constant function $\bar{q}_h \in \mathbb{P}_0(\mathbb{T}_h)$ that takes values q_P inside P . From [88], we know that there exists a positive constant $C_{\mathbb{RT}_0}$, independent of h , such that for every scalar function $\bar{q}_h \in \mathbb{P}_0(\mathbb{T}_h)$ there exists a vector function $\mathbf{H}_h \in \mathbb{RT}_0(\mathbb{T}_h)$ satisfying

$$\operatorname{div} \mathbf{H}_h = \bar{q}_h \quad (5.44)$$

and

$$\|\mathbf{H}_h\|_{L^2(\Omega)}^2 + \|\operatorname{div} \mathbf{H}_h\|_{L^2(\Omega)}^2 \leq C_{\mathbb{RT}_0} \|\bar{q}_h\|_{L^2(\Omega)}. \quad (5.45)$$

Let us define the discrete field $\mathbf{v}_h = \mathbf{H}_h^I \in \mathcal{F}_h$. The commuting diagram property (see Eq. (5.8)) gives

$$\operatorname{div}_h \mathbf{v}_h = \operatorname{div}_h \mathbf{H}_h^I = (\operatorname{div} \mathbf{H}_h)^I = (\bar{q}_h)^I = q_h.$$

Thus, \mathbf{v}_h satisfies (5.42). Applying the result of Lemma 5.3 to the restriction of \mathbf{H}_h^I to element P , an inverse inequality from $H^1(P)$ to $L^2(P)$, and inequality (5.45) yield:

$$\begin{aligned} \|\|\mathbf{v}_h\|\|_{\mathcal{F}_h}^2 &= \sum_{P \in \Omega_h} \|\|(\mathbf{H}_h^I)_P\|\|_P^2 \leq C \sum_{P \in \Omega_h} \left(\|\mathbf{H}_h\|_{L^2(P)}^2 + h_P^2 \|\mathbf{H}_h\|_{H^1(P)}^2 \right) \\ &\leq C \sum_{P \in \Omega_h} \|\mathbf{H}_h\|_{L^2(P)}^2 \leq C \|\bar{q}_h\|_{L^2(\Omega)}^2. \end{aligned}$$

Inequality (5.43) follows by setting $\beta = C$. Note that β depends on the stability constant $C_{\mathbb{RT}_0}$. \square

Second proof. For this proof, we assume that the problem is H^2 -regular, which is true, for instance, when the domain Ω is a convex polyhedron. Let $\psi \in H^2(\Omega)$ be the solution of

$$\operatorname{div}(\mathbb{K} \nabla \psi) = \bar{q}_h \quad \text{in } \Omega, \quad (5.46)$$

$$\psi = 0 \quad \text{in } \partial \Omega. \quad (5.47)$$

The regularity result states that

$$\|\psi\|_{H^2(\Omega)} \leq C_\Omega \|\bar{q}_h\|_{L^2(\Omega)}. \quad (5.48)$$

We define $\mathbf{v}_h = (K\nabla\psi)^I$. Using the commuting diagram property expressed in Lemma 5.1 and the fact that \bar{q}_h is piecewise-constant on Ω_h , gives

$$\operatorname{div}_h \mathbf{v}_h = \operatorname{div}_h (K\nabla\psi)^I = (\operatorname{div}(K\nabla\psi))^I = (\bar{q}_h)^I = q_h.$$

This proves (5.42). A straightforward calculation applying the result of Lemma 5.3 and the regularity result (5.48) yields

$$\begin{aligned} \|\|\mathbf{v}_h\|\|_{\mathcal{F}_h} &= \|\|(K\nabla\psi)^I\|\|_{\mathcal{F}_h} \leq C \left(\|\psi\|_{H^1(\Omega)} + Ch\|\psi\|_{H^2(\Omega)} \right) \\ &\leq C\|\psi\|_{H^2(\Omega)} \leq C\|\bar{q}_h\|_{L^2(\Omega)}. \end{aligned}$$

This proves (5.43) since $\|\bar{q}_h\|_{L^2(\Omega)} = \|\|q_h\|\|_{\mathcal{P}_h}$. \square

The uniform stability of the method can be shown by combining the stability property (S1) and the inf-sup condition from Lemma 5.7 with the classical theory of mixed discretizations of saddle-point problems, see [88]. In particular, a unique solution exists to problem (5.17)–(5.18).

5.2.3 Convergence of the vector variable

We prove the linear convergence of the numerical flux to the exact flux in Theorem 5.2 below.

Theorem 5.2. *Let (\mathbf{u}, p) with $p \in H^2(\Omega)$ be the exact solution of problem (5.1)–(5.4) and $(\mathbf{u}_h, p_h) \in \mathcal{F}_h \times \mathcal{P}_h$ be the mimetic solution of problem (5.17)–(5.18) under assumptions (MR1)–(MR3) and (S1)–(S2). Then,*

$$\mathbf{u}^I - \mathbf{u}_h \Big|_{\mathcal{F}_h} \leq Ch\|p\|_{H^2(\Omega)}, \quad (5.49)$$

where C is independent of h .

Proof. Let $p^{(1)}$ be a piecewise polynomial such that $p_{\mathbb{P}}^{(1)} = p^{(1)}|_{\mathbb{P}}$ is the linear approximation of $p|_{\mathbb{P}}$ over element \mathbb{P} that satisfies (5.34). Let $\mathbf{v}_h = \mathbf{u}^I - \mathbf{u}_h$. We observe that

$$\|\|\mathbf{u}_h - \mathbf{u}^I\|\|_{\mathcal{F}_h}^2 = [\mathbf{u}_h - \mathbf{u}^I, \mathbf{v}_h]_{\mathcal{F}_h} = [\mathbf{u}_h, \mathbf{v}_h]_{\mathcal{F}_h} - [\mathbf{u}^I, \mathbf{v}_h]_{\mathcal{F}_h}.$$

Let us develop further the last two terms. We use Eq. (5.17) (with $p|_{\partial\Omega}$ instead of g^D) and Eq. (5.41) to obtain:

$$[\mathbf{u}_h, \mathbf{v}_h]_{\mathcal{F}_h} = [p_h, \operatorname{div}_h \mathbf{v}_h]_{\mathcal{P}_h} - \langle p|_{\partial\Omega}, \mathbf{v}_h \rangle_h = -\langle p|_{\partial\Omega}, \mathbf{v}_h \rangle_h.$$

Note that the discretization error \mathbf{v}_h is orthogonal to \mathbf{u}_h with respect to the inner product of \mathcal{F}_h if $g^D = 0$.

Substituting $\mathbf{u}^I = (-\mathbb{K}\nabla p)^I$, and adding and subtracting the terms $(\mathbb{K}\nabla p^{(1)})^I$ and $(\overline{\mathbb{K}}\nabla p^{(1)})^I$ yields

$$\begin{aligned} [\mathbf{u}^I, \mathbf{v}_h]_{\mathcal{F}_h} &= - [(\mathbb{K}\nabla(p - p^{(1)}))^I, \mathbf{v}_h]_{\mathcal{F}_h} - [((\mathbb{K} - \overline{\mathbb{K}})\nabla p^{(1)})^I, \mathbf{v}_h]_{\mathcal{F}_h} \\ &\quad - [(\overline{\mathbb{K}}\nabla p^{(1)})^I, \mathbf{v}_h]_{\mathcal{F}_h}. \end{aligned}$$

The last term in the right-hand side is further developed by using the consistency condition, more precisely equations (5.20)–(5.21) with $q = p_P^{(1)}$, and noting again that $\operatorname{div}_h \mathbf{v}_h = 0$:

$$\begin{aligned} [(\overline{\mathbb{K}}\nabla p^{(1)})^I, \mathbf{v}_h]_{\mathcal{F}_h} &= \sum_{P \in \Omega_h} \left(- \int_P p_P^{(1)} \operatorname{div}_h \mathbf{v}_h dV + \sum_{f \in \partial P} \alpha_{P,f} \nu_f \int_f p_P^{(1)} dS \right) \\ &= \sum_{P \in \Omega_h} \sum_{f \in \partial P} \alpha_{P,f} \nu_f \int_f p_P^{(1)} dS. \end{aligned} \quad (5.50)$$

Combining the above developments, we have

$$\begin{aligned} \|\mathbf{u}_h - \mathbf{u}^I\|_{\mathcal{F}_h}^2 &= [\mathbf{u}_h - \mathbf{u}^I, \mathbf{v}_h]_{\mathcal{F}_h} \\ &= [(\mathbb{K}\nabla(p - p^{(1)}))^I, \mathbf{v}_h]_{\mathcal{F}_h} + [((\mathbb{K} - \overline{\mathbb{K}})\nabla p^{(1)})^I, \mathbf{v}_h]_{\mathcal{F}_h} \\ &\quad + \left(\sum_{P \in \Omega_h} \sum_{f \in \partial P} \alpha_{P,f} \nu_f \int_f p_P^{(1)} dS - \langle p|_{\partial\Omega}, \mathbf{v}_h \rangle_h \right) \\ &= A_1 + A_2 + A_3. \end{aligned}$$

Term A_1 is bounded by Lemma 5.4. Term A_2 is bounded by Lemma 5.5. Term A_3 is bounded by Lemma 5.6. This proves the assertion of the theorem. \square

5.2.4 Convergence of the scalar variable

One estimate of $\|p_h - p^I\|_{\mathcal{P}_h}$ is given in [90], where a linear convergence rate is proved for convex-shaped domains. The convexity of the computational domain is required since the analysis uses an H^2 -regularity estimate for solutions of elliptic problems. The convexity assumption has been removed in [48] using the analysis based on the *inf-sup* condition of Lemma 5.7. This approach is adopted in this section to obtain a more general result.

Theorem 5.3. *Let (\mathbf{u}, p) with $p \in H^2(\Omega)$ be the solution of the problem (5.1)–(5.4) and $(\mathbf{u}_h, p_h) \in \mathcal{F}_h \times \mathcal{P}_h$ be the solution of the mimetic discretization (5.17)–(5.18) under assumptions (MR1)–(MR3) and (S1)–(S2). Then, there exists a positive constant C independent of h such that*

$$\|p_h - p^I\|_{\mathcal{P}_h} \leq Ch \|p\|_{H^2(\Omega)}. \quad (5.51)$$

Proof. Let $\mathbf{v}_h \in \mathcal{F}_h$ be the discrete flux field provided by Lemma 5.7 for $q_h = p_h - p^I$. Equation (5.42) implies that $\operatorname{div}_h \mathbf{v}_h = p_h - p^I$, from which we obtain that

$$p_h - p^I \stackrel{2}{\mathcal{D}_h} = [p_h - p^I, p_h - p^I]_{\mathcal{D}_h} = [p_h - p^I, \operatorname{div}_h \mathbf{v}_h]_{\mathcal{D}_h}. \quad (5.52)$$

Using the discrete Eq. (5.17) yields

$$[p_h, \operatorname{div}_h \mathbf{v}_h]_{\mathcal{D}_h} = [\mathbf{u}_h, \mathbf{v}_h]_{\mathcal{F}_h} + \langle p | \partial \Omega, \mathbf{v}_h \rangle_h. \quad (5.53)$$

Let $p^{(1)}$ be a piecewise polynomial such that $p_P^{(1)} = p^{(1)}|_P$ is the linear approximation of p over element P satisfying (5.34). Let \mathbf{v}_P be the restriction of \mathbf{v}_h to P . Using first the definition of the inner product in \mathcal{D}_h , then the definition of the projection operator and the fact that $\operatorname{div}_P \mathbf{v}_P$ is a constant, and finally adding and subtracting $p_P^{(1)}$ yield

$$\begin{aligned} [p^I, \operatorname{div}_h \mathbf{v}_h]_{\mathcal{D}_h} &= \sum_{P \in \Omega_h} |P| p_P^I \operatorname{div}_P \mathbf{v}_P = \sum_{P \in \Omega_h} \int_P p \operatorname{div}_P \mathbf{v}_P dV \\ &= \sum_{P \in \Omega_h} \int_P (p - p_P^{(1)}) \operatorname{div}_P \mathbf{v}_P dV + \sum_{P \in \Omega_h} \int_P p_P^{(1)} \operatorname{div}_P \mathbf{v}_P dV. \end{aligned} \quad (5.54)$$

We transform the last term in (5.54) using the consistency condition, more precisely equations (5.20)–(5.21) with $q = p_P^{(1)}$, as

$$\sum_{P \in \Omega_h} \int_P p_P^{(1)} \operatorname{div}_P \mathbf{v}_P dV = - \sum_{P \in \Omega_h} [(\mathbf{K}_P \nabla p_P^{(1)})^I, \mathbf{v}_P]_P + \sum_{P \in \Omega_h} \sum_{f \in \partial P} \alpha_{P,f} \nu_f \int_f p_P^{(1)} dS.$$

Now, we add and subtract $\bar{\mathbf{K}} \nabla p$ and $\mathbf{K} \nabla p^{(1)}$ to obtain:

$$\begin{aligned} \sum_{P \in \Omega_h} [(\mathbf{K}_P \nabla p^{(1)})^I, \mathbf{v}_P]_P &= [(\bar{\mathbf{K}} \nabla p^{(1)})^I, \mathbf{v}_h]_{\mathcal{F}_h} = [(\mathbf{K} \nabla p)^I, \mathbf{v}_h]_{\mathcal{F}_h} \\ &+ [(\mathbf{K} \nabla (p^{(1)} - p))^I, \mathbf{v}_h]_{\mathcal{F}_h} + [((\bar{\mathbf{K}} - \mathbf{K}) \nabla p^{(1)})^I, \mathbf{v}_h]_{\mathcal{F}_h}. \end{aligned}$$

Noting that $\mathbf{u}^I = -(\mathbf{K} \nabla p)^I$ and substituting the above developments into (5.54), we have

$$\begin{aligned} [p^I, \operatorname{div}_h \mathbf{v}_h]_{\mathcal{D}_h} &= \sum_{P \in \Omega_h} \int_P (p - p_P^{(1)}) \operatorname{div}_P \mathbf{v}_P dV + \sum_{P \in \Omega_h} \sum_{f \in \partial P} \alpha_{P,f} \nu_f \int_f p_P^{(1)} dS \\ &+ [\mathbf{u}^I, \mathbf{v}_h]_{\mathcal{F}_h} - [(\mathbf{K} \nabla (p^{(1)} - p))^I, \mathbf{v}_h]_{\mathcal{F}_h} - [((\bar{\mathbf{K}} - \mathbf{K}) \nabla p^{(1)})^I, \mathbf{v}_h]_{\mathcal{F}_h}. \end{aligned} \quad (5.55)$$

Finally, using relation (5.55) and (5.53) into (5.52), and suitably collecting the right-hand side terms yield

$$\begin{aligned}
p_h - p^I &= [\mathbf{u}_h - \mathbf{u}^I, \mathbf{v}_h]_{\mathcal{F}_h} - \sum_{P \in \Omega_h} \int_P (p - p_P^{(1)}) \operatorname{div}_P \mathbf{v}_P \, dV \\
&\quad + [(\mathbf{K} \nabla (p^{(1)} - p))^I, \mathbf{v}_h]_{\mathcal{F}_h} + [((\bar{\mathbf{K}} - \mathbf{K}) \nabla p^{(1)})^I, \mathbf{v}_h]_{\mathcal{F}_h} \\
&\quad + \langle p|_{\partial\Omega}, \mathbf{v}_h \rangle_h - \sum_{P \in \Omega_h} \sum_{f \in \partial P} \alpha_{P,f} \nu_f \int_f p_P^{(1)} \, dS \\
&= T_1 + T_2 + T_3 + T_4 + T_5.
\end{aligned} \tag{5.56}$$

We bound each term in (5.56) separately. The term T_1 is bounded by applying the Cauchy-Schwarz inequality, the convergence result of Theorem 5.2, and the *inf-sup* property (5.43) with $q_h = p_h - p^I$:

$$|T_1| \leq \|\mathbf{u}_h - \mathbf{u}^I\|_{\mathcal{F}_h} \|\mathbf{v}_h\|_{\mathcal{F}_h} \leq Ch \|p\|_{H^2(\Omega)} \|p_h - p^I\|_{\mathcal{F}_h}. \tag{5.57}$$

The term T_2 is bounded by applying twice the Cauchy-Schwarz inequality, the approximation result in (5.34), and property (5.42):

$$\begin{aligned}
|T_2| &\leq \sum_{P \in \Omega_h} \|p - p_P^{(1)}\|_{L^2(P)} \|\operatorname{div}_P \mathbf{v}_P\|_{L^2(P)} \\
&\leq \left(\sum_{P \in \Omega_h} \|p - p_P^{(1)}\|_{L^2(P)}^2 \right)^{\frac{1}{2}} \|\operatorname{div}_h \mathbf{v}_h\|_{\mathcal{F}_h} \\
&\leq \left(C \sum_{P \in \Omega_h} h_P^4 |p|_{H^2(P)}^2 \right)^{\frac{1}{2}} \|p_h - p^I\|_{\mathcal{F}_h} \\
&\leq Ch^2 |p|_{H^2(\Omega)} \|p_h - p^I\|_{\mathcal{F}_h}.
\end{aligned} \tag{5.58}$$

The term T_3 is bounded by using the result of Lemma 5.4 with $q = p$ and $q^{(1)} = p^{(1)}$, and the *inf-sup* property (5.43):

$$|T_3| \leq C_2 h \|p\|_{H^2(\Omega)} \|\mathbf{v}_h\|_{\mathcal{F}_h} \leq Ch \|p\|_{H^2(\Omega)} \|p_h - p^I\|_{\mathcal{F}_h}. \tag{5.59}$$

The term T_4 is bounded by using Lemma 5.5 with $q = p$ and inequality (5.43) with $q_h = p_h - p^I$:

$$|T_4| \leq Ch (|p|_{H^1(\Omega)} + h |p|_{H^2(\Omega)}) \|\mathbf{v}_h\|_{\mathcal{F}_h} \leq Ch |p|_{H^2(\Omega)} \|p_h - p^I\|_{\mathcal{F}_h}. \tag{5.60}$$

The term T_5 is bounded by using Lemma 5.6, with $q = p$ and inequality (5.43):

$$|T_5| \leq C_1 h \|p\|_{H^2(\Omega)} \|\mathbf{v}_h\|_{\mathcal{F}_h} \leq Ch \|p\|_{H^2(\Omega)} \|p_h - p^I\|_{\mathcal{F}_h}. \tag{5.61}$$

The assertion of the theorem follows by combining inequalities (5.57)–(5.61) into (5.56) and simplifying by $\|p_h - p^I\|_{\mathcal{F}_h}$. \square

5.3 Exact reconstruction operators

In this section we prove a superconvergence estimate for the scalar variable under the condition that an *exact* reconstruction operator exists for the mimetic scheme. The exact reconstruction operator reproduces exactly the mimetic inner product; however, its existence can be shown only for a subfamily of mimetic inner products. An exact reconstruction operator is more restrictive than the reconstruction operators of Chap. 3.

Recall the space $S_{h,P}$ used in the consistency condition **(S2)**. It satisfies assumptions **(B1)** – **(B3)** and the additional restriction (5.22). A local exact reconstruction operator $R_P: \mathcal{F}_{h,P} \rightarrow S_{h,P}$ must satisfy the three conditions below.

(L1) For every discrete field $\mathbf{v}_P \in \mathcal{F}_{h,P}$ it holds

$$\operatorname{div} R_P(\mathbf{v}_P) = \operatorname{div}_P \mathbf{v}_P, \quad (5.62)$$

$$R_P(\mathbf{v}_P) \cdot \mathbf{n}_f = v_f \quad \forall f \in \partial P. \quad (5.63)$$

(L2) The reconstruction operator R_P is the left-inverse of the projection operator on the space \mathcal{F}_P of constant vector functions:

$$R_P(\mathbf{c}_P^1) = \mathbf{c} \quad \forall \mathbf{c} \in (L^2(P))^d. \quad (5.64)$$

(L3) For a given mimetic inner product, the reconstruction operator R_P reproduces it exactly:

$$[\mathbf{u}_P, \mathbf{v}_P]_P = \int_P \mathcal{K}_P^{-1} R_P(\mathbf{u}_P) \cdot R_P(\mathbf{v}_P) dV \quad \forall \mathbf{u}_P, \mathbf{v}_P \in \mathcal{F}_{h,P}. \quad (5.65)$$

A reconstruction operator satisfying **(L1)**–**(L3)** is related to the reconstruction operators of Chap. 3. In fact, the first condition in **(L1)** corresponds to the commuting property **(R3)**. The second condition is the right-inverse property **(R1)**, i.e. $\Pi_P^{\mathcal{F}} \circ R_P^{\mathcal{F}} = \mathbf{l}$. Assumption **(L2)** is the accuracy property **(R2)**.

In contrast, assumption **(L3)** is a stronger condition and does not correspond to any assumption among **(R1)**–**(R5)**. The existence of such an operator is not always guaranteed, although it is often true in most practical cases, as we will discuss in Sect. 5.3.1.

Remark 5.5. The reconstruction operator R_P defines a finite dimensional space of functions, $S_{h,P} = R_P(\mathcal{F}_{h,P})$, that is isomorphic to $\mathcal{F}_{h,P}$. In the finite element framework, the analog of such a space satisfies the unisolvency condition. In the mimetic finite difference framework, this space and the related reconstruction operator are not unique.

Remark 5.6. We show later that assumption **(L3)** is too strong and the exact reconstruction operator is not the only functional analysis tool available for proving the superconvergence of mimetic schemes.

The global exact reconstruction operator $R: \mathcal{F}_h \rightarrow X(\Omega)$ is defined such that its restriction to every $P \in \Omega_h$ is the local exact reconstruction operator, $R(\mathbf{v}_h)|_P = R_P(\mathbf{v}_P)$. From the definition of the mimetic inner product (5.10) and property **(L3)** it immediately follows that

$$[\mathbf{u}_h, \mathbf{v}_h]_{\mathcal{F}_h} = \int_{\Omega} \bar{K}^{-1} R(\mathbf{u}_h) \cdot R(\mathbf{v}_h) dV \quad \forall \mathbf{u}_h, \mathbf{v}_h \in \mathcal{F}_h. \quad (5.66)$$

We conclude this introductory part with two technical lemmas. The first lemma states the uniform stability of the reconstruction operator. The second lemma gives an approximation result.

Lemma 5.8. *Let R_P be an exact reconstruction operator. Then, for every vector-valued function $\mathbf{v} \in (H^\sigma(P))^d$ with $\sigma > 1/2$ it holds*

$$\|R_P(\mathbf{v}_P^I)\|_{L^2(P)} \leq C \|\mathbf{v}\|_{\sigma, h, P}, \quad (5.67)$$

where C is a positive constant independent of P and $\|\mathbf{v}\|_{\sigma, h, P}^2 = \|\mathbf{v}\|_{L^2(P)}^2 + h_P^{2\sigma} |\mathbf{v}|_{H^\sigma(P)}^2$.

Proof. Due to the trace theorem, the projection of a function $\mathbf{v} \in (H^\sigma(P))^d$ with $\sigma > 1/2$ is well defined. We now recall the strong ellipticity of K_P and, hence, of K_P^{-1} , see Assumption **(H1)** in Sect. 1.4.1. Using property **(L3)** and the stability property **(S1)** of the inner product yield

$$\begin{aligned} \|R_P(\mathbf{v}_P^I)\|_{L^2(P)}^2 &\leq \kappa^* \|K_P^{-1/2} R_P(\mathbf{v}_P^I)\|_{L^2(P)}^2 = \kappa^* \int_P K_P^{-1} R_P(\mathbf{v}_P^I) \cdot R_P(\mathbf{v}_P^I) dV \\ &= \kappa^* [\mathbf{v}_P^I, \mathbf{v}_P^I]_P \leq \kappa^* \sigma^* |P| \sum_{f \in \partial P} |v_f^I|^2. \end{aligned}$$

Applying the definition of the projection operator on $\mathcal{F}_{h, P}$ and using the Cauchy-Schwarz inequality, yield

$$|v_f^I| \leq |f|^{-1/2} \|\mathbf{v}\|_{L^2(f)}.$$

Inserting this in the previous inequality and using property **(M2)** from Sect. 1.6.2, we derive the following bound:

$$\|R_P(\mathbf{v}_P^I)\|_{L^2(P)}^2 \leq C \sum_{f \in \partial P} h_P \|\mathbf{v}\|_{L^2(f)}^2. \quad (5.68)$$

The assertion of the lemma follows from the trace inequality (5.35) applied to each component of \mathbf{v} in (5.68) and property **(M1)**. \square

Lemma 5.9. *Let R_P be an exact reconstruction operator. For every vector-valued function $\mathbf{v} \in (H^\sigma(\Omega))^d$ with $\sigma > 1/2$ it holds*

$$\|\mathbf{v} - R(\mathbf{v}^I)\|_{L^2(\Omega)} \leq C h^t |\mathbf{v}|_{H^t(\Omega)}, \quad (5.69)$$

where $t = \min\{1, \sigma\}$ and the positive constant C is independent of h .

Proof. Let \mathbf{v}_0 be the constant vector function whose components are the cell averages on P of the corresponding components of \mathbf{v} . We use the triangle inequality, the accuracy property (5.64) and bound (5.67) to derive

$$\begin{aligned} \|\mathbf{v} - R_P(\mathbf{v}_P^1)\|_{L^2(P)} &\leq \|\mathbf{v} - \mathbf{v}_0\|_{L^2(P)} + \|\mathbf{v}_0 - R_P(\mathbf{v}_P^1)\|_{L^2(P)} \\ &= \|\mathbf{v} - \mathbf{v}_0\|_{L^2(P)} + \|R_P(\mathbf{v}_0 - \mathbf{v})^1\|_{L^2(P)} \\ &\leq C \|\mathbf{v} - \mathbf{v}_0\|_{\sigma, h, P}. \end{aligned} \quad (5.70)$$

Now, we apply the estimate (5.34) to every component of \mathbf{v} :

$$\|\mathbf{v} - \mathbf{v}_0\|_{L^2(P)} \leq C h_P^t |\mathbf{v}|_{H^t(P)} \quad (5.71)$$

where $t = \min(1, \sigma)$. The assertion of the lemma follows by first substituting (5.71) into (5.70), then observing that $|\mathbf{v} - \mathbf{v}_0|_{H^t(P)} = |\mathbf{v}|_{H^t(P)}$, and finally summing up all inequalities for cells P of Ω_h . \square

5.3.1 Existence of exact reconstruction operators

Property **(L3)** can be reformulated as follows: given a symmetric positive definite matrix M_P , which represents a mimetic inner product in the sense discussed in Sect. 5.1.4, does it exist a reconstruction operator R_P such that

$$\mathbf{u}_P^T M_P \mathbf{v}_P = \int_P K_P^{-1} R_P(\mathbf{u}_P) \cdot R_P(\mathbf{v}_P) dV \quad \forall \mathbf{u}_P, \mathbf{v}_P \in \mathcal{F}_{h,P}. \quad (5.72)$$

We consider a minimal reconstruction operator defined in Chap. 3, which is denoted here as \tilde{R}_P . Let $\tilde{S}_{h,P} = \tilde{R}_P(\mathcal{F}_{h,P})$. In view of property **(L2)**, the space $\tilde{S}_{h,P}$ contains all constant vector functions. Let \mathbf{c}_i , $1 \leq i \leq d$, be linearly independent constant functions. For example, in the three-dimensional case, $\mathbf{c}_1 = (1, 0, 0)^T$, $\mathbf{c}_2 = (0, 1, 0)^T$, and $\mathbf{c}_3 = (0, 0, 1)^T$. We will find it convenient to choose a special basis in $\tilde{S}_{h,P}$. The basis functions \mathbf{w}_i are defined as follows:

- (i) $\mathbf{w}_i = \mathbf{c}_i$ for $i = 1, \dots, d$;
- (ii) \mathbf{w}_i for $i = d+1, \dots, N_P^{\mathcal{F}}$, are orthogonal to constant vector functions \mathbf{c}_i with respect to the weighted L^2 inner product in (5.72):

$$\int_P K_P^{-1} \mathbf{w}_i \cdot \mathbf{w}_j dV = 0, \quad 1 \leq i \leq d < j \leq N_P^{\mathcal{F}}.$$

From properties (i)-(ii) it follows that the weighted mass matrix G_P for the basis $\{\mathbf{w}_i\}$ has the block diagonal structure:

$$G_P = \begin{pmatrix} |P| K_P^{-1} & 0 \\ 0 & \hat{G}_P \end{pmatrix}, \quad (\hat{G}_P)_{i-d, j-d} = \int_P K_P^{-1} \mathbf{w}_i \cdot \mathbf{w}_j dV \quad i, j > d. \quad (5.73)$$

Let us define a transformation matrix A with columns $(\mathbf{w}_i)_P^1$ which form a new basis in $\mathcal{F}_{h,P}$. In this new basis, the mimetic inner product matrix is given by $\tilde{M}_P =$

$A^{-T} M_P A^{-1}$. Since $\tilde{S}_{h,P}$ satisfies properties **(B1)**–**(B2)**, the consistency condition **(S2)** implies that the matrix \tilde{M}_P must have the same block diagonal structure as matrix G_P :

$$\tilde{M}_P = \begin{pmatrix} |P| K_P^{-1} & 0 \\ 0 & \hat{M}_P \end{pmatrix}, \quad (5.74)$$

where, of course, \hat{G}_P and \hat{M}_P are generally different. Indeed, the mimetic inner product must return the exact value of the L^2 inner product when one of the entries corresponds to a constant function and the other one is either from $S_{h,P}$ or $\tilde{S}_{h,P}$. Thus, the first d rows and the first d columns in matrices G_P and \tilde{M}_P must coincide.

Lemma 5.10. *Let \tilde{R}_P be the minimal reconstruction operator and M_P be a mimetic inner product matrix. Furthermore, let matrices \hat{M}_P and \hat{G}_P be given by formulas (5.74) and (5.73), respectively. If $\hat{M}_P - \hat{G}_P$ is a symmetric semi-positive definite matrix, then, there exists an exact reconstruction operator R_P satisfying (5.72).*

Proof. Starting from \tilde{R}_P we will build an exact reconstruction operator by changing its action on basis vectors $(\mathbf{w}_i)_P^1$ without breaking properties **(L1)**–**(L2)**. Let $\boldsymbol{\varphi}$ be independent functions such that

$$\begin{aligned} \operatorname{div} \boldsymbol{\varphi} &= 0 && \text{in } P, \\ \boldsymbol{\varphi} \cdot \mathbf{n}_f &= 0 && \forall f \in \partial P. \end{aligned}$$

The space of such functions is infinite dimensional so that we can select a finite number of linearly independent functions $\boldsymbol{\varphi}_i$, $i = d+1, \dots, N_P^{\mathcal{F}}$, such that

$$\int_P K_P^{-1} \boldsymbol{\varphi}_i \cdot \boldsymbol{\varphi}_j dV = \delta_{ij} \quad \text{and} \quad \int_P K_P^{-1} \boldsymbol{\varphi}_i \cdot \mathbf{w}_j dV = 0 \quad \forall i, j > d.$$

Let us define a reconstruction operator that satisfies properties **(L1)**–**(L2)** as follows:

$$R_P((\mathbf{w}_i)_P^1) = \mathbf{w}_i + \sum_{j=d+1}^i z_{i-d,j-d} \boldsymbol{\varphi}_j,$$

where $z_{i-d,j-d}$ are some real numbers. Since $(\mathbf{w}_i)_P^1$ form a basis in $\mathcal{F}_{h,P}$, the action of this reconstruction operator can be calculated for any $\mathbf{v}_P \in \mathcal{F}_{h,P}$. Let us define matrix \overline{M}_P with entries

$$(\overline{M}_P)_{ij} = \int_P K_P^{-1} R_P((\mathbf{w}_i)_P^1) \cdot R_P((\mathbf{w}_j)_P^1) dV.$$

The orthogonality properties of functions $\boldsymbol{\varphi}_i$ imply that

$$\overline{M}_P = \begin{pmatrix} |P| K_P^{-1} & 0 \\ 0 & \hat{G}_P + Z Z^T \end{pmatrix},$$

where Z is the matrix with entries $z_{i-d,j-d}$. This matrix coincides with the given matrix M_P when $\widehat{M}_P = \widehat{G}_P + ZZ^T$. This proves the assertion of the lemma. \square

Remark 5.7. An exact reconstruction operator is not unique, because we have many options for selecting linearly independent functions $\boldsymbol{\varphi}_i$.

Remark 5.8. The exact reconstruction operator may not satisfy some of the properties **(R1)**–**(R5)** that are not equivalent to **(L1)**–**(L2)**.

5.3.2 Superconvergence of the scalar variable

The existence of an exact reconstruction operator R_P that fulfills conditions **(L1)**–**(L3)** in each cell P of Ω_h allows us to prove a better estimate (superconvergence) for the discretization error $p^I - p_h$. For simplicity of exposition, we consider the case of a piecewise constant diffusion tensor and homogeneous Dirichlet boundary conditions. The case of a general tensor satisfying **(H1)** and **(H1b)** (cf. Sect. 5.2.1) and heterogeneous boundary conditions also admits a superconvergent scheme but its analysis is more involved. The superconvergence property will be used in Sect. 5.4.1 to derive a post-processed discontinuous piecewise linear function with good approximation properties.

Theorem 5.4. *Let (\mathbf{u}, p) with $p \in H^2(\Omega)$ be the solution of problem (5.1)–(5.4) defined on a convex polyhedral domain Ω with the homogeneous Dirichlet boundary condition on $\partial\Omega$. Furthermore, let K be the piecewise constant diffusion tensor, $K = \overline{K}$, and the source term $b \in H^1(\Omega)$. Finally, let $(\mathbf{u}_h, p_h) \in \mathcal{F}_h \times \mathcal{P}_h$ be the solution of the mimetic discretization (5.17)–(5.18) under assumptions **(MR1)**–**(MR3)**, **(S1)**–**(S2)**, and **(L1)**–**(L3)**. Then, there exists a positive constant C independent of h such that*

$$\|p_h - p^I\|_{\mathcal{P}_h} \leq Ch^2 (\|p\|_{H^2(\Omega)} + |b|_{H^1(\Omega)}). \quad (5.75)$$

Proof. Let $\mathbf{v}_h \in \mathcal{F}_h$ satisfy the *inf-sup* condition of Lemma 5.7 for $q_h = p_h - p^I$. Let $\psi \in H^2(\Omega)$ be the solution of the auxiliary dual problem (5.46)–(5.47). It holds that $\mathbf{v}_h = (K\nabla\psi)^I$ and $\operatorname{div}_h \mathbf{v}_h = p_h - p^I$. Using (5.42) and the Eq. (5.17) with $g^D = 0$ yields

$$\|p_h - p^I\|_{\mathcal{P}_h}^2 = [\operatorname{div}_h \mathbf{v}_h, p_h - p^I]_{\mathcal{P}_h} = [\mathbf{u}_h, \mathbf{v}_h]_{\mathcal{F}_h} - [\operatorname{div}_h \mathbf{v}_h, p^I]_{\mathcal{P}_h}. \quad (5.76)$$

The second term in the right-hand side of (5.76) is further developed by applying the definition of the inner product, cf. (5.9), and integrating by parts element by element:

$$\begin{aligned} [\operatorname{div}_h \mathbf{v}_h, p^I]_{\mathcal{P}_h} &= \sum_{P \in \Omega_h} |P| (\operatorname{div}_P \mathbf{v}_P) p_P^I = \sum_{P \in \Omega_h} \int_P p \operatorname{div} R_P(\mathbf{v}_P) dV \\ &= \sum_{P \in \Omega_h} \left(- \int_P \nabla p \cdot R_P(\mathbf{v}_P) dV + \int_{\partial P} p \mathbf{n}_P \cdot R_P(\mathbf{v}_P) dV \right). \end{aligned} \quad (5.77)$$

Since $p \in H^2(\Omega)$ and $R(\mathbf{v}_h) \cdot \mathbf{n}_{P,f}$ is constant on each face f , the inter-element face integrals sum up to zero and the boundary terms are zero due to the homogeneous Dirichlet boundary condition. Now, $\nabla p = -\mathbf{K}^{-1}\mathbf{u}$ implies that

$$[\operatorname{div}_h \mathbf{v}_h, p^I]_{\mathcal{F}_h} = - \int_{\Omega} \nabla p \cdot R_P(\mathbf{v}_P) dV = \int_{\Omega} \mathbf{K}^{-1}\mathbf{u} \cdot R_P(\mathbf{v}_P) dV. \quad (5.78)$$

Substituting (5.78) into (5.76) and using property **(L3)**, allows us to connect the error for the scalar variable with that for the flux variable:

$$\| \| p_h - p^I \| \|_{\mathcal{F}_h}^2 = \int_{\Omega} \mathbf{K}^{-1}(R(\mathbf{u}_h) - \mathbf{u}) \cdot R(\mathbf{v}_h) dV. \quad (5.79)$$

By adding and subtracting $\mathbf{K}\nabla\psi$, we break the error into two terms:

$$\begin{aligned} \| \| p_h - p^I \| \|_{\mathcal{F}_h}^2 &= \int_{\Omega} \mathbf{K}^{-1}(R(\mathbf{u}_h) - \mathbf{u}) \cdot (R(\mathbf{v}_h) - \mathbf{K}\nabla\psi) dV \\ &\quad + \int_{\Omega} \mathbf{K}^{-1}(R(\mathbf{u}_h) - \mathbf{u}) \cdot \mathbf{K}\nabla\psi dV \\ &= T_1 + T_2. \end{aligned} \quad (5.80)$$

To bound the term T_1 , we first apply the Cauchy-Schwarz inequality and condition **(H1)** to obtain:

$$|T_1| \leq (\kappa_*)^{-1} \| (R(\mathbf{u}_h) - \mathbf{u}) \|_{L^2(\Omega)} \| R(\mathbf{v}_h) - \mathbf{K}\nabla\psi \|_{L^2(\Omega)}. \quad (5.81)$$

The first factor in the right-hand side is transformed by adding and subtracting $R(\mathbf{u}^I)$ and using the triangular inequality:

$$\| R(\mathbf{u}_h) - \mathbf{u} \|_{L^2(\Omega)} \leq \| R(\mathbf{u}_h - \mathbf{u}^I) \|_{L^2(\Omega)} + \| R(\mathbf{u}^I) - \mathbf{u} \|_{L^2(\Omega)}. \quad (5.82)$$

We bound the first term in the right-hand side of (5.82) by using the strong ellipticity of \mathbf{K} , cf. **(H1)** in Sect. 1.4.1, property **(L3)**, and the error estimate of Theorem 5.2:

$$\begin{aligned} \| R(\mathbf{u}_h - \mathbf{u}^I) \|_{L^2(\Omega)}^2 &\leq \kappa^* \| \mathbf{K}^{-1/2} R(\mathbf{u}_h - \mathbf{u}^I) \|_{L^2(\Omega)}^2 \\ &= \kappa^* \int_P \mathbf{K}^{-1} R(\mathbf{u}_h - \mathbf{u}^I) \cdot R(\mathbf{u}_h - \mathbf{u}^I) dV \\ &= \kappa^* \| \| \mathbf{u}_h - \mathbf{u}^I \| \|_{\mathcal{F}_h}^2 \\ &\leq Ch^2 \| p \|_{H^2(\Omega)}^2. \end{aligned}$$

Bounding the second term in the right-hand side of (5.82) by using Lemma 5.9 with $\sigma = 1$, we obtain:

$$\| R(\mathbf{u}_h) - \mathbf{u} \|_{L^2(\Omega)} \leq Ch \| p \|_{H^2(\Omega)}. \quad (5.83)$$

The second factor in the right-hand side of (5.81) is estimated by recalling the definition of \mathbf{v}_h , using the result of Lemma 5.9 with $\sigma = 1$, assumption **(H1)**, and the

elliptic regularity estimate (5.48):

$$\begin{aligned} \|R(\mathbf{v}_h) - \mathbf{K}\nabla\psi\|_{L^2(\Omega)} &= \|R((\mathbf{K}\nabla\psi)^1) - \mathbf{K}\nabla\psi\|_{L^2(\Omega)} \\ &\leq Ch|\mathbf{K}\nabla\psi|_{H^1(\Omega)} \\ &\leq Ch\|p_h - p^1\|_{\mathcal{P}_h}. \end{aligned} \quad (5.84)$$

To bound the term T_2 , we first integrate by parts, note that the boundary integral is zero due to (5.47), then substitute $\operatorname{div}R(\mathbf{u}_h) = \operatorname{div}_h\mathbf{u}_h = b^1$ (cf. property **(L1)**) and $\operatorname{div}\mathbf{u} = b$ (cf. Eq. (5.2)), and finally observe that $(b^1 - b)$ is L^2 -orthogonal to constant functions:

$$\begin{aligned} T_2 &= \int_{\Omega} (R(\mathbf{u}_h) - \mathbf{u}) \cdot \nabla\psi \, dV = - \int_{\Omega} \psi \operatorname{div}(R(\mathbf{u}_h) - \mathbf{u}) \, dV \\ &= - \int_{\Omega} \psi(b^1 - b) \, dV = \int_{\Omega} (\psi - \psi^1)(b - b^1) \, dV. \end{aligned}$$

Applying the Cauchy-Schwarz inequality yields

$$|T_2| \leq \|\psi - \psi^1\|_{L^2(\Omega)} \|b - b^1\|_{L^2(\Omega)}. \quad (5.85)$$

We apply the standard estimate for the interpolation error and the H^2 -regularity estimate (5.48) to obtain:

$$\|\psi - \psi^1\|_{L^2(\Omega)} \leq Ch|\psi|_{H^1(\Omega)} \leq Ch\|p_h - p^1\|_{L^2(\Omega)} = Ch\|p_h - p^1\|_{\mathcal{P}_h}. \quad (5.86)$$

Similarly, using again the estimate for the interpolation error, we have:

$$\|b^1 - b\|_{L^2(\Omega)} \leq Ch|b|_{H^1(\Omega)}. \quad (5.87)$$

The assertion of the theorem follows by combining (5.83) and (5.84) in (5.81) to obtain an estimate for T_1 , then by combining (5.86) and (5.87) in (5.85) to obtain an estimate for T_2 , and finally using these two bounds in (5.80). \square

5.4 A posteriori estimates

In this section we will derive an a-posteriori error estimator for the mimetic discretization described above. We refer to [8, 9, 355] for a detailed expositions of the a posteriori error estimation methodology for finite element methods. We will discuss the reliability and efficiency of our error indicator with respect to a suitably defined energy-type norm. This indicator uses a post-processed solution p_h^* , which is also interesting on its own, as it provides a better approximation of p . The results of this section are based on the work in [41, 53].

5.4.1 Post-processing of the scalar variable

The approximation property $\mathbf{u}_h \approx \mathbf{u} = -K\nabla p$ suggests that the discrete flux variable \mathbf{u}_h carries some knowledge of the gradient of the scalar variable p . Such knowledge can be exploited to build a discontinuous piecewise linear functions p_h^* with better convergence properties than p_h , similarly to what is done in the Raviart-Thomas or BDM finite elements on simplicial meshes [334].

The post-processed scalar field p_h^* is defined as the unique piecewise linear polynomial that satisfies (c.f. [41, 106])

$$\int_{\mathbb{P}} p_h^* dV = |\mathbb{P}| p_{\mathbb{P}}, \quad (5.88)$$

$$\int_{\mathbb{P}} \nabla p_h^* \cdot \nabla q dV = -[\mathbf{u}_h, (\nabla q)_{\mathbb{P}}]_{\mathbb{P}} \quad \forall q \in \mathbb{P}_1(\mathbb{P}), \quad (5.89)$$

for all $\mathbb{P} \in \Omega_h$. The post-processed gradient solving (5.89) can be easily computed by using the mimetic inner product matrix $M_{\mathbb{P}}$. First note that

$$R^T (\nabla q)_{\mathbb{P}}^{\perp} = \sum_{f \in \partial \mathbb{P}} \alpha_{\mathbb{P},f} |f| (\mathbf{x}_f - \mathbf{x}_{\mathbb{P}}) \mathbf{n}_f^T \nabla q = \left(\sum_{f \in \partial \mathbb{P}} |f| (\mathbf{x}_f - \mathbf{x}_{\mathbb{P}}) \mathbf{n}_{\mathbb{P},f}^T \right) \nabla q = \nabla q.$$

Second, note that $(\nabla q)_{\mathbb{P}}^{\perp}$ is the linear combination of columns of matrix $N_{\mathbb{P}}$. Since $M_{\mathbb{P}}^{(1)} N_{\mathbb{P}} = 0$ by the definition, we have

$$|\mathbb{P}| (\nabla q)^T \nabla p_{h|\mathbb{P}}^* = ((\nabla q)_{\mathbb{P}}^{\perp})^T \left(R_{\mathbb{P}} K_{\mathbb{P}}^{-1} R_{\mathbb{P}}^T + |\mathbb{P}| M_{\mathbb{P}}^{(1)} \right) \mathbf{u}_{\mathbb{P}} = (\nabla q)^T K_{\mathbb{P}}^{-1} R_{\mathbb{P}}^T \mathbf{u}_{\mathbb{P}}.$$

Since q is arbitrary, we have

$$\nabla p_{h|\mathbb{P}}^* = -\frac{1}{|\mathbb{P}|} K_{\mathbb{P}}^{-1} R_{\mathbb{P}}^T \mathbf{u}_{\mathbb{P}} = -\frac{1}{|\mathbb{P}|} K_{\mathbb{P}}^{-1} \sum_{f \in \partial \mathbb{P}} |f| \alpha_{\mathbb{P},f} u_f (\mathbf{x}_f - \mathbf{x}_{\mathbb{P}}).$$

This formula is applied element-wise and therefore carries negligible computational cost. Moreover, the post-processed function p_h^* does not depend on the particular inner product.

The proof of the following theorem, that is based on the superconvergence result of the previous section, is found in [41, 106].

Theorem 5.5. *Let the hypotheses of Theorem 5.4 hold. Then, there exists a positive constant C independent of h such that*

$$\|p_h^* - p\|_{L^2(\Omega)} \leq C h^2 (\|p\|_{H^2(\Omega)} + |b|_{H^1(\Omega)}). \quad (5.90)$$

5.4.2 A residual-based a posteriori estimator

The difficulty in deriving a residual based a posteriori error estimator for the mimetic discretization is related to the lack of complete knowledge of functions in space $S_{h,\mathbb{P}}$. In [41], this problem is solved by using the post-processed solution introduced in the previous section.

Let \mathcal{F}^{ext} denote the set of boundary faces and \mathcal{F}^{in} the set of internal faces of mesh Ω_h . We denote the jump of the post-processed function p_h^* on an internal face f as $[[p_h^*]]_f$. Often, we will drop out the superscript f . Following [41, 53], we consider the error indicator η given by:

$$\eta^2 = \sum_{P \in \Omega_h} \eta_P^2, \quad (5.91)$$

$$\begin{aligned} \eta_P^2 &= \kappa_P \| (K \nabla p_h^*)_P^I + \mathbf{u}_P \|_P^2 + h_P^2 \| b_h - b_P^I \|_{L^2(P)}^2 \\ &+ \frac{1}{2} \sum_{f \in \partial P \cap \mathcal{F}^{in}} \kappa_f^2 h_f^{-1} \| [[p_h^*]] \|_{L^2(f)}^2 + \sum_{f \in \partial P \cap \mathcal{F}^{ext}} \kappa_f^2 h_f^{-1} \| p_h^* - p_{b,h} \|_{L^2(f)}^2, \end{aligned} \quad (5.92)$$

where b_h and $p_{b,h}$ are some piecewise polynomial approximations of the source term b and the boundary function g^D , respectively, and

$$\kappa_P = \frac{d}{\text{trace}(K_P^{-1})}, \quad \kappa_f = \begin{cases} \kappa_P & f \in \partial P \cap \mathcal{F}^{ext}, \\ \max(\kappa_P, \kappa_{P'}) & f \in \partial P \cap \partial P'. \end{cases} \quad (5.93)$$

The degrees of the piecewise polynomial approximations b_h and $p_{b,h}$ depend in practice on the quadrature rule used, see Remark 5.9 below. The local coefficients κ_P and κ_f ensure that the indicator terms are properly scaled with respect to the magnitude of the diffusion tensor K . The error indicator η mimics the energy-like error \mathbf{err} given by

$$\mathbf{err}^2 = \sum_{P \in \Omega_h} \mathbf{err}_P^2, \quad (5.94)$$

$$\begin{aligned} \mathbf{err}_P^2 &= \| \mathbf{u} - R_P(\mathbf{u}_P) \|_{L^2(P)}^2 + h_P^2 \| \text{div}(\mathbf{u} - R_P(\mathbf{u}_P)) \|_{L^2(P)}^2 \\ &+ \kappa_P^2 \| \nabla(p - p_h^*) \|_{L^2(P)}^2 + \frac{1}{2} \sum_{f \in \partial P} \kappa_f^2 h_f^{-1} \| [[p - p_h^*]] \|_{L^2(f)}^2, \end{aligned} \quad (5.95)$$

The local coefficients κ_P and κ_f are again included to achieve a uniform scaling of the error terms with respect to K .

Remark 5.9. We do not need to compute the polynomial approximations b_h and $p_{b,h}$. In theory, the quantities $\| b_h - b_P^I \|_{L^2(P)}$ and $\| p_h^* - p_{b,h} \|_{L^2(f)}$ are defined as the result of a quadrature rule, exact for polynomial of high order, applied to $\| b - b_P^I \|_{L^2(P)}$ and $\| p_h^* - g^D \|_{L^2(f)}$, respectively. The higher the order of the quadrature rule, the smaller will be in general the oscillation terms introduced below.

Let us introduce the *oscillation terms*:

$$\begin{aligned} \text{osc}^2 &= \sum_{P \in \Omega_h} \text{osc}_P^2 + \sum_{f \in \mathcal{F}^{ext}} \text{osc}_f^2, \\ \text{osc}_P^2 &= h_P^2 \| b - b_h \|_{L^2(P)}^2 \quad \forall P \in \Omega_h, \\ \text{osc}_f^2 &= h_f \kappa_f^2 |g^D - p_{b,h}|_{H^1(f)}^2 \quad \forall f \in \mathcal{F}^{ext}. \end{aligned} \quad (5.96)$$

These oscillation terms are of higher order with respect to η_P , provided that the source term and boundary data are sufficiently regular. The theorem below states the reliability and local efficiency of the proposed a posteriori error indicator. Its proof can be found in [41, 53].

Theorem 5.6. *There exist two positive constants C_u and C_l depending only on K and the constants appearing in assumptions (MR1)–(MR2) (see Sect. 1.6.2) and (S1) such that*

$$\mathit{err} \leq C_u (\eta + \mathit{osc}). \quad (5.97)$$

and

$$\eta_P \leq C_l (\mathit{err}_P + \mathit{osc}_P + \sum_{f \in \partial P \cap \mathcal{F}^{ext}} \mathit{osc}_f) \quad \forall P \in \Omega_h. \quad (5.98)$$

The constant C_u is *homogeneous of degree zero* with respect to the magnitude of K , i.e. it is not changed if K is multiplied by a positive constant on the whole domain Ω . Likewise, the constant C_l is homogeneous of degree zero with respect to the magnitude of $K|_P$ for each element $P \in \Omega_h$.

The reliability and efficiency estimates (5.97)–(5.98) give the upper and lower bounds, respectively, of the numerical error (5.94)–(5.95). The first two terms in (5.95) compare the exact flux \mathbf{u} with its numerical approximation $R(\mathbf{u}_h)$ involving the reconstruction operator R which is never built explicitly. Even if $R(\mathbf{u}_h)$ is in general unknown, the flux error norm in (5.95) is still meaningful. In fact, Lemma 5.3 give

$$\| \mathbf{u}^I - \mathbf{u}_h \|_{\mathcal{F}_h} \leq C (\| \mathbf{u} - R(\mathbf{u}_h) \|_{L^2(\Omega)} + h | \mathbf{u} - R(\mathbf{u}_h) |_{H^1(\Omega)}).$$

We infer from this inequality that the convergence of $R(\mathbf{u}_h)$ to \mathbf{u} in the L^2 -norm implies the convergence of \mathbf{u}_h to \mathbf{u}^I .

From the computational standpoint, it would be more efficient to avoid storing the elemental inner product matrices that are required by the first term in the right-hand side of (5.92). Using the stability condition, we can replace the local inner product by the equivalent quantity:

$$\| (K \nabla p_h^*)|_P + \mathbf{u}_P \|_P^2 \simeq |P| \sum_{f \in \partial P} (K \nabla p_h^*)|_f + u_f^2. \quad (5.99)$$

The error indicator η_P is reliable, efficient, local and computable; hence, it can be used to develop adaptive strategies for mesh refinement. The mesh refinement process turns out to be simpler and efficient than in the case of standard finite element methods since the MFD method works on non-conforming meshes such as meshes with “hanging nodes”. This claim is verified with extensive numerical tests in [53]. In particular, the adaptive strategy driven by the indicator η_P shows optimal convergence rates with respect to the number of degrees of freedom.

Example 5.2. In this example we consider the Poisson problem on the L-shaped domain, see Fig. 5.4. The source term $b = 0$ and the Dirichlet boundary conditions are

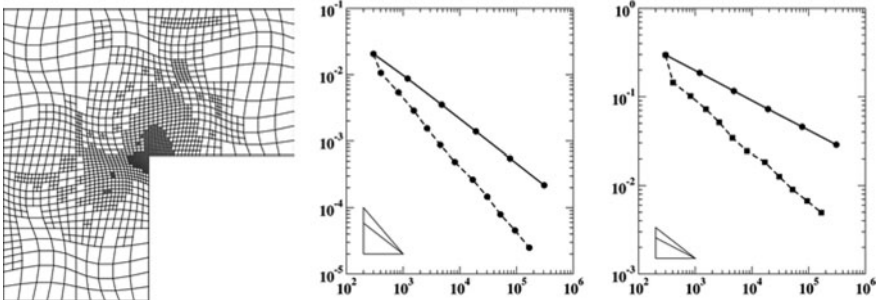


Fig. 5.4. Adaptive mesh (left), convergence rates for p (middle) and \mathbf{u} (right). Dashed line corresponds to adaptive strategy. The continuous line corresponds to the uniform refinement strategy

set by the exact solution written in cylindrical coordinates:

$$p(r, \theta) = r^{2/3} \sin(2\theta/3).$$

It is easy to check that the exact solution is only in $H^{5/3}(\Omega)$ due to the presence of the re-entrant corner. Thus, the expected asymptotic rates of convergence on uniformly refined meshes are

$$\mathbf{u}^I - \mathbf{u}_h \mathcal{F}_h \sim N_P^{-1/3} \quad \text{and} \quad p^I - p_h \mathcal{P}_h \sim N_P^{-2/3},$$

where N_P is the number of mesh cells. A successful adaptive strategy should recover the optimal convergence rates similar to that for a regular problem:

$$\mathbf{u}^I - \mathbf{u}_h \mathcal{F}_h \sim N_P^{-1/2} \quad \text{and} \quad p^I - p_h \mathcal{P}_h \sim N_P^{-1}. \tag{5.100}$$

The adaptive mesh in Fig. 5.4 shows the correct behavior of the adaptive strategy, the mesh is refined near the re-entrant corner. Note, that the computational mesh contains polygonal cells with four to seven edges. All these cells are shape-regular according to mesh assumptions **(MR1)**–**(MR2)**. The numerically calculated convergence rates agree with the predictions (5.100).

5.5 Second-order approximation of the flux

We illustrate the flexibility of the mimetic discretization framework by building a scheme that is second-order accurate for both the scalar p and vector \mathbf{u} unknowns. The new scheme uses the same space \mathcal{P}_h to approximate p and an enriched space \mathcal{F}_h^* to approximate \mathbf{u} . The major difference between \mathcal{F}_h and \mathcal{F}_h^* is that the latter has more degrees of freedom on each face f , which are sufficient to represent a linear function. This enrichment resembles the **BDIM** mixed finite element method [86,87,283]. The construction of the new mimetic scheme is based on a new consistency condition that

uses linear vector functions as test functions, in contrast to the low order case that uses constant vector functions. The new scheme also requires a special treatment of non-constant diffusion tensors.

We present a short description of the new scheme and formulate main theoretical results without proofs. Additional details concerning the scheme implementation and analysis can be found in [48, 54, 192].

5.5.1 Derivation of the mimetic scheme

5.5.1.1 Degrees of freedom and projection operators

Discrete spaces for the scalar and vector unknowns are formally defined as follows, see also Fig. 5.5.

- The space of discrete scalar fields \mathcal{P}_h is defined by attaching one degree of freedom to every mesh cell. The value associated with cell P is denoted by q_P . The collection of all degrees of freedom form the algebraic vector $q_h \in \mathcal{P}_h$,

$$q_h = (q_P)_{P \in \Omega_h}.$$

The dimension of \mathcal{P}_h equals the number of mesh cells.

- The space of discrete vector fields \mathcal{F}_h^* is defined by attaching d degrees of freedom to each mesh face. The values associated with face f are denoted by $v_f^0 \in \mathbb{R}$ and $\mathbf{v}_f^1 \in \mathbb{R}^{d-1}$. The collection of all degrees of freedom form the algebraic vector $\mathbf{v}_h \in \mathcal{F}_h^*$,

$$\mathbf{v}_h = (v_f^0, \mathbf{v}_f^1)_{f \in \mathcal{F}}.$$

The dimension of \mathcal{F}_h^* equals to d times the number of mesh faces.

The restriction of $\mathbf{v}_h \in \mathcal{F}_h^*$ to a mesh face f can be associated with a linear function:

$$\mathbf{v}_f(\boldsymbol{\xi}) = v_f^0 + \mathbf{v}_f^1 \cdot \frac{\boldsymbol{\xi} - \boldsymbol{\xi}_f}{h_f}, \tag{5.101}$$

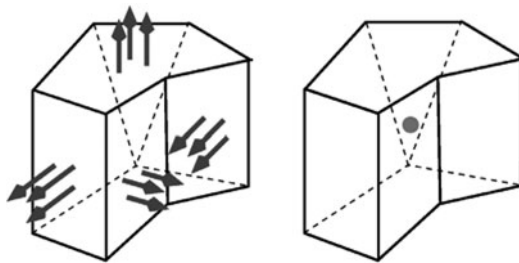


Fig. 5.5. Geometric location of degrees of freedom in the low-order MFD scheme: arrows represent fluxes u_f (on four visible faces), dot represents p_P

where $\boldsymbol{\xi} \in \mathbb{R}^{d-1}$ is the position vector in the local coordinate system on face f and $\boldsymbol{\xi}_f \in \mathbb{R}^{d-1}$ is the barycenter of f with respect to such coordinate system. Note that setting all \mathbf{v}_f^1 for $f \in \mathcal{F}$ to zero gives a subspace of \mathcal{F}_h^* that is isometric to space \mathcal{F}_h of Sect. 5.1. Since the degrees of freedom are uniquely defined on each mesh face, the discrete flux continuity across inter-element faces is naturally embodied into the definition of \mathcal{F}_h^* .

The projection operator from $L^1(\Omega)$ onto \mathcal{P}_h is given by (5.7):

$$q_P^1 := q^1|_P = \frac{1}{|P|} \int_P q dV.$$

The projection operator from $X(\Omega)$ (see (5.5)) onto \mathcal{F}_h^* is defined as follows. For any $\mathbf{v} \in X$, $\mathbf{v}^1 \in \mathcal{F}_h^*$ is defined by the linear functions \mathbf{v}_f^1 living on f :

$$\int_f \mathbf{v}_f^1(\boldsymbol{\xi}) q(\boldsymbol{\xi}) dS = \int_f \mathbf{n}_f \cdot \mathbf{v} q(\boldsymbol{\xi}) dS \quad \forall f \in \mathcal{F}, q \in \mathbb{P}_1(f). \quad (5.102)$$

When $q \in \mathbb{P}_0(f)$, we obtain the definition of the projection operator in the low-order mimetic scheme, see Eq. (5.6),

$$(\mathbf{v}^1)_f^0 = \frac{1}{|f|} \int_f \mathbf{v} \cdot \mathbf{n}_f dS.$$

When $q \in \mathbb{P}_1(f)/\mathbb{P}_0(f)$, we obtain the additional condition defining the high-order components of the discrete flux:

$$\int_f (\mathbf{v}^1)_f^1 \cdot \frac{\boldsymbol{\xi} - \boldsymbol{\xi}_f}{h_f} q(\boldsymbol{\xi}) dS = \int_f \mathbf{v} \cdot \mathbf{n}_f q(\boldsymbol{\xi}) dS \quad \forall q \in \mathbb{P}_1(f)/\mathbb{P}_0(f).$$

5.5.1.2 The primary divergence operator

The mimetic discrete divergence operator $\text{div}_h : \mathcal{F}_h^* \rightarrow \mathcal{P}_h$ is analogous to the one of the low order case. It is defined element by element as $\text{div}_h \mathbf{v}_h = \{\text{div}_P \mathbf{v}_P\}_{P \in \Omega_h}$ where \mathbf{v}_P is the restriction of \mathbf{v}_h to cell P and

$$\text{div}_P \mathbf{v}_P = \frac{1}{|P|} \sum_{f \in \partial P} \alpha_{P,f} \int_f \mathbf{v}_f(\boldsymbol{\xi}) dS = \frac{1}{|P|} \sum_{f \in \partial P} \alpha_{P,f} |f| v_f^0. \quad (5.103)$$

This definition is consistent with the Gauss divergence theorem. Furthermore,

$$\begin{aligned} (\text{div } \mathbf{v})_P^1 &= \frac{1}{|P|} \int_P \text{div } \mathbf{v} dV = \frac{1}{|P|} \int_{\partial P} \mathbf{v} \cdot \mathbf{n}_P dV = \frac{1}{|P|} \sum_{f \in \partial P} \int_f \mathbf{v} \cdot \mathbf{n}_{P,f} dS \\ &= \frac{1}{|P|} \sum_{f \in \partial P} \alpha_{P,f} \int_f \mathbf{v}_f(\boldsymbol{\xi}) \cdot \mathbf{n}_f dS = \text{div}_P \mathbf{v}_P^1, \end{aligned}$$

and the commuting property of the projection operators still holds:

$$(\text{div } \mathbf{v})^1 = \text{div}_h(\mathbf{v}^1). \quad (5.104)$$

Let us now introduce the L^2 -orthogonal projector $\mathcal{P}_P^{(1)}: (L^2(P))^d \rightarrow (\mathbb{P}_1(P))^d$. Let $\mathbf{u} \in (L^2(P))^d$, then

$$\int_P (\mathcal{P}_P^{(1)}(\mathbf{u}) - \mathbf{u}) \cdot \mathbf{v} dV = 0 \quad \forall \mathbf{v} \in (\mathbb{P}_1(P))^d. \quad (5.105)$$

This operator is clearly bounded, i.e. $\|\mathcal{P}_P^{(1)}(\mathbf{u})\|_{L^2(P)} \leq \|\mathbf{u}\|_{L^2(P)}$ and its approximation properties are characterized by the following lemma.

Lemma 5.11. *Under the mesh shape-regularity assumptions (MR1)–(MR2) of Sect. 1.6.2, the projection operator $\mathcal{P}_P^{(1)}$ provides a second-order accurate approximation of vector functions from $(H^2(P))^d$:*

$$\|\mathbf{u} - \mathcal{P}_P^{(1)}(\mathbf{u})\|_{L^2(P)} + h_P \|\mathbf{u} - \mathcal{P}_P^{(1)}(\mathbf{u})\|_{H^1(P)} \leq Ch_P^2 |\mathbf{u}|_{H^2(P)}. \quad (5.106)$$

The proof of this lemma is the direct consequence of property (5.34), see [48] for more details.

5.5.1.3 Mimetic inner products

We equip spaces \mathcal{P}_h and \mathcal{F}_h^* with the inner products $[\cdot, \cdot]_{\mathcal{P}_h}$ and $[\cdot, \cdot]_{\mathcal{F}_h^*}$. Let $\|\cdot\|_{\mathcal{P}_h}$ and $\|\cdot\|_{\mathcal{F}_h^*}$ be the norms induced by these inner products. The inner product on \mathcal{P}_h is the same one already introduced in (5.9). The inner product of \mathcal{F}_h^* is given by

$$[\mathbf{u}_h, \mathbf{v}_h]_{\mathcal{F}_h^*} = \sum_{P \in \Omega_h} [\mathbf{u}_P, \mathbf{v}_P]_P, \quad (5.107)$$

where we keep the same notation for the local inner product $[\cdot, \cdot]_P$. It is required to satisfy the stability and consistency conditions. Let

$$S_{h,P} = \{\mathbf{v} \in (L^s(P))^d, s > 2, \text{ with } \operatorname{div} \mathbf{v} = \text{const}, \mathbf{v} \cdot \mathbf{n}_f \in \mathbb{P}_1(f) \quad \forall f \in \partial P\}.$$

According to the theory developed in Part I of this book, this space must satisfy the following properties.

(B1) The local projection operator $(\cdot)^I$ from $S_{h,P}$ to $\mathcal{F}_{h,P}^*$ must be surjective.

(B2) The space $S_{h,P}$ must contain the trial space

$$\mathcal{T}_P = \{\mathbf{v}: P \rightarrow \mathbb{R}^d \text{ such that } \mathbf{v} = \mathcal{P}_P^{(1)}(\mathbf{K}\nabla q) \text{ with } q \in \mathbb{P}_2(P)\}.$$

Note that the space \mathcal{T}_P is contained in $[\mathbb{P}_1(P)]^d$ but may not be the whole $[\mathbb{P}_1(P)]^d$ (see Remark 5.10).

It is immediate to verify that the space $S_{h,P}$ above satisfies both conditions. The space $S_{h,P}$ is used in defining the consistency condition here below.

(S1) (Stability condition). There exist two positive constants σ_* and σ^* independent of h_P such that for all $\mathbf{v}_P \in \mathcal{F}_{h,P}^*$ and for every element P we have

$$\sigma_* h_P \sum_{f \in \partial P} \int_f \mathbf{v}_f(\boldsymbol{\xi})^2 dS \leq [\mathbf{v}_P, \mathbf{v}_P]_P \leq \sigma^* h_P \sum_{f \in \partial P} \int_f \mathbf{v}_f(\boldsymbol{\xi})^2 dS, \quad (5.108)$$

where $\mathbf{v}_f(\boldsymbol{\xi})$ is the local linear function defined on f by (5.101).

(S2) (Consistency condition). For every element P and every $q \in \mathbb{P}_2(P)$, we have

$$\left[(\mathcal{P}_P^{(1)}(K\nabla q))_P^I, \mathbf{v}_P^I \right]_P = \int_P \nabla q \cdot \mathbf{v} dV \quad \forall \mathbf{v} \in S_{h,P}. \quad (5.109)$$

Integrating the right-hand side of (5.109) we obtain

$$\left[(\mathcal{P}_P^{(1)}(K\nabla q))_P^I, \mathbf{v}_P^I \right]_P = - \int_P q \operatorname{div} \mathbf{v} dV + \sum_{f \in \partial P} \int_f (\mathbf{v} \cdot \mathbf{n}_{P,f}) q dS. \quad (5.110)$$

The definition of space $S_{h,P}$ implies that the integral arguments in the right-hand side are polynomials. Hence, they can be calculated using components of \mathbf{v}_P^I (our degrees of freedom), that is property **(B3)** from Chap. 4. In particular, this allows us to write the right-hand side of (5.110) as $R(q)^T \mathbf{v}_P$, where $R(q)^T$ is the computable vector from $\mathcal{F}_{h,P}^*$. To ensure the symmetry of the resulting inner product, condition **(S2)** uses the projected function $\mathcal{P}_P^{(1)}(K\nabla q)$ instead of $K_P \nabla q$ as it is done in the low-order scheme, see (5.19). This approximation is critical for proving the second-order convergence of the flux in the new scheme [48].

As we already did a few times in this book, once the consistency condition is specified, we follow the standard path. First, we select a few basis functions q^i in $\mathbb{P}_2(P)$. Second, we define vectors $N_i = (\mathcal{P}_P^{(1)}(K\nabla q^i))_P^I$ and $R_i = R(q^i)$. Then, the consistency condition can be written in the equivalent form as the system of matrix equations,

$$M_P N_i = R_i,$$

with respect to unknown inner product matrix M_P . Solution of this system of algebraic equations has been discussed in Sect. 5.1.4 and also in Part I.

The following bilinear form, whose arguments are a function from $L^1(\Gamma^D)$ and a vector from \mathcal{F}_h^* , is introduced in order to take into account non-homogeneous Dirichlet boundary conditions:

$$\langle g^D, \mathbf{v}_h \rangle_h = \sum_{f \in \Gamma^D} \int_f \mathbf{v}_f(\boldsymbol{\xi}) g^D(\boldsymbol{\xi}) dS = \sum_{f \in \Gamma^D} \left(v_f^0 \int_f g^D dS + \mathbf{v}_f^1 \cdot \int_f g^D(\boldsymbol{\xi}) \frac{\boldsymbol{\xi} - \boldsymbol{\xi}_f}{h_f} dS \right).$$

Remark 5.10. Note that, even in the case where K_P is constant, the trial space \mathcal{T}_P does not cover all functions in $[\mathbb{P}_1(P)]^d$. For instance, in the case K equal to the identity, the space \mathcal{T}_P is given by all vectors $\mathbf{v} = \nabla q$ with $q \in \mathbb{P}_2(P)$. Since all such vectors \mathbf{v} satisfy $\operatorname{curl}(\mathbf{v}) = 0$, the space \mathcal{T}_P will not contain the whole $[\mathbb{P}_1(P)]^d$. Nevertheless, since the solution to the problem satisfies $\mathbf{u} = -K\nabla p$, the approximation provided by the test space \mathcal{T}_P turns out to be sufficient to obtain the desired order of accuracy.

5.5.1.4 Weak formulation

Let the boundary data g^D and g^N be integrable on Γ^D and Γ^N , respectively. Moreover, let $(g^N)_f^l$, for all $f \in \Gamma^N$, represent a linear approximation to g^N on face f . Using this, we introduce the following space:

$$\mathcal{F}_{h,l}^* = \left\{ \mathbf{v}_h \in \mathcal{F}_h^* : \mathbf{v}_f(\boldsymbol{\xi}) = (g^N)_f^l \quad \forall f \in \Gamma^N \right\}.$$

As usual, $\mathcal{F}_{h,0}^*$ indicates the space given by setting $g^N = 0$ on Γ^N . The weak mimetic formulation of problem (5.1)–(5.4) reads as

Find $(\mathbf{u}_h, p_h) \in \mathcal{F}_{h,l}^* \times \mathcal{P}_h$ such that

$$[\mathbf{u}_h, \mathbf{v}_h]_{\mathcal{F}_h^*} - [p_h, \operatorname{div}_h \mathbf{v}_h]_{\mathcal{P}_h} = - \langle g^D, \mathbf{v}_h \rangle_h \quad \forall \mathbf{v}_h \in \mathcal{F}_{h,0}^*, \quad (5.111)$$

$$[\operatorname{div}_h \mathbf{u}_h, q_h]_{\mathcal{P}_h} = [b^l, q_h]_{\mathcal{P}_h} \quad \forall q_h \in \mathcal{P}_h. \quad (5.112)$$

5.5.2 Convergence analysis

We prove that the new numerical approximation of the vector variable converges quadratically. Regarding the scalar variable, since the discrete space is the same as in the low order case, a better rate cannot be expected in principle. Nevertheless, in Theorem 5.10 we show that some improvement can be still obtained for the scalar variable, using a piecewise quadratic post-processed solution.

Let us consider a local reconstruction operator $R_P : \mathcal{F}_{h,P}^* \rightarrow S_{h,P}$ that satisfies three conditions. As usual, the global reconstruction operator R combines all local reconstruction operators.

(L1a) For all $\mathbf{v}_P \in \mathcal{F}_{h,P}^*$, it holds

$$\operatorname{div} R_P(\mathbf{v}_P) = \operatorname{div}_P \mathbf{v}_P \quad \text{in } P, \quad (5.113)$$

$$R_P(\mathbf{v}_P)|_f \cdot \mathbf{n}_f = \mathbf{v}_f \quad \forall f \in \partial P. \quad (5.114)$$

(L2a) The reconstruction operator is the left-inverse of the projection operator given by (5.102) on the space of linear vector functions:

$$R_P(\mathbf{c}_P^l) = \mathbf{c}, \quad \forall \mathbf{c} \in (\mathbb{P}_1(P))^d. \quad (5.115)$$

(L3a) The reconstruction operator is uniformly bounded from below and above, i.e. there exist positive constants ρ_* and ρ^* independent of P such that

$$\rho_* h_P \sum_{f \in \partial P} \int_f |\mathbf{v}_f(\boldsymbol{\xi})|^2 dS \leq R_P(\mathbf{v}_P) \Big|_{L^2(P)}^2 \leq \rho^* h_P \sum_{f \in \partial P} \int_f |\mathbf{v}_f(\boldsymbol{\xi})|^2 dS \quad (5.116)$$

for any $\mathbf{v}_P \in \mathcal{F}_{h,P}^*$.

Requirements **(L1a)**–**(L3a)** are weaker than requirements **(L1)**–**(L3)** used in the analysis of the low-order scheme. Indeed, the new reconstruction operator does not

reproduce the mimetic inner product. Instead, it has to be stable with respect to the elemental norm as expressed by (5.116). In contrast to the low-order case, the existence of a reconstruction operator satisfying **(L1a)**–**(L3a)** can be always proved using only the mesh shape-regularity assumptions **(MR1)**–**(MR3)** of Sect. 1.6. For example, one could immediately build R_P by solving an discrete $\mathbb{BDM}_1 - \mathbb{P}_0$ problem on an auxiliary simplicial partition of element P , see [42, 192, 240]. We have the following approximation result [48].

Lemma 5.12. *There exists a constant C independent of h_P such that*

$$\mathbf{v} - R_P(\mathbf{v}_P^1) \Big|_{L^2(P)} \leq Ch_P^2 \|\mathbf{v}\|_{H^2(P)} \quad \forall \mathbf{v} \in (H^2(P))^d. \quad (5.117)$$

Let q be a function such that $q|_P \in H^1(P)$. We denote the jump of q across the internal face f by $[[q]]_f$ and extend this definition to the boundary faces by setting $[[q]]_f = q|_f$ for $f \subset \partial\Omega$. All a priori estimates will be given using the mesh-dependent norm:

$$q \Big|_{1,h}^2 = \sum_{P \in \Omega_h} \left(\|\nabla q\|_{L^2(P)}^2 + \sum_{f \in \partial P} h_P^{-1} \|[q]\|_f^2 \right). \quad (5.118)$$

When q is continuous across the internal faces and zero on the domain boundary, the norm $q \Big|_{1,h}$ coincides with the H^1 -seminorm of q which is also the norm on $H_0^1(\Omega)$. Thus, norm (5.118) can be interpreted as a discrete extension of the H^1 -norm to the “broken” H^1 Sobolev space. Indeed, both the reconstructed and post-processed numerical solutions are discontinuous functions on Ω_h and for this reason do not belong to $H^1(\Omega)$.

Since the space \mathcal{P}_h is unchanged with respect to the low-order case and the space \mathcal{F}_h^* is only enriched (it contains the flux space of the low-order scheme), the *inf-sup* condition proved in Lemma 5.7 holds immediately in the high-order case.

Lemma 5.13. *There exists a positive constant C independent of h such that for any $q_h \in \mathcal{P}_h$ there exists a discrete flux field $\mathbf{v}_h \in \mathcal{F}_h^*$ satisfying*

$$[\text{div}_h \mathbf{v}_h, q_h]_{\mathcal{P}_h} = \|q_h\|_{\mathcal{P}_h}^2 \quad \text{and} \quad \|\mathbf{v}_h\|_{\mathcal{F}_h^*} \leq C \|q_h\|_{\mathcal{P}_h}. \quad (5.119)$$

Furthermore, an *inf-sup* condition holds with respect to the norm $\|\cdot\|_{1,h}$, see [48].

Lemma 5.14. *There exists a positive constant C' independent of h such that for any $q_h \in \mathcal{P}_h$ there exists a discrete flux field $\mathbf{v}_h \in \mathcal{F}_h^*$ satisfying*

$$[\text{div}_h \mathbf{v}_h, q_h]_{\mathcal{P}_h} = \|q_h\|_{1,h}^2 \quad \text{and} \quad R(\mathbf{v}_h) \Big|_{L^2(\Omega)} \leq C' \|q_h\|_{1,h}. \quad (5.120)$$

Remark 5.11. From the *inf-sup* condition of Lemma 5.13 and the stability assumption **(S1)** in Sect. 5.5, using the standard theory of mixed discretization methods [88], the uniform stability of the proposed scheme follows.

The following convergence result holds for the vector variable [48].

Theorem 5.7. Let (\mathbf{u}, p) with $p \in H^3(\Omega)$ be the exact solution of (5.1)–(5.4), and $(\mathbf{u}_h, p_h) \in \mathcal{F}_h^* \times \mathcal{P}_h$ be the mimetic solution of (5.111)–(5.112) under assumptions (MR1)–(MR3) and (S1)–(S2). Then,

$$\mathbf{u}^1 - \mathbf{u}_h \Big|_{\mathcal{F}_h^*} \leq Ch^2 \|p\|_{H^3(\Omega)}, \quad (5.121)$$

where C is independent of h .

Inserting the projection of the exact solution on $\mathcal{F}_h^* \times \mathcal{P}_h$, i.e. (\mathbf{u}^1, p^1) , in equations (5.111)–(5.112), we obtain the consistency error of the mimetic scheme. By comparing the result with the mimetic scheme, we can write explicitly the error equation for $p_h - p^1$ (see Lemma 5.15) and then prove an estimate of the flux consistency error (see Theorem 5.8).

Lemma 5.15 (Error equation). Let (\mathbf{u}, p) be the solution of problem (5.1)–(5.4) and $(\mathbf{u}_h, p_h) \in \mathcal{F}_h^* \times \mathcal{P}_h$ be the solution of the mimetic scheme (5.111)–(5.112). Under assumptions (L1a)–(L3a), for every $\mathbf{v}_h \in \mathcal{F}_h^*$, there holds:

$$[p_h - p^1, \text{div}_h \mathbf{v}_h]_{\mathcal{P}_h} = [\mathbf{u}_h, \mathbf{v}_h]_{\mathcal{F}_h^*} + \int_{\Omega} \nabla p \cdot R(\mathbf{v}_h) dV. \quad (5.122)$$

Theorem 5.8 (Consistency flux error). Let (\mathbf{u}, p) with $p \in H^3(\Omega)$ be the solution of problem (5.1)–(5.4), and $(\mathbf{u}_h, p_h) \in \mathcal{F}_h^* \times \mathcal{P}_h$ be the solution of the mimetic scheme (5.111)–(5.112) under assumptions (MR1)–(MR3), (S1)–(S2), and (L1a)–(L3a). Then, there exists a constant C independent of h such that for every $\mathbf{v}_h \in \mathcal{F}_h^*$ there holds:

$$\sum_{P \in \Omega_h} [\mathbf{u}_h, \mathbf{v}_P]_P + \int_P \nabla p \cdot R_P(\mathbf{v}_P) dV \leq Ch^2 \|p\|_{H^3(\Omega)} \left(\sum_{P \in \Omega_h} R_P(\mathbf{v}_P) \Big|_{L^2(P)} \right)^{1/2}. \quad (5.123)$$

Theorem 5.9 below states the discretization error estimates for p in the mesh-dependent norms $\|\cdot\|_{1,h}$ and $\|\|\cdot\|\|_{\mathcal{P}_h}$. Its proof relies on Lemma 5.15 and Theorem 5.8. Theorem 5.9 is more general than the similar approximation result given in Theorem 5.4. More precisely, here we do not require that Ω is convex, that the mimetic inner product is reproduced by an exact reconstruction operator, and that the source term belongs to $H^1(\Omega)$. Nonetheless, the higher-order approximation of the fluxes requires the H^3 -regularity of the exact solution in order to achieve the optimal convergence rate. This requirement is needed for both $\|\cdot\|_{1,h}$ and $\|\|\cdot\|\|_{\mathcal{P}_h}$ norms of the error.

Theorem 5.9. Let $p \in H^3(\Omega)$ be the exact solution of problem (5.1)–(5.4), and $p_h \in \mathcal{P}_h$ be its mimetic approximation. Then,

$$p_h - p^1 \Big|_{1,h} \leq Ch^2 \|p\|_{H^3(\Omega)}, \quad (5.124)$$

$$\|\|p_h - p^1\|\|_{\mathcal{P}_h} \leq Ch^2 \|p\|_{H^3(\Omega)}, \quad (5.125)$$

where constant C is independent of h .

Since the new mimetic formulation approximates the scalar solution by a piecewise constant function, the convergence rate of p_h to the solution p cannot exceed that for the low-order scheme [48]. The advantage of Theorem 5.9 with respect to Theorem 5.4 lays in the weaker assumptions and in the stronger norm, but not in the order of convergence.

5.5.3 Solution post-processing

The post-processing technique is based on an element-by-element reconstruction of a solution gradient from the discrete flux solution. It generalizes the analogous technique for the low-order mimetic scheme in Sect. 5.4.1. Using the higher-order scheme we can get a better approximation of the gradient within each mesh element by exploiting the more accurate representation of the discrete flux solution.

The post processed scalar field p_h^* is defined as the unique piecewise quadratic polynomial that satisfies

$$\int_{\mathbb{P}} p_h^* dV = |\mathbb{P}| p_{\mathbb{P}}, \quad (5.126)$$

$$\int_{\mathbb{P}} \nabla p_h^* \cdot \nabla q dV = -[\mathbf{u}_h, (\nabla q)_{\mathbb{P}}]_{\mathbb{P}} \quad \forall q \in \mathbb{P}_2(\mathbb{P}), \quad (5.127)$$

for all $\mathbb{P} \in \Omega_h$.

Note that the computational cost of the post-processing procedure is negligible since it is calculated element-by-element and, in addition, the related local matrix to be inverted turns out to be diagonal. Details concerning the implementation can be found in [54].

We close this section with an error bound for p_h^* , see [48].

Theorem 5.10. *Let p_h^* be defined by (5.126)–(5.127). Then,*

$$\|p - p_h^*\|_{1,h} \leq Ch^2 \|p\|_{H^3(\Omega)}, \quad (5.128)$$

where constant C is independent of h .

The diffusion problem in primal form

Diffusion is one of the fundamental processes by which material moves.

The diffusion problem in primal form for the scalar variable u is governed by the Poisson problem, which we rewrite from Sect. 1.4.1:

$$-\operatorname{div}(\mathbb{K}\nabla u) = b \quad \text{in } \Omega, \quad (6.1)$$

$$u = g^D \quad \text{on } \Gamma^D, \quad (6.2)$$

$$(\mathbb{K}\nabla u) \cdot \mathbf{n} = g^N \quad \text{on } \Gamma^N. \quad (6.3)$$

Here, $\Omega \subset \mathbb{R}^d$ is a polyhedral domain with the Lipschitz boundary $\Gamma = \Gamma^D \cup \Gamma^N$, \mathbb{K} is the symmetric and strongly elliptic diffusion tensor, b is the forcing term, g^D and g^N are the given boundary data.

The primal mimetic low-order discretization of (6.1)–(6.3) proposed in [84] can be considered as an extension of the linear Galerkin method for simplicial meshes to general polygonal and polyhedral meshes. Later, an extension of the mimetic framework to arbitrary-order discretizations was introduced in [50] for polygonal meshes. Both low-order and arbitrary-order discretizations were unified in a Galerkin framework dubbed as the *virtual element method* [43].

In Sect. 6.1, we present the main idea of the mimetic finite difference (MFD) method for problem (6.1)–(6.3) from two points of view. The low-order and arbitrary-order discretizations are described in Sects. 6.2 and 6.3, respectively. In Sect. 6.4, we carry out the convergence analysis and derive a priori error estimates in mesh-dependent norms. In Sect. 6.5, we present a residual-based error indicator [16] that can be used to drive adaptive mesh refinement algorithms and derive a posteriori error estimates.

6.1 Overview of the method

In this section, we introduce two approaches to the construction of the mimetic method for the diffusion problem in primal form. The first approach is based on the discrete vector and tensor calculus, see Chap. 2. The second approach is based on the results of Chap. 4 and starts with the variational formulation of the diffusion problem.

For the considered diffusion problem, the second approach is computationally more efficient. Both approaches complement each other and in general selection of a particular discretization strategy must be driven by the application at hand.

6.1.1 Discretization of the strong form of the equations

In this short section, for simplicity, we assume that $\Gamma^N = \emptyset$. Let us rewrite Eq. (6.1) in rather unusual mixed form:

$$\mathbf{F} = \nabla u, \tag{6.4}$$

$$-\operatorname{div}(\mathbf{K}\mathbf{F}) = b, \tag{6.5}$$

subject to the Dirichlet boundary conditions (6.2). In contrast, to the mixed formulation considered in the previous chapter, the vector function \mathbf{F} has continuous tangential components across material interfaces.

We discretize (6.4)–(6.5) using a pair of primary and derived operators from Chap. 2. The discrete unknowns are given by (see Fig. 6.1)

- the node-based field $u_h \in \mathcal{V}_h$ whose components u_ν approximate the nodal values of u , i.e. $u_h = (u_\nu)_{\nu \in \mathcal{V}}$;
- the edge-based field $\mathbf{F}_h \in \mathcal{E}_h$ whose components F_e approximate the tangential components of \mathbf{F} on mesh edges e , i.e. $\mathbf{F}_h = (F_e)_{e \in \mathcal{E}}$.

With such a selection of degrees of freedom, it is natural to use the primary mimetic gradient operator $\nabla_h: \mathcal{V}_h \rightarrow \mathcal{E}_h$ and the derived mimetic divergence operator $\widetilde{\operatorname{div}}_h: \mathcal{E}_h \rightarrow \mathcal{V}_h$ as approximations of the continuum operators ∇ and $\operatorname{div}(\mathbf{K}\cdot)$, respectively:

$$\nabla \approx \nabla_h \quad \text{and} \quad \operatorname{div}(\mathbf{K}\cdot) \approx \widetilde{\operatorname{div}}_h.$$

The primary gradient operator is given by Eq. (2.19). According to the main principles of the discrete vector and tensor calculus developed in Chap. 2, the derived divergence operator is dual to the primary gradient operator with respect to inner

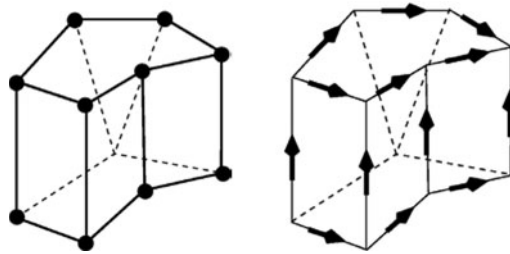


Fig. 6.1. Geometric location of degrees of freedom in the low-order MFD scheme: dots represent u_ν and arrows represent u_e (on 11 visible edges)

products in spaces \mathcal{V}_h and \mathcal{E}_h (see also Remark 2.5). This gives formula (2.32):

$$\widetilde{\operatorname{div}}_h = -M_{\mathcal{V}}^{-1} \nabla_h^T M_{\mathcal{E}}, \quad (6.6)$$

where matrices $M_{\mathcal{V}}$ and $M_{\mathcal{E}}$ represent inner products in the corresponding discrete spaces. The mimetic operators allow us to write down the following discrete problem:

$$\mathbf{F}_h - \nabla_h u_h = 0, \quad (6.7)$$

$$-\widetilde{\operatorname{div}}_h \mathbf{F}_h = \Pi^{\mathcal{V}}(b), \quad (6.8)$$

subject to the Dirichlet boundary conditions. Here $\Pi^{\mathcal{V}}$ is the vertex projection operator defined by (2.14).

In a finite difference setting, the boundary conditions are imposed by setting prescribed values $g^D(\mathbf{x}_v)$ to the components of u_h at the boundary nodes \mathbf{x}_v and eliminating the corresponding equations from the global system. Formally, equations (6.7)–(6.8) have the same structure as equations (5.12)–(5.13).

Remark 6.1. There exist two approaches for treating heterogeneous Neumann boundary conditions. The first one is based on an extension of the mimetic operators and a modification of the inner products [206], which is not pursued in this book. The second approach is based on the direct approximation of a weak formulation and is presented in subsequent sections.

The linear system arising from (6.7)–(6.8) reads:

$$M_{\mathcal{V}}^{-1} \nabla_h^T M_{\mathcal{E}} \nabla_h u_h = \Pi^{\mathcal{V}}(b),$$

subject to the Dirichlet boundary conditions. The last formula can be written as

$$A u_h = \widetilde{b}_h \quad \text{where} \quad A = \nabla_h^T M_{\mathcal{E}} \nabla_h \quad \text{and} \quad \widetilde{b}_h = M_{\mathcal{V}} \Pi^{\mathcal{V}}(b). \quad (6.9)$$

A more elegant way for treating boundary conditions that avoids the convoluted statement “subject to the Dirichlet boundary conditions” is to write (6.9) in a variational-like form. Let $\mathcal{V}_{h,g^D} \subset \mathcal{V}_h$ be a subspace of mesh functions whose values at boundary vertices \mathbf{x}_v are set to $g^D(\mathbf{x}_v)$. First, we define a *semi-inner product* on \mathcal{V}_h through the bilinear form:

$$\mathcal{A}_h(v_h, u_h) := [\nabla_h v_h, \nabla_h u_h]_{\mathcal{E}_h} = v_h^T \nabla_h^T M_{\mathcal{E}} \nabla_h u_h.$$

The bilinear form \mathcal{A}_h represents the energy semi-norm in space \mathcal{V}_h . Then, the discrete problem (6.9) subject to the Dirichlet boundary conditions is equivalent to the variational formulation:

Find $u_h \in \mathcal{V}_{h,g^D}$ such that

$$[\nabla_h u_h, \nabla_h v_h]_{\mathcal{E}_h} = [\Pi^{\mathcal{V}}(b), v_h]_{\mathcal{V}_h} \quad \forall v_h \in \mathcal{V}_{h,0}, \quad (6.10)$$

where we recall that the scalar product $[\cdot, \cdot]_{\mathcal{V}_h}$ is given by matrix $M_{\mathcal{V}}$.

According to the discrete Helmholtz decomposition Theorem 2.65, the discrete gradient operator acts from \mathcal{V}_h onto a proper subspace of \mathcal{E}_h . This subspace is much smaller than \mathcal{E}_h and only the action of matrix $M_{\mathcal{E}}$ in this subspace is needed to define matrix A . In the following section we will show that A can be calculated more efficiently, bypassing the calculation of $M_{\mathcal{E}}$.

6.1.2 Discretization of the weak formulation

Let us derive a mimetic discretization of problem (6.1)–(6.3) using the framework developed in Chap. 4. Let

$$X_g(\Omega) = \{v \in H^1(\Omega) : v|_{\Gamma^D} = g^D\}.$$

The weak formulation of problem (6.1)–(6.3) reads:

Find $u \in X_g(\Omega)$ such that

$$\int_{\Omega} \kappa \nabla u \cdot \nabla v dV = \int_{\Omega} b v dV + \int_{\Gamma^N} g^N v dS \quad \forall v \in X_0(\Omega). \quad (6.11)$$

Under assumptions **(H1)**–**(H2)**, see Sect. 1.4.1, the existence and uniqueness of the weak solution u can be proved [190].

The numerical approximation of (6.11) is performed on a sequence of polygonal or polyhedral conformal partitions $\{\Omega_h\}_h$ of the domain Ω for the mesh size parameter $h \rightarrow 0$. The mesh size parameter is given by $h = \max_{P \in \Omega_h} h_P$ where h_P is the diameter of element P . We assume that each mesh in the sequence is shape-regular, i.e. it satisfies assumptions **(MR1)**–**(MR2)** of Sect. 1.6. On a mesh Ω_h , we approximate the scalar functions from X_g through a set of suitable degrees of freedom:

$$u, v \in H^1(\Omega) \cap C^0(\overline{\Omega}) \longrightarrow u_h, v_h \in \mathcal{V}_h. \quad (6.12)$$

The definition of the linear space \mathcal{V}_h for the low-order and the high-order methods is different and is described in the next sections. It will be convenient to use a shorter notation for the formal projection operator $\Pi^{\mathcal{V}} : H^1(\Omega) \cap C^0(\overline{\Omega}) \rightarrow \mathcal{V}_h$. The degrees of freedom of function v are given by a discrete field $v^I \in \mathcal{V}_h$, which means that $v^I = \Pi^{\mathcal{V}}(v)$. Now, we introduce a bilinear form $\mathcal{A}_h : \mathcal{V}_h \times \mathcal{V}_h \rightarrow \mathbb{R}$ that approximates the left-hand side of (6.11),

$$\mathcal{A}_h(u^I, v^I) \approx \int_{\Omega} \kappa \nabla u \cdot \nabla v dV,$$

and a linear functional $\mathcal{L}_h : \mathcal{V}_h \rightarrow \mathbb{R}$ that approximates the right-hand side,

$$\mathcal{L}_h(v^I) \approx \int_{\Omega} b v dV + \int_{\Gamma^N} g^N v dS. \quad (6.13)$$

The construction of \mathcal{A}_h and \mathcal{L}_h is described in the next sections.

The Dirichlet boundary conditions are embedded in the definition of the subspace $\mathcal{V}_{h,g}$ of \mathcal{V}_h , which is formed by the discrete scalar fields of \mathcal{V}_h whose degrees of free-

dom associated with the Dirichlet boundary are calculated explicitly using function g^D . The mimetic finite difference method for problem (6.11) reads:

Find $u_h \in \mathcal{V}_{h,g}$ such that:

$$\mathcal{A}_h(u_h, v_h) = \mathcal{L}_h(v_h) \quad \forall v_h \in \mathcal{V}_{h,0}. \quad (6.14)$$

As proved in the next sections, the coercivity and the continuity of the bilinear form \mathcal{A}_h imply the well-posedness of discrete problem (6.14).

Remark 6.2. At this moment, the second mimetic approach resembles a finite element method. The essential difference between the two methods lies in the construction of the bilinear form \mathcal{A}_h .

6.2 Low-order mimetic method

6.2.1 Degrees of freedom

In the low-order MFD method, the linear space \mathcal{V}_h coincides with that introduced in Chap. 2, i.e. the degrees of freedom are associated with mesh vertices. A discrete scalar field $v_h \in \mathcal{V}_h$ consists of one real number $v_v = v_h|_v$ for every vertex $v \in \mathcal{V}$. Thus, the dimension of \mathcal{V}_h equals the number of mesh vertices. The restriction of v_h to element P is denoted by v_P and includes values v_v at vertices of P:

$$v_P = (v_v)_{v \in \mathcal{V}_P}.$$

We say that v_P belongs to the local approximation space $\mathcal{V}_{h,P} := \mathcal{V}_h|_P$, whose dimension is $\#(\mathcal{V}_P)$, the number of items forming the local set \mathcal{V}_P , see Fig. 6.1. We will treat non-homogeneous boundary conditions by using the space $\mathcal{V}_{h,g} \subset \mathcal{V}_h$:

$$\mathcal{V}_{h,g} = \{v_h \in \mathcal{V}_h : v_v = g^D(\mathbf{x}_v) \quad \forall \mathbf{x}_v \in \bar{\Gamma}^D\}.$$

The subspace $\mathcal{V}_{h,0}$ is defined by setting $g^D = 0$ in the definition of $\mathcal{V}_{h,g}$.

Remark 6.3. The definition of $\mathcal{V}_{h,g}$ requires more regularity of function g^D than it is needed to prove the well-posedness of the continuum problem. This limitation can be mitigated by using an average value of g^D in a neighborhood of vertex \mathbf{x}_v to define v_v .

Let v and v' be two vertices connected by an edge e , i.e. $e = (v, v')$. The space of the discrete scalar fields \mathcal{V}_h is endowed with the H^1 -like mesh-dependent norm

$$\|v_h\|_{1,h}^2 = \sum_{P \in \Omega_h} \|v_h\|_{1,h,P}^2, \quad (6.15)$$

where each local norm in the right-hand side must be equivalent (with constants that are uniformly bounded on the mesh) to

$$\|v_h\|_{1,h,P}^2 \simeq |P| \sum_{e=(v,v') \in \partial P} \frac{v_{v'} - v_v}{|e|}^2.$$

The assumption **(M2)** of mesh shape-regularity implies that $|P|/|e|^2 \succeq h_P^{d-2}$. Thus, the local norm can be defined also as follows:

$$\|v_h\|_{1,h,P}^2 = \begin{cases} \sum_{e=(v,v') \in \partial P} v_{v'} - v_v^2 & \text{for } d = 2, \\ h_P \sum_{e=(v,v') \in \partial f} v_{v'} - v_v^2 & \text{for } d = 3. \end{cases} \quad (6.16)$$

We define the projection operator $(\cdot)^I: H^1(\Omega) \cap C^0(\overline{\Omega}) \rightarrow \mathcal{V}_h$ as the unique discrete scalar field $v^I \in \mathcal{V}_h$ associated with the function v and such that

$$v_V^I = v^I|_V = v(\mathbf{x}_V) \quad \forall V \in \mathcal{V}.$$

The local projection operator from $H^1(P) \cap C^0(P)$ to $\mathcal{V}_{h,P}$ is denoted by using the symbol v_P^I .

6.2.2 The consistency and stability conditions

The bilinear form \mathcal{A}_h is built element-by-element using the following representation that reflects the additivity of the integration:

$$\mathcal{A}_h(u_h, v_h) = \sum_{P \in \Omega_h} \mathcal{A}_{h,P}(u_P, v_P).$$

To derive an accurate local bilinear form $\mathcal{A}_{h,P}$ and characterize its properties, we proceed along three steps. In the *first step*, we introduce a face quadrature rule $\mathcal{I}_f(v_P)$ that satisfies two conditions of *data locality* and \mathbb{P}_1 -*exactness*.

(Q1.A) *Data locality*: The quadrature rule \mathcal{I}_f uses only the degrees of freedom $\{v_v\}_{v \in \partial f}$ at the vertices forming the polygonal boundary of face f .

(Q1.B) \mathbb{P}_1 -*exactness*: The quadrature rule \mathcal{I}_f is exact for linear functions.

Assumption **(Q1.B)** implies that \mathcal{I}_f yields at least a second-order accurate approximation of the face integral of a sufficiently smooth scalar function ψ :

$$\int_f \psi dS = \mathcal{I}_f(\psi_P^I) + |f| \mathcal{O}(h_P^2). \quad (6.17)$$

In the *second step*, we approximate the diffusion tensor K on the element P by the constant tensor K_P , which is either K evaluated at the center of gravity of P or the (component-wise) average of K over P . Although assumption **(H1)** (see Sect. 1.4.1) is sufficient to ensure the existence and uniqueness of the numerical solution, a stronger

regularity assumption on K that holds often in practice assumes that each component K_{ij} is locally Lipschitz continuous. This stronger assumption allows us to derive the following upper bound:

$$\max_{1 \leq i, j \leq d} \sup_{\mathbf{x} \in P} |(K_P)_{ij} - K_{ij}(\mathbf{x})| \leq C_K^* h_P, \quad (6.18)$$

where C_K^* is a non-negative constant independent of h_P and P . In this chapter, we use the modified assumption **(H1)**.

(H1a) The diffusion tensor $K : \Omega \rightarrow \mathbb{R}^{2 \times 2}$ is a $d \times d$ bounded, measurable, and symmetric tensor. Its components K_{ij} belong to $W^{1, \infty}(P)$ for every $P \in \Omega_h$. Moreover, K is *strongly elliptic*, i.e., there exist two positive constants κ_* and κ^* such that for every $\mathbf{x} \in \Omega$ it holds

$$\kappa_* \|\mathbf{v}\|^2 \leq \mathbf{v} \cdot K(\mathbf{x}) \mathbf{v} \leq \kappa^* \|\mathbf{v}\|^2 \quad \forall \mathbf{v} \in \mathbb{R}^d, \quad (6.19)$$

where $\|\mathbf{v}\| = (\mathbf{v} \cdot \mathbf{v})^{1/2}$ is the Euclidean norm of vector \mathbf{v} .

In the *third step*, we require that the bilinear form $\mathcal{A}_{h,P}$ satisfies two conditions of *spectral stability* and *local consistency*. Let $S_{h,P}$ be a subspace of $H^1(P) \cap C^0(P)$ that satisfies assumptions **(B1)**–**(B3)** formulated in Part I of this book. For the considered mimetic discretization, they read as follows.

(B1) The projection operator $(\cdot)^I$ is surjective from $S_{h,P}$ to $\mathcal{V}_{h,P}$.

(B2) The space $S_{h,P}$ contains the space of linear functions.

(B3) Functions from $S_{h,P}$ are integrated exactly on faces f of P with the quadrature rule **(Q1)**.

In general, a space $S_{h,P}$ satisfying all assumptions is infinite dimensional. However, as we noticed in Chaps. 3 and 4, it is not restrictive (and often useful) to assume that

$$\dim(S_{h,P}) = \dim(\mathcal{V}_{h,P}). \quad (6.20)$$

In such a case the projection operator $(\cdot)^I$ restricted to $S_{h,P}$ becomes an invertible mapping $(\cdot)^I : S_{h,P} \rightarrow \mathcal{V}_{h,P}$ and thus the two spaces are isomorphic.

(S1) Spectral stability: There exists two positive constants σ_* and σ^* such that for every $v_P \in \mathcal{V}_{h,P}$ there holds:

$$\sigma_* \|v_P\|_{1,h,P}^2 \leq \mathcal{A}_{h,P}(v_P, v_P) \leq \sigma^* \|v_P\|_{1,h,P}^2.$$

(S2) Local consistency: For every $\psi \in \mathbb{P}_1(P)$ and every $v \in S_{h,P}$ there holds:

$$\mathcal{A}_{h,P}(v_P^I, \psi_P^I) = \int_P K_P \nabla v \cdot \nabla \psi dV.$$

Note that, for any sufficiently regular function v and for any $\psi \in \mathbb{P}_1(P)$, the integration by parts gives

$$\int_P K_P \nabla v \cdot \nabla \psi dV = K_P \nabla \psi \cdot \sum_{f \in \partial P} \mathbf{n}_{P,f} \int_f v dS. \quad (6.21)$$

Condition **(S2)** expresses the exactness of the discrete bilinear form when one of its arguments is the projection of a linear polynomial and the other one belongs to $S_{h,P}$. Due to property **(B3)** the right-hand side of (6.21) can be computed exactly. Formula (6.21) will be used in Sect. 6.2.5 to derive an algebraic form of the consistency condition.

Remark 6.4. Let us write an explicit form of the integration formula \mathcal{I}_f using weights $\{\omega_{f,v}\}_{v \in \partial f}$:

$$\mathcal{I}_f(v_P) = \sum_{v \in \partial f} \omega_{f,v} v_v. \quad (6.22)$$

Then, assumptions **(Q1.A)**–**(Q1.B)** are equivalent to the assumption **(Q1.AB)** introduced in [84].

(Q1.AB) For every face f there exists a set of non-negative weights $\{\omega_{f,v}\}_{v \in \partial f}$ associated with the vertices v of face f such that

$$\sum_{v \in \partial f} \omega_{f,v} = |f| \quad \text{and} \quad \sum_{v \in \partial f} (\mathbf{x}_v - \mathbf{x}_f) \omega_{f,v} = 0, \quad (6.23)$$

where \mathbf{x}_v is the position vector of vertex v and \mathbf{x}_f is the barycenter of face f .

We can find weights $\omega_{f,v}$ satisfying assumption **(Q1.AB)** by expressing \mathbf{x}_f as a linear combination of the vectors \mathbf{x}_v for $v \in \partial f$.

Remark 6.5. In the two-dimensional case the obvious choice for the numerical integration rule \mathcal{I}_f is given by the trapezoidal rule:

$$\mathcal{I}_f(v_P) = \frac{|f|}{2} (v_v + v_{v'}), \quad (6.24)$$

where v and v' are the end-points of edge f .

6.2.3 Discretization of linear functional \mathcal{L}_h

To discretize the volume integral in (6.13), we need one additional quadrature rule. Note that the quadrature below is not unique.

(Q2) For every polyhedron $P \in \Omega_h$ there exists a set of non-negative weights $\{\omega_{P,v}\}_{v \in \partial P}$ associated with its vertices v such that their sum equals $|P|$.

The corresponding numerical integration formula,

$$\int_P \psi dV \approx \sum_{v \in \partial P} \psi(\mathbf{x}_v) \omega_{P,v}, \quad (6.25)$$

is exact for constant function ψ . A simple choice of weights that satisfy **(Q2)** is given by $\omega_{\mathbf{P},\mathbf{v}} = |\mathbf{P}|/N_{\mathbf{P}}^{\mathcal{V}}$, where $N_{\mathbf{P}}^{\mathcal{V}}$ is the number of vertices in \mathbf{P} .

Using **(Q2)**, we approximate the forcing term in (6.13) by a linear functional $(b, \cdot)_h : \mathcal{V}_h \rightarrow \mathbb{R}$ given by

$$(b, v_h)_h = \sum_{\mathbf{P} \in \Omega_h} \left(\frac{1}{|\mathbf{P}|} \int_{\mathbf{P}} b dV \right) \sum_{\mathbf{v} \in \mathcal{V}_{\mathbf{P}}} v_{\mathbf{v}} \omega_{\mathbf{P},\mathbf{v}}. \quad (6.26)$$

Only a low-order approximation of the integral of b is required. For instance, using the barycenter of \mathbf{P} , we obtain

$$\frac{1}{|\mathbf{P}|} \int_{\mathbf{P}} b dV \approx b(\mathbf{x}_{\mathbf{P}}). \quad (6.27)$$

The boundary integral in (6.13) corresponding to the Neumann boundary condition is approximated using the quadrature rule \mathcal{S}_f for faces $f \in \Gamma^N$. This leads to a linear functional $\langle g^N, \cdot \rangle_h : \mathcal{V}_h \rightarrow \mathbb{R}$ given by

$$\langle g^N, v_h \rangle_h = \sum_{f \in \Gamma^N} \omega_{f,\mathbf{v}} g^N(\mathbf{x}_{\mathbf{v}}) v_{\mathbf{v}}. \quad (6.28)$$

Summarizing, the right-hand side of (6.11) is approximated by the linear functional $\mathcal{L}_h : \mathcal{V}_h \rightarrow \mathbb{R}$ that is defined by

$$\mathcal{L}_h(v_h) = (b, v_h)_h + \langle g^N, v_h \rangle_h.$$

6.2.4 Convergence theorem

The convergence of the low-order mimetic method has been analyzed in [84] for the case of homogeneous Dirichlet boundary conditions. Here, we present only the main result. In Sect. 6.4 we will prove a more general convergence theorem for the arbitrary order mimetic method of [50].

Theorem 6.1. *Let $\Gamma^N = \emptyset$ and $g^D = 0$. Furthermore, let $u \in H_0^1(\Omega) \cap H^2(\Omega)$ be the solution of variational problem (6.11), and $u_h \in \mathcal{V}_{h,0}$ be the solution of discrete problem (6.14) under assumptions **(MR1)**–**(MR2)** (see Chap. 1), **(H1a)**, **(Q1)**–**(Q2)**, and **(S1)**–**(S2)**. Then, there exists a positive constant C independent of h such that*

$$\|u_h - u^I\|_{1,h} \leq Ch \left(|u|_{H^1(\Omega)} + |u|_{H^2(\Omega)} + \|b\|_{L^2(\Omega)} \right).$$

6.2.5 Derivation of bilinear form \mathcal{A}_h

Let us consider the stiffness matrix $M_{\mathbf{P}}$ associated with the local bilinear form $\mathcal{A}_{h,\mathbf{P}}(u_{\mathbf{P}}, v_{\mathbf{P}})$:

$$\mathcal{A}_{h,\mathbf{P}}(u_{\mathbf{P}}, v_{\mathbf{P}}) = (u_{\mathbf{P}})^T M_{\mathbf{P}} v_{\mathbf{P}} \quad \forall u_{\mathbf{P}}, v_{\mathbf{P}} \in \mathcal{V}_{h,\mathbf{P}}. \quad (6.29)$$

We assume that the quadrature rule in (6.17) is given in Assumption **(Q1.AB)**. Using it in Assumption **(S2)** and rearranging the summation terms, we obtain:

$$\mathcal{A}_{h,P}(\boldsymbol{\psi}_P^I, \boldsymbol{v}_P) = \sum_{\boldsymbol{v} \in \partial P} \boldsymbol{v}_\boldsymbol{v} \sum_{\boldsymbol{f} \in \partial P: \boldsymbol{v} \in \partial \boldsymbol{f}} \boldsymbol{\omega}_{\boldsymbol{f},\boldsymbol{v}} \boldsymbol{n}_{P,\boldsymbol{f}} \cdot \boldsymbol{K}_P \nabla \boldsymbol{\psi} \quad \forall \boldsymbol{v}_P \in \mathcal{V}_{h,P}. \quad (6.30)$$

This relationship must hold for every linear polynomial $\boldsymbol{\psi}$. Since $\mathcal{A}_{h,P}$ is bilinear, it is sufficient that (6.30) is true for a finite number of linearly independent functions $\{\boldsymbol{\psi}_i\}_{i=0,\dots,d}$ spanning $\mathbb{P}_1(P)$. In three-dimensions, we can take $\boldsymbol{\psi}_0 = 1$, $\boldsymbol{\psi}_1 = x$, $\boldsymbol{\psi}_2 = y$ and $\boldsymbol{\psi}_3 = z$. Note that for $\boldsymbol{\psi}_0$ we have

$$(\boldsymbol{v}_P)^T \boldsymbol{M}_P (\boldsymbol{\psi}_0)_P^I = \int_P \boldsymbol{K}_P \nabla \boldsymbol{v} \cdot \nabla (1) dV = 0. \quad (6.31)$$

Since $(\boldsymbol{\psi}_0)_P^I = (1, 1, \dots, 1)^T$, Eq. (6.30) implies that the constant vector is in the kernel of matrix \boldsymbol{M}_P . Following the same arguments as in Chap. 4, we combine equations (6.29) and (6.30) to obtain

$$(\boldsymbol{v}_P)^T \boldsymbol{M}_P (\boldsymbol{\psi}_i)_P^I = (\boldsymbol{v}_P)^T \boldsymbol{R}_i,$$

where $\boldsymbol{R}_i \in \mathcal{V}_{h,P}$ and its components (each one associated to a vertex $\boldsymbol{v} \in \partial P$) are given by

$$(\boldsymbol{R}_i)_\boldsymbol{v} = \sum_{\boldsymbol{f} \in \partial P: \boldsymbol{v} \in \partial \boldsymbol{f}} \boldsymbol{\omega}_{\boldsymbol{f},\boldsymbol{v}} \boldsymbol{n}_{P,\boldsymbol{f}} \cdot \boldsymbol{K}_P \nabla \boldsymbol{\psi}_i.$$

Let $\boldsymbol{N}_i = (\boldsymbol{\psi}_i)_P^I$, where $i = 0, \dots, d$. We define the rectangular matrices \boldsymbol{R}_P and \boldsymbol{N}_P of size $\mathcal{N}_P^f \times (d+1)$ that collect the columns \boldsymbol{R}_i and \boldsymbol{N}_i , respectively. Then, the local consistency condition can be written in the compact matrix form:

$$\boldsymbol{M}_P \boldsymbol{N}_P = \boldsymbol{R}_P. \quad (6.32)$$

Lemma 6.1. *The matrices \boldsymbol{N}_P and \boldsymbol{R}_P satisfy the following identity:*

$$\boldsymbol{N}_P^T \boldsymbol{R}_P = \begin{pmatrix} 0 & \mathbf{0}^T \\ \mathbf{0} & |\boldsymbol{P}| \boldsymbol{K}_P \end{pmatrix}. \quad (6.33)$$

Proof. Since $\nabla x = (1, 0, 0)^T$, $\nabla y = (0, 1, 0)^T$, and $\nabla z = (0, 0, 1)^T$ it holds that

$$\int_P \boldsymbol{K}_P \nabla \boldsymbol{\psi}_i \cdot \nabla \boldsymbol{\psi}_j dV = |\boldsymbol{P}| (\boldsymbol{K}_P)_{ij}, \quad i, j > 0. \quad (6.34)$$

Now, we apply (6.21) for $\boldsymbol{v} = \boldsymbol{\psi}_j$ and $\boldsymbol{\psi} = \boldsymbol{\psi}_i$; then, we use Assumption **(Q1.B)** and, finally, we re-arrange the summations to obtain

$$\begin{aligned} \int_P \boldsymbol{K}_P \nabla \boldsymbol{\psi}_i \cdot \nabla \boldsymbol{\psi}_j dV &= \boldsymbol{K}_P \nabla \boldsymbol{\psi}_i \cdot \sum_{\boldsymbol{f} \in \partial P} \int_{\boldsymbol{f}} \boldsymbol{n}_{P,\boldsymbol{f}} \boldsymbol{\psi}_j dS \\ &= \boldsymbol{K}_P \nabla \boldsymbol{\psi}_i \cdot \sum_{\boldsymbol{f} \in \partial P} \boldsymbol{n}_{P,\boldsymbol{f}} \sum_{\boldsymbol{v} \in \partial \boldsymbol{f}} \boldsymbol{\omega}_{\boldsymbol{f},\boldsymbol{v}} \boldsymbol{\psi}_j(\boldsymbol{x}_\boldsymbol{v}) \\ &= \sum_{\boldsymbol{v} \in \partial P} \boldsymbol{\psi}_j(\boldsymbol{x}_\boldsymbol{v}) \sum_{\boldsymbol{f} \in \partial P: \boldsymbol{v} \in \partial \boldsymbol{f}} \boldsymbol{\omega}_{\boldsymbol{f},\boldsymbol{v}} \boldsymbol{n}_{P,\boldsymbol{f}} \cdot \boldsymbol{K}_P \nabla \boldsymbol{\psi}_i = (\boldsymbol{N}_j)^T \boldsymbol{R}_i. \end{aligned}$$

This proves the assertion of the lemma for $i, j > 0$. If $i = 0$ or $j = 0$ the assertion follows from the symmetry of matrix $N^T R$, e.g., $(N_j)^T R_i = (N_i)^T R_j$, and $R_0 = (0, \dots, 0)^T$. \square

Matrix N_P has the following explicit form

$$N_P = \begin{pmatrix} 1 & (\mathbf{x}_{v_1})^T \\ 1 & (\mathbf{x}_{v_2})^T \\ \vdots & \vdots \\ 1 & (\mathbf{x}_{v_{N_P^y}})^T \end{pmatrix}, \tag{6.35}$$

which holds for any number of spatial dimensions. The expression for matrix R_P depends on the quadrature weights introduced in (6.22). In two-dimensions, a simple formula, which is the consequence of the trapezoidal rule, is available. Let the edges and vertices of polygon P be ordered either clockwise or counter clockwise. Then,

$$R_P = (\mathbf{0}, \hat{R}_P), \quad \hat{R}_P = \frac{1}{2} \begin{pmatrix} |f_{N_P^y}| \mathbf{n}_{f_{N_P^y}}^T + f_1 \mathbf{n}_{f_1}^T \\ |f_1| \mathbf{n}_{f_1}^T + f_2 \mathbf{n}_{f_2}^T \\ \vdots \\ |f_{N_P^y-1}| \mathbf{n}_{f_{N_P^y-1}}^T + f_{N_P^y} \mathbf{n}_{f_{N_P^y}}^T \end{pmatrix} K_P.$$

According to the general theory (see Lemma 4.7), a solution to (6.32) is given by

$$M_P = M_P^{(0)} + M_P^{(1)}, \quad M_P^{(0)} = \frac{1}{|P|} R_P K_P^{-1} R_P^T, \quad M_P^{(1)} = D_P U_P D_P^T, \tag{6.36}$$

where D_P is a $N_P^y \times (N_P^y - (d + 1))$ -sized matrix such that $N_P^T D_P = 0$, and U_P a symmetric and positive definite $(N_P^y - (d + 1)) \times (N_P^y - (d + 1))$ -sized matrix. Formula (6.36) can be verified by a direct substitution.

Matrix U_P cannot be totally arbitrary. To comply with the stability condition (S2), the positive eigenvalues of matrix $M_P^{(1)}$ should be uniformly bounded by that of matrix $M_P^{(0)}$. There are many ways to achieve that. For example, after making the columns of D_P orthonormal, we can use the scalar matrix $U_P = \lambda^+(M_P^{(0)}) I$ where $\lambda^+(M_P^{(0)})$ is a positive eigenvalue of $M_P^{(0)}$.

Remark 6.6. Let us consider the two dimensional case with $K_P = I$. Then, formula (6.33) implies that $N_i^T R_j = \delta_{ij} |P|$ for $i, j > 0$. This vector-vector products coincide with the *shoe-lace* formula for the calculation of the area of polygon P . For example,

$$|P| = N_1^T R_1 = \sum_{i=1}^{N_P^y} x_i \frac{1}{2} (f_{i-1} n_{f_{i-1},x} + f_i n_{f_i,x}).$$

Let $\mathbf{x}_{v_i} = (x_i, y_i)$ and the vertices be ordered counter clockwise. From a simple geometric argument we find that $|\mathbf{f}_{i-1}| \mathbf{n}_{\mathbf{f}_{i-1}} = (y_i - y_{i-1}, x_{i-1} - x_i)^T$, and a similar formula holds for $|\mathbf{f}_i| \mathbf{n}_{\mathbf{f}_i}$. Using the above formula, we obtain:

$$\begin{aligned} |\mathbf{P}| &= \sum_{i=1}^{N_{\mathbf{P}}^{\mathcal{Y}}} x_i \frac{1}{2} ((y_i - y_{i-1}) + (y_{i+1} - y_i)) = \frac{1}{2} \sum_{i=1}^{N_{\mathbf{P}}^{\mathcal{Y}}} x_i (y_{i+1} - y_{i-1}) \\ &= \frac{1}{2} \sum_{i=1}^{N_{\mathbf{P}}^{\mathcal{Y}}} x_i y_{i+1} - \frac{1}{2} \sum_{i=1}^{N_{\mathbf{P}}^{\mathcal{Y}}} x_i y_{i-1} = \frac{1}{2} \sum_{i=1}^{N_{\mathbf{P}}^{\mathcal{Y}}} x_i y_{i+1} - \frac{1}{2} \sum_{i=1}^{N_{\mathbf{P}}^{\mathcal{Y}}} x_{i+1} y_i \\ &= \frac{1}{2} \sum_{i=1}^{N_{\mathbf{P}}^{\mathcal{Y}}} (x_i y_{i+1} - x_{i+1} y_i). \end{aligned}$$

6.2.6 A family of mimetic schemes

The size of matrix $\mathbf{U}_{\mathbf{P}}$ grows linearly with the number of vertices in element \mathbf{P} , and the number of its entries grows quadratically. A treatment of these entries as parameters leads to the development a new adaptation strategy dubbed *m-adaptation* [249]. For example, each element in a hexahedral mesh contributes 10 parameters. In this section, we consider a few simple examples showing the potential of the new adaptation strategy and leave the in-depth discussion to Chap. 11.

6.2.6.1 Admissible parameters

If matrix $\mathbf{U}_{\mathbf{P}}$ satisfies the stability condition with uniformly bounded constants σ_* and σ^* , the corresponding mimetic discretization has the optimal convergence properties. However, it is intuitively clear that the constant C in the convergence estimate of Theorem 6.1 depends on ratio σ^*/σ_* . The effectiveness of the *m-adaptation* depends on how much the stability constants affect the accuracy of a mimetic scheme.

Let us consider again the model problem from Example 5.1. In particular, we consider formula (6.36) where matrix $\mathbf{D}_{\mathbf{P}}$ has orthonormal columns and $\mathbf{U}_{\mathbf{P}}$ is the scalar matrix,

$$\mathbf{U}_{\mathbf{P}} = \tilde{\gamma} \frac{1}{N_{\mathbf{P}}^{\mathcal{Y}}} \text{trace}(\mathbf{M}_{\mathbf{P}}^{(0)}) \mathbf{I}.$$

By varying the scaling factor $\tilde{\gamma}$, we affect the stability constants. We apply this scheme to the numerical resolution of the diffusion problem (6.1)–(6.3) in a unit square Ω with the Dirichlet conditions. The diffusion tensor is given by

$$\mathbf{K}(x, y) = \begin{pmatrix} (x+1)^2 + y^2 & -xy \\ -xy & (x+1)^2 \end{pmatrix}.$$

The source term b and the boundary function $g^{\mathcal{D}}$ are defined by the exact solution

$$p = x^3 y^2 + x \sin(2\pi xy) \sin(2\pi y).$$

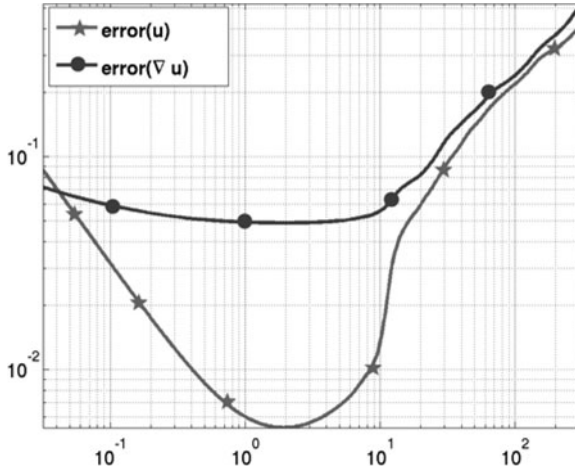


Fig. 6.2. Dependence of the approximation errors on the parameter $\tilde{\gamma}$

Figure 6.2 shows the dependence of the approximation errors for u and ∇u on the scaling parameter $\tilde{\gamma}$. The errors are calculated using discrete L^2 -norms that are independent of the definition of matrix M_P . The error for ∇u remains almost flat when $\tilde{\gamma}$ changes 300 times. The error for u has a well-defined minimum around $\tilde{\gamma} = 2$. This example shows that if the error in the gradient is our primary objective, there is a big room to optimize the method.

6.2.6.2 Special cases

Applying the previous formulas on meshes of rectangles having size $h_x \times h_y$, we rediscover several well-known finite difference and finite element schemes [303, 304]. Thus, these schemes belong to the family of mimetic schemes. Let us introduce two auxiliary quantities:

$$D = \frac{1}{2} \left(\frac{h_x}{h_y} + \frac{h_y}{h_x} \right) \quad \text{and} \quad E = \frac{1}{2} \left(\frac{h_x}{h_y} - \frac{h_y}{h_x} \right).$$

A straightforward calculation shows that

$$M_P^{(0)} = \frac{1}{2} \begin{pmatrix} +D & +E & -D & -E \\ +E & +D & -E & -D \\ -D & -E & +D & +E \\ -E & -D & +E & +D \end{pmatrix}, \quad N_P = \begin{pmatrix} 1 & 0 & 0 \\ 1 & h_x & 0 \\ 1 & h_x & h_y \\ 1 & 0 & h_y \end{pmatrix}.$$

The rank of matrix $M_P^{(0)}$ is 2. Indeed, we have that $M_P^{(0)} \mathbf{z}^0 = M_P^{(0)} \mathbf{z}^1 = 0$, where $\mathbf{z}^0 = (1, 1, 1, 1)^T$ and $\mathbf{z}^1 = (1, -1, 1, -1)^T$. The matrix D_P has a single column, and U_P is a 1×1 matrix. Let $U_P = (s)$ and $D_P = (a, b, c, d)^T$. The orthogonality condition

yields:

$$N_P^T D_P = \begin{pmatrix} 1 & 1 & 1 & 1 \\ 0 & h_x & h_x & 0 \\ 0 & 0 & h_y & h_y \end{pmatrix} \begin{pmatrix} a \\ b \\ c \\ d \end{pmatrix} = \begin{pmatrix} a+b+c+d \\ h_x b+h_x c \\ h_y c+h_y d \end{pmatrix} = \begin{pmatrix} 0 \\ 0 \\ 0 \end{pmatrix}.$$

Taking $c = 1$ yields $b = d = -1$ and $a = 1$. Hence, $D_P = (1, -1, 1, -1)^T$ and

$$M_P^{(1)} = \begin{pmatrix} 1 \\ -1 \\ 1 \\ -1 \end{pmatrix} (s) (1 \ -1 \ 1 \ -1) = s \begin{pmatrix} 1 & -1 & 1 & -1 \\ -1 & 1 & -1 & 1 \\ 1 & -1 & 1 & -1 \\ -1 & 1 & -1 & 1 \end{pmatrix}.$$

The formula of matrix M_P becomes:

$$M_P = \begin{pmatrix} \frac{D}{2} + s & \frac{E}{2} - s & -\frac{D}{2} + s & -\frac{E}{2} - s \\ \frac{E}{2} - s & \frac{D}{2} + s & -\frac{E}{2} - s & -\frac{D}{2} + s \\ -\frac{D}{2} + s & -\frac{E}{2} - s & \frac{D}{2} + s & \frac{E}{2} - s \\ -\frac{E}{2} - s & -\frac{D}{2} + s & \frac{E}{2} - s & \frac{D}{2} + s \end{pmatrix}.$$

Let us enumerate the vertices in rectangles as shown in Fig. 6.3. Let v be the central vertex marked by a filled circle. When a global assembly is performed, the diagonal entry in the equation of v takes contributions from matrix entries $(M_P)_{ii}$, $i = 1, \dots, 4$. Summing up these entries, we obtain $2D + 4s$ which is the central term of the stencil shown in Fig. 6.4. The other entries in the stencil are calculated similarly. For example, when we consider the global entry connecting vertex v with vertex v' being the top-middle node, we sum up entries $(M_P)_{23}$ and $(M_P)_{14}$. This gives $-E - 2s$. Different schemes are presented in Figs. 6.6–6.9.

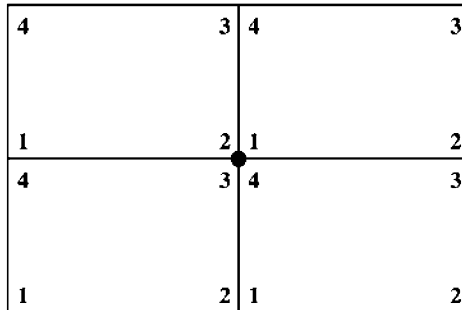


Fig. 6.3. Local numbering of a rectangle vertices

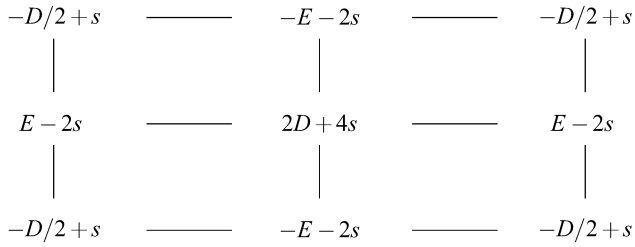


Fig. 6.4. The two parameter stencil for a mesh of rectangles; h_x may differ from h_y

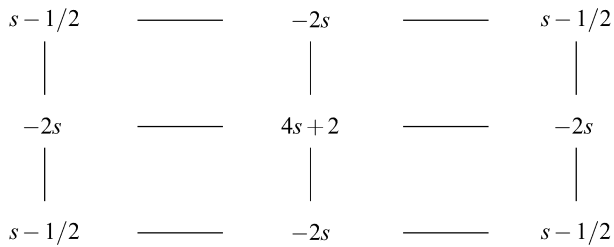


Fig. 6.5. The one-parameter stencil for a mesh of squares; $h_x = h_y$ implies $D = 1$ and $E = 0$

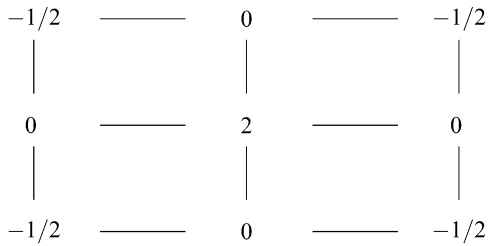


Fig. 6.6. The stencil for a square mesh with $s = 0$ corresponds to the hourglass scheme

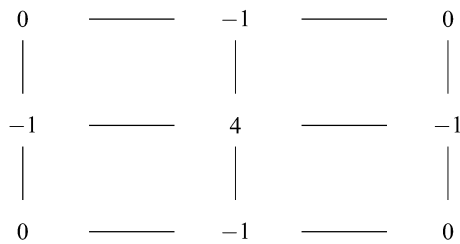


Fig. 6.7. The stencil for a square mesh with $s = 1/2$ corresponds to the 5-point Laplacian

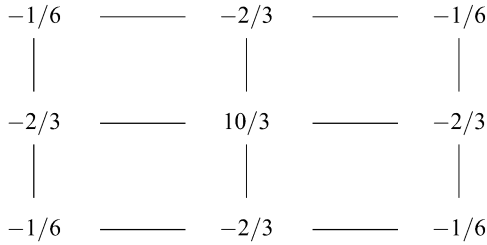


Fig. 6.8. The stencil for a square element with $s = 1/3$ corresponds to the 9-point Laplacian

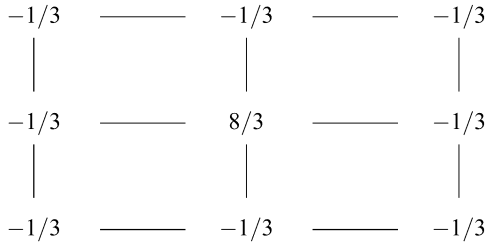


Fig. 6.9. The stencil for a square element with $s = 1/6$ corresponds to the bilinear FEM

6.3 Arbitrary-order mimetic method

In two dimensions, the arbitrary-order mimetic method has been formulated in [50]. In three dimensions, the construction is also feasible, as noted without detailed explanations in [50]. In the present section, we focus on the two dimensional case.

The theoretical convergence analysis of the arbitrary-order discretization requires to modify mesh regularity assumption **(MR)** by including assumption **(MR3)** as discussed in Sect. 1.6.2. With a slight abuse of notation, in the rest of this chapter, we will refer to the extended set of mesh regularity conditions **(MR1)–(MR3)** as assumption **(MR)**.

Assumption **(MR3)** limits slightly the set of admissible polygonal meshes by requiring each polygon to be star-shaped with respect to a special point $\bar{\mathbf{x}}_P \in P$. However, a great generality of cell shapes is allowed, e.g. non-convex polygons are still admissible. Also, a mesh may contain degenerate polygons like those encountered in the AMR methods [339] which divide a straight edge in two or more sub-edges. When P is a convex polygon, the arithmetic average of the position vectors of its vertices, $\bar{\mathbf{x}}_P = (1/N_P^V) \sum_{v \in \partial P} \mathbf{x}_v$, provides a convenient choice for the special point.

To extend the low-order mimetic method to an arbitrary-order method, we have to enrich the original set of the degrees of freedom. For simplicity of exposition, we assume temporary that K is a constant tensor inside each polygonal cell P . We remove this restriction in the next subsection. Integrating by parts and splitting the boundary

integral into a sum of face/edge contributions, we obtain the fundamental relation:

$$\int_{\mathbb{P}} \mathbb{K} \nabla \psi \cdot \nabla v dV = - \int_{\mathbb{P}} \operatorname{div}(\mathbb{K} \nabla \psi) v dV + \sum_{f \in \partial \mathbb{P}} \int_f \mathbb{K} \nabla \psi \cdot \mathbf{n}_{\mathbb{P},f} v dS. \quad (6.37)$$

If ψ is a given polynomial of degree m on \mathbb{P} , then

- $\operatorname{div}(\mathbb{K} \nabla \psi)$ is a polynomial of degree $m - 2$;
- $\mathbb{K} \nabla \psi \cdot \mathbf{n}_{\mathbb{P},f}$ is a polynomial of degree $m - 1$.

We express the divergence of $\mathbb{K} \nabla \psi$ as a linear combination of the canonical basis of $\mathbb{P}_{m-2}(\mathbb{P})$, i.e.,

$$\operatorname{div}(\mathbb{K} \nabla \psi) = a_0 1 + a_1 x + a_2 y + \dots \in \mathbb{P}_{m-2}(\mathbb{P}). \quad (6.38)$$

Since ψ and \mathbb{K} are known, so is $\operatorname{div}(\mathbb{K} \nabla \psi)$ and the coefficients a_0, a_1, a_2 , etc. A different basis with better properties is considered in the formal construction in the next subsection, but right now, the monomials of the canonical basis, e.g., $\{1, x, y, x^2, xy, y^2, \dots\}$, are making a good job. Using (6.38), allows us to reformulate the integral over \mathbb{P} in terms of the *moments of the function* v as

$$\begin{aligned} \int_{\mathbb{P}} \operatorname{div}(\mathbb{K} \nabla \psi) v dV &= a_0 \int_{\mathbb{P}} 1 v dV + a_1 \int_{\mathbb{P}} x v dV + a_2 \int_{\mathbb{P}} y v dV + \dots \\ &= a_0 \hat{v}_{\mathbb{P},0} + a_1 \hat{v}_{\mathbb{P},1} + a_2 \hat{v}_{\mathbb{P},2} + \dots \end{aligned}$$

Since ψ is known, the expression above is *exact* for any function v once we know its moments $\hat{v}_{\mathbb{P},0}, \hat{v}_{\mathbb{P},1}, \hat{v}_{\mathbb{P},2}$, etc. This fact suggests us to take these quantities as the degrees of freedom. By doing so, the integration of the divergence term introduces $m(m-1)/2$ degrees of freedom, as many as there are linearly independent polynomials in $\mathbb{P}_{m-2}(\mathbb{P})$.

Each face integral in (6.37) is evaluated by using the Gauss-Lobatto formula with $m+1$ nodes $\mathbf{x}_{f,q}$ and weights $w_{f,q}$:

$$\int_f v \mathbf{n}_{\mathbb{P},f} \cdot \mathbb{K} \nabla \psi dV \approx \sum_{q=0}^{m+1} w_{f,q} v(\mathbf{x}_{f,q}) \mathbf{n}_{\mathbb{P},f} \cdot \mathbb{K} \nabla \psi(\mathbf{x}_{f,q}). \quad (6.39)$$

Since $\mathbb{K} \nabla \psi(\mathbf{x}_{f,q}) \cdot \mathbf{n}_{\mathbb{P},f}$ is a known polynomial on degree $m-1$, we can calculate this integral *exactly* when the trace of function v on f is a polynomial of order at most m . We introduce a subspace $S_{h,\mathbb{P}}$ of functions $v \in H_0^1(\mathbb{P}) \cap C^0(\mathbb{P})$ with such polynomial trace on faces f so that (6.39) becomes the identity. This suggests us to define the following degrees of freedom

$$v_{f,q} = v(\mathbf{x}_{f,q}), \quad q = 0, 1, \dots, m, \quad (6.40)$$

where $\mathbf{x}_{f,0}$ and $\mathbf{x}_{f,m}$ are the end-points of edge f .

Remark 6.7. We emphasize two important steps in the construction of this and other mimetic schemes, see Chaps. 3 and 4 for a general discussion. First, the degrees of

freedom are selected to support polynomials of order m . Second, the test space $S_{h,P}$ is selected to be rich enough and integrate exactly all integrals in the right-hand side of (6.37).

Remark 6.8. The MFD method has enough flexibility to mix and match various degrees of freedom. For instance, face-based moments can be used instead on point-based values (6.40). Such a selection leads to a new family of mimetic schemes [247].

6.3.1 Degrees of freedom

Let m be a positive integer number. We define a new discrete space \mathcal{V}_h . A discrete field $v_h \in \mathcal{V}_h$ is written as

$$v_h = ((v_v)_{v \in \mathcal{V}}, (v_{f,i})_{f \in \mathcal{F}, i=1, \dots, m-1}, (v_{P,k,i})_{P \in \mathcal{P}, k=0, \dots, m-2, i=0, \dots, k}), \tag{6.41}$$

where

- (i) $(v_v)_{v \in \mathcal{V}}$ consists of one real number v_v per mesh vertex $v \in \mathcal{V}$;
- (ii) $(v_{f,i})_{f \in \mathcal{F}, i=1, \dots, m-1}$ consists of $(m-1)$ real numbers $v_{f,i}$ per mesh face $f \in \mathcal{F}$;
- (iii) $(v_{P,k,i})_{P \in \mathcal{P}, k=0, \dots, m-2, i=0, \dots, k}$ consists of $m(m-1)/2$ real numbers $v_{P,k,i}$ per mesh element $P \in \mathcal{P}$.

Examples for $m = 2, 3, 4, 5$ are shown in Fig. 6.10 for the case of a single pentagonal element. The first two sets of degrees of freedom can be combined together and written as $(v_{f,i})_{f \in \mathcal{F}, i=0, \dots, m}$. Their represent the *nodal* values of a scalar field. The last

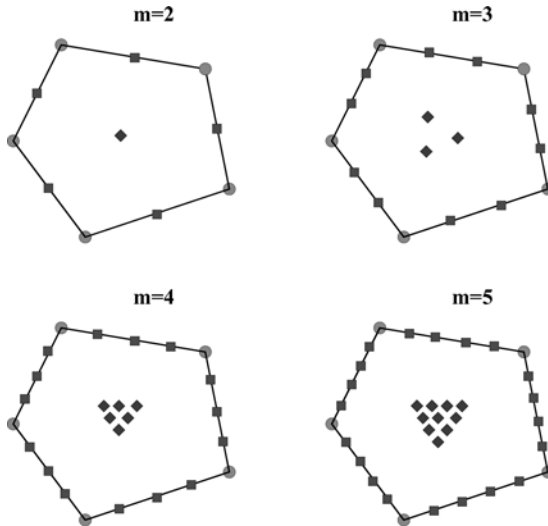


Fig. 6.10. Degrees of freedom for $m = 2, 3, 4, 5$; vertex degrees of freedom are symbolically denoted by circles, nodal degrees of freedom at the Gauss-Lobatto nodes inside each face are denoted by squares, and interior moment degrees of freedom are denoted by diamonds

set $(v_{\mathbb{P},k,i})_{\mathbb{P} \in \mathcal{P}, k=0, \dots, m-2, i=0, \dots, k}$ contains the moments of a scalar field over polygons \mathbb{P} . We will refer to them as the *internal* degrees of freedom. In a computer program, they can be eliminated locally.

The nodal values are associated with the Gauss-Lobatto numerical integration rule with $m+1$ nodes, cf. Formula 25.4.32 and Table 25.6 of [6]. The Gauss-Lobatto quadrature nodes are defined uniquely and symmetrically on face f and the first node and the last node always coincide with the end-points of f . Consistently with our notation, the values at the end-points are labeled by $v_{f,0}$ and $v_{f,m}$. Furthermore, the $(m+1)$ -sized set $(v_{f,i})_{i=0, \dots, m}$ of the nodal values can be identified with a polynomial $v_{h,f} \in \mathbb{P}_m(f)$, which is the unique one-dimensional polynomial of degree m that interpolates these values along f .

The dimension of the global approximation space \mathcal{V}_h is equal to $N^{\mathcal{V}} + N^{\mathcal{F}}(m-1) + N^{\mathcal{D}}m(m-1)/2$, where $N^{\mathcal{V}}$ is the number of mesh vertices, $N^{\mathcal{F}}$ the number of mesh faces, and $N^{\mathcal{D}}$ the number of mesh elements. Let $\mathcal{V}_{h,\mathbb{P}}$ denote the restriction of \mathcal{V}_h to element \mathbb{P} . The discrete field $v_{\mathbb{P}} \in \mathcal{V}_{h,\mathbb{P}}$ collects the degrees of freedom associated with the vertices, faces and interior of \mathbb{P} . The dimension of $\mathcal{V}_{h,\mathbb{P}}$ is equal to $m_{\mathcal{V}_{h,\mathbb{P}}} = N_{\mathbb{P}}^{\mathcal{F}}m + m(m-1)/2$, where $N_{\mathbb{P}}^{\mathcal{F}}$ is the number of faces in \mathbb{P} , $N_{\mathbb{P}}^{\mathcal{F}} = 5$ in Fig. 6.10.

Let us define, for every \mathbb{P} , a local projection operator $(\cdot)_{\mathbb{P}}^{\downarrow} : H^1(\mathbb{P}) \cap C^0(\mathbb{P}) \rightarrow \mathcal{V}_{h,\mathbb{P}}$. As usual, a global projection operator $(\cdot)^{\downarrow}$ is a combination of all the local ones so that for any $v \in H^1(\Omega) \cap C^0(\overline{\Omega})$ and any $\mathbb{P} \in \Omega_h$ it holds that $v^{\downarrow}|_{\mathbb{P}} = v|_{\mathbb{P}}$. For simplicity, we shall write $v_{\mathbf{v}}^{\downarrow}$ instead of $(v_{\mathbb{P}}^{\downarrow})_{\mathbf{v}}$ and $v_{f,i}^{\downarrow}$ instead of $(v_{\mathbb{P}}^{\downarrow})_{f,i}$ for particular vector components. For the nodal degrees of freedom, we set

$$v_{\mathbf{v}}^{\downarrow} = v(\mathbf{x}_{\mathbf{v}}) \quad \forall \mathbf{v} \in \partial \mathbb{P}; \quad (6.42)$$

$$v_{f,i}^{\downarrow} = v(\mathbf{x}_{f,i}) \quad \forall f \in \partial \mathbb{P}, i = 1, 2, \dots, m-1. \quad (6.43)$$

For the internal degrees of freedom, we set

$$v_{\mathbb{P},k,i}^{\downarrow} = \frac{1}{|\mathbb{P}|} \int_{\mathbb{P}} v \varphi_{k,i} dV \quad k = 0, \dots, m, i = 0, 1, \dots, k, \quad (6.44)$$

where $\varphi_{k,i}$ are linearly independent polynomials forming a basis of $\mathbb{P}_{m-2}(\mathbb{P})$. In this section, we introduce a different basis than before. It turns out that a very convenient choice for such functions is given by the following construction:

- for $k = i = 0$ we take the constant function $\varphi_{0,0} = 1$;
- for $k = 1, \dots, m$ and $i = 0, \dots, k$ we choose $(k+1)$ polynomial functions $\varphi_{k,i}$ that form an L^2 -orthogonal basis for

$$\widehat{\mathbb{P}}_k(\mathbb{P}) = \left\{ \varphi \in \mathbb{P}_k(\mathbb{P}) \text{ such that } \int_{\mathbb{P}} \varphi \psi dV = 0 \quad \forall \psi \in \mathbb{P}_{k-1}(\mathbb{P}) \right\}.$$

The linear space $\widehat{\mathbb{P}}_k(\mathbb{P})$ is formed by the polynomials of degree exactly equal to k . The polynomials $\varphi_{k,i}$ are normalized by imposing that $\|\varphi_{k,i}\|_{L^2(\mathbb{P})} = h_{\mathbb{P}}$.

Since the polynomials in $\widehat{\mathbb{P}}_k(\mathbb{P})$ for $k \geq 1$ are orthogonal to all the polynomials of lower degree, they are also orthogonal to $\varphi_{0,0} = 1$ and, consequently, to constant functions. Furthermore, we have that $\mathbb{P}_m(\mathbb{P}) = \bigoplus_{k=0}^m \widehat{\mathbb{P}}_k(\mathbb{P})$.

The convergence analysis in Sect. 6.4 measures the approximation error in the mesh-dependent norm:

$$\|v_h\|_{1,h}^2 = \sum_{\mathbb{P} \in \Omega_h} \|v_{\mathbb{P}}\|_{1,h,\mathbb{P}}^2, \quad (6.45)$$

where each local term $\|v_{\mathbb{P}}\|_{1,h,\mathbb{P}}^2$ is designed to mimic the H^1 seminorm on the element \mathbb{P} . We consider the following seminorm:

$$\|v_{\mathbb{P}}\|_{1,h,\mathbb{P}}^2 = \sum_{f \in \partial \mathbb{P}} h_{\mathbb{P}} \frac{\partial v_{h,f}}{\partial s} \Big|_{L^2(f)}^2 + (v_{\mathbb{P},0,0} - \bar{v}_{\mathbb{P}})^2 + \sum_{k=1}^{m-2} \sum_{i=0}^k |v_{\mathbb{P},k,i}|^2, \quad (6.46)$$

where $\partial v_{h,f}/\partial s$ is the derivative along edge f of the one-dimensional polynomial $v_{h,f}$ of degree $(m+1)$ that interpolates the values $v_{f,i}$ for $i = 0, \dots, m$, and

$$\bar{v}_{\mathbb{P}} = \frac{1}{N_{\mathbb{P}}^{\mathcal{V}}} \sum_{v \in \partial \mathbb{P}} v_v. \quad (6.47)$$

To enforce the Dirichlet boundary condition on Γ^D , we consider the subset $\mathcal{V}_{h,g}$ of discrete fields from \mathcal{V}_h whose restriction to a Dirichlet boundary edge is fully specified by function g^D . Assuming that g^D is continuous, we require that for each vertex $v \in \Gamma^D$ and each face $f \in \Gamma^D$ it holds that

$$v_v = g^D(\mathbf{x}_v), \quad v_{f,i} = g^D(\mathbf{x}_{f,i}), \quad i = 1, 2, \dots, m-1.$$

6.3.2 The consistency and stability conditions

The local bilinear form $\mathcal{A}_{h,\mathbb{P}}$ is defined in three steps. In the first step, we introduce the L^2 orthogonal projector on the linear space of two-dimensional vectors of polynomials of degree k :

$$\mathcal{P}_{\mathbb{P}}^k : (L^2(\mathbb{P}))^2 \rightarrow (\mathbb{P}_k(\mathbb{P}))^2.$$

For $w \in H^1(\mathbb{P})$ and $K \in L^\infty(\mathbb{P})$, the divergence $\text{div}(\mathcal{P}_{\mathbb{P}}^{m-1}(K\nabla w))$ belongs to $\mathbb{P}_{m-2}(\mathbb{P})$ and its expansion in the polynomial basis functions $\varphi_{k,i} \in \mathbb{P}_{m-2}(\mathbb{P})$ takes the form

$$\text{div}(\mathcal{P}_{\mathbb{P}}^{m-1}(K\nabla w)) = \sum_{k=0}^{m-2} \sum_{i=0}^k \alpha_{k,i} \varphi_{k,i}, \quad (6.48)$$

where the coefficients $\alpha_{k,i}$ depend on w .

In the second step, we define the quadrature formula $\mathcal{I}_P(v_P, w)$ by

$$\mathcal{I}_P(v_P, w) = \sum_{k=0}^{m-2} \sum_{i=0}^k |P| \alpha_{k,i} v_{P,k,i}, \quad (6.49)$$

where $v_{P,k,i}$ are the internal degrees of freedom of the discrete field v_P and the coefficients $\alpha_{k,i}$ are those used in expansion (6.48). The following argument explains the meaning of this quadrature rule. Let v_P^I be the projection of the scalar function $v \in H^1(P) \cap C^0(P)$ in $\mathcal{V}_{h,P}$ (see Sect. 6.3.1). Recalling (6.44) and inserting (6.48) in (6.49) yields

$$\begin{aligned} \mathcal{I}_P(v_P^I, w) &= \sum_{k=0}^{m-2} \sum_{i=0}^k \alpha_{k,i} \int_P v \varphi_{k,i} dV = \int_P v \left(\sum_{k=0}^{m-2} \sum_{i=0}^k \alpha_{k,i} \varphi_{k,i} \right) dV \\ &= \int_P v \operatorname{div}(\mathcal{P}_P^{m-1}(K\nabla w)) dV. \end{aligned} \quad (6.50)$$

Thus, the bilinear operator $\mathcal{I}_P(v_P^I, w)$ is an approximation of the last volume integral in (6.50).

In the third step, the discrete symmetric bilinear form $\mathcal{A}_{h,P}$ on $\mathcal{V}_{h,P} \times \mathcal{V}_{h,P}$ is required to satisfy the stability and consistency conditions. Let $S_{h,P}$ be a subspace of $H^1(P) \cap C^0(P)$ that satisfies assumptions **(B1)**–**(B3)** formulated in Part I of this book. For the considered mimetic discretization, they read as follows.

(B1) The projection operator $(\cdot)_P^I$ is surjective from $S_{h,P}$ to $\mathcal{V}_{h,P}$.

(B2) The space $S_{h,P}$ contains the space of polynomial of degree at most m .

(B3) The trace of $v \in S_{h,P}$ on face f of P is a polynomial of degree at most m .

In general, a space $S_{h,P}$ satisfying all requirements is infinite dimensional. However, the complete convergence theory can be built using a finite dimensional space such that $\dim(S_{h,P}) = \dim(\mathcal{V}_{h,P})$, i.e. $S_{h,P}$ is isomorphic to $\mathcal{V}_{h,P}$. In the sequel, we assume the latter.

(S1) Spectral stability: There exists two positive constants σ_* and σ^* such that for every $v_P \in \mathcal{V}_{h,P}$ there holds:

$$\sigma_* \|v_P\|_{1,h,P}^2 \leq \mathcal{A}_{h,P}(v_P, v_P) \leq \sigma^* \|v_P\|_{1,h,P}^2.$$

(S2) Local consistency: For every $\psi \in \mathbb{P}_m(P)$ and every $v_P \in S_{h,P}$ there holds:

$$\mathcal{A}_{h,P}(v_P^I, \psi_P^I) = \int_P \nabla v \cdot \mathcal{P}_P^{m-1}(K\nabla \psi) dV. \quad (6.51)$$

Note that, for any $v \in S_{h,P}$, the integration by parts gives

$$\int_P \nabla v \cdot \mathcal{P}_P^{m-1}(K\nabla \psi) dV = -\mathcal{I}_P(v_P^I, \psi) + \sum_{f \in \partial P} \int_f v \mathcal{P}_P^{m-1}(K\nabla \psi) \cdot \mathbf{n}_{P,f} ds.$$

The one-dimensional polynomial $\mathcal{P}_P^{m-1}(\mathbf{K}\nabla\psi) \cdot \mathbf{n}_{P,f}$ has degree at most $m-1$ and the trace of v on f is a polynomial of degree at most m . Since the Gauss-Lobatto formula of order m mentioned above is exact for polynomials up to degree $(2m-1)$ [6], it integrates exactly the product of $\mathcal{P}_P^{m-1}(\mathbf{K}\nabla\psi) \cdot \mathbf{n}_{P,f}$ and v . Thus,

$$\int_P \nabla v \cdot \mathcal{P}_P^{m-1}(\mathbf{K}\nabla\psi) dV = -\mathcal{I}_P(v_P^I, \psi) + \sum_{f \in \partial P} \sum_{i=0}^m v_{f,i}^I \omega_{f,i} (\mathcal{P}_P^{m-1}(\mathbf{K}\nabla\psi) \cdot \mathbf{n}_{P,f})(\mathbf{x}_{f,i}), \quad (6.52)$$

where $\omega_{f,i}$ are the weights in the Gauss-Lobatto formula. Thus the right hand side of (6.51) is exactly computable on the basis of the existing degrees of freedom.

Let now $\psi, \varphi \in \mathbb{P}_m(P)$. Since $\varphi \in S_{h,P}$ then we can take $v = \varphi$ in the consistency condition. Using the fact that \mathcal{P}_P^{m-1} is the orthogonal projection onto the polynomials of degree at most $m-1$ yields:

$$\mathcal{A}_{h,P}(\varphi_P^I, \psi_P^I) = \int_P \nabla \varphi \cdot \mathcal{P}_P^{m-1}(\mathbf{K}\nabla\psi) dV = \int_P \nabla \varphi \cdot \mathbf{K}\nabla\psi dV. \quad (6.53)$$

This relation implies that the bilinear form $\mathcal{A}_{h,P}(\cdot, \cdot)$ is exact for polynomials of order at most m and does not violate the symmetry requirement. Moreover, property (S1) combined with the boundary conditions allows us to prove that the bilinear form \mathcal{A}_h is coercive on the vector space $\mathcal{V}_{h,0}$, from which we can deduce that there exists a unique solution to the discrete problem (6.14).

6.3.3 Discretization of linear functional \mathcal{L}_h

In the present section we focus on the $m \geq 2$ case since for $m = 1$ one can follow the same construction shown in Sect. 6.2.3. Let us consider the L^2 -orthogonal projector $\mathcal{P}_P^k : L^2(P) \rightarrow \mathbb{P}_k(P)$ onto the space of polynomials of degree at most k . With a small abuse of notation, we use the same symbol for this projector as in Sect. 6.3.2, since its action is always clear from the type of its argument. Let $\hat{b}_P = \mathcal{P}_P^{m-2}(b)$ be the projection of the forcing term b in (6.11) on the polynomial space. We expand \hat{b}_P as a linear combination of the basis functions $\varphi_{k,i}$ for $k = 0, \dots, m-2$ and $i = 0, \dots, k$:

$$\hat{b}_P = \sum_{k=0}^{m-2} \sum_{i=0}^k c_{k,i} \varphi_{k,i}. \quad (6.54)$$

This expansion uses $m(m-1)/2$ coefficients $c_{k,i}$ depending on b . Using these coefficients and the internal degrees of freedom $v_{P,i,k}$ of the discrete field v_P , we define the local linear functional

$$\mathcal{L}_P(v_P) = |P| \sum_{k=0}^{m-2} \sum_{i=0}^k c_{k,i} v_{P,k,i}$$

and the global one by the assembly process:

$$\mathcal{L}_h(v_h) = \sum_{P \in \Omega_h} \mathcal{L}_P(v_P).$$

Remark 6.9. For any $v \in L^2(\mathbb{P})$ and any loading term $b \in L^2(\Omega)$ it holds that

$$\mathcal{L}_{\mathbb{P}}(v_{\mathbb{P}}^{\mathbb{I}}) = \int_{\mathbb{P}} \mathcal{D}_{\mathbb{P}}^{m-2}(b) \mathcal{D}_{\mathbb{P}}^{m-2}(v) dV = \int_{\mathbb{P}} \hat{b}_{\mathbb{P}} v dV \quad \forall \mathbb{P} \in \Omega_h. \quad (6.55)$$

6.3.4 Derivation of bilinear form \mathcal{A}_h

The construction of the arbitrary-order method coincides with that of the low-order method when we simply set $m = 1$. Again, we will follow the guidelines described in Chap. 4. Given $\mathbb{P} \in \Omega_h$, we will build an elemental stiffness matrix $M_{\mathbb{P}}$ such that

$$\mathcal{A}_{h,\mathbb{P}}(u_{\mathbb{P}}, v_{\mathbb{P}}) = u_{\mathbb{P}}^T M_{\mathbb{P}} v_{\mathbb{P}} \quad \forall u_{\mathbb{P}}, v_{\mathbb{P}} \in \mathcal{V}_{h,\mathbb{P}}.$$

The global stiffness matrix is obtained by the standard assembly process.

The construction of the elemental stiffness matrix is reduced to an algebraic equation of the form $M_{\mathbb{P}} N_{\mathbb{P}} = R_{\mathbb{P}}$, as in all other mimetic discretizations. Let

$\{\psi_1, \psi_2, \dots, \psi_n\}$ with $n = (m+1)(m+2)/2$ be a basis for polynomial space $\mathbb{P}_m(\mathbb{P})$. We select the following basis functions:

$$\begin{aligned} \psi_1(x, y) &= 1, \\ \psi_2(x, y) &= \frac{x - x_{\mathbb{P}}}{h_{\mathbb{P}}}, \quad \psi_3(x, y) = \frac{y - y_{\mathbb{P}}}{h_{\mathbb{P}}}, \\ \psi_4(x, y) &= \frac{(x - x_{\mathbb{P}})^2}{h_{\mathbb{P}}^2}, \quad \psi_5(x, y) = \frac{(x - x_{\mathbb{P}})(y - y_{\mathbb{P}})}{h_{\mathbb{P}}^2}, \quad \psi_6(x, y) = \frac{(y - y_{\mathbb{P}})^2}{h_{\mathbb{P}}^2}, \\ &\dots \end{aligned}$$

Here $\mathbf{x}_{\mathbb{P}} = (x_{\mathbb{P}}, y_{\mathbb{P}})^T$ is the barycenter of \mathbb{P} .

Remark 6.10. Note that $\|\psi_i\|_{L^2(\mathbb{P})} \sim h_{\mathbb{P}}$, so that the theory developed later still applies, but these basis functions suit better for the practical implementation of the method than the orthogonal basis used in the theory. Of course, the coefficients $\alpha_{k,i}$ (see (6.48)) and $c_{k,i}$ (see (6.54)) must be calculated with respect to the basis $\{\psi_i\}_{i=1}^n$.

Let $N_i = (\psi_i)_{\mathbb{P}}^{\mathbb{I}}$ be the i -th column of matrix $N_{\mathbb{P}}$. This matrix is easily calculated by evaluating ψ_i at the Gauss-Lobatto points and computing its moments over polygon \mathbb{P} . Using the divergence theorem, the calculation of the moments is reduced to integration of polynomials over edges f of \mathbb{P} .

A formula for the matrix $R_{\mathbb{P}}$ follows from the right-hand side of (6.52). For a given ψ_i , it represents a linear functional of $v_{\mathbb{P}}^{\mathbb{I}}$, i.e. it can be written as $(v_{\mathbb{P}}^{\mathbb{I}})^T R_i$. Let $\boldsymbol{\varepsilon}_{\mathbb{P}}^j$ denote the vector in $\mathcal{V}_{h,\mathbb{P}}$ whose j -th component equals to one and the other components are zero. Then,

$$(R_i)_j = -\mathcal{I}_{\mathbb{P}}(\boldsymbol{\varepsilon}_{\mathbb{P}}^j, \psi_i) + \sum_{f \in \partial \mathbb{P}} \sum_{q=0}^m \boldsymbol{\varepsilon}_{f,q}^j \boldsymbol{\omega}_{f,q}(\mathcal{D}_{\mathbb{P}}^{m-1}(\mathbb{K} \nabla \psi_i) \cdot \mathbf{n}_{\mathbb{P},f})(\mathbf{x}_{f,q}).$$

This implies that R_1 is the zero vector. Combining formulas (6.51), (6.52) and using the matrix representation of the local bilinear form, we obtain

$$(v_P^1)^T M_P N_i = (v_P^1)^T R_i \quad \forall v_P^1 \in \mathcal{V}_{h,P}.$$

These n matrix equations can be written in the compact form

$$M_P N_P = R_P \quad (6.56)$$

with rectangular $(N_P^{\mathcal{Y}} \times n)$ -sized matrices N_P and R_P .

Lemma 6.2. *The matrices N_P and R_P satisfy the following identity:*

$$(N_P^T R_P)_{ij} = \int_P K \nabla \psi_i \cdot \nabla \psi_j dV \quad (6.57)$$

for $i, j = 1, \dots, n$. The matrix $N_P^T R_P$ is symmetric and semi-positive definite.

Proof. The first assertion of the lemma follows from Eq. (6.53). The second assertion is the direct consequence of the first one. \square

Let $Q_P = N_P^T R_P$. This matrix represents the bilinear form $\mathcal{A}(\cdot, \cdot)$ restricted to space $\mathbb{P}_m(P)$. It is clear from (6.57) that matrix Q_P has the form

$$Q_P = \begin{pmatrix} 0 & \mathbf{0}^T \\ \mathbf{0} & \widehat{Q}_P \end{pmatrix},$$

where \widehat{Q}_P is a positive definite $(n-1) \times (n-1)$ -sized matrix. More precisely, the entries of \widehat{Q}_P are given by (6.57) for $i > 1$ and $j > 1$, i.e., when we exclude the constant polynomial $\psi_1(x, y) = 1$. Let $Q_P^\dagger \in \mathbb{R}^{n \times n}$ be the pseudo-inverse of matrix Q , which we define as

$$Q_P^\dagger = \begin{pmatrix} 0 & \mathbf{0}^T \\ \mathbf{0} & \widehat{Q}_P^{-1} \end{pmatrix}.$$

Since, the first column of matrix R_P is zero, we can easily verify that the solution of the matrix Eq. (6.56) is given by

$$M_P = R_P Q_P^\dagger R_P^T + D_P U_P D_P^T, \quad (6.58)$$

where U_P is an arbitrary positive definite matrix of size $(N_P^{\mathcal{Y}} - n - 1)$ and D_P is a rectangular matrix with the largest rank such that $D_P^T N_P$ is the zero matrix.

The stability condition **(S1)** imposes bounds on positive eigenvalues of $D_P U_P D_P^T$ as discussed in Chap. 4. In practice, a simple formula can be used:

$$M_P = R_P Q_P^\dagger R_P^T + u_P P_P, \quad (6.59)$$

where P_P is the orthogonal projector on $\ker(N_P^T)$ and positive scalar u_P is determined by the consistency term:

$$P = I - N_P(N_P^T N_P)^{-1} N_P^T, \quad u_P = \frac{1}{N_P^T} \text{trace}(R_P Q_P^\dagger R_P^T).$$

6.4 Convergence analysis

The main result of this section is given in Theorem 6.2. This theorem provides an estimate for the discretization error in the mesh-dependent norm $\|\cdot\|_{1,h}$ defined in (6.45)–(6.46). For simplicity of exposition, we assume that problem (6.1)–(6.3) is formulated with the homogeneous Dirichlet boundary conditions. Thus, we assume that $\Gamma^N = \emptyset$ in (6.3) and $g^D = 0$ in (6.2). Consistently, we have $u \in H_0^1(\Omega)$ and $u_h \in \mathcal{V}_{h,0}$.

Theorem 6.2. *Let $u \in H^{m+1}(\Omega) \cap H_0^1(\Omega)$ be the solution of variational problem (6.11) under assumptions **(H1)**–**(H2)**, $\Gamma^N = \emptyset$ and $g^D = 0$. Let $u^I \in \mathcal{V}_{h,0}$ be its projector defined by (6.42)–(6.43) and (6.44). Let $u_h \in \mathcal{V}_{h,0}$ be the solution of the mimetic problem (6.14) under assumption **(MR1)**–**(MR3)** and **(S1)**–**(S2)**. Let us assume that $K_P \in W^{m,\infty}(P)$ for any polygonal element P . Then, there exists a positive constant C , which is independent of h , such that*

$$\|u_h - u^I\|_{1,h} \leq Ch^m |u|_{H^{m+1}(\Omega)}. \quad (6.60)$$

The proof of Theorem 6.2 uses two theoretical tools, the reconstruction operator and the stability Lemma 6.5, that are presented in Sects. 6.4.1 and 6.4.2, respectively. For this reason, the proof is postponed to Sect. 6.4.3.

6.4.1 Reconstruction operator

In this subsection, we prove the existence of a local reconstruction operator

$$R_P : \mathcal{V}_{h,P} \rightarrow S_{h,P}$$

with the following three properties.

(L1) The reconstruction operator R_P is the right-inverse to the projection operator on $\mathcal{V}_{h,P}$:

$$(R_P(v_P))^I = v_P \quad \forall v_P \in \mathcal{V}_{h,P}.$$

(L2) The trace of the reconstruction operator R_P on face f coincides with the interpolation polynomial of degree m that is uniquely defined by the degrees of freedom associated with the Gauss-Lobatto quadrature nodes:

$$R_P(v_P)|_f = v_{h,f} \in \mathbb{P}_m(f) \quad \forall f \in \partial P, \forall v_P \in \mathcal{V}_{h,P}.$$

(L3) The reconstruction operator R_P is stable with respect to the mesh-dependent norm (6.46), i.e., there exists a positive constant C independent of P such that

$$|R_P(v_P)|_{H^1(P)} \leq C \|v_P\|_{1,h,P}.$$

Assumption **(L1)** is equivalent to assumption **(R1)** discussed in Chap. 3 (see also [67]). Assumption **(L2)** is much weaker than assumption **(R2)** stating that the reconstruction operator is the left-inverse of the projection operator on a polynomial space over element P .

Let us write the reconstruction operator as the sum of two distinct terms:

$$R_P(v_P) = R_P^{(1)}(v_P) + R_P^{(2)}(v_P). \quad (6.61)$$

The term $R_P^{(1)}(v_P)$ is built as follows. Let us consider the auxiliary decomposition $T_{h|P}$, which is provided by the mesh assumption **(MR3)**. This decomposition contains a unique triangle for each face f of ∂P , which is labeled as T_f . For each triangle T_f , we consider the function $v_{h,f}^\partial$ defined on ∂T_f that has the following properties:

- on face f , function $v_{h,f}^\partial$ coincides with the polynomial $v_{h,f}$;
- on the two other edges connecting the internal point \bar{x}_P with vertices of f , function $v_{h,f}^\partial$ is the linear interpolant between \bar{v}_P at \bar{x}_P (see (6.47)) and $v_{f,0}$ or $v_{f,m}$.

Now, we consider a linear map $\mathcal{F} : \widehat{T} \rightarrow T_f$ from the reference triangle \widehat{T} onto T_f . On \widehat{T} , we first solve the harmonic problem

$$-\Delta(\mathcal{H}(v_P)) = 0 \quad \text{in } \widehat{T}, \quad (6.62)$$

$$\mathcal{H}(v_P) = v_{h,f}^\partial \circ \mathcal{F} \quad \text{on } \partial \widehat{T}, \quad (6.63)$$

and then, set

$$R_P^{(1)}(v_P)|_{T_f} := \mathcal{H}(v_P) \circ \mathcal{F}^{-1} \quad \forall f \in \partial P. \quad (6.64)$$

A stability result holds for $R_P^{(1)}(v_P)$, whose proof is omitted since it is a consequence of a simple scaling argument and the mesh regularity assumptions **(MR)**.

Lemma 6.3. *There exists a constant C , independent of h_P and of the shape of P , such that*

$$\|\nabla R_P^{(1)}(v_P)\|_{L^2(P)} \leq C \|v_P\|_{1,h,P} \quad \forall v_P \in \mathcal{V}_{h,P}. \quad (6.65)$$

This lemma is used below to prove condition **(L3)**. For the moment, let us note that, by construction, the reconstruction operator $R_P^{(1)}$ is exact for constant fields:

$$R_P^{(1)}(c_P^1) = c \quad \forall c \in \mathbb{P}_0(P). \quad (6.66)$$

Furthermore, it also satisfies condition **(L2)**. Nonetheless, we cannot consider $R_P^{(1)}$ as the final reconstruction operator because condition **(L1)** is satisfied only for the

nodal degrees of freedom but not for the internal ones. In order to fix this deficiency, we need the second operator $R_{\mathbf{P}}^{(2)}$, which is built as follows.

Let us consider the $m(m-1)/2$ functions $\mathcal{B}_{k,i} \in H_0^1(\mathbf{P})$ labeled by the index pair (k, i) , where $k = 0, \dots, m-2$ and $i = 0, \dots, k$, that are such that

$$(i) \quad \int_{\mathbf{P}} \mathcal{B}_{k,i} \varphi_{l,j} = |\mathbf{P}| \delta_{kl} \delta_{ij} \quad \text{for } l = 0, \dots, m-2 \text{ and } j = 0, \dots, l; \quad (6.67)$$

$$(ii) \quad \|\nabla \mathcal{B}_{k,i}\|_{L^2(\mathbf{P})} \leq C \quad \text{for } k = 0, \dots, m-2 \text{ and } i = 0, \dots, k. \quad (6.68)$$

Note that relations (6.67)–(6.68) are consistent with $\|\varphi_{k,i}\|_{L^2(\mathbf{P})} = h_{\mathbf{P}}$. The existence of such functions can be proved using, for instance, reference polygons; details are found in [51]. The second term of the reconstruction operator is given by

$$R_{\mathbf{P}}^{(2)}(v_{\mathbf{P}}) = \sum_{k=0}^{m-2} \sum_{i=0}^k c_{k,i} \mathcal{B}_{k,i}, \quad (6.69)$$

where the coefficients $c_{k,i}$ are such that the condition **(L1)** holds true, i.e.

$$\frac{1}{|\mathbf{P}|} \int_{\mathbf{P}} \left(R_{\mathbf{P}}^{(1)}(v_{\mathbf{P}}) + R_{\mathbf{P}}^{(2)}(v_{\mathbf{P}}) \right) \varphi_{k,i} dV = v_{\mathbf{P},k,i}. \quad (6.70)$$

Substituting (6.69) in (6.70) and using the orthogonality relations (6.67) yield:

$$c_{k,i} = v_{\mathbf{P},k,i} - \frac{1}{|\mathbf{P}|} \int_{\mathbf{P}} R_{\mathbf{P}}^{(1)}(v_{\mathbf{P}}) \varphi_{k,i} dV. \quad (6.71)$$

Similarly to Lemma 6.4, a stability result holds for $R_{\mathbf{P}}^{(2)}(v_{\mathbf{P}})$. This result is also needed to prove condition **(L3)**.

Lemma 6.4. *There exists a constant C , which is independent of $h_{\mathbf{P}}$ and of the shape of \mathbf{P} , such that*

$$\|\nabla R_{\mathbf{P}}^{(2)}(v_{\mathbf{P}})\|_{L^2(\mathbf{P})} \leq C \|v_{\mathbf{P}}\|_{1,h,\mathbf{P}}. \quad (6.72)$$

Proof. We start by taking the gradient of both sides of (6.69):

$$\begin{aligned} \|\nabla R_{\mathbf{P}}^{(2)}(v_{\mathbf{P}})\|_{L^2(\mathbf{P})} &= \sum_{k=0}^{m-2} \sum_{i=0}^k c_{k,i} \|\nabla \mathcal{B}_{k,i}\|_{L^2(\mathbf{P})} \quad [\text{apply the triangle inequality}] \\ &\leq \sum_{k=0}^{m-2} \sum_{i=0}^k |c_{k,i}| \|\nabla \mathcal{B}_{k,i}\|_{L^2(\mathbf{P})} \quad [\text{use inequality (6.68)}] \\ &\leq C \sum_{k=0}^{m-2} \sum_{i=0}^k |c_{k,i}|. \end{aligned} \quad (6.73)$$

To estimate $|c_{k,i}|$ we reformulate (6.71). Let us identify the real number $\bar{v}_{\mathbf{P}}$ provided by (6.47) with the constant field taking this value over \mathbf{P} . For $(k, i) = (0, 0)$, we

apply the exactness property (6.66), which gives

$$\frac{1}{|\mathbb{P}|} \int_{\mathbb{P}} R_{\mathbb{P}}^{(1)}(\bar{v}_{\mathbb{P}}^I) \varphi_{0,0} dV = \frac{1}{|\mathbb{P}|} \int_{\mathbb{P}} \bar{v}_{\mathbb{P}} \varphi_{0,0} dV = \bar{v}_{\mathbb{P}} \frac{1}{|\mathbb{P}|} \int_{\mathbb{P}} \varphi_{0,0} dV = \bar{v}_{\mathbb{P}}.$$

It allows us to write

$$c_{0,0} = v_{\mathbb{P},0,0} - \bar{v}_{\mathbb{P}} - \frac{1}{|\mathbb{P}|} \int_{\mathbb{P}} R_{\mathbb{P}}^{(1)}(v_{\mathbb{P}} - (\bar{v}_{\mathbb{P}})^I) dV. \quad (6.74)$$

For any pair (k, i) with $k = 1, \dots, m-2$ and $i = 0, \dots, k$, the corresponding polynomial $\varphi_{k,i}$ is orthogonal to constant fields by construction. Thus,

$$c_{k,i} = v_{\mathbb{P},k,i} - \frac{1}{|\mathbb{P}|} \int_{\mathbb{P}} R_{\mathbb{P}}^{(1)}(v_{\mathbb{P}} - (\bar{v}_{\mathbb{P}})^I) \varphi_{k,i} dV. \quad (6.75)$$

Now, we use the Jensen and Cauchy-Schwarz inequalities, and the trivial geometric bound $|\mathbb{P}| \leq h_{\mathbb{P}}^2$ to start the development:

$$\begin{aligned} & \frac{1}{|\mathbb{P}|} \int_{\mathbb{P}} R_{\mathbb{P}}^{(1)}(v_{\mathbb{P}} - (\bar{v}_{\mathbb{P}})^I) \varphi_{k,i}^2 dV \\ & \leq h_{\mathbb{P}}^{-2} \|R_{\mathbb{P}}^{(1)}(v_{\mathbb{P}} - (\bar{v}_{\mathbb{P}})^I)\|_{L^2(\mathbb{P})} \|\varphi_{k,i}\|_{L^2(\mathbb{P})} \quad [\text{use } \|\varphi_{k,i}\|_{L^2(\mathbb{P})} = h_{\mathbb{P}}] \\ & \leq h_{\mathbb{P}}^{-1} \|R_{\mathbb{P}}^{(1)}(v_{\mathbb{P}} - (\bar{v}_{\mathbb{P}})^I)\|_{L^2(\mathbb{P})} \quad [R_{\mathbb{P}}^{(1)} \text{ preserves constants}] \\ & \leq h_{\mathbb{P}}^{-1} \|R_{\mathbb{P}}^{(1)}(v_{\mathbb{P}}) - \bar{v}_{\mathbb{P}}\|_{L^2(\mathbb{P})} \quad [\text{see below}] \\ & \leq C \|\nabla R_{\mathbb{P}}^{(1)}(v_{\mathbb{P}})\|_{L^2(\mathbb{P})} \quad [\text{use Lemma 6.3}] \\ & \leq C \|v_{\mathbb{P}}\|_{1,h,\mathbb{P}}. \end{aligned} \quad (6.76)$$

Let us show the fourth bound above for each triangle \mathbb{T}_f . By the construction of $R_{\mathbb{P}}^{(1)}$, it holds that $\bar{v}_{\mathbb{P}} = R_{\mathbb{P}}^{(1)}(v_{\mathbb{P}})(\bar{\mathbf{x}}_{\mathbb{P}})$. The space of harmonic functions $\mathcal{H}(v_{\mathbb{P}})$ defined by (6.62)–(6.63) is finite dimensional and is independent of the particular triangle \mathbb{T}_f . Assuming that $\bar{\mathbf{x}}_{\mathbb{P}}$ is mapped to point $(0, 0)$, a scaling argument gives

$$\begin{aligned} \|R_{\mathbb{P}}^{(1)}(v_{\mathbb{P}}) - R_{\mathbb{P}}^{(1)}(v_{\mathbb{P}})(\bar{\mathbf{x}}_{\mathbb{P}})\|_{L^2(\mathbb{T})} &= \mathbb{T}^{-1/2} \|R_{\mathbb{P}}^{(1)}(v_{\mathbb{P}}) \circ \mathcal{F} - R_{\mathbb{P}}^{(1)}(v_{\mathbb{P}}) \circ \mathcal{F}(0, 0)\|_{L^2(\hat{\mathbb{T}})} \\ &\leq C \mathbb{T}^{-1/2} \|\widehat{\nabla}(R_{\mathbb{P}}^{(1)}(v_{\mathbb{P}}) \circ \mathcal{F})\|_{L^2(\hat{\mathbb{T}})} \\ &\leq Ch_{\mathbb{P}} \|\nabla R_{\mathbb{P}}^{(1)}(v_{\mathbb{P}})\|_{L^2(\mathbb{T})}. \end{aligned}$$

We substitute (6.76) into (6.74) and (6.75) to derive upper bounds for the coeffi-

icients $c_{k,i}$:

$$|c_{k,i}| \leq C \left(|v_{P,k,i}|^2 + \left(\frac{1}{|\mathbb{P}|} \int_{\mathbb{P}} R_{\mathbb{P}}^{(1)}(v_h - (\bar{v}_{\mathbb{P}})^1) \varphi_{k,i} \right)^2 \right) \leq C \|v_h\|_{1,h,\mathbb{P}}, \quad (6.77)$$

with the obvious modification for $k = i = 0$. The assertion of the lemma is proved by applying estimate (6.77) in the final step of (6.73). \square

Eventually, property **(L3)** follows from definition (6.61), the triangle inequality

$$\|\nabla R_{\mathbb{P}}(v_{\mathbb{P}})\|_{L^2(\mathbb{P})} \leq \|\nabla R_{\mathbb{P}}^{(1)}(v_{\mathbb{P}})\|_{L^2(\mathbb{P})} + \|\nabla R_{\mathbb{P}}^{(2)}(v_{\mathbb{P}})\|_{L^2(\mathbb{P})},$$

and the stability results in Lemmas 6.3 and 6.4.

6.4.2 Stability of the projection operator

The stability of the projection operator is proved in Lemma 6.5 using the mesh-dependent norm of Sect. 6.3.1.

Lemma 6.5. *Let $v \in H^2(\mathbb{P})$. Then, there exists a constant C independent of h such that for any $\mathbb{P} \in \mathcal{Q}_h$ we have*

$$\|v_{\mathbb{P}}^{\downarrow}\|_{1,h,\mathbb{P}}^2 \leq C \left(|v|_{H^1(\mathbb{P})}^2 + h_{\mathbb{P}}^2 |v|_{H^2(\mathbb{P})}^2 \right).$$

Proof. We estimate separately each one of the three terms in (6.46) that form $\|v_{\mathbb{P}}^{\downarrow}\|_{1,h,\mathbb{P}}^2$. For the first term we apply a scaling argument that provides an estimate that holds for every polynomial q in $\mathbb{P}_m(\mathbf{f})$:

$$\frac{\partial q}{\partial s} \Big|_{L^2(\mathbf{f})}^2 \leq C |\mathbf{f}|^{-1} \max_{i=0,\dots,m} |q(\mathbf{x}_{\mathbf{f},i})|^2, \quad (6.78)$$

where the right-hand side is evaluated at the Gauss-Lobatto nodes $\mathbf{x}_{\mathbf{f},i}$. Let $\bar{v}_{\mathbf{f}} = \frac{1}{|\mathbf{f}|} \int_{\mathbf{f}} v ds$ be the average of v evaluated over \mathbf{f} . We identify $\bar{v}_{\mathbf{f}}$ with a constant function over \mathbf{f} , consequently, $\bar{v}_{\mathbf{f}}$ takes the same value at the Gauss-Lobatto nodes. Inequality (6.78) and a scaling argument yield:

$$\begin{aligned} \frac{\partial v_{h,\mathbf{f}}}{\partial s} \Big|_{L^2(\mathbf{f})}^2 &= \frac{\partial (v_{h,\mathbf{f}} - \bar{v}_{\mathbf{f}})}{\partial s} \Big|_{L^2(\mathbf{f})}^2 \leq C |\mathbf{f}|^{-1} \max_{i=0,\dots,m} |v(\mathbf{x}_{\mathbf{f},i}) - \bar{v}_{\mathbf{f}}|^2 \\ &\leq C |\mathbf{f}|^{-1} \|v - \bar{v}_{\mathbf{f}}\|_{L^\infty(\mathbf{f})}^2 \\ &\leq C |\mathbf{f}| \frac{\partial v}{\partial s} \Big|_{L^\infty(\mathbf{f})}^2 \\ &\leq C \frac{\partial v}{\partial s} \Big|_{L^2(\mathbf{f})}^2. \end{aligned} \quad (6.79)$$

Let T_f be the triangle in $T_{h|P}$ associated with face $f \in \partial P$. We use (6.79) and the Agmon inequality (see **(M3)** of Sect. 1.6.2) to obtain:

$$\begin{aligned} \sum_{f \in \partial P} h_P \frac{\partial v_{h,f}}{\partial s} \Big|_{L^2(f)}^2 &\leq C \sum_{f \in \partial P} h_P \frac{\partial v}{\partial s} \Big|_{L^2(f)}^2 \\ &\leq C \sum_{f \in \partial P} \left(\|\nabla v\|_{L^2(T_f)}^2 + h_P^2 \|\nabla v\|_{H^1(T_f)}^2 \right) \\ &= C \left(|v|_{H^1(P)}^2 + h_P^2 |v|_{H^2(P)}^2 \right). \end{aligned} \quad (6.80)$$

We estimate the second term in (6.46) by using the definition of $v_{P,0,0}$ and (6.47). Let us select any vertex $v' \in \partial P$. Applying a standard inequality and Jensen's inequality, we obtain

$$\begin{aligned} |v_{P,0,0}^I - \bar{v}_P|^2 &= \frac{1}{|P|} \int_P v dV - \frac{1}{N_P^{\mathcal{V}}} \sum_{v \in \partial P} v(\mathbf{x}_v) \Big|^2 \\ &= \frac{1}{|P|} \int_P (v - v(\mathbf{x}_{v'})) dV - \frac{1}{N_P^{\mathcal{V}}} \sum_{v \in \partial P} (v(\mathbf{x}_v) - v(\mathbf{x}_{v'})) \Big|^2 \\ &\leq C \frac{1}{|P|} \left(\|v - v(\mathbf{x}_{v'})\|_{L^2(P)}^2 + \frac{1}{N_P^{\mathcal{V}}} \sum_{v \in \partial P} |v(\mathbf{x}_v) - v(\mathbf{x}_{v'})|^2 \right). \end{aligned} \quad (6.81)$$

Now, the standard approximation result [78] gives us the following estimate:

$$\|v - v(\mathbf{x}_{v'})\|_{L^2(P)} \leq C \left(h_P |v|_{H^1(P)} + h_P^2 |v|_{H^2(P)} \right).$$

For every vertex v of ∂P , we apply first Jensen's inequality and then Agmon's inequality (cf. property **(M3)** in Sect. 1.6.2) to obtain:

$$\begin{aligned} |v(\mathbf{x}_v) - v(\mathbf{x}_{v'})|^2 &\leq h_P \int_{\partial P} \frac{\partial v}{\partial s} \Big|_{L^2(f)}^2 ds = h_P \sum_{f \in \partial P} \frac{\partial v}{\partial s} \Big|_{L^2(f)}^2 \\ &\leq C^{Agm} \left(|v|_{H^1(P)}^2 + h_P^2 |v|_{H^2(P)}^2 \right). \end{aligned}$$

Using the last two inequalities in (6.81) together with the normalization relation $\sum_{v \in \partial P} 1 = N_P^{\mathcal{V}}$ give us the estimate

$$|v_{P,0,0}^I - \bar{v}_P|^2 \leq C \left(|v|_{H^1(P)}^2 + h_P^2 |v|_{H^2(P)}^2 \right). \quad (6.82)$$

To estimate the third term in (6.46), we use the fact that the basis functions $\varphi_{k,i}$ for $k = 1, \dots, m-2$ and $0 \leq i \leq k$ are orthogonal to the constant fields:

$$\begin{aligned} \sum_{k=1}^{m-2} \sum_{i=0}^k |v_{\mathbb{P},k,i}^{\mathbb{I}}|^2 &= \sum_{k=1}^{m-2} \sum_{i=0}^k \left(\frac{1}{|\mathbb{P}|} \int_{\mathbb{P}} v \varphi_{k,i} dV \right)^2 \\ &= \sum_{k=1}^{m-2} \sum_{i=0}^k \left(\frac{1}{|\mathbb{P}|} \int_{\mathbb{P}} (v - v_{\mathbb{P},0,0}) \varphi_{k,i} dV \right)^2. \end{aligned} \quad (6.83)$$

Using the Cauchy-Schwarz inequality, the normalization $\|\varphi_{k,i}\|_{L^2(\mathbb{P})} = h_{\mathbb{P}}$, the fact that $C_* h_{\mathbb{P}}^2 \leq |\mathbb{P}|$ for some constant C_* independent of $h_{\mathbb{P}}$ (which is a consequence of properties (M2)–(M3), see Sect. 1.6.2), and the estimate of the interpolation error in (M5) yield:

$$\begin{aligned} \sum_{k=1}^{m-2} \sum_{i=0}^k |v_{\mathbb{P},k,i}^{\mathbb{I}}|^2 &\leq \sum_{k=1}^{m-2} \sum_{i=0}^k \left(\frac{1}{|\mathbb{P}|} \|v - v_{\mathbb{P},0,0}\|_{L^2(\mathbb{P})} \|\varphi_{k,i}\|_{L^2(\mathbb{P})} \right)^2 \\ &\leq C \sum_{k=1}^{m-2} \sum_{i=0}^k |v|_{H^1(\mathbb{P})}^2 = C \frac{(m+1)(m+2)}{2} |v|_{H^1(\mathbb{P})}^2. \end{aligned} \quad (6.84)$$

The assertion of the lemma follows from estimates (6.80), (6.82) and (6.84). \square

6.4.3 Proof of the convergence theorem

Let u^m be a piecewise polynomial over Ω_h such that its restriction, $u_{\mathbb{P}}^m$, to \mathbb{P} belongs to $\mathbb{P}_m(\mathbb{P})$. Let also $(u^m)_{\mathbb{P}}^{\mathbb{I}} \in \mathcal{V}_{h,\mathbb{P}}$ be the projection of u^m defined by (6.42)–(6.44) and restricted to \mathbb{P} . Let $e_h = u_h - u^{\mathbb{I}}$ denote the discretization error and $v_h = e_h / \|e_h\|_{1,h}$. The left inequality in the stability condition (S1) leads to the following developments:

$$\begin{aligned} \sigma_* \|e_h\|_{1,h} &\leq \mathcal{A}_h(e_h, v_h) && [\text{use } e_h = u_h - u^{\mathbb{I}}] \\ &= \mathcal{A}_h(u_h, v_h) - \mathcal{A}_h(u^{\mathbb{I}}, v_h) && [\text{use (6.14)}] \\ &= \mathcal{L}_h(v_h) - \mathcal{A}_h(u^{\mathbb{I}}, v_h) && [\text{add/subtract } (u^m)_{\mathbb{P}}^{\mathbb{I}}] \\ &= \mathcal{L}_h(v_h) + \mathbb{T}_1 - \sum_{\mathbb{P} \in \Omega_h} \mathcal{A}_{h,\mathbb{P}}((u^m)_{\mathbb{P}}^{\mathbb{I}}, v_{\mathbb{P}}) \end{aligned} \quad (6.85)$$

where

$$\mathbb{T}_1 = \sum_{\mathbb{P} \in \Omega_h} \mathcal{A}_{h,\mathbb{P}}((u^m - u)_{\mathbb{P}}^{\mathbb{I}}, v_{\mathbb{P}}). \quad (6.86)$$

Using the consistency condition (S2) (see formula (6.51)) with $\psi = u_{\mathbb{P}}^m$ and $v = R_{\mathbb{P}}(v_h)$ yields:

$$\sum_{\mathbb{P} \in \Omega_h} \mathcal{A}_{h,\mathbb{P}}(v_{\mathbb{P}}, (u^m)_{\mathbb{P}}^{\mathbb{I}}) = \sum_{\mathbb{P} \in \Omega_h} \int_{\mathbb{P}} \nabla(R_{\mathbb{P}}(v_h)) \cdot \mathcal{D}_{\mathbb{P}}^{m-1}(\mathbb{K} \nabla u_{\mathbb{P}}^m) dV. \quad (6.87)$$

Substituting (6.87) in (6.85) and adding/subtracting $\nabla(R_P(v_P)) \cdot K \nabla u$, we obtain:

$$\sigma_* \|e_h\|_{1,h} \leq \mathcal{L}_h(v_h) + T_1 - T_2 - \sum_{P \in \Omega_h} \int_P K \nabla u \cdot \nabla(R_P(v_P)) dV, \quad (6.88)$$

where

$$T_2 = \sum_{P \in \Omega_h} \int_P (\mathcal{P}_P^{m-1}(K \nabla u_P^m) - K \nabla u) \cdot \nabla R_P(v_P) dV. \quad (6.89)$$

The variational formulation (6.11) with $v|_P = R_P(v_P)$ allows us to write:

$$\sum_{P \in \Omega_h} \int_P K \nabla u \cdot \nabla R_P(v_P) dV = \sum_{P \in \Omega_h} \int_P b R_P(v_P) dV,$$

which substituted in (6.88) gives the final inequality

$$\|e_h\|_{1,h} \leq C(|T_1| + |T_2| + |T_3|), \quad (6.90)$$

where

$$T_3 = \mathcal{L}_h(v_h) - \sum_{P \in \Omega_h} \int_P b R_P(v_P) dV. \quad (6.91)$$

Estimate of term T_1 . Using the continuity of the bilinear forms $\mathcal{A}_{h,P}(\cdot, \cdot)$ with respect to the local mesh-dependent norms $\|\cdot\|_{1,h,P}$, then applying the Cauchy-Schwarz inequality, and finally using the fact that $\|v_h\|_{1,h} = 1$ leads to the following chain of inequalities:

$$\begin{aligned} |T_1| &\leq \sum_{P \in \Omega_h} (u^m - u)|_P \cdot \|v_h\|_{1,h,P} \leq \left(\sum_{P \in \Omega_h} (u^m - u)|_P^2 \right)^{1/2} \|v_h\|_{1,h} \\ &= \left(\sum_{P \in \Omega_h} (u^m - u)|_P^2 \right)^{1/2}. \end{aligned} \quad (6.92)$$

Now, we define u_P^m as the L^2 -orthogonal projection of u on $\mathbb{P}_m(P)$. Applying Lemma 6.5 to each summation argument of (6.92), and using the interpolation error estimate of (M5) (see Sect. 1.6.2) gives the following upper bound:

$$|T_1| \leq \left(\sum_{P \in \Omega_h} |u_P^m - u|_{H^1(P)}^2 + h_P^2 |u_P^m - u|_{H^2(P)}^2 \right)^{1/2} \leq \left(\sum_{P \in \Omega_h} h_P^{2m} |u_P^m - u|_{H^{m+1}(P)}^2 \right)^{1/2}. \quad (6.93)$$

Estimate of term T_2 . Assumption (L3) and the fact that $\|v_h\|_{1,h} = 1$ imply that

$$\sum_{P \in \Omega_h} \|\nabla R_P(v_h)\|_{L^2(P)}^2 \leq C \sum_{P \in \Omega_h} \|v_P\|_{1,h,P}^2 = C \|v_h\|_{1,h}^2 = C. \quad (6.94)$$

To bound T_2 , we apply the Cauchy-Schwarz inequality and estimate (6.94):

$$\begin{aligned} |T_2| &\leq C \sum_{P \in \Omega_h} \|\mathcal{P}_P^{m-1}(\mathcal{K}\nabla u_P^m) - \mathcal{K}\nabla u\|_{L^2(P)} \|\nabla R_P(v_P)\|_{L^2(P)} \\ &\leq C \left(\sum_{P \in \Omega_h} \|\mathcal{P}_P^{m-1}(\mathcal{K}\nabla u_P^m) - \mathcal{K}\nabla u\|_{L^2(P)}^2 \right)^{1/2}. \end{aligned} \quad (6.95)$$

In order to estimate the summation arguments of (6.95) we first add and subtract the quantity $\mathcal{P}_P^{m-1}(\mathcal{K}\nabla u)$, then apply a standard inequality, and finally note that

$$\|\mathcal{P}_P^{m-1}(v)\|_{L^2(P)} \leq \|v\|_{L^2(P)} \quad \forall v \in L^2(P).$$

We obtain the following development:

$$\begin{aligned} &\|\mathcal{P}_P^{m-1}(\mathcal{K}\nabla u_P^m) - \mathcal{K}\nabla u\|_{L^2(P)}^2 \\ &\leq 2 \left(\|\mathcal{P}_P^{m-1}(\mathcal{K}\nabla u_P^m) - \mathcal{P}_P^{m-1}(\mathcal{K}\nabla u)\|_{L^2(P)}^2 + \|\mathcal{P}_P^{m-1}(\mathcal{K}\nabla u) - \mathcal{K}\nabla u\|_{L^2(P)}^2 \right) \\ &\leq 2 \left(\|\mathcal{K}\nabla u_P^m - \mathcal{K}\nabla u\|_{L^2(P)}^2 + \|\mathcal{P}_P^{m-1}(\mathcal{K}\nabla u) - \mathcal{K}\nabla u\|_{L^2(P)}^2 \right). \end{aligned} \quad (6.96)$$

Finally, we substitute (6.96) into (6.95), and apply the interpolation error estimate from **(M5)** (see Sect. 1.6.2) to obtain:

$$\begin{aligned} |T_2| &\leq C \left(\sum_{P \in \Omega_h} \|\mathcal{K}\|_{L^\infty(P)}^2 h_P^{2m} |u|_{H^{m+1}(P)} + h_P^{2m} |\mathcal{K}\nabla u|_{H^m(P)} \right)^{1/2} \\ &\leq C \left(\sum_{P \in \Omega_h} h_P^{2m} \|\mathcal{K}\|_{W^{m,\infty}(P)}^2 \|\nabla u\|_{H^m(P)}^2 \right)^{1/2}. \end{aligned} \quad (6.97)$$

Estimate of term T_3 . Assumption **(L1)** implies that $v_P = (R_P(v_P))^I$ for any discrete field v_P . In particular, we have

$$v_{P,k,i} = \frac{1}{|P|} \int_P R_P(\mathbf{v}_h) \varphi_{k,i} dV \quad k = 0, \dots, m-2 \text{ and } i = 0, 1, \dots, k.$$

Consequently,

$$\begin{aligned} \mathcal{L}_P(v_P) &= |P| \sum_{k=0}^{m-2} \sum_{i=0}^k c_{k,i} \left(\frac{1}{|P|} \int_P R_P(v_P) \varphi_{k,i} dV \right) \quad [\text{rearrange the terms}] \\ &= \int_P R_P(v_P) \sum_{k=0}^{m-2} \sum_{i=0}^k c_{k,i} \varphi_{k,i} dV \quad [\text{use (6.54)}] \\ &= \int_P R_P(v_P) \hat{b}_P dV. \end{aligned}$$

Inserting this into definition (6.91) yields:

$$T_3 = \sum_{P \in \Omega_h} \int_P (b - \hat{b}_P) R_P(v_P) dV. \quad (6.98)$$

The definition of \hat{b}_P in (6.54) implies that $\int_P b dV = \int_P \hat{b}_P dV$. Thus, the integrand function $(b - \hat{b}_P)$ is $L^2(P)$ -orthogonal to every constant function. Let $\overline{R_P(v_P)}$ denote the average of the reconstructed function $R_P(v_P)$ over P . Then,

$$|\mathbb{T}_3| \leq \sum_{P \in \Omega_h} \int_P (b - \hat{b}_P)(R_P(v_P) - \overline{R_P(v_P)}) dV .$$

Using the Cauchy-Schwarz inequality, the error estimate for $\|b - \hat{b}_P\|_{L^2(P)}$, assumption **(L3)**, and the fact that $\|v_h\|_{1,h} = 1$, give us the following development:

$$\begin{aligned} \mathbb{T}_3 &\leq \sum_{P \in \Omega_h} \|b - \hat{b}_P\|_{L^2(P)} \|R_P(v_P) - \overline{R_P(v_P)}\|_{L^2(P)} \\ &\leq C \sum_{P \in \Omega_h} h_P^m |b|_{H^{m-1}(P)} \|\nabla R_P(v_P)\|_{L^2(P)} \\ &\leq C \left(\sum_{P \in \Omega_h} h_P^{2m} |b|_{H^{m-1}(P)}^2 \right)^{1/2} \|v_h\|_{1,h} \\ &\leq C \left(\sum_{P \in \Omega_h} h_P^{2m} |u|_{H^{m+1}(P)}^2 \right)^{1/2} . \end{aligned} \quad (6.99)$$

The estimate (6.60) stated in Theorem 6.2 is deduced by combining inequalities (6.93), (6.97) and (6.99) in (6.90). \square

6.4.4 L^2 -estimate of the approximation error

In this subsection we discuss how to estimate the discretization error in the arbitrary-order mimetic method in the L^2 norm. The convergence analysis of this section is based on the existence of an exact reconstruction operator

$$R_P : \mathcal{V}_{h,P} \rightarrow S_{h,P}$$

that satisfies the three conditions **(L1)**–**(L3)** of Sect. 6.4.1 plus the two additional conditions.

(L4) The reconstruction operator reproduces the mimetic bilinear form:

$$\int_P \nabla R_P(v_P) \cdot \nabla R_P(u_P) dV = \mathcal{A}_{h,P}(u_P, v_P) \quad \forall u_P, v_P \in \mathcal{V}_{h,P} .$$

(L5) The reconstruction operator provides a proper approximation of scalar functions on every polygon P :

$$\|v - R_P(v_P^I)\|_{L^2(P)} + h_P |v - R_P(v_P^I)|_{H^1(P)} \leq C h_P^\sigma |v|_{H^\sigma(P)} \quad \forall v \in H^\sigma(P) ,$$

where C is a uniformly bounded constant and $2 \leq \sigma \leq m + 1$, $\sigma \in \mathbb{N}$.

The qualifier "exact" in front of the reconstruction operator indicates that for a given mimetic scheme, there exists a reconstruction operator that produces the same stiffness matrix. We refer to Sect. 5.3 where the existence of the exact reconstruction operator is analyzed for the diffusion problem in the mixed form. Existence of such

an operator has been shown for a subfamily of mimetic schemes. We expect that a similar conclusion holds for the mimetic discretization of the diffusion problem in the primary form; however, a formal proof has not been yet published.

Theorem 6.3. *Let Ω be a convex domain and the loading $b \in H^{m-1}(\Omega)$. Let $u \in H^{m+1}(\Omega)$ be the solution of the variational problem (6.11) under assumptions **(H1)**–**(H2)**, and u_h be the solution of the mimetic problem (6.14) under assumptions **(MR1)**–**(MR3)**, **(S1)**–**(S2)**, and **(L1)**–**(L5)**. Then, there exists a positive constant C independent of h such that:*

$$\|u - R(u_h)\|_{L^2(\Omega)} \leq Ch^{m+v_m} |u|_{H^{m+1}(\Omega)},$$

where the integer $v_m = 0$ for $m = 2$ and $v_m = 1$ for $m \geq 3$.

The proof can be found in [51]. Note that the error estimate in the L^2 norm is suboptimal in the case $m = 2$, a phenomenon confirmed by numerical tests. The reason for that is the approximation of the source term b . Indeed, as shown in [44], a more accurate approximation of this term allows one to prove the optimal $O(h^3)$ convergence rate in the L^2 norm.

6.5 A posteriori estimates

In this section, we present an a posteriori error estimator for the low-order mimetic scheme in the space dimension $d = 2$ described in Sect. 6.2. This error estimator, together with the associated reliability and efficiency theory, was introduced in [16]; we refer to this work for the proofs of the results shown below. In contrast to the error estimator from Sect. 5.4, the estimator in this section is of a non-residual type. More precisely, it falls in to the class of hierarchical error estimators, see e.g. [9, 37] and the references therein for the finite element methods. In the following, we state also some preliminary key results concerning the mesh refinement.

6.5.1 Mesh refinement and related results

Let as usual Ω_h represent a polygonal mesh. We start by showing how to build a uniformly refined mesh $\hat{\Omega}_h$, that will be used to compute the error indicator. We make an additional mesh regularity assumption that holds only for the end of this chapter.

(MR4) All polygons $P \in \Omega_h$ are convex.

Let us define point $\bar{\mathbf{x}}_P \in P$ as follows:

$$\bar{\mathbf{x}}_P := \frac{1}{N_P'} \sum_{\mathbf{v} \in \partial P} \mathbf{x}_v. \quad (6.100)$$

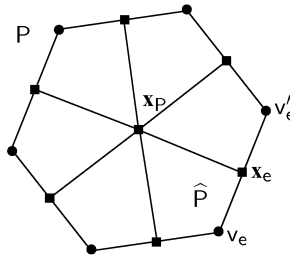


Fig. 6.11. The refinement strategy: coarse element P and the related fine element \widehat{P} . Circles denote vertices in the coarse, while diamonds refer to new vertices in the finer mesh

Note that assumption **(MR4)** is made essentially for the sake of exposition simplicity. The subsequent derivations can be modified in order to cover the case of more general meshes, for instance, meshes with polygons that are star-shaped with respect to a ball. The definition of point \bar{x}_P has to be modified and (6.103) below has to be changed in such a way that the operator preserves linear functions.

We build the uniformly refined mesh $\widehat{\Omega}_h$ by subdividing each element P of Ω_h into quadrilaterals. The midpoint \mathbf{x}_e of each edge $e \in \partial P$ is connected with the point \bar{x}_P , as shown in Fig. 6.11. The quadrilaterals for all $P \in \Omega_h$ form the new mesh $\widehat{\Omega}_h$. In the sequel, we will use the symbol "hat" for objects associated with mesh $\widehat{\Omega}_h$ to distinguish them from similar objects associated with the original mesh. For example, \widehat{P} will stand for a generic element of $\widehat{\Omega}_h$, $\widehat{\mathcal{V}}$ will denote the set of all mesh vertices, and \widehat{h} will indicate the maximum element size. Note that the edge midpoints \mathbf{x}_e and the internal points \bar{x}_P become additional vertices in the new mesh $\widehat{\Omega}_h$, i.e.

$$\widehat{\mathcal{V}} = \mathcal{V} \cup \{\mathbf{x}_e\}_{e \in \mathcal{E}} \cup \{\bar{x}_P\}_{P \in \Omega_h}.$$

Let us employ the construction described in Sect. 6.2 on mesh $\widehat{\Omega}_h$. We introduce a discrete space $\widehat{\mathcal{V}}_h$ associated with $\widehat{\Omega}_h$, a bilinear form $\widehat{\mathcal{A}}_h : \widehat{\mathcal{V}}_h \times \widehat{\mathcal{V}}_h \rightarrow \mathbb{R}$ and a suitable discrete loading term. The fine-grid discrete mimetic problem (compare with (6.14)) reads:

Find $\widehat{u}_h \in \widehat{\mathcal{V}}_{h,g}$ such that

$$\widehat{\mathcal{A}}_h(\widehat{u}_h, v_h) = \widehat{\mathcal{L}}_h(v_h) \quad \forall v_h \in \widehat{\mathcal{V}}_{h,0}. \tag{6.101}$$

Let us introduce two operators mapping the fine-grid space onto the coarser one and viceversa. Let $\Pi : \widehat{\mathcal{V}}_h \rightarrow \mathcal{V}_h$ be defined by

$$(\Pi(v_h))_v = v_v \quad \forall v \in \mathcal{V}, \forall v_h \in \widehat{\mathcal{V}}_h. \tag{6.102}$$

Given edge $e \in \mathcal{E}$ and its midpoint \mathbf{x}_e , we denote by v_e and v'_e the mesh vertices which

are the endpoints of \mathbf{e} , see Fig. 6.11. We then define $\Pi^\dagger : \mathcal{V}_h \rightarrow \widehat{\mathcal{V}}_h$ by

$$(\Pi^\dagger(v_h))_{\mathbf{v}} = \begin{cases} v_{\mathbf{v}} & \forall \mathbf{v} \in \mathcal{V}, \\ \frac{1}{2}(v_h(\mathbf{v}_e) + v_h(\mathbf{v}'_e)) & \text{if } \mathbf{x}_{\mathbf{v}} = \mathbf{x}_e, \mathbf{e} \in \mathcal{E}, \\ \frac{1}{k_P} \sum_{\mathbf{v} \in \partial P} v_{\mathbf{v}} & \text{if } \mathbf{x}_{\mathbf{v}} = \bar{\mathbf{x}}_P, P \in \Omega_h. \end{cases} \quad (6.103)$$

Thus, the operator Π^\dagger interpolates a coarse-space discrete field v_h by the linearity preserving averaging of its vertex values. Let $\widehat{\mathcal{V}}_h^c$ denote the subspace of $\widehat{\mathcal{V}}_h$ given by the image of operator Π^\dagger ; we will refer to it as to the interpolated coarse-grid space. As a complement to $\widehat{\mathcal{V}}_h^c$, we consider the fluctuation space

$$\widehat{\mathcal{V}}_h^f = \{v_h \in \widehat{\mathcal{V}}_h : v_{\mathbf{v}} = 0 \quad \forall \mathbf{v} \in \mathcal{V}\}.$$

It clearly holds that

$$\widehat{\mathcal{V}}_h = \widehat{\mathcal{V}}_h^c \oplus \widehat{\mathcal{V}}_h^f. \quad (6.104)$$

The global and local mesh-dependent norms on space $\widehat{\mathcal{V}}_h$ are denoted by $\|\cdot\|_{1,\widehat{h}}$ and $\|\cdot\|_{1,\widehat{h},\widehat{P}}$, respectively (see also (6.15)). In addition, we introduce an intermediate norm $\|\cdot\|_{1,\widehat{h},P}$ which is the restriction of the global norm to a coarse element $P \in \Omega_h$,

$$\|v_P\|_{1,\widehat{h},P}^2 := \sum_{\widehat{P} \in \widehat{\Omega}_h : \widehat{P} \subset P} \|v_{\widehat{P}}\|_{1,\widehat{h},\widehat{P}}^2 \quad \forall v_P \in \widehat{\mathcal{V}}_{h,P}.$$

We have the following lemma, stating the minimum angle condition between the spaces $\widehat{\mathcal{V}}_{h,P}^c$ and $\widehat{\mathcal{V}}_{h,P}^f$ that are the restrictions of the related global spaces in (6.104) to element P .

Lemma 6.6. *There exists a positive constant C_m independent of h such that*

$$\|v_P^c\|_{1,\widehat{h},P} + \|v_P^f\|_{1,\widehat{h},P} \leq C_m (\|v_P^c\| + \|v_P^f\|)_{1,\widehat{h},P} \quad (6.105)$$

for all $P \in \Omega_h$ and all $v_P^c \in \widehat{\mathcal{V}}_{h,P}^c$ and $v_P^f \in \widehat{\mathcal{V}}_{h,P}^f$.

Let Π_P^\dagger denote restriction of the operator Π^\dagger to element P . The following simple lemma holds [16].

Lemma 6.7. *There exist positive constants C and C' independent of mesh such that for all $P \in \Omega_h$ we have*

$$C \|v_P\|_{1,h,P} \leq \Pi_P^\dagger(v_P)_{1,\widehat{h},P} \leq C' \|v_P\|_{1,h,P} \quad \forall v_P \in \mathcal{V}_{h,P}. \quad (6.106)$$

6.5.2 A consistent coarse-grid problem

In this section we introduce a particular coarse-grid bilinear form \mathcal{A}_h consistent with the fine-grid bilinear form $\widehat{\mathcal{A}}_h$. This will allow us to simplify the a posteriori error analysis, see Corollary 6.1. Although such choice is convenient, it is not mandatory and the generality of the analysis is not affected by it.

As usual, the bilinear form $\widehat{\mathcal{A}}_h$ is defined as the sum of local forms $\widehat{\mathcal{A}}_{h,\widehat{P}}$, for $\widehat{P} \in \widehat{\Omega}_h$, that satisfy the consistency and stability conditions of Sect. 6.2.2 or, more precisely, their counterparts for the new discrete space and refined mesh. The local forms can be assembled over coarse-grid elements $P \in \Omega_h$ into bilinear forms $\widehat{\mathcal{A}}_{h,P}$. For all $P \in \Omega_h$, we then define a coarse-grid bilinear form $\mathcal{A}_{h,P}$ as follows:

$$\mathcal{A}_{h,P}(v_h, w_h) = \widehat{\mathcal{A}}_{h,P}(\Pi_P^\dagger(v_P), \Pi_P^\dagger(w_P)) \quad \forall v_P, w_P \in \mathcal{V}_{h,P}. \quad (6.107)$$

Note that the bilinear form (6.107) satisfies both the consistency and stability conditions; the proof can be found in [16]. Using the same argument, we define the following coarse-grid loading term:

$$\mathcal{L}_h(v_h) = \sum_{P \in \Omega_h} \widehat{\mathcal{L}}_{h,P}(\Pi_P^\dagger(v_P)),$$

with $\widehat{\mathcal{L}}_{h,P}(\Pi_P^\dagger(\cdot))$ being the local linear functional built using a construction analogous to Sect. 6.2.3.

We can now define a coarse-grid mimetic problem (6.14) by assembling the global bilinear form \mathcal{A}_h from the local forms (6.107) and taking the load term defined above. The advantage of such a coarse-grid problem is to be fully consistent with the fine-grid problem, in a sense that will be clarified in the next section.

6.5.3 A posteriori error analysis

Let us consider the following *fluctuation* discrete mimetic problem:

Find $\widehat{e}_h^f \in \widehat{\mathcal{V}}_h^f$ such that

$$\widehat{\mathcal{A}}_h(\widehat{e}_h^f, v_h^f) = \widehat{\mathcal{L}}_h(v_h^f) - \widehat{\mathcal{A}}_h(\Pi^\dagger(u_h), v_h^f) \quad \forall v_h^f \in \widehat{\mathcal{V}}_h^f. \quad (6.108)$$

We observe that the right-hand side in (6.108) represents the residual of the approximate solution u_h when tested with the fluctuation space $\widehat{\mathcal{V}}_h^f$.

We assume that the exact solution u is sufficiently regular, e.g. it belongs at least to $H^{3/2}(\Omega)$. In such a case, the vertex-based projection $\widehat{u}^\dagger \in \widehat{\mathcal{V}}_h$ is well defined. In the following, we assume that the following *saturation assumption* holds true.

(SAT) There exists $\beta < 1$ such that

$$\|\widehat{u}^\dagger - \widehat{u}_h\|_{1,\widehat{h}} \leq \beta \|\widehat{u}^\dagger - \Pi^\dagger(u_h)\|_{1,\widehat{h}}. \quad (6.109)$$

Assumption (SAT) means that the fine-grid solution \widehat{u}_h converges (uniformly) more rapidly to \widehat{u}^\dagger than the coarser solution u_h . Although such an assumption is not negli-

gible, it is widely accepted in the a posteriori error analysis of finite element methods [9, 38, 71].

Theorem 6.4 (Upper bound). *Let assumptions (MR1)–(MR4) and (SAT) hold. Furthermore, let u solve the continuum problem (6.1)–(6.3), u_h solve the discrete problem (6.14), and \widehat{e}_h^f solve (6.108). Finally, let $c^* = (C_m(1 - \beta)\widehat{c}_1)^{-1}$ with C_m from (6.105). Then,*

$$\|\widehat{u}^\dagger - \Pi^\dagger(u_h)\|_{1,\widehat{h}} \leq c^* \left(\widehat{c}_2 \|\widehat{e}_h^f\|_{1,\widehat{h}} + \sup_{v_h \in \mathcal{V}_h} \frac{\widehat{\mathcal{L}}_h(\Pi^\dagger(v_h)) - \widehat{\mathcal{A}}_h(\Pi^\dagger(u_h), \Pi^\dagger(v_h))}{|\Pi^\dagger(v_h)|_{1,\widehat{h}}} \right). \quad (6.110)$$

The above result holds for any bilinear forms \mathcal{A}_h and $\widehat{\mathcal{A}}_h$. If we choose the consistent bilinear \mathcal{A}_h introduced in (6.107), we obtain the following simpler result.

Corollary 6.1 (Upper bound). *In addition to the assumption of Theorem 6.4, let the coarse-grid bilinear form \mathcal{A}_h be given by (6.107). Then,*

$$\|\widehat{u}^\dagger - \Pi^\dagger(u_h)\|_{1,\widehat{h}} \leq c^* \widehat{c}_2 \|\widehat{e}_h^f\|_{1,\widehat{h}}. \quad (6.111)$$

Observe that

$$\Pi(\widehat{u}^\dagger - \Pi^\dagger(u_h)) = u^\dagger - u_h.$$

Using the triangle inequality applied edge-by-edge, we can show easily that

$$\Pi_{\mathbb{P}}(v_{\mathbb{P}}) \Big|_{1,h,\mathbb{P}} \leq C \ v_{\mathbb{P}} \Big|_{1,\widehat{h},\mathbb{P}} \quad \forall v_{\mathbb{P}} \in \widehat{\mathcal{V}}_{h,\mathbb{P}}.$$

The above two observations, allow us replace the left-hand sides of the upper bounds (6.110) and (6.111) by a slightly more natural error $\|u^\dagger - u_h\|_{1,h}$.

Theorem 6.5 (Lower bound). *Let assumptions (MR1)–(MR4) and (SAT) hold true. Furthermore, let u solve (6.1)–(6.3), u_h solve (6.14), and \widehat{e}_h^f solve (6.108). If $c_* = \widehat{c}_2(1 + \beta)(\widehat{c}'_1)^{-1}$, then*

$$\|\widehat{e}_h^f\|_{1,\widehat{h}} \leq c_* \|\widehat{u}^\dagger - \Pi^\dagger(u_h)\|_{1,\widehat{h}}. \quad (6.112)$$

The upper bound (6.111) can be rewritten as follows:

$$\|\widehat{u}^\dagger - \Pi^\dagger(u_h)\|_{1,\widehat{h}}^2 \leq (c^* \widehat{c}_2)^2 \sum_{\mathbb{P} \in \Omega_h} \eta_{\mathbb{P}}^2 \quad (6.113)$$

with the local terms

$$\eta_{\mathbb{P}}^2 = \sum_{\widehat{\mathbb{P}} \in \widehat{\Omega}_h: \widehat{\mathbb{P}} \subset \mathbb{P}} \|e_h^f\|_{1,\widehat{h},\widehat{\mathbb{P}}}^2. \quad (6.114)$$

Therefore, we can use quantities $\eta_{\mathbb{P}}$ as the local a posteriori error indicators in a mesh refinement strategy of an adaptive algorithm.

6.5.4 An inexpensive error indicator

The computation of the error indicator η_P in (6.114) requires to solve the fluctuation problem (6.108). Since the cost of solving such a problem is comparable to that of solving the original one, the computation of η_P turns out to be quite demanding. Here, we present an inexpensive estimate of η_P .

We make a preliminary observation. Let (6.108) be replaced by a more general fluctuation problem of the form

$$\widehat{\mathcal{B}}_h(\widehat{\mathcal{E}}_h^f, v_h^f) = \widehat{\mathcal{L}}_h(v_h^f) - \widehat{\mathcal{A}}_h(\Pi^\dagger(u_h), v_h^f) \quad \forall v_h^f \in \widehat{\mathcal{V}}_h^f, \quad (6.115)$$

with a suitable bilinear form $\widehat{\mathcal{B}}_h$ satisfying the stability assumption **(S1)**. Then, the upper bound (6.110) and the lower bound (6.112) still hold, but possibly with different constants. We define this bilinear form as follows:

$$\widehat{\mathcal{B}}_h(v_h, w_h) = \sum_{\widehat{v} \in \widehat{\mathcal{V}} \setminus \mathcal{V}} v_{\widehat{v}} w_{\widehat{v}}. \quad (6.116)$$

This form is continuous and coercive on the space $\widehat{\mathcal{V}}_h^f$, with respect to the discrete energy norm, as stated in the lemma below.

Lemma 6.8. *The bilinear form $\widehat{\mathcal{B}}_h$ defined in (6.116) satisfies **(S1)**, i.e.*

$$\widehat{\mathcal{B}}_h(v_h, v_h) \simeq \|v_h\|_{1, \widehat{h}}^2 \quad \forall v_h \in \widehat{\mathcal{V}}_h^f. \quad (6.117)$$

We are now ready to introduce an new inexpensive error indicator η_P^D :

$$(\eta_P^D)^2 = \sum_{\widehat{P} \subset P} \|\widehat{\mathcal{E}}_h^f\|_{1, \widehat{h}, \widehat{P}}^2, \quad (6.118)$$

with $\widehat{\mathcal{E}}_h^f$ being the solution to the generalized fluctuation problem (6.115) with the bilinear form $\widehat{\mathcal{B}}_h$ instead of $\widehat{\mathcal{A}}_h$. Due to definition (6.116), the matrix of the induced algebraic problem is the identity matrix. Hence, the cost of computing η_P^D is negligible.

The numerical results presented in [16] for both estimators, η_P and η_P^D , indicate a satisfactory behavior of η_P^D . Therefore, the estimator η_P^D may be preferable to η_P in many problems of practical interest.

Example 6.1. We close this chapter by presenting a single adaptive test. We consider the same L-shaped domain problem studied in Example 5.2. We remind that the solution u is in $H^{5/3}$ and not better; therefore, uniform adaptive strategies are expected to yield a sub-optimal convergence rate (in terms of degrees of freedom) when compared to more regular problems. We solve the problem applying a fixed fraction refinement strategy (with fraction set at 30%, see [16] for the details) driven by the inexpensive error estimator η_P^D . The initial grid is a regular mesh composed mainly of hexagons. In Fig. 6.12, we plot the total error estimator η^D and the true error $\|\widehat{u}^\dagger - \Pi^\dagger u_h\|_{1, \widehat{h}}$, both with respect to the total number of degrees of freedom N .

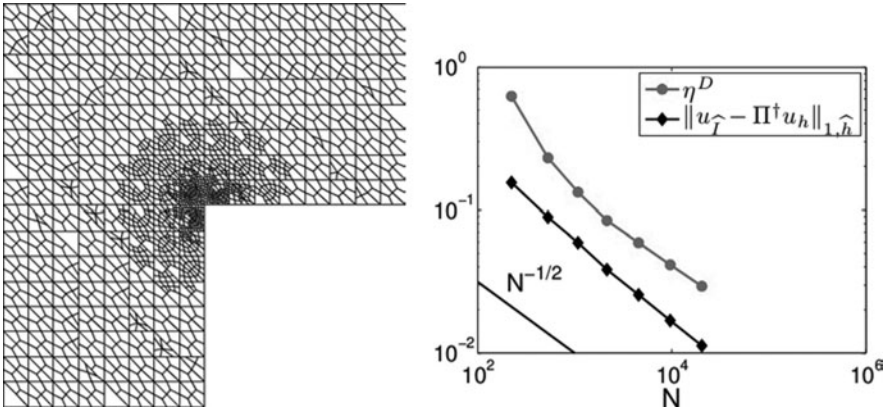


Fig. 6.12. Estimator η^D . Left picture shows a sample mesh after 3 refinement steps. Right picture shows the actual and estimated errors versus the number of degrees of freedom

From this figure, we conclude that the adaptive method is able to recover the $N^{-1/2}$ rate of convergence typical of regular problems.

Maxwell's equations

*“Maxwell's equations have had a greater impact
on human history than any ten presidents”*
(Carl Sagan)

Maxwell's equations together with the Lorentz force law form the foundation of classical electrodynamics, optics, and electric circuits. Maxwell's equations are named after the Scottish physicist and mathematician James Clerk Maxwell. In this chapter, we consider three problems derived from original Maxwell's equations. Numerical treatment of these problems will exercise most tools of the discrete vector and tensor calculus from Chap. 2.

7.1 Maxwell's equations

Let \mathbf{H} be the magnetic field and \mathbf{E} the electric field. The constitutive relations give the magnetic flux density $\mathbf{B} = \mu\mathbf{H}$, where μ is the magnetic permeability, and the dielectric displacement $\mathbf{D} = \varepsilon\mathbf{E}$, where ε is the electric permittivity. The magnetic permeability μ and the electric permittivity ε can be full tensors discontinuous at material interfaces. The basic laws of electromagnetics in differential forms are summarized by these four equations:

$$\text{Coulomb's law:} \quad \operatorname{div} \mathbf{D} = \rho, \quad (7.1)$$

$$\text{Faraday's law:} \quad \operatorname{curl} \mathbf{E} = -\frac{\partial \mathbf{B}}{\partial t}, \quad (7.2)$$

$$\text{Amperes's law:} \quad \operatorname{curl} \mathbf{H} = \mathbf{J} + \frac{\partial \mathbf{D}}{\partial t}, \quad (7.3)$$

$$\text{Gauss's law:} \quad \operatorname{div} \mathbf{B} = 0, \quad (7.4)$$

where \mathbf{J} is the current density and ρ is the charge density.

Let Ω be a bounded domain. The first problem that we consider in this chapter is that of the *Maxwell's equations for a perfect conductor*. We consider the four equations (7.1)–(7.4) with $\mathbf{J} = 0$ and $\rho = 0$ and the homogeneous boundary condition $\mathbf{n} \times \mathbf{E} = 0$ on $\partial\Omega$.

The second problem is the *magnetic diffusion*. Let us take the divergence of (7.3) and use the Coulomb's law. A straightforward calculation yields the charge continu-

ity equation $\operatorname{div} \mathbf{J} + \partial \rho / \partial t = 0$. Following a general magnetohydrodynamics (MHD) assumption, we assume that the materials of interest are sufficiently conducting so that the assumption of quasi-neutrality (negligible charge density, i.e., $\partial \rho / \partial t \approx 0$) is reasonable. With this assumption, the charge continuity Eq. (7.1) reduces to $\operatorname{div} \mathbf{J} = 0$. Additionally, the displacement current term $\partial \mathbf{D} / \partial t$ in Ampere's law is neglected so that we can use the classical Ampere's law to relate the magnetic field to the current density. Finally, the MHD form of Ohm's law relates the electric field to the current vector and is derived from a simplified form of the electron momentum equation, $\mathbf{E} = \sigma^{-1} \mathbf{J}$. The resulting governing equations are

$$\operatorname{curl} \mathbf{E} = -\frac{\partial \mathbf{B}}{\partial t} \quad \text{and} \quad \sigma^{-1} \operatorname{curl} \mathbf{H} = \mathbf{E} \quad \text{in } \Omega, \quad (7.5)$$

where the conductivity σ can be a symmetric positive definite discontinuous tensor, and the divergence-free conditions (7.1) (for $\rho = 0$) and (7.4). We consider again the homogeneous boundary condition $\mathbf{n} \times \mathbf{E} = 0$ on $\partial \Omega$.

The third problem is the *magnetostatic problem in div-curl form*. We assume that the charges are either fixed or move as a steady current. Thus, the governing equations are

$$\operatorname{div} \mathbf{B} = 0, \quad \operatorname{curl} \mathbf{H} = \mathbf{J} \quad \text{in } \Omega.$$

The boundary condition is obtained by approximating the radiation condition that \mathbf{H} vanishes at infinity by taking the non-homogeneous condition $\mathbf{n} \times \mathbf{H} = \mathbf{g}$ on $\partial \Omega$. More details on the magnetostatic problem in div-curl form can be found in Sect. 1.5.4.

We will discuss a mimetic discretization of the first two problems in Sect. 7.2 and a mimetic discretization of the third problem in Sect. 7.3. This presentation is mainly focused on the three dimensional case.

7.2 Mimetic discretizations

7.2.1 Degrees of freedom and projection operators

In electromagnetism, the tangential component of \mathbf{E} and the normal component of \mathbf{B} are continuous across media discontinuities [218, 241, 335]. Thus, these components are the natural choice for the discretization of these fields. We recall briefly the definition of the degrees of freedom, see also Chap. 2 and Fig. 7.1.

- The space of edge-based vector fields \mathcal{E}_h is defined by attaching one degree of freedom to every mesh edge $e \in \mathcal{E}$. The value associated with edge e is denoted by E_e . The collection of all the degrees of freedom forms the algebraic vector $\mathbf{E}_h \in \mathcal{E}_h$,

$$\mathbf{E}_h = (E_e)_{e \in \mathcal{E}}.$$

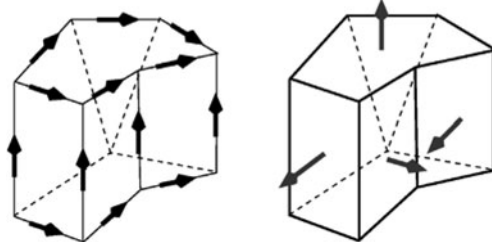


Fig. 7.1. Geometric location of degrees of freedom in the low-order MFD scheme: arrows on edges represent E_e (on thirteen visible edges), arrows on faces represent B_f (on four visible faces)

- The space of face-based vector fields \mathcal{F}_h is defined by attaching one degree of freedom to every mesh face $f \in \mathcal{F}$. The value associated with face f is denoted by B_f . The collection of all the degrees of freedom forms the algebraic vector $\mathbf{B}_h \in \mathcal{F}_h$,

$$\mathbf{B}_h = (B_f)_{f \in \mathcal{F}}.$$

The restriction of \mathbf{E}_h to cell P is denoted by $\mathbf{E}_P = (E_e)_{e \in \partial P}$ and represents a collection of degrees of freedom on the edges of P . The set of these discrete fields forms the linear space $\mathcal{E}_{h,P}$. The restriction of \mathbf{B}_h to cell P is defined similarly, $\mathbf{B}_P = (B_f)_{f \in \partial P}$, and \mathbf{B}_P belongs to the linear space $\mathcal{F}_{h,P}$.

The edge-based projection operator from a sufficiently smooth space to \mathcal{E}_h is defined by (2.15). In the sequel, it will be convenient to use a shorter symbol for this projection operator, $\mathbf{E}^I = \Pi^{\mathcal{E}}(\mathbf{E})$. According to the definition of the projection operator, we have

$$\mathbf{E}^I = (E_e^I)_{e \in \mathcal{E}}, \quad E_e^I = \frac{1}{|e|} \int_e \mathbf{E} \cdot \boldsymbol{\tau}_e dL, \quad (7.6)$$

where $\boldsymbol{\tau}_e$ is a unit vector describing the fixed orientation of mesh edge e .

The face-based projection operator $\Pi^{\mathcal{F}} : X(\Omega) \rightarrow \mathcal{F}_h$ is defined by (2.16) and is stable for vector functions in $(L^s(\Omega))^d$ with $s > 2$ and divergence in $L^2(\Omega)$. Again, it will be convenient to use a shorter symbol for the projection operator, $\mathbf{B}^I = \Pi^{\mathcal{F}}(\mathbf{B})$:

$$\mathbf{B}^I = (B_f^I)_{f \in \mathcal{F}}, \quad B_f^I = \frac{1}{|f|} \int_f \mathbf{B} \cdot \mathbf{n}_f dS, \quad (7.7)$$

where \mathbf{n}_f is the unit vector normal to mesh face f . Its orientation is fixed once and for all.

The edge-based mesh functions are natural for discretizing the primary mimetic curl operator $\text{curl}_h : \mathcal{E}_h \rightarrow \mathcal{F}_h$ (see Chap. 2, Sect. 2.3.2):

$$(\text{curl}_h \mathbf{E}_h)_f = \frac{1}{|f|} \sum_{e \in \mathcal{E}_f} \alpha_{f,e} |e| E_e, \quad (7.8)$$

where $\alpha_{f,e} = \pm 1$ is determined by the mutual orientation of the tangent vector $\boldsymbol{\tau}_e$ and

the normal vector $\mathbf{n}_{P,f}$. The discrete curl operator restricted to cell P is denoted by $\text{curl}_P \mathbf{E}_P \in \mathcal{F}_{h,P}$ and uses only the degrees of freedom in \mathbf{E}_P .

The face-based mesh functions are natural for discretizing the primary mimetic divergence operator $\text{div}_h: \mathcal{F}_h \rightarrow \mathcal{P}_h$ (see Chap. 2, Sect. 2.3.3):

$$(\text{div}_h \mathbf{B}_h)_P = \frac{1}{|P|} \sum_{f \in \mathcal{F}_P} \alpha_{P,f} |f| B_f, \quad (7.9)$$

where $\alpha_{P,f} = \mathbf{n}_f \cdot \mathbf{n}_{P,f} = \pm 1$ is determined by the mutual orientation of the fixed normal vector \mathbf{n}_f and the exterior normal vector $\mathbf{n}_{P,f}$ to face f .

7.2.2 Strong form of discrete equations

Let us consider the first problem given by (7.1)–(7.4) with $\mathbf{J} = 0$ and $\rho = 0$. Inserting the constitutive relations of fields \mathbf{D} and \mathbf{H} , we reformulate equations (7.2)–(7.3) as follows:

$$\text{curl} \mathbf{E} = -\frac{\partial \mathbf{B}}{\partial t} \quad \text{and} \quad \varepsilon^{-1} \text{curl}(\mu^{-1} \mathbf{B}) = \frac{\partial \mathbf{E}}{\partial t} \quad \text{in } \Omega. \quad (7.10)$$

The primary mimetic operator curl_h can be used to discretize the curl operator in the first equation, while a derived mimetic operator, denoted by $\widetilde{\text{curl}}_h$, must approximate the differential operator $\varepsilon^{-1} \text{curl} \mu^{-1}$, which includes the material properties. To derive $\widetilde{\text{curl}}_h$ according to the framework of Chap. 2, we need a discrete analog of a Green formula that yields a duality relation between curl and $\varepsilon^{-1} \text{curl} \mu^{-1}$. Let us start by establishing the relationship between the differential operators. Due to the homogeneous boundary conditions, the integration by parts formula reads:

$$\int_{\Omega} \text{curl} \mathbf{E} \cdot \mu^{-1} \mathbf{B} dV = \int_{\Omega} (\varepsilon \mathbf{E}) \cdot \varepsilon^{-1} \text{curl}(\mu^{-1} \mathbf{B}) dV. \quad (7.11)$$

Thus, the operator $\varepsilon^{-1} \text{curl} \mu^{-1}$ is dual to the operator curl with respect to the weighted inner products in (7.11) that use the tensorial coefficients μ^{-1} and ε as weights. To build a discrete analog of (7.11), we introduce two modified inner products for spaces \mathcal{E}_h and \mathcal{F}_h that approximate the weighted inner products:

$$[\mathbf{E}_h, \widetilde{\mathbf{E}}_h]_{\mathcal{E}_h} \approx \int_{\Omega} \mathbf{E} \cdot \varepsilon \widetilde{\mathbf{E}} dV \quad \text{and} \quad [\mathbf{B}_h, \widetilde{\mathbf{B}}_h]_{\mathcal{F}_h} \approx \int_{\Omega} \mathbf{B} \cdot \mu^{-1} \widetilde{\mathbf{B}} dV, \quad (7.12)$$

where $\mathbf{E}_h = (\mathbf{E})^I$, $\widetilde{\mathbf{E}}_h = (\widetilde{\mathbf{E}})^I$, $\mathbf{B}_h = (\mathbf{B})^I$, and $\widetilde{\mathbf{B}}_h = (\widetilde{\mathbf{B}})^I$. In the mimetic method, the duality relation between the primary operator curl_h and the derived operator $\widetilde{\text{curl}}_h$ is formulated with respect to these inner products:

$$[\text{curl}_h \mathbf{E}_h, \mathbf{B}_h]_{\mathcal{F}_h} = [\mathbf{E}_h, \widetilde{\text{curl}}_h \mathbf{B}_h]_{\mathcal{E}_h} \quad \forall \mathbf{B}_h \in \mathcal{F}_h, \mathbf{E}_h \in \mathcal{E}_h. \quad (7.13)$$

This is the discrete analog of Green's formula (7.11) mentioned above. The accuracy of this approximation depends on the accuracy of the inner products. The theory presented in Chaps. 3 and 4 requires these inner products to satisfy the consistency and stability conditions. We consider them in details in the subsequent sections. For

the moment, we assume that the matrices $M_{\mathcal{E}}$ and $M_{\mathcal{F}}$ representing the inner products are known:

$$[\mathbf{E}_h, \tilde{\mathbf{E}}_h]_{\mathcal{E}_h} = \mathbf{E}_h^T M_{\mathcal{E}} \tilde{\mathbf{E}}_h \quad \text{and} \quad [\mathbf{B}_h, \tilde{\mathbf{B}}_h]_{\mathcal{F}_h} = \mathbf{B}_h^T M_{\mathcal{F}} \tilde{\mathbf{B}}_h. \quad (7.14)$$

Inserting these formulas into (7.13), we obtain the explicit matrix formula for the derived curl operator:

$$\widetilde{\text{curl}}_h = M_{\mathcal{E}}^{-1} \text{curl}_h^T M_{\mathcal{F}}. \quad (7.15)$$

The conditions $\text{div } \mathbf{B} = 0$ and $\text{div } \varepsilon \mathbf{E} = 0$ are discretized using the discrete analogs of the operators div and $\text{div } \varepsilon$. To this purpose, we use the integration by part formula with the weight ε and the natural homogeneous boundary condition $\mathbf{D} \cdot \mathbf{n} = 0$ on $\partial\Omega$:

$$\int_{\Omega} u \text{div}(\varepsilon \mathbf{E}) \, dV = - \int_{\Omega} \nabla u \cdot \varepsilon \mathbf{E} \, dV. \quad (7.16)$$

This suggests us to define the discrete analog of operator $\text{div } \varepsilon$ as the negative adjoint of the primary mimetic operator $\nabla_h: \mathcal{V}_h \rightarrow \mathcal{E}_h$ (see Chap. 2, Sect. 2.3.1):

$$(\nabla_h p_h)_e = \frac{p_v - p_{v'}}{|e|}, \quad \mathbf{e} = (v, v'). \quad (7.17)$$

Space \mathcal{V}_h is defined in Sect. 2.2 and contains all vertex-based functions of the form

$$q_h = (q_v)_{v \in \mathcal{V}},$$

which associates a value with each mesh vertex $v \in \mathcal{V}$. The derived divergence operator is given implicitly by

$$[u_h, \widetilde{\text{div}}_h \mathbf{E}_h]_{\mathcal{E}_h} = -[\nabla_h u_h, \mathbf{E}_h]_{\mathcal{E}_h} \quad \forall u_h \in \mathcal{V}_h, \mathbf{E}_h \in \mathcal{E}_h, \quad (7.18)$$

which is a discrete analog of (7.16). Let matrix $M_{\mathcal{V}}$ represents the inner product $[\cdot, \cdot]_{\mathcal{V}_h}$ in \mathcal{V}_h , so that the left-hand side of (7.18) can be written as the vector-matrix-vector product:

$$[q_h, p_h]_{\mathcal{V}_h} = q_h^T M_{\mathcal{V}} p_h \quad \forall q_h, p_h \in \mathcal{V}_h. \quad (7.19)$$

Using (7.19) and the first relation of (7.14) in (7.18) yields the matrix form of the derived divergence operator:

$$\widetilde{\text{div}}_h = -M_{\mathcal{V}}^{-1} \nabla_h^T M_{\mathcal{E}}. \quad (7.20)$$

The derived operators $\widetilde{\text{curl}}_h$ and $\widetilde{\text{div}}_h$ are different from those introduced in Chap. 2 as they incorporate the material properties. Nonetheless, they still satisfy important relations of the DVTC; in particular, a discrete analog of $\text{div curl} = 0$ holds true again:

$$\widetilde{\text{div}}_h \widetilde{\text{curl}}_h = -M_{\mathcal{V}}^{-1} \nabla_h^T M_{\mathcal{E}} M_{\mathcal{E}}^{-1} \text{curl}_h^T M_{\mathcal{F}} = -M_{\mathcal{V}}^{-1} (\text{curl}_h \nabla_h)^T M_{\mathcal{F}} = 0.$$

It is easy to verify that analogs of Lemmas 2.6 and 2.4 also hold true.

We use the derived operators $\widetilde{\text{curl}}_h$ and $\widetilde{\text{div}}_h$ in combination with the primary operators curl_h and div_h to build a mimetic approximation of the Maxwell's equations.

More precisely, let \mathcal{E}_h^0 denote a proper subspace of \mathcal{E}_h consisting of the edge-based mesh functions whose values are zero at the boundary edges. The mimetic discretization of the first problem reads:

Find $\mathbf{E}_h \in \mathcal{E}_h^0$ and $\mathbf{B}_h \in \mathcal{F}_h$ such that

$$\operatorname{curl}_h \mathbf{E}_h = -\frac{\partial \mathbf{B}_h}{\partial t}, \quad \widetilde{\operatorname{curl}}_h \mathbf{B}_h = \frac{\partial \mathbf{E}_h}{\partial t} \quad (7.21)$$

and

$$\widetilde{\operatorname{div}}_h \mathbf{E}_h = 0, \quad \operatorname{div}_h \mathbf{B}_h = 0. \quad (7.22)$$

A mimetic discretization of the second problem, which is given by (7.5), (7.1) and (7.4) with homogeneous boundary condition, is derived similarly. We reformulate the two equations in (7.5) as

$$\operatorname{curl} \mathbf{E} = -\frac{\partial \mathbf{B}}{\partial t} \quad \text{and} \quad \sigma^{-1} \operatorname{curl} \mu^{-1} \mathbf{B} = \mathbf{E}. \quad (7.23)$$

To discretize (7.23), we use the primary mimetic operator curl_h and define a new derived operator $\widetilde{\operatorname{curl}}_h$ that approximates the differential operator $\sigma^{-1} \operatorname{curl} \mu^{-1}$ instead of $\varepsilon^{-1} \operatorname{curl} \mu^{-1}$ as before. As the development is identical (just substitute ε with σ in the previous formulas), we omit it. The mimetic semi-discretization of problem (7.23) reads:

Find $\mathbf{E}_h \in \mathcal{E}_h^0$ and $\mathbf{B}_h \in \mathcal{F}_h$ such that

$$\operatorname{curl}_h \mathbf{E}_h = -\frac{\partial \mathbf{B}_h}{\partial t}, \quad \widetilde{\operatorname{curl}}_h \mathbf{B}_h = \mathbf{E}_h \quad (7.24)$$

and the divergence-free constraints (7.22). Note that the divergence-free constraint for the discrete analog of the electric field \mathbf{E}_h follows from the second relation in (7.24). Indeed, using the second equation in (7.24) and Lemma 2.6, i.e. $\widetilde{\operatorname{div}}_h \circ \widetilde{\operatorname{curl}}_h = 0$, yields $\widetilde{\operatorname{div}}_h \mathbf{E}_h = \widetilde{\operatorname{div}}_h \widetilde{\operatorname{curl}}_h \mathbf{B}_h = 0$. This condition is satisfied exactly at any time moment $t \geq 0$.

We will present a mimetic discretization and detailed analysis of the third problem in Sect. 7.3.

7.2.3 Divergence constraints and energy conservation

An important property of these mimetic discretizations concerns *the invariance of the divergence constraint*. As a consequence, if the divergence-free condition holds at the initial time $t = 0$, it is exactly preserved at any subsequent time moment. Let us consider the various cases. Using the second equation in (7.21) and Lemma 2.6, i.e. $\widetilde{\operatorname{div}}_h \circ \widetilde{\operatorname{curl}}_h = 0$, yields

$$\frac{\partial}{\partial t} (\widetilde{\operatorname{div}}_h \mathbf{E}_h) = \widetilde{\operatorname{div}}_h \frac{\partial \mathbf{E}_h}{\partial t} = \widetilde{\operatorname{div}}_h \widetilde{\operatorname{curl}}_h \mathbf{B}_h = 0.$$

If we use, for example, the backward Euler time discretization, we obtain

$$\widetilde{\operatorname{div}}_h \frac{\mathbf{E}_h^{n+1} - \mathbf{E}_h^n}{\Delta t} = 0,$$

which implies that the divergence of the electric field is conserved. Similarly, using the first equation in (7.21) and Lemma 2.4, we obtain

$$\frac{\partial}{\partial t} (\operatorname{div}_h \mathbf{B}_h) = \operatorname{div}_h \frac{\partial \mathbf{B}_h}{\partial t} = -\operatorname{div}_h \operatorname{curl}_h \mathbf{B}_h = 0. \quad (7.25)$$

The property of invariance of the divergence constraints also holds for the second problem as $\operatorname{div}_h \mathbf{E}_h = 0$ for any $t \geq 0$ as discussed in the final comments of the previous section. The condition on \mathbf{B}_h is the same of the first problem.

Another important property of the mimetic method is the *conservation of the electromagnetic energy*. The electromagnetic energy is defined as

$$\mathbb{E} = \frac{1}{2} \left(\int_{\Omega} \mathbf{E} \cdot \mathbf{D} dV + \int_{\Omega} \mathbf{B} \cdot \mathbf{H} dV \right). \quad (7.26)$$

The energy conservation for a conducting medium is connected with the fundamental mathematical property that the operator curl is self-adjoint. Let us multiply Faraday's law (7.2) by $\mu^{-1} \mathbf{B}$ and Ampere's law (7.3) by \mathbf{E} . Then, we sum them up, and integrate the result over the computational domain Ω . In the left-hand side we easily recognize the time derivative of the electromagnetic energy. The right-hand side is zero due to (7.11):

$$\begin{aligned} \frac{\partial \mathbb{E}}{\partial t} &= \int_{\Omega} \mathbf{E} \cdot \frac{\partial \mathbf{D}}{\partial t} dV + \int_{\Omega} \mathbf{B} \cdot \frac{\partial \mathbf{H}}{\partial t} dV \\ &= - \int_{\Omega} \operatorname{curl} \mathbf{E} \cdot \mathbf{H} dV + \int_{\Omega} \mathbf{E} \cdot \operatorname{curl} \mathbf{H} dV = 0. \end{aligned} \quad (7.27)$$

Since the primary and derive discrete curl operators mimic this property, we may expect that some discrete analog of (7.27) holds true. We define the discrete electromagnetic energy as

$$\mathbb{E}_h = \frac{1}{2} \left([\mathbf{E}_h, \mathbf{E}_h]_{\mathcal{E}_h} + [\mathbf{B}_h, \mathbf{B}_h]_{\mathcal{F}_h} \right), \quad (7.28)$$

where the inner products, which include the material properties, are defined in (7.14). The conservation of the discrete electromagnetic energy \mathbb{E}_h is stated by the following theorem.

Theorem 7.1. *The discrete electromagnetic energy \mathbb{E}_h defined by (7.28) is conserved in the mimetic scheme.*

Proof. The argument used in this proof is very similar to the argument that shows the conservation of electromagnetic energy (7.26) in the continuous case. We take the product of \mathbf{B}_h with both sides of the first equation in (7.21) using the inner product

in \mathcal{F}_h , and the product of \mathbf{E}_h with both sides of the second equation using the inner product in \mathcal{E}_h to obtain:

$$\left[\frac{\partial \mathbf{B}_h}{\partial t}, \mathbf{B}_h \right]_{\mathcal{F}_h} = -[\operatorname{curl} \mathbf{E}_h, \mathbf{B}_h]_{\mathcal{F}_h}, \quad \left[\frac{\partial \mathbf{E}_h}{\partial t}, \mathbf{E}_h \right]_{\mathcal{E}_h} = [\widetilde{\operatorname{curl}}_h \mathbf{B}_h, \mathbf{E}_h]_{\mathcal{F}_h}.$$

Summing up these equations and using definition (7.28) and the duality property of mimetic operators (2.29), we obtain:

$$\begin{aligned} \frac{\partial \mathbf{E}_h}{\partial t} &= \left[\frac{\partial \mathbf{B}_h}{\partial t}, \mathbf{B}_h \right]_{\mathcal{F}_h} + \left[\frac{\partial \mathbf{E}_h}{\partial t}, \mathbf{E}_h \right]_{\mathcal{E}_h} \\ &= -[\operatorname{curl} \mathbf{E}_h, \mathbf{B}_h]_{\mathcal{F}_h} + [\widetilde{\operatorname{curl}}_h \mathbf{B}_h, \mathbf{E}_h]_{\mathcal{F}_h} = 0. \end{aligned}$$

This proves the assertion of the theorem. \square

A fully discrete method can be obtained by introducing a suitable time-stepping scheme for the time derivative, which can be either implicit, semi-implicit, or explicit. The effectiveness of the resulting mimetic discretizations is shown by numerical experiments on logically rectangular meshes in [207].

7.2.4 Stability and consistency conditions

In this section we extend the fundamental conditions of stability and consistency to the inner products with tensorial weights. The case of space \mathcal{F}_h is considered in Chap. 5; therefore, here we will focus on space \mathcal{E}_h .

Let ε_P be the approximation of the permittivity tensor ε on cell P :

$$\varepsilon_P = \frac{1}{|P|} \int_P \varepsilon dV. \quad (7.29)$$

Using (7.29), we define a discontinuous piecewise constant tensorial field $\bar{\varepsilon}$ such that $\bar{\varepsilon}|_P = \varepsilon_P$.

Let $[\cdot, \cdot]_{\mathcal{E}_h, P}$ be the inner product on the local space $\mathcal{E}_{h, P}$. The global inner product is assembled from local ones in the usual manner. The local inner product induces a norm that must satisfy the stability condition below.

(S1) (Stability condition). There exist two positive constants σ_* and σ^* independent of the mesh size h such that for every P it holds

$$\sigma_* |P| \sum_{\mathbf{e} \in \partial P} |E_{\mathbf{e}}|^2 \leq [\mathbf{E}_P, \mathbf{E}_P]_{\mathcal{E}_h, P} \leq \sigma^* |P| \sum_{\mathbf{e} \in \partial P} |E_{\mathbf{e}}|^2 \quad \forall \mathbf{E}_P \in \mathcal{E}_{h, P}.$$

Let us define the functional space

$$\begin{aligned} S_{h, P} = \mathbf{E} \in H(\operatorname{curl}, P) : & \int_P (\operatorname{curl} \mathbf{E}) \cdot \mathbf{q} dV = 0 \quad \forall \mathbf{q} \in \mathcal{O}_P^{\mathcal{F}}, \\ & \mathbf{E} \cdot \boldsymbol{\tau}_{\mathbf{e}} \in \mathbb{P}_0(\mathbf{e}) \quad \forall \mathbf{e} \in \partial P, \quad \operatorname{curl} \mathbf{E} \cdot \mathbf{n}_{\mathbf{f}} \in \mathbb{P}_0(\mathbf{f}) \quad \forall \mathbf{f} \in \partial P, \\ & \int_{\mathbf{f}} \mathbf{E}_{\mathbf{f}} \cdot \mathbf{p}^1 dS = 0 \quad \forall \mathbf{p}^1 \in \mathcal{O}_{\mathbf{f}}^{\mathcal{E}} \quad \forall \mathbf{f} \in \partial P \}. \end{aligned} \quad (7.30)$$

Here, $\mathcal{O}_P^{\mathcal{F}}$ is the space of polynomials $\mathbf{c} \times (\mathbf{x} - \mathbf{x}_P)$ where \mathbf{c} is a constant vector; $\mathcal{O}_f^{\mathcal{E}}$ is the space of linear polynomials $\mathbf{p}^1(\boldsymbol{\xi}) = c(\boldsymbol{\xi} - \boldsymbol{\xi}_f)$ defined on the plane (ξ_1, ξ_2) of face f where c is a constant, $\boldsymbol{\xi}_f$ is the centroid of f , and the two-dimensional vector $\mathbf{E}_f = \mathbf{E} - (\mathbf{E} \cdot \mathbf{n}_{P,f})\mathbf{n}_{P,f}$ is the orthogonal projection of \mathbf{E} onto f . This selection of space $S_{h,P}$ has been inspired by the definition of the reconstruction operator $R_P^{\mathcal{E}}$ in Chap. 3.

Note that $S_{h,P}$ is an infinite dimensional space. The conditions imposed on it are consistent with the definition of the reconstruction operator $R_P^{\mathcal{E}}$ in Chap. 3. Note, that $S_{h,P}$ does not depend on the material properties.

According to the theory developed in Part I of this book, this space must satisfy three assumptions **(B1)**–**(B3)**. We recall the first two assumptions, while the third assumption will be addressed below.

(B1) The local projection operator from $S_{h,P}$ to $\mathcal{E}_{h,P}$ must be subjective.

(B2) The space $S_{h,P}$ must contain the trial space of constant vector functions.

It can be checked that that the space $S_{h,P}$ above satisfies both conditions.

(S2) (*Consistency condition*). For any vector function $\mathbf{E} \in S_{h,P}$, any linear vector function $\mathbf{q} = \mathbf{c} \times (\mathbf{x} - \mathbf{x}_P)$, and every element P of Ω_h it holds

$$[(\varepsilon_P^{-1} \operatorname{curl} \mathbf{q})_P^1, \mathbf{E}_P^1]_P = \int_P (\operatorname{curl} \mathbf{q}) \cdot \mathbf{E} dV. \quad (7.31)$$

The consistency condition is an exactness property, since it ensures the accuracy of the resulting mimetic scheme. To make it useful, the right-hand side of (7.31) must be computable easily and be independent of the values of \mathbf{E} inside P . Integrating by parts and using the properties of space $S_{h,P}$, we obtain

$$\begin{aligned} \int_P (\operatorname{curl} \mathbf{q}) \cdot \mathbf{E} dV &= \int_P \mathbf{q} \operatorname{curl} \mathbf{E} dV + \sum_{f \in \partial P} \int_f (\mathbf{q} \times \mathbf{E}) \cdot \mathbf{n}_{P,f} dS \\ &= \sum_{f \in \partial P} \int_f (\mathbf{n}_{P,f} \times \mathbf{q}) \cdot \mathbf{E} dS. \end{aligned} \quad (7.32)$$

Here, we used only the first property of space $S_{h,P}$ to eliminate the volume integral. The other properties are designed to calculate explicitly the right-hand side of (7.32), so to have property **(B3)** of Chap. 4 satisfied by the bilinear form

$$\mathcal{B}_P(\mathbf{E}, \mathbf{q}) = [(\operatorname{curl} \mathbf{q})_P^1, \mathbf{E}_P^1]_{\mathcal{E}_{h,P}}$$

for any $\mathbf{E} \in S_{h,P}$ and any linear vector function \mathbf{q} .

To prove this statement, we need the result of the following lemma.

Lemma 7.1. *Let f be a face of P . Then, for any $\mathbf{E} \in S_{h,P}$ and $\mathbf{q}(\mathbf{x}) = \mathbf{c} \times (\mathbf{x} - \mathbf{x}_f)$, $\mathbf{c} \in \mathbb{R}^3$, it holds that*

$$\int_f (\mathbf{n}_{P,f} \times \mathbf{q}) \cdot \mathbf{E} dS = \int_f \mathbf{c}_f \cdot \mathbf{E}_f dS, \quad (7.33)$$

where the two-dimensional vectors \mathbf{c}_f and \mathbf{E}_f are the orthogonal projections of $\mathbf{n}_{P,f} \times (\mathbf{c} \times (\mathbf{x}_f - \mathbf{x}_P))$ and \mathbf{E} onto f , respectively.

Proof. Adding and subtracting $\mathbf{q}(\mathbf{x}_f)$ yields:

$$\mathbf{n}_{P,f} \times \mathbf{q}(\mathbf{x}) = \mathbf{n}_{P,f} \times \mathbf{q}(\mathbf{x}_f) + \mathbf{n}_{P,f} \times (\mathbf{q}(\mathbf{x}) - \mathbf{q}(\mathbf{x}_f)). \quad (7.34)$$

Using (7.34) in the left-hand side of (7.33)

$$\int_f (\mathbf{n}_{P,f} \times \mathbf{q}) \cdot \mathbf{E} \, dS = \int_f (\mathbf{n}_{P,f} \times \mathbf{q}(\mathbf{x}_f)) \cdot \mathbf{E} \, dS + \int_f (\mathbf{n}_{P,f} \times (\mathbf{q}(\mathbf{x}) - \mathbf{q}(\mathbf{x}_f))) \cdot \mathbf{E} \, dS. \quad (7.35)$$

Vector $\mathbf{n}_{P,f} \times \mathbf{q}(\mathbf{x}_f) = \mathbf{n}_{P,f} \times (\mathbf{c} \times (\mathbf{x}_f - \mathbf{x}_P))$ lies on face f ; hence, it holds that $\mathbf{n}_{P,f} \times \mathbf{q}(\mathbf{x}_f) \cdot \mathbf{E} = \mathbf{c}_f \cdot \mathbf{E}_f$, with the definitions of \mathbf{c}_f and \mathbf{E}_f given in the lemma. Then, we rewrite the first integral in the right-hand side of (7.35) as

$$\int_f (\mathbf{n}_{P,f} \times \mathbf{q}(\mathbf{x}_f)) \cdot \mathbf{E} \, dS = \int_f \mathbf{c}_f \cdot \mathbf{E}_f \, dS,$$

which is the right-hand side of (7.33)

To complete the proof we must show that the second integral of the right-hand side of (7.35) is zero. A useful property of the cross product implies that

$$\begin{aligned} \mathbf{n}_{P,f} \times (\mathbf{q}(\mathbf{x}) - \mathbf{q}(\mathbf{x}_f)) &= \mathbf{n}_{P,f} \times (\mathbf{c} \times (\mathbf{x} - \mathbf{x}_f)) \\ &= \mathbf{c}(\mathbf{n}_{P,f} \cdot (\mathbf{x} - \mathbf{x}_f)) - (\mathbf{x} - \mathbf{x}_f)(\mathbf{n}_{P,f} \cdot \mathbf{c}). \end{aligned} \quad (7.36)$$

The first term in the right-hand side of (7.36) is zero for every $\mathbf{x} \in f$ because $\mathbf{x} - \mathbf{x}_f$ lies on f and $\mathbf{n}_{P,f}$ is orthogonal to f . Thus,

$$\int_f \mathbf{E} \cdot \mathbf{n}_{P,f} \times (\mathbf{q}(\mathbf{x}) - \mathbf{q}(\mathbf{x}_f)) \, dS = - \int_f \mathbf{E} \cdot (\mathbf{x} - \mathbf{x}_f)(\mathbf{n}_{P,f} \cdot \mathbf{c}) \, dS.$$

As $\mathbf{x} - \mathbf{x}_f$ lies on f for any $\mathbf{x} \in f$, we can write $\mathbf{x} - \mathbf{x}_f \equiv \boldsymbol{\xi} - \boldsymbol{\xi}_f$, where $\boldsymbol{\xi}$ and $\boldsymbol{\xi}_f$ are the two-dimensional vectors on f that points to the same position of \mathbf{x} on f and \mathbf{x}_f , respectively. The vectors $\boldsymbol{\xi}$ and $\boldsymbol{\xi}_f$ are defined with respect to a local coordinate system (ξ_1, ξ_2) and an arbitrary origin that we can take at \mathbf{x}_f for convenience. From a simple geometric argument, we note that $\mathbf{E} \cdot (\mathbf{x} - \mathbf{x}_f) = \mathbf{E}_f \cdot (\boldsymbol{\xi} - \boldsymbol{\xi}_f)$, where \mathbf{E}_f is the two-dimensional projection of \mathbf{E} onto f . Therefore, we have

$$\int_f \mathbf{E} \cdot \mathbf{n}_{P,f} \times (\mathbf{q}(\mathbf{x}) - \mathbf{q}(\mathbf{x}_f)) \, dS = - \int_f \mathbf{E}_f \cdot (\boldsymbol{\xi} - \boldsymbol{\xi}_f)(\mathbf{n}_{P,f} \cdot \mathbf{c}) \, dS = 0 \quad (7.37)$$

due to the second orthogonality property of space $S_{h,P}$ (take $c = \mathbf{n}_{P,f} \cdot \mathbf{c}$). \square

As the previous lemma suggests, the right-hand side integral of (7.33) can be calculated in the local two-dimensional coordinate system $\boldsymbol{\xi} = (\xi_1, \xi_2)$ associated with the plane of f . Using a two-dimensional curl operator, we have $\mathbf{c}_f = (c_1, c_2) = \text{Curl}_{\boldsymbol{\xi}} q_f$ where $q_f(\boldsymbol{\xi}) = -c_1(\xi_2 - \xi_{f,2}) + c_2(\xi_1 - \xi_{f,1})$. Inserting this expression in the right-hand side of (7.33), integrating by parts, and using the remaining properties of space

$S_{h,P}$, we obtain

$$\begin{aligned} \int_f (\mathbf{n}_{P,f} \times \mathbf{q}) \cdot \mathbf{E} dS &= \int_f \text{Curl}_\xi q_f(\boldsymbol{\xi}) \cdot \mathbf{E}_f dS = \sum_{e \in \partial f} \int_e q_f(\boldsymbol{\xi}) \mathbf{E}_f \cdot \boldsymbol{\tau}_{f,e} \\ &= \sum_{e \in \partial f} |e| q_f(\boldsymbol{\xi}_e) \alpha_{f,e} E_e. \end{aligned}$$

To return back to the global coordinate system, let us first note that

$$q_f(\boldsymbol{\xi}_e) = (c_2, -c_1) \begin{pmatrix} \xi_{e,1} - \xi_{f,1} \\ \xi_{e,2} - \xi_{f,2} \end{pmatrix} = \mathcal{R}_{\pi/2} \mathbf{c}_f \cdot (\boldsymbol{\xi}_e - \boldsymbol{\xi}_f) = \mathbf{c}_f \cdot \mathcal{R}_{\pi/2}^T (\boldsymbol{\xi}_e - \boldsymbol{\xi}_f), \quad (7.38)$$

where $\mathcal{R}_{\pi/2} = \begin{pmatrix} 0 & 1 \\ -1 & 0 \end{pmatrix}$ is a 2×2 -sized rotation matrix in the (ξ_1, ξ_2) plane of face f . Let $\tilde{\mathcal{R}}_{\pi/2}$ be the 3×3 rotation matrix that rotates the vectors lying in the (ξ_1, ξ_2) plane of face f , so that $\tilde{\mathcal{R}}_{\pi/2}^T (\mathbf{x}_e - \mathbf{x}_f)$ and $\mathcal{R}_{\pi/2}^T (\boldsymbol{\xi}_e - \boldsymbol{\xi}_f)$ actually represent the same geometric vector. Let us also denote

$$\tilde{\mathbf{c}}_f = \mathbf{n}_{P,f} \times (\mathbf{c} \times (\mathbf{x}_f - \mathbf{x}_P)) = -(\mathbf{n}_{P,f} \cdot \mathbf{c})(\mathbf{x}_f - \mathbf{x}_P).$$

Vector $\tilde{\mathbf{c}}_f$ lies on face f and geometrically coincides with \mathbf{c}_f . This construction allows us to express $q_f(\boldsymbol{\xi}_e)$ as

$$q_f(\boldsymbol{\xi}_e) = \mathbf{c}_f \cdot \mathcal{R}_{\pi/2}^T (\boldsymbol{\xi}_e - \boldsymbol{\xi}_f) = \tilde{\mathbf{c}}_f \cdot \tilde{\mathcal{R}}_{\pi/2}^T (\mathbf{x}_e - \mathbf{x}_f).$$

Returning back to global coordinate system and using the definition of $\tilde{\mathbf{c}}_f$, we obtain

$$\begin{aligned} \int_f (\mathbf{n}_{P,f} \times \mathbf{q}) \cdot \mathbf{E} dS &= \sum_{e \in \partial f} |e| \tilde{\mathbf{c}}_f \cdot \tilde{\mathcal{R}}_{\pi/2}^T (\mathbf{x}_e - \mathbf{x}_f) \alpha_{f,e} E_e \\ &= -\mathbf{n}_{P,f} \cdot \mathbf{c} \tilde{\mathcal{R}}_{\pi/2} (\mathbf{x}_f - \mathbf{x}_P) \cdot \sum_{e \in \partial f} |e| (\mathbf{x}_e - \mathbf{x}_f) \alpha_{f,e} E_e. \end{aligned} \quad (7.39)$$

This formula shows that the right-hand side of the consistency condition depends only on \mathbf{c} , the geometry of cell P and the degrees of freedom E_e .

Remark 7.1. Combining (7.31) with (7.32) and (7.39), recalling the surjectivity property **(B1)**, we therefore obtain a more practical form of the consistency condition. For all $\mathbf{E}_P \in \mathcal{E}_{h,P}$ and for all $\mathbf{c} \in \mathbb{R}^3$ it holds

$$2[(\varepsilon_P^{-1} \mathbf{c})]_P, \mathbf{E}_P]_P = - \sum_{f \in \partial P} \mathbf{n}_{P,f} \cdot \mathbf{c} \tilde{\mathcal{R}}_{\pi/2} (\mathbf{x}_f - \mathbf{x}_P) \cdot \sum_{e \in \partial f} |e| (\mathbf{x}_e - \mathbf{x}_f) \alpha_{f,e} E_e,$$

where, as usual, $\mathbf{E}_P = (E_e)_{e \in \partial P}$ and where we used that $\mathbf{q} = \mathbf{c} \times (\mathbf{x} - \mathbf{x}_P)$ and thus $\text{curl} \mathbf{q} = 2\mathbf{c}$. The auxiliary space $S_{h,P}$ is needed only for constructive purposes and has completely disappeared from the consistency condition.

Remark 7.2. Note that space $S_{h,P}$ is infinite dimensional. However, nothing forbids us from choosing its finite dimensional subspace, still denoted by $S_{h,P}$, e.g. by requiring that

$$\dim(S_{h,P}) = \dim(\mathcal{E}_{h,P}). \quad (7.40)$$

Such an assumption moves the mimetic framework closer to the finite element framework with the important difference that we never calculate the basis functions in $S_{h,P}$ explicitly.

7.2.5 A family of mimetic schemes

Let us consider a polyhedron P . The local inner product in $\mathcal{E}_{h,P}$ can be represented by a symmetric and positive definite matrix M_P :

$$[\mathbf{E}_P, \tilde{\mathbf{E}}_P]_{\mathcal{E}_{h,P}} = \mathbf{E}_P^T M_P \tilde{\mathbf{E}}_P. \quad (7.41)$$

We have shown in Chap. 3 that the local inner product matrix satisfies the algebraic equation $M_P N_P = R_P$ where N_P and R_P are rectangular matrices. Let us show that a similar matrix equation holds for the weighted inner product. Combining Remark 7.1 with (7.41) yields

$$\begin{aligned} 2(\mathbf{E}_P^1)^T M_P (\varepsilon_P^{-1} \mathbf{c})_P^1 &= - \sum_{f \in \partial P} \left[(\mathbf{n}_{P,f} \cdot \mathbf{c}) \tilde{\mathcal{H}}_{\pi/2}(\mathbf{x}_f - \mathbf{x}_P) \cdot \sum_{e \in \partial f} |e| (\mathbf{x}_e - \mathbf{x}_f) \alpha_{f,e} E_e \right] \\ &= \sum_{e \in \partial P} R_{\mathbf{c},e} E_e, \end{aligned} \quad (7.42)$$

where the final term is given by switching the summations on f and e and including all summations on f in the definition of the column vector $R_{\mathbf{c}} = (R_{\mathbf{c},e})_{e \in \partial P}$. We have

$$R_{\mathbf{c},e} = -|e| \sum_{f: e \in \partial f} (\mathbf{n}_{P,f} \cdot \mathbf{c}) \tilde{\mathcal{H}}_{\pi/2}(\mathbf{x}_f - \mathbf{x}_P) \cdot (\mathbf{x}_e - \mathbf{x}_f) \alpha_{f,e} \quad (7.43)$$

Let us consider three constant vectors that form the canonical basis of \mathbb{R}^d , i.e., $\mathbf{c}_1 = (1, 0, 0)^T$, $\mathbf{c}_2 = (0, 1, 0)^T$, $\mathbf{c}_3 = (0, 0, 1)^T$. We define vectors $N_i = 2(\varepsilon_P^{-1} \mathbf{c}_i)_P^1$. If we enumerate the edges of P by an index running from 1 to $N_P^{\mathcal{E}}$, the explicit formula for the j -th component of N_i is

$$(N_i)_j = \frac{2}{|e_j|} \int_{e_j} \varepsilon_P^{-1} \mathbf{c}_i \cdot \boldsymbol{\tau}_e dS.$$

Let us define the $N_P^{\mathcal{E}} \times 3$ matrix $N_P = (N_1, N_2, N_3)$. Note that we can pull out the full tensor ε_P^{-1} (like we did in Chaps. 5 and 6) to get a simpler representation of

this matrix:

$$N_P = 2 \begin{pmatrix} \boldsymbol{\tau}_{\mathbf{e}_1}^T \\ \boldsymbol{\tau}_{\mathbf{e}_2}^T \\ \vdots \\ \boldsymbol{\tau}_{\mathbf{e}_{N_P^e}}^T \end{pmatrix} \boldsymbol{\varepsilon}_P^{-1}.$$

Let us define the $N_P^e \times 3$ matrix $R_P = (R_1, R_2, R_3)$ from (7.43) by setting $R_i = R_{\mathbf{e}_i}$ for $i = 1, 2, 3$. Now formula (7.42) gives us the desired algebraic equation

$$M_P N_P = R_P.$$

Lemma 7.2. *For any polyhedron P , matrix $N_P^T R_P$ is symmetric and positive definite. Moreover,*

$$N_P^T R_P = 4|P| \boldsymbol{\varepsilon}_P^{-1}.$$

Proof. Note that constant vector functions belong to space $S_{h,P}$. Let $\mathbf{q}_i = \mathbf{c}_i \times (\mathbf{x} - \mathbf{x}_P)$, $i \leq 3$, where \mathbf{c}_i form the canonical basis of \mathbb{R}^d . Then, the consistency condition gives

$$\begin{aligned} N_i^T R_j &= N_i^T M_P N_j = [(\boldsymbol{\varepsilon}_P^{-1} \operatorname{curl} \mathbf{q}_i)]_P^1, (\boldsymbol{\varepsilon}_P^{-1} \operatorname{curl} \mathbf{q}_j)]_P^1 \\ &= \int_P \operatorname{curl} \mathbf{q}_i \cdot (\boldsymbol{\varepsilon}_P^{-1} \operatorname{curl} \mathbf{q}_j) dV. \end{aligned}$$

Since $\operatorname{curl} \mathbf{q}_i = 2\mathbf{c}_i$, the last integral is nothing else but $4|P|(\boldsymbol{\varepsilon}_P^{-1})_{ij}$. This proves the assertion of the lemma. \square

Example 7.1. In two dimensions, the derivation of matrices N_P and R_P becomes much simpler. Let us consider a polygon P . In two dimensions there are two curl operators:

$$\operatorname{Curl} B = \begin{pmatrix} -\frac{\partial B}{\partial x_2} \\ \frac{\partial B}{\partial x_1} \end{pmatrix} \quad \text{and} \quad \operatorname{curl} \mathbf{E} = \frac{\partial E_1}{\partial x_2} - \frac{\partial E_2}{\partial x_1}.$$

for $B \in H^1(P)$ and $\mathbf{E} \in H(\operatorname{curl}, P)$. The space $S_{h,P}$ has a much simpler form:

$$S_{h,P} = \{ \mathbf{E} \in H(\operatorname{curl}, P) : \operatorname{curl} \mathbf{E} \in \mathbb{P}_0(P), \mathbf{E} \cdot \boldsymbol{\tau}_e \in \mathbb{P}_0(e) \quad \forall e \in \partial P \}.$$

The consistency condition is transformed as follows. For any vector function $\mathbf{E} \in S_{h,P}$ and any linear function $q = \mathbf{c} \cdot (\mathbf{x} - \mathbf{x}_P)$, it holds

$$[(\boldsymbol{\varepsilon}_P^{-1} \operatorname{Curl} q)]_P^1, \mathbf{E}_P^1]_P = \int_P (\operatorname{Curl} q) \cdot \mathbf{E} dV = \sum_{e \in \partial P} \int_e q \mathbf{E} \cdot \boldsymbol{\tau}_e dS = \sum_{e \in \partial P} |e| q(\mathbf{x}_e) E_e.$$

Following the arguments used in three dimensions, we can write down explicit formulas for matrices N_P and R_P . Let $\boldsymbol{\tau}_e$ be the unit tangent vector oriented counter-

clockwise and $n_{P,e}$ be the exterior normal to edge e . Note that

$$\varepsilon_P^{-1} \text{Curl} q \cdot \boldsymbol{\tau}_e = \varepsilon_P^{-1} \begin{pmatrix} -c_2 \\ c_1 \end{pmatrix} \cdot \boldsymbol{\tau}_e = \mathcal{R}_{\pi/2}^T \varepsilon_P^{-1} \mathcal{R}_{\pi/2} \begin{pmatrix} c_1 \\ c_2 \end{pmatrix} \cdot \mathbf{n}_{P,e},$$

where $\mathcal{R}_{\pi/2}$ is the 2×2 -sized rotation matrix by $\pi/2$. Then,

$$N_P = \begin{pmatrix} \mathbf{n}_{P,e_1}^T \\ \mathbf{n}_{P,e_2}^T \\ \vdots \\ \mathbf{n}_{P,e_{N_P}^e}^T \end{pmatrix} \mathcal{R}_{\pi/2}^T \varepsilon_P^{-1} \mathcal{R}_{\pi/2}, \quad R_P = \begin{pmatrix} |e_1| (\mathbf{x}_{e_1} - \mathbf{x}_P)^T \\ |e_2| (\mathbf{x}_{e_2} - \mathbf{x}_P)^T \\ \vdots \\ |e_{N_P}^e| (\mathbf{x}_{e_{N_P}^e} - \mathbf{x}_P)^T \end{pmatrix}.$$

These matrices differ from similar matrices in Chap. 5 by a rotation of the tensor ε_P^{-1} . Thus, in two dimensions, in the case of a scalar tensor, the mimetic inner product in spaces \mathcal{F}_h and \mathcal{E}_h are defined by the same matrix. \square

7.3 Magnetostatics equations

Let $\Omega \subset \mathbb{R}^3$ be a simply connected domain with the Lipschitz continuous boundary Γ . In this section, we consider in more details the magnetostatics problem:

$$\text{curl } \mathbf{H} = \mathbf{J} \quad \text{in } \Omega, \quad (7.44)$$

$$\text{div}(\mu \mathbf{H}) = 0 \quad \text{in } \Omega, \quad (7.45)$$

$$\mathbf{H} \times \mathbf{n} = \mathbf{g}' \quad \text{on } \Gamma, \quad (7.46)$$

for the unknown magnetic field intensity \mathbf{H} . We assume that \mathbf{J} is a divergence-free current density.

From a physical standpoint, the domain Ω should be the whole space \mathbb{R}^d , and the magnetic field should satisfy a radiation condition like $\mathbf{H} \rightarrow 0$ at infinity instead of the Dirichlet boundary condition. In practice, we assume that Ω is a bounded domain and approximate the radiation condition.

The divergence-free condition allows us to introduce the vector potential \mathbf{u} such that $\text{curl } \mathbf{u} = \mu \mathbf{H}$. The choice of \mathbf{u} is not unique as we can always add the gradient of a scalar function to the vector potential \mathbf{u} and leave the relation with \mathbf{H} unaltered. To obtain a weak formulation that admits a unique solution we consider the *Coulomb gauge*, which leads to a divergence-free vector potential. More precisely, we require the vector field \mathbf{u} to be the solution of the set of equations:

$$\text{curl}(\mu^{-1} \text{curl } \mathbf{u}) + \nabla p = \mathbf{J} \quad \text{in } \Omega, \quad (7.47)$$

$$\text{div } \mathbf{u} = 0 \quad \text{in } \Omega, \quad (7.48)$$

$$\mathbf{u} \times \mathbf{n} = 0 \quad \text{on } \partial\Omega, \quad (7.49)$$

where p is the Lagrange multiplier. The variational formulation of this problem reads (see, e.g. [225]):

Find $\mathbf{u} \in H_0(\text{curl}, \Omega)$ and $p \in H_0^1(\Omega)$ such that

$$\int_{\Omega} \mu^{-1} \text{curl} \mathbf{u} \cdot \text{curl} \mathbf{v} dV + \int_{\Omega} \mathbf{v} \cdot \nabla p dV = \int_{\Omega} \mathbf{J} \cdot \mathbf{v} dV \quad \forall \mathbf{v} \in H_0(\text{curl}, \Omega), \quad (7.50)$$

$$\int_{\Omega} \mathbf{u} \cdot \nabla q dV = 0 \quad \forall q \in H_0^1(\Omega). \quad (7.51)$$

Under assumptions **(H8)**–**(H9)** (see Sect. 1.5.4) the well-posedness of (7.50)–(7.51) can be proved in the framework of Brezzi-Babuska theory for saddle-point problems.

Let us choose $\mathbf{v} = \nabla p \in H_0(\text{curl}, \Omega)$ in (7.50). Then, the first integral of (7.50) is zero due to the exact identity $\text{curl} \circ \nabla = 0$. If current density \mathbf{J} is a sufficiently smooth function, we also have

$$\int_{\Omega} \mathbf{J} \cdot \nabla p dV = - \int_{\Omega} p \text{div} \mathbf{J} dV + \int_{\Gamma} p \mathbf{n} \cdot \mathbf{J} dS = 0 \quad (7.52)$$

since \mathbf{J} is a divergence-free field and p is zero on the boundary. Thus, the right-hand side of (7.50) is zero, and this equation becomes:

$$\int_{\Omega} |\nabla p|^2 dV = 0,$$

from which it follows that p is constant. The homogeneous Dirichlet condition implies that $p = 0$ in Ω . This fact ensures that (7.50)–(7.51) are weakly consistent with the strong formulation (7.47)–(7.49).

7.3.1 Strong and weak forms of discrete equations

We use the following spaces to approximate \mathbf{u} and p , see Fig. 7.2:

- The vector \mathbf{u}_h belongs to the space \mathcal{E}_h of edge-based fields defined in Sect. 7.2.1:

$$\mathbf{u}_h = (u_e)_{e \in \mathcal{E}}.$$

The value associated with edge e is denoted by u_e and may represent the tangential component of a vector field defined on Ω .

- The scalar p_h belongs to the space \mathcal{V}_h of vertex-based fields:

$$p_h = (p_v)_{v \in \mathcal{V}}.$$

The value associated with node v is denoted by p_v and may represent the pointwise value of a scalar field defined on Ω . We also use the symbol \mathcal{V}_h^0 to denote a proper subspace of \mathcal{V}_h consisting of vectors whose components are zero at the boundary nodes.

The restriction of \mathbf{u}_h to cell $P \in \Omega_h$ is denoted by $\mathbf{u}_P = (u_e)_{e \in \partial P}$. Similarly, we define the restriction $p_P = (p_v)_{v \in \partial P}$. Note that $\mathbf{u}_P \in \mathcal{E}_{h,P}$ and $p_P \in \mathcal{V}_{h,P}$. These degrees of freedom are illustrated in Fig. 7.2. For the cell shown in this figure, the dimensions of the spaces \mathcal{E}_h and \mathcal{V}_h are 17 and 11, respectively.

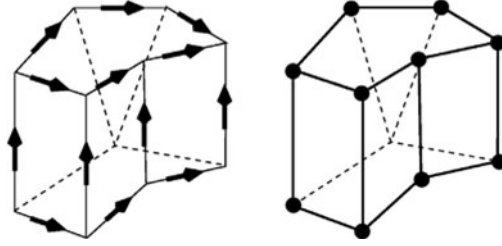


Fig. 7.2. Geometric location of degrees of freedom in the low-order MFD scheme for magnetostatics problem: arrows on edges represent u_e (on 13 visible edges), dots at nodes represent p_v (at 10 visible nodes)

We use again the symbol $(\cdot)^I$ to denote the projection operators from the functional spaces to the discrete spaces \mathcal{E}_h and \mathcal{V}_h . The edge-based projection operator is given by (7.6). The vertex-based projection operator is given by

$$p^I = (p_v^I)_{v \in \mathcal{V}}, \quad p_v^I = p(\mathbf{x}_v).$$

We represent the differential operators curl and $\text{curl} \mu^{-1}$ that appear in Eq. (7.47) by the primary discrete operator curl defined by (7.8) and the derived operator $\widetilde{\text{curl}}_h$ defined as in (7.15) using $\varepsilon = 1$. We represent the gradient operator in (7.47) by the primary discrete operator ∇_h defined in (7.17) and the divergence operator in (7.48) by the derived operator $\widetilde{\text{div}}_h$ defined as in (7.20) using $\varepsilon = 1$. Using these operators, the mimetic discretization of (7.47)–(7.49) in strong form reads:

Find $\mathbf{u}_h \in \mathcal{E}_h^0$ and $p_h \in \mathcal{V}_h^0$ such that

$$\widetilde{\text{curl}}_h \text{curl}_h \mathbf{u}_h + \nabla_h p_h = \mathbf{J}^I, \quad (7.53)$$

$$\widetilde{\text{div}}_h \mathbf{u}_h = 0, \quad (7.54)$$

where $\mathbf{J}^I \in \mathcal{E}_h$ is the projection onto \mathcal{E}_h of the current density vector \mathbf{J} . Due to the Dirichlet boundary conditions, equations (7.53) should be considered only for the interior mesh edges. Similarly, equations (7.54) should be considered only for the interior mesh nodes.

The linear algebraic formulation follows immediately by using the definition of the primary and derived operators:

$$\mathbf{M}_{\mathcal{E}}^{-1} \text{curl}^T \mathbf{M}_{\mathcal{F}} \text{curl} \mathbf{u}_h + \nabla_h p_h = \mathbf{J}^I,$$

$$\mathbf{M}_{\mathcal{V}}^{-1} \nabla_h^T \mathbf{M}_{\mathcal{E}} \mathbf{u}_h = 0.$$

Since $\mathbf{M}_{\mathcal{E}}^{-1}$ is in general dense on an unstructured mesh, a computationally tractable system is obtained by multiplying the first equation by $\mathbf{M}_{\mathcal{E}}$. A symmetric system is obtained by multiplying the second equation by $\mathbf{M}_{\mathcal{V}}$.

A weak formulation of (7.53)–(7.54) is obtained by multiplying (through the \mathcal{E}_h scalar product) the first equation by $\mathbf{v}_h \in \mathcal{E}_h^0$ and multiplying (through the \mathcal{V}_h scalar

product) the second one by $q_h \in \mathcal{V}_h^0$. Then, also using the definitions of the derived mimetic operators, we obtain:

Find $\mathbf{u}_h \in \mathcal{E}_h^0$ and $p_h \in \mathcal{V}_h^0$ such that

$$[\operatorname{curl}_h \mathbf{u}_h, \operatorname{curl}_h \mathbf{v}_h]_{\mathcal{F}_h} + [\mathbf{v}_h, \nabla_h p_h]_{\mathcal{E}_h} = [\mathbf{J}^I, \mathbf{v}_h]_{\mathcal{E}_h} \quad \forall \mathbf{v}_h \in \mathcal{E}_h^0, \quad (7.55)$$

$$[\mathbf{u}_h, \nabla_h q_h]_{\mathcal{E}_h} = 0 \quad \forall q_h \in \mathcal{V}_h^0. \quad (7.56)$$

The well-posedness of the mimetic scheme is stated by the following theorem.

Theorem 7.2. *Let Ω_h be a simply connected mesh. Then, problem (7.53)–(7.54) admits a unique solution.*

Proof. Let $\mathbf{J}^I = 0$. We have to prove that $\mathbf{u}_h = 0$ and $p_h = 0$. To this purpose, let us consider Eq. (7.55) with $\mathbf{v}_h = \mathbf{u}_h$ and Eq. (7.56) with $q_h = p_h$. We have

$$[\operatorname{curl}_h \mathbf{u}_h, \operatorname{curl}_h \mathbf{u}_h]_{\mathcal{F}_h} = 0.$$

Since the mimetic inner product defines a norm on \mathcal{F}_h , this implies that $\operatorname{curl}_h \mathbf{u}_h = 0$. Substituting this back into Eq. (7.55) and taking $\mathbf{v}_h = \nabla_h p_h$ yields:

$$[\nabla_h p_h, \nabla_h p_h]_{\mathcal{E}_h} = 0,$$

which implies that $\nabla_h p_h = 0$. Lemma 2.3 states that the null space of ∇_h consists of constant mesh functions. From the homogeneous Dirichlet conditions it immediately follows that $p_h = 0$.

Then, we observe that the condition $\operatorname{curl}_h \mathbf{u}_h = 0$ and the result of Lemma 2.4 imply that there exists a node function $w_h \in \mathcal{V}_h$ such that $\mathbf{u}_h = \nabla_h w_h$. From Eq. (7.56) with $q_h = w_h$, we have $\nabla_h w_h = 0$. Thus, we obtain $\mathbf{u}_h = \nabla_h w_h = 0$ which proves the assertion of the theorem. \square

From Theorem 7.2, we derive a discrete analog of the weak consistency between the variational and the strong form of the magnetostatic equations, which is discussed at the end of Sect. 7.3. We state such property in the following corollary.

Corollary 7.1. *Let us assume that $\widetilde{\operatorname{div}}_h \mathbf{J}^I = 0$. Then, $p_h = 0$.*

Proof. We take $\mathbf{v}_h = \nabla_h p_h$ and observe that $[\mathbf{J}^I, \mathbf{v}_h]_{\mathcal{E}_h} = [\widetilde{\operatorname{div}}_h \mathbf{J}^I, p_h]_{\mathcal{V}_h} = 0$. Since $\operatorname{curl}_h \nabla_h p_h$ is also zero, Eq. (7.55) becomes

$$[\nabla_h p_h, \nabla_h p_h]_{\mathcal{E}_h} = 0,$$

which implies that $\nabla_h p_h = 0$. By repeating the argument used in the proof of the theorem, we obtain the result. \square

Remark 7.3. The first term in (7.55) shows that the inner product needs to be defined only on a proper subspace of \mathcal{F}_h given by the image of the primary mimetic curl

operator. We met a similar problem in Chap. 5; however, the same approach does not work here. Direct calculation of the triple product $\text{curl}_h^T \mathbf{M}_{\mathcal{F}} \text{curl}_h$ that bypasses the calculation of matrix $\mathbf{M}_{\mathcal{F}}$ is an open problem.

7.3.2 Stability and consistency conditions

The proposed method makes use of the scalar product on the space \mathcal{F}_h introduced in Chap. 3 and extended to general material tensors in Chap. 5. In the present section we focus in particular on the framework of Chap. 5. Note that here we have a different notation for the material tensor (μ_P instead of \mathbf{K}_P). To avoid discussion of many technical details, herein and in the theoretical analysis of the next section we assume that μ is a positive definite piecewise constant tensor, e.g., $\mu = \mu_P$, over each mesh cell P .

Let us define the following norm on the space \mathcal{F}_h :

$$\|\mathbf{v}_h\|_{\mathcal{F}_h}^2 = \sum_{P \in \Omega_h} \|\mathbf{v}_P\|_{\mathcal{F}_{h,P}}^2, \quad \|\mathbf{v}_P\|_{\mathcal{F}_{h,P}}^2 = |P| \sum_{f \in \partial P} |v_f|^2$$

for all $\mathbf{v}_h = (v_f)_{f \in \mathcal{F}} \in \mathcal{F}_h$. The stability condition (S1) of Chap. 5 reads:

(S1) (*Stability condition*). There exist two positive constants σ_* and σ^* independent of the mesh size h such that for every P it holds

$$\sigma_* \|\mathbf{v}_P\|_{\mathcal{F}_{h,P}}^2 \leq [\mathbf{v}_P, \mathbf{v}_P]_{\mathcal{F}_{h,P}} \leq \sigma^* \|\mathbf{v}_P\|_{\mathcal{F}_{h,P}}^2 \quad \forall \mathbf{v}_P \in \mathcal{F}_{h,P}.$$

The above condition states that the discrete bilinear form $[\text{curl}_h \cdot, \text{curl}_h \cdot]_{\mathcal{F}_h}$ appearing in (7.55) has the correct kernel. In fact, Lemma 2.4 restricted to cell P implies that $\|\text{curl}_P \mathbf{v}_P\|_{\mathcal{F}_{h,P}}$ is zero if and only if $\mathbf{v}_P = \nabla_h q_P$ where $q_P \in \mathcal{V}_{h,P}$.

We now present a simple consequence of the consistency condition (S2) of Chap. 5 that will be useful in the theoretical analysis. Let us define the spaces

$$\mathcal{T}_P = \left\{ \mathbf{q} \in (\mathbb{P}_1(P))^3 : \mathbf{q}(\mathbf{x}) = \mathbf{c}' + \mathbf{c}'' \times (\mathbf{x} - \mathbf{x}_P), \mathbf{c}', \mathbf{c}'' \in (\mathbb{P}_0(P))^3 \right\}$$

and

$$S_{h,P} = \left\{ \mathbf{v} \in H(\text{curl}, P) : (\text{curl} \mathbf{v}) \cdot \mathbf{n}_f \in \mathbb{P}_0(f) \quad \forall f \in \partial P, \mathbf{v} \cdot \boldsymbol{\tau}_e \in \mathbb{P}_0(e) \quad \forall e \in \partial P \right\}.$$

Lemma 7.3. *For every $\mathbf{q} \in \mathcal{T}_P$ and every $\mathbf{v} \in S_{h,P}$ there holds:*

$$[\text{curl}_h \mathbf{q}_P^I, \text{curl}_h \mathbf{v}_P^I]_{\mathcal{F}_h} = \int_P \mu_P^{-1} \text{curl} \mathbf{q} \cdot \text{curl} \mathbf{v} dV. \quad (7.57)$$

Proof. We start from the consistency condition (5.20) in Chap. 5 with $\mu_P = \mathbf{K}_P$. By taking $q = \mathbf{c} \cdot (\mathbf{x} - \mathbf{x}_P)$ for $\mathbf{c} \in \mathbb{R}^3$ (and thus $\nabla q = \mathbf{c}$) we obtain

$$[(\mu_P \mathbf{c})_P^I, \mathbf{w}_P^I]_{\mathcal{F}_{h,P}} = \int_P \mathbf{c} \cdot \mathbf{w} dV \quad (7.58)$$

for all functions $\mathbf{w} \in (L^s(P))^3$, $s > 2$, and such that

$$\operatorname{div} \mathbf{w} = \text{const}, \quad \mathbf{w} \cdot \mathbf{n}_f = \text{const} \quad \forall f \in \partial P, \quad (7.59)$$

see Sect. 5.1.3. For any function $\mathbf{q} \in \mathcal{T}_P$, it clearly holds $\mu_P^{-1} \operatorname{curl} \mathbf{q} = \text{const}$. Moreover, for all $\mathbf{v} \in S_{h,P}$, $\operatorname{curl} \mathbf{v}$ satisfies all the conditions for the test space appearing in (7.59). Therefore, we can take $\mathbf{c} = \mu_P^{-1} \operatorname{curl} \mathbf{q}$ and $\mathbf{w} = \operatorname{curl} \mathbf{v}$ in (7.58) to obtain:

$$[(\operatorname{curl} \mathbf{q})_P^1, (\operatorname{curl} \mathbf{v})_P^1]_P = \int_P \mu_P^{-1} \operatorname{curl} \mathbf{q} \cdot \operatorname{curl} \mathbf{v} dV. \quad (7.60)$$

The assertion of the lemma follows from the commuting diagram property in Lemma 2.2. \square

7.3.3 Convergence analysis

The main result of this section is the convergence Theorem 7.3. We consider the mesh conditions **(MR1)**–**(MR3)** of Sect. 1.6.2. The proof of this theorem requires some tools that are introduced below. The first one is a reconstruction operator

$$R_P^\mathcal{E} : \mathcal{E}_{h,P} \rightarrow S_{h,P}$$

that satisfies the following six properties.

(L1) The reconstruction operator $R_P^\mathcal{E}$ is a right inverse of the projection operator defined by (7.6):

$$\mathbf{v}_P = (R_P^\mathcal{E}(\mathbf{v}_P))_P^1 \quad \forall \mathbf{v}_P \in \mathcal{E}_{h,P}.$$

(L2) The reconstruction operator is exact $R_P^\mathcal{E}$ on constant functions:

$$R_P^\mathcal{E}(\mathbf{c}_P^1) = \mathbf{c} \quad \forall \mathbf{c} \in (\mathbb{P}_0(P))^3.$$

(L3) The reconstruction operator $R_P^\mathcal{E}$ and the minimal reconstruction operator $R_P^\mathcal{F}$ defined in Chap. 3 commute with the continuum and discrete curl operators:

$$R_P^\mathcal{F}(\operatorname{curl}_P \mathbf{v}_P) = \operatorname{curl} R_P^\mathcal{E}(\mathbf{v}_P) \quad \forall \mathbf{v}_P \in \mathcal{E}_{h,P}.$$

(L4) The reconstructed functions are orthogonal to a special subspace of linear polynomials with zero average. Let \mathbf{x}_P be the barycenter of P , then

$$\int_P R_P^\mathcal{E}(\mathbf{v}_P) \cdot \mathbf{p}^1 dV = 0 \quad \forall \mathbf{v}_P \in \mathcal{E}_{h,P}, \quad \forall \mathbf{p}^1 \in \mathcal{O}_P^\mathcal{E} \equiv \{c(\mathbf{x} - \mathbf{x}_P), \forall c \in \mathbb{R}\}.$$

(L5) The trace of the reconstructed function on a face f of P (respectively, on an edge e of P) depends only on the degrees of freedom associated with f (respectively, with e):

$$R_P^\mathcal{E}(\mathbf{v}_P)|_f = R_f^\mathcal{E}(\mathbf{v}_P|_f), \quad R_f^\mathcal{E}(\mathbf{v}_P)|_e \cdot \boldsymbol{\tau}_e = v_e,$$

where $R_f^\mathcal{E}$ is the face-based reconstruction operator defined in Chap. 3.

(L6) The reconstruction operator satisfies the following stability condition: there exists a constant C independent of h such that

$$\|\operatorname{curl}(R_P^\mathcal{E}(\mathbf{v}_P))\|_{L^2(P)} \leq C \|\operatorname{curl}_P \mathbf{v}_P\|_{\mathcal{F}_{h,P}} \quad \forall \mathbf{v}_P \in \mathcal{E}_{h,P}.$$

The reconstruction operator $R_P^\mathcal{E}$ above is the one defined in Chap. 3. Indeed, the first five properties **(L1)**–**(L5)** were already proved there. The fact that $R_P^\mathcal{E}(\mathbf{v}_P) \in S_{h,P}$ follows from **(L5)** (the second condition states that the tangent components on cell edges are constant) and **(L3)** (the normal components of functions in the image of $R_P^\mathcal{E}$ are constant on faces of P , see Chap. 3). Finally, due to **(L3)**, in order to show property **(L6)**, we need to prove

$$\|R_P^\mathcal{F}(\operatorname{curl}_P \mathbf{v}_P)\|_{L^2(P)} \leq C \|\operatorname{curl}_P \mathbf{v}_P\|_{\mathcal{F}_{h,P}} \quad \forall \mathbf{v}_P \in \mathcal{E}_{h,P},$$

that is guaranteed if we show that

$$\|R_P^\mathcal{F}(\mathbf{w}_P)\|_{L^2(P)} \leq C \|\mathbf{w}_P\|_{\mathcal{F}_{h,P}} \quad \forall \mathbf{w}_P \in \mathcal{F}_{h,P}.$$

This continuity property of $R_P^\mathcal{F}$ can be easily proved using the definition of $R_P^\mathcal{F}$ and scaling arguments that make use of the mesh shape regularity assumptions **(MR1)**–**(MR3)** of Sect. 1.6.2. Therefore we omit the proof.

In Sect. 7.2.1, we introduced a projection operator $(\mathbf{v})^I$ from the space of continuous functions to the discrete space \mathcal{E}_h . It will be convenient to perform the convergence analysis using a different projection operator that preserves the divergence free condition.

Let $\operatorname{div} \mathbf{v} = 0$ in Ω , then there exists a vector potential $\boldsymbol{\psi}_\mathbf{v} \in (H^1(\Omega))^3$ such that $\mathbf{v} = \operatorname{curl} \boldsymbol{\psi}_\mathbf{v}$ (see, e.g. [184]). Moreover, $\operatorname{div} \boldsymbol{\psi}_\mathbf{v} = 0$. We define the second projection as follows:

$$\mathbf{v}^{\parallel} = \widetilde{\operatorname{curl}}_h \boldsymbol{\psi}_\mathbf{v}^I,$$

where $\boldsymbol{\psi}_\mathbf{v}^I$ is given by (7.7).

Thus, calculation of a divergence-free mesh function \mathbf{J}^{\parallel} requires a global solver with the mimetic mass matrix $M_{\mathcal{E}_h}$. In practice, we may use \mathbf{J}^I which leads to $p_h \neq 0$.

Theorem 7.3. *Let Ω be a simply connected Lipschitz polyhedron and Ω_h be a simply connected polyhedral mesh that satisfies the hypotheses **(MR1)**–**(MR3)** of Sect. 1.6.2. Furthermore, let (\mathbf{u}, p) be the solution of problem (7.44)–(7.46) with $\mathbf{u} \in (H^2(\Omega))^3 \cap H_0(\operatorname{curl}, \Omega)$ and $\mathbf{J} = \operatorname{curl} \boldsymbol{\psi}_\mathbf{J}$ where $\boldsymbol{\psi}_\mathbf{J} \in (H^1(\Omega))^3$. Finally, let $(\mathbf{u}_h, p_h) \in \mathcal{E}_h^0 \times \mathcal{V}_h^0$ be the solution of mimetic scheme (7.55)–(7.56) with the discrete current density \mathbf{J}^{\parallel} in place of \mathbf{J}^I . Then,*

$$\|\operatorname{curl}_h(\mathbf{u}^I - \mathbf{u}_h)\|_{\mathcal{F}_h} \leq Ch \left(\|\mathbf{u}\|_{H^2(\Omega)} + \|\boldsymbol{\psi}_\mathbf{J}\|_{H^1(\Omega)} \right).$$

Proof. Let us define the approximation error as $\boldsymbol{\varepsilon}_h = \mathbf{u}^I - \mathbf{u}_h$. Note that $\boldsymbol{\varepsilon}_h \in \mathcal{E}_h^0$ since the Dirichlet condition implies that $u_e = 0$ and $(\mathbf{u})_e^I = 0$ for any mesh edge e

that is on the boundary of Ω . Recall that $\mathbf{J}^{\parallel} = \widetilde{\text{curl}}_h \boldsymbol{\psi}_J^{\parallel}$ where $\boldsymbol{\psi}_J^{\parallel} \in \mathcal{F}_h$ is the discrete vector potential. Since $\widetilde{\text{div}}_h \mathbf{J}^{\parallel} = \widetilde{\text{div}}_h \widetilde{\text{curl}}_h \boldsymbol{\psi}_J^{\parallel} = 0$, Corollary 7.1 implies that $p_h = 0$, and using Assumption **(S1)** and (7.55) with $\boldsymbol{\varepsilon}_h$ instead of \mathbf{v}_h and the discrete current density \mathbf{J}^{\parallel} in place of \mathbf{J}^{\perp} yields

$$\begin{aligned} C \|\text{curl}_h \boldsymbol{\varepsilon}_h\|_{\mathcal{F}_h}^2 &\leq [\text{curl}_h \boldsymbol{\varepsilon}_h, \text{curl}_h \boldsymbol{\varepsilon}_h]_{\mathcal{F}_h} \\ &= [\text{curl}_h \mathbf{u}^{\perp}, \text{curl}_h \boldsymbol{\varepsilon}_h]_{\mathcal{F}_h} - [\text{curl}_h \mathbf{u}_h, \text{curl}_h \boldsymbol{\varepsilon}_h]_{\mathcal{F}_h} \\ &= \mathbb{T}_1 - [\mathbf{J}^{\parallel}, \boldsymbol{\varepsilon}_h]_{\mathcal{E}_h} = \mathbb{T}_1 - [\widetilde{\text{curl}}_h \boldsymbol{\psi}_J^{\parallel}, \boldsymbol{\varepsilon}_h]_{\mathcal{E}_h} \\ &= \mathbb{T}_1 - \mathbb{T}_2. \end{aligned} \quad (7.61)$$

Let $\mathbf{v} = \text{curl} \mathbf{u}$. Let $\mathbf{v}_{0,P}$ be the piecewise constant function defined on P whose value is the cell-average of \mathbf{v} on P and $(\mathbf{v}_{0,P})_P^{\perp} = ((\mathbf{v}_{0,P})_f^{\perp})_{f \in \partial P}$ its local projection on $\mathcal{F}_{h,P}$. Let $\boldsymbol{\varepsilon}_P = \boldsymbol{\varepsilon}_h|_P$. We split term \mathbb{T}_1 into the sum of the local contributions from each mesh cell, then use the commutative property stated by Lemma 2.2, i.e., $\text{curl}_P \mathbf{u}_P^{\perp} = (\text{curl} \mathbf{u})_P^{\perp} = \mathbf{v}_P^{\perp}$, and finally add and subtract $(\mathbf{v}_{0,P})_P^{\perp}$ to obtain:

$$\begin{aligned} \mathbb{T}_1 &= \sum_{P \in \Omega_h} [\text{curl}_P \mathbf{u}_P^{\perp}, \text{curl}_P \boldsymbol{\varepsilon}_P]_{\mathcal{F}_{h,P}} = \sum_{P \in \Omega_h} [(\text{curl} \mathbf{u})_P^{\perp}, \text{curl}_P \boldsymbol{\varepsilon}_P]_{\mathcal{F}_{h,P}} \\ &= \sum_{P \in \Omega_h} \left([(\mathbf{v}_P^{\perp} - \mathbf{v}_{0,P})_P^{\perp}, \text{curl}_P \boldsymbol{\varepsilon}_P]_{\mathcal{F}_{h,P}} + [(\mathbf{v}_{0,P})_P^{\perp}, \text{curl}_P \boldsymbol{\varepsilon}_P]_{\mathcal{F}_{h,P}} \right) \\ &= \mathbb{T}_{1a} + \mathbb{T}_{1b}. \end{aligned} \quad (7.62)$$

In view of the Cauchy-Schwarz inequality, we have

$$\begin{aligned} |\mathbb{T}_{1a}| &\leq C \left(\sum_{P \in \Omega_h} \|(\mathbf{v} - \mathbf{v}_{0,P})_P^{\perp}\|_{\mathcal{F}_{h,P}}^2 \right)^{1/2} \left(\sum_{P \in \Omega_h} \|\text{curl}_h \boldsymbol{\varepsilon}_P\|_{\mathcal{F}_{h,P}}^2 \right)^{1/2} \\ &= C \left(\sum_{P \in \Omega_h} \|(\mathbf{v} - \mathbf{v}_{0,P})_P^{\perp}\|_{\mathcal{F}_{h,P}}^2 \right)^{1/2} \|\text{curl}_h \boldsymbol{\varepsilon}_h\|_{\mathcal{F}_h}. \end{aligned} \quad (7.63)$$

The spectral bound on the mimetic inner product $[\cdot, \cdot]_{\mathcal{F}_{h,P}}$ gives:

$$\|(\mathbf{v} - \mathbf{v}_{0,P})_P^{\perp}\|_{\mathcal{F}_{h,P}}^2 \leq C|P| \sum_{f \in \partial P} |(\mathbf{v} - \mathbf{v}_{0,P})_f^{\perp}|^2$$

for some constant C independent of h . Now, we apply the Agmon's inequality **(M4)** and the approximation result **(M5)** to each component of function \mathbf{v} and we have

$$\begin{aligned} |P| \|(\mathbf{v} - \mathbf{v}_0)_f^{\perp}\|^2 &= \frac{|P|}{|f|^2} \int_f (\mathbf{v} - \mathbf{v}_0) \cdot \mathbf{n}_f dS \leq Ch_P \| \mathbf{v} - \mathbf{v}_0 \|_{L^2(f)}^2 \\ &\leq C \left(\| \mathbf{v} - \mathbf{v}_0 \|_{L^2(P)}^2 + h_P^2 | \mathbf{v} |_{H^1(P)}^2 \right) \leq Ch_P^2 | \mathbf{v} |_{H^1(P)}^2. \end{aligned} \quad (7.64)$$

Combining the last three estimates, we obtain

$$|\mathbb{T}_{1a}| \leq Ch \|\mathbf{u}\|_{H^2(\Omega)} \|\operatorname{curl}_h \boldsymbol{\varepsilon}_h\|_{\mathcal{F}_h}. \quad (7.65)$$

Let $\mathbf{v}_1(\mathbf{x}) = \frac{1}{2} \mathbf{v}_{0,P} \times (\mathbf{x} - \mathbf{x}_P)$, so that $\mathbf{v}_{0,P} = \operatorname{curl} \mathbf{v}_1$. In view of property **(R1)** of the reconstruction operator $R_P^\mathcal{E}$ it holds that $\boldsymbol{\varepsilon}_P = (R_P^\mathcal{E}(\boldsymbol{\varepsilon}_P))_P^\perp$. We use the commutative property stated by Lemma 2.2 to obtain:

$$\operatorname{curl}_P \boldsymbol{\varepsilon}_P = \operatorname{curl}_P (R_P^\mathcal{E}(\boldsymbol{\varepsilon}_P))_P^\perp = (\operatorname{curl} R_P^\mathcal{E}(\boldsymbol{\varepsilon}_P))_P^\perp, \quad (7.66)$$

where the last projection operator acts to space $\mathcal{F}_{h,P}$. Now, we split \mathbb{T}_{1b} in the sum of the local contributions from each cell P , then substitute $\mathbf{v}_{0,P} = \operatorname{curl} \mathbf{v}_1$, use (7.66), and finally apply the consistency condition of Lemma 7.3:

$$\begin{aligned} |\mathbb{T}_{1b}| &= \sum_{P \in \Omega_h} [(\mathbf{v}_{0,P})_P^\perp, \operatorname{curl}_P \boldsymbol{\varepsilon}_P]_{\mathcal{F}_{h,P}} = \sum_{P \in \Omega_h} [(\operatorname{curl} \mathbf{v}_1)_P^\perp, (\operatorname{curl} R_P^\mathcal{E}(\boldsymbol{\varepsilon}_P))_P^\perp]_{\mathcal{F}_{h,P}} \\ &= \sum_{P \in \Omega_h} \int_P \mu_P^{-1} \operatorname{curl} \mathbf{v}_1 \cdot \operatorname{curl} R_P^\mathcal{E}(\boldsymbol{\varepsilon}_P) dV. \end{aligned} \quad (7.67)$$

Then, we add and subtract $\mathbf{v} = \operatorname{curl} \mathbf{u}$ and note that $\operatorname{curl}(\mathbf{v}_1 - \mathbf{u}) = \mathbf{v}_{0,P} - \mathbf{v}$:

$$\begin{aligned} |\mathbb{T}_{1b}| &= \sum_{P \in \Omega_h} \left(\int_P \mu_P^{-1} \operatorname{curl}(\mathbf{v}_1 - \mathbf{u}) \cdot \operatorname{curl} R_P^\mathcal{E}(\boldsymbol{\varepsilon}_P) dV + \int_P \mu_P^{-1} \operatorname{curl} \mathbf{u} \cdot \operatorname{curl} R_P^\mathcal{E}(\boldsymbol{\varepsilon}_P) dV \right) \\ &= \sum_{P \in \Omega_h} \left(\int_P \mu_P^{-1} (\mathbf{v}_0 - \mathbf{v}) \cdot \operatorname{curl} R_P^\mathcal{E}(\boldsymbol{\varepsilon}_P) dV + \int_P \mu_P^{-1} \operatorname{curl} \mathbf{u} \cdot \operatorname{curl} R_P^\mathcal{E}(\boldsymbol{\varepsilon}_P) dV \right) \\ &= \mathbb{T}_{1c} + \mathbb{T}_{1d}. \end{aligned} \quad (7.68)$$

Each integral in \mathbb{T}_{1c} is bounded using the Cauchy-Schwarz inequality, the assumption that μ_P is uniformly bounded from above and below, the approximation results **(M5)**, and property **(L6)**:

$$|\mathbb{T}_{1c}| \leq C \sum_{P \in \Omega_h} \|\mathbf{v}_0 - \mathbf{v}\|_{L^2(P)} \|\operatorname{curl} R_P^\mathcal{E}(\boldsymbol{\varepsilon}_P)\|_{L^2(P)} \leq Ch \|\mathbf{u}\|_{H^2(\Omega)} \|\operatorname{curl}_h \boldsymbol{\varepsilon}_h\|_{\mathcal{F}_h},$$

where all constants denoted by C are independent of h and may depend only on the mesh shape regularity constants and the approximation constant of **(M5)**.

Let $\boldsymbol{\psi}_0$ be a piecewise constant function on mesh Ω_h with values $\boldsymbol{\psi}_{0,P}$ on cell P . We define $\boldsymbol{\psi}_{0,P}$ as the L^2 projection of the vector potential $\boldsymbol{\psi}_J$ onto $\mathbb{P}_0(P)$. Let $\boldsymbol{\psi}_1(\mathbf{x}) = \frac{1}{2} (\mu_P \boldsymbol{\psi}_{0,P}) \times (\mathbf{x} - \mathbf{x}_P)$. Using again (7.66) and the consistency condition in Lemma 7.3, the same argument used to develop \mathbb{T}_{1b} gives the identities:

$$\begin{aligned} \int_P \boldsymbol{\psi}_{0,P} \cdot \operatorname{curl} R_P^\mathcal{E}(\boldsymbol{\varepsilon}_P) dV &= \int_P \mu_P^{-1} \operatorname{curl} \boldsymbol{\psi}_1 \cdot \operatorname{curl} R_P^\mathcal{E}(\boldsymbol{\varepsilon}_P) dV \\ &= [(\operatorname{curl} \boldsymbol{\psi}_1)_P^\perp, (\operatorname{curl} R_P^\mathcal{E}(\boldsymbol{\varepsilon}_P))_P^\perp]_{\mathcal{F}_{h,P}} \\ &= [(\boldsymbol{\psi}_{0,P})_P^\perp, \operatorname{curl}_h \boldsymbol{\varepsilon}_P]_{\mathcal{F}_{h,P}}. \end{aligned} \quad (7.69)$$

Using Eq. (7.50) with $\mathbf{v} = R^\mathcal{E}(\boldsymbol{\varepsilon}_h)$, the observation that $p = 0$, and $\mathbf{J} = \text{curl } \boldsymbol{\psi}_J$, we obtain

$$T_{1d} = \int_{\Omega} \mu^{-1} \text{curl } \mathbf{u} \cdot \text{curl } R^\mathcal{E}(\boldsymbol{\varepsilon}_h) dV = \int_{\Omega} \mathbf{J} \cdot R^\mathcal{E}(\boldsymbol{\varepsilon}_h) dV = \int_{\Omega} \text{curl } \boldsymbol{\psi}_J \cdot R^\mathcal{E}(\boldsymbol{\varepsilon}_h) dV.$$

Then, we split the integral in the sum of the local contributions from each cell P , and we integrate by parts

$$T_{1d} = \sum_{P \in \Omega_h} \int_P \text{curl } \boldsymbol{\psi}_J \cdot R_P^\mathcal{E}(\boldsymbol{\varepsilon}_P) dV = \sum_{P \in \Omega_h} \int_P \boldsymbol{\psi}_J \cdot \text{curl } R_P^\mathcal{E}(\boldsymbol{\varepsilon}_P) dV.$$

The last step holds because the sum of the boundary terms of ∂P is zero. Indeed, the internal faces gives integrands with opposite signs, while on the mesh faces of the domain boundary $R_P^\mathcal{E}(\boldsymbol{\varepsilon}_h)$ is zero as it interpolates all zero values. Finally, we split T_2 in the sum of the local contributions from each cell P , combine terms T_{1d} and T_2 together, and subtract both sides of (7.69) to obtain

$$T_{1d} - T_2 = \sum_{P \in \Omega_h} \left(\int_P (\boldsymbol{\psi}_J - \boldsymbol{\psi}_{0,P}) \cdot \text{curl } R_P^\mathcal{E}(\boldsymbol{\varepsilon}_P) dV - \left[(\boldsymbol{\psi}_J - \boldsymbol{\psi}_{0,P}) \Big|_P, \text{curl}_P \boldsymbol{\varepsilon}_P \right]_{\mathcal{F}_h, P} \right) = T_{2a} - T_{2b}.$$

Term T_{2a} is bounded like term T_{1c} . Term T_{2b} is bounded like term T_{1a} . Thus,

$$|T_{2a}| + |T_{2b}| \leq Ch |\boldsymbol{\psi}_J|_{H^1(\Omega)} \|\text{curl}_h \boldsymbol{\varepsilon}_h\|_{\mathcal{F}_h}.$$

The assertion of the theorem follows by combining all estimates in (7.61). \square

Remark 7.4. Extension of error analysis to the L^2 norm is currently a work in progress. It requires to prove the discrete Maxwell inequality stating that for any mesh function $\mathbf{v}_h \in \mathcal{E}_h^0$ we have

$$\|\mathbf{v}_h\|_{\mathcal{E}_h} \leq C (\|\text{curl}_h \mathbf{v}_h\|_{\mathcal{F}_h} + \|\widetilde{\text{div}}_h \mathbf{v}_h\|_{\mathcal{V}_h}),$$

with constant C independent of \mathbf{v}_h and the mesh.

The Stokes problem

When working toward the solution of a problem, it always helps to know the answer. Provided, of course, you know there is a problem.
(Known as the “rule of accuracy”)

The incompressible Stokes problem for the vector field \mathbf{u} and the scalar pressure field p is governed by the following equations:

$$-\operatorname{div}(\nu \boldsymbol{\varepsilon}(\mathbf{u})) + \nabla p = \mathbf{b} \quad \text{in } \Omega, \quad (8.1)$$

$$\operatorname{div} \mathbf{u} = 0 \quad \text{in } \Omega, \quad (8.2)$$

$$\mathbf{u} = \mathbf{g}^D \quad \text{on } \Gamma^D, \quad (8.3)$$

$$\nu \boldsymbol{\varepsilon}(\mathbf{u}) \cdot \mathbf{n} = \mathbf{g}^N \quad \text{on } \Gamma^N, \quad (8.4)$$

where $\nu > 0$ is the fluid viscosity, the vector-valued field \mathbf{b} is the forcing term, the vector-valued fields \mathbf{g}^D and \mathbf{g}^N are the boundary data, and $\boldsymbol{\varepsilon}(\mathbf{u}) = (\nabla \mathbf{u} + (\nabla \mathbf{u})^T)/2$ is the symmetric strain tensor. We refer the reader to Sect. 1.5.1 for a more detailed presentation of the Stokes problem.

The numerical approximation of the Stokes problem with the finite element and the finite volume methods has raised much attention in the literature over the years. Since it is impossible to mention all the papers on the subject, we cite only [31, 59, 95, 125, 173, 204, 332] and address the reader to the references in [88] for a more complete list. From the numerical standpoint, the main difficulty in the approximation of the Stokes problem is the incompressibility condition (8.2). An abrupt approach most certainly leads to a bad approximation and possibly spurious pressure modes. In stable finite elements (that satisfy the inf-sup condition), the discrete spaces for \mathbf{u} and p are chosen carefully in order to derive a stable and converging scheme, see for example [88]. Other viable numerical approaches leading to good results use a stabilization technique, see e.g. [175].

The Stokes problem is a starting point for more complex models such as the Navier-Stokes equations [184]. It moreover shares similar numerical difficulties with the displacement-pressure formulation of incompressible and almost-incompressible elasticity (see Sect. 9.1).

In this chapter, we will introduce and analyze a mimetic discretization the Stokes problem. It does not adopt any stabilization procedure and the robustness of the resulting scheme follows from a careful choice of the degrees of freedom. The mimetic scheme presented here will be extended to the linear elasticity problem in Sect. 9.1. We will also present a modified mimetic scheme which attains the same convergence rate but uses a smaller number of degrees of freedom. The discussion in this chapter is mainly based on [46, 47, 49].

8.1 The mimetic formulation

In this section, we mostly focus on the three-dimensional case. A two-dimensional scheme can be derived in a straightforward way by repeating the presented arguments using mesh edges in place of mesh faces. Without loss of generality, when the viscosity ν in (8.1) is constant, we assume that its value equals to one.

Let us consider the functional space $V = (H^1(\Omega))^3$ and its subspace

$$V_{\mathbf{g}} = \mathbf{u} \in V \text{ such that } \mathbf{u} = \mathbf{g} \text{ on } \Gamma^D. \quad (8.5)$$

The space Q of admissible pressures depends on the Neumann boundary condition:

$$Q = \begin{cases} L^2(\Omega) & \text{if } \Gamma^N \neq \emptyset, \\ L_0^2(\Omega) & \text{if } \Gamma^N = \emptyset, \end{cases} \quad (8.6)$$

where

$$L_0^2(\Omega) \equiv L^2(\Omega)/\mathbb{R} = \left\{ q \in L^2(\Omega) : \int_{\Omega} q dV = 0 \right\}.$$

By multiplying equations (8.1)–(8.2) by the test functions $\mathbf{v} \in V_0$ and $q \in Q$, respectively, and integrating by parts we obtain their weak variational formulation:

Find $\mathbf{u} \in V_{\mathbf{g}^D}$ and $p \in Q$ such that

$$\int_{\Omega} \mathbf{v} \boldsymbol{\varepsilon}(\mathbf{u}) : \boldsymbol{\varepsilon}(\mathbf{v}) dV - \int_{\Omega} p \operatorname{div} \mathbf{v} dV = \langle \mathbf{b}, \mathbf{v} \rangle_{\Omega} + \langle \mathbf{g}^N, \mathbf{v} \rangle_{\Gamma^N} \quad \forall \mathbf{v} \in V_0, \quad (8.7)$$

$$\int_{\Omega} q \operatorname{div} \mathbf{u} dV = 0 \quad \forall q \in Q, \quad (8.8)$$

where the symbol “:” stands for the standard contraction operator between two tensors.

8.1.1 Degrees of freedom and projection operators

To discretize (8.7)–(8.8), we select the following degrees of freedom for scalar and vector functions.

- The space of discrete scalar fields \mathcal{P}_h is defined by attaching one degree of freedom to every mesh cell. The value of $q_h \in \mathcal{P}_h$ associated with cell P is denoted by q_P :

$$q_h = (q_P)_{P \in \Omega_h}.$$

- The space of discrete vector fields $X_h = (\mathcal{V}_h)^3 \times \mathcal{F}_h$ is defined by attaching three degrees of freedom to each mesh vertex and one degree of freedom to each mesh face. For $\mathbf{v}_h \in X_h$, the values associated with vertex v form a three-dimensional vector denoted by \mathbf{v}_v and the value associated with face f is denoted by v_f :

$$\mathbf{v}_h = (\mathbf{v}_v, v_f)_{v \in \mathcal{V}_h, f \in \mathcal{F}_h}.$$

Remark 8.1. In two-dimensions, a similar definition of the degrees of freedom associates two numbers with each mesh vertex and one number with each edge. This is sufficient to define, for each edge, a unique vector-valued function that has a linear tangential and a quadratic normal components.

The dimension of space \mathcal{P}_h equals to the number of mesh elements. This space can be identified with the space of piecewise constant functions defined on Ω_h . We consider the cell-based projection operator $\Pi^{\mathcal{P}} : L^1(\Omega) \rightarrow \mathcal{P}_h$ defined by (2.17):

$$q_P^I := q^I|_P = \frac{1}{|P|} \int_P q dV. \quad (8.9)$$

To ease the notation, we will use the symbol $(\cdot)^I$ for this operator, i.e. $q^I = \Pi^{\mathcal{P}}(q)$.

The dimension of space X_h equals to three times the number of mesh vertices plus the number of mesh faces. We assume that for every face f there exists a set of non-negative weights $\{\omega_{f,v}\}_{v \in \partial f}$ associated with the vertices v of f such that

$$\sum_{v \in \partial f} \omega_{f,v} = |f| \quad \text{and} \quad \sum_{v \in \partial f} (\mathbf{x}_v - \mathbf{x}_f) \omega_{f,v} = 0, \quad (8.10)$$

where \mathbf{x}_v is the position vector of vertex v and \mathbf{x}_f is the centroid of face f . For instance, we can determine this set of weights by taking coefficients in the well known expression of \mathbf{x}_f as a linear combination of $\{\mathbf{x}_v\}$.

Remark 8.2. In two dimensions, a natural choice for the weights is provided by the trapezoidal rule, i.e., $\omega_{e,v} = |e|/2$.

Remark 8.3. This set of weights satisfies the conditions **(Q1.AB)**, see Chap. 6, after Remark 6.4. By using these weights, we can derive a second-order accurate approximation of integrals over face f . \square

The degrees of freedom of X_h contains both nodal and face values. Due to this the projection operator $(\cdot)^{\mathbb{H}}$ from $(H^1(\Omega))^3 \cap (C^0(\overline{\Omega}))^3$ into X_h is a combination of two

projection operators $\Pi^{\mathcal{V}}$ and $\Pi^{\mathcal{F}}$ introduced in Chap. 2. We define it in two steps. In the first step we define the nodal and face projection operators.

- For any $\mathbf{v} \in (H^1(\Omega))^3 \cap (C^0(\overline{\Omega}))^3$, the *nodal projection operator* returns vector $\mathbf{v}^I \in X_h$ such that

$$\mathbf{v}_v^I = \mathbf{v}|_v = \mathbf{v}(\mathbf{x}_v) \quad \forall v \in \mathcal{V} \quad \text{and} \quad v_f^I = \mathbf{v}|_f = 0 \quad \forall f \in \mathcal{F}. \quad (8.11)$$

- The *face projection operator* returns vector $\mathbf{v}^b \in X_h$ such that

$$\mathbf{v}_v^b = \mathbf{v}|_v = 0 \quad \forall v \in \mathcal{V} \quad (8.12)$$

and the face-based components $v_f^b = \mathbf{v}^b|_f$ are defined by the relation:

$$\int_f \mathbf{v} \cdot \mathbf{n}_f dS = \sum_{v \in \partial f} \mathbf{v}(\mathbf{x}_{f,v}) \cdot \mathbf{n}_f \omega_{f,v} + |f| v_f^b \quad \forall f \in \mathcal{F}. \quad (8.13)$$

In the second step, we define the aforementioned projection operator:

$$\mathbf{v}^{\mathbb{I}} = \mathbf{v}^I + \mathbf{v}^b. \quad (8.14)$$

The vector $\mathbf{v}^{\mathbb{I}}$ clearly satisfies:

$$\mathbf{v}_v^{\mathbb{I}} = \mathbf{v}_v^I \quad \forall v \in \mathcal{V} \quad \text{and} \quad v_f^{\mathbb{I}} = v_f^b \quad \forall f \in \mathcal{F}.$$

As the integration rule provided by the face weights $\{\omega_{f,v}\}$ is exact for linear functions, we see from (8.13) that $\mathbf{\psi}^b = 0$ for any linear function $\mathbf{\psi} \in (\mathbb{P}_1(\mathbb{P}))^3$. Therefore,

$$\mathbf{\psi}^{\mathbb{I}} = \mathbf{\psi}^I \quad \forall \mathbf{\psi} \in (\mathbb{P}_1(\mathbb{P}))^3. \quad (8.15)$$

Boundary conditions. For the numerical treatment of the Dirichlet boundary condition (8.3), we need the subspaces $X_{h,\mathbf{g}}$ and $X_{h,0}$ of X_h . A mesh function $\mathbf{v}_h \in X_{h,\mathbf{g}}$ if

- $\mathbf{v}_v = \mathbf{g}^D(\mathbf{x}_v)$ for every $v \in \Gamma^D$;
- v_f is given by

$$\int_f \mathbf{g}^D \cdot \mathbf{n}_f dS = \sum_{v \in \partial f} \mathbf{g}^D(\mathbf{x}_{f,v}) \cdot \mathbf{n}_f \omega_{f,v} + |f| v_f \quad \forall f \subset \Gamma^D.$$

The subspace $X_{h,0}$ is defined by setting $\mathbf{g}^D = 0$. When $\Gamma^D = \Gamma$, i.e. $\Gamma^N = \emptyset$, instead of $L^2(\Omega)$, we consider the space of pressures with zero average on Ω denoted by $L_0^2(\Omega)$. If $q \in L_0^2(\Omega)$, we have

$$0 = \int_{\Omega} q dV = \sum_{P \in \Omega_h} \int_P q dV = \sum_{P \in \Omega_h} |P| q_P^I.$$

In the discrete setting, instead of \mathcal{P}_h we consider its subspace $\mathcal{P}_{h,0}$ formed by projection of functions from $L^2_0(\Omega)$ to \mathcal{P}_h :

$$\mathcal{P}_{h,0} = \left\{ q_h \in \mathcal{P}_h : \sum_{P \in \Omega_h} |P| q_P = 0 \right\}.$$

Consistently with (8.6), we define the discrete space

$$Q_h = \begin{cases} \mathcal{P}_h & \text{if } \Gamma^N \neq \emptyset, \\ \mathcal{P}_{h,0} & \text{if } \Gamma^N = \emptyset. \end{cases} \quad (8.16)$$

As usual, we will indicate the restrictions of the degrees of freedom to a geometrical object by using either one or two indices. For instance, given $P \in \Omega_h$, the symbol $X_{h,P}$ represents $X_h|_P$, while \mathbf{v}_P represents $\mathbf{v}_h|_P$, $\mathbf{v}_h \in X_h$. The symbol $\mathbf{v}_{P,v}$ indicates the degrees of freedom related to vertex v for $\mathbf{v}_P \in X_{h,P}$.

8.1.2 Mimetic operators, inner products and bilinear forms

We endow the space Q_h with the inner product constructed in Sect. 3.4:

$$[p_h, q_h]_{Q_h} = \sum_{P \in \Omega_h} |P| p_P q_P \quad \forall p_h, q_h \in Q_h. \quad (8.17)$$

Formula (8.17) can be interpreted as the $L^2(\Omega)$ inner product of piecewise constant functions on Ω_h . This inner product induces the following norm:

$$\|q\|_{Q_h} = [q_h, q_h]_{Q_h}^{1/2} \quad \forall q_h \in Q_h. \quad (8.18)$$

A discrete bilinear form on $X_h \times X_h$ is defined by the summation of local discrete bilinear forms:

$$\mathcal{A}_h(\mathbf{u}_h, \mathbf{v}_h) = \sum_{P \in \Omega_h} \mathcal{A}_{h,P}(\mathbf{u}_P, \mathbf{v}_P) \quad \forall \mathbf{u}_h, \mathbf{v}_h \in X_h.$$

It requires a proper definition of the *mimetic* bilinear form $\mathcal{A}_{h,P} : X_{h,P} \times X_{h,P} \rightarrow \mathbb{R}$ that approximates the continuum form and satisfies the stability and consistency conditions (see Sect. 8.1.4). For sufficiently regular functions \mathbf{u} , \mathbf{v} , and the related projections \mathbf{u}_P^\parallel , \mathbf{v}_P^\parallel , we have

$$\mathcal{A}_{h,P}(\mathbf{u}_P, \mathbf{v}_P) \approx \int_P \mathbf{v} \boldsymbol{\varepsilon}(\mathbf{u}) : \boldsymbol{\varepsilon}(\mathbf{v}) dV. \quad (8.19)$$

We will show the construction of the bilinear form $\mathcal{A}_{h,P}$ in Sect. 8.1.4. The discrete divergence operator $\text{div}_h : X_h \rightarrow \mathcal{P}_h$ is the primary mimetic operator and its definition follows from the divergence theorem:

$$\frac{1}{|P|} \int_P \text{div} \mathbf{v} dV = \sum_{f \in \partial P} \int_f \mathbf{v} \cdot \mathbf{n}_{P,f} dS.$$

By using the face weights $\{\omega_{f,v}\}$, for any $\mathbf{v}_h \in X_h$, we define

$$\operatorname{div}_h \mathbf{v}_h = (\operatorname{div}_P \mathbf{v}_P)_{P \in \mathcal{P}}, \quad \operatorname{div}_P \mathbf{v}_P = \frac{1}{|P|} \sum_{f \in \partial P} s_{P,f} \left(\sum_{v \in \partial f} \mathbf{v}_{f,v} \cdot \mathbf{n}_f \omega_{f,v} + |f| v_f \right), \quad (8.20)$$

where $s_{P,f} = \mathbf{n}_f \cdot \mathbf{n}_{P,f}$. The consistency of this definition with the Gauss theorem is reflected in the commuting property that we state for future reference in the following lemma.

Lemma 8.1. *The projection and the divergence operators commute for every sufficiently regular vector-valued function \mathbf{v} :*

$$\operatorname{div}_h \mathbf{v}^{\mathbb{I}} = (\operatorname{div} \mathbf{v})^{\mathbb{I}}. \quad (8.21)$$

Proof. Using definition (8.20), we start the following developments:

$$\begin{aligned} \operatorname{div}_P \mathbf{v}_P^{\mathbb{I}} &= \frac{1}{|P|} \sum_{f \in \partial P} s_{P,f} \left(\sum_{v \in \partial f} \mathbf{v}_{f,v} \cdot \mathbf{n}_f \omega_{f,v} + |f| v_f \right) \quad [\text{use (8.13)}] \\ &= \frac{1}{|P|} \sum_{f \in \partial P} s_{P,f} \int_f \mathbf{v} \cdot \mathbf{n}_f dS \quad [\text{use Gauss theorem}] \\ &= \frac{1}{|P|} \int_P \operatorname{div} \mathbf{v} dV \quad [\text{use (8.9)}] \\ &= (\operatorname{div} \mathbf{v})_P^{\mathbb{I}}. \end{aligned}$$

This proves the assertion of the lemma. □

Remark 8.4. The incompressibility condition (8.2) implies that the velocity solution \mathbf{u} satisfies

$$\operatorname{div}_h \mathbf{u}^{\mathbb{I}} = (\operatorname{div} \mathbf{u})^{\mathbb{I}} = 0. \quad (8.22)$$

8.1.3 Discrete strong and weak formulations

The conventional mimetic approach leads to a strong form of discrete equations. It requires two pairs of primary and derived mimetic operators and three approximation spaces; therefore, it is less efficient than the approach based on a weak formulation. However, there exist applications where the closed form representation of the derived operators is needed. The strong formulation will be derived for the case of constant viscosity ν , Dirichlet boundary conditions and $X_h = (\mathcal{V}_h)^3$. Under the above conditions, it is well known that the first operator in (8.1) can be replaced by the vector Laplacian operator $\nu \Delta$. Note that while the first assumption is considered only for the sake of a simpler exposition, the remaining conditions are not immediate to handle with the strong formulation; this is one of the reasons why we will focus on the weak formulation for the rest of the chapter.

Let us define an inner product $[\cdot, \cdot]_{X_h}$ in space X_h as the generalization to the vector case of the inner product in space \mathcal{Y}_h described in Chap. 3. The trivial generalization consists in applying this inner product to each component of the velocity vector. The derived gradient operator $\widetilde{\nabla}_h : X_h \rightarrow \mathcal{Q}_h$, dual to the primary mimetic operator (8.20) is given through the duality relationship;

$$[\widetilde{\nabla}_h q_h, \mathbf{v}_h]_{X_h} = [q_h, \operatorname{div}_h \mathbf{v}_h]_{\mathcal{Q}_h} \quad \forall q_h \in \mathcal{Q}_h, \mathbf{v}_h \in X_h.$$

The mimetic discretization of the vector Laplacian starts with writing it as a combination of two first-order operators:

$$\Delta \mathbf{u} \implies \boldsymbol{\sigma} = \operatorname{div} \mathbf{u}, \quad \boldsymbol{\sigma} = \nabla \mathbf{u}.$$

We select discrete gradient $\nabla_h : X_h \rightarrow \mathcal{E}_h^3$ as the primary mimetic operator. Let $\Sigma_h = \mathcal{E}_h^3$. Again ∇_h is the trivial generalization to the vector case of the similar operator defined in (2.18). The inner product in space Σ_h is define by replicating three times the inner product in space \mathcal{E}_h derived in Chap. 3. The vector case of the derived divergence operator is given by the discrete duality relationship:

$$[\boldsymbol{\sigma}_h, \nabla_h \mathbf{v}_h]_{\Sigma_h} = [\widetilde{\operatorname{div}}_h \boldsymbol{\sigma}_h, \mathbf{v}_h]_{X_h} \quad \forall \boldsymbol{\sigma}_h \in \Sigma_h, \forall \mathbf{v}_h \in X_h.$$

Once the above ingredients have been established, the mimetic approximation of the Stokes problems (8.1)–(8.2) reads:

Find $\mathbf{u}_h \in X_{h,g}$ and $p_h \in \mathcal{Q}_h$ such that:

$$\begin{aligned} -v \widetilde{\operatorname{div}}_h \nabla_h \mathbf{u}_h + \widetilde{\nabla}_h p_h &= \mathbf{b}^I, \\ \operatorname{div}_h \mathbf{u}_h &= 0. \end{aligned}$$

The nodal approximation of the vector Laplacian provided by this construction requires to know only the part of the inner product in Σ_h restricted to gradients of mesh functions in X_h . A more efficient construction of this operator is discussed in the rest of this chapter using a different framework.

Remark 8.5. The above strong formulation may be unstable on some meshes. In two dimensions, a stable scheme is obtained through the enrichment of space \mathcal{Y}_h by adding additional mesh vertices to the selected mesh edges, see Sect. 8.3. In three dimensions, additional velocity unknowns can be introduced on mesh faces (like in the weak formulation) and the primary gradient operator can be generalized accordingly.

Now we drop-off all assumptions made for the strong formulation. Let us consider the weights $\{\omega_{f,v}\}_{v \in \partial f}$ in (8.10). Similarly, for every P there exists a set of non-negative weights $\{\omega_{P,v}\}_{v \in \partial P}$ associated with the vertices v of P such that

$$\sum_{v \in \partial P} \omega_{P,v} = |P| \quad \text{and} \quad \sum_{v \in \partial P} (\mathbf{x}_v - \mathbf{x}_P) \omega_{P,v} = 0, \quad (8.23)$$

where \mathbf{x}_P is the centroid of P . Using these weights, we define two linear operators that represent the loading and the Neumann boundary condition terms:

$$(\mathbf{b}, \mathbf{v}_h)_h = \sum_{P \in \Omega_h} \left(\frac{1}{|\mathbf{P}|} \int_P \mathbf{b} dV \right) \cdot \sum_{\mathbf{v} \in \mathcal{V}_P} \mathbf{v}_{P,\mathbf{v}} \omega_{P,\mathbf{v}}, \quad (8.24)$$

$$\langle \mathbf{g}^N, \mathbf{v}_h \rangle_h = \sum_{f \in \mathcal{F}^\partial \cap \Gamma^N} \left(\frac{1}{|f|} \int_f \mathbf{g}^N dV \right) \cdot \sum_{\mathbf{v} \in \partial f} \mathbf{v}_{P,\mathbf{v}} \omega_{f,\mathbf{v}}, \quad (8.25)$$

The mimetic discretization of the Stokes problem reads:

Find $\mathbf{u}_h \in X_{h,\mathbf{g}}$ and $p_h \in Q_h$ such that:

$$\mathcal{A}_h(\mathbf{u}_h, \mathbf{v}_h) - [\operatorname{div}_h \mathbf{v}_h, p_h]_{Q_h} = (\mathbf{b}, \mathbf{v}_h)_h + \langle \mathbf{g}^N, \mathbf{v}_h \rangle_h \quad \forall \mathbf{v}_h \in X_{h,0}, \quad (8.26)$$

$$[\operatorname{div}_h \mathbf{u}_h, q_h]_{Q_h} = 0 \quad \forall q_h \in Q_h. \quad (8.27)$$

Remark 8.6. Since $\operatorname{div}_h \mathbf{u}_h \in \mathcal{P}_h$, we obtain immediately the identity $\operatorname{div}_h \mathbf{u}_h = 0$ which is the discrete counterpart of the incompressibility constraint (8.2).

8.1.4 Stability and consistency conditions

In this section, we derive the explicit representation of the discrete bilinear form $\mathcal{A}_{h,P}(\mathbf{u}_P, \mathbf{v}_P)$. First, we introduce the mesh-dependent semi-norm:

$$\begin{aligned} \|\mathbf{v}_h\|_{X_h}^2 &= \sum_{P \in \Omega_h} \|\mathbf{v}_P\|_{X_{h,P}}^2, \\ \|\mathbf{v}_P\|_{X_{h,P}}^2 &= \begin{cases} \sum_{e=(\mathbf{v},\mathbf{v}') \in \partial f} \frac{1}{2} \|\mathbf{v}_{\mathbf{v}'} - \mathbf{v}_{\mathbf{v}}\|^2 + |v_f|^2 & \text{if } d = 2, \\ \sum_{f \in \partial P} \left(|\mathbf{P}| \sum_{e=(\mathbf{v},\mathbf{v}') \in \partial f} \frac{1}{2} \frac{\|\mathbf{v}_{\mathbf{v}'} - \mathbf{v}_{\mathbf{v}}\|^2}{|e|^2} + h_P |v_f|^2 \right) & \text{if } d = 3, \end{cases} \end{aligned} \quad (8.28)$$

where \mathbf{v} and \mathbf{v}' are the end-points of edge e . This is the discrete H^1 -type semi-norm on space X_h and coincides with the semi-norm appearing in (6.15)–(6.16), except for terms that take into account the face degrees of freedom. Since it becomes a norm on the space $X_{h,0}$, we will often refer to it as a norm.

In the coming theoretical developments, we will also use a slightly weaker semi-norm. Let Θ represent the space of (linearized) rigid body rotations:

$$\Theta = \begin{cases} \operatorname{span} \{ (-y, x, 0)^T, (-z, 0, x)^T, (0, -z, y)^T \} & \text{if } d = 3, \\ \operatorname{span} \{ (-y, x)^T \} & \text{if } d = 2, \end{cases}$$

where x, y, z are the Cartesian coordinates with the origin at the centroid of P . Using the projector (8.14), we define

$$\|\mathbf{v}_h\|_{\tilde{X}_h}^2 = \sum_{P \in \Omega_h} \|\mathbf{v}_P\|_{\tilde{X}_{h,P}}^2 \quad \text{where} \quad \|\mathbf{v}_P\|_{\tilde{X}_{h,P}} = \inf_{\boldsymbol{\theta} \in \Theta} \|\mathbf{v}_P - \boldsymbol{\theta}_P\|_{\tilde{X}_{h,P}}. \quad (8.29)$$

Then, we require that the symmetric bilinear form $\mathcal{A}_{h,P}$ satisfies the stability and consistency conditions.

(S1) (*Stability conditions*). For every $\mathbf{v}_P \in X_{h,P}$ it holds:

$$\sigma_* \|\mathbf{v}_P\|_{X_{h,P}}^2 \leq \mathcal{A}_{h,P}(\mathbf{v}_P, \mathbf{v}_P) \leq \sigma^* \|\mathbf{v}_P\|_{X_{h,P}}^2,$$

where σ_* and σ^* are two positive constants independent of h and P .

This condition states that the bilinear form is coercive on a subspace of $X_{h,P}$. We employ the norm $\|\cdot\|_{X_{h,P}}$ and not $|||\cdot|||_{X_{h,P}}$, since the latter one does not have the correct kernel. Also, using $|||\cdot|||_{X_h}$ here would lead to a contradiction with the consistency condition below.

Let \mathbf{v}_P be a constant approximation of \mathbf{v} in cell P , e.g. $\mathbf{v}_P = \mathbf{v}(\mathbf{x}_P)$. We define the following space:

$$S_{h,P} = \left\{ \mathbf{v} \in (H^1(P) \cap C^0(P))^3 : \int_f \mathbf{v} \cdot \boldsymbol{\tau}_f dS = \sum_{\mathbf{v} \in \partial f} \mathbf{v}_\mathbf{v} \cdot \boldsymbol{\tau}_f \omega_{f,\mathbf{v}} \quad \forall f \in P, \forall \boldsymbol{\tau}_f \right\}.$$

According to the theory in Chap. 4, this space must satisfy three conditions **(B1)**–**(B3)**. The first one states that $S_{h,P}$ is rich enough, so that the local projection operator from $S_{h,P}$ to $X_{h,P}$ is surjective. The second condition states that this space has some approximation properties, e.g., it contains linear functions. The last condition must allow us to compute easily the consistency condition for any $\mathbf{v} \in S_{h,P}$. It can be checked that the selected space satisfies conditions **(B1)** and **(B2)**. Note in particular that condition **(B2)** follows from the fact that formula (8.10) is exact for linear functions.

(S2) (*Consistency Condition*). For every $\boldsymbol{\psi} \in (\mathbb{P}_1(P))^3$ and every $\mathbf{v} \in S_{h,P}$ there holds:

$$\mathcal{A}_{h,P}(\mathbf{v}_P^{\mathbb{I}}, \boldsymbol{\psi}_P^{\mathbb{I}}) = \int_P \mathbf{v}_P \boldsymbol{\varepsilon}(\mathbf{v}) : \boldsymbol{\varepsilon}(\boldsymbol{\psi}) dV, \quad (8.30)$$

The consistency condition is an exactness property, i.e., the discrete bilinear form returns the exact value when their arguments are the projections of a linear function and a function from $S_{h,P}$. To verify the condition **(B3)**, we integrate by parts in (8.30):

$$\mathcal{A}_{h,P}(\mathbf{v}_P^{\mathbb{I}}, \boldsymbol{\psi}_P^{\mathbb{I}}) = \sum_{f \in \partial P} \int_f \mathbf{v} \cdot (\mathbf{v}_P \boldsymbol{\varepsilon}(\boldsymbol{\psi}) \cdot \mathbf{n}_{P,f}) dS = \sum_{f \in \partial P} (\mathbf{v}_P \boldsymbol{\varepsilon}(\boldsymbol{\psi}) \cdot \mathbf{n}_{P,f}) \cdot \int_f \mathbf{v} dS. \quad (8.31)$$

Due to the linearity of the dot product, it is sufficient to enforce the integrability property of functions in $S_{h,P}$ for a fixed pair of orthonormal vectors $\boldsymbol{\tau}_{f,1}$ and $\boldsymbol{\tau}_{f,2}$ for each face f . Recall that

$$\mathbb{I}_{3 \times 3} = \mathbf{n}_f^T \mathbf{n}_f + \boldsymbol{\tau}_{f,1}^T \boldsymbol{\tau}_{f,1} + \boldsymbol{\tau}_{f,2}^T \boldsymbol{\tau}_{f,2}.$$

We use the definition of $S_{h,P}$ to integrate the tangential components of \mathbf{v} and the definition (8.13) to integrate its normal components:

$$\begin{aligned} \int_f \mathbf{v} dV &= \mathbf{n}_f \int_f \mathbf{v} \cdot \mathbf{n}_f dV + \boldsymbol{\tau}_{f,1} \int_f \mathbf{v} \cdot \boldsymbol{\tau}_{f,1} dV + \boldsymbol{\tau}_{f,2} \int_f \mathbf{v} \cdot \boldsymbol{\tau}_{f,2} dV \\ &= \sum_{f \in \partial P} \omega_{f,v} \mathbf{v}_v^\parallel + |f| v_f^\parallel \mathbf{n}_{P,f}. \end{aligned}$$

Inserting this into (8.31), we obtain:

$$\mathcal{A}_{h,P}(\mathbf{v}_P^\parallel, \boldsymbol{\psi}_P^\perp) = \sum_{f \in \partial P} \sum_{v \in \partial f} \mathbf{v}_v^\parallel \cdot (\nu_P \boldsymbol{\varepsilon}(\boldsymbol{\psi}) \cdot \mathbf{n}_{P,f}) \omega_{f,v} + |f| v_f^\parallel \mathbf{n}_f \cdot (\nu_P \boldsymbol{\varepsilon}(\boldsymbol{\psi}) \cdot \mathbf{n}_{P,f}). \quad (8.32)$$

The right-hand side of this formula depends on the degrees of freedom, cell geometry and fluid properties, e.g. it is computable.

Remark 8.7. Making use of (8.32) and recalling the surjectivity property **(B1)**, the consistency condition **(S2)** can be written in the following more practical form. For all $\mathbf{v}_P \in X_{h,P}$ and $\boldsymbol{\psi} \in (\mathbb{P}_1(P))^3$

$$\mathcal{A}_{h,P}(\mathbf{v}_P, \boldsymbol{\psi}_P^\perp) = \sum_{f \in \partial P} \sum_{v \in \partial f} \mathbf{v}_v \cdot (\nu_P \boldsymbol{\varepsilon}(\boldsymbol{\psi}) \cdot \mathbf{n}_{P,f}) \omega_{f,v} + |f| v_f \mathbf{n}_f \cdot (\nu_P \boldsymbol{\varepsilon}(\boldsymbol{\psi}) \cdot \mathbf{n}_{P,f}),$$

where we follow the usual notation $\mathbf{v}_h = (\mathbf{v}_v, v_f)_{v \in \partial P, f \in \partial P}$. The above condition shows that the space $S_{h,P}$ is only introduced for constructive reasons but does not appear in the practical definition of the bilinear form.

8.1.5 Formula for the stiffness matrix

Given $P \in \Omega_h$, the local stiffness matrix M_P satisfies

$$\mathcal{A}_{h,P}(\mathbf{u}_P, \mathbf{v}_P) = \mathbf{u}_P^T M_P \mathbf{v}_P \quad \forall \mathbf{u}_P, \mathbf{v}_P \in X_{h,P}.$$

The global stiffness matrix is assembled from these matrices in the usual manner.

Let $m = 3N_P^v + N_P^f$ be the number of degrees of freedom in cell P , i.e. the dimension of the discrete velocity space $X_{h,P}$. Let $\mathbf{p}_1, \mathbf{p}_2, \dots, \mathbf{p}_k$, with $k = d(d+1)$ form a basis for the space $(\mathbb{P}_1(P))^d$ of linear vector-valued functions. We assume that the first $k/2$ functions span the kernel of the symmetric gradient operator:

$$\boldsymbol{\varepsilon}(\mathbf{p}_i) = \mathbf{0} \quad i = 1, 2, \dots, d(d+1)/2. \quad (8.33)$$

Let $N_i = (\mathbf{p}_i)_P^\perp$. Using the basis functions in (8.32), we obtain

$$\mathcal{A}_{h,P}(\mathbf{v}_P, N_i) = \mathbf{v}_P^T M_P N_i = \mathbf{v}_P^T R_i \quad \forall \mathbf{v}_P \in X_{h,P}, \quad (8.34)$$

where $R_i = (R_{i,v}, R_{i,f})_{v \in P, f \in P}$ and

$$R_{i,v} = \sum_{f \ni v} (\nu_P \boldsymbol{\varepsilon}(\mathbf{p}_i) \cdot \mathbf{n}_{P,f}) \omega_{f,v}, \quad R_{i,f} = |f| \mathbf{n}_f \cdot (\nu_P \boldsymbol{\varepsilon}(\mathbf{p}_i) \cdot \mathbf{n}_{P,f}). \quad (8.35)$$

Let us define rectangular matrices $N_P = (N_1, \dots, N_m)$ and $R_P = (R_1, \dots, R_m)$. Then, Eq. (8.34) can be written as the typical mimetic matrix equation

$$M_P N_P = R_P.$$

Analyzing (8.35), we observe that the first $k/2$ vectors R_i are zero vectors. Hence, we can write $R_P = (\mathbf{0}, \widehat{R}_P)$ and $N_P = (\widetilde{N}_P, \widehat{N}_P)$ where the columns of matrix \widetilde{N}_P correspond to the vector-valued linear functions that are in the kernel of $\boldsymbol{\varepsilon}(\cdot)$.

Now, we can apply the theory in Chap. 4 (see Sect. 4.3) to write the general solution of the matrix equation as

$$M_P = \widehat{R}_P (\widehat{N}_P^T \widehat{R}_P)^{-1} \widehat{R}_P^T + M_P^{(1)}, \quad (8.36)$$

where $M_P^{(1)}$ is a symmetric and positive semi-definite matrix such that $\ker(M_P^{(1)}) = \text{img}(N_P)$. As the choice of $M_P^{(1)}$ is not unique, formula (8.36) represents a family of admissible stiffness matrices, and, thus, a family of numerical schemes. As discussed in Sect. 4.5, the stability condition limits the number of good choices. The recommended choice is given by

$$M_P^{(1)} = \gamma_P (I - N_P (N_P^T N_P)^{-1} N_P^T), \quad \gamma_P = \frac{1}{m} \text{trace}(\widehat{R}_P (\widehat{N}_P^T \widehat{R}_P)^{-1} \widehat{R}_P^T). \quad (8.37)$$

Furthermore, from Chap. 4 we know that the symmetric $k \times k$ matrix $N_P^T R_P$ represents the bilinear form restricted to the space $(\mathbb{P}_1(P))^d$. Due to condition (8.33), it can be easily checked that this matrix has the form

$$N_P^T R_P = \begin{pmatrix} \mathbf{0} & \mathbf{0} \\ \mathbf{0} & \widehat{N}_P^T \widehat{R}_P \end{pmatrix},$$

where matrix $\widehat{N}_P^T \widehat{R}_P$ has size $(k/2) \times (k/2)$ and is symmetric and positive definite. It represents the bilinear form restricted to the polynomials of $(\mathbb{P}_1(P))^d / \ker(\boldsymbol{\varepsilon})$.

Example 8.1. Let P be a quadrilateral with vertices $\mathbf{x}_i = (x_i, y_i)^T$, $i = 1, \dots, 4$, enumerated counter-clock wise. We assume that its centroid is at the origin, $\mathbf{x}_P = (0, 0)^T$. Let $v_P = 1$. The linear functions forming a basis $(\mathbb{P}_1(P))^2$ are

$$\mathbf{p}_1 = \begin{pmatrix} 1 \\ 0 \end{pmatrix}, \quad \mathbf{p}_2 = \begin{pmatrix} 0 \\ 1 \end{pmatrix}, \quad \mathbf{p}_3 = \begin{pmatrix} y \\ -x \end{pmatrix}, \quad \mathbf{p}_4 = \begin{pmatrix} x \\ 0 \end{pmatrix}, \quad \mathbf{p}_5 = \begin{pmatrix} 0 \\ y \end{pmatrix}, \quad \mathbf{p}_6 = \begin{pmatrix} y \\ x \end{pmatrix}.$$

The first three functions correspond to the rigid-body translations and rotation and generate the kernel of the bilinear form $\mathcal{A}_{h,P}$. The columns of matrix N_P are obtained by applying the projection operator to these functions. We enumerate the degrees of freedom as follows: first we consider all the x -components of vertex vectors, then the y -components and finally the edge degrees of freedom. A straightforward calcu-

lation yields:

$$N_P = \begin{pmatrix} 1 & 0 & y_1 & x_1 & 0 & y_1 \\ 1 & 0 & y_2 & x_2 & 0 & y_2 \\ 1 & 0 & y_3 & x_3 & 0 & y_3 \\ 1 & 0 & y_4 & x_4 & 0 & y_4 \\ 0 & 1 & -x_1 & 0 & y_1 & x_1 \\ 0 & 1 & -x_2 & 0 & y_2 & x_2 \\ 0 & 1 & -x_3 & 0 & y_3 & x_3 \\ 0 & 1 & -x_4 & 0 & y_4 & x_4 \\ 0 & 0 & 0 & 0 & 0 & 0 \\ 0 & 0 & 0 & 0 & 0 & 0 \\ 0 & 0 & 0 & 0 & 0 & 0 \\ 0 & 0 & 0 & 0 & 0 & 0 \end{pmatrix}.$$

The first four rows are obtained by evaluating the x components of \mathbf{p}_i at the vertices of P . The next four rows are obtained by evaluating the y components of \mathbf{p}_i at the vertices of P . The last four rows contain only zeroes due to property (8.15).

To calculate the entries of matrix R_P , we start with the formulas for symmetrized gradients:

$$\begin{aligned} \boldsymbol{\varepsilon}(\mathbf{p}_1) = \boldsymbol{\varepsilon}(\mathbf{p}_2) = \boldsymbol{\varepsilon}(\mathbf{p}_3) &= \begin{pmatrix} 0 & 0 \\ 0 & 0 \end{pmatrix}, \quad \boldsymbol{\varepsilon}(\mathbf{p}_4) = \begin{pmatrix} 1 & 0 \\ 0 & 0 \end{pmatrix}, \quad \boldsymbol{\varepsilon}(\mathbf{p}_5) = \begin{pmatrix} 0 & 0 \\ 0 & 1 \end{pmatrix}, \\ \boldsymbol{\varepsilon}(\mathbf{p}_6) &= \begin{pmatrix} 0 & 1 \\ 1 & 0 \end{pmatrix}. \end{aligned}$$

Thus, according to (8.35), the first three columns of matrix R_P are zero vectors. Let $\mathbf{e}_i = (\mathbf{x}_i, \mathbf{x}_{i+1})$ be the i -th edge of P , $i = 1, \dots, 4$, $\mathbf{n}_{P, \mathbf{e}_i} = (n_{i,x}, n_{i,y})^T$ be its exterior normal vector, and $s_i = \mathbf{n}_{P, \mathbf{e}_i} \cdot \mathbf{n}_{\mathbf{e}_i} = \pm 1$ denote the orientation of the fixed normal vector $\mathbf{n}_{\mathbf{e}_i}$. We use the trapezoidal quadrature rule which is exact for linear functions. Its weights are given by $\omega_{\mathbf{e}_i, \mathbf{v}} = \frac{1}{2}|\mathbf{e}_i|$. Now, formula (8.35) gives

$$\widehat{R}_P = \frac{1}{2} \begin{pmatrix} n_{1,x}|\mathbf{e}_1| + n_{4,x}|\mathbf{e}_4| & 0 & n_{1,y}|\mathbf{e}_1| + n_{4,y}|\mathbf{e}_4| \\ n_{2,x}|\mathbf{e}_2| + n_{1,x}|\mathbf{e}_1| & 0 & n_{2,y}|\mathbf{e}_2| + n_{1,y}|\mathbf{e}_1| \\ n_{3,x}|\mathbf{e}_3| + n_{2,x}|\mathbf{e}_2| & 0 & n_{3,y}|\mathbf{e}_3| + n_{2,y}|\mathbf{e}_2| \\ n_{4,x}|\mathbf{e}_4| + n_{3,x}|\mathbf{e}_3| & 0 & n_{4,y}|\mathbf{e}_4| + n_{3,y}|\mathbf{e}_3| \\ 0 & n_{1,y}|\mathbf{e}_1| + n_{4,y}|\mathbf{e}_4| & n_{1,x}|\mathbf{e}_1| + n_{4,x}|\mathbf{e}_4| \\ 0 & n_{2,y}|\mathbf{e}_2| + n_{1,y}|\mathbf{e}_1| & n_{2,x}|\mathbf{e}_2| + n_{1,x}|\mathbf{e}_1| \\ 0 & n_{3,y}|\mathbf{e}_3| + n_{2,y}|\mathbf{e}_2| & n_{3,x}|\mathbf{e}_3| + n_{2,x}|\mathbf{e}_2| \\ 0 & n_{4,y}|\mathbf{e}_4| + n_{3,y}|\mathbf{e}_3| & n_{4,x}|\mathbf{e}_4| + n_{3,x}|\mathbf{e}_3| \\ 2s_1|\mathbf{e}_1|(n_{1,x})^2 & 2s_1|\mathbf{e}_1|(n_{1,y})^2 & 2s_1|\mathbf{e}_1| \\ 2s_2|\mathbf{e}_2|(n_{2,x})^2 & 2s_2|\mathbf{e}_2|(n_{2,y})^2 & 2s_2|\mathbf{e}_2| \\ 2s_3|\mathbf{e}_3|(n_{3,x})^2 & 2s_3|\mathbf{e}_3|(n_{3,y})^2 & 2s_3|\mathbf{e}_3| \\ 2s_4|\mathbf{e}_4|(n_{4,x})^2 & 2s_4|\mathbf{e}_4|(n_{4,y})^2 & 2s_4|\mathbf{e}_4| \end{pmatrix}.$$

The formulas for matrices N_P and \widehat{R}_P show once again that the construction of the mimetic scheme is not limited by the shape complexity of polygonal cells. The minimal required geometric information includes the position of mesh vertices and their enumeration. □

8.2 Convergence analysis and error estimates

In this section, we prove optimal convergence of the mimetic discretization, see Theorem 8.1. The convergence analysis is performed on a sequence of meshes that satisfy the shape regularity conditions (MR1)–(MR3) stated in Sect. 1.6.2. Thus, we can use properties (M1)–(M5) discussed in this section. For the sake of presentation, we consider the three-dimensional case; analysis of the two-dimensional case follows readily.

8.2.1 Preliminaries and technical lemmas

The mesh property (M2) implies that the discrete norm (8.28) is spectrally equivalent to

$$\| \mathbf{v}_h \|_{X_{h,P}}^2 \succeq h_P \sum_{f \in \partial P} \left(\sum_{e=(v,v') \in \partial f} \frac{1}{2} \| \mathbf{v}_{v'} - \mathbf{v}_v \|^2 + v_f^2 \right). \tag{8.38}$$

We present three technical lemmas that are used in the proof of Theorem 8.1. The first two lemmas are the vector versions of the similar lemmas proved in [84] for the scalar case. Their extension to the vector case is discussed in [49] and we omit the proofs here.

Lemma 8.2. *For every polyhedron P , every face f of P , and any vertex $\bar{v} \in f$, there exists a positive constant γ_1 , which depends only on \mathcal{N}^s and ρ_s and is independent of h , such that*

$$\sum_{v \in \partial f} \| \mathbf{v}_v - \mathbf{v}_{\bar{v}} \|^2 \omega_{f,v} \leq \gamma_1 h_P \| \mathbf{v}_P \|_{X_{h,P}}^2 \quad \forall \mathbf{v}_P \in X_{h,P}.$$

Let $\boldsymbol{\varphi} \in (H^2(\Omega))^3$ be a vector-valued function and $\boldsymbol{\psi}$ be the discontinuous piecewise linear on Ω_h vector-valued function such that its restriction to cell P is the $L^2(P)$ -projection of $\boldsymbol{\varphi}$ onto $(\mathbb{P}_1(P))^3$. The projections of these functions satisfy the following lemma.

Lemma 8.3. *For every vector-valued function $\boldsymbol{\varphi} \in (H^2(\Omega))^3$ and its piecewise linear approximation $\boldsymbol{\psi}$ there holds*

$$\| \boldsymbol{\varphi}_P^I - \boldsymbol{\psi}_P^I \|_{X_{h,P}} \leq \gamma_2 h_P \| \boldsymbol{\varphi} \|_{H^2(P)},$$

where γ_2 is a positive constant that depends only on the constants \mathcal{N}^s and ρ_s appeared in assumption (MR1).

Let f be an internal mesh face and P_1, P_2 be the two polyhedra that share this face, so that $f \subseteq \partial P_1 \cap \partial P_2$. Furthermore, let us define the jump of the normal component of the strain $\boldsymbol{\varepsilon}(\boldsymbol{\psi})$ across f as follows:

$$J_f(\boldsymbol{\psi}) = \boldsymbol{\varepsilon}(\boldsymbol{\psi}_{P_1}) \cdot \mathbf{n}_{P_1,f} + \boldsymbol{\varepsilon}(\boldsymbol{\psi}_{P_2}) \cdot \mathbf{n}_{P_2,f}. \quad (8.39)$$

Lemma 8.4. *For every vector-valued function $\boldsymbol{\varphi} \in (H^2(\Omega))^3$ and its piecewise linear approximation $\boldsymbol{\psi}$ there holds:*

$$\sum_{f \in \mathcal{F}^0} \|J_f(\boldsymbol{\psi})\|_{L^2(f)}^2 \leq \gamma_3 h \|\boldsymbol{\varphi}\|_{H^2(\Omega)}^2, \quad (8.40)$$

where the positive constant γ_3 depends only on \mathcal{N}^s and ρ_s of assumption **(MR1)**.

Proof. We add and subtract $\boldsymbol{\varphi}$ and we apply the triangular inequality to obtain

$$\begin{aligned} \|\boldsymbol{\varepsilon}(\boldsymbol{\psi}_{P_1}) \cdot \mathbf{n}_{P_1,f} + \boldsymbol{\varepsilon}(\boldsymbol{\psi}_{P_2}) \cdot \mathbf{n}_{P_2,f}\|_{L^2(f)}^2 &\leq 3 \left(\|\boldsymbol{\varepsilon}(\boldsymbol{\psi}_{P_1} - \boldsymbol{\varphi}) \cdot \mathbf{n}_{P_1,f}\|_{L^2(f)}^2 \right. \\ &\quad \left. + \|\boldsymbol{\varepsilon}(\boldsymbol{\psi}_{P_2} - \boldsymbol{\varphi}) \cdot \mathbf{n}_{P_2,f}\|_{L^2(f)}^2 + \|\boldsymbol{\varepsilon}(\boldsymbol{\varphi}) \cdot \mathbf{n}_{P_1,f} + \boldsymbol{\varepsilon}(\boldsymbol{\varphi}) \cdot \mathbf{n}_{P_2,f}\|_{L^2(f)}^2 \right). \end{aligned} \quad (8.41)$$

All components of $\boldsymbol{\varphi}$ belong to $H^2(\Omega)$ and their normal derivatives are continuous across the mesh faces. Thus, the last term in the right-hand side of (8.41) is zero. For $i = 1, 2$, from the Cauchy-Schwarz inequality and the Agmon inequality **(M4)** it follows that

$$\begin{aligned} \|\boldsymbol{\varepsilon}(\boldsymbol{\psi}_{P_i} - \boldsymbol{\varphi}) \cdot \mathbf{n}_{P_i,f}\|_{L^2(f)}^2 &\leq \|\boldsymbol{\varepsilon}(\boldsymbol{\psi}_{P_i} - \boldsymbol{\varphi})\|_{L^2(f)}^2 \\ &\leq C^{Agm} \left(h_{P_i}^{-1} \|\boldsymbol{\varepsilon}(\boldsymbol{\psi}_{P_i} - \boldsymbol{\varphi})\|_{L^2(P_i)}^2 + h_{P_i} \|\boldsymbol{\varepsilon}(\boldsymbol{\psi}_{P_i} - \boldsymbol{\varphi})\|_{H^1(P_i)}^2 \right). \end{aligned} \quad (8.42)$$

The interpolation error estimate of assumption **(M5)** and the inequality $\|\boldsymbol{\varepsilon}(\boldsymbol{\psi}_{P_i} - \boldsymbol{\varphi})\|_{H^1(P_i)} \leq \|\boldsymbol{\varphi}\|_{H^2(P_i)}$ give:

$$\|\boldsymbol{\varepsilon}(\boldsymbol{\psi}_{P_i} - \boldsymbol{\varphi}) \cdot \mathbf{n}_{P_i,f}\|_{L^2(f)}^2 \leq C^{Agm} (C^I + 1) h_{P_i} \|\boldsymbol{\varphi}\|_{H^2(P_i)}^2. \quad (8.43)$$

To prove the lemma, we combine bounds (8.42)–(8.43) with (8.41), then apply the resulting inequality to the left-hand side of (8.40), and finally change the summation from faces to polyhedra. The assertion follows immediately with $\gamma_3 = 3C^{Agm}(C^I + 1)N^{\mathcal{F}}$, where $N^{\mathcal{F}}$ is the uniform bound on the number of faces in a cell (see assumption **(M1)**). \square

8.2.2 Stability analysis

In this section, we prove the discrete *inf-sup* condition and the discrete Korn-type inequality. According to the theory of mixed methods [88], the uniform stability of the mimetic discretization follows from these two properties. For simplicity of exposition, we consider the homogeneous Dirichlet boundary conditions, i.e. $\Gamma^D = \Gamma$ and $\mathbf{g}^D = 0$ in (8.3). Hence, we search for the discrete velocity field $\mathbf{u}_h \in X_{h,0}$.

8.2.2.1 The reconstruction operator

A reconstruction operator R_P associated with the polyhedral cell P is a useful theoretical tool for the stability analysis. It is never constructed in the practical implementation of the mimetic scheme. Let

$$R_P : X_{h,P} \rightarrow (H^1(P) \cap C^0(P))^3.$$

We assume that this operator satisfies the six conditions listed below.

(L1) The reconstruction operator is the right-inverse of the nodal projection operator on a subspace of $X_{h,P}$:

$$(R_P(\mathbf{v}_P))_{P,v}^I = \mathbf{v}_{P,v} \quad \forall \mathbf{v}_P \in X_{h,P}. \quad (8.44)$$

(L2) The reconstruction operator is stable with respect to the mesh dependent norm (8.28), i.e. there exists a constant C^R independent of h_P and P such that

$$|R_P(\mathbf{v}_P)|_{H^1(P)} \leq C^R \|\mathbf{v}_P\|_{X_{h,P}} \quad \forall \mathbf{v}_P \in X_{h,P}. \quad (8.45)$$

(L3) The reconstruction operator has minimal approximation properties, specifically, for every $\mathbf{v}_P \in X_{h,P}$ it holds:

$$\|R_P(\mathbf{v}_P) - \mathbf{v}_v\|_{L^2(P)} \leq C^R h_P \|\mathbf{v}_P\|_{X_{h,P}} \quad \forall \mathbf{v} \in P. \quad (8.46)$$

(L4) For every $\mathbf{v}_P \in X_{h,P}$ it holds:

$$\int_P \operatorname{div} R_P(\mathbf{v}_P) dV = |P| \operatorname{div}_P \mathbf{v}_P. \quad (8.47)$$

(L5) The reconstruction operator is exact for linear vector-valued functions:

$$R_P(\boldsymbol{\Psi}_P^I) = \boldsymbol{\Psi} \quad \forall \boldsymbol{\Psi} \in (\mathbb{P}_1(P))^3. \quad (8.48)$$

(L6) The restriction of the reconstructed function $R_P(\mathbf{v}_P)$ to a face f of P depends only on the degrees of freedom $\mathbf{v}_{P|f}$.

Collecting all local operators yields the global reconstruction operator R such that $R|_P(\mathbf{v}_h) = R_P(\mathbf{v}_P)$.

Let us discuss a few properties of these assumptions. Condition **(L6)** implies that the local reconstructions inside any two adjacent cells have the same trace on the common interface; hence, the global reconstructed function is continuous. Consequently, the range of the global reconstruction operator is inside the functional space $(H^1(\Omega) \cap C^0(\overline{\Omega}))^3$. Equation (8.47) implies that the reconstruction operator preserves the discrete divergence in the following sense:

$$(R_P(\mathbf{v}_P))_P^I = \operatorname{div}_P \mathbf{v}_P. \quad (8.49)$$

Equation (8.48) guarantees that R_P preserves the kernel of the symmetrized gradient operator. Indeed, the kernel of $\boldsymbol{\epsilon}$ contains the constant functions (rigid-body translations) and the subspace $\Theta \subset (\mathbb{P}_1(P))^3$ (rigid-body rotations) defined by (8.29). The

existence of a reconstruction operator is proved in Sect. 8.4. We have the following Lemma proved in [49].

Lemma 8.5. *There exists a positive constant γ_4 , which depends only on the constants \mathcal{N}^s and ρ_s appeared in assumption (MR1), such that for every $\mathbf{b} \in (L^2(\Omega))^3$ and $\mathbf{v}_h \in X_h$ there holds*

$$(\mathbf{b}, \mathbf{v}_h)_h - \int_{\Omega} \mathbf{b} \cdot \mathbf{R}(\mathbf{v}_h) dV \leq \gamma_4 h \|\mathbf{b}\|_{L^2(\Omega)} \|\mathbf{v}_h\|_{X_h}. \quad (8.50)$$

8.2.2.2 A discrete inf-sup condition

A key condition in the convergence analysis of mixed schemes is the *inf-sup condition* that is stated and proved in the following lemma.

Lemma 8.6. *There exists a positive constant β independent of h such that for every $q_h \in \mathcal{P}_h$ there exists a discrete velocity $\mathbf{v}_h \in X_{h,0}$ satisfying:*

$$[\operatorname{div}_h \mathbf{v}_h, q_h]_{Q_h} \geq \beta \|q_h\|_{Q_h}, \quad (8.51)$$

$$\|\mathbf{v}_h\|_{X_h} \leq 1. \quad (8.52)$$

Proof. Let us identify the mesh function q_h with the piecewise constant function $\tilde{q}_h \in L^2(\Omega)$. We prove this lemma using the inf-sup condition (1.32) of the continuum problem which states that there exist a positive constant β and a vector field $\mathbf{v} \in (H_0^1(\Omega))^3$ such that

$$\int_{\mathcal{P}} \tilde{q}_h \operatorname{div} \mathbf{v} dV \geq \beta \|\tilde{q}_h\|_{L^2(\Omega)} \quad \text{and} \quad \|\mathbf{v}\|_{H^1(\Omega)} \leq 1. \quad (8.53)$$

Let \mathbf{v}^c be a piecewise linear Clément-type interpolant of \mathbf{v} built on the tetrahedral sub-mesh \mathcal{T}_h (see assumption (M2)). As shown for instance in [322], there holds

$$h_{\mathcal{P}}^{-1} \|\mathbf{v}^c - \mathbf{v}\|_{L^2(\mathcal{P})} + \|\nabla \mathbf{v}^c\|_{L^2(\mathcal{P})} \leq C \|\nabla \mathbf{v}\|_{L^2(\mathcal{P})} \quad \forall \mathcal{P} \in \Omega_h. \quad (8.54)$$

Let $(\mathbf{v}^c)^I$ be the nodal projection of \mathbf{v}^c into $X_{h,0}$. We define the vector $\mathbf{v}_h \in X_{h,0}$ such that

$$\mathbf{v}_v = \mathbf{v}^c(\mathbf{x}_v) \quad \forall v \in \mathcal{V}, \quad (8.55)$$

$$\int_{\mathcal{f}} \mathbf{v} \cdot \mathbf{n}_{\mathcal{f}} dS = \sum_{v \in \partial \mathcal{f}} \mathbf{v}_v \cdot \mathbf{n}_{\mathcal{f}} \omega_{\mathcal{f},v} + |\mathcal{f}| v_{\mathcal{f}} \quad \forall \mathcal{f} \in \mathcal{F}^0. \quad (8.56)$$

Since the integral argument in the left-hand side of (8.56) is not $\mathbf{v}^c \cdot \mathbf{n}_{\mathcal{f}}$, vector \mathbf{v}_h differs from $(\mathbf{v}^c)^I$. To show that \mathbf{v}_h satisfies (8.51) we insert (8.55)–(8.56) into the definition of the discrete divergence operator (8.20):

$$|\mathcal{P}| \operatorname{div}_{\mathcal{P}} \mathbf{v}_{\mathcal{P}} = \sum_{\mathcal{f} \in \mathcal{P}} s_{\mathcal{P},\mathcal{f}} \int_{\mathcal{f}} \mathbf{v} \cdot \mathbf{n}_{\mathcal{f}} dS = \int_{\mathcal{P}} \operatorname{div} \mathbf{v} dV. \quad (8.57)$$

In view of the scalar product definition (8.17), Eq. (8.57), and the first inequality in (8.53), we derive:

$$[\operatorname{div}_h \mathbf{v}_h, q_h]_{Q_h} = \sum_{P \in \Omega_h} |P| (\operatorname{div}_P \mathbf{v}_P) q_P = \sum_{P \in \Omega_h} \int_P (\operatorname{div} \mathbf{v}) q_P dV \quad (8.58)$$

$$= \int_{\Omega} \tilde{q}_h \operatorname{div} \mathbf{v} dV \geq \beta \|\tilde{q}_h\|_{L^2(\Omega)} = \beta \|q_h\|_{Q_h}. \quad (8.59)$$

To show that \mathbf{v}_h satisfies (8.52), we consider a polyhedron P and note that

$$\|\mathbf{v}_P\|_{X_{h,P}}^2 = \|(\mathbf{v}^c)_P\|_{X_{h,P}}^2 + h_P \sum_{f \in \partial P} v_f^2, \quad (8.60)$$

since the edge-based degrees of freedom of the nodal projection are zero. For an edge $e = (v, v_1)$ of P , let f be a face containing e . Let K_e be a specific triangle (chosen once and for all) which belongs to the triangular partition $\mathcal{T}_{h|f}$ of f and contains at least a part of e . Let K_e be a tetrahedron of $\mathcal{T}_{h|P}$ containing K_e . We denote the tangential derivative of \mathbf{v}^c along e by $\partial \mathbf{v}^c / \partial \boldsymbol{\tau}_e$ and the two-dimensional gradient of \mathbf{v}^c with respect to a local coordinate system $\boldsymbol{\xi}$ on f by $\nabla_{\boldsymbol{\xi}} \mathbf{v}^c$.

By construction, $\nabla \mathbf{v}^c$ is constant in each tetrahedron of \mathcal{T}_h . The standard scaling arguments and property **(M3)** give the following bound:

$$\begin{aligned} |\mathbf{v}^c(\mathbf{x}_{v_1}) - \mathbf{v}^c(\mathbf{x}_v)| &\leq \int_e \frac{\partial \mathbf{v}^c}{\partial \boldsymbol{\tau}_e} dS \leq h_e^{1/2} \left(\int_e \frac{\partial \mathbf{v}^c}{\partial \boldsymbol{\tau}_e}^2 dS \right)^{1/2} \\ &\leq C \|\nabla_{\boldsymbol{\xi}} \mathbf{v}^c\|_{L^2(K_e)} \leq Ch_P^{-1/2} \|\nabla \mathbf{v}^c\|_{L^2(T_e)}. \end{aligned} \quad (8.61)$$

The face-based components of $(\mathbf{v}^c)^I$ are zero, c.f. (8.11). Hence, using definition (8.38), inequality (8.61), and the continuity property of the Clément interpolant (8.54), yields the upper bound for the first term in (8.60):

$$\|(\mathbf{v}^c)_P^I\|_{X_{h,P}}^2 = h_P \sum_{e \in \partial P} |\mathbf{v}^c(\mathbf{x}_{v_1}) - \mathbf{v}^c(\mathbf{x}_v)|^2 \leq C \|\nabla \mathbf{v}^c\|_{L^2(P)}^2 \leq C \|\nabla \mathbf{v}\|_{L^2(P)}^2. \quad (8.62)$$

To control the second term in (8.60), for every face f of P we choose a vertex $\bar{v}_f \in f$ and fix it for the following developments. We recall that the quadrature rule provided by the set of weights $\{\omega_{f,v}\}$ is exact for linear polynomials. Starting from (8.56), we add and subtract \mathbf{v}^c and then the constant vector function $\mathbf{v}^c(\mathbf{x}_{\bar{v}_f})$:

$$\begin{aligned} |f| |v_f| &= \int_f \mathbf{v} \cdot \mathbf{n}_f dS - \sum_{v \in \partial f} \mathbf{v}^c(\mathbf{x}_v) \cdot \mathbf{n}_f \omega_{f,v} \leq \int_f (\mathbf{v}(\mathbf{x}) - \mathbf{v}^c(\mathbf{x})) \cdot \mathbf{n}_f dS \\ &\quad + \int_f (\mathbf{v}^c(\mathbf{x}) - \mathbf{v}^c(\mathbf{x}_{\bar{v}_f})) \cdot \mathbf{n}_f dS + \sum_{v \in \partial f} (\mathbf{v}^c(\mathbf{x}_{\bar{v}_f}) - \mathbf{v}^c(\mathbf{x}_v)) \cdot \mathbf{n}_f \omega_{f,v} \\ &= R_1 + R_2 + R_3. \end{aligned} \quad (8.63)$$

We bound the term R_1 by using the Cauchy-Schwartz inequality, inequality **(M4)** and, finally, inequality (8.54):

$$R_1 \leq Ch_P^{3/2} \|\nabla \mathbf{v}\|_{L^2(P)}. \quad (8.64)$$

To estimate the term R_2 , we consider the continuous piecewise linear function

$$\varphi_f(\mathbf{x}) = (\mathbf{v}^c(\mathbf{x}) - \mathbf{v}^c(\mathbf{x}_{\bar{v}_f})) \cdot \mathbf{n}_f \quad \forall \mathbf{x} \in f. \quad (8.65)$$

Let γ be a polygonal curve that connects the points $\mathbf{x}_{\bar{v}_f}$ and $\mathbf{x} \in f$. If f is convex, γ is simply the straight segment. Otherwise, γ can be built such that its length $|\gamma|$ is bounded, $|\gamma| \leq Ch_P$, where C is a positive constant independent of h . Let $\gamma(s)$ be a parameterization of γ such that $\gamma(0) = \mathbf{x}_{\bar{v}_f}$ and $\gamma(|\gamma|) = \mathbf{x}$. Then,

$$\varphi_f(\mathbf{x}) = \int_{\gamma} \frac{\partial \varphi_f(s)}{\partial s} dL \quad \forall \mathbf{x} \in f.$$

Using this, we obtain the following bound:

$$|\varphi_f(\mathbf{x})| \leq \int_{\gamma} \frac{\partial \varphi_f(s)}{\partial s} dL \leq |\gamma| \|\nabla \varphi_f\|_{L^\infty(f)} \leq Ch_P \|\nabla \varphi_f\|_{L^\infty(f)}. \quad (8.66)$$

Since $\varphi_f(\mathbf{x})$ is piecewise linear on f , its gradient is piecewise constant. Due to definition (8.65), we have $|\varphi_f|_{H^1(f)} = |\mathbf{v}^c|_{H^1(f)}$. Using this and **(M3)**, we continue the chain of inequalities:

$$\begin{aligned} |\varphi_f(\mathbf{x})| &\leq Ch_P \|\nabla \varphi_f\|_{L^\infty(f)} \leq Ch_P \max_{\top} \|\nabla \varphi_f\|_{L^\infty(\top)} \leq Ch_P \max_{\top} h_{\top}^{-3/2} \|\nabla \varphi_f\|_{L^2(\top)} \\ &\leq Ch_P^{-1/2} \max_{\top} \|\nabla \varphi_f\|_{L^2(\top)} \leq Ch_P^{-1/2} |\mathbf{v}^c|_{H^1(P)}, \end{aligned} \quad (8.67)$$

where C is the generic constant that may change at any occurrence. We use inequality (8.67), the scaling $|f| \approx h_P^2$ provided by **(M2)** and the continuity of the Clément interpolation (8.54) to derive the following bound for R_2 :

$$\begin{aligned} R_2 &= \int_f (\mathbf{v}^c - \mathbf{v}^c(\mathbf{x}_{\bar{v}_f})) \cdot \mathbf{n}_f dS \leq \int_f |\varphi_f(\mathbf{x})| dS \\ &\leq C |f| h_P^{-1/2} |\mathbf{v}^c|_{H^1(P)} \leq Ch_P^{3/2} |\mathbf{v}|_{H^1(P)}. \end{aligned} \quad (8.68)$$

To estimate term R_3 , we use the triangular inequality, the Cauchy-Schwartz inequality, the result of Lemma 8.2, equations (8.10), the scaling $|f| \approx h_P^2$ given by **(M2)**, and inequality (8.62):

$$\begin{aligned} R_3 &= \sum_{\mathbf{v} \in \partial f} (\mathbf{v}^c(\mathbf{x}_{\bar{v}_f}) - \mathbf{v}^c(\mathbf{x}_v)) \cdot \mathbf{n}_f \omega_{f,v} \leq \sum_{\mathbf{v} \in \partial f} |\mathbf{v}^c(\mathbf{x}_{\bar{v}_f}) - \mathbf{v}^c(\mathbf{x}_v)| \omega_{f,v} \\ &\leq \left(\sum_{\mathbf{v} \in \partial f} |(\mathbf{v}^c)_{\bar{v}_f}^I - (\mathbf{v}^c)_v^I|^2 \omega_{f,v} \right)^{1/2} \left(\sum_{\mathbf{v} \in \partial f} \omega_{f,v} \right)^{1/2} \\ &\leq Ch_P^{1/2} \|(\mathbf{v}^c)_P^I\|_{X_{h,P}} |f|^{1/2} \leq Ch_P^{3/2} \|(\mathbf{v}^c)_P^I\|_{X_{h,P}} \leq Ch_P^{3/2} |\mathbf{v}|_{H^1(P)}. \end{aligned} \quad (8.69)$$

Thus, all terms in the right-hand side of (8.63) have similar bounds. We use once more the scaling $|f| \approx h_P^2$ and recall that the number of faces in P is uniformly bounded. We have

$$h_P \sum_{f \in \partial P} |v_f|^2 = \sum_{f \in \partial P} \frac{h_P}{|f|^2} (|f| |v_f|)^2 \leq Ch_P^{-3} (R_1 + R_2 + R_3)^2 \leq C |v|_{H^1(P)}^2. \quad (8.70)$$

Inserting (8.62) and (8.70) in (8.60), and summing over cells, we obtain:

$$\|v_h\|_{X_h}^2 = \sum_{P \in \Omega_h} \|v_P\|_{X_{h,P}}^2 \leq C \sum_{P \in \Omega_h} |v|_{H^1(P)}^2 \leq C. \quad (8.71)$$

The lemma’s inequality (8.52) follows by scaling the discrete velocity v_h by \sqrt{C} , where $C > 0$ is the mesh independent constant appeared in (8.71). \square

8.2.2.3 The discrete Korn-type inequality

By assumption **(S1)**, the discrete bilinear form $\mathcal{A}_h(\cdot, \cdot)$ is coercive with respect to the weaker semi-norm $\|\cdot\|_{X_h}$. In the convergence analysis, we need a stronger coercivity which is the consequence of the discrete Korn-type inequality stated in the following lemma.

Lemma 8.7. *It exists a positive constant C' independent of h such that*

$$\|v_h\|_{X_h} \leq C' \|v_h\|_{X_{h,0}} \quad \forall v_h \in X_{h,0}. \quad (8.72)$$

Proof. This proof uses the results of Sect. 8.4. Note that, since the space Θ used in (8.29) is contained in $(\mathbb{P}_1(P))^3$, it holds $\theta_f^\Pi = 0$ for all $\theta \in \Theta$ and all $f \in \mathcal{F}$, see (8.15). Thus, both norms have a common part related the face-based degrees of freedom. Therefore, in order to prove (8.72) it is sufficient to show that

$$\|v_h\|_* \leq C \|v_h\|_{X_{h,0}} \quad \forall v_h \in X_{h,0}, \quad (8.73)$$

where

$$\|v_h\|_*^2 = \sum_{P \in \Omega_h} \|v_h\|_{*,P}^2, \quad \|v_h\|_{*,P}^2 = |P| \sum_{f \in \partial P} \sum_{e=(v,v') \in \partial f} \frac{1}{2} \left\| \frac{v_{v'} - v_v}{|e|} \right\|^2. \quad (8.74)$$

Consider a polyhedron P . Let \tilde{R}_P be the reconstruction operator introduced at the beginning of Sect. 8.4.2. One of its properties is that the function $\tilde{R}_P(v_P)$ is linear on all mesh edges. Also, \tilde{R}_P satisfies condition **(L1)**. Thus,

$$\|v_h\|_{*,P}^2 = |P| \sum_{f \in \partial P} \sum_{e \in \partial f} \frac{1}{2} \|\nabla \tilde{R}_P(v_P) \cdot \tau_{f,e}\|^2. \quad (8.75)$$

Since $\nabla \tilde{R}_P(\mathbf{v}_P) \cdot \boldsymbol{\tau}_{f,e}$ is constant on each edge, we can also write

$$\|\mathbf{v}_h\|_{*,P}^2 = |P| \sum_{f \in \partial P} \sum_{e \in \partial f} \frac{1}{2h_e} \|\nabla \tilde{R}_P(\mathbf{v}_h) \cdot \boldsymbol{\tau}_{f,e}\|_{L^2(e)}^2. \quad (8.76)$$

Every edge $e \in \partial P$ can be split into edges of tetrahedra of the submesh $\mathbb{T}_{h|P}$. By the construction, function $\nabla \tilde{R}_P(\mathbf{v}_h)$ is constant inside each tetrahedron; hence, the usual scaling argument allows us to obtain the following bound:

$$\begin{aligned} \|\mathbf{v}_h\|_{*,P}^2 &\leq C|P| \sum_{e \in \partial P} \sum_{T \in \mathbb{T}_h: e \cap \partial T \neq \emptyset} h_e^{-1} \|\nabla \tilde{R}_P(\mathbf{v}_h) \cdot \boldsymbol{\tau}_{f,e}\|_{L^2(e \cap \partial T)}^2 \\ &\leq C|P| \sum_{e \in \partial P} \sum_{T \in \mathbb{T}_h: e \cap \partial T \neq \emptyset} h_e^{-1} h_T^{-2} \|\nabla \tilde{R}_P(\mathbf{v}_P)\|_{L^2(T)}^2, \end{aligned}$$

where h_T is the diameter of T . From this equation, using first **(M2)** ($|P| \sim h_P^3$) and then **(M3)** of Sect. 1.6.2 yields

$$\|\mathbf{v}_h\|_{*,P}^2 \leq C \|\nabla \tilde{R}_P(\mathbf{v}_P)\|_{L^2(P)}^2. \quad (8.77)$$

By the construction, $\tilde{R}(\mathbf{v}_h) \in (H_0^1(\Omega))^3$. Therefore, applying bound (8.77) in (8.74), summing up the terms, and using the conventional Korn inequality, see for instance [116], we have

$$\|\mathbf{v}_h\|_*^2 \leq C \|\tilde{R}(\mathbf{v}_h)\|_{L^2(\Omega)}^2 \leq C \|\boldsymbol{\varepsilon}(\tilde{R}(\mathbf{v}_h))\|_{L^2(\Omega)}^2. \quad (8.78)$$

Recall that $\boldsymbol{\varepsilon}(\boldsymbol{\theta}) = 0$ for all $\boldsymbol{\theta} \in \Theta$. By the construction \tilde{R}_P preserves linear functions. Hence, we can continue (8.78) as follows:

$$\begin{aligned} \|\mathbf{v}_h\|_*^2 &\leq C \sum_{P \in \Omega_h} \inf_{\boldsymbol{\theta} \in \Theta} \|\boldsymbol{\varepsilon}(\tilde{R}_P(\mathbf{v}_P) - \boldsymbol{\theta})\|_{L^2(P)}^2 = C \sum_{P \in \Omega_h} \inf_{\boldsymbol{\theta} \in \Theta} \|\boldsymbol{\varepsilon}(\tilde{R}_P(\mathbf{v}_P - \boldsymbol{\theta}_P^{\parallel}))\|_{L^2(P)}^2 \\ &\leq C \sum_{P \in \Omega_h} \inf_{\boldsymbol{\theta} \in \Theta} \|\nabla(\tilde{R}_P(\mathbf{v}_P - \boldsymbol{\theta}_P^{\parallel}))\|_{L^2(P)}^2. \end{aligned} \quad (8.79)$$

The final property of \tilde{R}_P that we are going to use is **(L3s)** which states

$$\|\nabla \tilde{R}_P(\mathbf{v}_P)\|_{L^2(P)} \leq C \|\mathbf{v}_P\|_{X_{h,P}}.$$

Inserting this bound into (8.79) and using definition (8.29), we have

$$\|\mathbf{v}_h\|_*^2 \leq C \sum_{P \in \Omega_h} \inf_{\boldsymbol{\theta} \in \Theta} \|\mathbf{v}_P - \boldsymbol{\theta}_P^{\parallel}\|_{X_{h,P}}^2 \leq C \|\mathbf{v}_h\|_{X_h}^2. \quad (8.80)$$

This proves the assertion of the lemma. \square

Remark 8.8. Combining Lemma 8.7 with the stability assumption **(S1)**, we obtain

$$\mathcal{A}_h(\mathbf{v}_h, \mathbf{v}_h) \geq C \|\mathbf{v}_h\|_{X_h}^2 \quad \forall \mathbf{v}_h \in X_{h,0}, \quad (8.81)$$

which represents the discrete coercivity property of the bilinear form. In accordance with the theory of mixed methods [88], this coercivity property combined with the inf-sup condition proved in Lemma 8.6 yield the uniform stability of the mimetic discretization with respect to the norm (8.28) for $X_{h,0}$ and the norm (8.18) for \mathcal{Q}_h . \square

8.2.3 Error estimates

We now prove the main convergence result for the mimetic discretization. The approximation error is measured using the mesh-dependent norm (8.28) for the velocity solution and the mesh-dependent norm (8.18) for the pressure solution.

Theorem 8.1. *Let $\mathbf{u} \in (H^2(\Omega) \cap H_0^1(\Omega))^3$ and $p \in H^1(\Omega)$ be the solution of problem (8.7)–(8.8) with $\Gamma^D = \partial\Omega$ and $\mathbf{g}^D = \mathbf{0}$. Furthermore, let $\mathbf{u}_h \in X_{h,0}$ and $p_h \in \mathcal{Q}_h$ be the solution of the mimetic scheme (8.26)–(8.27) under the assumptions (MR1)–(MR2) (see Sects. 1.6.2) and (S1)–(S2) (see Sect. 8.1.4). Then, there exists a positive constant C independent of h such that*

$$\|\|\mathbf{u}_h - \mathbf{u}^{\mathbb{I}}\|\|_{X_h} + \|p_h - p^{\mathbb{I}}\|_{\mathcal{Q}_h} \leq Ch \left(\|\mathbf{u}\|_{H^2(\Omega)} + \|p\|_{H^1(\Omega)} \right). \quad (8.82)$$

Proof. As observed in Remark 8.8, the mimetic discretization is uniformly stable with respect to the mesh size h . Hence, according to [88], there exist a positive constant α and two discrete fields $\mathbf{v}_h \in X_{h,0}$ and $q_h \in \mathcal{P}_h$ such that

$$\|\|\mathbf{v}_h\|\|_{X_h} \leq 1, \quad \|q_h\|_{\mathcal{Q}_h} \leq 1, \quad (8.83)$$

and

$$\alpha \left(\|\|\mathbf{u}_h - \mathbf{u}^{\mathbb{I}}\|\|_{X_h} + \|p_h - p^{\mathbb{I}}\|_{\mathcal{Q}_h} \right) \leq \mathcal{A}_h(\mathbf{u}_h - \mathbf{u}^{\mathbb{I}}, \mathbf{v}_h) - [\operatorname{div}_h \mathbf{v}_h, p_h - p^{\mathbb{I}}]_{\mathcal{Q}_h} + [\operatorname{div}_h(\mathbf{u}_h - \mathbf{u}^{\mathbb{I}}), q_h]_{\mathcal{Q}_h}. \quad (8.84)$$

Equations (8.22) and (8.27) imply that $\operatorname{div}_h(\mathbf{u}_h - \mathbf{u}^{\mathbb{I}}) = 0$. Thus, inequality (8.84) becomes:

$$\alpha \left(\|\|\mathbf{u}_h - \mathbf{u}^{\mathbb{I}}\|\|_{X_h} + \|p_h - p^{\mathbb{I}}\|_{\mathcal{Q}_h} \right) \leq A - B + C, \quad (8.85)$$

where we set (using also (8.26))

$$A = \mathcal{A}_h(\mathbf{u}_h, \mathbf{v}_h) - [\operatorname{div}_h \mathbf{v}_h, p_h]_{\mathcal{Q}_h} = (\mathbf{b}, \mathbf{v}_h)_h, \quad (8.86)$$

$$B = \mathcal{A}_h(\mathbf{u}^{\mathbb{I}}, \mathbf{v}_h), \quad (8.87)$$

$$C = [\operatorname{div}_h \mathbf{v}_h, p^{\mathbb{I}}]_{\mathcal{Q}_h}. \quad (8.88)$$

Let $\boldsymbol{\psi}$ be a discontinuous piecewise linear function on Ω_h such that $\boldsymbol{\psi}_P = \boldsymbol{\psi}|_P$ is the L^2 -projection of \mathbf{u} onto $(\mathbb{P}_1(P))^3$. We define $\boldsymbol{\psi}_P^{\mathbb{I}}$ as the nodal projection of $\boldsymbol{\psi}_P$ into

$X_{h,P}$. We developed further the term B by adding and subtracting $\boldsymbol{\psi}_P^I$:

$$B = \sum_{P \in \Omega_h} (\mathcal{A}_{h,P}(\mathbf{u}^I - \boldsymbol{\psi}_P^I, \mathbf{v}_P) + \mathcal{A}_{h,P}(\boldsymbol{\psi}_P^I, \mathbf{v}_h)) = T_1 + \sum_{P \in \Omega_h} \mathcal{A}_{h,P}(\boldsymbol{\psi}_P^I, \mathbf{v}_h). \quad (8.89)$$

For each face $f \in \mathcal{F}$, we choose and fix one of its vertices \bar{v} , and indicate the corresponding degrees of freedom, $\mathbf{v}_{f,\bar{v}} \in \mathbb{R}^3$, by $\mathbf{v}_{f,\bar{v}}$. We use the consistency property (S2) to transform the last term of (8.89) by adding and subtracting $\mathbf{v}_{f,\bar{v}}$:

$$\begin{aligned} \sum_{P \in \Omega_h} \mathcal{A}_{h,P}(\boldsymbol{\psi}_P^I, \mathbf{v}_h) &= \sum_{P \in \Omega_h} \sum_{f \in \partial P} \sum_{v \in \partial f} (\mathbf{v}_{f,v} - \mathbf{v}_{f,\bar{v}}) \cdot (\boldsymbol{\varepsilon}(\boldsymbol{\psi}_P) \cdot \mathbf{n}_{P,f}) \omega_{f,v} \\ &+ \sum_{P \in \Omega_h} \sum_{f \in \partial P} |f| \mathbf{v}_f \mathbf{n}_f \cdot (\boldsymbol{\varepsilon}(\boldsymbol{\psi}_P) \cdot \mathbf{n}_{P,f}) + \sum_{P \in \Omega_h} \sum_{f \in \partial P} \sum_{v \in \partial f} \mathbf{v}_{f,\bar{v}} \cdot (\boldsymbol{\varepsilon}(\boldsymbol{\psi}_P) \cdot \mathbf{n}_{P,f}) \omega_{f,v} \\ &= T_2 + T_3 + \sum_{P \in \Omega_h} \sum_{f \in \partial P} \sum_{v \in \partial f} \mathbf{v}_{f,\bar{v}} \cdot (\boldsymbol{\varepsilon}(\boldsymbol{\psi}_P) \cdot \mathbf{n}_{P,f}) \omega_{f,v}. \end{aligned} \quad (8.90)$$

We recall that the quadrature rule for face integrals provided by the set of nodal weights $\{\omega_{f,v}\}$ is exact for linear functions. Since, the derivative $\boldsymbol{\varepsilon}(\boldsymbol{\psi}_P) \cdot \mathbf{n}_{P,f}$ is constant over f , we have

$$\sum_{v \in \partial f} \mathbf{v}_{f,\bar{v}} \cdot (\boldsymbol{\varepsilon}(\boldsymbol{\psi}_P) \cdot \mathbf{n}_{P,f}) \omega_{f,v} = |f| \mathbf{v}_{f,\bar{v}} \cdot (\boldsymbol{\varepsilon}(\boldsymbol{\psi}_P) \cdot \mathbf{n}_{P,f}) = \int_f \mathbf{v}_{f,\bar{v}} \cdot (\boldsymbol{\varepsilon}(\boldsymbol{\psi}_P) \cdot \mathbf{n}_{P,f}) dS.$$

We insert this in the last term of (8.90), then add and subtract $R_P(\mathbf{v}_P)$, integrate by parts, and finally observe that $\operatorname{div}(\boldsymbol{\varepsilon}(\boldsymbol{\psi}_P)) = 0$ as $\boldsymbol{\varepsilon}(\boldsymbol{\psi}_P)$ is constant:

$$\begin{aligned} \sum_{P \in \Omega_h} \sum_{f \in \partial P} \sum_{v \in \partial f} \mathbf{v}_{f,\bar{v}} \cdot (\boldsymbol{\varepsilon}(\boldsymbol{\psi}_P) \cdot \mathbf{n}_{P,f}) \omega_{f,v} &= \sum_{P \in \Omega_h} \sum_{f \in \partial P} \int_f \mathbf{v}_{f,\bar{v}} \cdot (\boldsymbol{\varepsilon}(\boldsymbol{\psi}_P) \cdot \mathbf{n}_{P,f}) dS \\ &= \sum_{P \in \Omega_h} \sum_{f \in \partial P} \int_f (\mathbf{v}_{f,\bar{v}} - R_P(\mathbf{v}_P)) \cdot (\boldsymbol{\varepsilon}(\boldsymbol{\psi}_P) \cdot \mathbf{n}_{P,f}) dS \\ &\quad + \sum_{P \in \Omega_h} \sum_{f \in \partial P} \int_f R_P(\mathbf{v}_P) \cdot (\boldsymbol{\varepsilon}(\boldsymbol{\psi}_P) \cdot \mathbf{n}_{P,f}) dS \\ &= T_4 + \sum_{P \in \Omega_h} \int_P \boldsymbol{\varepsilon}(R_P(\mathbf{v}_P)) : \boldsymbol{\varepsilon}(\boldsymbol{\psi}_P) dV. \end{aligned} \quad (8.91)$$

Finally, adding and subtracting $\boldsymbol{\varepsilon}(\mathbf{u})$ yields

$$\begin{aligned} \sum_{P \in \Omega_h} \int_P \boldsymbol{\varepsilon}(R_P(\mathbf{v}_P)) : \boldsymbol{\varepsilon}(\boldsymbol{\psi}_P) dV \\ &= \sum_{P \in \Omega_h} \left(\int_P \boldsymbol{\varepsilon}(R_P(\mathbf{v}_P)) : (\boldsymbol{\varepsilon}(\boldsymbol{\psi}_P) - \boldsymbol{\varepsilon}(\mathbf{u})) dV + \int_P \boldsymbol{\varepsilon}(R_P(\mathbf{v}_P)) : \boldsymbol{\varepsilon}(\mathbf{u}) dV \right) \\ &= T_5 + \int_{\Omega} \boldsymbol{\varepsilon}(R(\mathbf{v}_h)) : \boldsymbol{\varepsilon}(\mathbf{u}) dV = T_5 + A_1. \end{aligned} \quad (8.92)$$

Now, we develop term C in (8.88) by using definition (8.17), condition **(L4)**, and adding and subtracting the pressure solution p :

$$\begin{aligned}
C &= [\operatorname{div}_h \mathbf{v}_h, p^I]_{Q_h} = \sum_{P \in \Omega_h} |P| (\operatorname{div}_P \mathbf{v}_P) p_P^I = \sum_{P \in \Omega_h} \int_P \operatorname{div} R_P(\mathbf{v}_P) p_P^I dV \\
&= \sum_{P \in \Omega_h} \int_P (\operatorname{div} R_P(\mathbf{v}_P)) (p^I - p) dV + \sum_{P \in \Omega_h} \int_P (\operatorname{div} R_P(\mathbf{v}_P)) p dV \\
&= T_6 + A_2.
\end{aligned} \tag{8.93}$$

Using (8.7) with $\mathbf{v} = R(\mathbf{v}_h)$, we obtain

$$A_1 - A_2 = \int_{\Omega} \boldsymbol{\varepsilon}(R(\mathbf{v}_h)) : \boldsymbol{\varepsilon}(\mathbf{u}) dV - \int_{\Omega} p \operatorname{div} R(\mathbf{v}_h) dV = \int_{\Omega} \mathbf{b} \cdot R(\mathbf{v}_h) dV$$

and

$$A - (A_1 - A_2) = (\mathbf{b}, \mathbf{v}_h)_h - \int_{\Omega} \mathbf{b} \cdot R(\mathbf{v}_h) dV = T_7. \tag{8.94}$$

Finally, we substitute the expressions for the terms T_1, \dots, T_7 into the terms A, B, C and the resulting expressions into (8.85) to derive the error bound

$$\alpha \left(\|\mathbf{u}_h - \mathbf{u}^{\mathbb{I}}\|_{X_h} + \|p_h - p^I\|_{Q_h} \right) \leq \sum_{i=1}^7 |T_i|. \tag{8.95}$$

Estimate of T_1 . We apply the Cauchy-Schwarz inequality and bound (8.83) to have

$$\begin{aligned}
|T_1| &\leq \sum_{P \in \Omega_h} \mathcal{A}_{h,P}(\mathbf{u}^{\mathbb{I}} - \boldsymbol{\psi}_P^I, \mathbf{v}_P) \leq \sum_{P \in \Omega_h} \|\mathbf{u}^{\mathbb{I}} - \boldsymbol{\psi}_P^I\|_{X_{h,P}} \|\mathbf{v}_P\|_{X_{h,P}} \\
&\leq \left[\sum_{P \in \Omega_h} \|\mathbf{u}^{\mathbb{I}} - \boldsymbol{\psi}_P^I\|_{X_{h,P}}^2 \right]^{1/2} \|\mathbf{v}_h\|_{X_h} \leq \left[\sum_{P \in \Omega_h} \|\mathbf{u}^{\mathbb{I}} - \mathbf{u}_P^I\|_{X_{h,P}}^2 \right]^{1/2}.
\end{aligned} \tag{8.96}$$

Since $\mathbf{u}^{\mathbb{I}} = \mathbf{u}^I + \mathbf{u}^b$ with $\mathbf{u}^I|_f = 0$ for every face f and $\mathbf{u}^b|_v = 0$ for every vertex v , in accordance with norm definition (8.38), it follows that

$$\|\mathbf{u}^{\mathbb{I}} - \boldsymbol{\psi}_P^I\|_{X_{h,P}}^2 = \|\mathbf{u}^I - \boldsymbol{\psi}_P^I\|_{X_{h,P}}^2 + h_P \sum_{f \in \partial P} |u_f^b|^2. \tag{8.97}$$

The first term is bounded by Lemma 8.3:

$$\|\mathbf{u}^I - \boldsymbol{\psi}_P^I\|_{X_{h,P}} \leq \gamma_2 h_P \|\mathbf{u}\|_{H^2(\Omega)}. \tag{8.98}$$

To bound the second term, we apply definition (8.13) with $\mathbf{u}(\mathbf{x}_{f,v}) = \mathbf{u}_{f,v}^1$ instead of $\mathbf{v}(\mathbf{x}_{f,v})$ and recall that the quadrature rule is exact for linear functions:

$$\begin{aligned} |f|^2 |u_f^b|^2 &= \int_f \mathbf{u} \cdot \mathbf{n}_f dS - \sum_{v \in \partial f} \mathbf{u}(\mathbf{x}_{f,v}) \cdot \mathbf{n}_f \omega_{f,v}^2 \\ &\leq 2 \int_f (\mathbf{u} - \boldsymbol{\psi}_P) \cdot \mathbf{n}_f dS^2 + 2 \sum_{v \in \partial f} (\mathbf{u}(\mathbf{x}_{f,v}) - \boldsymbol{\psi}_P(\mathbf{x}_{f,v})) \cdot \mathbf{n}_f \omega_{f,v}^2. \end{aligned} \quad (8.99)$$

We use Jensen's inequality, the Cauchy-Schwarz inequality, the Agmon inequality from (M4), the estimate of the interpolation error from (M5), and finally the scaling $\alpha_* h_P^2 \leq |f|$ from (M2) to obtain

$$\begin{aligned} \int_f (\mathbf{u} - \boldsymbol{\psi}_P) \cdot \mathbf{n}_f dS^2 &\leq |f| C^{Agm} \left(h_P^{-1} \|\mathbf{u} - \boldsymbol{\psi}_P\|_{L^2(P)}^2 + h_P \|\mathbf{u} - \boldsymbol{\psi}_P\|_{H^1(P)}^2 \right) \\ &\leq C^{Agm} C^{Int} |f| h_P^3 |\mathbf{u}|_{H^2(P)}^2 \leq C |f|^2 h_P |\mathbf{u}|_{H^2(P)}^2, \end{aligned}$$

where C is the generic constant independent of the mesh. Now, we apply an L^∞ -estimate of the interpolation error extended to polyhedrons (see for instance [78, 115]) to obtain an upper bound for the second term in (8.99):

$$\sum_{v \in \partial f} (\mathbf{u}(\mathbf{x}_{f,v}) - \boldsymbol{\psi}_P(\mathbf{x}_{f,v})) \cdot \mathbf{n}_f \omega_{f,v}^2 \leq |f|^2 \|\mathbf{u} - \boldsymbol{\psi}_P\|_{L^\infty(P)}^2 \leq C |f|^2 h_P |\mathbf{u}|_{H^2(P)}^2.$$

Inserting the last two estimates into (8.99) yields

$$|u_f^b|^2 \leq C h_P |\mathbf{u}|_{H^2(P)}^2. \quad (8.100)$$

Since the number of faces in a polyhedron is uniformly bounded by $N^{\mathcal{F}}$, c.f. (M1), from Eq. (8.100) we obtain

$$\sum_{P \in \Omega_h} h_P \sum_{f \in \partial P} |u_f^b|^2 \leq C N^{\mathcal{F}} \sum_{P \in \Omega_h} h_P^2 |\mathbf{u}|_{H^2(P)}^2 \leq C h^2 |\mathbf{u}|_{H^2(\Omega)}^2. \quad (8.101)$$

We use inequalities (8.98), (8.101) in (8.97) and substitute the resulting expression into (8.96) in order to obtain the final estimate of T_1 :

$$|T_1| \leq C h \|\mathbf{u}\|_{H^2(\Omega)}. \quad (8.102)$$

Estimate of T_2 . Let us change the summation over the polyhedra into the summation over the mesh faces. To this purpose, we define the jump of the normal strain across mesh faces. Let f be an internal mesh face shared by polyhedra P_1 and P_2 . Then, we set

$$J_f(\boldsymbol{\psi}) = \boldsymbol{\varepsilon}(\boldsymbol{\psi}_{P_1}) \cdot \mathbf{n}_{P_1,f} + \boldsymbol{\varepsilon}(\boldsymbol{\psi}_{P_2}) \cdot \mathbf{n}_{P_2,f}, \quad (8.103)$$

which is a constant vector. The boundary faces do not contribute to T_2 because $\mathbf{v}_h \in X_{h,0}$. Thus,

$$T_2 = \sum_{f \in \mathcal{F}^0} \sum_{v \in \partial f} \omega_{f,v} (\mathbf{v}_{f,v} - \mathbf{v}_{f,\bar{v}}) \cdot J_f(\boldsymbol{\psi}).$$

We apply the Cauchy-Schwarz inequality twice, note that $J_f(\boldsymbol{\psi})$ is the same quantity for all vertices of f , and use the first relation in (8.10) to obtain:

$$\begin{aligned} |T_2| &\leq \sum_{f \in \mathcal{F}^0} \sum_{v \in \partial f} \|\mathbf{v}_{f,v} - \mathbf{v}_{f,\bar{v}}\| \|J_f(\boldsymbol{\psi})\| \omega_{f,v} \\ &\leq \left(\sum_{f \in \mathcal{F}^0} \sum_{v \in \partial f} \|\mathbf{v}_{f,v} - \mathbf{v}_{f,\bar{v}}\|^2 \omega_{f,v} \right)^{1/2} \left(\sum_{f \in \mathcal{F}^0} \|J_f(\boldsymbol{\psi})\|^2 \sum_{v \in \partial f} \omega_{f,v} \right)^{1/2} \\ &\leq \left(\sum_{P \in \Omega_h} \sum_{f \in \partial P} \sum_{v \in \partial f} \|\mathbf{v}_{f,v} - \mathbf{v}_{f,\bar{v}}\|^2 \omega_{f,v} \right)^{1/2} \left(\sum_{f \in \mathcal{F}^0} |f| \|J_f(\boldsymbol{\psi})\|^2 \right)^{1/2}. \end{aligned}$$

Due to Lemma 8.4, it holds

$$\sum_{f \in \mathcal{F}^0} |f| \|J_f(\boldsymbol{\psi})\|^2 = \sum_{f \in \mathcal{F}^0} \|J_f(\boldsymbol{\psi})\|_{L^2(f)}^2 \leq \gamma_3 h \|\mathbf{u}\|_{H^2(\Omega)}^2. \quad (8.104)$$

Lemma 8.2 allows us to estimate the other factor. Recall that the number of faces in P is uniformly bounded by $N^{\mathcal{F}}$, c.f. **(M1)**. We use this, Eq. (8.104) and inequality $\|\mathbf{v}_h\|_{X_{h,P}} \leq 1$ to obtain the estimate:

$$|T_2| \leq \left(N^{\mathcal{F}} \gamma_1 \sum_{P \in \Omega_h} h_P \|\mathbf{v}_h\|_{X_{h,P}}^2 \right)^{1/2} \left(\gamma_3 h \|\mathbf{u}\|_{H^2(\Omega)}^2 \right)^{1/2} \leq Ch \|\mathbf{u}\|_{H^2(\Omega)}. \quad (8.105)$$

Estimate of T_3 . We start with definition (8.103) and note again that $v_f = 0$ on the boundary faces. This allows us to reformulate T_3 as

$$T_3 = \sum_{P \in \Omega_h} \sum_{f \in \partial P} |f| v_f \mathbf{n}_f \cdot (\boldsymbol{\varepsilon}(\boldsymbol{\psi}_P) \cdot \mathbf{n}_{P,f}) = \sum_{f \in \mathcal{F}^0} |f| v_f \mathbf{n}_f \cdot J_f(\boldsymbol{\psi}). \quad (8.106)$$

Now, by applying the Cauchy-Schwarz inequality twice, we immediately obtain

$$|T_3| \leq \sum_{f \in \mathcal{F}^0} |f| |v_f| \|J_f(\boldsymbol{\psi})\| \leq \left(\sum_{f \in \mathcal{F}^0} |f| |v_f|^2 \right)^{1/2} \left(\sum_{f \in \mathcal{F}^0} |f| \|J_f(\boldsymbol{\psi})\|^2 \right)^{1/2}. \quad (8.107)$$

We note that $|f| \approx h_P^2$ due to **(M2)** and $\|\mathbf{v}_h\|_{X_{h,P}} \leq 1$. The definition of this norm given in (8.38) leads to a chain of simple inequalities:

$$\sum_{f \in \mathcal{F}^0} |f| |v_f|^2 \leq C \sum_{P \in \Omega_h} h_P^2 \sum_{f \in \partial P} |v_f|^2 \leq C \sum_{P \in \Omega_h} h_P \|\mathbf{v}_h\|_{X_{h,P}}^2 \leq Ch. \quad (8.108)$$

Substituting (8.108) and (8.104) into (8.106) provides the final bound on T_3 :

$$|T_3| \leq Ch \|\mathbf{u}\|_{H^2(\Omega)}.$$

Estimate of T_4 . Due to **(L6)**, the traces of $R_{P_1}(\mathbf{v}_{P_1})$ and $R_{P_2}(\mathbf{v}_{P_2})$ on the common face $f \subseteq \partial P_1 \cap \partial P_2$ coincide. Therefore, we consider again the jump of the normal strain and rewrite T_4 as

$$T_4 = \sum_{f \in \mathcal{F}^0} \int_f (\mathbf{v}_{f,\bar{\nu}} - R(\mathbf{v}_h)) \cdot J_f(\boldsymbol{\psi}) dS. \quad (8.109)$$

We apply the Cauchy-Schwarz inequality twice to obtain

$$\begin{aligned} |T_4| &\leq \sum_{f \in \mathcal{F}^0} \|\mathbf{v}_{f,\bar{\nu}} - R(\mathbf{v}_h)\|_{L^2(f)} \|J_f(\boldsymbol{\psi})\|_{L^2(f)} \\ &\leq \left(\sum_{f \in \mathcal{F}^0} \|\mathbf{v}_{f,\bar{\nu}} - R(\mathbf{v}_h)\|_{L^2(f)}^2 \right)^{1/2} \left(\sum_{f \in \mathcal{F}^0} \|J_f(\boldsymbol{\psi})\|_{L^2(f)}^2 \right)^{1/2}. \end{aligned} \quad (8.110)$$

We develop (8.110) further by using the Agmon inequality from **(M4)** with the constant function $\mathbf{v}_{f,\bar{\nu}}$. Also, we use the reconstruction properties **(L2)**–**(L3)** and $\|\mathbf{v}_h\|_{X_h} \leq 1$ to obtain:

$$\begin{aligned} \|\mathbf{v}_{f,\bar{\nu}} - R(\mathbf{v}_h)\|_{L^2(f)}^2 &\leq C^{Agm} \left(h_P^{-1} \|\mathbf{v}_{f,\bar{\nu}} - R(\mathbf{v}_h)\|_{L^2(P)}^2 + h_P |R(\mathbf{v}_h)|_{H^1(P)}^2 \right) \\ &\leq C^{Agm} (C^R)^2 h_P \|\mathbf{v}_h\|_{X_h}^2 \leq C^{Agm} (C^R)^2 h_P. \end{aligned} \quad (8.111)$$

The second factor in the right-hand side of (8.110) is bounded by Lemma 8.4. Applying this upper bound and (8.111) yields

$$|T_4| \leq Ch \|\mathbf{u}\|_{H^2(\Omega)}. \quad (8.112)$$

Estimate of T_5 . To estimate this term, we apply the triangular inequality, the Cauchy-Schwarz inequality, and property **(L2)** of the reconstruction operator. Again, we use $\|\mathbf{v}_h\|_{X_h} \leq 1$ and the interpolation error estimate given by **(M5)**. This yields

$$\begin{aligned} |T_5| &\leq \sum_{P \in \Omega_h} \int_P \boldsymbol{\varepsilon}(R_P(\mathbf{v}_P)) : \boldsymbol{\varepsilon}(\boldsymbol{\psi}_P - \mathbf{u}) dV \leq \sum_{P \in \Omega_h} |R_P(\mathbf{v}_P)|_{H^1(P)} |\boldsymbol{\psi}_P - \mathbf{u}|_{H^1(P)} \\ &\leq \left(\sum_{P \in \Omega_h} |R_P(\mathbf{v}_P)|_{H^1(P)}^2 \right)^{1/2} \left(\sum_{P \in \Omega_h} |\boldsymbol{\psi}_P - \mathbf{u}|_{H^1(P)}^2 \right)^{1/2} \\ &\leq C^R \|\mathbf{v}_h\|_{X_h} \left(C^{Int} \sum_{P \in \Omega_h} h_P^2 |\mathbf{u}|_{H^2(P)}^2 \right)^{1/2} \leq Ch \|\mathbf{u}\|_{H^2(\Omega)}. \end{aligned} \quad (8.113)$$

Estimate of T_6 . To estimate this term, we use the triangular inequality, the Cauchy-Schwarz inequality, and property **(L2)** of the reconstruction operator. In addition, we use $\|\mathbf{v}_h\|_{X_h} \leq 1$ and the interpolation error estimate from **(M5)**, but now for a scalar

function:

$$\begin{aligned}
|\mathbb{T}_6| &\leq \sum_{P \in \Omega_h} \int_P (\operatorname{div} R_P(\mathbf{v}_P))(p^I - p) dV \leq \sum_{P \in \Omega_h} |R_P(\mathbf{v}_P)|_{H^1(P)} \|p^I - p\|_{L^2(P)} \\
&\leq \left(\sum_{P \in \Omega_h} |R_P(\mathbf{v}_P)|_{H^1(P)}^2 \right)^{1/2} \left(\sum_{P \in \Omega_h} \|p^I - p\|_{L^2(P)}^2 \right)^{1/2} \\
&\leq C^R \|\mathbf{v}_h\|_{X_h} \left(C^{Int} \sum_{P \in \Omega_h} h_P^2 |p|_{H^1(P)}^2 \right)^{1/2} \leq Ch |p|_{H^1(\Omega)}. \tag{8.114}
\end{aligned}$$

Estimate of \mathbb{T}_7 . To estimate the last term, we apply Lemma 8.5:

$$|\mathbb{T}_7| \leq \gamma_4 h \|\mathbf{b}\|_{L^2(\Omega)} \|\mathbf{v}_h\|_{X_h} \leq Ch (\|\mathbf{u}\|_{H^2(\Omega)} + \|p\|_{H^1(\Omega)}). \tag{8.115}$$

Combining all estimates in (8.95), we prove the theorem. \square

8.3 Reduced edge bubbles formulation

In the mimetic formulation of the previous sections, the discrete velocity space X_h contains both the vertex-based and face-based degrees of freedom. The latter are referred to as bubbles and are introduced only to stabilize the numerical scheme, i.e. to prove the discrete *inf-sup* condition (8.51)–(8.52). This condition asserts that the velocity space X_h is sufficiently rich to control the pressure space Q_h . Although the resulting mimetic scheme is stable, there is a subtle issue.

The number of vertices in a polyhedral mesh is usually bigger than that in a tetrahedral mesh with a same number of cells. If the number of vertices increases without a significant change in the number of cells, the velocity space gets richer while the pressure space stays essentially the same. Hence, on a polyhedral mesh the fulfillment of the *inf-sup* condition may be expected to be easier and the face degrees of freedom might not be necessary. In two dimensions, this is often the case and we can modify the mimetic discretization so that the bubble degrees of freedom are added only when they are really necessary, thus yielding a more efficient numerical scheme. As shown in Fig. 8.1, on the mesh of square cells, the edge bubbles are needed roughly to every fourth edge and on the polygonal mesh they are not needed at all.

To determine sufficient conditions for adding edge bubbles to the discretization, we extend the macroelement technology of [333] to polygonal meshes. In the developments of this section, we require the mesh to satisfy assumption **(MR3)** from Sect. 1.7 in addition to assumptions **(MR1)**–**(MR2)**. For simplicity of the exposition, we consider the homogeneous Dirichlet boundary conditions, i.e. $\Gamma^D = \partial\Omega$ and $\mathbf{g}^D = 0$ in problem (8.1)–(8.4). The notation introduced earlier are easily adjusted to the two-dimensional case by using edges instead of faces. For example, X_h still denotes the space of the discrete velocity fields and $X_{h,0}$ is its subspace corresponding to zero boundary conditions.

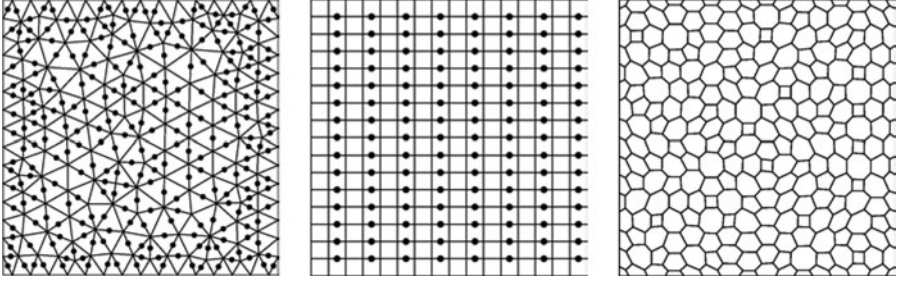


Fig. 8.1. Dots mark the location of bubble-type degrees of freedom on three different meshes

We note that even if this section considers the two-dimensional case, the arguments used herein can be extended to the three-dimensional case. The results of this section are based on [47].

8.3.1 The modified mimetic discretization

Formally, the modified mimetic scheme reads exactly as in (8.26)–(8.27). The major difference is in the definition of the discrete velocity field X_h . This difference requires some adjustments in the mimetic framework that we discuss below.

Let us decompose \mathcal{E}^0 , the set of the internal edges of a polygonal mesh, in the union of two disjoint subsets, namely, \mathcal{E}^b and \mathcal{E}^x , so that $\mathcal{E}^0 = \mathcal{E}^b \cup \mathcal{E}^x$. A practical construction of \mathcal{E}^b and \mathcal{E}^x is discussed later in the section.

- The space of discrete velocity fields X_h is defined by attaching two degrees of freedom to each vertex and one degree of freedom to each edge from \mathcal{E}^b . For $\mathbf{v}_h \in X_h$, the degrees of freedom associated with vertex \mathbf{v} form a two-dimensional vector $\mathbf{v}_\mathbf{v}$ that approximates velocity at the vertex. The edge-based degrees of freedom $v_\mathbf{e}$ represent corrections to the normal velocity components on mesh edges:

$$\mathbf{v}_h = (\mathbf{v}_\mathbf{v}, v_\mathbf{e})_{\mathbf{v} \in \mathcal{V}, \mathbf{e} \in \mathcal{E}^b}.$$

Similarly to Remark 8.1, the edge-based degrees of freedom can be used to define a continuum vector-values function $\mathbf{v}_{h,\mathbf{e}}$ of each mesh edge \mathbf{e} such that:

(A1) On edge $\mathbf{e} \in \mathcal{E}^0$, the tangential component of $\mathbf{v}_{h,\mathbf{e}}$ is linear and is uniquely determined by the values of \mathbf{v}_h at two end-points of \mathbf{e} .

(A2) On edge $\mathbf{e} \in \mathcal{E}^x$, the normal component of $\mathbf{v}_{h,\mathbf{e}}$ is linear and is uniquely determined by the values of \mathbf{v}_h at two end-points of \mathbf{e} .

(A3) On edge $\mathbf{e} = (\mathbf{v}, \mathbf{v}_1) \in \mathcal{E}^b$, the normal component of $\mathbf{v}_{h,\mathbf{e}}$ is a quadratic function and is uniquely determined by the values of \mathbf{v}_h at the end-points of \mathbf{e} and edge-based value $v_\mathbf{e}$. The following relationship holds

$$\int_{\mathbf{e}} \mathbf{v}_{h,\mathbf{e}} \cdot \mathbf{n}_\mathbf{e} dS = \frac{|\mathbf{e}|}{2} (\mathbf{v}_\mathbf{v} + \mathbf{v}_{\mathbf{v}_1}) \cdot \mathbf{n}_\mathbf{e} + |\mathbf{e}| v_\mathbf{e}. \quad (8.116)$$

The first term in the right-hand side of (8.116) is the one-dimensional analog of the face integration rule in (8.13).

We define the projection operator $(\cdot)^{\parallel}$ from a sufficiently smooth space into X_h by restricting (8.14) to the edges of \mathcal{E}^b . A mesh-dependent energy-like norm on X_h is defined by

$$\| \mathbf{v}_h \|_{X_h}^2 = \sum_{P \in \Omega_h} \| \mathbf{v}_P \|_{X_{h,P}}^2, \quad \| \mathbf{v}_P \|_{X_{h,P}}^2 = \sum_{e \in \partial P} |e| \left\| \frac{\partial \mathbf{v}_{h,e}}{\partial s} \right\|_{L^2(e)}^2 \quad \forall \mathbf{v}_h \in X_h, \quad (8.117)$$

where s is the local coordinate along e . This norm is equivalent to the norm given in (8.28) for $d = 2$.

The space of the discrete pressures is equipped with norm (8.18), which is induced by the mimetic inner product (8.17). We also need the mesh-dependent semi-norm

$$|q_h|_h^2 = \sum_{e \in \mathcal{E}^0} |e|^2 \llbracket q_h \rrbracket_e^2 \quad \forall q_h \in \mathcal{P}_h,$$

where $\llbracket q_h \rrbracket_e = q_{P_1} - q_{P_2}$ is the jump of q_h across the internal edge e shared by two polygons P_1 and P_2 . The assume that the normal vector \mathbf{n}_e points from P_1 to P_2 .

The discrete divergence operator $\text{div}_h : X_h \rightarrow Q_h$ restricted to cell P can be written using the old and new definitions:

$$\text{div}_P \mathbf{v}_P = \frac{1}{|P|} \sum_{e=(v,v_1) \in \partial P} |e| \left(\frac{\mathbf{v}_v + \mathbf{v}_{v_1}}{2} \cdot \mathbf{n}_{P,e} + v_e \right) = \frac{1}{|P|} \sum_{e \in \partial P} \int_e \mathbf{v}_{h,e} \cdot \mathbf{n}_{P,e} dS.$$

The bilinear form $\mathcal{A}_h : X_h \times X_h \rightarrow \mathbb{R}$ is required to satisfy the same stability and consistency conditions (S1) and (S2) of Sect. 8.1.4.

8.3.2 Stability of the modified scheme

As noted in Remark 8.8, the uniform stability of the mimetic discretization is guaranteed provided that the following *inf-sup* condition holds [88]:

Condition 8.2. *There exists a positive constant β , independent of h , such that*

$$\sup_{\mathbf{v}_h \in X_h \setminus \{\mathbf{0}\}} \frac{[\text{div}_h \mathbf{v}_h, q_h]_{Q_h}}{\| \mathbf{v}_h \|_{X_h}} \geq \beta \| q_h \|_{Q_h} \quad \forall q_h \in \mathcal{P}_h. \quad (8.118)$$

This condition is crucial. If it holds, the convergence of the solution $(\mathbf{u}_h, p_h) \in X_h \times Q_h$ of the modified mimetic scheme to the exact solution can be proved as shown in Sect. 8.2.3. Conversely, when it fails, spurious pressure modes may pollute the numerical solution leading to an unsatisfactory result.

The equivalent *inf-sup* condition in Lemma 8.6 is proved for the case $\mathcal{E}^b = \mathcal{E}^0$. A key role in the analysis is played by the edge-based degrees of freedom that are introduced to stabilize the scheme. Later, we show that Condition 8.2 may hold when \mathcal{E}^b is much smaller than \mathcal{E}^0 .

8.3.3 A macroelement technique

In this section, we extend the finite element results of [333] for simplicial meshes to mimetic discretizations on polygonal meshes that satisfy (MR1)–(MR3). The main result of this section, Theorem 8.3, follows from four preliminary lemmas, whose proofs can be found in [333] and [47].

Let us introduce the concepts of a macroelement and the equivalence class of macroelements. In view of assumption (MR1), for each integer $3 \leq n \leq \mathcal{N}^\varepsilon$ there exists a reference polygon \widehat{P}_n such that the following results hold. Each cell $P \in \Omega_h$ with exactly n edges is the image of an invertible and continuous map

$$\Phi_P : \widehat{P}_n \longrightarrow P. \quad (8.119)$$

Furthermore, map Φ_P and its inverse are piecewise $W^{1,\infty}$ -regular with respect to the triangular partition $T_{h|P}$ introduced in (MR2)–(MR3).

To prove these results, we define \widehat{P}_n as a convex regular polygon with n edges and build a triangulation of \widehat{P}_n by connecting its vertices with its centroid \widehat{x}_P . Then, for every element $P \in \Omega_h$ with n edges, the mapping Φ_P is the only $T_{h|P}$ -piecewise linear function that maps the ordered vertices of \widehat{P}_n to the ordered vertices of P and \widehat{x}_P to the point \bar{x}_P defined in (MR3). The $W^{1,\infty}$ regularity of Φ_P can be proved by using the standard arguments from the finite element literature (see, e.g. [78, 115]) based on the shape-regularity assumption (MR2).

A *macroelement* M is a connected collection of polygons P . Let \mathcal{M} denote a set of macroelements that cover completely the mesh Ω_h , i.e. for any $P \in \Omega_h$ there exists $M \in \mathcal{M}$ containing it. Given $M \in \mathcal{M}$, we introduce the local spaces:

$$\begin{aligned} X_{h,M}^0 &= \left\{ \mathbf{v}_h \in X_{h|M} : \mathbf{v}_v = \mathbf{0} \quad \forall v \in \mathcal{V} \cap \partial M, \quad v_f = 0 \quad \forall e \in \mathcal{E}^b \cap \partial M \right\}, \\ Q_{h,M} &= \mathcal{P}_{h|M}. \end{aligned}$$

Let \mathbf{v}_M be the restriction of \mathbf{v}_h to macroelement M . Furthermore, let \mathcal{E}^M indicate the set of all the internal edges of M . We will make use of the following local norm and seminorm:

$$\begin{aligned} \|\mathbf{v}_M\|_M^2 &= \sum_{P \in M} \|\mathbf{v}_P\|_{X_{h,P}}^2 \quad \forall \mathbf{v}_M \in X_{h,M}^0, \\ |q_M|_M^2 &= \sum_{e \in \mathcal{E}^M} |e|^2 [|q_M]_e]^2 \quad \forall q_M \in Q_{h,M}. \end{aligned}$$

Now, we introduce the *equivalence class of macroelements*. Note that the reference macroelement used the definition below is not necessarily formed by the reference polygons.

Definition 8.1. We say that a macroelement M is equivalent with a given reference macroelement \widetilde{M} if there exists a continuous and invertible map $\Phi_M : \widetilde{M} \rightarrow M$ that satisfies four conditions below.

- The map is surjective, $\Phi_M(\widetilde{M}) = M$.

- Let $\tilde{M} = \cup_{i=1}^m \tilde{P}_i$ and $M = \cup_{i=1}^m P_i$. Moreover, let P_i and \tilde{P}_i have the same number of edges, n_i . Then $P_i = \Phi_M(\tilde{P}_i)$.
- For each $i = 1, 2, \dots, m$, we have $(\Phi_M)|_{\tilde{P}_i} = \Phi_{P_i} \circ \Phi_{\tilde{P}_i}^{-1}$, where Φ_{P_i} and $\Phi_{\tilde{P}_i}$ are the maps from the reference element \hat{P}_{n_i} , introduced in (8.119), onto P_i and \tilde{P}_i , respectively.
- If \tilde{e} is an interior edge of \tilde{M} , then $e = \Phi_M(\tilde{e})$ is an interior edge of M .

We say that two macroelements are equivalent when they are equivalent to the same reference macroelement. \square

The following lemma has been proved in [333, Lemma 1].

Lemma 8.8. *Assume that there exists a macroelement partition \mathcal{M} such that each $e \in \mathcal{E}^0$ is an interior edge of at least one and not more than L_* macroelements, where L_* is independent of h . Moreover, assume that there exists a positive constant β_1 such that*

$$\sup_{\mathbf{v}_M \in X_{h,M}^0 \setminus \{0\}} \frac{[q_M, \operatorname{div}_M \mathbf{v}_M]_{Q_{h,M}}}{\|\mathbf{v}_M\|_M} \geq \beta_1 |q_M|_M \quad \forall q_M \in Q_{h,M},$$

for all $M \in \mathcal{M}$. Then, there exist a positive constant β_2 such that

$$\sup_{\mathbf{v}_h \in X_h \setminus \{0\}} \frac{[q_h, \operatorname{div}_h \mathbf{v}_h]_{Q_h}}{\|\mathbf{v}_h\|_{X_h}} \geq \beta_2 |q_h|_h \quad \forall q_h \in \mathcal{P}_h. \quad (8.120)$$

The following result extends [333, Lemma 2] to the case of mimetic discretizations on polygonal meshes. Its proof can be found in [47].

Lemma 8.9. *There exist two positive constants β_3 and β_4 , independent of h , such that*

$$\sup_{\mathbf{v}_h \in X_h \setminus \{0\}} \frac{[q_h, \operatorname{div}_h \mathbf{v}_h]_{Q_h}}{\|\mathbf{v}_h\|_{X_h}} \geq \beta_3 \|q_h\|_{Q_h} - \beta_4 |q_h|_h \quad \forall q_h \in \mathcal{P}_h.$$

The next result follows easily using Lemma 8.9. The proof, which is identical to the finite element case, can be found in [333, Lemma 3].

Lemma 8.10. *Let the stability estimate (8.120) hold. Then, condition (8.118) is true.*

The following fundamental lemma is the extension of [333, Lemma 4] to the mimetic discretization on a polygonal mesh. Its proof based on the compactness argument can be found in [47].

Lemma 8.11. *Let Σ be a class of equivalent macroelements. Suppose that for every $M \in \Sigma$ the space*

$$\mathcal{N}_M = \{q_M \in Q_{h,M} : [q_M, \operatorname{div}_M \mathbf{v}_M]_{Q_{h,M}} = 0 \quad \forall \mathbf{v}_M \in X_{h,M}^0\} \quad (8.121)$$

is one dimensional and consist of mesh functions that are constant on M . Then, there exists a constant β_5 , independent of h , such that

$$\sup_{\mathbf{v}_M \in X_{h,M}^0 \setminus \{0\}} \frac{[q_M, \operatorname{div}_M \mathbf{v}_M]_{Q_{h,M}}}{\|\mathbf{v}_M\|_M} \geq \beta_5 |q_M|_M \quad \forall q_M \in Q_{h,M} \quad (8.122)$$

holds for all $M \in \Sigma$.

The main result of this section follows by combining Lemmas 8.8, 8.10 and 8.11.

Theorem 8.3. *Let \mathcal{M} be a macroelement partition of Ω_h . Suppose that*

1. \mathcal{M} is composed of a finite set of equivalence classes Σ_i , $i = 1, 2, \dots, l$, of macroelements.
2. For each $M \in \Sigma_i$ for some i , the space \mathcal{N}_M in (8.121) is one-dimensional and consists of mesh functions that are constant on M .
3. There exists $L_* \in \mathbb{N}$ such that each $e \in \mathcal{E}^0$ is an interior edge of at least one and no more than L_* macroelements.

Then, the inf-sup condition (8.118) holds.

8.3.4 Sufficient conditions for the stability

The results in this section provide a practical tool for identifying the stabilizing set \mathcal{E}^b of edge bubbles. Given a polygonal mesh Ω_h satisfying (MR1)–(MR3), we construct a macroelement partition \mathcal{M} that verifies the hypotheses of Theorem 8.3. Let $v \in \mathcal{V}^0$ be an internal mesh node that shared by at least three mesh edges and M_v be the macroelement collecting all polygons P that have vertex v , see Fig. 8.2. All such macroelements M_v , $v \in \mathcal{V}^0$, cover (possibly with overlaps) the mesh Ω_h .

For any internal edge $e \in \mathcal{E}^0$, there exists at least one macroelement M such that e is an internal edge of M . The only exceptions are meshes which include cells with all vertices on the boundary, a case which is always possible (and wise) to avoid. In addition, it is easy to verify that each internal edge $e \in \mathcal{E}^0$ belongs to at most two macroelements. Thus, the third condition of Theorem 8.3 is verified.

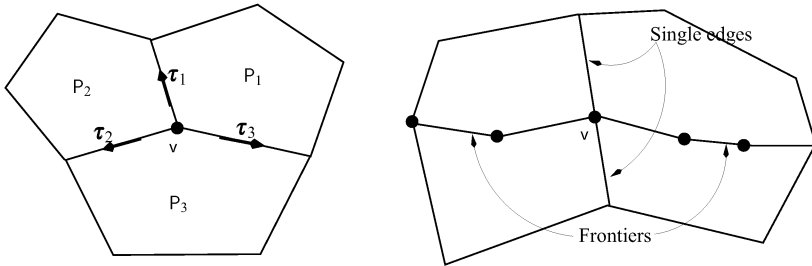


Fig. 8.2. Two examples of macroelements

In order to check the first condition of Theorem 8.3, we need to count the number of equivalence classes Σ_i in \mathcal{M} . Two macroelements M_v and $M_{v'}$ are equivalent if

1. The number of polygons in M_v equals to the number of polygons in $M_{v'}$. We denote this number by $k(v)$.
2. The number of edges in polygons $P_1, P_2, \dots, P_{k(v)}$, ordered counter-clockwise around vertex v , is the same as that in polygons $P'_1, P'_2, \dots, P'_{k(v)}$, ordered counter-clockwise around vertex v' .
3. The number of edges in $\partial P_i \cap \partial P_{i+1}$ is equal to the number of edges in $\partial P'_i \cap \partial P'_{i+1}$ for $i = 1, 2, \dots, k(v)$ (modulo $k(v)$).
4. The number of internal edges in M_v which are in \mathcal{E}_v^b is equal to that in $M_{v'}$. The same holds for their relative positions.

Due to assumption **(MR1)** of Chap. 1, each polygon has no more than $\mathcal{N}^\mathcal{E}$ edges and any set $\partial P_i \cap \partial P_j$ has at most $\mathcal{N}^\mathcal{E} - 1$ edges. The shape regularity assumption **(MR2)** implies that all angles in the mesh are uniformly bounded from below. Therefore, $k(v) \leq K_*$ with K_* independent of h . As the consequence of the above arguments, there exist a finite number of equivalence classes in \mathcal{M} , i.e. the first condition in Theorem 8.3 is satisfied.

The second condition of Theorem 8.3 is more involved and we need additional notations. Given an internal node v and the respective macroelement M_v , we denote by \mathcal{E}_v the set of mesh edges that join at v . We also introduce subsets $\mathcal{E}_v^x = \mathcal{E}_v \cap \mathcal{E}^x$ and $\mathcal{E}_v^b = \mathcal{E}_v \cap \mathcal{E}^b$. Let the integers N_v, N_v^x , and N_v^b indicate the cardinality of the sets $\mathcal{E}_v, \mathcal{E}_v^x$, and \mathcal{E}_v^b , respectively.

Lemma 8.12. *Assume that v is the only internal vertex in M_v . Let either (a) $N_v^x < 3$ or (b) $N_v^x = 3$ and the three angles naturally defined by the three edges in \mathcal{E}_v^x be less or equal than π . Then, the space \mathcal{N}_M defined in (8.121) consists of constant mesh functions.*

Proof. The proof is divided into three steps. *Step 1.* Let $N_v^x = 3$ as shown, for example, on the left panel in Fig. 8.2. We enumerate the three edges in \mathcal{E}_v^x as e_1, e_2, e_3 , their normals as $\mathbf{n}_1, \mathbf{n}_2, \mathbf{n}_3$ and their tangents as $\boldsymbol{\tau}_1, \boldsymbol{\tau}_2, \boldsymbol{\tau}_3$. We assume that $\boldsymbol{\tau}_i$ points outwards of v and the corresponding normal \mathbf{n}_i is obtained by its clockwise rotation by the angle $\pi/2$:

$$\boldsymbol{\tau}_i = (\boldsymbol{\tau}_{i,x}, \boldsymbol{\tau}_{i,y}) = (-n_{i,y}, n_{i,x}).$$

Thus, the jump of q_M across e_i is given by $[[q_M]]_{e_i} = q_{P_{i+1}} - q_{P_i}$. Without loss of generality, we can assume that $\boldsymbol{\tau}_1$ and $\boldsymbol{\tau}_2$ are linearly independent. The remaining edges in \mathcal{E}_v are enumerated as e_4, e_5, \dots , and the same indices are used for their tangents and normals.

Let $q_M \in \mathcal{N}_M$. Since arbitrary vector \mathbf{v}_M in the definition of \mathcal{N}_M is zero on the boundary of M , the straightforward calculation yields

$$0 = [q_M, \operatorname{div}_M \mathbf{v}_M]_{Q_{h,M}} = \sum_{P \in M} \sum_{e \in \partial P} q_P \int_e \mathbf{v}_{h,e} \cdot \mathbf{n}_{P,e} dS = \sum_{e \in \mathcal{E}_v} [[q_M]]_e \int_e \mathbf{v}_{h,e} \cdot \mathbf{n}_e dS.$$

We define $\mathbf{w} = \mathbf{v}_v$. Using identity (8.116), the above equation gives

$$0 = \frac{1}{2} \sum_{e \in \mathcal{E}_v} |e| [[q_M]]_e \mathbf{w} \cdot \mathbf{n}_e + \sum_{e \in \mathcal{E}_v^b} |e| [[q_M]]_e \nu_e \quad \forall \mathbf{v}_M \in X_{h,M}^0. \quad (8.123)$$

The formula for the jump mentioned above gives immediately

$$\sum_{e \in \mathcal{E}_v} [[q_M]]_e = 0. \quad (8.124)$$

Thus, in order to prove the lemma, we need to show that equations (8.124) and (8.123) with respect to the jumps have only the trivial solution, $[[q_M]]_e = 0$.

Step 2. By taking $\mathbf{w} = 0$, $\nu_e = 1$ for any particular edge in \mathcal{E}_v^b , and $\nu_e = 0$ for all the remaining edges, it follows that $[[q_M]]_e = 0$ for all edges in \mathcal{E}_v^b .

Let now $\mathbf{w}_1, \mathbf{w}_2$ form a basis in \mathbb{R}^2 . We test condition (8.123) separately for \mathbf{w}_1 and \mathbf{w}_2 . Combining the resulting equations with condition (8.124), we obtain a system of equations

$$\mathbf{S} \mathbf{q} = \mathbf{0}, \quad (8.125)$$

where $\mathbf{q} = ([[q_M]]_{e_1}, [[q_M]]_{e_2}, [[q_M]]_{e_3})$, and the $\mathbb{R}^{3 \times 3}$ matrix \mathbf{S} has the form

$$\mathbf{S} = \begin{pmatrix} |e_1| \mathbf{w}_1 \cdot \mathbf{n}_1 & |e_2| \mathbf{w}_1 \cdot \mathbf{n}_2 & |e_3| \mathbf{w}_1 \cdot \mathbf{n}_3 \\ |e_1| \mathbf{w}_2 \cdot \mathbf{n}_1 & |e_2| \mathbf{w}_2 \cdot \mathbf{n}_2 & |e_3| \mathbf{w}_2 \cdot \mathbf{n}_3 \\ 1 & 1 & 1 \end{pmatrix}.$$

We need to show that \mathbf{S} is the full rank matrix. Since that $\boldsymbol{\tau}_1$ and $\boldsymbol{\tau}_2$ are linearly independent by the hypothesis, it holds

$$\boldsymbol{\tau}_1 \cdot \mathbf{n}_1 = \boldsymbol{\tau}_2 \cdot \mathbf{n}_2 = 0, \quad \boldsymbol{\tau}_1 \cdot \mathbf{n}_2 = -\boldsymbol{\tau}_2 \cdot \mathbf{n}_1 \neq 0. \quad (8.126)$$

We set $\mathbf{w}_1 = \boldsymbol{\tau}_1$ and $\mathbf{w}_2 = \boldsymbol{\tau}_2$, calculate the determinant of \mathbf{S} and use (8.126), to obtain the equivalent condition

$$|e_3| \mathbf{n}_3 \cdot (|e_2| \boldsymbol{\tau}_2 - |e_1| \boldsymbol{\tau}_1) \neq |e_1| |e_2| \boldsymbol{\tau}_2 \cdot \mathbf{n}_1. \quad (8.127)$$

Due to the angle hypothesis of the lemma, there exist two non-negative numbers α_1 and α_2 such that

$$\boldsymbol{\tau}_3 = -\alpha_1 \boldsymbol{\tau}_1 - \alpha_2 \boldsymbol{\tau}_2, \quad \alpha_1 \geq 0, \alpha_2 \geq 0.$$

This equation immediately yields that $\mathbf{n}_3 = -\alpha_1 \mathbf{n}_1 - \alpha_2 \mathbf{n}_2$. Inserting this identity into (8.127) and applying (8.126), we obtain another equivalent condition:

$$|e_3| (-\alpha_1 |e_2| - \alpha_2 |e_1|) \boldsymbol{\tau}_2 \cdot \mathbf{n}_1 \neq |e_1| |f_2| \boldsymbol{\tau}_2 \cdot \mathbf{n}_1. \quad (8.128)$$

Since α_1 and α_2 are non-negative, (8.128) holds true. Therefore, the matrix \mathbf{S} is non-singular, which proves the lemma for $N_V^X = 3$.

Step 3. The case $N_V^x = 2$ is actually simpler. Repeating the above arguments, we end up with showing that the matrix

$$\tilde{\mathbf{S}} = \begin{pmatrix} |e_1| \mathbf{w}_1 \cdot \mathbf{n}_1 & |e_2| \mathbf{w}_1 \cdot \mathbf{n}_2 \\ |e_1| \mathbf{w}_2 \cdot \mathbf{n}_1 & |e_2| \mathbf{w}_2 \cdot \mathbf{n}_2 \\ 1 & 1 \end{pmatrix} \tag{8.129}$$

has full rank. Note that it could be rank deficient only when $\mathbf{n}_1 = \mathbf{n}_2$, which is the impossible condition. Finally, the cases $N_V^x = 0$ and $N_V^x = 1$ are even more simpler and therefore are not shown. \square

Remark 8.9. Let $N_V^x = 3$ and assume that the triple $\boldsymbol{\tau}_1, \boldsymbol{\tau}_2, \boldsymbol{\tau}_3$ does not satisfy the angle condition. Then, there exists a macroelement with edges e_1, e_2, e_3 that have the tangents $\boldsymbol{\tau}_i$ such that the matrix \mathbf{S} is singular. Therefore, the angle condition in Lemma 8.12 is sharp.

A stronger result can be obtained from Lemma 8.12. We define a *frontier* \tilde{E} as a collection of *at least two* adjoint edges such that $\tilde{E} = \partial P_1 \cap \partial P_2$ and $P_1, P_2 \in M_V$. An example of two frontiers is given on the right panel in Fig. 8.2.

In Lemma 8.12 we assume that v is the only internal vertex of M_V ; thus, the macroelements have no frontiers. In the case of more general macroelements, when the frontiers appear, a distinction must be made: every internal boundary between polygons in M is either a frontier or a standard (single) edge. The result below shows that the frontiers can be essentially ignored.

Lemma 8.13. *Let \bar{N}_V^x indicate the number of edges in \mathcal{E}_V^x which are not a part of a frontier. Let either (a) $\bar{N}_V^x < 3$ or (b) $\bar{N}_V^x = 3$ and the three angles naturally defined by the three respective edges be less or equal than π . Then, the space \mathcal{N}_M defined in (8.121) consists of constant mesh functions.*

Proof. Let \tilde{E} indicate any frontier in M_V and $\tilde{E} = \partial P_1 \cap \partial P_2$ with $P_1, P_2 \in M_V$. Moreover, let $v' \neq v$ be one of the interior vertices in \tilde{E} and e_1, e_2 be two edges in \tilde{E} adjacent to v' . We take $\mathbf{v}_M \in X_{h,M}^0$ to be zero in all interior vertices except v' , and $v_e = 0$ for all edges in \mathcal{E}_V^{b} . We set $\mathbf{w} = \mathbf{v}_{v'}$ for clarity of notation. By testing condition (8.121) with the selected \mathbf{v}_M , we obtain

$$\begin{aligned} 0 &= [q_M, \operatorname{div}_M \mathbf{v}_M]_{\mathcal{Q}_{h,M}} = \llbracket q_M \rrbracket_{\tilde{E}} \left(\int_{e_1} \mathbf{v}_{h,e_1} \cdot \mathbf{n}_{P_1,e_1} dS + \int_{e_2} \mathbf{v}_{h,e_2} \cdot \mathbf{n}_{P_1,e_2} dS \right) \\ &= \llbracket q_M \rrbracket_{\tilde{E}} \frac{1}{2} \left(|e_1| \mathbf{w} \cdot \mathbf{n}_{P_1,e_1} + |e_2| \mathbf{w} \cdot \mathbf{n}_{P_1,e_2} \right) \quad \forall \mathbf{w} \in \mathbb{R}^2, \end{aligned}$$

where $\llbracket q_M \rrbracket_{\tilde{E}} = q_{P_1} - q_{P_2}$ denotes the jump across the frontier. It is obvious that this equation holds true only when the jump is zero, i.e. $q_{P_1} = q_{P_2}$. Thus, for the purpose of this proof the polygons P_1 and P_2 can be considered as a single element, and the frontier \tilde{E} can be completely ignored.

This argument does not use any degree of freedom related to v nor the degrees of freedom related to edge bubbles. Applying it to all frontiers in M_v , we conclude that all of them can be ignored and the respective pairs of polygons treated as single elements. The rest of the proof follows the proof Lemma 8.12. \square

We have shown that, when the set \mathcal{E}^b is defined such that the conditions of Lemma 8.13 are satisfied, the second condition in Theorem 8.3 holds true and thus the inf-sup condition (8.118) is satisfied. This in turn implies the stability and (linear) convergence of the mimetic scheme, following essentially the proofs in Sects. 8.2.2 and 8.2.3 for the three dimensional case.

The results of this section indicate that there exists a large variety of polygonal meshes for which no bubble-type degrees of freedom are needed in order to have stability. This is true, for instance, for any mesh with convex polygons where each node belongs to at most three edges. The Voronoi meshes satisfy often this property. For such meshes, we can set $\mathcal{E}^b = \emptyset$, i.e. use only the nodal degrees of freedom in the mimetic discretization.

For a general mesh, it is sufficient to add bubble-type degrees of freedom only where they are needed, as dictated by Lemma 8.13. A few such degrees of freedom are often sufficient to stabilize the scheme and kill spurious pressure modes. For example, on a logically square mesh one needs to add them approximately to every fourth edge.

8.4 Existence of the reconstruction operator

Here, we construct a reconstruction operator R_P of Sect. 8.2.2 that satisfies properties (L1)–(L6). The construction starts with an auxiliary scalar reconstruction operator and then extends it to the vector case to obtain R_P .

8.4.1 Construction of the scalar reconstruction operator

Let us show that for every cell $P \in \Omega_h$, there exists a reconstruction operator $\tilde{R}_P : \mathcal{V}_{h,P} \rightarrow H^1(P) \cap C^0(P)$ satisfying the five properties below. We remind that $\mathcal{V}_{h,P}$ denotes the restriction of the vertex-based space \mathcal{V}_h to cell P . Let $v_P = (v_v)_{v \in \partial P}$ be the restriction of the discrete field $v_h \in \mathcal{V}_h$ of P . A two dimensional version of the present reconstruction operator is shown later in Sect. 10.2.3.

(L1s) The reconstruction operator R_P is the right inverse of the nodal projection operator:

$$\tilde{R}_P(v_P)(\mathbf{x}_v) = v_v \quad \forall v \in \mathcal{V}_P. \quad (8.130)$$

(L2s) The reconstruction operator is exact for linear functions:

$$\tilde{R}_P(\psi^l) = \psi \quad \forall \psi \in \mathbb{P}_1(P).$$

(L3s) The reconstruction operator is stable with respect to the H^1 -type mesh dependent norm defined by equations (6.15)–(6.16), i.e. there exists a positive con-

stant C^R , independent of h and P , such that

$$|\tilde{R}_P(v_P)|_{H^1(P)} \leq C^R \|v_P\|_{1,h,P}.$$

(L4s) The reconstruction operator has minimal approximation properties, specifically, for every $v_P \in \mathcal{V}_{h,P}$ we have:

$$\tilde{R}_P(v_P) - v_P \quad_{L^2(P)} \leq C^R h_P \|v_P\|_{1,h,P} \quad \forall v_P \in \mathcal{V}_P. \quad (8.131)$$

(L5s) The restriction of $\tilde{R}_P(v_P)$ to a face f of P depends only on the values v_v at the vertices v of f .

Let $v_P \in \mathcal{V}_{h,P}$. We construct a scalar function $\tilde{R}_P(v_P)$ which is globally continuous and piecewise linear on the auxiliary simplicial partition $\mathcal{T}_{h|P}$ of **(MR2)**. Partition $\mathcal{T}_{h|P}$ may have additional nodes inside element P , in the interior of its faces, and in the interior of its edges.

For each vertex v of P , we naturally set that $\tilde{R}_P(v_P)(\mathbf{x}_v) = v_v$. The restriction of $\tilde{R}_P(v_P)$ to edge $e = (v, v')$ is the linear interpolation of the vertex values v_v and $v_{v'}$.

For a face f of P we proceed as follows. Let v of $\mathcal{T}_{h|f}$ be a node located inside it and Ξ_v be the set of all the other nodes in $\mathcal{T}_{h|f}$ that share an edge of $\mathcal{T}_{h|f}$ with v . Node v belongs to the convex hull of the nodes in Ξ_v ; hence, its position is a convex linear combination of the positions of these nodes. Thus, there exists a set of nonnegative numbers $\{\omega_{v,v'}\}$ such that

$$\mathbf{x}_v = \sum_{v' \in \Xi_v} \omega_{v,v'} \mathbf{x}_{v'}, \quad \sum_{v' \in \Xi_v} \omega_{v,v'} = 1. \quad (8.132)$$

We use these coefficients to define the reconstructed function inside f :

$$\tilde{R}_P(v_P)(\mathbf{x}_v) - \sum_{v' \in \Xi_v} \omega_{v,v'} \tilde{R}_P(v_P)(\mathbf{x}_{v'}) = 0. \quad (8.133)$$

Repeating this construction for all the internal nodes of $\mathcal{T}_{h|f}$ yields a linear system with as many unknowns as Eqs. (8.133). The unknowns are the values of the reconstructed function $\tilde{R}_P(v_P)$ at the internal nodes of f . The matrix of this linear system is an M -matrix by the construction. It is nonsingular, and its inverse has nonnegative entries [60]. Thus, a unique solution exists; moreover, it satisfies a discrete maximum principle.

Similarly, we determine the values of $\tilde{R}_P(v_P)$ at the internal nodes of $\mathcal{T}_{h|P}$. For any such node v , we consider the set (denoted again by Ξ_v) of the other nodes in $\mathcal{T}_{h|P}$ connected to v by an edge. The node v belongs to the convex hull of the nodes in Ξ_v and we can write:

$$\mathbf{x}_v = \sum_{v' \in \Xi_v} \tilde{\omega}_{v,v'} \mathbf{x}_{v'}, \quad \sum_{v' \in \Xi_v} \tilde{\omega}_{v,v'} = 1, \quad \tilde{\omega}_{v,v'} \geq 0. \quad (8.134)$$

We use these coefficients to define the reconstructed function inside P :

$$\tilde{R}_P(v_P)(\mathbf{x}_v) - \sum_{v' \in \Xi_v} \tilde{\omega}_{v,v'} \tilde{R}_P(v_P)(\mathbf{x}_{v'}) = 0. \quad (8.135)$$

The reconstructed function is already defined on the boundary ∂P and we can use its values there. Repeating this construction for all the internal nodes of $T_{h|P}$ yields a linear system with an M -matrix. Thus, it has a unique solution that satisfies a discrete maximum.

Once the values $\tilde{R}_P(v_P)(\mathbf{x}_v)$ have been determined for all nodes of $T_{h|P}$, the reconstructed function inside each simplex of $T_{h|P}$ is given by the linear interpolation of its nodal values. The maximum principle implies the following property:

$$\max_{v,v' \in T_{h|P}} |\tilde{R}_P(v_P)(\mathbf{x}_v) - \tilde{R}_P(v_P)(\mathbf{x}_{v'})| \leq \max_{v,v' \in \partial P} |v_v - v_{v'}| \quad \forall v_P \in \mathcal{Y}_{h,P}. \quad (8.136)$$

Properties **(L1s)**, **(L2s)**, and **(L5s)** follows immediately from the construction. To show property **(L3s)**, we use the fact that $\tilde{R}_P(v_P)$ is the piecewise linear function, inequality (8.136), and the estimates **(M2)**–**(M3)** from Sect. 1.6.2:

$$\begin{aligned} |\tilde{R}_P(v_P)|_{H^1(P)}^2 &\leq C|P| \max_{T \in T_{h|P}} \|\nabla \tilde{R}_P(v_P)\|_{L^\infty(T)}^2 \\ &\leq C|P| \max_{T \in T_{h|P}} \left(\max_{v,v' \in T} \frac{|\tilde{R}_P(v_P)(\mathbf{x}_v) - \tilde{R}_P(v_P)(\mathbf{x}_{v'})|^2}{|\mathbf{x}_v - \mathbf{x}_{v'}|^2} \right) \\ &\leq C \frac{|P|}{h_P^2} \left(\max_{v,v' \in \partial P} |v_v - v_{v'}|^2 \right) \leq C \|v_P\|_{1,h,P}^2. \end{aligned}$$

Property **(L4s)** is the consequence of the following chain of inequalities,

$$\begin{aligned} \|\tilde{R}_P(v_P) - v_v\|_{L^2(P)}^2 &\leq |P| \max_{T \in T_{h|P}} \|\tilde{R}_P(v_P) - v_v\|_{L^\infty(T)}^2 \\ &\leq |P| \max_{T \in T_{h|P}} \left(\max_{v' \in T} |\tilde{R}_P(v_P)(\mathbf{x}_{v'}) - \tilde{R}_P(v_P)(\mathbf{x}_v)|^2 \right), \end{aligned}$$

and the argument used in the proof of **(L3s)**.

8.4.2 Construction of the vector reconstruction operator

Let us construct a reconstruction operator R_P that satisfies properties **(L1)**–**(L6)** of Sect. 8.2.2. With a slight abuse of notation, we now use the symbol \tilde{R}_P to indicate the reconstruction operators of Sect. 8.4.1 applied separately to each component of \mathcal{Y}_h^3

$$\tilde{R}_P : (\mathcal{Y}_{h,P})^3 \rightarrow (H^1(P) \cap C^0(P))^3.$$

This operator ignores the bubble-type degrees of freedom associated with mesh faces.

It is easy to verify that, for any face $f \in \partial P$, there exists a function $\phi_f^b : P \rightarrow \mathbb{R}$ satisfying the four properties below.

- (a) Function φ_f^b is non negative and continuous on P .
 (b) Function φ_f^b is zero on $\overline{\partial P}/f$. The trace of φ_f^b on f depends only on the geometry of f (and not the whole P).
 (c) $\int_f \varphi_f^b dS = 1$.
 (d) Function φ_f^b is scaled uniformly for all P and f :

$$1 = \|\varphi_f^b\|_{L^1(f)} \approx h_P^{1/2} \|\varphi_f^b\|_{L^2(P)} \approx h_P^{3/2} |\varphi_f^b|_{H^1(P)}.$$

Let $\mathbf{v}_P \in X_{h,P}$. We define $R_P(\mathbf{v}_P) = \tilde{R}_P(\mathbf{v}_P) + R_P^b(\mathbf{v}_P)$, where

$$R_P^b(\mathbf{v}_P) \in \text{span}\{\varphi_f^b \mathbf{n}_f\}_{f \in \mathcal{F}^0 \cap \partial P}$$

and is such that:

$$\int_f R(\mathbf{v}_P) \cdot \mathbf{n}_f dS = \sum_{v \in \partial f} \mathbf{v}_v \cdot \mathbf{n}_f \omega_{f,v} + |f| v_f \quad \forall f \in \mathcal{F}^0 \cap \partial P, \quad (8.137)$$

where $\omega_{f,v}$ are the weights in the integration rule (8.10).

It is immediate to see that property **(L4)** follows from the above definition and the divergence theorem. Property **(L1)** follows from the construction, since the functions φ_f^b are zero at all mesh vertices. To show property **(L2)**, it is sufficient to bound R_P^b , since the H^1 -seminorm of \tilde{R}_P is already bounded by **(L3s)** of the previous section. It holds

$$R_P^b(\mathbf{v}_P) = \sum_{f \in \mathcal{F}^0 \cap \partial P} \alpha_f \varphi_f^b \mathbf{n}_f \quad \text{with } \alpha_f \in \mathbb{R}, \quad (8.138)$$

which implies

$$|R_P^b(\mathbf{v}_P)|_{H^1(P)}^2 \leq C \sum_{f \in \partial P} |\alpha_f|^2 |\varphi_f^b|_{H^1(P)}^2 \leq C \sum_{f \in \partial P} |\alpha_f|^2 h_P^{-3}, \quad (8.139)$$

where C is the generic constant independent of h_P and P . The coefficient α_f can be bounded by repeating some of the arguments used frequently in the convergence analysis of Sect. 8.2.3. More precisely, first noting that

$$|\alpha_f| = \int_f \alpha_f \varphi_f^b \mathbf{n}_f \cdot \mathbf{n}_f dS \leq \sum_{v \in \partial f} \mathbf{v}_v \cdot \mathbf{n}_f \omega_{f,v} - \int_f \tilde{R}_P(\mathbf{v}_P) \cdot \mathbf{n}_f dS + |f| |v_f|, \quad (8.140)$$

then adding and subtracting $\mathbf{v}_{f,\bar{v}}$ in the first term, using Lemma 8.2, the approximation properties of \tilde{R}_P and finally applying the scaling $|f| \approx h_P^2$, we derive

$$|\alpha_f| \leq h_P^{3/2} \|\mathbf{v}_P\|_{X_{h,P}}. \quad (8.141)$$

Inserting this bound into (8.139) yields

$$|R_P^b(\mathbf{v}_P)|_{H^1(P)} \leq C \|\mathbf{v}_P\|_{X_{h,P}} \quad \forall P \in \Omega_h. \quad (8.142)$$

To show property **(L3)**, we observe that

$$\|R_P(\mathbf{v}_P) - v_v\|_{L^2(P)}^2 = \|\tilde{R}_P(\mathbf{v}_P) - v_v\|_{L^2(P)}^2 + \|R_P^b(\mathbf{v}_P)\|_{L^2(P)}^2. \quad (8.143)$$

The first term in the right hand side is controlled by using the approximation property **(L4s)** of \tilde{R}_P . The second term is bounded as follows:

$$R_P^b(\mathbf{v}_P) \Big|_{L^2(P)}^2 \leq C \sum_{f \in \partial P} |\alpha_f|^2 \|\phi_f^b\|_{L^2(P)}^2 \leq C \sum_{f \in \partial P} |\alpha_f|^2 h_P^{-1} \leq C h_P^2 \|\mathbf{v}_P\|_{X_{h,P}}^2.$$

Let us consider property **(L5)**. Recall that $\boldsymbol{\psi}_f^{\parallel} = 0$ for any $\boldsymbol{\psi} \in (\mathbb{P}_1(P))^3$ and any $f \in \mathcal{F}$. Thus, using definition (8.137) and observing that \tilde{R}_P preserves linear functions, we obtain that $R_P^b(\boldsymbol{\psi}^{\parallel})$ is zero. Hence, property **(L5)** follows directly from the analogous property **(L2s)** of \tilde{R}_P .

Finally, property **(L6)** follows from **(L5s)** and property (b) of ϕ_f^b .

Part III
Further Developments

Elasticity and plates

“All progress is precarious, and the solution of one problem brings us face to face with another problem”
(Martin Luther King, Jr)

In this chapter we consider two different linear problems in structural mechanics. The first one is the *linear elasticity problem*, which we study in both the displacement-pressure and the stress-displacement formulations. In both cases, we take a particular care in devising mimetic schemes that are also stable in the incompressible limit. As the second problem, we consider the *bending of Reissner-Mindlin plates*, which is a very popular problem in engineering applications.

9.1 Displacement-pressure formulation of linear elasticity

Let us remind the equations for the mixed displacement-pressure formulation of the linear elasticity (see Sect. 1.5.2 for more details):

$$-\operatorname{div}(2\mu\varepsilon(\mathbf{u})) + \nabla p = \mathbf{b} \quad \text{in } \Omega, \quad (9.1)$$

$$\operatorname{div} \mathbf{u} - \lambda^{-1} p = 0 \quad \text{in } \Omega, \quad (9.2)$$

$$\mathbf{u} = \mathbf{g}^D \quad \text{on } \Gamma^D, \quad (9.3)$$

$$(2\mu\varepsilon(\mathbf{u}) + \mathbb{I}p) \cdot \mathbf{n} = \mathbf{g}^N \quad \text{on } \Gamma^N, \quad (9.4)$$

where \mathbf{u} is the displacement and $\varepsilon(\mathbf{u})$ its symmetric gradient, p the pressure, \mathbf{b} the forcing term, μ, λ the two positive Lamè functions describing the material properties, \mathbf{g}^D the boundary displacement, and \mathbf{g}^N the boundary force.

The mimetic finite difference scheme for the Stokes problem introduced and analyzed in Sects. 8.1 and 8.2 can be easily extended to the displacement-pressure formulation (9.1)–(9.4).

Let us define the space $V = (H^1(\Omega))^d$, where d as usual is the dimension of the problem, and its subspace $V_{\mathbf{g}^D}$ of functions that equal to \mathbf{g}^D of Γ^D . Let $Q = L^2(\Omega)$ if $\Gamma^N \neq \emptyset$ or $Q = L_0^2(\Omega)$ otherwise. These spaces are defined in (8.5) and (8.6). The variational formulation of problem (9.1)–(9.4) reads:

Find $\mathbf{u} \in V_{\mathbf{g}^D}$ and $p \in Q$ such that

$$\int_{\Omega} 2\mu \boldsymbol{\varepsilon}(\mathbf{u}) : \boldsymbol{\varepsilon}(\mathbf{v}) dV - \int_{\Omega} p \operatorname{div} \mathbf{v} dV = \langle \mathbf{b}, \mathbf{v} \rangle_{\Omega} + \langle \mathbf{g}^N, \mathbf{v} \rangle_{\Gamma^N} \quad \forall \mathbf{v} \in V_0, \quad (9.5)$$

$$\int_{\Omega} q \operatorname{div} \mathbf{u} dV - \int_{\Omega} \lambda^{-1} p q dV = 0 \quad \forall q \in Q. \quad (9.6)$$

Let $\bar{\mu}$ and $\bar{\lambda}^{-1}$ be the piecewise constant functions defined on Ω_h whose restriction to a given polyhedral cell P is given by

$$\bar{\mu}_P = \frac{1}{|P|} \int_P \mu dV, \quad (\bar{\lambda}^{-1})_P = \frac{1}{|P|} \int_P \lambda^{-1} dV.$$

To discretize the linear elasticity problem (9.5)–(9.6), we consider the same discrete spaces X_h and Q_h of Sect. 8.1. We also consider the same bilinear form $\mathcal{A}_{h,P}$, but with the slightly modified consistency condition given below (that we describe briefly, referring to Sect. 8.1 for more details).

(S2) Consistency condition. Let $\mathbf{v} \in [H^1(P) \cap C^0(P)]^d$ be a vector field with the property that the integration rule associated to the weights in (8.10) is exact for any tangent component $\mathbf{v} \cdot \boldsymbol{\tau}_{P,f}$ on every face $f \in \partial P$, see the definition of the space $S_{h,P}$ in Sect. 8.1.4. For every such function and every $\boldsymbol{\psi} \in (\mathbb{P}_1(P))^d$ there holds:

$$\mathcal{A}_{h,P}(\mathbf{v}_P^{\mathbb{I}}, \boldsymbol{\psi}_P^{\mathbb{I}}) = \int_P 2\bar{\mu}_P \boldsymbol{\varepsilon}(\mathbf{v}) : \boldsymbol{\varepsilon}(\boldsymbol{\psi}) dV. \quad (9.7)$$

where the projection operators $(\cdot)^{\mathbb{I}}$ and $(\cdot)^{\mathbb{II}}$ are defined in Sect. 8.1.

In order to show that the right hand side in (9.7) is computable, we follow the same identical steps as in Sect. 8.1.4. Integrating by parts, recalling (8.13) and applying the quadrature rule (8.10) to each face f of P , we have

$$\begin{aligned} \mathcal{A}_{h,P}(\mathbf{v}_P^{\mathbb{I}}, \boldsymbol{\psi}_P^{\mathbb{I}}) &= 2\bar{\mu}_P \int_{\partial P} (\boldsymbol{\varepsilon}(\boldsymbol{\psi}) \cdot \mathbf{n}_P) \cdot \mathbf{v} dS \\ &= 2\bar{\mu}_P \sum_{f \in \partial P} \alpha_{P,f} \left(\sum_{v \in df} \mathbf{v}_{f,v} \cdot (\boldsymbol{\varepsilon}(\boldsymbol{\psi}) \cdot \mathbf{n}_f) \omega_{f,v} + |f| v_f \mathbf{n}_f \cdot (\boldsymbol{\varepsilon}(\boldsymbol{\psi}) \cdot \mathbf{n}_f) \right), \end{aligned}$$

where the coefficient $\alpha_{P,f} = \mathbf{n}_{P,f} \cdot \mathbf{n}_f = \pm 1$ takes into account the orientation of the outward face normal $\mathbf{n}_{P,f}$ with respect to the fixed face normal \mathbf{n}_f . As in all mimetic schemes, the right-hand side can be calculated using the degrees of freedom of the discrete space $X_{h,g}$. The discrete weak mimetic formulation of problem (9.5)–(9.6) reads as (we refer again to Sect. 8.1 for notation):

Find $\mathbf{u}_h \in X_{h,g}$ and $p_h \in Q_h$ such that:

$$\mathcal{A}_h(\mathbf{u}_h, \mathbf{v}_h) + [\operatorname{div}_h \mathbf{v}_h, p_h]_{Q_h} = (\mathbf{b}, \mathbf{v}_h)_h + \langle \mathbf{g}^N, \mathbf{v}_h \rangle_h \quad \forall \mathbf{v}_h \in X_{h,0}, \quad (9.8)$$

$$[\operatorname{div}_h \mathbf{u}_h, q_h]_{Q_h} - \sum_{P \in \Omega_h} (\bar{\lambda}^{-1})_P |P| p_P q_P = 0 \quad \forall q_h \in Q_h. \quad (9.9)$$

Due to the similarity of the discrete weak formulations for the Stokes and linear elasticity problems, the stability and convergence of the mimetic scheme (9.8)-(9.9) can be proved repeating the arguments of Sect. 8.2. Thus, we have the following convergence result.

Theorem 9.1. *Let $\mathbf{u} \in (H^2(\Omega))^d \cap V_{\mathbf{g}^D}$ and $p \in H^1(\Omega)$ be the solution of the variational problem (9.5)–(9.6), with the material coefficient $\mu \in W^{1,\infty}(\mathbb{P})$ for all $\mathbb{P} \in \Omega_h$. Furthermore, let $\mathbf{u}_h \in X_{h,\mathbf{g}}$ and $p_h \in Q_h$ be the solution of the mimetic finite difference formulation (9.8)–(9.9). Under assumptions (MR1)–(MR2) (see Sect. 1.6.2), (S1) (see Sect. 8.1), and (S2) there exists a positive constant C independent of h and λ , such that*

$$\|\|\mathbf{u}_h - \mathbf{u}^{\mathbb{I}}\|\|_{X_h} + \|p_h - p^{\mathbb{I}}\|_{Q_h} \leq Ch \left(\|\mathbf{u}\|_{H^2(\Omega)} + \|p\|_{H^1(\Omega)} \right).$$

This convergence result is uniform in λ , thus guaranteeing the good behavior of the discretization scheme in the limiting case of incompressible elasticity (i.e., $\lambda = +\infty$) and almost incompressible elasticity (i.e., $\lambda \gg \mu$).

Remark 9.1. In [44] a VEM scheme of arbitrary polynomial order on general polygonal meshes is proposed for the linear elasticity problem (9.1)–(9.4). Such scheme, that for the velocity variable makes use of a vector version of the discrete space introduced in Sect. 6.3, can be easily recast in the mimetic framework, thus leading to a MFD scheme of arbitrary order for the elasticity problem.

9.2 Stress-displacement formulation of linear elasticity

In this section we present a mimetic discretization of the linear elasticity problem following the mixed, or Hellinger-Reissner, formulation. Such a formulation, presented in Sect. 1.5.2, uses stresses and displacements as the primary unknowns:

$$\boldsymbol{\sigma} = \mathbb{C}\boldsymbol{\varepsilon}(\mathbf{u}) \quad \text{in } \Omega, \tag{9.10}$$

$$-\text{div } \boldsymbol{\sigma} = \mathbf{b} \quad \text{in } \Omega, \tag{9.11}$$

$$\mathbf{u} = \mathbf{g}^D \quad \text{on } \Gamma^D, \tag{9.12}$$

$$\boldsymbol{\sigma} \cdot \mathbf{n} = \mathbf{g}^N \quad \text{on } \Gamma^N, \tag{9.13}$$

where $\boldsymbol{\sigma}$ is the stress tensor, \mathbf{b} the external loading term, \mathbf{u} the displacement vector, \mathbb{C} the tensor of elastic moduli, \mathbf{g}^D the boundary displacement, and \mathbf{g}^N the boundary force.

This problem has a strong similarity with the mixed formulation of the diffusion problem. Indeed, up to a substitution of vectors with tensors and scalars with vectors, the structure of the two problems is very similar. On the other hand, there are two obstacles that make the numerical discretization and analysis of the elasticity problem more involved. The first one is the symmetry of the stress tensor, which in most

methods is enforced weakly through a variational equation rather than directly in the discrete space. The second one is the lack of uniform coercivity of the main bilinear form in the important case of almost incompressible materials.

The approach considered here allows us to construct a mimetic scheme that is uniformly stable and convergent. In particular, we have to derive new discrete anti-symmetry and trace operators that respect given properties and develop an inner product that mimics properly the non-uniform coercivity of the inverse elastic moduli (1.41). The results in this section are based on [42].

The advantage of the stress-displacement formulation with respect to the displacement-pressure formulation of Sect. 9.1 is a better approximation of the stress. In addition, the numerical stress satisfies a discrete form of the equilibrium condition (9.11) on each mesh cell $P \in \Omega_h$. The price to pay for these properties is that we have to use a larger number of degrees of freedom. This trade-off between accuracy and complexity is observed in many discretization methods.

Let \mathbf{as} be the anti-symmetric operator defined in (1.40). The weak formulation of the problem is as follows:

Find $(\boldsymbol{\sigma}, \mathbf{u}, \mathbf{s}) \in H_{\mathbf{g},N}(\text{div}, \Omega) \times (L^2(\Omega))^d \times (L^2(\Omega))^d$ such that:

$$\int_{\Omega} \mathbb{C}^{-1} \boldsymbol{\sigma} : \boldsymbol{\tau} dV + \int_{\Omega} \mathbf{u} \cdot \text{div } \boldsymbol{\tau} dV + \int_{\Omega} \mathbf{s} \cdot \mathbf{as}(\boldsymbol{\tau}) dV = \langle \mathbf{g}^D, \boldsymbol{\tau} \cdot \mathbf{n} \rangle_{\Gamma^D} \quad \forall \boldsymbol{\tau} \in H_0(\text{div}, \Omega), \quad (9.14)$$

$$\int_{\Omega} \text{div } \boldsymbol{\sigma} \cdot \mathbf{v} dV = \langle \mathbf{b}, \mathbf{v} \rangle_{\Omega} \quad \forall \mathbf{v} \in (L^2(\Omega))^d, \quad (9.15)$$

$$\int_{\Omega} \mathbf{as}(\boldsymbol{\sigma}) \cdot \mathbf{q} dV = 0 \quad \forall \mathbf{q} \in L^2(\Omega). \quad (9.16)$$

In the rest of this section we focus on the three-dimensional problem, i.e. $d = 3$. The numerical analysis of the two-dimensional problem follows the same steps.

9.2.1 Assumptions on mesh and data

We consider the mesh shape regularity assumptions introduced in Chap. 1. For simplicity, we assume that the material properties μ and λ are piecewise constant functions on mesh Ω_h with values μ_P and λ_P , respectively, $P \in \Omega_h$. This assumption can be interpreted as a data approximation. Moreover, we assume that there exist two positive constants μ_* and μ^* independent of h such that

$$\mu_* \leq \mu(\mathbf{x}) \leq \mu^* \quad \forall \mathbf{x} \in \Omega. \quad (9.17)$$

We do not make any further assumption on λ in order to include the important case of almost incompressible materials.

The above assumptions imply that the tensor \mathbb{C} is piecewise constant with respect to mesh Ω_h . Let \mathbb{C}_P be its value over cell P . Moreover, we have

$$\mathbb{C}^{-1} \boldsymbol{\tau} : \boldsymbol{\tau} = \frac{1}{2\mu} \|\text{dev} \boldsymbol{\tau}\|^2 + \frac{1}{2\mu + 3\lambda} |\text{tr}(\boldsymbol{\tau})|^2 \geq \frac{1}{2\mu^*} \|\text{dev} \boldsymbol{\tau}\|^2 \quad \forall \boldsymbol{\tau}, \quad (9.18)$$

where dev stands for the deviatoric operator and $\|\cdot\|$ is the standard Euclidean norm on tensors.

Finally, for simplicity of exposition we assume homogeneous boundary conditions, i.e. $\mathbf{g}^D = 0$ and $\mathbf{g}^N = 0$.

9.2.2 Degrees of freedom and projection operators

Let us introduce the discrete spaces for stresses, displacements and anti-symmetry Lagrange multipliers. These finite dimensional spaces are represented by a set of degrees of freedom associated with mesh elements or faces.

- Let Q_h denote the finite dimensional space whose degrees of freedom are collections of discrete vectors in \mathbb{R}^3 associated with the elements P of Ω_h :

$$\mathbf{q}_h \in Q_h \implies \mathbf{q}_h = (\mathbf{q}_P)_{P \in \Omega_h}, \quad \mathbf{q}_P \in \mathbb{R}^3. \quad (9.19)$$

The dimension of Q_h is three times the number of elements, and each vector $\mathbf{q}_h \in Q_h$ can be naturally associated with a piecewise constant vector function whose restriction to P coincides with \mathbf{q}_P . With a small abuse of notation, we identify the discrete fields in Q_h with the respective piecewise constant vector functions.

- Let X_h denote the finite dimensional space whose degrees of freedom are a collection of vectors in \mathbb{R}^9 associated with the mesh faces f :

$$\boldsymbol{\tau}_h \in X_h \implies \boldsymbol{\tau}_h = (\widehat{\boldsymbol{\tau}}_f, \widetilde{\boldsymbol{\tau}}_f^1, \widetilde{\boldsymbol{\tau}}_f^2)_{f \in \mathcal{F}}, \quad \widehat{\boldsymbol{\tau}}_f, \widetilde{\boldsymbol{\tau}}_f^1, \widetilde{\boldsymbol{\tau}}_f^2 \in \mathbb{R}^3. \quad (9.20)$$

The dimension of X_h is nine times the number of mesh faces. The restriction of $\boldsymbol{\tau}_h$ to P is denoted by $\boldsymbol{\tau}_P = (\widehat{\boldsymbol{\tau}}_f, \widetilde{\boldsymbol{\tau}}_f^1, \widetilde{\boldsymbol{\tau}}_f^2)_{f \in P}$ and $\boldsymbol{\tau}_P$ belongs to the linear space $X_{h,P}$.

The projection operator from $(L^1(\Omega))^3$ onto Q_h is defined by

$$\mathbf{q}^1|_P = \frac{1}{|P|} \int_P \mathbf{q} dV \quad \forall P \in \Omega_h,$$

where the integrals of vectors are interpreted componentwisely. Hereafter, we will use a shorter notation \mathbf{q}_P^1 .

Given a mesh face $f \in \mathcal{F}$, let $\boldsymbol{\xi} = (\xi_1, \xi_2) \in \mathbb{R}^2$ denote the position vector of face points with respect to a local coordinate system chosen on f with the origin at the barycenter of f . Each local vector $(\widehat{\boldsymbol{\tau}}_f, \widetilde{\boldsymbol{\tau}}_f^1, \widetilde{\boldsymbol{\tau}}_f^2)$ can be associated with the linear vector field defined on face f as follows:

$$\boldsymbol{\tau}_f(\boldsymbol{\xi}) = \widehat{\boldsymbol{\tau}}_f + \frac{1}{h_f} \widetilde{\boldsymbol{\tau}}_f^1 \xi_1 + \frac{1}{h_f} \widetilde{\boldsymbol{\tau}}_f^2 \xi_2. \quad (9.21)$$

Hereafter, the symbol $\boldsymbol{\tau}_f$ may denote both the vector $(\widehat{\boldsymbol{\tau}}_f, \widetilde{\boldsymbol{\tau}}_f^1, \widetilde{\boldsymbol{\tau}}_f^2)$ and the respective linear function (9.21). Thus, any discrete field $\boldsymbol{\tau}_h \in X_h$ can also be written as $\boldsymbol{\tau}_h = (\boldsymbol{\tau}_f)_{f \in \Omega_h}$ and for any face f it represents the normal component of a piecewise regular stress tensor field defined on Ω . In this respect, we also use the notation

$$\boldsymbol{\tau}_{P,f} = (\mathbf{n}_{P,f} \cdot \mathbf{n}_f) \boldsymbol{\tau}_f = \alpha_{P,f} \boldsymbol{\tau}_f \quad (9.22)$$

which represents the outward normal component of the discrete tensor field with respect to the element P .

For any tensor field $\boldsymbol{\tau} \in (L^s(\Omega))^{3 \times 3}$, $s > 2$, with $\mathbf{div} \boldsymbol{\tau} \in (L^2(\Omega))^3$, we define the projection $\boldsymbol{\tau}^I$ in X_h by

$$\int_f \boldsymbol{\tau}^I|_f \cdot \mathbf{p}^1 d\xi = \int_f (\boldsymbol{\tau} \cdot \mathbf{n}_f) \cdot \mathbf{p}^1 d\xi \quad \forall \mathbf{p}^1 \in (\mathbb{P}_1(f))^3, \forall f \in \mathcal{F}, \quad (9.23)$$

where $\mathbb{P}_1(f)$ is the space of polynomial of degree at most one defined on f . The tensor-vector dot product $\boldsymbol{\tau} \cdot \mathbf{n}_f$ is the conventional matrix-vector product:

$$(\boldsymbol{\tau} \cdot \mathbf{n}_f)_i = \sum_{j=1}^3 \tau_{ij} n_{f,j}.$$

Even if we use the same notation $(\cdot)^I$ for the projection operators in X_h and Q_h , no confusion is possible between them since in the former case the projection operator is applied to tensor fields while in the latter case the projection operator is applied to vector fields. Finally, the symbol $X_{h,0}$ denotes the subspace of the discrete fields in X_h that vanish on all Neumann boundary faces $f \in \Gamma^N$.

9.2.3 Discrete mimetic operators

We define three discrete operators acting on X_h that mimic the divergence, trace, and anti-symmetry operators. Consistently with the Gauss divergence theorem, the discrete divergence operator $\mathbf{div}_h: X_h \rightarrow Q_h$ is defined by

$$(\mathbf{div}_h \boldsymbol{\tau}_h)|_P = \mathbf{div}_P(\boldsymbol{\tau}_P) = \frac{1}{|P|} \sum_{f \in \partial P} \int_f \boldsymbol{\tau}_{P,f} \cdot \mathbf{n}_f dS \quad \forall P \in \Omega_h. \quad (9.24)$$

Following the same argument as in (2.25), we can easily prove the following commuting diagram property:

$$\mathbf{div}_h \boldsymbol{\tau}^I = (\mathbf{div} \boldsymbol{\tau})^I \quad \forall \boldsymbol{\tau} \in (L^s(\Omega))^{3 \times 3} \cap H(\mathbf{div}, \Omega), s > 2. \quad (9.25)$$

Let $\mathbf{x} = (x, y, z)$ represent the coordinates in the global Cartesian coordinate system and $\mathbf{x}_P = (x_P, y_P, z_P)$ the barycenter of element P in this coordinate system. For each P , we consider the vector-valued linear functions

$$\boldsymbol{\varphi}_P(\mathbf{x}) = \begin{pmatrix} x - x_P \\ y - y_P \\ z - z_P \end{pmatrix} \quad (9.26)$$

and

$$\boldsymbol{\psi}_P^1(\mathbf{x}) = \begin{pmatrix} y - y_P \\ x_P - x \\ 0 \end{pmatrix}, \quad \boldsymbol{\psi}_P^2(\mathbf{x}) = \begin{pmatrix} z - z_P \\ 0 \\ x_P - x \end{pmatrix}, \quad \boldsymbol{\psi}_P^3(\mathbf{x}) = \begin{pmatrix} 0 \\ z - z_P \\ y_P - y \end{pmatrix}. \quad (9.27)$$

Note that $\nabla \boldsymbol{\varphi}_P$ is the identity matrix. Until the end of this section, we assume that $\boldsymbol{\tau} \in (L^s(P))^{3 \times 3}$, $s > 2$, and its divergence is constant. Using the integration by parts and observing that the integral of $\boldsymbol{\varphi}_P$ on P is zero yield:

$$\int_P \text{tr}(\boldsymbol{\tau}) dV = \int_P \boldsymbol{\tau} : \nabla \boldsymbol{\varphi}_P dV = \sum_{f \in \partial P} \int_f (\boldsymbol{\tau} \cdot \mathbf{n}_{P,f}) \cdot \boldsymbol{\varphi}_P dS. \quad (9.28)$$

Consistently, we define the discrete trace operator tr_h from X_h to the space of scalar functions that are piecewise constant on Ω_h :

$$\text{tr}_h(\boldsymbol{\tau}_h)|_P = \text{tr}_P(\boldsymbol{\tau}_P) = \frac{1}{|P|} \sum_{f \in \partial P} \int_f \boldsymbol{\tau}_{P,f} \cdot \boldsymbol{\varphi}_P dS \quad \forall P \in \Omega_h. \quad (9.29)$$

From definition (9.23) and observing that $\boldsymbol{\varphi}_P$ is linear, it follows that

$$\sum_{f \in \partial P} \int_f (\boldsymbol{\tau} \cdot \mathbf{n}_{P,f}) \cdot \boldsymbol{\varphi}_P dS = \sum_{f \in \partial P} \int_f \boldsymbol{\tau}_{P,f}^I \cdot \boldsymbol{\varphi}_P dS. \quad (9.30)$$

By combining definition (9.29) with identities (9.28) and (9.30), we have

$$\text{tr}_h(\boldsymbol{\tau}^I)|_P = \frac{1}{|P|} \int_P \text{tr}(\boldsymbol{\tau}) dV \quad \forall P \in \Omega_h. \quad (9.31)$$

Recalling definition (1.40) of the anti-symmetry operator, we now observe that

$$(\mathbf{as}(\boldsymbol{\theta}))_i = \boldsymbol{\theta} : \nabla \boldsymbol{\psi}_P^i \quad \forall \boldsymbol{\theta} \in \mathbb{R}^{3 \times 3}, \quad i = 1, 2, 3.$$

Therefore, the same argument as in (9.28) gives

$$\int_P (\mathbf{as}(\boldsymbol{\tau}))_i dV = \sum_{f \in \partial P} \int_f (\boldsymbol{\tau} \cdot \mathbf{n}_{P,f}) \cdot \boldsymbol{\psi}_P^i dS. \quad (9.32)$$

This formula leads to the consistent definition of the discrete anti-symmetry operator acting from X_h into Q_h :

$$(\mathbf{as}_h(\boldsymbol{\tau}_h))_i = (\mathbf{as}_P(\boldsymbol{\tau}_P))_i = \frac{1}{|P|} \sum_{f \in \partial P} \int_f \boldsymbol{\tau}_{P,f} \cdot \boldsymbol{\psi}_P^i dS, \quad i = 1, 2, 3, \quad \forall P \in \Omega_h. \quad (9.33)$$

By applying the same argument used to show (9.31), we obtain

$$\mathbf{as}_h(\boldsymbol{\tau}^I)|_P = \frac{1}{|P|} \int_P \mathbf{as}(\boldsymbol{\tau}) dV \quad \forall P \in \Omega_h. \quad (9.34)$$

In the next sections, we will use the restrictions of the aforementioned discrete operators to cell P denoted by \mathbf{div}_P , tr_P and \mathbf{as}_P .

9.2.4 Weak form of discrete equations

We equip space Q_h with the following inner product:

$$[\mathbf{q}_h, \mathbf{p}_h]_{Q_h} = \sum_{P \in \Omega_h} [\mathbf{q}_P, \mathbf{p}_P]_P, \quad [\mathbf{q}_P, \mathbf{p}_P]_P = |P| \mathbf{q}_P \cdot \mathbf{p}_P. \quad (9.35)$$

We denote the global and local norms induced by (9.35) by $\|\cdot\|_{Q_h}$ and $\|\cdot\|_P$, respectively. Regarding space X_h , we define the following norm

$$\|\boldsymbol{\tau}_h\|_{X_h}^2 = \sum_{P \in \Omega_h} \|\boldsymbol{\tau}_P\|_P^2, \quad \|\boldsymbol{\tau}_P\|_P^2 = \sum_{f \in \partial P} h_f \|\boldsymbol{\tau}_f\|_{L^2(f)}^2. \quad (9.36)$$

Definition of a consistent inner product on space X_h requires more work. This inner product must mimic the natural form of the continuous problem as explained below. For a moment, we assume the existence of an inner product with special properties and leave its detailed construction to the next subsection. Let

$$[\boldsymbol{\tau}_h, \boldsymbol{\delta}_h]_{X_h} = \sum_{P \in \Omega_h} [\boldsymbol{\tau}_P, \boldsymbol{\delta}_P]_P \quad \forall \boldsymbol{\tau}_h, \boldsymbol{\delta}_h \in X_h, \quad (9.37)$$

where the local bilinear forms $[\cdot, \cdot]_P$ satisfy the stability and consistency conditions.

(S1) (Stability Condition). There exist two positive constants C_* , C^* independent of h and λ such that

$$[\boldsymbol{\tau}_P, \boldsymbol{\delta}_P]_P \leq C^* \|\boldsymbol{\tau}_P\|_P \|\boldsymbol{\delta}_P\|_P \quad \forall \boldsymbol{\tau}_P, \boldsymbol{\delta}_P \in X_{h,P}, \quad (9.38)$$

and

$$C_* \|\boldsymbol{\tau}_P - \frac{1}{3} \text{tr}_P(\boldsymbol{\tau}_P) \mathbb{I}_P\|_P^2 \leq [\boldsymbol{\tau}_P, \boldsymbol{\tau}_P]_P \quad \forall \boldsymbol{\tau}_P \in X_{h,P} \text{ with } \mathbf{div}_P \boldsymbol{\tau}_P = 0, \quad (9.39)$$

where \mathbb{I}_P is the projection of the constant tensor \mathbb{I} .

This condition enforces the correct scaling of the inner product with respect to the size of the element and the coercivity of the deviatoric part of the tensor, mimicking the continuum bilinear form.

Let us define the following space

$$S_{h,P} = \{\boldsymbol{\tau} \in (L^s(P))^{3 \times 3}, s > 2, \mathbf{div} \boldsymbol{\tau} \in (\mathbb{P}_0(P))^3, \boldsymbol{\tau} \cdot \mathbf{n}_f \in (\mathbb{P}_1(f))^3 \quad \forall f \in P\}.$$

(S2) (Consistency Condition). For all $\boldsymbol{\tau} \in S_{h,P}$ and any function $\mathbf{p}^1 \in (\mathbb{P}_1(P))^3$ there holds

$$[(C_P \nabla \mathbf{p}^1)_P, \boldsymbol{\tau}_P]_P = \int_P \nabla \mathbf{p}^1 : \boldsymbol{\tau} dV. \quad (9.40)$$

The consistency condition states that the inner product is exact when one of its two entries is the projection of a linear function. The space $S_{h,P}$ is infinite dimensional and its functions cannot be calculated explicitly. Following the general approach described in Chap. 4, the space $S_{h,P}$ has been designed to be rich enough in order to

satisfy **(B1)** (the interpolation operator is surjective from $S_{h,P}$ to $X_{h,P}$) and **(B2)** (contains the constant tensors $\mathbb{C}_P \nabla \mathbf{p}^1$ with $\mathbf{p}^1 \in (\mathbb{P}_1(P))^3$). At the same time the space $S_{h,P}$ must allow us to calculate the right-hand side of (9.40) using only the degrees of freedom of $\boldsymbol{\tau}_P$ and the fact that \mathbf{p}^1 is a linear vector-valued field (property **(B3)**). Indeed, integrating by parts, using the properties of this space and recalling (9.23), (9.25), we easily have

$$\begin{aligned} [(\mathbb{C}_P \nabla \mathbf{p}^1)_P, \boldsymbol{\tau}_P]_P &= -(\mathbf{div} \boldsymbol{\tau}) \cdot \int_P \mathbf{p}^1 dV + \sum_{f \in \partial P} \int_f (\boldsymbol{\tau} \cdot \mathbf{n}_{P,f}) \cdot \mathbf{p}^1 dS \\ &= -(\mathbf{div}_P \boldsymbol{\tau}_P) \cdot \int_P \mathbf{p}^1 dV + \sum_{f \in \partial P} \int_f \boldsymbol{\tau}_{P,f} \cdot \mathbf{p}^1 dS. \end{aligned} \quad (9.41)$$

We can now present the weak formulation of the mimetic scheme:

Find $(\boldsymbol{\sigma}_h, \mathbf{u}_h, \mathbf{s}_h) \in X_{h,0} \times Q_h \times Q_h$ such that

$$[\boldsymbol{\sigma}_h, \boldsymbol{\tau}_h]_{X_h} + [\mathbf{u}_h, \mathbf{div}_h \boldsymbol{\tau}_h]_{Q_h} + [\mathbf{s}_h, \mathbf{as}_h(\boldsymbol{\tau}_h)]_{Q_h} = 0 \quad \forall \boldsymbol{\tau}_h \in X_{h,0}, \quad (9.42)$$

$$[\mathbf{div}_h \boldsymbol{\sigma}_h, \mathbf{v}_h]_{X_h} = [\mathbf{b}^I, \mathbf{v}_h]_{Q_h} \quad \forall \mathbf{v}_h \in Q_h, \quad (9.43)$$

$$[\mathbf{as}_h \boldsymbol{\sigma}_h, \mathbf{q}_h]_{Q_h} = 0 \quad \forall \mathbf{q}_h \in Q_h. \quad (9.44)$$

Note that the second two equations are equivalent to $\mathbf{div}_h \boldsymbol{\sigma}_h = \mathbf{b}^I$ and $\mathbf{as}_h \boldsymbol{\sigma}_h = \mathbf{0}$.

Remark 9.2. Making use of (9.41) and recalling the surjectivity property **(B1)**, the consistency condition **(S2)** can be written in the following more practical form. For all $\boldsymbol{\tau}_P \in X_{h,P}$ and $\mathbf{p}^1 \in (\mathbb{P}_1(P))^3$

$$[(\mathbb{C}_P \nabla \mathbf{p}^1)_P, \boldsymbol{\tau}_P]_P = -(\mathbf{div}_P \boldsymbol{\tau}_P) \cdot \int_P \mathbf{p}^1 dV + \sum_{f \in \partial P} \int_f \boldsymbol{\tau}_{P,f} \cdot \mathbf{p}^1 dS.$$

where we follow the usual notation $\boldsymbol{\tau} = (\boldsymbol{\tau}_{P,f})_{f \in \partial P}$. The above condition shows that the space $S_{h,P}$ is only introduced for constructive reasons but does not appear in the practical definition of the bilinear form.

Remark 9.3. To ease the presentation, we assume that the measures of both Γ^D and Γ^N are strictly positive. The first condition avoids a floating domain. Regarding the second condition, when the measure of Γ^N is zero, the discrete stresses must be restricted to the subspace

$$\left\{ \boldsymbol{\tau}_h \in X_h \text{ such that } \sum_{P \in \Omega_h} |P| \operatorname{tr}_h(\boldsymbol{\tau}_h)|_P = 0 \right\}$$

and the subsequent statements (including their proofs) have to be modified accordingly, see [42] for details.

9.2.5 Practical construction of the scalar product

The inner product (9.37), which satisfies properties **(S1)** and **(S2)**, can be built following essentially the same steps of the previous chapters. Let \mathbf{p}_i^1 , $i = 1, 2, \dots, 12$, be basis functions in $(\mathbb{P}_1(\mathcal{P}))^3$ such that the first three ones are constants and the remaining ones have zero mean value on \mathcal{P} . Let $\mathbf{N}_i = (\mathbb{C}_\mathcal{P} \nabla \mathbf{p}_i^1)_\mathcal{P}$ and $\mathbf{N}_\mathcal{P} = (N_1, N_2, \dots, N_{12})$ be the $9N_\mathcal{P}^\mathcal{F} \times 12$ rectangular matrix. Then, the left-hand side of (9.40) can be written as

$$[(\mathbb{C}_\mathcal{P} \nabla \mathbf{p}_i^1)_\mathcal{P}, \boldsymbol{\tau}_\mathcal{P}^1]_\mathcal{P} = (\boldsymbol{\tau}_\mathcal{P}^1)^T M_\mathcal{P} N_i. \quad (9.45)$$

Since the $\mathbb{C}_\mathcal{P} \nabla \mathbf{p}_i^1$ is constant over the element, $6N_\mathcal{P}^\mathcal{F}$ components of vector N_i vanish, see (9.23). The remaining components can be easily computed using the mid-point quadrature rule on each face f of \mathcal{P} .

Using definition of the discrete divergence operator, the right-hand side of Eq. (9.41) can be written as a dot product of two vectors:

$$-(\text{div}_h \boldsymbol{\tau}_\mathcal{P}^1) \cdot \int_\mathcal{P} \mathbf{p}_i^1 dV + \sum_{f \in \partial \mathcal{P}} \int_f \boldsymbol{\tau}_{\mathcal{P},f}^1 \cdot \mathbf{p}_i^1 dS = (\boldsymbol{\tau}_\mathcal{P}^1)^T R_i,$$

where

$$R_i = \begin{pmatrix} R_{i,0} \\ R_{i,1} \\ R_{i,2} \end{pmatrix} \quad (9.46)$$

and

$$R_{i,0} = \begin{pmatrix} \int_{f_1} \mathbf{p}_i^1 dS \\ \vdots \\ \int_{f_{N_\mathcal{P}^\mathcal{F}}} \mathbf{p}_i^1 dS \end{pmatrix}, \quad R_{i,k} = \begin{pmatrix} \int_{f_1} \frac{\xi_k}{h_{f_1}} \mathbf{p}_i^1 dS \\ \vdots \\ \int_{f_n} \frac{\xi_k}{h_{f_{N_\mathcal{P}^\mathcal{F}}}} \mathbf{p}_i^1 dS \end{pmatrix}, \quad k = 1, 2. \quad (9.47)$$

Let $R_\mathcal{P} = (R_1, R_2, \dots, R_{12})$. Inserting (9.45)–(9.47) into the consistency condition (9.40), we obtain the matrix equation

$$M_\mathcal{P} N_\mathcal{P} = R_\mathcal{P}.$$

The following property follows immediately from the consistency condition and is a consequence of the more general result of Lemma 4.1.

Lemma 9.1. *The matrices $N_\mathcal{P}$ and $R_\mathcal{P}$ satisfy*

$$N_\mathcal{P}^T R_\mathcal{P} = |\mathcal{P}| \bar{K}_\mathcal{P}, \quad (9.48)$$

where $\bar{K}_\mathcal{P}$ is the symmetric semi-positive definite matrix:

$$\bar{K}_\mathcal{P} = (\bar{K}_{ij})_{i,j=1}^{12}, \quad \bar{K}_{ij} = \frac{1}{|\mathcal{P}|} \int_\mathcal{P} \mathbb{C}_\mathcal{P} \nabla \mathbf{p}_i^1 : \nabla \mathbf{p}_j^1 dV.$$

Once the local matrices N_P and R_P are computed, the local stiffness matrix M_P can be built following the construction shown in Corollary 4.2:

$$M_P = R_P (R_P^T N_P)^\dagger R_P^T + \gamma_P (I - N_P (N_P^T N_P)^{-1} N_P^T),$$

where $(\cdot)^\dagger$ is a pseudo-inverse matrix and γ_P is a positive parameter. To satisfy the stability condition (S1), we can take

$$\gamma_P = \frac{1}{12N_P^2} \text{trace} \left(R_P (R_P^T N_P)^\dagger R_P^T \right).$$

The theory developed in Chap. 4 guarantees the upper bound (9.38). To show the lower bound (9.39), we need to modify slightly the proof of Theorem 4.2 using the following lemma.

Lemma 9.2. *Let $M_P^0 = R_P (R_P^T N_P)^\dagger R_P^T$. Then, there exists a positive constant C , independent of h , λ , and μ , such that*

$$\boldsymbol{\tau}_P^T M_P^0 \boldsymbol{\tau}_P = [\boldsymbol{\tau}_P, \boldsymbol{\tau}_P]_P \geq \frac{C}{\mu_P} \|\boldsymbol{\tau}_P - \frac{1}{3} \text{tr}_P(\boldsymbol{\tau}_P) \mathbb{I}_P^1\|_P^2 \quad (9.49)$$

for all $\boldsymbol{\tau}_P \in \text{img}(N_P)$.

Proof. The first identity in (9.49) follows immediately from the properties of the λ -term in matrix M_P . Moreover, since $\boldsymbol{\tau}_P \in \text{img}(N_P)$, it exists a linear function \mathbf{p}^1 such that $\boldsymbol{\tau}_P = (\mathbb{C}_P \nabla \mathbf{p}^1)_P^1$. The consistency condition (see also Lemma 4.6) gives

$$\boldsymbol{\tau}_P^T M_P^0 \boldsymbol{\tau}_P = \int_P \nabla \mathbf{p}^1 : (\mathbb{C}_P \nabla \mathbf{p}^1) dV. \quad (9.50)$$

Recall that $\mathbb{C}_P \boldsymbol{\tau} = 2\mu_P \boldsymbol{\tau} + \lambda_P \text{tr}(\boldsymbol{\tau}) \mathbb{I}$ for any tensor $\boldsymbol{\tau}$. Inserting this expression for $\boldsymbol{\tau} = \nabla \mathbf{p}^1$ in (9.50) and noting that $\text{tr}(\nabla \mathbf{p}^1) = \nabla \mathbf{p}^1 : \mathbb{I} = \text{div} \mathbf{p}^1$, we obtain

$$\boldsymbol{\tau}_P^T M_P^0 \boldsymbol{\tau}_P = 2\mu_P \|\nabla \mathbf{p}^1\|_{L^2(P)}^2 + \lambda_P \|\text{div} \mathbf{p}^1\|_{L^2(P)}^2 \geq 2\mu_P \|\nabla \mathbf{p}^1\|_{L^2(P)}^2. \quad (9.51)$$

Using property (9.31) of the discrete trace operator and the definition of interpolant in (9.23), we have

$$\text{tr}_P(\boldsymbol{\tau}_P) = \frac{1}{|P|} \int_P \text{tr}(\mathbb{C}_P \nabla \mathbf{p}^1) dV = \text{tr}(\mathbb{C}_P \nabla \mathbf{p}^1) = (2\mu_P + 3\lambda_P) \text{div} \mathbf{p}^1.$$

Using this formula, we obtain

$$\begin{aligned} \|\boldsymbol{\tau}_P - \frac{1}{3} \text{tr}_P(\boldsymbol{\tau}_P) \mathbb{I}_P^1\|_P^2 &= \|(\mathbb{C}_P \nabla \mathbf{p}^1 - \frac{1}{3}(2\mu_P + 3\lambda_P) (\text{div} \mathbf{p}^1) \mathbb{I})_P^1\|_P^2 \\ &= 4\mu_P^2 \|(\nabla \mathbf{p}^1 + \frac{1}{3} (\text{div} \mathbf{p}^1) \mathbb{I})_P^1\|_P^2. \end{aligned}$$

Finally, using the standard projection-scaling arguments based on Agmon's inequality and the mesh shape regularity assumptions, we conclude that

$$\|\boldsymbol{\tau}_P - \frac{1}{3} \text{tr}_P(\boldsymbol{\tau}_P) \mathbb{I}_P\|_P^2 \leq C \mu_P^2 \|\nabla \mathbf{p}^1 + \frac{1}{3}(\text{div} \mathbf{p}^1) \mathbb{I}\|_{L^2(P)}^2 \leq C \mu_P^2 \|\nabla \mathbf{p}^1\|_{L^2(P)}^2. \quad (9.52)$$

The assertion of the lemma follows by combining bounds (9.51) and (9.52). \square

9.2.6 Stability and convergence analysis

Let us show the uniform stability of mimetic scheme (9.42)–(9.44) on $X_{h,0} \times Q_h \times Q_h$ and discuss its convergence properties. The discrete spaces are equipped with the norms introduced above. Following the general theory of saddle-point systems [88], the stability result stems directly from the discrete *inf-sup* condition (Lemma 9.3) and the coercivity condition on the kernel (Lemma 9.4). Detailed proofs of these results can be found in [42].

Lemma 9.3. (*inf-sup condition*). *There exists a positive constant β independent of h such that, for all $\mathbf{v}_h, \mathbf{q}_h \in Q_h$, there exists $\boldsymbol{\tau}_h \in X_h$ such that*

$$[\mathbf{v}_h, \text{div}_h \boldsymbol{\tau}_h]_{Q_h} + [\mathbf{q}_h, \text{as}_h(\boldsymbol{\tau}_h)]_{Q_h} \geq \beta (\|\mathbf{v}_h\|_{Q_h} + \|\mathbf{q}_h\|_{Q_h}), \quad (9.53)$$

$$\|\boldsymbol{\tau}_h\|_{X_h} \leq 1. \quad (9.54)$$

We note that proof of this lemma uses the auxiliary simplicial partition T_h introduced in assumption (MR) and the stability result similar to (9.53)–(9.54) for the $\mathbb{B}\mathbb{D}\mathbb{M}$ finite elements of order 1, see Theorem 4.6 in [82] and Example 7 in the same paper.

Lemma 9.4. *There exists a positive constant α , independent of h and λ , such that for all $\boldsymbol{\tau}_h \in X_{h,0}$ with $\text{div}_h \boldsymbol{\tau}_h = \mathbf{0}$ it holds*

$$[\boldsymbol{\tau}_h, \boldsymbol{\tau}_h]_{X_h} \geq \alpha \|\boldsymbol{\tau}_h\|_{X_h}^2. \quad (9.55)$$

By combining Lemmas 9.3 and 9.4 with the classical theory of [88], we can prove the uniform stability of the method.

Lemma 9.5. *The solution to problem (9.42)–(9.44) exists and is unique. Moreover, it holds*

$$\|\boldsymbol{\sigma}_h\|_{X_h} + \|\mathbf{u}_h\|_{Q_h} + \|\mathbf{s}_h\|_{Q_h} \leq C \sup_{\mathbf{v}_h \in Q_h} \frac{[\mathbf{b}', \mathbf{v}_h]_{Q_h}}{\|\mathbf{v}_h\|_{Q_h}} \leq C \|\mathbf{b}\|_{L^2(\Omega)}, \quad (9.56)$$

where constant C is independent of h and λ .

The convergence of the mimetic scheme is shown in the following theorem that uses the broken semi-norm [42]

$$|\mathbf{b}|_{H^{1,h}(\Omega)}^2 = \sum_{P \in \Omega_h} |\mathbf{b}|_{H^1(P)}^2.$$

Theorem 9.2. *Let $(\boldsymbol{\sigma}, \mathbf{u})$ be the solution of continuum problem (9.14)–(9.16) with $\boldsymbol{\sigma} \in (H^1(\Omega))^{3 \times 3}$ and $\mathbf{u} \in (H^2(\Omega))^3$. Furthermore, let $(\boldsymbol{\sigma}_h, \mathbf{u}_h) \in X_{h,0} \times Q_h$ be the solution of the discrete problem (9.42)–(9.44) under assumptions (MR) and (S1)–(S2). Then, it holds that*

$$\|\boldsymbol{\sigma}_h - \boldsymbol{\sigma}^I\|_{X_h} \leq Ch (\|\mathbf{u}\|_{H^2(\Omega)} + \|\boldsymbol{\sigma}\|_{H^1(\Omega)} + |\mathbf{b}|_{H^{1,h}(\Omega)}), \quad (9.57)$$

$$\mathbf{div}_h \boldsymbol{\sigma}_h = (\mathbf{div} \boldsymbol{\sigma})^I, \quad (9.58)$$

$$\|\mathbf{u}_h - \mathbf{u}^I\|_{Q_h} \leq Ch (\|\mathbf{u}\|_{H^2(\Omega)} + |\mathbf{b}|_{H^{1,h}(\Omega)}), \quad (9.59)$$

where the constant C is independent of h and λ .

Since the constant C is independent of λ , the scheme is robust at the limit $\lambda \rightarrow \infty$, i.e., for almost-incompressible materials. Note moreover that Eq. (9.58) implies that

$$\|\mathbf{div}_h(\boldsymbol{\sigma}_h - \boldsymbol{\sigma}^I)\|_{Q_h} \leq Ch |\mathbf{b}|_{H^{1,h}(\Omega)}. \quad (9.60)$$

The solution regularity required for Theorem 9.2 is the standard one for the discretization methods converging with the linear order. For example, such regularity holds on all convex domains whenever $\mathbf{b} \in (L^2(\Omega))^3$, see Theorem 1.3. Here, in addition, we are assuming that $\mathbf{b} \in H^1(P)$ for all $P \in \Omega$. This condition is expected to be satisfied for most problems, since it still allows the load to jump across mesh faces.

Let us assume the existence of an exact reconstruction operator, i.e. an operator

$$R_P : X_{h,P} \rightarrow S_{h,P}.$$

that satisfies the following properties

(L1) For every discrete field $\boldsymbol{\tau}_h \in X_{h,P}$ it holds

$$\begin{aligned} \mathbf{div} R_P(\boldsymbol{\tau}_P) &= \mathbf{div}_P \boldsymbol{\tau}_P, \\ R_P(\boldsymbol{\tau}_P) \cdot \mathbf{n}_f &= \boldsymbol{\tau}_f \quad \forall f \in \partial P. \end{aligned}$$

(L2) The reconstruction operator R_P is the left-inverse of the projection operator on the space of constant tensors:

$$R_P(\mathbf{c}_P^I) = \mathbf{c} \quad \forall \mathbf{c} \in (\mathbb{P}_0(P))^{3 \times 3}.$$

(L3) For the considered mimetic inner product, the reconstruction operator R_P reproduces it exactly:

$$[\boldsymbol{\tau}_P, \boldsymbol{\delta}_P]_P = \int_P \mathbb{C}_P^{-1} R_P(\boldsymbol{\tau}_P) : R_P(\boldsymbol{\delta}_P) dV \quad \forall \boldsymbol{\tau}_P, \boldsymbol{\delta}_P \in X_{h,P}.$$

The label “exact” refers to property **(L3)**. We recall that the above operator is usually not unique and not always guaranteed to exist, see Sect. 5.3 for a deeper study of exact reconstruction operators. Under this exactness assumption, it is possible to show the superconvergence of the discrete solution, like in Sect. 5.3.

Theorem 9.3. *For any $P \in \Omega_h$, let R_P be the reconstruction operator satisfying properties **(L1)**–**(L3)**. Then, under assumptions of Theorem 9.2, it holds*

$$\| \mathbf{u}_h - \mathbf{u}^1 \|_{Q_h} \leq Ch^{1+s} (\| \mathbf{u} \|_{H^2(\Omega)} + | \mathbf{b} |_{H^{1,h}(\Omega)}), \quad (9.61)$$

where the constant C is independent of h and λ , and $0 \leq s \leq 1$ depends on the domain Ω and tensor \mathbb{C} . In particular, $s = 1$ if Ω is convex and \mathbb{C} is constant.

9.3 Reissner-Mindlin plates

In this section, we present the mimetic discretization of the Reissner-Mindlin plate bending problem, described in Sect. 1.5.3. We remind the strong form of the equations for a clamped plate subjected to a normal loading b :

$$-\operatorname{div}(\mathbb{C}\boldsymbol{\varepsilon}(\boldsymbol{\beta})) - \boldsymbol{\gamma} = \mathbf{0} \quad \text{in } \Omega, \quad (9.62)$$

$$-\operatorname{div} \boldsymbol{\gamma} = b \quad \text{in } \Omega, \quad (9.63)$$

$$\boldsymbol{\gamma} = \kappa t^{-2}(\nabla w - \boldsymbol{\beta}) \quad \text{in } \Omega, \quad (9.64)$$

$$\boldsymbol{\beta} = \mathbf{0} \quad \text{on } \partial\Omega, \quad (9.65)$$

$$w = 0 \quad \text{on } \partial\Omega, \quad (9.66)$$

where $\boldsymbol{\beta} = (\beta_1, \beta_2)$ represents the rotations, w is the transverse displacement, $\boldsymbol{\gamma} = (\gamma_1, \gamma_2)$ denotes the scaled shear stress, and \mathbb{C} is the tensor of bending moduli,

$$\mathbb{C}\boldsymbol{\tau} = \frac{E}{12(1-\nu^2)}((1-\nu)\boldsymbol{\tau} + \nu \operatorname{tr}(\boldsymbol{\tau})\mathbb{I}). \quad (9.67)$$

This problem has attracted much attention in the last decades both in the engineering and mathematical communities, mainly due to its wide applicability and many difficulties hidden in its numerical approximation. Nowadays, there exists a large variety of finite element schemes for the Reissner-Mindlin plate bending problem, the most famous and popular ones being the Mixed Interpolation of Tensorial Components (MITC) class of methods.

The mimetic scheme presented below is based on [57] and follows the MITC philosophy. As usual for mimetic discretizations, the scheme can be applied to general polygonal meshes with possibly non-convex elements. The scheme uses one degree of freedom per mesh vertex to represent the scalar displacement variable and two degrees of freedom per mesh vertex plus one additional degree of freedom per mesh edge to represent the vector rotation variable. Under certain mesh assumptions, the

degrees of freedom associated with the edges can be dropped out, leading to a scheme that uses only vertex degrees of freedom for displacement and rotations. Inspired by the MITC approach, the mimetic scheme adopts a reduction of the shear energy in order to avoid locking. All the reductions and differential operators, bilinear forms, and degrees of freedom are defined carefully in order to preserve the important properties of the continuum problem.

Let $\mathcal{H} = (H_0^1(\Omega))^2 \times H_0^1(\Omega)$. We recall the weak formulation of the problem stated in Chap. 1:

Find $(\boldsymbol{\beta}, w) \in \mathcal{H}$ and $\boldsymbol{\gamma} \in (L^2(\Omega))^2$ such that

$$a(\boldsymbol{\beta}, \boldsymbol{\eta}) + \int_{\Omega} \boldsymbol{\gamma} \cdot (\nabla v - \boldsymbol{\eta}) dV = \langle b, v \rangle_{\mathcal{Q}} \quad \forall (\boldsymbol{\eta}, v) \in \mathcal{H}, \quad (9.68)$$

$$\int_{\Omega} (\nabla w - \boldsymbol{\beta}) \cdot \boldsymbol{\delta} dV - \kappa^{-1} t^2 \int_{\Omega} \boldsymbol{\gamma} \cdot \boldsymbol{\delta} dV = 0 \quad \forall \boldsymbol{\delta} \in (L^2(\Omega))^2. \quad (9.69)$$

where

$$\begin{aligned} a(\boldsymbol{\beta}, \boldsymbol{\eta}) &= \int_{\Omega} \mathbb{C} \boldsymbol{\varepsilon}(\boldsymbol{\beta}) : \boldsymbol{\varepsilon}(\boldsymbol{\eta}) dV \\ &= \frac{E}{12(1-\nu^2)} \int_{\Omega} ((1-\nu) \boldsymbol{\varepsilon}(\boldsymbol{\beta}) : \boldsymbol{\varepsilon}(\boldsymbol{\eta}) + \nu \operatorname{div} \boldsymbol{\beta} \operatorname{div} \boldsymbol{\eta}) dV. \end{aligned} \quad (9.70)$$

9.3.1 Assumptions on mesh and data

We consider again the mesh shape regularity assumptions **(MR1)**–**(MR3)** introduced in Chap. 1. Let $\boldsymbol{\tau}_{P,e}$ be the unit tangent vector to edge e of cell P . We assume that these vectors are oriented counter-clockwise in each cell P .

We assume that the Young modulus E and the Poisson ratio ν in (9.67) are piecewise constant functions on mesh Ω_h . Moreover, there exist two positive constants C_* and C^* such that

$$C_* < E(\mathbf{x}) < C^* \quad \forall \mathbf{x} \in \Omega.$$

This uniform bounds are sufficient for many applications, while the condition of being piecewise constant can be interpreted as an approximation of the data and is introduced only for simplicity. In general, it is enough to assume that E and ν are (piecewise) $W^{1,\infty}$ and use their cell averages in the numerical scheme.

The above assumptions imply that the tensor \mathbb{C} is piecewise constant with respect to mesh Ω_h . Let \mathbb{C}_P be its value over cell P .

9.3.2 Degrees of freedom and projection operators

To discretize problem (9.68)–(9.69), we introduce a linear space of discrete transverse displacements, \mathcal{V}_h , a linear space of discrete rotations, H_h , and a linear space of discrete shears, Γ_h (see Fig. 9.1).

- The space \mathcal{V}_h is defined by attaching one degree of freedom to each mesh vertex v . The value associated with v is denoted by v_v . The collection of all degrees of

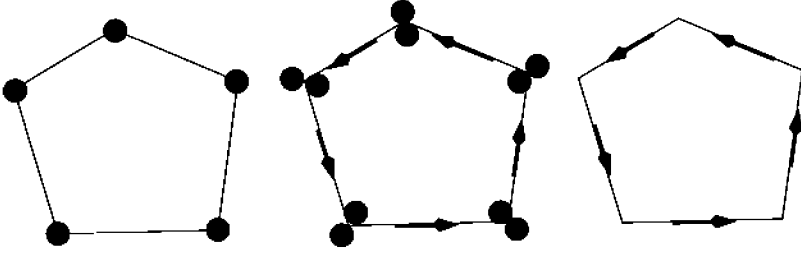


Fig. 9.1. Degrees of freedom for the transverse displacement (left), rotations (center) and shear stress (right)

freedom from the vector $v_h \in \mathcal{V}_h$:

$$v_h = (v_v)_{v \in \mathcal{V}}.$$

The number of unknowns is equal to the number of mesh vertices.

- The space H_h is defined by attaching two degrees of freedom (i.e., a vector $\boldsymbol{\eta}_v \in \mathbb{R}^2$) to each mesh vertex v and one degree of freedom $\eta_{P,e}$ to each mesh edge of each cell P :

$$\boldsymbol{\eta}_h = (\boldsymbol{\eta}_v)_{v \in \mathcal{V}^0} \cup (\eta_{P,e})_{P \in \Omega_h, e \in \partial P}.$$

For each edge e shared by two elements P_1 and P_2 , we assume

$$\eta_{P_1,e} = -\eta_{P_2,e}, \quad (9.71)$$

so that, effectively, we have only one degree of freedom per edge. The scalar $\eta_{P,e}$ represents a bubble-type correction to the tangent component of the rotations on edge e . The total number of unknowns is equal to twice the number of mesh vertices plus the number of mesh edges.

- The space Γ_h is defined by attaching one degree of freedom $\delta_{P,e}$ to every edge e of every element P :

$$\boldsymbol{\delta}_h = (\delta_{P,e})_{P \in \Omega_h, e \in \partial P}.$$

Again, we assume that for each edge e shared by two elements P_1 and P_2 , we have

$$\delta_{P_1,e} = -\delta_{P_2,e}. \quad (9.72)$$

The scalar $\delta_{P,e}$ represents the average of the tangential shear on edge e . The total number of unknowns is equal to the number of edges.

The negative sign in (9.71) and (9.72) is due to the opposite orientation of tangent vectors $\boldsymbol{\tau}_{P_1,e}$ and $\boldsymbol{\tau}_{P_2,e}$. The restrictions of the above spaces to cell P are denoted by $\mathcal{V}_{h,P}$, $H_{h,P}$, and $\Gamma_{h,P}$. We also introduce the proper subspaces $\mathcal{V}_{h,0} \subset \mathcal{V}_{h,P}$, $H_{h,0} \subset H_{h,P}$, and $\Gamma_{h,0} \subset \Gamma_{h,P}$ that collect the vectors whose components associated with the boundary vertices and edges are zero.

Now, we define the projection operators from spaces of sufficiently smooth functions to the discrete spaces \mathcal{V}_h , H_h and Γ_h . For every function $v \in C^0(\overline{\Omega}) \cap H^1(\Omega)$, we define $v^I \in \mathcal{V}_h$ by

$$v^I = (v_v^I)_{v \in \mathcal{V}}, \quad v_v^I = v(\mathbf{x}_v).$$

For every vector-valued function $\boldsymbol{\eta} \in (C^0(\overline{\Omega}) \cap H^1(\Omega))^2$, we define $\boldsymbol{\eta}^I \in H_h$ by

$$\boldsymbol{\eta}^I = (\boldsymbol{\eta}_v^I)_{v \in \mathcal{V}} \cup (\boldsymbol{\eta}_{P,e}^I)_{P \in \Omega_h, e \in \partial P}, \quad \boldsymbol{\eta}_v^I = \boldsymbol{\eta}(\mathbf{x}_v),$$

and

$$\boldsymbol{\eta}_{P,e}^I = \frac{1}{|e|} \int_e \boldsymbol{\eta} \cdot \boldsymbol{\tau}_{P,e} dL - \frac{1}{2} (\boldsymbol{\eta}_{v_1}^I + \boldsymbol{\eta}_{v_2}^I) \cdot \boldsymbol{\tau}_{P,e},$$

where v_1 and v_2 are the vertices of edge e . For every vector-valued function $\boldsymbol{\delta} \in H(\text{curl}, \Omega) \cap (L^s(\Omega))^2$, $s > 2$, we define $\boldsymbol{\delta}^{\text{II}} \in \Gamma_h$ by

$$\boldsymbol{\delta}^{\text{II}} = (\boldsymbol{\delta}_{P,e}^{\text{II}})_{P \in \Omega_h, e \in \partial P}, \quad \boldsymbol{\delta}_{P,e}^{\text{II}} = \frac{1}{|e|} \int_e \boldsymbol{\delta} \cdot \boldsymbol{\tau}_{P,e} dL.$$

Remark 9.4. The edge-based degrees of freedom for space H_h are included for a stability reason. As for the analysis of the mimetic scheme for the Stokes problem in Sect. 8.3, these degrees of freedom can be omitted for the same class of polygonal meshes. On such meshes, we obtain a scheme where only vertex-based degrees of freedom (for both the displacement and rotations) are used. We refer to [57] for a thorough investigation.

9.3.3 Discrete operators and norms

Let v_1 and v_2 be the vertices of edge e such that $\boldsymbol{\tau}_{P,e}$ points from v_1 to v_2 . We endow the space \mathcal{V}_h with the following norm:

$$\|v_h\|_{\mathcal{V}_h}^2 = \sum_{P \in \Omega_h} \|v_P\|_{\mathcal{V}_h,P}^2, \quad \|v_P\|_{\mathcal{V}_h,P}^2 = |P| \sum_{e \in \partial P} \left[\frac{1}{|e|} (v_{v_2} - v_{v_1}) \right]^2. \quad (9.73)$$

In space H_h , we consider the norm

$$\|\boldsymbol{\eta}_h\|_{H_h}^2 = \sum_{P \in \Omega_h} \|\boldsymbol{\eta}_P\|_{H_h,P}^2, \quad \|\boldsymbol{\eta}_P\|_{H_h,P}^2 = |P| \sum_{e \in \partial P} \left(\frac{1}{|e|} (\|\boldsymbol{\eta}_{v_1} - \boldsymbol{\eta}_{v_2}\| + |\eta_{P,e}|) \right)^2,$$

where $\|\cdot\|$ is the Euclidean norm on vectors. Finally, in space Γ_h , we consider the following norm:

$$\|\boldsymbol{\delta}_h\|_{\Gamma_h}^2 = \sum_{P \in \Omega_h} \|\boldsymbol{\delta}_P\|_{\Gamma_h,P}^2, \quad \|\boldsymbol{\delta}_P\|_{\Gamma_h,P}^2 = |P| \sum_{e \in \partial P} |\boldsymbol{\delta}_{P,e}|^2. \quad (9.74)$$

The norms on \mathcal{V}_h and H_h are H^1 -type discrete semi-norms. They become norms on the subspaces $\mathcal{V}_{h,0}$ and $H_{h,0}$ due to the homogeneous Dirichlet boundary conditions.

Indeed, the finite differences appearing in both norms represent gradients on edges and the scaling factors $|P|$ were chosen to mimic the $H^1(P)$ local semi-norms. Note that for the edge-based degrees of freedom in H_h no finite difference is needed since it already represents a bubble correction. The norm on Γ_h is a discrete L^2 -type norm.

Let $\boldsymbol{\eta}^{rot} = (y_P - y, x - x_P)^T$ represent the linearized rigid body rotation about the centroid of P . We define the following L^2 -type discrete seminorm on H_h :

$$\|\boldsymbol{\eta}_h\|_{H_h}^2 = \sum_{P \in \Omega_h} \|\boldsymbol{\eta}_P\|_{H_h, P}^2, \quad \|\boldsymbol{\eta}_P\|_{H_h, P}^2 = \min_{c \in \mathbb{R}} \| \|\boldsymbol{\eta}_P - c(\boldsymbol{\eta}^{rot})_P^I \|_{H_h, P}^2. \quad (9.75)$$

Due to this definition, we have

$$\|\boldsymbol{\eta}_P\|_{H_h, P} \leq \| \|\boldsymbol{\eta}_P \|_{H_h, P} \|, \quad \forall \boldsymbol{\eta}_P \in H_h, P. \quad (9.76)$$

The primary discrete gradient operator $\nabla_h : \mathcal{V}_h \rightarrow \Gamma_h$ is defined as

$$(\nabla_h v_h)_{|P, e} = \frac{v_{v_2} - v_{v_1}}{|e|}.$$

It is immediate to check that

$$\|v_h\|_{\mathcal{V}_h} = \|\nabla_h v_h\|_{\Gamma_h}. \quad (9.77)$$

The primary discrete curl operator $\text{curl}_h : \Gamma_h \rightarrow \mathcal{P}_h$ is defined as

$$(\text{curl}_h \boldsymbol{\delta}_h)_{|P} = \frac{1}{|P|} \sum_{e \in \partial P} \delta_{P, e} |e|.$$

In two dimensions, this operator can be considered as a rotated version of the discrete divergence operator of Chap. 2. We also have the modified version of the commuting property:

$$\text{curl}_h \boldsymbol{\delta}^{\parallel} = (\text{curl} \boldsymbol{\delta})^I, \quad (9.78)$$

where the second projection operator on \mathcal{P}_h is defined in (2.17).

The reduction operator $\Pi_h : H_h \rightarrow \Gamma_h$ is defined as

$$(\Pi_h \boldsymbol{\eta}_h)_{|P, e} = \eta_{P, e} + \frac{1}{2} [\boldsymbol{\eta}_{v_1} + \boldsymbol{\eta}_{v_2}] \cdot \boldsymbol{\tau}_{P, e} \quad \forall P \in \Omega_h, \forall e \in P.$$

9.3.4 Mimetic inner products and bilinear forms

We equip the space Γ_h with the inner product:

$$[\boldsymbol{\gamma}_h, \boldsymbol{\delta}_h]_{\Gamma_h} = \sum_{P \in \Omega_h} [\boldsymbol{\gamma}_P, \boldsymbol{\delta}_P]_{\Gamma_h, P}. \quad (9.79)$$

The local inner product on the element P must satisfy the stability and consistency conditions.

(S1) (Stability Condition). There exist two positive constants σ_* and σ^* , which are independent of h , such that for every $\boldsymbol{\delta}_P \in \Gamma_{h,P}$ and every $P \in \Omega_h$, it holds

$$\sigma_* \|\boldsymbol{\delta}_P\|_{\Gamma_{h,P}}^2 \leq [\boldsymbol{\delta}_h, \boldsymbol{\delta}_h]_{\Gamma_{h,P}} \leq \sigma^* \|\boldsymbol{\delta}_P\|_{\Gamma_{h,P}}^2. \quad (9.80)$$

This condition mimics the coercivity of the continuum L^2 product and ensures the stability of the mimetic scheme.

Let us define the following space:

$$S_{h,P} = \{\boldsymbol{\delta} \in H(\text{curl}, P) : \text{curl } \boldsymbol{\delta} \in \mathbb{P}_0(P), \boldsymbol{\delta} \cdot \boldsymbol{\tau}_{P,e} \in \mathbb{P}_0(e) \quad \forall e \in \partial P\}.$$

According to the constructive path developed in Chap. 4, this space must satisfy three assumptions **(B1)**–**(B3)**. It is easy to verify the first condition **(B1)** that the local projection operator from $S_{h,P}$ to $\Gamma_{h,P}$ is surjective, by building ad-hoc problems on P . The second condition **(B2)** is also trivial, since clearly $S_{h,P}$ contains the smallest approximation space consisting of constant vector functions. The third condition **(B3)**, stating that the right-hand side of the consistency condition can be calculated explicitly using only the degrees of freedom of $\boldsymbol{\delta}$ and the fact that $p^{(1)}$ is a linear polynomial, is verified below.

(S2) (Consistency Condition). For every element P , every scalar linear function $p^{(1)}$, and every $\boldsymbol{\delta} \in S_{h,P}$, it holds

$$[(\text{Curl } p^{(1)})^{\mathbb{I}}, \boldsymbol{\delta}_P^{\mathbb{I}}]_{\Gamma_{h,P}} = \int_P \text{Curl } p^{(1)} \cdot \boldsymbol{\delta} \, dV. \quad (9.81)$$

This condition asserts that the mimetic inner product is exact when one of its arguments is the curl of a linear function (i.e. a constant vector field) and the other is a function from $S_{h,P}$. Integrating the right hand side of (9.81) by parts, using the properties of $S_{h,P}$ and (9.78), we have

$$\begin{aligned} [(\text{Curl } p^{(1)})^{\mathbb{I}}, \boldsymbol{\delta}_P^{\mathbb{I}}]_{\Gamma_{h,P}} &= \int_P p^{(1)} \text{curl } \boldsymbol{\delta} \, dV - \sum_{e \in \partial P} \int_e p^{(1)} (\boldsymbol{\delta} \cdot \boldsymbol{\tau}_{P,e}) \, dL \\ &= \text{curl}_P \boldsymbol{\delta}_P^{\mathbb{I}} \int_P p^{(1)} \, dV - \sum_{e \in \partial P} \delta_{P,e}^{\mathbb{I}} \int_e p^{(1)} \, dL. \end{aligned} \quad (9.82)$$

Thus, the right hand-side can be calculated using only the degrees of freedom of the discrete field $\boldsymbol{\delta} \in \Gamma_h$ and various integrals of a linear function.

Let $a_h : H_h \times H_h \rightarrow \mathbb{R}$ denote an approximation of the bilinear form a defined in (9.70). We break it into the sum of discrete local forms:

$$a_h(\boldsymbol{\beta}_h, \boldsymbol{\eta}_h) = \sum_{P \in \Omega_h} a_{h,P}(\boldsymbol{\beta}_P, \boldsymbol{\eta}_P) \quad \forall \boldsymbol{\beta}_h, \boldsymbol{\eta}_h \in H_h, \quad (9.83)$$

where

$$a_{h,P}(\boldsymbol{\beta}_P, \boldsymbol{\eta}_P) \approx \int_P \mathbb{C} \boldsymbol{\varepsilon}(\boldsymbol{\beta}) : \boldsymbol{\varepsilon}(\boldsymbol{\eta}) \, dV.$$

According to the general theory developed in Chap. 4, the local bilinear form $a_{h,P}$ is required to satisfy the stability and consistency conditions. The stability condition ensures the coercivity property on the subspace orthogonal to its kernel. It also uses the correct scaling with respect to the cell size.

(S1a) (Stability Condition). There exist two positive constants σ_* and σ^* , which are independent of h , such that for every $\boldsymbol{\eta}_P \in H_{h,P}$ and each $P \in \Omega_h$ it holds

$$\sigma_* \|\boldsymbol{\eta}_P\|_{H_{h,P}}^2 \leq a_{h,P}(\boldsymbol{\eta}_P, \boldsymbol{\eta}_P) \leq \sigma^* \|\boldsymbol{\eta}_P\|_{H_{h,P}}^2. \quad (9.84)$$

Note that we make use of the weaker norm (9.75) in order to guarantee that the discrete bilinear form has the correct kernel, spanned not only by the constant vector fields but also by the “linearized rotation” $\boldsymbol{\eta}^{rot}$.

Let us define a functional space $S_{h,P}$ of test functions (with a slight abuse of notation, we use the same name for all problems):

$$S_{h,P} = \{\boldsymbol{\eta} \in (H^1(P))^2 : \boldsymbol{\eta} \cdot \mathbf{n}_{P,e} \in \mathbb{P}_1(e) \ \forall e \in P\}.$$

This space is rich enough so that the projection operator $(\cdot)^I$ on $H_{h,P}$ is surjective, which gives property **(B1)** of Chap. 4. It contains the space of linear functions (property **(B2)**). The last property is verified below.

(S2a) (Consistency Condition). For every element P , every linear vector-valued function \mathbf{p}^1 , and every $\boldsymbol{\eta} \in S_{h,P}$, it holds

$$a_{h,P}((\mathbf{p}^1)_P^I, \boldsymbol{\eta}_P^I) = \int_P \mathbb{C}_P \boldsymbol{\varepsilon}(\mathbf{p}^1) : \boldsymbol{\varepsilon}(\boldsymbol{\eta}) dV. \quad (9.85)$$

The consistency condition is the exactness property; namely, the discrete bilinear form is exact when one of its arguments is a linear vector-valued function and the other one is from space $S_{h,P}$. The integration by parts yields

$$\begin{aligned} a_{h,P}((\mathbf{p}^1)_P^I, \boldsymbol{\eta}_P^I) &= \sum_{e \in \partial P} \int_e (\mathbb{C}_P \boldsymbol{\varepsilon}(\mathbf{p}^1) \cdot \mathbf{n}_{P,e}) \cdot \boldsymbol{\eta} dL \\ &= \sum_{e \in \partial P} (\mathbb{C}_P \boldsymbol{\varepsilon}(\mathbf{p}^1) \cdot \mathbf{n}_{P,e}) \cdot \int_e \boldsymbol{\eta} dL. \end{aligned}$$

Using $\mathbb{I}_2 = \mathbf{n}_{P,e}^T \mathbf{n}_{P,e} + \boldsymbol{\tau}_{P,e}^T \boldsymbol{\tau}_{P,e}$, we develop the edge integral as follows:

$$\begin{aligned} \int_e \boldsymbol{\eta} dL &= \mathbf{n}_{P,e} \int_e \boldsymbol{\eta} \cdot \mathbf{n}_{P,e} dL + \boldsymbol{\tau}_{P,e} \int_e \boldsymbol{\eta} \cdot \boldsymbol{\tau}_{P,e} dL \\ &= \mathbf{n}_{P,e} \left(\frac{|e|}{2} (\boldsymbol{\eta}_{v_1} + \boldsymbol{\eta}_{v_2}) \cdot \mathbf{n}_{P,e} \right) + \boldsymbol{\tau}_{P,e} \left(|e| \eta_{P,e} + \frac{|e|}{2} (\boldsymbol{\eta}_{v_1} + \boldsymbol{\eta}_{v_2}) \cdot \boldsymbol{\tau}_{P,e} \right). \end{aligned} \quad (9.86)$$

Inserting the last two formulas in (9.85), we conclude that the right-hand side of the consistency condition can be calculated exactly using the degrees of freedom in H_h , the cell geometry, and the linear function \mathbf{p}^1 , which is the property **(B3)** of Chap. 4. The construction of the discrete bilinear form will be completed in Sect. 9.4.

We finally note that we do not need to build an inner product for the deflection space \mathcal{V}_h in order to formulate the numerical scheme.

Remark 9.5. Making use of (9.82), (9.86) and recalling the surjectivity properties **(B1)**, the consistency conditions **(S2)**, **(S2a)** can be written in the more practical form that does not make use of the spaces $S_{h,P}$, exactly as in Remark 8.7. Therefore, as usual, the spaces $S_{h,P}$ are introduced for constructive reasons but do not appear in the practical definition of the bilinear form.

9.3.5 Weak form of discrete equations

The mimetic scheme for the Reissner-Mindlin plate is defined as follows. First, we introduce the following approximation of the loading term:

$$(b, v_h)_h = \sum_{P \in \Omega_h} b_P^I \sum_{v \in \partial P} \omega_{P,v} v_v \quad \forall v_h \in \mathcal{V}_h, \quad (9.87)$$

where $b_P^I = |P|^{-1} \int_P b dV$ by the definition of the projector and $\{\omega_{P,v}\}_{v \in \partial P}$ is a set of positive weights such that $\sum_{v \in \partial P} \omega_{P,v} = |P|$. This approximation of the loading term is exact for constant loads. Then, the mimetic scheme reads:

Find $(\boldsymbol{\beta}_h, w_h, \boldsymbol{\gamma}_h) \in H_{h,0} \times \mathcal{V}_{h,0} \times \Gamma_{h,0}$ such that

$$a_h(\boldsymbol{\beta}_h, \boldsymbol{\eta}_h) + [\boldsymbol{\gamma}_h, \nabla_h v_h - \Pi_h \boldsymbol{\eta}_h]_{\Gamma_h} = (b, v_h)_h \quad \forall (\boldsymbol{\eta}_h, v_h) \in H_{h,0} \times \mathcal{V}_{h,0}, \quad (9.88)$$

$$[\nabla_h w_h - \Pi_h \boldsymbol{\beta}_h, \boldsymbol{\delta}_h]_{\Gamma_h} - \kappa^{-1} t^2 [\boldsymbol{\gamma}_h, \boldsymbol{\delta}_h]_{\Gamma_h} = 0 \quad \forall \boldsymbol{\delta}_h \in \Gamma_{h,0}. \quad (9.89)$$

It is immediate to check that the scheme (9.88)–(9.89) is equivalent to the following scheme:

Find $(\boldsymbol{\beta}_h, w_h) \in H_{h,0} \times \mathcal{V}_{h,0}$ such that

$$\begin{aligned} a_h(\boldsymbol{\beta}_h, \boldsymbol{\eta}_h) + \frac{\kappa}{t^2} [\nabla_h w_h - \Pi_h \boldsymbol{\delta}_h, \nabla_h v_h - \Pi_h \boldsymbol{\eta}_h]_{\Gamma_h} \\ = (b, v_h)_h \quad \forall (\boldsymbol{\eta}_h, v_h) \in H_{h,0} \times \mathcal{V}_{h,0}. \end{aligned} \quad (9.90)$$

The discrete operator associated with scheme (9.90) is positive definite and involves only two unknowns, namely the displacement and rotation variables. Therefore, it is generally more suitable to practical implementations.

9.3.6 A priori error estimates

The stability conditions **(S1)** and **(S1a)** imply that the bilinear form in the left-hand side of (9.90) is semi-positive definite on $H_h \times \mathcal{V}_h$. Moreover, again due to the Dirichlet boundary conditions, it is easy to verify that

$$a_h(\boldsymbol{\eta}_h, \boldsymbol{\eta}_h) + \frac{\kappa}{t^2} [\nabla_h v_h - \Pi_h \boldsymbol{\eta}_h, \nabla_h v_h - \Pi_h \boldsymbol{\eta}_h]_{\Gamma_h} = 0$$

only when both $\boldsymbol{\eta}_h$ and v_h are zero mesh functions. Therefore, the bilinear form is positive definite on $H_{h,0} \times \mathcal{V}_{h,0}$ and scheme (9.90) has a unique solution for all h and $t > 0$.

We now present the following convergence result. The proof makes use of the analysis tools discussed in the previous chapters combined with technical arguments from the MITC Finite Element literature and can be found in [57].

Theorem 9.4. *Let $(\boldsymbol{\beta}, w, \boldsymbol{\gamma})$ be the solution of (9.68)–(9.69) with $\boldsymbol{\beta} \in (H^2(\Omega) \cap H_0^1(\Omega))^2$, $w \in H^2(\Omega) \cap H_0^1(\Omega)$, and $\boldsymbol{\gamma} \in (H_0^1(\Omega))^2$. Furthermore, let $(\boldsymbol{\beta}_h, w_h, \boldsymbol{\gamma}_h)$ be the solution of the mimetic problem (9.88)–(9.89) under the assumptions (S1)–(S2), (S1a)–(S2a), and the mesh shape regularity assumptions (MR1)–(MR2) of Sect. 1.6.2. Then, there exists a constant C independent of h and t such that*

$$\|\boldsymbol{\beta}^I - \boldsymbol{\beta}_h\|_{H_h} + \|w^I - w_h\|_{\gamma_h} + t\|\boldsymbol{\gamma}^I - \boldsymbol{\gamma}_h\|_{\Gamma_h} \leq Ch\|b\|_{L^2(\Omega)}. \quad (9.91)$$

This theorem states the linear convergence of the method uniformly in the thickness parameter t . The approximation properties of the method do not deteriorate when the (relative) thickness of the plate is small. The scheme presented here is therefore locking free. Extensive numerical verification of the converge estimate can be found in [52], together with an extension to plate vibration and plate buckling problems.

9.4 Implementation of the method

In this section, we complete the construction of the local bilinear forms introduced in the previous sections. We assume that the mesh satisfies the conditions of Remark 9.4, i.e. we consider the case of only vertex-based degrees of freedom.

Let P be a polygon. In order to shorten the notation, we will use the symbol m to denote the number of vertices in P , i.e. $m = N_P^V$. The vertices are enumerated counter-clockwise as v_1, \dots, v_m and $v_{m+1} = v_1$. The polygon edges are also enumerated counter-clockwise and $\mathbf{e}_i = (v_i, v_{i+1})$.

In total, $3m$ degrees of freedom are associated with P , three with each vertex. We order them as follows: first all the rotations, then all the deflections. The local vector of unknowns $(\boldsymbol{\eta}_P \in H_{h,P}$ and $w_P \in W_{h,P})$ becomes

$$\{\boldsymbol{\eta}_{v_1}, \boldsymbol{\eta}_{v_2}, \dots, \boldsymbol{\eta}_{v_m}, w_{v_1}, w_{v_2}, \dots, w_{v_m}\}.$$

According to (9.90), the matrix that represents the local bilinear form, denoted by $M_P \in \mathbb{R}^{3m \times 3m}$, can be broken into two terms:

$$M_P = M_{P,a} + \kappa t^{-2} M_{P,b}. \quad (9.92)$$

The first matrix is associated with the bilinear form $a_{h,P}$; the second matrix is associated with the shear energy term. Once the elemental matrices M_P are built, the global stiffness matrix is assembled in the conventional finite element way.

9.4.1 Stiffness matrix for the bilinear form $a_{h,P}$

The local bilinear form $a_{h,P}$ uses only $2m$ degrees of freedom. Therefore, it can be represented by a $2m \times 2m$ matrix still denoted by $M_{P,a}$:

$$a_{h,P}(\boldsymbol{\beta}_P, \boldsymbol{\eta}_P) = \boldsymbol{\beta}_P^T M_{P,a} \boldsymbol{\eta}_P \quad \forall \boldsymbol{\beta}_P, \boldsymbol{\eta}_P \in H_{h,P}.$$

The construction of matrix $M_{P,a}$ is based on the stability and consistency conditions (S1a)–(S2a). Let $\mathbf{q}_1, \mathbf{q}_2, \dots, \mathbf{q}_6$ form a basis in $(\mathbb{P}_1(P))^2$, for example,

$$\begin{pmatrix} 1 \\ 0 \end{pmatrix}, \quad \begin{pmatrix} 0 \\ 1 \end{pmatrix}, \quad \begin{pmatrix} y - y_P \\ x_P - x \end{pmatrix}, \quad \begin{pmatrix} y - y_P \\ x - x_P \end{pmatrix}, \quad \begin{pmatrix} x - x_P \\ y - y_P \end{pmatrix}, \quad \begin{pmatrix} x - x_P \\ y_P - y \end{pmatrix},$$

where $\mathbf{x}_P = (x_P, y_P)^T$ is the barycenter of P . Let $N_i = (\mathbf{q}_i)_P^I$. Since, according to Remark 9.4, no edge-based degrees of freedom are considered here, the explicit expression of vector N_i is available:

$$(N_i)_{2j-1} = (\mathbf{q}_i(v_j))_x, \quad (N_i)_{2j} = (\mathbf{q}_i(v_j))_y, \quad j = 1, \dots, m.$$

Thus, the components of vector N_i are the x and y values of the linear polynomial \mathbf{q}_i at the vertices of P .

Formulas (9.85)–(9.86) imply that

$$a_{h,P}((\mathbf{q}_i)_P^I, \boldsymbol{\eta}_P^I) = N_i^T M_{P,a} \boldsymbol{\eta}_P^I = R_i^T \boldsymbol{\eta}_P^I \quad \forall \boldsymbol{\eta}_P^I \in H_{h,P}, \quad (9.93)$$

where the components of vector R_i are defined implicitly by

$$R_i^T \boldsymbol{\eta}_P^I = \frac{1}{2} \sum_{e_i=1}^m |e_i| (\mathbb{C}_P \boldsymbol{\varepsilon}(\mathbf{q}_i) \mathbf{n}_{P,e_i}) \cdot (\boldsymbol{\eta}_{v_i} + \boldsymbol{\eta}_{v_{i+1}}).$$

Since $\boldsymbol{\varepsilon}(\mathbf{q}_i) = \mathbf{0}$ for $i = 1, 2, 3$, the column vectors R_1, R_2 , and R_3 are the zero vector.

Let us introduce two rectangular $2m \times 6$ matrices $N_P = (N_1, \dots, N_6)$ and $R_P = (R_1, \dots, R_6)$. Due to the arbitrariness of $\boldsymbol{\eta}_P^I$, Eq. (9.93) implies that

$$M_{P,a} N_i = R_i, \quad i = 1, \dots, 6,$$

which can be written in the compact matrix form:

$$M_{P,a} N_P = R_P. \quad (9.94)$$

Matrix equations of this type appear in every mimetic scheme. Typically, it has a family of solutions, whose derivation is discussed in Chap. 4. Here, we present the member of this family that leads to the simplest practical implementation of the mimetic scheme.

Remark 9.6. If edge-based degrees of freedom are required for stability, additional rows are added to matrices N_P and R_P . The remaining derivations are modified accordingly.

Let us introduce the 6×6 -sized real matrix $K_P = N_P^T R_P$. According to Lemma 4.1, this matrix is symmetric and semi-positive definite. Moreover, it has the following block structure:

$$K_P = \begin{pmatrix} O_3 & O \\ O & K_* \end{pmatrix},$$

where K_* is positive definite, O is a generic zero rectangular matrix, and O_3 is a zero 3×3 square matrix. Then, Corollary 4.2 gives

$$M_{P,a} = R_P K_P^\dagger R_P^T + \gamma_P (I - N_P (N_P^T N_P)^{-1} N_P^T),$$

where γ_P is a scaling coefficient and K_P^\dagger is a pseudo-inverse matrix:

$$\gamma_P = \frac{1}{2m} \text{trace}(R_P K_P^\dagger R_P^T), \quad K_P^\dagger = \begin{pmatrix} O_3 & O \\ O & K_*^{-1} \end{pmatrix}.$$

It is immediate to check that $M_{P,a}$ satisfies Eq. (9.94). The uniform semi-positive definiteness expressed by the stability condition (**S1a**) can be proved with the techniques described in Chap. 4.

Note that matrix $M_{P,a} \in \mathbb{R}^{2m \times 2m}$ is defined for the rotational degrees of freedom, since the bilinear form $a_{h,P}$ is independent of the deflection variable. When it comes to building the local matrix M_P in (9.92) one simply needs to augment $M_{P,a}$ with m zero rows and m zero columns.

9.4.2 Stiffness matrix for the shear energy term

The matrix $M_{P,b}$ for the shear energy term is obtained as a product of matrices representing the operators ∇_h and Π_h with the inner product matrix $\overline{M}_P \in \mathbb{R}^{m \times m}$ representing the local bilinear form $[\cdot, \cdot]_{\Gamma_{h,P}}$, see (9.90):

$$[\gamma_P, \delta_P]_{\Gamma_{h,P}} = \gamma_P^T \overline{M}_P \delta_P \quad \forall \gamma_P, \delta_P \in \Gamma_{h,P}.$$

We enumerate the local degrees of freedom in $\Gamma_{h,P}$ following the enumeration of edges in P . The construction of \overline{M}_P repeats the steps of the previous section and therefore is presented briefly.

Let $q_1 = x - x_P$, $q_2 = y - y_P$, and $q_3 = 1$ denote the basis functions of the space of linear polynomials on P . We set $\overline{N}_i = (\text{Curl } q_i)_{\mathbb{P}}$. The consistency condition (**S2**) (see formulas (9.81) and (9.82)) and the definition of the discrete curl operator imply

$$(\overline{N}_i)^T \overline{M}_P \delta_P^{\mathbb{I}} = (\overline{R}_i)^T \delta_P^{\mathbb{I}} \quad \forall \delta_P^{\mathbb{I}} \in \Gamma_{h,P}.$$

where

$$(\overline{R}_i)_j = \frac{|e_j|}{|P|} \int_P q_i dV - \int_e q dL = |e_j| (q_i(\mathbf{x}_P) - q_i(\mathbf{x}_{e_j})).$$

Since $\overline{N}_3 = \overline{R}_3 = 0$, the consistency condition is trivially satisfied for q_3 . Let $\overline{N}_P = (\overline{N}_1, \overline{N}_2)$ and $\overline{R}_P = (\overline{R}_1, \overline{R}_2)$. Due to arbitrariness of vector $\delta_P^{\mathbb{I}}$, we have two matrix

equations:

$$\overline{M}_P \overline{N}_i = \overline{R}_i, \quad i = 1, 2,$$

that can be written as $\overline{M}_P \overline{N}_P = \overline{R}_P$.

Next, we introduce the symmetric semi-positive definite matrix $K_P = \overline{N}_i^T \overline{R}_P$. Now, Corollary 4.2 gives the solution to the matrix equation:

$$\overline{M}_P = \overline{R}_P \overline{K}_P^{-1} \overline{R}_P^T + \overline{\gamma}_P (I - \overline{N}_P (\overline{N}_P^T \overline{N}_P)^{-1} \overline{N}_P^T),$$

where $\overline{\gamma}_P = \text{trace}(\overline{R}_P \overline{K}_P^{-1} \overline{R}_P^T)$. The consistency condition **(S2)** gives immediately that $\overline{K}_P = |P| \mathbb{I}_2$.

The matrix $M_{P,b}$ appearing in (9.92) can be built by combining \overline{M}_P with a matrix $C_P \in \mathbb{R}^{m \times 3m}$ representing both the discrete gradient operator ∇_h , and the reduction operator Π_h . Therefore, we set

$$C_P = (-C_1, C_2)$$

where matrix $C_1 \in \mathbb{R}^{m \times 2m}$ represents the Π_h operator,

$$C_1 = \frac{1}{2} \begin{pmatrix} \boldsymbol{\tau}_{P,e_1}^T & \boldsymbol{\tau}_{P,e_1}^T & \mathbf{0}_{1 \times 2} & \mathbf{0}_{1 \times 2} & \cdots & \boldsymbol{\tau}_{P,e_1}^T \\ \mathbf{0}_{1 \times 2} & \boldsymbol{\tau}_{P,e_2}^T & \boldsymbol{\tau}_{P,e_2}^T & \mathbf{0}_{1 \times 2} & \cdots & \mathbf{0}_{1 \times 2} \\ \mathbf{0}_{1 \times 2} & \mathbf{0}_{1 \times 2} & \boldsymbol{\tau}_{P,e_3}^T & \boldsymbol{\tau}_{P,e_3}^T & \cdots & \mathbf{0}_{1 \times 2} \\ \vdots & \vdots & \vdots & \vdots & \vdots & \vdots \\ \boldsymbol{\tau}_{P,e_m}^T & \mathbf{0}_{1 \times 2} & \mathbf{0}_{1 \times 2} & \mathbf{0}_{1 \times 2} & \cdots & \boldsymbol{\tau}_{P,e_m}^T \end{pmatrix},$$

and matrix $C_2 \in \mathbb{R}^{m \times m}$ represents the ∇_h operator,

$$C_2 = \begin{pmatrix} -|e_1|^{-1} & |e_1|^{-1} & 0 & 0 & \cdots & 0 \\ 0 & -|e_2|^{-1} & |e_2|^{-1} & 0 & \cdots & 0 \\ 0 & 0 & -|e_3|^{-1} & |e_3|^{-1} & \cdots & 0 \\ \vdots & \vdots & \vdots & \vdots & \vdots & \vdots \\ -|e_m|^{-1} & 0 & 0 & \cdots & 0 & |e_m|^{-1} \end{pmatrix}.$$

Finally, the local matrix for the shear energy term is given by

$$M_{P,b} = C_P^T \overline{M}_P C_P.$$

Other linear and nonlinear mimetic schemes

“Classification of mathematical problems as linear and nonlinear is like classification of the Universe as bananas and non-bananas”

(Unknown source)

10.1 Advection-diffusion equation

Let Ω be a bounded, open, polygonal (polyhedral) subset of \mathbb{R}^d , $d = 2, 3$, with the Lipschitz continuous boundary Γ . We consider the mimetic discretization of the advection-diffusion equation for the scalar field p introduced in Sect. 1.4.3:

$$\operatorname{div}(\beta p - K\nabla p) = b \quad \text{in } \Omega, \quad (10.1)$$

$$p = g^D \quad \text{on } \Gamma, \quad (10.2)$$

where K is a bounded, measurable, symmetric and uniformly elliptic tensor, $b \in L^2(\Omega)$, $g^D \in H^{1/2}(\Gamma)$, $\beta \in C^1(\overline{\Omega})^d$ is such that $\operatorname{div} \beta \geq 0$, cf. assumptions **(H1)**–**(H3)** in Sect. 1.4.1. The diffusive and the total fluxes are given by

$$\mathbf{u} = -K\nabla p \quad \text{and} \quad \tilde{\mathbf{u}} = \mathbf{u} + \beta p. \quad (10.3)$$

For simplicity, we will restrict the presentation of the mimetic schemes and their theoretical analysis to the case of the homogeneous Dirichlet boundary condition $g^D = 0$. However, we will consider non-homogeneous boundary conditions in the numerical experiments in Sect. 10.1.4.

Under these assumptions, the existence and uniqueness of a weak solution in $H_0^1(\Omega)$ follows from the fact that the bilinear form associated with problem (10.1)–(10.2) is continuous and coercive. The advection-diffusion equation can be discretized by considering various techniques from the literature on finite volume and finite element schemes. There are two possible approaches:

1. The diffusive flux is approximated by the low order mimetic discretization of Chap. 5 and the advective term is treated numerically using a centered or an up-wind discretization.
2. The total flux is selected as the primary variable, which leads often to a scheme with a centered-type approximation of the advection term.

The first approach is, seems, more popular in the finite difference and finite volume (FV) communities, cf. [113, 147]. The second one is often used in the finite element community. Nevertheless, it is worth mentioning that both approaches have been considered in the framework of mixed finite element methods, see [143, 144, 220]. In the mimetic finite difference framework, a numerical discretization of the total flux has been proposed in [107]. A proper reformulation of the mimetic scheme as a conforming method, using a finite dimensional subspace of $H(\operatorname{div}, \Omega)$, makes it possible to perform the convergence analysis in a way very similar to that presented in [143].

A systematic study of the two possible approaches, their advantages and drawback, has been carried out in [45], in which the advective term is treated numerically using the unified formulation for the hybrid FV, the mixed FV and the MFD methods dubbed as the hybrid mimetic method (HMM), cf. [148]. We review the main approaches in the next subsections. In Sect. 10.2.3, we present the convergence analysis and a priori error estimates. In Sect. 10.1.4, we illustrate the shock-capturing behavior of the various mimetic discretizations.

10.1.1 Discretization of the advective term

We introduce a few geometric quantities that will be useful in the definition of the numerical advection flux. Let $d_{P,f}$ be the distance between centroid \mathbf{x}_P of cell P and the hyperplane containing the face f . Furthermore, let

$$d_f = \begin{cases} d_{P,f} + d_{P',f} & \text{for any internal face } f \in \mathcal{F}^0 \text{ shared by } P \text{ and } P', \\ d_{P,f} & \text{for any boundary face } f \in \mathcal{F}^\partial. \end{cases}$$

As in Chap. 5, the degrees of freedom of the vector variable \mathbf{u} are associated with the mesh faces and approximate the normal component of \mathbf{u} on each face. In contrast to Chap. 5, here, we prescribe one flux value $u_{P,f}$ to each pair (P, f) . Thus, each internal face f shared by cells P_1 and P_2 has two fluxes, $u_{P_1,f}$ and $u_{P_2,f}$. We denote the linear space of the discrete fields collecting these fluxes by $\widehat{\mathcal{F}}_h$:

$$\mathbf{v}_h \in \widehat{\mathcal{F}}_h \implies \mathbf{v}_h = (v_{P,f})_{P \in \mathcal{P}, f \in \partial P}.$$

Let $\widehat{\mathcal{F}}_{h,P}$ denote the restriction of $\widehat{\mathcal{F}}_h$ to cell P . Note that the discrete space \mathcal{F}_h introduced in Chap. 5 is isomorphic to a subspace of $\widehat{\mathcal{F}}_h$ which is given by

$$\widetilde{\mathcal{F}}_h = \left\{ \mathbf{v}_h \in \widehat{\mathcal{F}}_h : v_{P_1,f} = -v_{P_2,f} \quad \forall f = P_1 \cap P_2, f \in \mathcal{F}^0 \right\}.$$

In each cell P , we approximate the velocity field by a vector $\boldsymbol{\beta}_P^1 \in \widehat{\mathcal{F}}_{h,P}$:

$$\boldsymbol{\beta}_P^1 = (\beta_{P,f}^1)_{f \in \partial P}, \quad \beta_{P,f}^1 = \frac{1}{|f|} \int_f \boldsymbol{\beta} \cdot \mathbf{n}_{P,f} dS. \quad (10.4)$$

FV-inspired mimetic discretizations. Several discretization schemes for the advection term are available in the FV literature including *the second-order cell-centered scheme, the first-order upwind scheme, the θ -scheme, and the Scharfetter-Gummel scheme*. In these schemes, the advective flux of the exact solution p is approximated by the numerical advective flux $\mathbf{u}^a(p_h) \in \widehat{\mathcal{F}}_h$ of the discrete scalar field $p_h \in \mathcal{P}_h$:

$$\mathbf{u}^a(p_h) = ((\mathbf{u}^a(p_h))_{P,f})_{P \in \mathcal{P}, f \in \partial P}, \quad (\mathbf{u}^a(p_h))_{P,f} \approx \frac{1}{|f|} \int_f \beta p \cdot \mathbf{n}_{P,f} dS. \quad (10.5)$$

We list below the schemes that we will consider in the section with numerical experiments. Let $f = P \cap P'$ if $f \in \mathcal{F}^0$ and that $p_{P'} = 0$ if $f \in \mathcal{F}^\partial$.

- The second-order cell-centered scheme is given by the approximation

$$(\mathbf{u}^a(p_h))_{P,f} = \beta_{P,f} \frac{p_P + p_{P'}}{2}.$$

- The first-order upwind scheme is given by the approximation

$$(\mathbf{u}^a(p_h))_{P,f} = \beta_{P,f}^+ p_P - \beta_{P,f}^- p_{P'},$$

where $s^\pm = \max(\pm s, 0)$.

- The θ -scheme is given by the approximation

$$\begin{aligned} (\mathbf{u}^a(p_h))_{P,f} &= \beta_{P,f}^+ ((1 - \theta)p_P + \theta p_{P'}) - \beta_{P,f}^- ((1 - \theta)p_{P'} + \theta p_P) \\ &= (1 - 2\theta)((\beta_{P,f}^+ p_P - \beta_{P,f}^- p_{P'}) + \theta \beta_{P,f}(p_P + p_{P'})), \end{aligned}$$

where $\theta \in [0, 1/2]$. This scheme is clearly intermediate between the cell-centered and the upwind schemes.

- The Scharfetter-Gummel scheme [321] is given by the approximation

$$(\mathbf{u}^a(p_h))_{P,f} = \frac{1}{d_f} (A_{\text{sg}}(d_f \beta_{P,f}) p_P - A_{\text{sg}}(-d_f \beta_{P,f}) p_{P'}), \quad (10.6)$$

where

$$A_{\text{sg}}(s) = \frac{-s}{e^{-s} - 1} - 1. \quad (10.7)$$

Note that the first three scheme above can be also found in the FE literature, see for instance [128, 219]. As pointed out in [113], the Scharfetter-Gummel scheme was written for an isotropic homogeneous material, i.e., $K = I$. This definition of the advective flux is somewhat basic in the general case $K \neq I$, especially if some eigenvalues of K are small. Although the above definition of A_{sg} ensures the L^2 -stability of the scheme, it can produce quite bad solutions in the advection-dominated cases. A better choice is provided by scaling A_{sg} locally in accordance with the smallest eigenvalue of K . If λ_f is the smallest eigenvalue of K_P and $K_{P'}$, we take

$$A_{\text{sg},K,f}(s) = \min(1, \lambda_f) A_{\text{sg}}\left(\frac{s}{\min(1, \lambda_f)}\right) \quad (10.8)$$

instead of $A_{\text{sg}}(s)$ in (10.6). In this way, the numerical flux automatically and locally adjusts the upwinding of the advection term depending on its relative strength with respect to the diffusive term, without perturbing the consistency property of A_{sg} . More details and background of this choice can be found in [45].

Once a FV-based discretization of the advective term has been chosen, the term $\text{div } \beta p$ in (10.1) is approximated by

$$(\text{div } \beta p)|_{\mathcal{P}} \approx \frac{1}{|\mathcal{P}|} \sum_{f \in \partial \mathcal{P}} |f| (\mathbf{u}^a(p_h))_{\mathcal{P},f} = \text{div}_{\mathcal{P}} (\mathbf{u}^a(p_h))|_{\mathcal{P}}$$

where $\text{div}_{\mathcal{P}}$ is defined as in Sect. 2.2. The inner product on space \mathcal{F}_h introduced in Chap. 5 is the sum of cell-based contributions; therefore, it can be naturally extended to an inner product on space $\widehat{\mathcal{F}}_h$. The mimetic approximation of the problem (10.1)–(10.2) reads:

Find $(\mathbf{u}_h, p_h) \in \widehat{\mathcal{F}}_h \times \mathcal{P}_h$ such that

$$[\mathbf{u}_h, \mathbf{v}_h]_{\widehat{\mathcal{F}}_h} = [\text{div}_h \mathbf{v}_h, p_h]_{\mathcal{P}_h} \quad \forall \mathbf{v}_h \in \widehat{\mathcal{F}}_h, \quad (10.9)$$

$$[\text{div}_h (\mathbf{u}_h + \mathbf{u}^a(p_h)), q_h]_{\mathcal{P}_h} = [b^I, q_h]_{\mathcal{P}_h} \quad \forall q_h \in \mathcal{P}_h. \quad (10.10)$$

FE-inspired discretizations. In [107] a different approach, that uses the total flux as the primary variable, is considered. The authors start with the mixed variational formulation of problem (10.1)–(10.2) that reads (see [88]):

Find $(\tilde{\mathbf{u}}, p) \in H(\text{div}, \Omega) \times L^2(\Omega)$ such that

$$(\mathcal{K}^{-1} \tilde{\mathbf{u}}, \mathbf{v}) - (p, \text{div } \mathbf{v}) - (\mathcal{K}^{-1} \beta p, \mathbf{v}) = 0 \quad \forall \mathbf{v} \in H(\text{div}, \Omega), \quad (10.11)$$

$$(\text{div } \tilde{\mathbf{u}}, q) = (b, q) \quad \forall q \in L^2(\Omega), \quad (10.12)$$

where $\tilde{\mathbf{u}}$ is the total flux defined in (10.3).

The mimetic discretization of the first term in (10.11) is considered in Chap. 5. To discretize the advection term, we approximate the variational term as

$$(\mathcal{K}^{-1} \beta p, \mathbf{v}) = \sum_{\mathcal{P} \in \Omega_h} \int_{\mathcal{P}} \mathcal{K}^{-1} \beta p \cdot \mathbf{v} dV \approx \sum_{\mathcal{P} \in \Omega_h} p_{\mathcal{P}} [\beta_{\mathcal{P}}^I, \mathbf{v}_{\mathcal{P}}]_{\mathcal{P}},$$

where the interpolated velocity field $\beta^I \in \widehat{\mathcal{F}}_h$ is given by (10.4) and the local inner products are the same inner product used to assemble $[\cdot, \cdot]_{\widehat{\mathcal{F}}_h}$. The weak form of the mimetic scheme proposed in [107] reads:

Find $(\tilde{\mathbf{u}}_h, p_h) \in \widehat{\mathcal{F}}_h \times \mathcal{P}_h$ such that

$$[\tilde{\mathbf{u}}_h, \mathbf{v}_h]_{\widehat{\mathcal{F}}_h} - [p_h, \text{div}_h \mathbf{v}_h]_{\mathcal{P}_h} - \sum_{\mathcal{P} \in \Omega_h} p_{\mathcal{P}} [\beta_{\mathcal{P}}^I, \mathbf{v}_h]_{\mathcal{P}} = 0 \quad \forall \mathbf{v}_h \in \widehat{\mathcal{F}}_h, \quad (10.13)$$

$$[\text{div}_h \tilde{\mathbf{u}}_h, q_h]_{\mathcal{P}_h} = [b^I, q_h]_{\mathcal{P}_h} \quad \forall q_h \in \mathcal{P}_h. \quad (10.14)$$

The convergence analysis of this scheme is carried out in [107] under certain assumptions on the mesh shape regularity. When $p \in H^2(\Omega)$, this analysis provides the following estimate:

$$\|\|\|\tilde{\mathbf{u}}_h - \tilde{\mathbf{u}}^I\|\|\|_{\mathcal{F}_h} + \|\|p_h - p^I\|\|_{\mathcal{P}_h} \leq Ch \|p\|_{H^2(\Omega)}, \quad (10.15)$$

where $\|\|\|\cdot\|\|\|_{\mathcal{F}_h}$ and $\|\|\|\cdot\|\|\|_{\mathcal{P}_h}$ are the norms induced by the respective inner products. It is worth mentioning that the approximation of the scalar variable is superconvergent, the result that can be shown theoretically under additional assumptions on the domain shape, the source term, and the velocity field.

The convergence is proved for $h \rightarrow 0$, but for larger h the scheme is expected to become unstable when the problem is advection-dominated. This instability manifests itself through various numerical artifacts such as undershoots, overshoots, and especially oscillations. To improve the stability of the scheme, we modify the divergence equation by adding a stabilization term that depends on the solution jumps across mesh faces. Let $f = P \cap P'$ be an internal mesh face and $\mathbf{n}_{P,f} \cdot \mathbf{n}_f = 1$. The jump of the discrete scalar field $q_h \in \mathcal{P}_h$ is defined by

$$[[q_h]]_f = \begin{cases} q_P - q_{P'} & \text{for } f \in \mathcal{F}^0, \\ q_P & \text{for } f \in \mathcal{F}^d. \end{cases} \quad (10.16)$$

Now, Eq. (10.14) is substituted by

$$[\text{div}_h \tilde{\mathbf{u}}_h + J_h(p_h), q_h]_{\mathcal{P}_h} = [b^I, q_h]_{\mathcal{P}_h} \quad \forall q_h \in \mathcal{P}_h. \quad (10.17)$$

The stabilization term $J_h(p_h) \in \mathcal{P}_h$ is given by

$$J_h(p_h)|_P = \frac{\alpha}{2|P|} \sum_{f \in \partial P} |f| |\beta_{P,f}^I| [[p_h]]_f, \quad (10.18)$$

where α is a non-negative parameter that can be tuned to control the amount of numerical dissipation added to the scheme.

The scheme (10.13), (10.17) formally differs from the scheme introduced earlier, since the advection term is now imbedded in the total flux. However, it is still possible to extract an explicit form of the numerical advection flux and reformulate the new scheme like a FV scheme. To this purpose, we define the vector

$$\mathbf{u}_h = (u_{P,f})_{P \in \mathcal{P}_h, f \in \partial P}, \quad u_{P,f} = \tilde{u}_{P,f} - p_P \beta_{P,f}^I. \quad (10.19)$$

with this definition, Eq. (10.13) resembles Eq. (10.9); therefore, \mathbf{u}_h plays the role of a pure diffusive flux. Noting that the stabilization term $J_h(p_h)|_P$ is written as a balance of fluxes, allows us to identify the advective flux as

$$(\mathbf{u}^a(p_h))_{P,f} = p_P \beta_{P,f}^I + \frac{\alpha}{2} \beta_{P,f}^I [[p_h]]_f, \quad (10.20)$$

so that (10.17) is equivalent to $\text{div}_h(\mathbf{u}_h + \mathbf{u}^a(p_h)) = b^I$. The stabilized scheme (10.13), (10.17) can therefore be written as:

Find $(\mathbf{u}_h, p_h) \in \widehat{\mathcal{F}}_h \times \mathcal{P}_h$ such that

$$[\mathbf{u}_h, \mathbf{v}_h]_{\widehat{\mathcal{F}}_h} = [\operatorname{div}_h \mathbf{v}_h, p_h]_{\mathcal{P}_h} \quad \forall \mathbf{v}_h \in \widehat{\mathcal{F}}_h, \quad (10.21)$$

$$[\operatorname{div}_h(\mathbf{u}_h + \mathbf{u}^a(p_h)), q_h]_{\mathcal{P}_h} = [b^I, q_h]_{\mathcal{P}_h} \quad \forall q_h \in \mathcal{P}_h, \quad (10.22)$$

$$(\mathbf{u}_h + (\mathbf{u}^a(p_h)))_{\mathcal{P},f} + (\mathbf{u}_h + (\mathbf{u}^a(p_h)))_{\mathcal{P}',f} = 0 \quad \forall f \in \mathcal{F}^0. \quad (10.23)$$

Note that the diffusive flux \mathbf{u}_h and the advective flux $\mathbf{u}^a(p_h)$ are not conservative when considered separately and, therefore, belong to the linear space $\widehat{\mathcal{F}}_h$ but not to \mathcal{F}_h . However, their sum is conservative in view of Eq. (10.23).

10.1.1.1 Unified setting

We present a unified formulation for the numerical discretization of the advection term. It includes the FV-based discretizations, as was noted in [113], and the MFD-based discretization (10.21)–(10.23). The unified formulation allows us to simplify the software implementation and carry out a unified theoretical analysis.

Let us consider two functions $A, B: \mathbb{R} \rightarrow \mathbb{R}$ and define the numerical advective flux as the collection of real numbers

$$\mathbf{u}^a(p_h) = (\mathbf{u}^a(p_h)_{\mathcal{P},f})_{\mathcal{P} \in \mathcal{P}_h, f \in \partial \mathcal{P}} \quad (10.24)$$

such that

$$(\mathbf{u}^a(p_h))_{\mathcal{P},f} = \frac{1}{d_f} (A(d_f \beta_{\mathcal{P},f}^I) p_{\mathcal{P}} + B(d_f \beta_{\mathcal{P},f}^I) p_{\mathcal{P}'}). \quad (10.25)$$

We consider the scheme (10.21)–(10.23) with this definition of the advective flux. The schemes presented earlier correspond to different choices of A and B :

- *Centered scheme*: $A(s) = \frac{s}{2}$ and $B(s) = \frac{s}{2}$.
- *Upwind scheme*: $A(s) = s^+$ and $B(s) = -s^-$.
- θ -*scheme*: $A(s) = (1 - 2\theta)s^+ + \theta s$ and $B(s) = -A(-s)$.
- *Scharfetter-Gummel scheme*: $A(s) = A_{\text{sg}}(s)$ is defined by (10.7) and $B(s) = -A_{\text{sg}}(-s)$. The locally scaled Scharfetter-Gummel scheme is obtained by using $A_{\text{sg},K,f}$ defined by (10.8) instead of A_{sg} .
- *Stabilized MFD scheme*: $A(s) = s + \frac{\alpha}{2}|s|$ and $B(s) = -\frac{\alpha}{2}|s|$.

The first four choices lead to a conservative definition of the numerical advective flux, whereas the last one does not. However, in all five cases, the total conservation is ensured by (10.23). Note that functions A and B have the following properties:

(AB1) A and B are Lipschitz-continuous functions and $A(0) = B(0) = 0$.

(AB2) $A(s) + B(s) = s$ for any real number s .

(AB3) One of the following two alternatives holds:

(AB3s) $A(s) + B(-s) = 0$ and $A(s) - B(s) \geq 0$ for any s .

(AB3w) The function $s \rightarrow A(s) + B(-s)$ is odd and there exists $C > 0$ such that $A(s) - B(s) \geq -C|s|$ for any s .

We will refer to **(AB3s)** as the *strong* **(AB3)** condition, and to **(AB3w)** as the *weak* **(AB3)** condition. Condition **(AB3s)** is satisfied by all FV-based discretizations listed above, whereas the MFD-based discretization satisfies **(AB3w)**. In fact, condition $A(s) + B(-s) = 0$ is the one that ensures the conservation of the numerical advective flux (10.25). As noted in [45], conditions **(AB1)**–**(AB3)** are sufficient to carry out the theoretical analysis of the scheme (10.21)–(10.25), with slightly different results depending on which alternative in **(AB3)** is satisfied.

Remark 10.1. Equation (10.22) can be rewritten in the finite volume form as the local (cell-based) flux balance equation:

$$\sum_{f \in \partial P} |f| (\mathbf{u}_{P,f} + (\mathbf{u}^a(p_h))_{P,f}) = \int_P b dV \quad \forall P \in \Omega_h. \quad (10.26)$$

Remark 10.2. Nothing prevent us from choosing in (10.25) different functions $A = A^f$ and $B = B^f$ for different edges f , provided that they satisfy conditions **(AB1)**–**(AB3)** and that their Lipschitz constants remain uniformly bounded as $h \rightarrow 0$. This setting would allow us to make a finer tuning of the scheme, e.g. to reduce the numerical diffusion due to upwinding or to adapt the scheme to the mesh geometry.

10.1.2 An alternative hybrid discretization of the advection term

Another discretization of the advection term is obtained by using face-based values p_f in (10.25) instead of p_P . These values appear in the hybrid mimetic scheme (see Chap. 11) and approximate average value of p on mesh edges. Let $\tilde{p}_h = (p_f)_{f \in \mathcal{F}_h}$. We define

$$\mathbf{u}^a(p_h, \tilde{p}_h) = ((\mathbf{u}^a(p_h, \tilde{p}_h))_{P,f})_{P \in \mathcal{P}_h, f \in \partial P} \quad (10.27)$$

such that

$$(\mathbf{u}^a(p_h, \tilde{p}_h))_{P,f} = \frac{1}{d_f} (A(d_f \beta_{P,f}^I) p_P + B(d_f \beta_{P,f}^I) p_f). \quad (10.28)$$

The substantial difference with the previous choice (10.25) is that no property imposed on A and B ensure that the fluxes $\mathbf{u}^a(p_h, \tilde{p}_h)$ are conservative. However, this does not bring additional difficulties in the theoretical analysis provided that the following weaker form of property **(AB3)** holds.

(AB3h) One of the following two alternatives holds:

(AB3hs) $A(s) - B(s) \geq 0$ for any s .

(AB3hw) There exists $C > 0$ such that $A(s) - B(s) \geq -C|s|$ for any s .

The hybrid-mixed mimetic formulation can then be written as:

Find $(p_h, \mathbf{u}_h, \tilde{p}_h) \in \mathcal{P}_h \times \widehat{\mathcal{F}}_h \times \Lambda_h$ such that

$$[\mathbf{u}_P, \mathbf{v}_P]_P = \sum_{f \in \partial P} |f| \mathbf{v}_{P,f} (p_P - p_f) \quad \forall \mathbf{v}_P \in \widehat{\mathcal{F}}_{h,P}, \quad (10.29)$$

$$\sum_{f \in \partial P} |f| (u_{P,f} + (\mathbf{u}^\alpha(p_h, \tilde{p}_h))_{P,f}) = \int_P b dV \quad \forall P \in \Omega_h, \quad (10.30)$$

$$(\mathbf{u}_h + (\mathbf{u}^\alpha(p_h, \tilde{p}_h))_{P,f})_{P,f} + (\mathbf{u}_h + (\mathbf{u}^\alpha(p_h, \tilde{p}_h))_{P',f})_{P',f} = 0 \quad \forall f \in \mathcal{F}^0, \quad (10.31)$$

where the local inner product is the same as above.

Remark 10.3. An important advantage of using (10.27)–(10.28) instead of (10.24)–(10.25) is that the unknowns p_h and \mathbf{u}_h can be eliminated locally by the static condensation. This procedure is common for hybrid-mixed discretizations and provides a reduced linear system with respect to the unknown \tilde{p}_h . Moreover, when the discretization of the advection term leads to a significant numerical diffusion, as for example in the case of the upwind scheme, the hybrid-mixed formulation is likely to be less diffusive.

10.1.3 Convergence analysis

The convergence analysis is based on the mesh regularity assumptions **(MR1)**–**(MR3)** of Sect. 1.6.2. Let us introduce the following mesh-dependent norms for the space $\widehat{\mathcal{F}}_h$:

$$\| \mathbf{v}_h \|_{\widehat{\mathcal{F}}_h}^2 = [\mathbf{v}_h, \mathbf{v}_h], \quad \| \mathbf{v}_P \|_{\widehat{\mathcal{F}}_{h,P}}^2 = [\mathbf{v}_P, \mathbf{v}_P] \quad \forall \mathbf{v}_h \in \widehat{\mathcal{F}}_h. \quad (10.32)$$

The mesh functions in \mathcal{P}_h can be identified with the Ω_h -piecewise constant functions and the inner product in \mathcal{P}_h is, in fact, the L^2 -scalar product for such functions. Therefore, it is quite natural to consider the L^2 norm. However, we will also find it useful to carry out the analysis by using the discrete H_0^1 -like norm:

$$\| q_h \|_{1,h}^2 = \sum_{P \in \Omega_h} \sum_{f \in \partial P} |f| d_{P,f} \left(\frac{|q_P - q_{P'}|}{d_f} \right)^2 \quad \forall q_h \in \mathcal{P}_h, \quad (10.33)$$

where P' is the cell on the other side of $f \in \partial P \cap \mathcal{F}^0$ and, to ease notation, we assume that $q_{P'} = 0$ if $f \in \partial P \cap \mathcal{F}^\partial$. We will also need a discrete H^1 norm on $\mathcal{P}_h \times \Lambda_h$:

$$\| (q_h, \tilde{q}_h) \|_{1,h}^2 = \sum_{P \in \Omega_h} \sum_{f \in \partial P} \frac{|f|}{d_{P,f}} |q_P - q_f|^2 \quad \forall (q_h, \tilde{q}_h) \in \mathcal{P}_h \times \Lambda_h. \quad (10.34)$$

It is easy to see that this norm is stronger than (10.33). More precisely, there exists a constant C that depends only on the mesh regularity constants in **(MR1)**–**(MR2)** such that

$$\| q_h \|_{1,h} \leq C \| (q_h, \tilde{q}_h) \|_{1,h} \quad \forall (q_h, \tilde{q}_h) \in \mathcal{P}_h \times \Lambda_h. \quad (10.35)$$

In the following, we will use the symbol \lesssim to indicate an upper bound that holds up to a positive multiplicative constant independent of h . Also, we will trace explicitly the constants that may be zero depending on which alternative, **(AB3s)** or **(AB3w)**, is considered. The proofs of the results in this section can be found in [45].

Lemma 10.1. *Assume that (H1)–(H3) of Chap. 1 hold. Let Ω_h satisfy the mesh assumptions (MR1)–(MR3) in Sect. 1.6.2. Furthermore, let $\mathbf{u}^a(q_h)$ be the advective flux, $q_h \in \mathcal{P}_h$, given by (10.24)–(10.25) with A and B satisfying conditions (AB1)–(AB3). Then, there exists a constant $C_1 \geq 0$ that only depends on β, A, B and the mesh regularity constants such that*

$$\frac{1}{2} \int_{\Omega} q_h^2 \operatorname{div} \beta \, dV \leq \sum_{P \in \Omega_h} \sum_{f \in \partial P} |f| (\mathbf{u}^a(q))_{P,f} (q_P - q_f) + C_1 h \| (q_h, \tilde{q}_h) \|_{1,h}^2, \quad (10.36)$$

for all $(q_h, \tilde{q}_h) \in \mathcal{P}_h \times \Lambda_h$. Moreover, $C_1 = 0$ if (AB3s) holds.

The lemma below is the key point in the *a priori* error analysis of scheme (10.21)–(10.25). To state it, we first notice that, thanks to (10.21), we can introduce the set of face values $\tilde{p}_h \in \Lambda_h$ such that (10.29) holds even if \mathbf{u}_h is not conservative. To this purpose, we simply define p_f through $|f| (p_P - p_f) = [\mathbf{u}_P, \tilde{\mathbf{v}}_P]_P$ where $\tilde{\mathbf{v}}_{P,f} = 1$ and $\tilde{\mathbf{v}}_{P,f'} = 0$ for $f' \neq f$. Then, taking the vector $\mathbf{v}_h \in \widehat{\mathcal{F}}_h$ in (10.21) that vanishes on all mesh faces except f and is such that $v_{P,f} = 1$ and $v_{P,f'} = -1$ allows us to show that p_f does not depend on P . This definition also ensures that $p_f = 0$ whenever $f \in \mathcal{F}^\partial$.

Lemma 10.2. *Assume that (H1)–(H3) of Chap. 1 hold. Let Ω_h satisfy the mesh assumptions (MR1)–(MR3) in Sect. 1.6.2. Furthermore, let $\mathbf{u}^a(q_h)$ be the advective flux given by (10.24)–(10.25) with A and B satisfying conditions (AB1)–(AB3). Then, for the solution (p_h, \mathbf{u}_h) to scheme (10.21)–(10.23) and \tilde{p}_h introduced above, we have:*

$$\sum_{P \in \Omega_h} [\mathbf{u}_P \mathbf{u}_P]_P + \frac{1}{2} \int_{\Omega} \operatorname{div} \beta p_h^2 \, dV \leq \int_{\Omega} b p_h \, dV + C_1 h \| (p_h, \tilde{p}_h) \|_{1,h}^2 \quad (10.37)$$

where C_1 is the constant of Lemma 10.1.

Corollary 10.1. *Under the assumptions of Lemma 10.2, we have*

$$\| (p_h, \tilde{p}_h) \|_{1,h}^2 \lesssim \| b \|_{L^2(\Omega)} \| p_h \|_{L^2(\Omega)} + C_1 h \| (p_h, \tilde{p}_h) \|_{1,h}^2. \quad (10.38)$$

In particular, for all h small enough (or any h if (AB3s) holds), the scheme (10.21)–(10.23) has a unique solution.

Remark 10.4. For the hybrid-mixed mimetic scheme (10.27)–(10.31) with A and B satisfying (AB1)–(AB2) and (AB3h) there hold results similar to that given in Lemma 10.2 and Corollary 10.1.

The main convergence result for $(p_h, \mathbf{u}_h, \tilde{p}_h) \in \mathcal{P}_h \times \widehat{\mathcal{F}}_h \times \Lambda_h$ is stated in the following theorem. This theorem uses projections $p^J \in \mathcal{P}_h$ and $\mathbf{u}^J \in \widehat{\mathcal{F}}_h$ of the exact solutions and the projection $p^J \in \Lambda_h$ given by

$$p^J = (p_f^J)_{f \in \mathcal{F}}, \quad p_f^J = \frac{1}{|f|} \int_f p \, dS. \quad (10.39)$$

Theorem 10.1. *Let $p \in H^2(\Omega)$ be the solution of the continuous problem (10.1)–(10.2) under assumptions **(H1)**–**(H3)** and \mathbf{u} be given by (10.3). In addition, let \mathbb{K} be locally Lipschitz continuous on Ω_h . Furthermore, let (\mathbf{u}_h, p_h) be the solution of problem (10.21)–(10.22) under assumptions **(MR1)**–**(MR3)** and **(AB1)**–**(AB3)** with either h small enough if **(AB3w)** holds or any h if **(AB3s)** holds. Then,*

$$\mathbf{u}_h - \mathbf{u}^I \underset{\widehat{\mathcal{F}}_h}{\lesssim} + \|p_h - p^I\|_{1,h} + \|(p_h - p^I, \widetilde{p}_h - p^I)\|_{1,h} \lesssim h \|p\|_{H^2(\Omega)}. \quad (10.40)$$

From Theorem 10.1 we get immediately two corollaries.

Corollary 10.2. *Under the hypotheses of Theorem 10.1, it holds*

$$\widetilde{\mathbf{u}}_h - \widetilde{\mathbf{u}}^I \underset{\widehat{\mathcal{F}}_h}{\lesssim} h \|p\|_{H^2(\Omega)}, \quad (10.41)$$

where $\widetilde{\mathbf{u}}^I = -(\mathbb{K}\nabla p + \beta p)^I$ and $\widetilde{\mathbf{u}}_h = \mathbf{u}_h + \mathbf{u}^a(p_h)$.

Corollary 10.3. *Under the hypotheses of Theorem 10.1, it holds*

$$\|p^I - p_h\|_{L^r(\Omega)} \lesssim h \|p\|_{H^2(\Omega)},$$

where $r = \frac{2d}{d-2}$ if $d > 2$ and $r < +\infty$ if $d = 2$.

Remark 10.5. Repeating the arguments used in [45] for proving Theorem 10.1, it is possible to show that a similar error estimate holds for the hybrid-mixed formulation (10.29)–(10.31), which is based on the numerical advective flux (10.27)–(10.28).

Remark 10.6. It must be noted that the results of this section are not uniform with respect to the Peclet number, i.e., the estimates degenerate when the advection becomes dominant. Uniform estimates cannot be derived under the unified framework considered here, since it includes the methods that are not stable in this limit. Nevertheless, numerical tests show the good behavior of the methods also in the advection-dominated case, see Sect. 10.1.4

10.1.4 Shock-capturing behavior

The shock-capturing capability of the discretization methods is illustrated with two test cases where strong layers are developed in the advection-dominated regime. More numerical tests can be found in [45]. We solve the advection-diffusion equation in $\Omega =]0, 1[\times]0, 1[$ using the mesh shown in Fig. 5.2.

For convenience, we use short labels for the schemes introduced above. Recall that these schemes use the same discretization of the diffusion term as described in Chap. 5 and differ by the numerical treatment of the advective flux:

- **Cnt**, two-point centered flux formula;
- **Upw**, first-order upwind flux formula;
- **SG**, the Scharfetter-Gummel flux formula with the local adjustment (10.8);
- **NoStab**, central mimetic scheme without any form of stabilization;
- **Jmp**, central mimetic scheme with the jump stabilization (10.17).

Exponential boundary layers. We study experimentally how different schemes approximate a solution with an exponential boundary layer, which is formed on the downwind sides (with respect to β) of the domain boundary. To this purpose, we solve problem (10.1)–(10.2) with the scalar diffusion tensor, $K = \nu I$, $\nu = 10^{-4}$, and velocity field $\beta = (2, 3)^T$. The Dirichlet boundary conditions and the loading term are such that the exact solution is:

$$p(x, y) = \left(x - e^{2(x-1)/\nu} \right) \left(y^2 - e^{3(y-1)/\nu} \right).$$

This problem is strongly advection-dominated and the solution has two exponential boundary layers near the top and right sides of Ω .

In Fig. 10.1, we compare the numerical solutions produced by four schemes: **SG**, **Upw**, **NoStab** and **Jmp**. Panel (a) and (b) show non-oscillatory solutions produced by schemes **Upw** and **SG**. From panel (c) it is evident that without a stabilization, the numerical solution produced by the **NoStab** scheme suffers from severe oscillations. These oscillations disappear (see panel (d)) when we add a stabilizing term to the divergence equation based on the solution jumps across mesh edges. However, this stabilization introduces significant numerical diffusion leading to a poor resolution of the boundary layers, worse than in the FV-based schemes.

Exponential and parabolic boundary layers. Now, we solve problem (10.1)–(10.2) with the Dirichlet boundary conditions on Γ :

$$p(x, 0) = (1 - x)^3, \quad p(x, 1) = (1 - x)^2, \quad p(0, y) = 1, \quad p(1, y) = 0.$$

Again, we take the scalar diffusion tensor, $K = \nu I$, $\nu = 10^{-4}$, but change the velocity field to $\beta = (1, 0)^T$. The solution has one exponential boundary layer at the side $x = 1$ and two parabolic boundary layers at $y = 0$ and $y = 1$. Figure 10.2 shows the discrete solutions produced by four schemes: **SG**, **Upw**, **NoStab**, and **Jmp**. The conclusions are similar to that in the previous case of the single exponential layer.

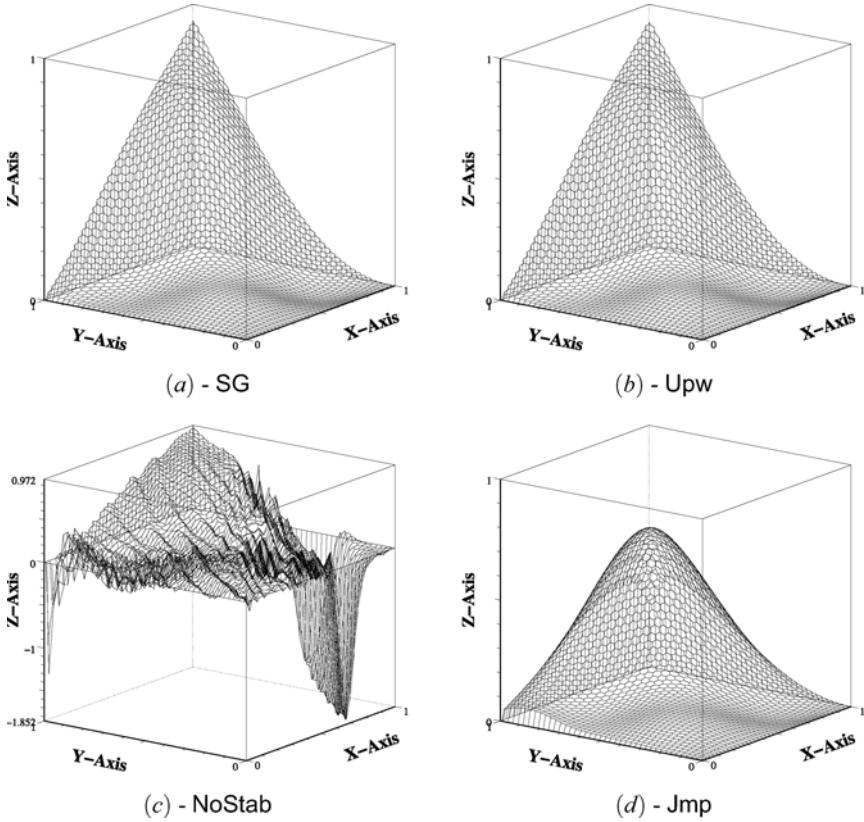


Fig. 10.1. The exact solution has two exponential boundary layers on the right and top sides of Ω . Numerical solution is displayed at mesh vertices using a linear interpolation of cell-centered data. Severe oscillations are visible in plot (c) for the central mimetic scheme without any stabilization (note the different scale along the axis Z). These artifacts disappear in plot (d) where the jump stabilization is turned on

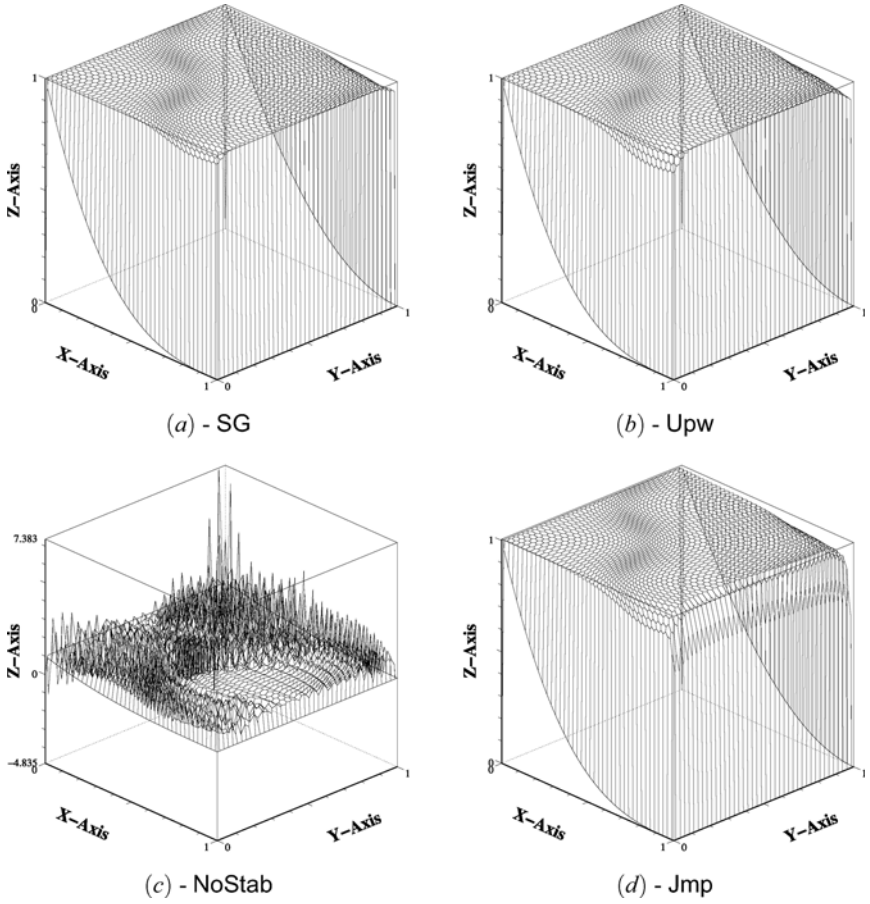


Fig. 10.2. The exact solution has the exponential boundary layer on the right side and two parabolic layers on top and bottom sides of Ω . Numerical solution is displayed at mesh vertices through a linear interpolation of cell-centered data. Severe oscillations are visible in plot (c) when we use the central mimetic scheme without any stabilization (note the different scale along the axis Z). These artifacts disappear in plot (d) where the jump stabilization is turned on

10.2 Obstacle problem

The elliptic obstacle problem can be considered as a model problem for variational inequalities (see, e.g. [176]). It is the problem of finding the equilibrium position of an elastic membrane which is constrained to lie above a given obstacle and whose boundary is held fixed. This problem has found applications in a number of different fields as structural and fluid dynamics. The examples include fluid filtration in porous media, optimal control, and financial mathematics [221, 226]. In this section we introduce a lower order mimetic scheme for the obstacle problem that is an extension of the mimetic scheme for the diffusion problem described in Sect. 6.2. The presented results are based on [17].

10.2.1 The problem formulation

Let Ω be an open, bounded, convex set of \mathbb{R}^2 , with either a polygonal or a C^2 -smooth boundary Γ . Let $g := \tilde{g}|_\Gamma$ with $\tilde{g} \in H^2(\Omega)$. We define the linear space

$$\mathcal{V}_g = \{v \in H^1(\Omega) : v = g \text{ on } \Gamma\}.$$

Let us introduce the function $\psi \in H^2(\Omega)$ such that $\psi \leq g$ on Γ , representing an obstacle, and the related convex space of admissible solutions:

$$\mathcal{K} = \{v \in \mathcal{V}_g : v \geq \psi \text{ a.e. in } \Omega\}. \quad (10.42)$$

We are interested in solving the following variational inequality:

Find $u \in \mathcal{K}$ such that

$$\mathcal{A}(u, v - u) \geq b(v - u) \quad \forall v \in \mathcal{K}. \quad (10.43)$$

where the bilinear form $\mathcal{A}(\cdot, \cdot) : H^1(\Omega) \times H^1(\Omega) \rightarrow \mathbb{R}$ and the linear functional $b(\cdot) : H^1(\Omega) \rightarrow \mathbb{R}$ are defined by

$$\mathcal{A}(u, v) = \int_{\Omega} \nabla u \cdot \nabla v dV, \quad b(v) = \int_{\Omega} b v dV.$$

Under the above data regularity assumption, the elliptic obstacle problem (10.43) is well posed (see e.g. [81] and [308, Corollary 5:2.3]) and has the unique solution $u \in H^2(\Omega) \cap \mathcal{V}_g$.

10.2.2 A mimetic discretization

Let $\tilde{\Omega} \subset \Omega$ be a polygonal approximation of Ω such that all the vertices of $\tilde{\Omega}$ that are on the boundary of $\tilde{\Omega}$ are also on the boundary of Ω . We denote a polygonal partition of $\tilde{\Omega}$ by Ω_i and we assume that this partition satisfies the assumptions (MR1)–(MR2) introduced in Chap. 1. Let, as usual, \mathcal{V} and \mathcal{E} denote the set of mesh vertices and edges. In addition, we denote the set of internal vertices and edges by \mathcal{V}^0 and \mathcal{E}^0 , and the set of boundary vertices and edges by \mathcal{V}^∂ and \mathcal{E}^∂ .

10.2.2.1 Degrees of freedom and projection operators

To discretize problem (10.43), we employ the construction of Sect. 6.2 which is summarized below. The first step is to select the degrees of freedom for the approximation space \mathcal{V}_h : a vector $v_h \in \mathcal{V}_h$ consists of vertex-based degrees of freedom, one per mesh vertex:

$$v_h = (v_v)_{v \in \mathcal{V}}.$$

Its restriction to cell P is denoted by $v_P \in \mathcal{V}_{h,P}$. The dimension of \mathcal{V}_h is equal to the number of mesh vertices. We also define the discrete space $\mathcal{V}_{h,g} \subset \mathcal{V}_h$

$$\mathcal{V}_{h,g} = \{v_h \in \mathcal{V}_h : v_v = g(\mathbf{x}_v) \forall v \in \mathcal{V}^\partial\}$$

of the functions that satisfy the Dirichlet boundary condition. Accordingly, $\mathcal{V}_{h,0}$ denotes the space of discrete functions that vanish at the boundary nodes.

We finally introduce the projection operator from the spaces of continuous functions $v \in C^0(\Omega) \cap H^1(\Omega)$ to the discrete space \mathcal{V}_h :

$$v^I = (v_v^I)_{v \in \mathcal{V}}, \quad v_v^I = v(\mathbf{x}_v).$$

10.2.2.2 Discrete norms and bilinear forms

We endow the space \mathcal{V}_h with the following discrete seminorm

$$\|v_h\|_{1,h}^2 = \sum_{P \in \Omega_h} \|v_h\|_{1,h,P}^2 = \sum_{P \in \Omega_h} P \sum_{e \in \partial P} \left[\frac{1}{|e|} (v_{v_2} - v_{v_1}) \right]^2, \quad (10.44)$$

where v_1 and v_2 are the two vertices of edge e . The finite difference $(v^{v_2} - v^{v_1})/|e|$ represents the tangential gradient along the edge. Therefore, $\|\cdot\|_{1,h}$ is a $H^1(\Omega)$ -type discrete seminorm, which becomes a norm on $\mathcal{V}_{h,0}$.

Let $\mathcal{A}_h : \mathcal{V}_h \times \mathcal{V}_h \rightarrow \mathbb{R}$ denote the mimetic approximation of the bilinear form \mathcal{A} . The discrete form \mathcal{A}_h is identical to the one introduced in Sect. 6.2 for the Poisson equation. It is built element-by-element:

$$\mathcal{A}_h(u_h, v_h) = \sum_{P \in \Omega_h} \mathcal{A}_{h,P}(u_P, v_P).$$

The local discrete bilinear forms satisfy the consistency and stability conditions. Let $\mathcal{S}_{h,P}$ be a subspace of $H^1(P) \cap C^0(P)$ of functions that are linear on the edges e of P .

(S1) (Stability Condition). There exists two positive constants σ_* and σ^* such that for every $v_P \in \mathcal{V}_{h,P}$ it holds:

$$\sigma_* \|v_P\|_{1,h,P}^2 \leq \mathcal{A}_{h,P}(v_P, v_P) \leq \sigma^* \|v_P\|_{1,h,P}^2.$$

(S2) (Consistency Condition). For every $\psi \in \mathbb{P}_1(P)$ and every $v \in S_{h,P}$ it holds:

$$\mathcal{A}_{h,P}(v_P^I, \psi_P^I) = \int_P \nabla v \cdot \nabla \psi \, dV = \nabla \psi \cdot \sum_{e \in \partial P} \mathbf{n}_{P,e} \int_e v \, dS.$$

Let $\omega_{P,1}, \dots, \omega_{P,N_P^\gamma}$ be positive weights associated with vertices $v_1, \dots, v_{N_P^\gamma}$ of polygon P and such that $\sum_{i=1}^{N_P^\gamma} \omega_{P,i} = |P|$. We use them to approximate the loading term:

$$(b, v_h)_h = \sum_{P \in \Omega_h} b_P^I \sum_{i=1}^{N_P^\gamma} v_{v_i} \omega_{P,i}, \quad b_P^I = \frac{1}{|P|} \int_P b \, dV. \quad (10.45)$$

10.2.2.3 The numerical scheme

Let us introduce the discrete convex space that approximates \mathcal{H} :

$$\mathcal{K}_h = \{v_h \in \mathcal{V}_{h,g} : v_v \geq \psi(\mathbf{x}_v) \quad \forall v \in \mathcal{V}\}.$$

The mimetic discretization of problem (10.43) reads:

Find $u_h \in \mathcal{K}_h$ such that

$$\mathcal{A}_h(u_h, v_h - u_h) \geq (b, v_h - u_h)_h \quad \forall v_h \in \mathcal{K}_h. \quad (10.46)$$

Due to the stability property (S1), the bilinear form \mathcal{A}_h is coercive on the subspace of \mathcal{V}_h of the mesh functions that are orthogonal to constant functions. Therefore, since $\mathcal{K}_h \subset \mathcal{V}_h$ is convex and closed, the existence and uniqueness of a solution for the discrete problem (10.46) follows from standard arguments [115]. The uniform stability of the discrete problem with respect to h is an implicit consequence of the analysis that follows.

10.2.3 Convergence of the method

In this section, we prove the linear convergence of the proposed mimetic scheme. In order to shorten the notation, we will use the symbols \succeq , \lesssim , and \gtrsim to represent equivalences and bounds that hold up to a constant uniformly in the mesh size.

10.2.3.1 A reconstruction operator

Let us show that for all $P \in \Omega_h$ there exists a local reconstruction operator

$$R_P : \mathcal{V}_{h,P} \rightarrow H^1(P) \cap C^0(P),$$

that satisfies the six properties listed below. The global reconstruction operator R is defined such that $R(v_h)|_P = R_P(v_P)$. A three dimensional version of this same reconstruction operator has been presented in Sect. 8.4.1.

(L1) The reconstruction operator is the right inverse of the projection operator:

$$R_P(v_P)(\mathbf{x}_v) = v_v \quad \forall v_P \in \mathcal{V}_{h,P}, \quad \forall v \in \partial P.$$

(L2) The reconstructed function $R_P(v_P)$ is linear on every edge e of P .

(L3) The reconstruction operator is exact on linear functions:

$$R_P((p^1)_P) = p^1 \quad \forall p^1 \in \mathbb{P}_1(P).$$

(L4) The reconstruction operator is uniformly bounded in the energy norm:

$$|R_P(v_P)|_{H^1(P)} \lesssim \|v_P\|_{1,h,P} \quad \forall v_P \in \mathcal{V}_{h,P}.$$

(L5) The reconstruction operator is uniformly bounded in the L^2 norm:

$$\|R_P(v_P^I)\|_{L^2(P)}^2 \lesssim \sum_{k=0}^2 h_P^{2k} |v|_{H^k(P)}^2 \quad \forall v \in H^2(P),$$

(L6) The reconstruction operator satisfies the maximum principle: if $v_v \geq 0$ for all $v \in \partial P$, then $R_P(v_P) \geq 0$ in P .

A local reconstruction operator satisfying these properties has been built in [57]. Let $P \in \Omega_h$ and $v_P \in \mathcal{V}_{h,P}$ be given. We define $R_P(v_P)$ as a globally continuous and piecewise linear function on the triangulation \mathbb{T}_h introduced in Sect. 1.6.2. Since such a reconstruction operator is uniquely defined by its values at the vertices of \mathbb{T}_h , it is sufficient to provide an algorithm to compute these values.

For each vertex v of P we set $R_P(v_P)(\mathbf{x}_v) = v_v$. On each edge e of P , the reconstructed function is defined by the linear interpolation of the two vertex values. Let \bar{v} be the internal node of $\mathbb{T}_h|_P$ and Ξ_v denote the set of other internal nodes connected to v by an edge of $\mathbb{T}_h|_P$. By construction, v is in the convex hull of the set of nodes $\{\bar{v}\}_{\bar{v} \in \Xi_v}$. Therefore, we have

$$\mathbf{x}_v = \sum_{\bar{v} \in \Xi_v} \omega_{v,\bar{v}} \mathbf{x}_{\bar{v}}, \quad \sum_{\bar{v} \in \Xi_v} \omega_{v,\bar{v}} = 1, \quad \omega_{v,\bar{v}} > 0. \quad (10.47)$$

Using these weights, we define

$$R_P(v_P)(\mathbf{x}_v) - \sum_{\bar{v} \in \Xi_v} \omega_{v,\bar{v}} R_P(v_P)(\mathbf{x}_{\bar{v}}) = 0. \quad (10.48)$$

This set of equations leads to a square linear system. The associated matrix is an M-matrix, which implies the existence of a unique solution and the discrete maximum principle. Thus, the resulting reconstructed function satisfies assumption **(L6)**.

Properties **(L1)** and **(L2)** are satisfied by construction. Property **(L3)** follows immediately from the linear relationship (10.47). Furthermore, the maximum principle implies the stability condition **(L4)**. This can be verified following the same arguments used in the proof of **(L3s)** in Sect. 8.4.1.

We are left to show property **(L5)**. The mesh shape regularity assumptions **(MR1)** and **(MR2)** imply that

$$h_P \lesssim h_T \leq h_P \quad \forall T \in \mathbb{T}_h|_P. \quad (10.49)$$

Due to the maximum principle, for any $v \in H^2(\mathbb{P})$ we have that

$$\|R_{\mathbb{P}}(v_{\mathbb{P}}^I)\|_{L^\infty(\mathbb{P})} \leq \max_{v \in \partial\mathbb{P}} |v_v^I| = \max_{v \in \partial\mathbb{P}} |v(\mathbf{x}_v)| \leq \|v\|_{L^\infty(\mathbb{P})}. \quad (10.50)$$

We now use (10.50), (10.49) and apply the standard scaling argument on each triangle $T \in \mathcal{T}_{h|\mathbb{P}}$, to obtain

$$\begin{aligned} \|R_{\mathbb{P}}(v_{\mathbb{P}}^I)\|_{L^2(\mathbb{P})}^2 &\leq |\mathbb{P}| \|v\|_{L^\infty(\mathbb{P})}^2 = |\mathbb{P}| \max_{T \in \mathcal{T}_{h|\mathbb{P}}} \|v\|_{L^\infty(T)}^2 \\ &\leq |\mathbb{P}| \max_{T \in \mathcal{T}_{h|\mathbb{P}}} \sum_{k=0}^2 h_T^{2k-2} |v|_{H^k(T)}^2 \lesssim |\mathbb{P}| \sum_{k=0}^2 h_{\mathbb{P}}^{2k-2} |v|_{H^k(\mathbb{P})}^2. \end{aligned}$$

Property **(L5)** follows from this bound and $|\mathbb{P}| \leq h_{\mathbb{P}}^2$.

We end this subsection with two bounds showing the approximation properties of $R_{\mathbb{P}}$ that will be useful later. Let be given $\mathbb{P} \in \Omega_h$, $v \in H^2(\mathbb{P})$, and $v^{(1)} \in \mathbb{P}_1(\mathbb{P})$, the linear approximation of v defined by **(M5)** after setting $m = 1$. We apply **(L3)**, **(L5)**, and, then, the approximation property **(M5)** to obtain

$$\begin{aligned} \|v - R_{\mathbb{P}}(v_{\mathbb{P}}^I)\|_{L^2(\mathbb{P})}^2 &\leq 2 \left(\|v - v^{(1)}\|_{L^2(\mathbb{P})}^2 + \|R_{\mathbb{P}}((v^{(1)} - v)_{\mathbb{P}}^I)\|_{L^2(\mathbb{P})}^2 \right) \\ &\lesssim \sum_{k=1}^2 h_{\mathbb{P}}^{2k} |v - v^{(1)}|_{H^k(\mathbb{P})}^2 \lesssim h_{\mathbb{P}}^4 |v|_{H^2(\mathbb{P})}^2. \end{aligned} \quad (10.51)$$

The definition of the discrete H^1 -norm in (10.44) and the maximum principle property **(L6)** give

$$\|R_{\mathbb{P}}(v_{\mathbb{P}}) - v_{\mathbb{P}}\|_{L^\infty(\mathbb{P})} \leq \max_{v' \in \partial\mathbb{P}} |v_{v'} - v_v| \lesssim \|v_{\mathbb{P}}\|_{1,h},$$

and, as its immediate consequence, also

$$\|R_{\mathbb{P}}(v_{\mathbb{P}}) - v_{\mathbb{P}}\|_{L^2(\mathbb{P})} \lesssim h_{\mathbb{P}} \|v_{\mathbb{P}}\|_{1,h}. \quad (10.52)$$

10.2.3.2 The main convergence result

In this subsection, we prove convergence of the mimetic scheme (10.46), see [17] for more details.

Theorem 10.2. *Let $u \in \mathcal{X} \cap H^2(\Omega)$ be the solution to the continuous problem (10.43) and $u_h \in \mathcal{X}_h$ be the solution of the discrete problem (10.46) under assumption **(MR1)**–**(MR2)** and **(S1)**–**(S2)**. Then, there exists a constant C independent of h such that*

$$\|u_h - u^I\|_{1,h} \leq Ch.$$

Proof. Let $e_h = u_h - u^I$. We consider a discontinuous piecewise linear function $u^{(1)}$ on Ω_h such that for every $\mathbb{P} \in \Omega_h$ the restriction $u^{(1)}|_{\mathbb{P}}$ is the $L^2(\mathbb{P})$ -projection of u on the space of polynomials of degree at most 1. With a little abuse of notation, we denote

by $(u^{(1)})^I$ a collection of vertex values for all elements P such that the restriction $(u^{(1)})^I_P$ is well defined and is given by the local projector. We further observe that the mesh dependent norm $\|\cdot\|_{1,h}$ and the bilinear form \mathcal{A}_h can be immediately extended to $(u^{(1)})^I$, since both operators are defined by summation of local terms. We now use **(S1)**–**(S2)** and the discrete problem (10.46) to derive the inequality chain:

$$\begin{aligned} \sigma_* \|e_h\|_{1,h}^2 &\leq \mathcal{A}_h(e_h, e_h) \\ &\leq (b, e_h)_h - \mathcal{A}_h(u^I, e_h) \\ &= (b, e_h)_h - \mathcal{A}_h(u^I - (u^{(1)})^I, e_h) - \mathcal{A}_h((u^{(1)})^I, e_h) \end{aligned} \quad (10.53)$$

Assumption **(L3)** states that $e_P = (R_P(e_P))^I$; assumption **(L2)** states that $R_P(e_P)|_e$ is a linear function on any edge e of P ; hence, assumption **(S2)** implies that

$$\mathcal{A}_{h,P}((u^{(1)})^I_P, e_P) = \mathcal{A}_{h,P}((u^{(1)})^I_P, (R_P(e_P))^I) = \sum_{e \in \partial P} \frac{\partial u^{(1)}}{\partial \mathbf{n}_{P,e}} \int_e R_P(e_P) dS. \quad (10.54)$$

Using the integration by parts twice and noting that function $R(e_h)$ vanishes on the boundary of Ω_h , we obtain

$$\begin{aligned} - \sum_{P \in \Omega_h} \sum_{e \in \partial P} \frac{\partial u^{(1)}}{\partial \mathbf{n}_{P,e}} \int_e R_P(e_P) dV &= - \sum_{P \in \Omega_h} \int_P \nabla R_P(e_P) \cdot \nabla u^{(1)} dV \\ &= \sum_{P \in \Omega_h} \int_P \nabla R_P(e_P) \cdot \nabla (u - u^{(1)}) dV - \int_{\tilde{\Omega}} \nabla R(e_h) \cdot \nabla u dV \\ &= \sum_{P \in \Omega_h} \int_P \nabla R_P(e_P) \cdot \nabla (u - u^{(1)}) dV + \int_{\tilde{\Omega}} \Delta u R(e_h) dV. \end{aligned} \quad (10.55)$$

We substitute (10.54)–(10.55) into (10.53), we use the Young inequality, we add and subtract $\int_{\tilde{\Omega}} b R(e_h) dV$ and we introduce the quantity $w = \Delta u + b$. From such manipulation it follows that

$$\begin{aligned} \sigma_* \|e_h\|_{1,h}^2 &\leq \left((b, e_h)_h - \int_{\tilde{\Omega}} b R(e_h) dV \right) + \sigma^* \|u^I - (u^{(1)})^I\|_{1,h} \|e_h\|_{1,h} \\ &\quad + \sum_{P \in \Omega_h} \int_P \nabla R_P(e_P) \cdot \nabla (u - u^{(1)}) dV + \int_{\tilde{\Omega}} w R(e_h) dV. \end{aligned} \quad (10.56)$$

Thus, we need to bound four terms in the right hand side of (10.56). By recalling (10.52) and using essentially the same steps as in the estimate of the *First Piece* in [84], it is easy to derive the following bound

$$(b, e_h)_h - \int_{\tilde{\Omega}} b R(e_h) dV \lesssim h \|b\|_{L^2(\tilde{\Omega})} \|e_h\|_{1,h} \lesssim h \|e_h\|_{1,h}. \quad (10.57)$$

To bound the second term, we set $v = u - u^{(1)}$, use definition (10.44), and the Cauchy-Schwarz inequality:

$$\begin{aligned} \|v^I\|_{1,h}^2 &= \sum_{P \in \Omega_h} |P| \sum_{e \in \partial P} \left[\frac{1}{|e|} (v_{v_2} - v_{v_1}) \right]^2 = \sum_{P \in \Omega_h} |P| \sum_{e \in \partial P} \left[\frac{1}{|e|} \int_e \frac{\partial v}{\partial \boldsymbol{\tau}_{P,e}} dS \right]^2 \\ &\leq \sum_{P \in \Omega_h} |P| \sum_{e \in \partial P} \left[\frac{1}{|e|} \|\nabla v\|_{L^2(e)}^2 \right]. \end{aligned}$$

The trace inequality **(M4)** applied to ∇v and the approximation error estimate **(M5)** give

$$\|(u - u^{(1)})^I\|_{1,h}^2 \lesssim \sum_{P \in \Omega_h} \left[\|\nabla(u - u^{(1)})\|_{L^2(P)}^2 + h_P^2 |u|_{H^2(P)}^2 \right] \lesssim h^2 |u|_{H^2(\tilde{\Omega})}^2 \lesssim h^2. \quad (10.58)$$

To bound the third term, we use the Cauchy-Schwarz inequality, property **(L4)** and the approximation result **(M5)**:

$$\begin{aligned} \sum_{P \in \Omega_h} \int_P \nabla R_P(e_P) \cdot \nabla(u - u^{(1)}) dV &\leq \|\nabla R(e_h)\|_{L^2(\tilde{\Omega})} \|\nabla(u - u^{(1)})\|_{L^2(\tilde{\Omega})} \\ &\lesssim h \|e_h\|_{1,h} |u|_{H^2(\tilde{\Omega})} \lesssim h \|e_h\|_{1,h}. \end{aligned} \quad (10.59)$$

Finally, let us bound the fourth term in (10.56). There holds, as shown in [79],

$$w \leq 0 \quad \text{and} \quad w(\boldsymbol{\psi} - u) = 0 \quad \text{a.e. in } \tilde{\Omega}. \quad (10.60)$$

where $\boldsymbol{\psi}$ is the function representing the obstacle according to the definition given in (10.42).

By a simple addition and subtraction of terms, we obtain

$$\begin{aligned} \int_{\tilde{\Omega}} w R(e_h) dV &= - \int_{\tilde{\Omega}} w (R(u^I) - u) dV + \int_{\tilde{\Omega}} w (\boldsymbol{\psi} - u) dV \\ &\quad + \int_{\tilde{\Omega}} w (R(u_h) - R(\boldsymbol{\psi}^I)) dV + \int_{\tilde{\Omega}} w (R(\boldsymbol{\psi}^I) - \boldsymbol{\psi}) dV. \end{aligned} \quad (10.61)$$

Due to (10.60), the second term in the right hand side is zero. Furthermore, since for every $v \in \mathcal{V}$ there holds $u_v \geq \boldsymbol{\psi}_v^I$, recalling assumption **(L6)** we have

$$R(u_h - \boldsymbol{\psi}^I) \geq 0 \quad \text{in } \tilde{\Omega}.$$

This and (10.60) imply that the third term in the right-hand side of (10.61) is non-positive. Thus, we can bound (10.61) as follows:

$$\int_{\tilde{\Omega}} w R(e_h) dV \leq \int_{\tilde{\Omega}} w (u - R(u^I)) dV + \int_{\tilde{\Omega}} w (R(\boldsymbol{\psi}^I) - \boldsymbol{\psi}) dV. \quad (10.62)$$

To bound the integrals in (10.62), we use the Cauchy-Schwarz inequality, estimate (10.51), and recall the definition of $w = \Delta u + b$:

$$\int_{\tilde{\Omega}} wR(e_h) dV \lesssim h^2 \|w\|_{L^2(\tilde{\Omega})} \left(\|\psi\|_{H^2(\tilde{\Omega})} + \|u\|_{H^2(\tilde{\Omega})} \right) \lesssim h^2. \tag{10.63}$$

We now insert bounds (10.57), (10.58), (10.59) and (10.63) in (10.56) to obtain

$$\|e_h\|_{1,h}^2 \lesssim h \|e_h\|_{1,h} + h^2,$$

which proves the theorem. □

The convexity assumption on Ω can be relaxed to include a more general class of domains. Indeed, we only need to know that the solution u belongs to $H^2(\Omega)$ and that $\tilde{\Omega}$ can be inscribed in Ω for every h . The latter is true, for instance, in the case of non-convex polygonal domains. After that, the convergence theorem can be generalized by following the argument in [89], which is based on a suitable extension of the mesh and the solution.

Remark 10.7. When the homogeneous Dirichlet boundary conditions are imposed, i.e. \mathcal{V}_g coincides with $H_0^1(\Omega)$, Theorem 10.2 can be proved in a different way by using the idea proposed in [166]. The details of this proof is found in [15, Appendix A].

10.2.4 Numerical test

We close our discussion with a numerical test for the obstacle problem that confirms the main convergence estimate, which was originally introduced in [290]. Other tests are found in [17]. Let $\Omega = \tilde{\Omega} =]-1, 1[^2$ and the obstacle be given by $\psi(x, y) = 0$. For a given parameter $0 < r < 1$, we define the continuous load

$$b(x, y) = \begin{cases} -8(2x^2 + 2y^2 - r^2) & \text{if } \sqrt{x^2 + y^2} > r, \\ -8r^2(1 - x^2 - y^2 + r^2) & \text{if } \sqrt{x^2 + y^2} \leq r. \end{cases} \tag{10.64}$$

The Dirichlet boundary data is set in accordance with $g(x, y) = (x^2 + y^2 - r^2)^2$. The analytic solution of problem (10.43) with the above data is known and given by

$$u(x, y) = (\max\{x^2 + y^2 - r^2, 0\})^2. \tag{10.65}$$

The discrete obstacle problem has been solved numerically by the Projected Successive Over Relaxation (PSOR) method, see [126, 156, 185]. We present the results for two different sequences of meshes that we label as *median-type 1* and *median-type 2*. The examples of these meshes are shown in Fig. 10.3.

In Fig. 10.4 (log-log scale) we plot the relative errors $\epsilon_{1,h}^r(u^I, u_h)$ in the discrete energy norm,

$$\epsilon_{1,h}^r(u^I, u_h) = \frac{\|u^I - u_h\|_{1,h}}{\|u^I\|_{1,h}},$$

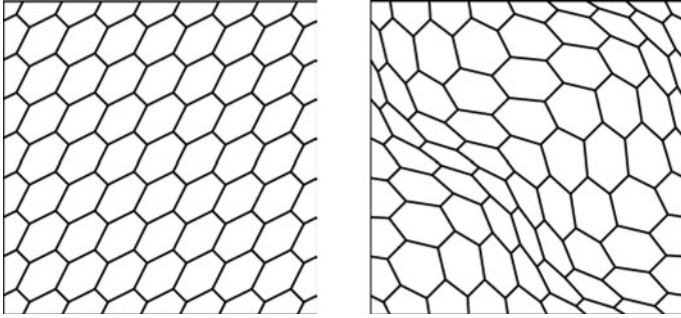


Fig. 10.3. Two samples of the considered meshes: median-type 1 (left) and median-type 2 (right)

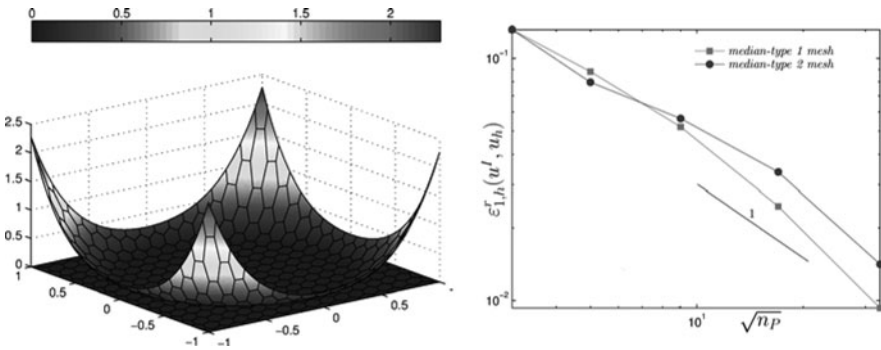


Fig. 10.4. Left panel: numerical solution. Right panel: relative error $\epsilon_{1,h}^r(u^I, u_h)$ as a function $\sqrt{n_P}$ for two the median-type 1 and median-type 2 polygonal meshes

for the two sequences of meshes. In this figure n_P denotes the number of polygons in the mesh. The results indicate the linear convergence of the scheme which verifies our theoretical developments.

Remark 10.8. Numerical tests that make use of an adaptive strategy and mesh refinement for the obstacle problem has been presented in [18].

Analysis of parameters and maximum principles

*“There is no smallest among the small
and no largest among the large;
but always something still smaller
and something still larger”*
(Anaxagoras)

A major property of the solutions of elliptic problems is the existence of the maximum and minimum principles [190, 203]. The strongest form of the minimum principle states that solution p cannot have a minimum in Ω when the source term is nonnegative. More precisely, if p takes a minimum value at point $\mathbf{x}_0 \in \Omega$, then p is constant in Ω . This classical result, also known as *Hopf’s lemma* [203], has been proved for $p \in C^2(\Omega)$ and locally uniformly positive definite tensor \mathbb{K} .

The existence of *discrete* maximum or minimum principles (DMP) for a numerical approximation p_h of p may be crucial for robustness and accuracy of simulations.

We recall a few other classical results. Let Ω be a bounded, simply-connected open subset of \mathbb{R}^d with the Lipschitz continuous boundary Γ . We split the boundary into two parts, Γ_D and Γ_N such that $\Gamma = \Gamma_D \cup \Gamma_N$.

Theorem 11.1 (Strong Maximum Principle). *Let $p \in C^2(\Omega)$ satisfy*

$$-\operatorname{div}(\mathbb{K}\nabla p) \leq 0 \quad \text{in } \Omega$$

under assumption (H1) (see Sect. 1.4.1) on \mathbb{K} . If p attains a nonnegative maximum \hat{p} at a point of Ω , then

$$p = \hat{p} \quad \text{in } \Omega.$$

Theorem 11.2 (Weak Maximum Principle). *Let $p \in C^2(\Omega) \cap C^0(\overline{\Omega})$ satisfy*

$$-\operatorname{div}(\mathbb{K}\nabla p) \leq 0 \quad \text{in } \Omega$$

under assumption (H1) (see Sect. 1.4.1) on \mathbb{K} . Then,

$$\max_{\mathbf{x} \in \overline{\Omega}} p(\mathbf{x}) \leq \max_{\mathbf{x} \in \Gamma} p(\mathbf{x}).$$

Remark 11.1. For functions with less regularity, e.g., $p \in H^1(\Omega) \cap C^0(\overline{\Omega})$, the weak maximum principle remains true by replacing \max with \sup (see, e.g. [182]).

From the weak maximum principle it is immediate to derive a *monotonicity property* for the Dirichlet boundary value problem. In case of mixed boundary conditions, the monotonicity property is as follows [223].

Corollary 11.1 (Monotonicity Property). *Let $p \in C^2(\Omega) \cap C^0(\overline{\Omega})$ satisfy*

$$\begin{aligned} -\operatorname{div}(K\nabla p) &\geq 0 \quad \text{in } \Omega, \\ \mathbf{n} \cdot K\nabla p &\geq 0 \quad \text{on } \Gamma^N, \\ p &\geq 0 \quad \text{on } \Gamma^D, \end{aligned}$$

under assumption (H1) (see Sect. 1.4.1) on K . Then,

$$p \geq 0 \quad \text{in } \Omega.$$

The possibility of reproducing these fundamental properties of the continuum solutions at the discrete level has been extensively investigated in the literature concerning the finite volume and finite element methods for linear and nonlinear parabolic and elliptic PDEs [77, 99, 157, 223, 234, 291, 353].

Since we may find different formulations of the maximum principle in the continuum [217], it is not surprising that there may exist a number of different formulations of the DMP. For example, another formulation of a DMP is based on the requirement that the inverse of the stiffness matrix arising from a discretization is a nonnegative matrix, i.e., a matrix with nonnegative coefficients. A sufficient condition for that is an M-matrix property [60], i.e. building a numerical scheme that leads to an M-matrix ensures the monotonicity of the discrete solution.

Definition 11.1. A matrix A is called a Z-matrix if $(A)_{ij} \leq 0$ for $i \neq j$. A nonsingular Z-matrix A is called an M-matrix if $(A^{-1})_{ij} \geq 0$.

In this chapter we show how to build an M-matrix in the context of mimetic schemes. In Sect. 11.2, we discuss the sufficient conditions that ensure the existence of monotone schemes in the family of mixed mimetic approximations. In Sect. 11.3, we present similar developments for the low order nodal mimetic schemes of Chap. 6. The development of monotone mimetic schemes is work in progress and the theoretical results are available only for a class of meshes. Therefore, in Sect. 11.4 we present a non-linear optimization strategy that allows us to analyze the family of mimetic schemes numerically.

11.1 Hybridization techniques

Let us consider again the diffusion problem and the family of mimetic schemes introduced in Chap. 5:

$$\mathbf{u} + K\nabla p = 0 \quad \text{in } \Omega, \quad (11.1)$$

$$\operatorname{div} \mathbf{u} = b \quad \text{in } \Omega, \quad (11.2)$$

$$p = g^D \quad \text{on } \Gamma^D, \quad (11.3)$$

$$-\mathbf{u} \cdot \mathbf{n} = g^N \quad \text{on } \Gamma^N, \quad (11.4)$$

where the vector variable \mathbf{u} represents the flux of the scalar unknown p , \mathbf{K} is the diffusion tensorial coefficient, b, g^D, g^N are given functions, and \mathbf{n} is the unit normal vector to Γ pointing out of Ω . We assume that $\Gamma^D = \bar{\Gamma}^D \subseteq \Gamma$ is non-empty. Under the assumptions introduced in Chap. 1, this problem is mathematically well-posed, cf. [190].

11.1.1 The mixed-hybrid mimetic formulation

The hybridization of the mixed mimetic schemes of Chap. 5 is the exact algebraic transformation of discrete equations. It introduces two new linear spaces, Λ_h and $\widetilde{\mathcal{F}}_h$, for the discrete scalar and vector fields. The former complements the cell-based degrees of freedom while the latter is used in place of space \mathcal{F}_h . The unknowns in Λ_h , called the Lagrange multipliers, approximate the scalar variable on mesh faces. The use of the additional degrees of freedom makes it possible to reduce the mixed mimetic discretization to an algebraic problem for the Lagrange multipliers through the process known as the static condensation.

Thus, the degrees of freedom for the scalar variable p are associated with cells P and mesh faces f and denoted by p_P and p_f , respectively. As in Chap. 5, we denote the linear space of cell-based discrete fields $p_h = (p_P)_{P \in \mathcal{P}}$ collecting p_P by \mathcal{P}_h . The space \mathcal{P}_h is equipped with the inner product $[\cdot, \cdot]_{\mathcal{P}_h}$ defined in (5.9). Similarly, we denote the linear space of face-based discrete fields $\lambda_h = (p_f)_{f \in \mathcal{F}}$ collecting p_f by Λ_h . The restriction of Λ_h to a cell P is denoted by $\Lambda_{h,P}$.

As in Sect. 10.1, the degrees of freedom of the vector variable \mathbf{u} are denoted by $u_{P,f}$. Each $u_{P,f}$ approximates the normal component of \mathbf{u} on a face f of P . We denote the linear space of face-based discrete fields collecting all $u_{P,f}$ by $\widetilde{\mathcal{F}}_h$. The restriction of $\widetilde{\mathcal{F}}_h$ to a cell P is denoted by $\widetilde{\mathcal{F}}_{h,P}$ which coincides with $\mathcal{F}_{h,P}$. The space $\widetilde{\mathcal{F}}_h$ is equipped with the inner product $[\cdot, \cdot]_{\widetilde{\mathcal{F}}_h}$ that is assembled from the same local inner products introduced in Chap. 5 for \mathcal{F}_h :

$$[\mathbf{u}_h, \mathbf{v}_h]_{\widetilde{\mathcal{F}}_h} = \sum_{P \in \Omega_h} [\mathbf{u}_P, \mathbf{v}_P]_{\mathcal{F}_{h,P}} \quad \forall \mathbf{u}_h, \mathbf{v}_h \in \widetilde{\mathcal{F}}_h,$$

where $\mathbf{u}_P, \mathbf{v}_P \in \widetilde{\mathcal{F}}_{h,P}$ are the restrictions of global vectors to cell P , e.g.

$$\mathbf{u}_P = (u_{P,f})_{f \in \mathcal{F}_P}.$$

The space $\widetilde{\mathcal{F}}_h$ uses two flux unknowns per interior mesh faces, e.g., $u_{P_1,f}$ and $u_{P_2,f}$, that are related to the cells P_1 and P_2 sharing face f . The flux continuity condition is imposed as the trivial constraint:

$$u_{P_1,f} + u_{P_2,f} = 0 \quad \forall f \in \mathcal{F}^0.$$

Note that such flux continuity condition is not enforced in the space $\widetilde{\mathcal{F}}_h$, that is therefore richer than the space \mathcal{F}_h of Chap. 5.

A numerical treatment of the Dirichlet and the Neumann boundary conditions in (11.3) and (11.4) requires to introduce proper subspaces of the linear spaces Λ_h and $\widetilde{\mathcal{F}}_h$. Let Π_f be the L^2 orthogonal projector onto the space of constant functions defined on face f :

$$\Pi_f(q) = \frac{1}{|f|} \int_f q dS. \quad (11.5)$$

The Dirichlet boundary condition (11.3) is taken into account by setting prescribed values to the components of λ_h corresponding to the boundary faces:

$$p_f = \Pi_f(g^D) \quad \forall f \in \Gamma^D. \quad (11.6)$$

Let Λ_{h,g^D} be the subspace of Λ_h of the discrete fields satisfying (11.6). The case of the homogeneous boundary conditions, $g^D = 0$, leads to the linear space $\Lambda_{h,0}$.

The Neumann boundary condition (11.4) is taken into account by setting the prescribed values to the numerical fluxes on boundary faces:

$$u_{P,f} = \Pi_f(g^N) \quad \forall f \in \Gamma^N \cap P. \quad (11.7)$$

Let $\widetilde{\mathcal{F}}_{h,g^N}$ be the subspace of $\widetilde{\mathcal{F}}_h$ of the discrete fields satisfying (11.7). The case of the homogeneous boundary conditions, $g^N = 0$, leads to the linear subspace $\widetilde{\mathcal{F}}_{h,0}$.

Let $b^I = (b_P)_{P \in \Omega_h} \in \mathcal{P}_h$ be the approximation of source term b . The primary mimetic divergence operator is defined locally like in Chap. 5:

$$\operatorname{div}_P \mathbf{u}_P = \frac{1}{|P|} \sum_{f \in P} |f| u_{P,f}.$$

With the above definitions, the mixed-hybrid mimetic scheme reads:

Find $(p_h, \lambda_h, \mathbf{u}_h) \in \mathcal{P}_h \times \Lambda_{h,g^D} \times \widetilde{\mathcal{F}}_{h,g^N}$ such that:

$$[\mathbf{u}_h, \mathbf{v}_h]_{\widetilde{\mathcal{F}}_h} - [\operatorname{div}_h \mathbf{v}_h, p_h]_{\mathcal{P}_h} + \sum_{P \in \Omega_h} \sum_{f \in \partial P} |f| v_{P,f} p_f = 0 \quad \forall \mathbf{v}_h \in \widetilde{\mathcal{F}}_h, \quad (11.8)$$

$$[\operatorname{div}_h \mathbf{u}_h, q_h]_{\mathcal{P}_h} = [b^I, q_h]_{\mathcal{P}_h} \quad \forall q_h \in \mathcal{P}_h, \quad (11.9)$$

$$u_{P,f} + u_{P',f} = 0 \quad \forall f \in \mathcal{F}^0. \quad (11.10)$$

Remark 11.2. Using the last Eq. (11.10) in the consistency Eq. (11.8) and the mass balance Eq. (11.9), we can verify that the mixed-hybrid formulation is equivalent to the mixed mimetic formulation (5.17)–(5.18).

11.1.2 Convergence analysis for Lagrange multipliers

Let \mathcal{F}^D be the set of mesh faces where we impose a Dirichlet boundary condition. The face degrees of freedom λ_h provide an accurate approximation of p on the mesh

faces as stated in the following theorem. We need to assume the existence of an exact reconstruction operator, see Sect. 5.3.

Theorem 11.3. *Let $R_{\mathbb{P}}^{\mathcal{F}}(\mathbf{u}_{\mathbb{P}})$ be the exact reconstruction operator defined in Sect. 5.3. Let $p^{\mathbb{I}} \in \mathcal{D}_h$ be the projection of the exact solution p using the projection operator defined by (5.7). Then, there exist a constant C independent of $h_{\mathbb{P}}$ such that for every face $f \in \partial\mathbb{P}/\mathcal{F}^D$ it holds*

$$\|p_f - \Pi_f(p)\|_{L^2(f)} \leq C \left(h_{\mathbb{P}}^{\frac{1}{2}} \|\mathbf{u} - R_{\mathbb{P}}^{\mathcal{F}}(\mathbf{u}_{\mathbb{P}})\|_{L^2(\mathbb{P})} + h_{\mathbb{P}}^{\frac{3}{2}} \|\mathbf{u}\|_{L^2(\mathbb{P})} + h_{\mathbb{P}}^{-\frac{1}{2}} \|p^{\mathbb{I}} - p_{\mathbb{P}}\|_{L^2(\mathbb{P})} \right). \quad (11.11)$$

Proof. Let f be a face of cell \mathbb{P} and $\mathbf{v}_{\mathbb{P}} \in \widetilde{\mathcal{F}}_{h,\mathbb{P}}$ be the vector associated with this face such that

$$\mathbf{v}_{\mathbb{P}|_{f'}} = \begin{cases} p_f - \Pi_f(p) & \text{if } f' = f, \\ 0 & \text{otherwise.} \end{cases} \quad (11.12)$$

Since $R_{\mathbb{P}}^{\mathcal{F}}(\mathbf{v}_{\mathbb{P}}) \in H(\text{div}, \mathbb{P})$, multiplying (11.1) by $K^{-1}R_{\mathbb{P}}^{\mathcal{F}}(\mathbf{v}_{\mathbb{P}})$, integrating over \mathbb{P} , and then integrating by parts, give

$$\int_{\mathbb{P}} K^{-1} \mathbf{u} \cdot R_{\mathbb{P}}^{\mathcal{F}}(\mathbf{v}_{\mathbb{P}}) dV - \int_{\mathbb{P}} p \text{div} R_{\mathbb{P}}^{\mathcal{F}}(\mathbf{v}_{\mathbb{P}}) dV + \int_f p R_{\mathbb{P}}^{\mathcal{F}}(\mathbf{v}_{\mathbb{P}}) \cdot \mathbf{n}_{\mathbb{P},f} dS = 0. \quad (11.13)$$

Let $\mathbf{v}_h \in \widetilde{\mathcal{F}}_h$ be the discrete vector field whose restriction to cell \mathbb{P} coincides with $\mathbf{v}_{\mathbb{P}}$ and is zero elsewhere. By using \mathbf{v}_h in (11.8) and the definition of the exact reconstruction operator (5.65), we obtain

$$\int_{\mathbb{P}} K_{\mathbb{P}}^{-1} R_{\mathbb{P}}^{\mathcal{F}}(\mathbf{u}_{\mathbb{P}}) \cdot R_{\mathbb{P}}^{\mathcal{F}}(\mathbf{v}_{\mathbb{P}}) dV - \int_{\mathbb{P}} p_{\mathbb{P}} \text{div} R_{\mathbb{P}}^{\mathcal{F}}(\mathbf{v}_{\mathbb{P}}) dV + \int_f p_f R_{\mathbb{P}}^{\mathcal{F}}(\mathbf{v}_{\mathbb{P}}) \cdot \mathbf{n}_{\mathbb{P},f} dS = 0.$$

Taking the difference of this equation with (11.13) and adding and subtracting $K_{\mathbb{P}}^{-1} \mathbf{u}$ yields

$$\begin{aligned} & \int_{\mathbb{P}} K_{\mathbb{P}}^{-1} (\mathbf{u} - R_{\mathbb{P}}^{\mathcal{F}}(\mathbf{u}_{\mathbb{P}})) \cdot R_{\mathbb{P}}^{\mathcal{F}}(\mathbf{v}_{\mathbb{P}}) dV + \int_{\mathbb{P}} (K^{-1} - K_{\mathbb{P}}^{-1}) \mathbf{u} \cdot R_{\mathbb{P}}^{\mathcal{F}}(\mathbf{v}_{\mathbb{P}}) dV \\ & - \int_{\mathbb{P}} (p - p_{\mathbb{P}}) \text{div} R_{\mathbb{P}}^{\mathcal{F}}(\mathbf{v}_{\mathbb{P}}) dV + \int_f (p - p_f) R_{\mathbb{P}}^{\mathcal{F}}(\mathbf{v}_{\mathbb{P}}) \cdot \mathbf{n}_{\mathbb{P},f} dS = 0. \end{aligned} \quad (11.14)$$

By the definition of the reconstructed function, its divergence is constant on \mathbb{P} . Thus, we can transform the third integral in (11.14) as:

$$\int_{\mathbb{P}} (p - p_{\mathbb{P}}) \text{div} R_{\mathbb{P}}^{\mathcal{F}}(\mathbf{v}_{\mathbb{P}}) dV = |\mathbb{P}| (p_{\mathbb{P}}^{\mathbb{I}} - p_{\mathbb{P}}) \text{div} R_{\mathbb{P}}^{\mathcal{F}}(\mathbf{v}_{\mathbb{P}}). \quad (11.15)$$

By the same definition, $R_{\mathbb{P}}^{\mathcal{F}}(\mathbf{v}_{\mathbb{P}}) \cdot \mathbf{n}_{\mathbb{P},f} = v_f$, and we have

$$\int_f (p_f - p) R_{\mathbb{P}}^{\mathcal{F}}(\mathbf{v}_{\mathbb{P}}) \cdot \mathbf{n}_{\mathbb{P},f} dS = \int_f (p_f - \Pi_f(p)) v_f dS = \|p_f - \Pi_f(p)\|_{L^2(f)}^2. \quad (11.16)$$

Now, we rearrange the terms in (11.14), use (11.15)–(11.16), the Cauchy-Schwarz inequality, and the bound provided by assumption **(H1b)** (see, formula (5.36)) to obtain:

$$\begin{aligned}
\|p_f - \Pi_f(p)\|_{L^2(f)}^2 &= \int_P \mathbf{K}_P^{-1}(\mathbf{u} - R_P^{\mathcal{F}}(\mathbf{u}_P)) \cdot R_P^{\mathcal{F}}(\mathbf{v}_P) dV \\
&\quad + \int_P (\mathbf{K}^{-1} - \mathbf{K}_P^{-1}) \mathbf{u} \cdot R_P^{\mathcal{F}}(\mathbf{v}_P) dV + |P| (p_P - p_P^1) \operatorname{div} R_P^{\mathcal{F}}(\mathbf{v}_P) \\
&\leq C \left(\|\mathbf{u} - R_P^{\mathcal{F}}(\mathbf{u}_P)\|_{L^2(P)} + h_P \|\mathbf{u}\|_{L^2(P)} \right) \|R_P^{\mathcal{F}}(\mathbf{v}_P)\|_{L^2(P)} \\
&\quad + |P| p_P - p_P^1 \operatorname{div} R_P^{\mathcal{F}}(\mathbf{v}_P). \tag{11.17}
\end{aligned}$$

Note that we have the following upper bound:

$$\|R_P^{\mathcal{F}}(\mathbf{v}_P)\|_{L^2(P)} \leq C \|\mathbf{K}_P^{-\frac{1}{2}} R_P^{\mathcal{F}}(\mathbf{v}_P)\|_{L^2(P)} = \|\mathbf{v}_P\|_{\mathcal{F}_{h,P}},$$

where norm $\|\cdot\|_{\mathcal{F}_{h,P}}$ is induced by the local mimetic inner product $[\cdot, \cdot]_{\mathcal{F}_{h,P}}$. Using property **(S1)** from Sect. 5.1.3 and the definition of \mathbf{v}_P yields

$$[\mathbf{v}_P, \mathbf{v}_P]_P \leq \sigma^* |P| \sum_{f \in \partial P} |v_f|^2 = \sigma^* |P| \|p_f - \Pi_f(p)\|^2 = \sigma^* \frac{|P|}{f} \|p_f - \Pi_f(p)\|_{L^2(f)}^2.$$

Combining the last two formulas, and using the mesh regularity property **(M2)** (see, Sect. 1.6.2) we obtain

$$\|R_P^{\mathcal{F}}(\mathbf{v}_P)\|_{L^2(P)} \leq C h_P^{\frac{1}{2}} \|p_f - \Pi_f(p)\|_{L^2(f)}. \tag{11.18}$$

To estimate the last term in (11.17), we recall the definition of the mimetic divergence operator and apply again the mesh regularity property **(M2)**:

$$\begin{aligned}
|\operatorname{div} R_P^{\mathcal{F}}(\mathbf{v}_P)| &= |\operatorname{div}_P \mathbf{v}_P| = \frac{1}{|P|} \sum_{f \in \partial P} |f| v_f = \frac{|f|}{|P|} p_f - \Pi_f(p) \\
&\leq C h_P^{-\frac{1}{2}} \|p_f - \Pi_f(p)\|_{L^2(f)}. \tag{11.19}
\end{aligned}$$

The assertion of the theorem follows by inserting (11.18) and (11.19) into (11.17) and simplifying $\|p_f - \Pi_f(p)\|_{L^2(f)}$ from both sides of the resulting inequality. \square

It is worth mentioning that a simple modification of the previous proof (just apply the Cauchy-Schwarz inequality to the left-hand side of (11.15)) gives another estimate:

$$\|p_f - \Pi_f(p)\|_{L^2(f)} \leq C \left(h_P^{\frac{1}{2}} \|\mathbf{u} - R_P(\mathbf{u}_h)\|_{L^2(P)} + h_P^{\frac{3}{2}} \|\mathbf{u}\|_{L^2(P)} + h_P^{-\frac{1}{2}} \|p - p_P\|_{L^2(P)} \right).$$

We introduce the following mesh-dependent norm to measure the discretization error for the Lagrange multipliers:

$$\|\lambda_h - \Pi_h^{\mathcal{F}}(p)\|_{h, \mathcal{F}}^2 = \sum_{f \in \mathcal{F} / \mathcal{F}^D} h_f \|p_f - \Pi_f(p)\|_{L^2(f)}^2, \tag{11.20}$$

where $\Pi_h^{\mathcal{F}}$ is the global projection operator whose restriction to face f is Π_f . A bound for this error follows immediately from Theorem 11.3.

Corollary 11.2. *Under the assumptions of Theorem 11.3, it holds:*

$$\|\lambda_h - \Pi_h^{\mathcal{F}}(p)\|_{h,\mathcal{F}} \leq C \left(h \|\mathbf{u} - R^{\mathcal{F}}(\mathbf{u}_h)\|_{L^2(\Omega)} + h^2 \|\mathbf{u}\|_{L^2(\Omega)} + \|P^I - p_h\|_{\mathcal{F}_h} \right).$$

It is remarkable that under the assumptions of Theorem 5.4, we also have the super-convergence result for the Lagrange multipliers:

$$\|\lambda_h - \Pi_h^{\mathcal{F}}(p)\|_{h,\mathcal{F}} \leq Ch^2 (\|p\|_{H^2(\Omega)} + \|b\|_{H^1(\Omega)}), \tag{11.21}$$

where C is independent of h .

11.2 Monotonicity conditions for the mixed-hybrid formulation

In this section, we discuss sufficient algebraic conditions for selecting monotone schemes within the family of mimetic schemes.

We consider a cell P and define two matrices

$$B_P = \begin{pmatrix} |f_1| \\ |f_2| \\ \vdots \\ |f_{N_P^{\mathcal{F}}}| \end{pmatrix} \quad \text{and} \quad C_P = \begin{pmatrix} |f_1| & & & \\ & |f_2| & & \\ & & \ddots & \\ & & & |f_{N_P^{\mathcal{F}}}| \end{pmatrix},$$

where $N_P^{\mathcal{F}}$ is the number of faces in P . Let us define a mesh function $\mathbf{v}_h \in \widetilde{\mathcal{F}}_h$ such that \mathbf{v}_P is zero for all cells except P . Inserting this function in (11.8), we obtain

$$M_P \mathbf{u}_P - B_P p_P + C_P \lambda_P = \mathbf{0}. \tag{11.22}$$

Let us define a mesh function $q_h \in \mathcal{D}_h$ such that q_P is zero for all cells except P . Inserting this function in (11.9), we obtain the local mass balance equation

$$B_P^T \mathbf{u}_P = |P| b_P^I. \tag{11.23}$$

It can be shown that the algebraic system appearing from the mixed-hybrid formulation (before applying the Dirichlet boundary conditions) is assembled from cell-based systems

$$\begin{pmatrix} M_P & -B_P & C_P \\ -B_P^T & 0 & 0 \\ C_P^T & 0 & 0 \end{pmatrix} \begin{pmatrix} \mathbf{u}_P \\ p_P \\ \lambda_P \end{pmatrix} = \begin{pmatrix} \mathbf{0} \\ -|P| b_P^I \\ \mathbf{g}_P \end{pmatrix},$$

where the components of vector \mathbf{g}_P are non-zero only for boundary faces on Γ_N and equal to the given Neumann fluxes. The Dirichlet boundary conditions can be enforced after any step of our derivations by prescribing given values to the Lagrange

multipliers and eliminating the corresponding equations. Typically, it is done after the last step.

Note that only the Lagrange multipliers share values across cell interfaces. The other unknowns can be eliminated locally. Elimination of \mathbf{u}_P ads to the following local systems that have to be assembled into the global system:

$$\begin{pmatrix} B_P^T M_P^{-1} B_P & -B_P^T M_P^{-1} C_P \\ -C_P^T M_P^{-1} B_P & C_P^T M_P^{-1} C_P \end{pmatrix} \begin{pmatrix} p_P \\ \lambda_P \end{pmatrix} = \begin{pmatrix} |P| b_P^1 \\ \mathbf{g}_P \end{pmatrix}. \quad (11.24)$$

We denote the matrix of this system by S_P . Let $W_P = M_P^{-1}$ and $\tilde{W}_P = (w_{ij})_{i,j=1}^{N_P^{\mathcal{F}}}$. Direct derivation of matrix W_P is possible and discussed in details in Sect. 4.6. We make two assumptions.

(W1) Matrix W_P satisfies the geometric constraint

$$\sum_j w_{ij} |f_j| \geq 0 \quad \forall i,$$

and the inequality is strict for at least one matrix row.

(W2) Matrix W_P is a Z-matrix, i.e., $w_{ij} \leq 0$ for $i \neq j$.

Lemma 11.1. *Under assumption (W1)–(W2), the matrix S_P in (11.24) is a singular M-matrix. Moreover, its null space consists of constant vectors.*

Proof. Let us consider the matrix $\tilde{W}_P = C_P^T W_P C_P$. This matrix has entries $\tilde{w}_{ij} = w_{ij} |f_i| |f_j|$ and is a weakly diagonally dominant Z-matrix by our assumptions. Matrix W_P is symmetric and positive definite; hence, its diagonal entries are strictly positive. Multiplying the i -th inequality in **(W1)** by $|f_i|$, we obtain

$$\sum_j w_{ij} |f_j| |f_i| \geq 0 \implies a_i \equiv \sum_j \tilde{w}_{ij} \geq 0 \quad \forall i.$$

One of the inequalities must be strict, i.e. $a_i > 0$.

Let us consider the column-matrix $\tilde{B}_P = C_P^T W_P B_P$. Its i -th entry is $-a_i \leq 0$; hence,

$$a_i + \sum_j \tilde{w}_{ij} = 0 \implies |\tilde{w}_{ii}| = |a_i| - \sum_{i \neq j} |\tilde{w}_{ij}| \quad \forall i.$$

Finally, let us consider matrix $B_P^T W_P B_P = \sum_i a_i > 0$. Since $\sum_i a_i = \sum_i |a_i|$, the entries in the first row of S_P sum up to zero. We conclude that a constant vector is in the null spaces of matrix S_P .

Let $\mathbf{b} = \alpha \mathbf{1} + \beta \mathbf{c}$ be a non-constant vector in the null space of S_P and $\mathbf{c}^T = (c_1, \mathbf{c}_2^T)$. Direct calculations show that

$$0 = \mathbf{b}^T S_P \mathbf{b} = (B_P \mathbf{c}_1 - C_P \mathbf{c}_2)^T W_P (B_P \mathbf{c}_1 - C_P \mathbf{c}_2).$$

Hence, $B_P \mathbf{c}_1 = C_P \mathbf{c}_2$. The structure of these matrices implies that \mathbf{c} is a constant vector, hence, the null space of S_P consists of only constant vectors.

We show by contradiction that matrix S_P is irreducible. Let us assume the opposite. Then, the matrix can be reduced to a block-diagonal matrix by re-arranging rows and columns. Since, we proved that the constant vector is the eigenvector, the block-diagonal matrix can have two distinct eigenvectors $(1, \dots, 1, 0, \dots, 0)^T$ and $(0, \dots, 0, 1, \dots, 1)^T$, which leads to the contradiction.

Observe, that if we add a small positive number to any diagonal entry of S_P , it becomes weakly a diagonally dominant irreducible Z-matrix with positive diagonal entries. This is the definition of a singular M-matrix. \square

Let S be the matrix obtained by assembling the elemental matrix S_P and applying the Dirichlet boundary conditions. A proof of the following results is left as an exercise, see [249] for details.

Theorem 11.4. *Let, for every element $P \in \Omega_h$, the matrix W_P satisfy assumptions (W1) and (W2). Furthermore, let mesh Ω_h be face-connected and $|\Gamma^D| \neq 0$. Then, S is an irreducible weakly diagonally dominant M-matrix.*

Now, we state two monotonicity results that we study in detail in the next subsections. The proofs are straightforward and are based on the properties of an M-matrix and the observation that the right-hand side vector is either non-negative or non-positive.

Theorem 11.5 (Discrete Maximum Principle). *Let $p_h = (p_P)_{P \in \Omega_h}$ and $\lambda_h = (p_f)_{f \in \mathcal{F}}$ be the solutions of the mixed-hybrid mimetic scheme under the assumptions of Theorem 11.4. If b is a nonnegative function in Ω and g^D and g^N are nonnegative functions on Γ^D and Γ^N , respectively, then $p_P \geq 0$ and $p_f \geq 0$ for all P and f .*

Theorem 11.6 (Discrete Minimum Principle). *Let $p_h = (p_P)_{P \in \Omega_h}$ and $\lambda_h = (p_f)_{f \in \mathcal{F}}$ be the solutions of the mixed hybrid mimetic scheme under the assumptions of Theorem 11.4. If b is a nonpositive function in Ω and g^D and g^N are nonpositive functions on Γ^D and Γ^N , respectively, then $p_P \leq 0$ and $p_f \leq 0$ for all P and f .*

Using both Theorems 11.5 and 11.6, we obtain a discrete version of Theorem 11.2.

Theorem 11.7. *Let $p_h = (p_P)_{P \in \Omega_h}$ and $\lambda_h = (p_f)_{f \in \mathcal{F}}$ be the solutions of the mixed hybrid mimetic scheme under the assumptions of Theorem 11.4. Furthermore, let $b = 0$ and $\Gamma^N = \emptyset$. Then, for all P and f , values p_P and p_f are bounded by the maximum and minimum values of the set $\{\Pi_f(g^D)\}_{f \in \partial\Omega}$.*

Let us recall the general formula of matrix W_P as stated by Eq. (4.67):

$$W_P = N_P \frac{K_P^{-1}}{|P|} N_P^T + D_P U_P D_P^T, \tag{11.25}$$

where matrices R_P and N_P for cell P are given by (5.29) and (5.25), respectively. Recall also that D_P is the full rank matrix such that $D_P^T R_P = 0$ and the size of matrix U_P is $N_P^{\mathcal{F}} - d$ where $N_P^{\mathcal{F}}$ is the number of faces in P .

In accordance with the spectral analysis of the mixed mimetic scheme, cf. Chap. 5 and also [93], matrix W_P is an SPD matrix and satisfies a stability condition similar to **(S1)** of Sect. 5.1.3:

$$\sigma_* \frac{1}{|P|} \mathbf{v}_P^T \mathbf{v}_P \leq \mathbf{v}_P^T W_P \mathbf{v}_P \leq \sigma^* \frac{1}{|P|} \mathbf{v}_P^T \mathbf{v}_P \quad \forall \mathbf{v}_P.$$

To satisfy these inequality, we can take a matrix U_P which is spectrally equivalent to $|P|^{-1} I_P$ and enforce uniform bounds on the norms of the columns of D_P .

Conditions **(W1)** and **(W2)** combined with the positive definiteness of matrix U_P allow us to obtain a set of inequalities forming a local optimization problem for every element P . These optimization problems can be solved analytically for a class of polygonal and polyhedral cells. In general, they have to be solved numerically.

11.2.1 Triangular and tetrahedral cells

If P is a simplex, then $N_P^{\mathcal{F}} = d + 1$ and U_P is a 1×1 matrix, i.e. we have a one-parameter family of matrices W_P in accordance with (11.25):

$$W_P = \frac{1}{|P|} N_P K_P^{-1} N_P^T + u_P D_P D_P^T,$$

where matrix N_P is given by (5.25). The column matrix D_P must be orthogonal to column of matrix R_P given by (5.29). It is easy to verify that

$$D_P^T = (|f_1|^{-1}, |f_2|^{-1}, \dots, |f_{d+1}|^{-1}).$$

The assumption **(W1)** is reduced to $u_P > 0$. The assumption **(W2)** reproduces the well established angle conditions for the $\mathbb{RT}_0 - \mathbb{P}_0$ finite element discretization [250]:

$$\mathbf{n}_i^T K_P \mathbf{n}_j \leq 0 \quad i \neq j.$$

For example, when P is a triangle and the diffusion tensor K_P is isotropic, the monotonicity requirement is that the angles are less than $\frac{\pi}{2}$. For a tetrahedron P , the monotonicity requirement is that the dihedral angles are less than $\frac{\pi}{2}$.

11.2.2 Parallelograms

Let us consider a parallelogram P . The formulas for the local matrices R_P , N_P , and D_P depend on the order in which we take the edges of cell P . A different enumeration of the edges corresponds to a permutation of the rows in these matrices. We consider the enumeration given in Fig. 11.1. Let \mathbf{x}_{BC} , \mathbf{x}_{AD} , etc. be the midpoint of edge f_{BC} , f_{AD} , etc., respectively, and \mathbf{n}_{BC} , \mathbf{n}_{AD} , etc. be the unit orthogonal vector to edge f_{BC} ,

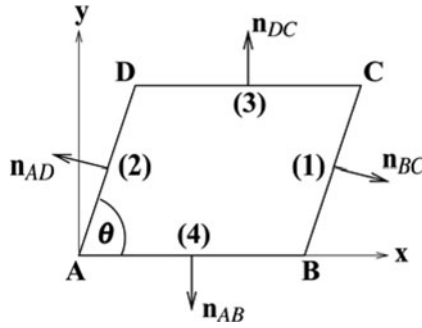


Fig. 11.1. Geometry of a parallelogram; the numbers in parenthesis, e.g., (1)-(4), indicate the order of the edges used in the construction of matrices R_P , N_P , D_P , and W_P

f_{AD} , etc., respectively, pointing out of cell P . We have:

$$R_P = \begin{pmatrix} |f_{BC}|(\mathbf{x}_{BC} - \mathbf{x}_P)^T \\ |f_{AD}|(\mathbf{x}_{AD} - \mathbf{x}_P)^T \\ |f_{DC}|(\mathbf{x}_{DC} - \mathbf{x}_P)^T \\ |f_{AB}|(\mathbf{x}_{AB} - \mathbf{x}_P)^T \end{pmatrix} = \frac{|P|}{2 \sin(\theta)} \begin{pmatrix} 1 & 0 \\ -1 & 0 \\ \cos(\theta) & \sin(\theta) \\ -\cos(\theta) & -\sin(\theta) \end{pmatrix} \quad (11.26)$$

and

$$N_P = \begin{pmatrix} \mathbf{n}_{BC}^T \\ \mathbf{n}_{AD}^T \\ \mathbf{n}_{DC}^T \\ \mathbf{n}_{AB}^T \end{pmatrix} K_P = \begin{pmatrix} \sin(\theta) & -\cos(\theta) \\ -\sin(\theta) & \cos(\theta) \\ 0 & 1 \\ 0 & -1 \end{pmatrix} K_P. \quad (11.27)$$

The definition of matrix D_P is not unique, and among the simplest ones we select the following:

$$D_P^T = \begin{pmatrix} 1 & 1 & 0 & 0 \\ 0 & 0 & 1 & 1 \end{pmatrix}. \quad (11.28)$$

For any $\theta \in (0, \pi/2)$, this matrix satisfies the orthogonality condition $R_P^T D_P = 0$ and the columns of the 4×4 matrix (R_P, D_P) form a basis of \mathbb{R}^4 . Regarding the 2×2 -sized parameter matrix $U_P = (u_{ij})_{i,j=1}^2$, the hypothesis that this matrix is SPD implies that $u_{12} = u_{21}$, $u_{11} > 0$, $u_{22} > 0$, and $u_{11} u_{22} > u_{12}^2$.

To simplify notations, we set $\mathbf{n}_1 = \mathbf{n}_{BC}$, $\mathbf{n}_2 = \mathbf{n}_{DC}$, $f_1 = f_{BC}$, and $f_2 = f_{DC}$. We define the transformed diffusion tensor $K^\theta = (K_{ij}^\theta)$ by setting $K_{ij}^\theta = \mathbf{n}_i^T K_P \mathbf{n}_j$:

$$K^\theta = \begin{pmatrix} K_{11}^\theta & \sin(\theta)K_{12} - \cos(\theta)K_{22} \\ \sin(\theta)K_{21} - \cos(\theta)K_{22} & K_{22} \end{pmatrix}, \quad (11.29)$$

where

$$K_{11}^\theta = \sin^2(\theta)K_{11} + \cos^2(\theta)K_{22} - \sin(\theta)\cos(\theta)(K_{12} + K_{21}).$$

From the strong ellipticity of K it follows immediately that matrix K^θ is semi-positive definite. A direct calculation shows that

$$\det(K^\theta) = \det(K_P) \sin^2(\theta) > 0,$$

i.e. K^θ is the SPD matrix.

Using formulas (11.26)–(11.28), we can calculate matrix W_P . It turns out that it has a very peculiar block structure characterized by the entries of the transformed diffusion matrix K^θ :

$$W_P = \begin{pmatrix} W^{11} & W^{12} \\ W^{21} & W^{22} \end{pmatrix}, \quad W^{ij} = \frac{K_{ij}^\theta}{|P|} \begin{pmatrix} 1 & -1 \\ -1 & 1 \end{pmatrix} + u_{ij} \begin{pmatrix} 1 & 1 \\ 1 & 1 \end{pmatrix}.$$

Note that $W^{12} = W^{21}$ and each matrix block W^{ij} is a symmetric matrix. Let us analyze conditions **(W1)** and **(W2)**. We set $\alpha := |f_1| = |f_3|$, $\beta := |f_2| = |f_4|$ and define vector $\mathbf{f} = (\alpha, \alpha, \beta, \beta)^T$. Note that $|P| = \alpha \beta \sin(\theta)$. Condition **(W1)** gives

$$W_P \mathbf{f} > 0.$$

This and similar inequalities mean that all vector components are nonpositive and at least one is strictly positive. Let $\boldsymbol{\alpha} = (\alpha, \alpha)^T$, $\boldsymbol{\beta} = (\beta, \beta)^T$, and $\mathbb{1} = (1, 1)^T$. Then, we have

$$W_P \mathbf{f} = \begin{pmatrix} W^{11} & W^{12} \\ W^{21} & W^{22} \end{pmatrix} \begin{pmatrix} \boldsymbol{\alpha} \\ \boldsymbol{\beta} \end{pmatrix} = 2 \begin{pmatrix} (\alpha u_{11} + \beta u_{12}) \mathbb{1} \\ (\alpha u_{21} + \beta u_{22}) \mathbb{1} \end{pmatrix} > 0. \quad (11.30)$$

We write these inequalities in the compact form:

$$U_P \begin{pmatrix} \boldsymbol{\alpha} \\ \boldsymbol{\beta} \end{pmatrix} > 0.$$

Let us introduce the 2×2 -sized matrix

$$\tilde{K}^\theta = \begin{pmatrix} K_{11}^\theta & -|K_{12}^\theta| \\ -|K_{21}^\theta| & K_{22}^\theta \end{pmatrix}.$$

Condition **(W2)** requires W_P to be a Z-matrix. Thus, the off-diagonal blocks W^{ij} for $i \neq j$ must be nonpositive matrices and the diagonal blocks W^{ii} must be Z-matrices. These requirements lead to the following matrix inequality:

$$|P| U_P \leq \tilde{K}^\theta. \quad (11.31)$$

Combining conditions **(W1)** and **(W2)** together gives

$$0 < |P| U_P \begin{pmatrix} \boldsymbol{\alpha} \\ \boldsymbol{\beta} \end{pmatrix} \leq \tilde{K}^\theta \begin{pmatrix} \boldsymbol{\alpha} \\ \boldsymbol{\beta} \end{pmatrix},$$

from which we derive the *necessary condition for parallelograms*:

$$\tilde{K}^\theta \begin{pmatrix} \alpha \\ \beta \end{pmatrix} > 0. \tag{11.32}$$

This condition imposes constraints on both the lengths of edges f_i and the range of values of entries in K_P . It is necessary because there cannot exist a parameter matrix U_P that satisfies **(W1)** and **(W2)** if condition (11.32) is violated.

By going one step further into the analysis, we recover the condition "C" for parallelograms, which is the monotonicity result for the family of nine-point difference schemes published in [291]. Let us introduce the three parameters a, b, c as follows:

$$\begin{pmatrix} a & c \\ c & b \end{pmatrix} = (|f_1| \mathbf{n}_1, |f_2| \mathbf{n}_2)^T K_P (|f_1| \mathbf{n}_1, |f_2| \mathbf{n}_2). \tag{11.33}$$

As matrix K^θ is SPD, matrix \tilde{K}^θ is also SPD. We multiply the first equation in (11.32) by α , the second equation by β , and use definition (11.33). It follows that a matrix U_P satisfying **(W1)** and **(W2)** can exist only if $|c| \leq \min(a, b)$, which is the condition "C" for parallelograms proposed in [291].

Let $K_{ij}^{\theta,\pm}$ for $i \neq j$ denote the positive and negative part of K_{ij}^θ , i.e., $K_{ij}^{\theta,\pm} = (K_{ij}^\theta \pm |K_{ij}^\theta|)/2$. Due to matrix symmetry, $K_{ij}^{\theta,\pm} = K_{ji}^{\theta,\pm}$. To maximize the sparsity structure of W_P , we may consider a matrix U_P given by

$$U_P = \frac{\tilde{K}^\theta}{|P|} \implies W_P = \frac{2}{|P|} \left(\begin{array}{cc|cc} K_{11}^\theta & 0 & K_{12}^{\theta,-} & -K_{12}^{\theta,+} \\ 0 & K_{11}^\theta & -K_{12}^{\theta,+} & K_{12}^{\theta,-} \\ \hline K_{21}^{\theta,-} & -K_{21}^{\theta,+} & K_{22}^\theta & 0 \\ -K_{21}^{\theta,+} & K_{21}^{\theta,-} & 0 & K_{22}^\theta \end{array} \right). \tag{11.34}$$

With this choice, matrix W_P is reducible. Indeed, if $K_{12}^\theta < 0$ exchanging the second and third rows and, then, the second and third columns gives a block diagonal matrix where each 2×2 diagonal blocks is equal to K^θ . Similarly, when $K_{12}^\theta > 0$ we obtain a block diagonal matrix with 2×2 diagonal blocks by exchanging the second and the fourth rows and, then, the second and the fourth columns. Nonetheless, irreducibility is not lost for matrix S_P , as can be verified by direct calculations.

The special case of a scalar diffusion coefficient, $K_P = k_P I_2$, worth detailed comments. By definition, we have that

$$\tilde{K}^\theta = k_P \begin{pmatrix} \mathbf{n}_1^T \mathbf{n}_1 & -|\mathbf{n}_1^T \mathbf{n}_2| \\ -|\mathbf{n}_2^T \mathbf{n}_1| & \mathbf{n}_2^T \mathbf{n}_2 \end{pmatrix} = k_P \begin{pmatrix} 1 & -\cos(\theta) \\ -\cos(\theta) & 1 \end{pmatrix},$$

and the necessary condition for parallelograms (11.32) becomes

$$\begin{cases} \alpha - \beta \cos(\theta) \geq 0, \\ -\alpha \cos(\theta) + \beta \geq 0. \end{cases} \tag{11.35}$$

Without loss of generality, let $\alpha \geq \beta$ (for $\beta \geq \alpha$ we will just exchange the role of α and β). The first inequality in (11.35) is obviously satisfied. The second inequality gives $\cos(\theta) \leq \beta/\alpha$. Since θ varies between 0 and $\pi/2$, we have

$$\arccos\left(\frac{\beta}{\alpha}\right) \leq \theta \leq \frac{\pi}{2}. \quad (11.36)$$

This necessary condition constrains the shape of the parallelogram and does not involve the diffusion coefficient k_P . Moreover, it is always satisfied for the whole range of the parameter θ when $\alpha = \beta$, i.e. when $\arccos(\beta/\alpha) = 0$. Therefore, the mixed mimetic scheme defined by (11.34) always provides a monotone discretization on a tilted mesh of originally square cells regardless of the angle of inclination.

Finally, let us analyze another special case of an elliptic problem with a scalar diffusion tensor and a mesh of rectangles, i.e., $\theta = \pi/2$. In view of Eq. (11.34), matrix W_P takes a very simple form:

$$W_P = \frac{2k_P}{|P|} |P|. \quad (11.37)$$

Inserting formula (11.37) in (11.22), we obtain a simple formula for the numerical flux in terms of edge and cell pressures:

$$u_{P,f_i} = -\frac{2k_P}{|P|} |f_i| (p_{f_i} - p_P), \quad i = 1, \dots, 4.$$

Let f be the edge shared by rectangles P and P' . The numerical fluxes for this edge are given by:

$$u_{P,f} = -\frac{2k_P}{|P|} |f| (p_f - p_P) \quad \text{and} \quad u_{P',f} = -\frac{2k_{P'}}{|P'|} |f| (p_f - p_{P'}).$$

Since $u_{P,f} + u_{P',f} = 0$ and $|P| = |P'|$ we solve for p_f and substitute the result in the formulas above. Since $|\mathbf{x}_{P'} - \mathbf{x}_P| |f| = |P|$, we obtain the well-known two-point flux approximation formula:

$$u_{P,f} = -k_f \frac{p_{P'} - p_P}{|\mathbf{x}_{P'} - \mathbf{x}_P|}, \quad k_f = \frac{2k_P k_{P'}}{k_P + k_{P'}}.$$

11.2.3 Oblique parallelepipeds

Let us consider a parallelepiped P . The formulas for local matrices R_P , N_P , and D_P depend on the order in which we consider the faces of P . We take the enumeration of faces shown in Fig. 11.2.

We denote the centroid of face f_{BCGF} by \mathbf{x}_{BCGF} , of face f_{ADHE} by \mathbf{x}_{ADHE} , and so on. Similarly, we denote the unit vector orthogonal to face f_{BCGF} by \mathbf{n}_{BCGF} , and so

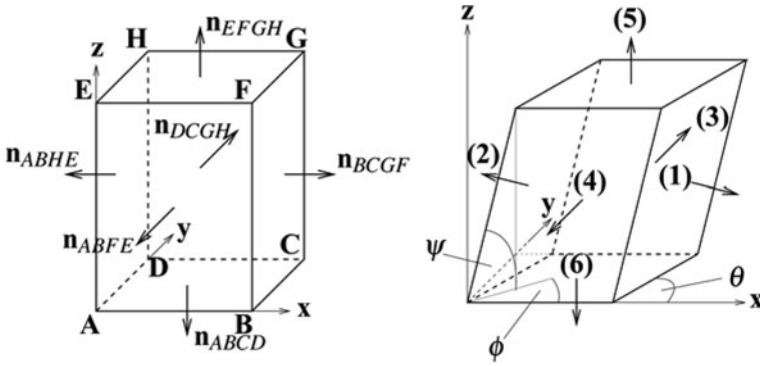


Fig. 11.2. Geometry of an orthogonal (left) and oblique (right) parallelepipeds. The labeling of points and normal vectors is the same for both plots and, for readability, is given only on the left plot. The numbers in parenthesis on the right plot, e.g., (1)-(6), indicate the enumeration of faces

on, and assume that all the normal vectors point out of P. Let

$$\begin{aligned} \rho' &= (\sin^2 \psi + \cos^2 \psi (\cos \theta \sin \phi - \sin \theta \cos \phi)^2)^{1/2}, \\ \rho'' &= (1 - \cos^2 \psi \cos^2 \phi)^{1/2}, \\ \rho''' &= \sin \theta \cos \psi, \\ \rho_P &= \frac{L_x L_y L_z}{2}. \end{aligned}$$

Then, matrix R_P takes the form:

$$R_P = \begin{pmatrix} |f_{BCGF}| (\mathbf{x}_{BCGF} - \mathbf{x}_P)^T \\ |f_{ADHE}| (\mathbf{x}_{ADHE} - \mathbf{x}_P)^T \\ |f_{DCGH}| (\mathbf{x}_{DCGH} - \mathbf{x}_P)^T \\ |f_{ABFE}| (\mathbf{x}_{ABFE} - \mathbf{x}_P)^T \\ |f_{EFGH}| (\mathbf{x}_{EFGH} - \mathbf{x}_P)^T \\ |f_{ABCD}| (\mathbf{x}_{ABCD} - \mathbf{x}_P)^T \end{pmatrix} = \rho_P \begin{pmatrix} \rho' & 0 & 0 \\ -\rho' & 0 & 0 \\ \rho'' \cos \theta & \rho'' \sin \theta & 0 \\ -\rho'' \cos \theta & -\rho'' \sin \theta & 0 \\ \rho''' \cos \phi & \rho''' \sin \phi & \sin \theta \sin \psi \\ -\rho''' \cos \phi & -\rho''' \sin \phi & -\sin \theta \sin \psi \end{pmatrix}.$$

Matrix N_P takes the form:

$$N_P = \begin{pmatrix} \mathbf{n}_{BCGF} \\ \mathbf{n}_{ADHE} \\ \mathbf{n}_{DCGH} \\ \mathbf{n}_{ABFE} \\ \mathbf{n}_{EFGH} \\ \mathbf{n}_{ABCD} \end{pmatrix} K_P = \begin{pmatrix} \frac{\sin \theta \sin \psi}{\rho'} & -\frac{\cos \theta \sin \psi}{\rho'} & \frac{\cos \psi (\cos \theta \sin \phi - \sin \theta \cos \phi)}{\rho'} \\ -\frac{\sin \theta \sin \psi}{\rho'} & \frac{\cos \theta \sin \psi}{\rho'} & -\frac{\cos \psi (\cos \theta \sin \phi - \sin \theta \cos \phi)}{\rho'} \\ 0 & \frac{\sin \psi}{\rho''} & -\frac{\cos \psi \sin \phi}{\rho''} \\ 0 & -\frac{\sin \psi}{\rho''} & \frac{\cos \psi \sin \phi}{\rho''} \\ 0 & 0 & 1 \\ 0 & 0 & -1 \end{pmatrix} K_P.$$

Matrix D_P is not defined uniquely. Among many possible choices, we select the following one which is also one of the simplest:

$$D_P^T = \begin{pmatrix} 1 & 1 & 0 & 0 & 0 & 0 \\ 0 & 0 & 1 & 1 & 0 & 0 \\ 0 & 0 & 0 & 0 & 1 & 1 \end{pmatrix}. \quad (11.38)$$

It is easy to verify that matrix D_P satisfies the orthogonality condition $R_P^T D_P = 0$. Indeed, the first couple of rows of R_P are formed by opposite vectors and the same is true for the second and the third couple of rows. Moreover, the columns of matrix (R_P, D_P) form a basis of \mathbb{R}^6 .

We assume that the 3×3 -sized parameter matrix $U_P = (u_{ij})_{i,j=1}^3$ is SPD, i.e. $u_{ij} = u_{ji}$, $u_{ii} > 0$, $u_{11}u_{22} - u_{12}^2 > 0$, and $\det(U_P) > 0$. For convenience, we shorten our notation:

$$\mathbf{n}_1 = \mathbf{n}_{BCGF}, \quad \mathbf{n}_2 = \mathbf{n}_{DCGH}, \quad \mathbf{n}_3 = \mathbf{n}_{EFGH},$$

and define the transformed diffusion tensor $K^\theta = (K_{ij}^\theta)_{i,j=1}^3$ with entries $K_{ij}^\theta = \mathbf{n}_i^T K_P \mathbf{n}_j$. Straightforward calculations using the matrices N_P and D_P provides us with the matrix W_P . Similar to the two-dimensional case, this matrix has a very peculiar 3×3 block structure:

$$W_P = \begin{pmatrix} W^{11} & W^{12} & W^{13} \\ W^{21} & W^{22} & W^{23} \\ W^{31} & W^{32} & W^{33} \end{pmatrix}, \quad W^{ij} = \frac{K_{ij}^\theta}{|P|} \begin{pmatrix} 1 & -1 \\ -1 & 1 \end{pmatrix} + u_{ij} \begin{pmatrix} 1 & 1 \\ 1 & 1 \end{pmatrix}.$$

Each block W^{ij} is a symmetric matrix and $W^{ij} = W^{ji}$ for $i \neq j$. Let us define a vector $\mathbf{f} = (\alpha, \alpha, \beta, \beta, \gamma, \gamma)^T$ where $\alpha := |f_{BCGF}| = |f_{ADHE}|$, $\beta := |f_{DCGH}| = |f_{ABFE}|$, and $\gamma := |f_{EFGH}| = |f_{ABCD}|$. Applying the same arguments as in the two-dimensional case, we can show that condition **(W1)** implies

$$W_P \mathbf{f} > 0. \quad (11.39)$$

Let again $\alpha = (\alpha, \alpha)^T$, $\beta = (\beta, \beta)^T$, and $\gamma = (\gamma, \gamma)^T$ (and recall that $\mathbb{1}_2 = (1, 1)^T$). We have

$$W_P \mathbf{f} = \begin{pmatrix} W^{11} \alpha + W^{12} \beta + W^{13} \gamma \\ W^{21} \alpha + W^{22} \beta + W^{23} \gamma \\ W^{31} \alpha + W^{32} \beta + W^{33} \gamma \end{pmatrix} = 2 \begin{pmatrix} (\alpha u_{11} + \beta u_{12} + \gamma u_{13}) \mathbb{1} \\ (\alpha u_{21} + \beta u_{22} + \gamma u_{23}) \mathbb{1} \\ (\alpha u_{31} + \beta u_{32} + \gamma u_{33}) \mathbb{1} \end{pmatrix} > 0,$$

which is equivalent to

$$U_P \begin{pmatrix} \alpha \\ \beta \\ \gamma \end{pmatrix} > 0.$$

Condition **(W2)** states that matrix W_P must be a Z-matrix. According to the block structure shown above, the off-diagonal blocks W^{ij} for $i \neq j$ must be nonpositive

matrices and the diagonal blocks W^{ii} must be Z -matrices. We define matrix $\tilde{K}^\theta = (\tilde{K}_{ij}^\theta)_{i,j=1}^3$ by setting $\tilde{K}_{ii}^\theta = K_{ii}^\theta$ and $\tilde{K}_{ij}^\theta = -|K_{ij}^\theta|$ for $i \neq j$. Then, condition **(W2)** can be restated in the compact form:

$$|P|U_P \leq \tilde{K}^\theta. \tag{11.40}$$

Combining conditions **(W1)** and **(W2)**, we obtain two inequality:

$$0 < |P|U_P \begin{pmatrix} \alpha \\ \beta \\ \gamma \end{pmatrix} \leq \tilde{K}^\theta \begin{pmatrix} \alpha \\ \beta \\ \gamma \end{pmatrix}.$$

From this and the assumptions on U_P , we derive two *necessary conditions* for parallelepipeds:

$$\tilde{K}^\theta \begin{pmatrix} \alpha \\ \beta \\ \gamma \end{pmatrix} > 0 \quad \text{and} \quad \tilde{K}^\theta \text{ is SPD.} \tag{11.41}$$

Note the difference with the two-dimensional case: the matrix \tilde{K}^θ is not always an SPD matrix. Conditions (11.41) constrain both the areas of faces f_i and the values of entries in K_P . They are necessary because no parameter matrix U_P satisfying **(W1)** and **(W2)** exists if these conditions are violated. The first inequality in (11.41) can be interpreted as an extension of the condition "C" derived in [291] to meshes of parallelepipeds.

Let \tilde{K}^θ be an SPD matrix. To maximize the sparsity structure of W_P , we can take a matrix U_P given by

$$U_P = \frac{\tilde{K}^\theta}{|P|}, \text{ which implies}$$

$$W_P = \frac{2}{|P|} \begin{pmatrix} K_{11}^\theta & 0 & K_{12}^{\theta,-} & -K_{12}^{\theta,+} & K_{13}^{\theta,-} & -K_{13}^{\theta,+} \\ 0 & K_{11}^\theta & -K_{12}^{\theta,+} & K_{12}^{\theta,-} & -K_{13}^{\theta,+} & K_{13}^{\theta,-} \\ \hline K_{21}^{\theta,-} & -K_{21}^{\theta,+} & K_{22}^\theta & 0 & K_{23}^{\theta,-} & -K_{23}^{\theta,+} \\ -K_{21}^{\theta,+} & K_{21}^{\theta,-} & 0 & K_{22}^\theta & -K_{23}^{\theta,+} & K_{23}^{\theta,-} \\ \hline K_{31}^{\theta,-} & -K_{31}^{\theta,+} & K_{32}^{\theta,-} & -K_{32}^{\theta,+} & K_{33}^\theta & 0 \\ -K_{31}^{\theta,+} & K_{31}^{\theta,-} & -K_{32}^{\theta,+} & K_{32}^{\theta,-} & 0 & K_{33}^\theta \end{pmatrix}, \tag{11.42}$$

where $K_{ij}^{\theta,\pm} = (K_{ij}^\theta \pm |K_{ij}^\theta|)/2$.

We have three off-diagonal entries in matrix K^θ that may be positive or negative; thus, we have six possible combinations of signs. In a special case of a scalar diffusion coefficient and a mesh of orthogonal bricks, we obtain the diagonal matrix (11.37).

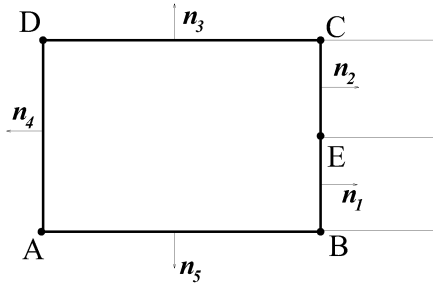


Fig. 11.3. Geometry of the AMR cell

11.2.4 AMR cells

In this subsection, we consider a special type of quadrilateral meshes that is used in the adaptive mesh refinement (AMR) strategy. The resulting AMR meshes have degenerate cells (see Fig. 11.3) and a discretization method should handle such cases. This makes the definition of discrete operators more challenging than that on regular quadrilateral meshes. In the MFD method, the AMR meshes are treated as general polygonal meshes and no special treatment of degenerate cells is required.

Let us consider the pentagon P shown in Fig. 11.3 as $ABECD$. The angle between the edges BE and EC is π ; therefore, we refer to this cell as the degenerate pentagon. We enumerate the cell edges as shown in this figure.

The size of the parameter matrix U_P is 3×3 ; hence, there are six parameters to be determined. Due to complexity of the analysis, we will focus on rectangular meshes and diagonal diffusion tensors. To further simplify the analysis, we impose additional constraints on the matrix W_P which mimic the geometric symmetry of P . Let us consider the following discrete solution:

$$p_P = 0, \quad p_{f_1} = p_{f_2} = 1, \quad \text{and} \quad p_{f_3} = p_{f_4} = p_{f_5} = 0.$$

This solution is symmetric with respect to the line parallel to edge AB and passing through the vertex E . We require that the discrete fluxes have the same symmetry, which means that $u_{P,f_1} = u_{P,f_2}$ and $u_{P,f_3} = -u_{P,f_5}$. Let $W_P = (w_{ij})_{i,j=1}^5$. Substituting the discrete solution into formula (11.22), we rewrite the first flux symmetry constraint as follows:

$$-u_{P,f_1} = w_{11}|f_1| + w_{12}|f_2| = w_{21}|f_1| + w_{22}|f_2| = -u_{P,f_2}.$$

Since $|f_1| = |f_2|$ and $w_{12} = w_{21}$, we obtain that $w_{11} = w_{22}$. We repeat this argument to derive symmetry constraints for the other entries of W_P :

$$w_{33} = w_{55}, \quad w_{23} = w_{15}, \quad \text{and} \quad w_{14} = w_{24}. \quad (11.43)$$

Without loss of generality, we assume temporarily that $|P| = 1$ and later rescale the matrix of parameters U_P to get a general formula. Let $r^2 = \frac{f_{AD}}{f_{AB}}$ denote the aspect ratio of P . Then, matrix R_P takes the form:

$$R_P = \begin{pmatrix} |f_{BE}| (\mathbf{x}_{BE} - \mathbf{x}_P)^T \\ |f_{EC}| (\mathbf{x}_{EC} - \mathbf{x}_P)^T \\ |f_{DC}| (\mathbf{x}_{DC} - \mathbf{x}_P)^T \\ |f_{AD}| (\mathbf{x}_{AD} - \mathbf{x}_P)^T \\ |f_{AB}| (\mathbf{x}_{AB} - \mathbf{x}_P)^T \end{pmatrix} = \frac{1}{8} \begin{pmatrix} 2 & -r^2 \\ 2 & r^2 \\ 0 & 4 \\ -4 & 0 \\ 0 & -4 \end{pmatrix}. \quad (11.44)$$

Matrix N_P takes the form:

$$N_P = \begin{pmatrix} \mathbf{n}_{BE}^T \\ \mathbf{n}_{EC}^T \\ \mathbf{n}_{DC}^T \\ \mathbf{n}_{AD}^T \\ \mathbf{n}_{AB}^T \end{pmatrix} K_P = \begin{pmatrix} K_{11} & 0 \\ K_{11} & 0 \\ 0 & K_{22} \\ -K_{11} & 0 \\ 0 & -K_{22} \end{pmatrix}. \quad (11.45)$$

Matrix D_P is not defined uniquely. Among many possible choice, we select the following:

$$D_P^T = \begin{pmatrix} 2 & -2 & r^2 & 0 & 0 \\ 1 & 1 & 0 & 1 & 0 \\ -2 & 2 & 0 & 0 & r^2 \end{pmatrix}. \quad (11.46)$$

It is easy to check that $D_P^T R_P = 0$. Let $U_P = (u_{ij})_{i,j=1}^3$. By calculating matrix W_P and using the symmetry relations (11.43), we prove that $u_{11} = u_{33}$ and $u_{12} = u_{23}$. These two conditions allows us to reduce the number of parameters from six to four. With this relations, the matrix W_P is given by:

$$\begin{pmatrix} w_{11} & w_{12} & w_{13} & u_{22} - K_{11} & w_{15} \\ w_{21} & w_{22} & w_{23} & u_{22} - K_{11} & w_{25} \\ w_{31} & w_{32} & u_{11}r^4 + K_{22} & u_{12}r^2 & u_{13}r^4 - K_{22} \\ u_{22} - K_{11} & u_{22} - K_{11} & u_{12}r^2 & u_{22} + K_{11} & u_{12}r^2 \\ w_{51} & w_{52} & u_{13}r^4 - K_{22} & u_{12}r^2 & u_{11}r^4 + K_{22} \end{pmatrix}.$$

where the remaining entries in the first row are given by

$$w_{11} = K_{11} + 8u_{11} - 8u_{13} + u_{22}, \quad w_{12} = K_{11} - 8u_{11} + 8u_{13} + u_{22}, \\ w_{13} = w_{31} = (2u_{11} + u_{12} - 2u_{13})r^2, \quad w_{15} = w_{51} = (2u_{13} + u_{12} - 2u_{11})r^2,$$

and in the second row by

$$w_{21} = K_{11} - 8u_{11} + 8u_{13} + u_{22}, \quad w_{22} = K_{11} + 8u_{11} - 8u_{13} + u_{22}, \\ w_{23} = w_{32} = (-2u_{11} + u_{12} + 2u_{13})r^2, \quad w_{25} = w_{52} = (-2u_{13} + u_{12} + 2u_{11})r^2.$$

Let us define a vector \mathbf{f} whose components are the edge lengths of the pentagon. Since $|\mathbf{P}| = 1$, we have $\mathbf{f} = (0.5r, 0.5r, r^{-1}, r, r^{-1})^T$. Condition **(W1)** implies that

$$W_P \mathbf{f} = \begin{pmatrix} 2r(u_{22} + u_{12}) \\ 2r(u_{22} + u_{12}) \\ r^3(2u_{12} + u_{11} + u_{13}) \\ 2r(u_{22} + u_{12}) \\ r^3(2u_{12} + u_{11} + u_{13}) \end{pmatrix} > 0.$$

This gives the first set of inequality constraints:

$$\begin{cases} u_{22} + u_{12} > 0, \\ 2u_{12} + u_{11} + u_{13} \geq 0 \end{cases} \quad \text{or} \quad \begin{cases} u_{22} + u_{12} \geq 0, \\ 2u_{12} + u_{11} + u_{13} > 0. \end{cases} \tag{11.47}$$

Condition **(W2)** adds the second set of inequality constraints:

$$\begin{cases} u_{11} > 0, \\ u_{13} \leq K_{22}r^{-4}, \\ 0 < u_{22} \leq K_{11}, \\ u_{12} \leq -2u_{11} - u_{13}, \\ u_{11} - u_{13} \geq \frac{1}{8}(u_{22} + K_{11}). \end{cases} \tag{11.48}$$

The third set of inequalities state that the matrix U_P is SPD, i.e., all major minors of U_P must be positive:

$$\begin{cases} u_{12}^2 < u_{11}u_{22}, \\ u_{12}^2 < \frac{1}{2}u_{22}(u_{11} + u_{13}). \end{cases} \tag{11.49}$$

By combining the third and fifth inequalities in (11.48), we conclude that $u_{11} - u_{13} > K_{11}/8$. Thus, the solution to the second inequality in (11.49) is always the solution of the first one. Analysis of the combined system of inequalities (11.47)–(11.49) results in the following lemma.

Lemma 11.2. *A matrix W_P satisfying conditions **(W1)** and **(W2)** exists if and only if*

$$r^4 < 4 \frac{K_{22}}{K_{11}}. \tag{11.50}$$

For each aspect ratio r satisfying (11.50), we obtain a family of monotone mimetic schemes. The closer the aspect ratio to the limiting value $4K_{22}/K_{11}$, the narrower this family. Among many of possible choices, we present two particular members of this family including the proper scaling for $|\mathbf{P}| \neq 1$. The first one reduces the number of nonzero entries in the matrix W_P . The matrix U_P and the sparsity structure of the matrix W_P are

$$U_P = \frac{1}{4|\mathbf{P}|} \begin{pmatrix} \frac{4}{r^4}K_{22} + K_{11} & -2K_{11} & \frac{4}{r^4}K_{22} \\ -2K_{11} & 4K_{11} & -2K_{11} \\ \frac{4}{r^4}K_{22} & -2K_{11} & \frac{4}{r^4}K_{22} + K_{11} \end{pmatrix}, \quad W_P = \begin{pmatrix} * & 0 & 0 & 0 & * \\ 0 & * & * & 0 & 0 \\ 0 & * & * & * & 0 \\ 0 & 0 & * & * & * \\ * & 0 & 0 & * & * \end{pmatrix}.$$

This choice requires a stronger condition on the aspect ration,

$$r^4 < \frac{8K_{22}}{3K_{11}}.$$

Otherwise, when the aspect ratio is close to this limiting value, we suggest another member in a family:

$$U_P = \frac{1}{6|P|} \begin{pmatrix} \frac{6}{r^4}K_{22} + K_{11} & -2K_{11} & \frac{6}{r^4}K_{22} \\ -2K_{11} & 2K_{11} & -2K_{11} \\ \frac{6}{r^4}K_{22} & -2K_{11} & \frac{6}{r^4}K_{22} + K_{11} \end{pmatrix}, \quad W_P = \begin{pmatrix} * & 0 & 0 & * & * \\ 0 & * & * & * & 0 \\ 0 & * & * & * & 0 \\ * & * & * & * & * \\ * & 0 & 0 & * & * \end{pmatrix}.$$

11.3 Monotonicity conditions for the nodal formulation

For a nodal mimetic discretization developed in Chap. 6, the sufficient condition for the monotonicity is that the global stiffness matrix is an M-matrix. This property can be achieved by requiring that each local stiffness matrix M_P is an M-matrix.

11.3.1 Geometric notation for a quadrilateral cell

Following [264], we define a few geometric objects on a quadrilateral cell P . Let $\mathbf{d}_i, i = 1, \dots, 4$, be four oriented diagonal vectors; T_i and \widehat{T}_i be four related pairs of triangles, $P = T_i \cup \widehat{T}_i$, see Fig. 11.4 for details. By definition, it holds that $\mathbf{d}_3 = -\mathbf{d}_1$ and $\mathbf{d}_4 = -\mathbf{d}_2$; therefore, later we will use only \mathbf{d}_1 and \mathbf{d}_2 . Furthermore, $\widehat{T}_1 = T_3, \widehat{T}_2 = T_4, \widehat{T}_3 = T_1$, and $\widehat{T}_4 = T_2$. To ease the notation, we denote the oriented areas of the triangles T_i and \widehat{T}_i by the same symbols T_i and \widehat{T}_i , respectively. Thus,

$$|P| = \widehat{T}_1 + \widehat{T}_3 = \widehat{T}_2 + \widehat{T}_4.$$

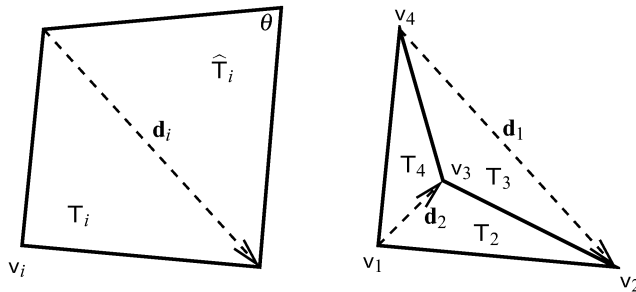


Fig. 11.4. The left picture shows the diagonal vector \mathbf{d}_i in a convex quadrilateral and the triangles T_i and \widehat{T}_i associated with the vertex v_i . The right picture shows the diagonal vectors \mathbf{d}_1 and \mathbf{d}_2 and the triangles T_2, T_3 , and T_4 in a concave quadrilateral. The triangle T_1 (not shown) is defined by vertices v_1, v_2 , and v_4 . Note that the oriented area of T_3 is negative. In both pictures, the subscript i runs from 1 to 4 counter clock-wise

When P is a nonconvex quadrilateral, one and only one of the four oriented areas \widehat{T}_i is negative.

11.3.2 Sufficient monotonicity conditions on quadrilaterals cells

Let \widetilde{K}_P be the rotated permeability tensor K_P :

$$\widetilde{K}_P = \mathcal{R}_{90}^T K_P \mathcal{R}_{90} \quad \text{with} \quad \mathcal{R}_{90} = \begin{pmatrix} 0 & 1 \\ -1 & 0 \end{pmatrix}. \quad (11.51)$$

As mentioned in Chap. 6, the total number of parameters appearing in matrix M_P is equal to $k = (N_P^{\mathcal{V}} - d)(N_P^{\mathcal{V}} - d - 1)/2$, where $N_P^{\mathcal{V}}$ is the number of vertices in P . For a quadrilateral, $N_P^{\mathcal{V}} = 4$ and $d = 2$, so that $k = 1$ and we have a one-parameter family of stiffness matrices M_P . Furthermore, we have a special representation of entries of matrix M_P derived in [264].

Lemma 11.3. *The ij -entry in the matrix M_P has the following representation:*

$$(M_P)_{ij} = (M_P^{(0)})_{ij} + (M_P^{(1)})_{ij} = \frac{1}{4|P|} \mathbf{d}_i \cdot \widetilde{K}_P \mathbf{d}_j + (-1)^{i+j} \frac{\widehat{T}_i \widehat{T}_j}{|P|^2} u_{11}, \quad (11.52)$$

where u_{11} is a nonnegative parameter.

Matrix M_P may be an M-matrix for some values of parameter u_{11} . Let us discuss how the range of such values of u_{11} depends on the shape of P and permeability tensor K_P .

Note that matrix $M_P^{(0)}$, which is the consistency term in matrix M_P , has the block-structured form:

$$M_P^{(0)} = \frac{1}{4|P|} \begin{pmatrix} S & -S \\ -S & S \end{pmatrix} \quad \text{where} \quad S = \begin{pmatrix} \mathbf{d}_1^T \widetilde{K}_P \mathbf{d}_1 & \mathbf{d}_1^T \widetilde{K}_P \mathbf{d}_2 \\ \mathbf{d}_2^T \widetilde{K}_P \mathbf{d}_1 & \mathbf{d}_2^T \widetilde{K}_P \mathbf{d}_2 \end{pmatrix}.$$

As stated in the next theorem, cell convexity is the necessary condition for M_P to be an M-matrix.

Theorem 11.8. (i) *Let P be a convex quadrilateral cell and parameter u_{11} satisfy two inequalities*

$$\max \left\{ \frac{-\mathbf{d}_1^T \widetilde{K}_P \mathbf{d}_2}{\min(\widehat{T}_1 \widehat{T}_4, \widehat{T}_2 \widehat{T}_3)}, \frac{\mathbf{d}_1^T \widetilde{K}_P \mathbf{d}_2}{\min(\widehat{T}_1 \widehat{T}_2, \widehat{T}_3 \widehat{T}_4)} \right\} \leq \frac{4u_{11}}{|P|}, \quad (11.53)$$

$$\frac{4u_{11}}{|P|} \leq \min \left\{ \frac{\mathbf{d}_1^T \widetilde{K}_P \mathbf{d}_1}{\widehat{T}_1 \widehat{T}_3}, \frac{\mathbf{d}_2^T \widetilde{K}_P \mathbf{d}_2}{\widehat{T}_2 \widehat{T}_4} \right\}. \quad (11.54)$$

Then, matrix M_P is an M-matrix.

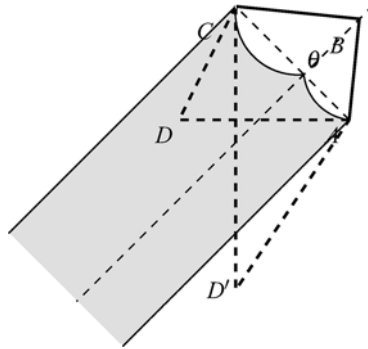


Fig. 11.5. A sketch of the monotonicity region (shaded region) for $K_P = I$ and three fixed vertices A, B, C

(ii) Let P be a non-convex quadrilateral cell. Then, there exist no parameter u_{11} for which M_P is an M -matrix.

Proof. From representation (11.52) it follows readily that inequalities (11.53)–(11.54) are sufficient conditions for M_P being an M -matrix. If P is a non-convex cell, then it holds that either $\widehat{T}_1 \widehat{T}_3 < 0$ or $\widehat{T}_2 \widehat{T}_4 < 0$. In such a case, the right-hand side of inequality (11.54) is strictly negative for a non-degenerate cell P . Therefore, it is impossible to find a positive number u_{11} that satisfies these inequalities. \square

Using Theorem 11.8, we introduce the concept of *monotonicity region*, which is illustrated in Fig. 11.5. Let us fix three vertices of the quadrilateral cell, for example, A, B and C , and vary the position of the fourth vertex D . The shaded region represents the monotonicity region of vertex D : when it lies inside this region, a non-empty set of values of u_{11} satisfying inequalities (11.53)–(11.54) exists for the quadrilateral cell $ABCD$. Otherwise, if vertex D lies outside the shaded region, as D' on the figure, inequalities (11.53)–(11.54) cannot be satisfied. Therefore, there is no value of u_{11} for which M_P can be an M -matrix for the quadrilateral cell $ABCD'$.

The shape of the monotonicity region depends on the angle $\theta = \widehat{ABC}$ and the diffusion tensor K_P . In Fig. 11.6, we plot monotonicity regions for the identity tensor and different angles θ . In Fig. 11.7, we plot monotonicity regions for the same angles but a full diffusion tensor K_P . By comparison of the plots in two figures, we observe that the full diffusion tensor rotates the monotonicity region.

For the identity diffusion tensor, the monotonicity region tends to an infinite strip whose base is the segment AC when θ becomes a very acute angle. Moreover, an infinite part of the ray originating at point B and orthogonal to segment AC is always inside the monotonicity region for any value of θ from very obtuse to very acute. Indeed, when D lies on this ray, the right-hand side of (11.54) is strictly positive and the left-hand side of (11.53) is always zero.

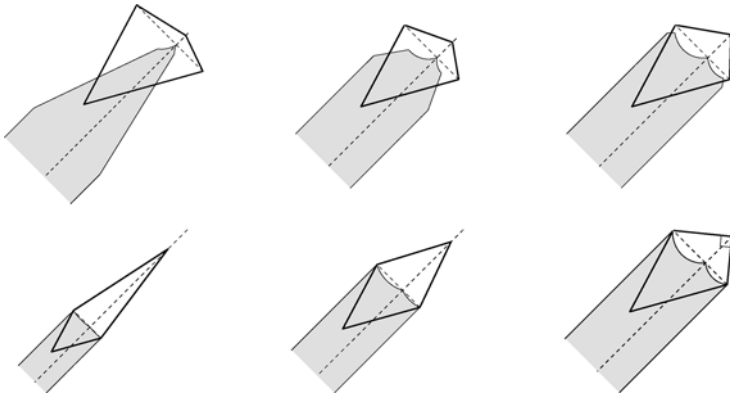


Fig. 11.6. Monotonicity regions (shaded area) for $K_P = I$ and different angles $\theta = \widehat{ABC}$ which take values 147° , 119° , and 98° in the top row, and 20° , 47° and 90° , in the bottom row

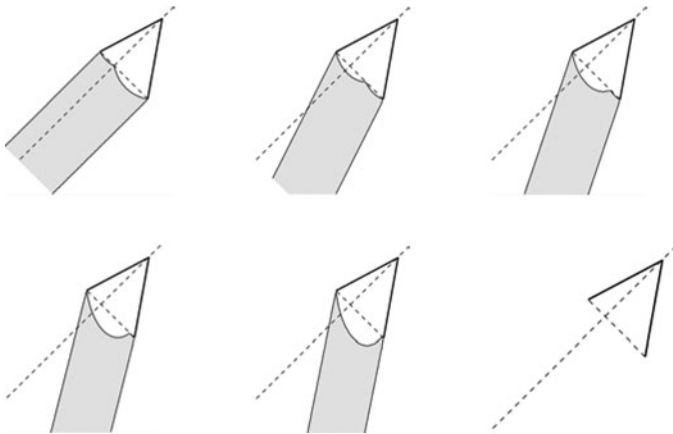


Fig. 11.7. Monotonicity regions (shaded area) for a full tensor K_P and the same angles $\theta = \widehat{ABC}$ as in Fig. 11.6. The full tensor rotates the monotonicity region. Note the existence of a limiting angle beyond which the monotonicity region is empty

Remark 11.3. The above analysis can be used in mesh generation algorithms to formulate an additional quality metric.

11.4 Non-linear optimization

In Sect. 11.2 we presented a set of results that hold for specially shaped cells such as simplexes, parallelograms, tilted parallelepipeds, and degenerate pentagons. Nonetheless, the theoretical developments leading to conditions **(W1)**–**(W2)** are

quite general and can be applied to arbitrarily shaped cells. In this section, we enforce these conditions by solving a nonlinear optimization problem. To this end, let us introduce two quantities:

$$E = \max_{i \neq j} w_{ij} \quad \text{and} \quad F = \min_i \sum_j w_{ij} |f_j|. \quad (11.55)$$

The quantity E controls the off-diagonal entries of matrix W_P , and is thus related to condition **(W2)**. The quantity F controls the property of W_P being a diagonally dominant matrix and is thus related to condition **(W1)**. The following simple lemma shows that we have to minimize E and maximize F to find an M-matrix.

Lemma 11.4. *Let matrix W_P be given by (11.25) and such that $E \leq 0$ and $F > 0$. Then, W_P satisfies conditions **(W1)**–**(W2)**.*

To control the SPD property of the parameter matrix U_P in the optimization strategy, we employ its Cholesky factorization $U_P = L_P L_P^T$, where L_P is a lower triangular matrix. The diagonal entries of $L_P = (\ell_{ij})$ must be positive real numbers since U_P is SPD. Let γ_P be the trace of W_P^0 . We denote by \tilde{U}_P one of the matrices listed below (note that the last choice does not always give an SPD matrix):

- (i) $\tilde{U}_P = \gamma_P I_P$;
- (ii) $\tilde{U}_P = \gamma_P (D_P D_P^T)^{-1}$;
- (iii) \tilde{U}_P is given by the least square solution of $\min_{i \neq j} |w_{ij}|^2$.

Let $\tilde{U}_P = \tilde{L}_P \tilde{L}_P^T$ be the Cholesky decomposition of \tilde{U}_P . We consider the following objective functional:

$$f(E, F, L_P) = v(E; \varepsilon_E) - \varepsilon_F F + \varepsilon_L \|\tilde{L}_P - L_P\|_{\mathbb{F}}^2, \quad (11.56)$$

where $\varepsilon_E > 0$, $\varepsilon_F \geq 0$, $\varepsilon_L \geq 0$ are tuning parameters, $\|\cdot\|_{\mathbb{F}}$ is the Frobenius norm of a matrix, and $v(E; \varepsilon_E)$ is the wall function:

$$v(E) = E + \sqrt{\varepsilon_E^2 + E^2}. \quad (11.57)$$

Now, we solve the following non-linear constrained optimization problem:

$$\begin{aligned} & \text{minimize} && f(E, F, L_P) \\ & \text{subject to:} && w_{ij} - E \geq 0 && \forall i \neq j, \\ & && F - \sum_j w_{ij} \geq 0 && \forall i, \\ & \text{and:} && E, F \in \mathbb{R} \\ & && 0 < \ell_{ii} \leq +\infty && \forall i, \\ & && \ell_{ij} \in \mathbb{R} && \forall i \neq j. \end{aligned} \quad (11.58)$$

Let us introduce the compact notation for the constraints:

$$g_{pq}(E, F, L_P) = \begin{cases} E - w_{pq} & \text{for } p < q, \\ \sum_j w_{pj} |f_j| - F & \text{for } p = q. \end{cases}$$

The Lagrangian of the minimization problem is given by:

$$\mathcal{L}(E, F, L_P, \boldsymbol{\mu}) = f(E, F, L_P) - \sum_{p \leq q} \mu_{pq} g_{pq}(E, F, L_P), \quad (11.59)$$

where $\boldsymbol{\mu} = (\mu_{pq})_{p \leq q}$ is the vector of Lagrange multipliers. A part of the Jacobian matrix related to the constraints has the following entries:

$$\begin{aligned} \frac{\partial g_{pq}}{\partial E} &= 1 \text{ for } p < q & \text{and} & \quad \frac{\partial g_{pp}}{\partial E} = 0 \\ \frac{\partial g_{pq}}{\partial F} &= 0 \text{ for } p < q & \text{and} & \quad \frac{\partial g_{pp}}{\partial F} = -1 \\ \frac{\partial g_{pq}}{\partial \ell_{ij}} &= -\frac{\partial w_{pq}}{\partial \ell_{ij}} \text{ for } p < q & \text{and} & \quad \frac{\partial g_{pp}}{\partial \ell_{ij}} = \sum_q \frac{\partial w_{pq}}{\partial \ell_{ij}} |f_q|. \end{aligned} \quad (11.60)$$

The last two terms can be computed efficiently using the formula provided by the following lemma.

Lemma 11.5. *Let $W_P = (w_{ij})$ be given by (11.25), where $D_P = (d_{ij})$, $U_P = L_P L_P^T$ and $L_P = (\ell_{ij})$ is the low triangular matrix. Then,*

$$\frac{\partial w_{pq}}{\partial \ell_{ij}} = \sum_{k \geq j} (d_{qk} d_{pi} + d_{pk} d_{qi}) \ell_{kj}. \quad (11.61)$$

Proof. Let \mathbf{e}_p be the p -th vector of the canonical basis of \mathbb{R}^p , i.e., this vector has 1 in the p -th position and zero elsewhere. Since $w_{pq} = w_{pq}^0 + ((D_P L_P)(D_P L_P)^T)_{pq}$ and w_{pq}^0 does not depend on L_P , we have:

$$\frac{\partial w_{pq}}{\partial \ell_{ij}} = \frac{\partial}{\partial \ell_{ij}} \left((D_P L_P)(D_P L_P)^T \right)_{pq} = \frac{\partial}{\partial \ell_{ij}} \left(\mathbf{e}_p^T (D_P L_P)(D_P L_P)^T \mathbf{e}_q \right)_{pq}.$$

Using the chain rule, the derivative becomes:

$$\frac{\partial w_{pq}}{\partial \ell_{ij}} = \mathbf{e}_p^T \left(D_P \frac{\partial L_P}{\partial \ell_{ij}} \right) (D_P L_P)^T \mathbf{e}_q + \mathbf{e}_p^T (D_P L_P) (D_P \frac{\partial L_P}{\partial \ell_{ij}})^T \mathbf{e}_q.$$

Since $\partial L_P / \partial \ell_{ij} = \mathbf{e}_i \mathbf{e}_j^T$, the straightforward calculations give:

$$\begin{aligned} \frac{\partial w_{pq}}{\partial \ell_{ij}} &= \mathbf{e}_p^T (D_P \mathbf{e}_i \mathbf{e}_j^T) (D_P L_P)^T \mathbf{e}_q + \mathbf{e}_p^T (D_P L_P) (D_P \mathbf{e}_i \mathbf{e}_j^T)^T \mathbf{e}_q \\ &= (\mathbf{e}_p^T D_P \mathbf{e}_i) \mathbf{e}_j^T (D_P L_P)^T \mathbf{e}_q + \mathbf{e}_p^T (D_P L_P) \mathbf{e}_j (\mathbf{e}_i^T D_P^T \mathbf{e}_q) \\ &= d_{pi} (D_P L_P)_{qj} + (D_P L_P)_{pj} d_{qi}. \end{aligned} \quad (11.62)$$

Equation (11.61) follows by noting that

$$(\mathbf{D}_P \mathbf{L}_P)_{sj} = \sum_{k \geq j} d_{sk} \ell_{kj}$$

since \mathbf{L}_P is a lower triangular matrix. □

Diffusion problem on generalized polyhedral meshes

The minimal surface area partition of space into cells of equal volume is a tiling by truncated octahedra with slightly curved faces.
(Lord Kelvin’s conjecture)

A *generalized polyhedron* is a topological polyhedron, i.e. a solid defined by a bi-Lipschitz mapping of a polyhedron. The faces of a generalized polyhedron are usually non-planar (or curved) but edges may remain straight line segments. A *generalized polyhedral mesh* is a mesh containing generalized polyhedra. Such a mesh often appears in Lagrangian fluid flow simulations where the computational mesh moves with flow.

It was shown experimentally in [254] that the MFD method for the diffusion problem in the mixed form described in Chap. 5 does not converge on generalized polyhedral meshes. A similar statement can be made for the lower-order Raviart-Thomas finite element method, see Fig. 12.1 where we solve a simple Poisson equation in a unit cube.

A straightforward solution is to approximate a strongly curved face by triangles to get a polyhedral mesh where all elements have planar faces. The number of

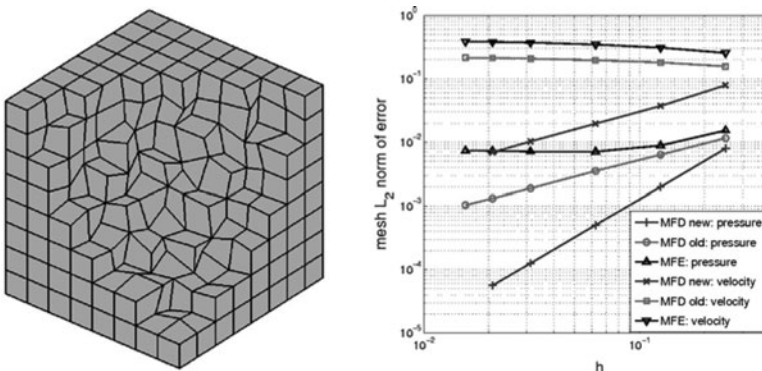


Fig. 12.1. Left picture shows a logically cubic mesh with randomly perturbed interior vertices. The right picture shows convergence graphs for the MFD method (+ and x) described in this chapter, mixed finite element method (triangles) and the MFD method described in Chap. 5 (squares and circles)

flux degrees of freedom grows linearly with the number of these triangles. Potential problem with such an approach is that an approximate piecewise-linear representation of smooth material interfaces and external boundaries may lead to profoundly non-physical numerical effects including spurious dispersion, anisotropy and reflection/scattering in simulations of acoustic, visco-elastic and electromagnetic waves. It may also break the symmetries of boundary and initial conditions and even change convergence properties with mesh refinement.

Another approach is considered in this chapter. It incorporates the face curvature into the discretization and uses only three degrees of freedom for every strongly curved face regardless of the number of its vertices. The new mimetic scheme is developed for a diffusion problem; however, the underlying ideas can be extended to other PDEs.

Other discretization schemes [2, 276] can be also used to solve diffusion problems on generalized polyhedral meshes; however, to the best of our knowledge, the convergent schemes result in non-symmetric discrete problems which reduces significantly the number of available efficient algebraic solvers. The MFD method, by its nature, results always in a symmetric discrete problem.

12.1 Diffusion problem in mixed form

Let Ω be an open connected subset of \mathfrak{R}^3 with a Lipschitz continuous boundary. We consider the diffusion problem in the mixed form:

$$\mathbf{u} + \mathbf{K}\nabla p = 0 \quad \text{in } \Omega, \quad (12.1)$$

$$\operatorname{div} \mathbf{u} = b \quad \text{in } \Omega, \quad (12.2)$$

$$p = g^D \quad \text{on } \partial\Omega, \quad (12.3)$$

where the vector variable \mathbf{u} represents the flux of the scalar unknown p , \mathbf{K} is a *full symmetric* tensor, and b is a source function. The unknown p may be a pressure, a temperature, or a flow density depending on the physical interpretation that we give to this mathematical model.

We assume for simplicity that the homogeneous Dirichlet boundary condition, $g^D = 0$, is imposed on $\partial\Omega$. Other types of boundary conditions can be also incorporated into the mimetic scheme, see for example [206] and Chap. 5. We also make the following assumption.

(H1b) Every component of tensor \mathbf{K} is in $W^{1,\infty}(\Omega)$ and \mathbf{K} is strongly elliptic, i.e. there exist two positive constants κ_* and κ^* such that

$$\kappa_* \|\boldsymbol{\xi}\|^2 \leq \boldsymbol{\xi}^T \mathbf{K}(\mathbf{x}) \boldsymbol{\xi} \leq \kappa^* \|\boldsymbol{\xi}\|^2 \quad \forall \boldsymbol{\xi} \in \mathfrak{R}^3, \quad \mathbf{x} \in \Omega. \quad (12.4)$$

12.2 Polyhedral meshes with curved faces

Let Ω_h be a non-overlapping conformal partition of Ω into generalized polyhedra P . For simplicity, we will often refer to them as polyhedra. Intersection of any two distinct generalized polyhedra is either empty, or a few mesh vertices, or a few mesh edges, or a few mesh faces. Two adjacent polyhedra may share more than one edge or more than one face.

As usual, we denote by $|P|$ the volume of P and by h_P its diameter. For every face f , we denote by $|f|$ its area and by h_f its diameter. We finally set $h = \sup_P h_P$ and consider a sequence of generalized polyhedral meshes $\{\Omega_h\}_h$ where $h \rightarrow 0$.

Since mesh faces can be curved, we cannot use the mesh regularity assumptions (MR) of Chap. 1. An alternative way to characterize the shape properties of a generalized polyhedron is based on the definition of a *generalized pyramid*.

Definition 12.1. Let $k \geq 3$ be an integer, and γ_* and τ_* be positive real numbers, with $\gamma_* < 1$. A generalized pyramid Q with k lateral faces and shape-regularity constants γ_* and τ_* is a subset of \mathfrak{R}^3 that can be constructed with the following three steps:

1. Take a pyramid \widehat{Q} whose base \widehat{f} is a convex polygon with k edges. Let $v_{\widehat{Q}}$ be the vertex of this pyramid, $h_{\widehat{Q}}$ be its diameter, and $H_{\widehat{Q}}$ be its height (see Fig. 12.2).

Up to a rigid-body displacement, we can assume that $v_{\widehat{Q}}$ is in the origin and \widehat{f} is a subset of the plane $z = H_{\widehat{Q}}$. We also assume that \widehat{Q} contains a sphere of radius

$$r \geq \gamma_* h_{\widehat{Q}}.$$

2. Define a *radial* one-to-one C^1 mapping Φ of the pyramid \widehat{Q} into itself. In a radial map a point \mathbf{x} and its image $\mathbf{x}' = \Phi(\mathbf{x})$ lie on the same ray emanating from the origin. We assume that

$$\max_{\mathbf{x} \in \widehat{Q}} \|\nabla \Phi(\mathbf{x})\| \leq \tau_* \quad \text{and} \quad \max_{\mathbf{x}' \in \widehat{Q}} \|\nabla(\Phi^{-1})(\mathbf{x}')\| \leq \tau_*. \quad (12.5)$$

The norms in (12.5) are the usual Euclidean norms of 3×3 matrices.

3. Define the generalized pyramid $Q \equiv \Phi(\widehat{Q})$. The image of the base \widehat{f} is a C^1 surface f , $f \equiv \Phi(\widehat{f})$, that we will refer to as the *base* of the generalized pyramid. Accordingly, the images of the k lateral faces of \widehat{Q} will be referred to as the lateral faces of Q .

The convexity assumption of \widehat{f} could be replaced with a star-shaped assumption (see [90] for more details). However, for simplicity of the presentation, we will not do it here. Nevertheless, the following definition of a generalized polyhedron allows us to keep the class of admissible generalized polyhedral meshes sufficiently large.

Definition 12.2. A generalized polyhedron P is formed by the generalized pyramids that have the same vertex \bar{x}_P . The vertex \bar{x}_P lies strictly inside P . The boundary ∂P

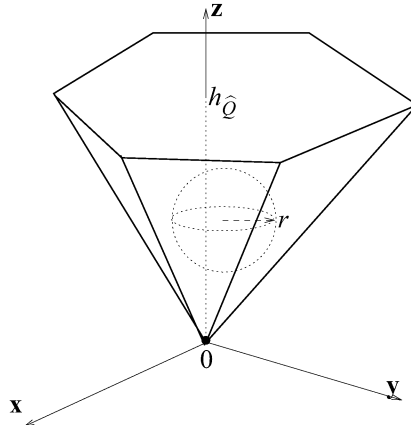


Fig. 12.2. Pyramid \widehat{Q} containing a sphere of radius r

is the union of the bases of the generalized pyramids. These bases will be referred to as the faces of P .

Consider a generalized pyramid Q . According to Definition 12.1, at each point of its base f , we can define a normal unit vector \mathbf{n}_f pointing outward of Q and varying continuously with the point. Thus, we can define the *average normal vector* $\widetilde{\mathbf{n}}_f$ as

$$\widetilde{\mathbf{n}}_f = \frac{1}{|f|} \int_f \mathbf{n}_f dS. \quad (12.6)$$

It is not difficult to see that $\|\widetilde{\mathbf{n}}_f\| \leq 1$. A lower bound for $\|\widetilde{\mathbf{n}}_f\|$ depends on γ_* , τ_* and is contained in the following technical lemma.

Lemma 12.1. *Let Q be a generalized pyramid with shape regularity constants γ_* and τ_* . Let f be its base and let $\widetilde{\mathbf{n}}_f$ be the average normal to f defined in (12.6). Then,*

$$\|\widetilde{\mathbf{n}}_f\| \geq \frac{2\gamma_*}{\tau_*^4}. \quad (12.7)$$

Proof. Definition 12.1 implies that there exists a bijective mapping $\varphi: \widehat{f} \rightarrow \mathfrak{R}$ such that the restriction of Φ to f can be written as

$$x' = x\varphi(x,y), \quad y' = y\varphi(x,y), \quad z' = H_{\widehat{Q}}\varphi(x,y). \quad (12.8)$$

Using assumption (12.5), it is not difficult to check that for every pair of points \mathbf{x}_1 and \mathbf{x}_2 on \widehat{f} , and their images $\mathbf{x}'_1 = \Phi(\mathbf{x}_1)$ and $\mathbf{x}'_2 = \Phi(\mathbf{x}_2)$ on f , we have

$$\|\mathbf{x}'_1 - \mathbf{x}'_2\| \leq \tau_* \|\mathbf{x}_1 - \mathbf{x}_2\| \quad \text{and} \quad \|\mathbf{x}_1 - \mathbf{x}_2\| \leq \tau_* \|\mathbf{x}'_1 - \mathbf{x}'_2\|. \quad (12.9)$$

By the basic vector calculus, we have

$$\int_{\hat{f}} \mathbf{n}_{\hat{f}} dS = \int_{\hat{f}} \frac{\partial \mathbf{x}'}{\partial x} \times \frac{\partial \mathbf{x}'}{\partial y} dx dy. \quad (12.10)$$

Differentiating (12.8), we obtain

$$\frac{\partial \mathbf{x}'}{\partial x} = (\varphi + x\varphi_x, y\varphi_x, H_{\hat{Q}}\varphi_x) \quad \text{and} \quad \frac{\partial \mathbf{x}'}{\partial y} = (x\varphi_y, \varphi + y\varphi_y, H_{\hat{Q}}\varphi_y).$$

A lengthy but easy calculation gives

$$\frac{\partial \mathbf{x}'}{\partial x} \times \frac{\partial \mathbf{x}'}{\partial y} = \left(-H_{\hat{Q}}\varphi\varphi_x, -H_{\hat{Q}}\varphi\varphi_y, \varphi^2 + \varphi(x\varphi_x + y\varphi_y) \right). \quad (12.11)$$

Now, let $\xi \equiv (\xi_1, \xi_2, H_{\hat{Q}})$ be a point in \hat{f} and $g = \varphi^2/2$. Using (12.11) and (12.10) in (12.6), and then integrating by parts, we get

$$\begin{aligned} \tilde{\mathbf{n}}_{\hat{f}} \cdot \xi &= \frac{1}{|\hat{f}|} \int_{\hat{f}} H_{\hat{Q}}(2g + (x - \xi_1)g_x + (y - \xi_2)g_y) dx dy \\ &= \frac{H_{\hat{Q}}}{|\hat{f}|} \left(\int_{\hat{f}} (2g - g - g) dx dy + \int_{\partial \hat{f}} g (x - \xi_1)v_x + (y - \xi_2)v_y \right), \end{aligned}$$

where (v_x, v_y) is the outward unit normal to $\partial \hat{f}$ lying in the plane $z = H_{\hat{Q}}$. Since ξ is internal to \hat{f} and \hat{f} is convex, we have

$$(x - \xi_1)v_x + (y - \xi_2)v_y \geq 0.$$

Let g_{min} be the minimum value of g on $\partial \hat{f}$. Using first the mean value theorem for integrals and then the divergence theorem in the plane $z = H_{\hat{Q}}$, we obtain

$$\tilde{\mathbf{n}}_{\hat{f}} \cdot \xi \geq g_{min} \frac{H_{\hat{Q}}}{|\hat{f}|} \int_{\partial \hat{f}} (x - \xi_1)v_x + (y - \xi_2)v_y dl = (\varphi^2)_{min} H_{\hat{Q}} \frac{|\hat{f}|}{|\hat{f}|}.$$

Thus, the Cauchy-Schwarz inequality implies that

$$\|\tilde{\mathbf{n}}_{\hat{f}}\| \geq (\varphi^2)_{min} \frac{H_{\hat{Q}}}{\|\xi\|} \frac{|\hat{f}|}{|\hat{f}|}. \quad (12.12)$$

To complete the proof, we have to estimate three factors in the right hand side of (12.12). From (12.9), we have easily that

$$|\hat{f}| \leq \tau_*^2 |\hat{f}|. \quad (12.13)$$

Next, using (12.5) and taking any point \mathbf{x} on $\partial \hat{f}$, its image point $\mathbf{x}' = \Phi(\mathbf{x})$ on ∂f , we have $\|\mathbf{x}\| \leq \tau_* \|\mathbf{x}'\|$. Thus, (12.8) implies that

$$(\varphi^2)_{min} \geq \frac{1}{\tau_*^2}. \quad (12.14)$$

Finally, we recall that the pyramid \widehat{Q} contains a sphere of radius $r \geq \gamma_* h_{\widehat{Q}}$. Since $\|\boldsymbol{\xi}\| \leq h_{\widehat{Q}}$ and $2r \leq h_{\widehat{Q}}$, we deduce that

$$\|\boldsymbol{\xi}\| \leq h_{\widehat{Q}} \leq \frac{r}{\gamma_*} \leq \frac{H_{\widehat{Q}}}{2\gamma_*}. \quad (12.15)$$

The assertion of the lemma follows from estimates (12.12)–(12.15). \square

Now we describe a class of shape-regular generalized polyhedral meshes. All convergence error estimates will be proved for these meshes. A generalized polyhedral mesh Ω_h is called shape-regular if it satisfies the following assumption.

(GR) We assume that there exist two positive constants γ_* and τ_* , and one integer number \mathcal{N}^s , independent of the mesh, such that every element P is the union of at most \mathcal{N}^s generalized pyramids with at most \mathcal{N}^s lateral faces and shape constants γ_* and τ_* .

Definition 12.3. (*Moderately and strongly curved faces*). Let η_* be a positive constant independent of the mesh Ω_h . We say that f is *moderately curved* if at every point $\mathbf{x} \in f$ it holds:

$$\|\mathbf{n}_f(\mathbf{x}) - \widetilde{\mathbf{n}}_f\| \leq \eta_* |f|^{1/2}, \quad (12.16)$$

where $\widetilde{\mathbf{n}}_f$ is defined in (12.6). Otherwise, we say that the face f is *strongly curved*.

Remark 12.1. The meshes generated with a smooth mapping or by a uniform refinement of a coarse mesh contain typically cells with moderately curved faces. In contrast, the meshes generated by moving mesh methods contain frequently cells with strongly curved faces. Definition 12.3 gives a simple computable measure of face curvature.

Assumption **(GR)** is close to the mesh shape regularity assumption **(MR)** introduced in Chap. 1. It implies immediately that every element P is star-shaped with respect to the common vertex $\bar{\mathbf{x}}_P$ of the generalized pyramids that form it; compare with the assumption **(MR3)**. Additional consequences of assumption **(GR)** are stated in the following lemma.

Lemma 12.2. *Let Ω_h be a generalized polyhedral mesh satisfying assumption **(GR)** and P be any element in Ω_h . Furthermore, let ρ_* and a_* denote positive constants that depend only on the constants γ_* , τ_* , and \mathcal{N}^s . Then P is star-shaped with respect to every point of a sphere centered at $\bar{\mathbf{x}}_P$ with radius $\rho_* h_P$. Moreover, we have the following bounds:*

$$a_* h_P^3 \leq |P| \leq h_P^3 \quad \text{and} \quad a_* h_P^2 \leq |f| \leq h_P^2 \quad (12.17)$$

for all faces f of P .

Proof. A conventional polyhedron \widetilde{P} is star-shaped with respect to every point in its feasible set. The feasible set is defined as the intersection of half-spaces formed

by all faces of \tilde{P} and containing \bar{x}_P . For a generalized polyhedron P , its feasible set is the intersection of the infinite number of half-spaces containing the point \bar{x}_P and tangential to all internal points of faces f of P . The radius of a sphere inscribed in the feasible set equals to the shortest distance from \bar{x}_P to the tangential planes.

Without loss of generality, we assume that \bar{x}_P is in the origin. Using the notation of Lemma 12.1, we consider a generalized pyramid Q built from a regular pyramid \hat{Q} via map Φ . Let f be the base of Q , \hat{f} the base of \hat{Q} , and $H_{\hat{Q}}$ the height of \hat{Q} . Let $\mathbf{x} \in \hat{f}$ and $\mathbf{x}' = \Phi(\mathbf{x})$. The normal vector to face f at point \mathbf{x}' is given by

$$\mathbf{n}_f(\mathbf{x}') = \left(-H_{\hat{Q}} \varphi \varphi_x, -H_{\hat{Q}} \varphi \varphi_y, \varphi^2 + \varphi(x\varphi_x + y\varphi_y) \right),$$

where map $\varphi(x,y)$ is defined by (12.8). Distance from the origin to the tangential plane defined by the normal vector $\mathbf{n}_f(\mathbf{x}')$ and passing through point \mathbf{x}' is

$$d(\mathbf{x}') = \frac{|\mathbf{x}' \cdot \mathbf{n}_f(\mathbf{x}')|}{\|\mathbf{n}_f(\mathbf{x}')\|} = \frac{|H_{\hat{Q}} \varphi^3|}{\|\mathbf{n}_f(\mathbf{x}')\|}. \tag{12.18}$$

Since Φ is a bounded operator, the absolute values of its components are bounded by τ_* . Thus,

$$\|\mathbf{n}_f(\mathbf{x}')\| \leq |\varphi| \left(|H_{\hat{Q}} \varphi_x| + |H_{\hat{Q}} \varphi_y| + |y\varphi_y + x\varphi_x + \varphi| \right) \leq |\varphi| 5\tau_*.$$

Inserting estimate (12.14) into (12.18), we obtain a lower bound for the distance independent of the position of point \mathbf{x}' :

$$d(\mathbf{x}') \geq H_{\hat{Q}} / (5\tau_*^3).$$

Using Definition 12.1, we obtain that $H_{\hat{Q}} \geq 2r \geq 2\gamma_* h_{\hat{Q}}$. Formula (12.9) implies that $h_{\hat{Q}} \leq \tau_* h_Q$ and $h_Q \leq \tau_* h_{\hat{Q}}$, where h_Q is the diameter of the generalized pyramid Q . These formulas give us a different lower bound:

$$d(\mathbf{x}') \geq \frac{1}{5\tau_*^3} H_{\hat{Q}} \geq \frac{2\gamma_*}{5\tau_*^4} h_Q.$$

Let us show that the diameters of the generalized pyramids $Q \in P$ are uniformly bounded from below. Let Q_1 have the largest diameter among all generalized pyramids and Q_2 be a generalized pyramid that has a common lateral face with Q_1 . Note that $\tau_* h_{Q_1} \geq h_{\hat{Q}_1} \geq H_{\hat{Q}_1}$. Since these two pyramids have a common face, a pessimistic estimate for the diameter of Q_2 is $H_{\hat{Q}_1} / \tau_*$. Thus,

$$h_{Q_2} \geq \frac{H_{\hat{Q}_1}}{\tau_*} \geq \frac{2\gamma_* h_{\hat{Q}_1}}{\tau_*} \geq \frac{2\gamma_*}{\tau_*^2} h_{Q_1}.$$

Since the generalized pyramids are connected with one another, a pessimistic estimate for the radius of a sphere inscribed in the feasible set is given by

$$d(\mathbf{x}') \geq \frac{2\gamma_*}{5\tau_*^4} \min_{Q \in P} h_Q \geq \frac{2\gamma_*}{5\tau_*^4} \left(\frac{2\gamma_*}{\tau_*^2} \right)^{N^s-1} h_{Q_1} \geq \frac{2}{5\tau_*^2} \left(\frac{2\gamma_*}{\tau_*^2} \right)^{N^s} \frac{h_P}{2} \equiv \rho_* h_P.$$

The volume of P is bounded from below by the volume of the inscribed sphere with radius ρ_* . This gives $a_* = 4\pi\rho_*^3/3$. The bound for $|f|$ follows from an estimate similar to (12.13) and the above arguments:

$$|f| \geq \frac{1}{\tau_*^2} |\widehat{f}| \geq \frac{\pi r^2}{\tau_*^2} \geq \frac{\pi \gamma_*^2}{\tau_*^2} h_{\widehat{Q}}^2 \geq \frac{\pi \gamma_*^2}{\tau_*^4} h_{\widehat{Q}}^2,$$

which gives $a_* = \pi(5\tau_*^4\rho_*/4)^2$. The assertion of the lemma follows by selecting the smallest of a_* . \square

A useful consequence of the proof of the last lemma is that

$$H_{\widehat{Q}} \geq \frac{2\gamma_*}{\tau_*} h_{\widehat{Q}} \geq \frac{2\gamma_*\rho_*}{\tau_*} h_P \quad \forall \widehat{Q} \in P. \quad (12.19)$$

12.3 Mimetic discretization

12.3.1 Degrees of freedom and projection operators

The mimetic approximation of (12.1)–(12.3) starts with the definition of the degrees of freedom for scalar and vector fields.

- The space of discrete scalar fields \mathcal{P}_h is defined by attaching one degree of freedom to every cell $P \in \Omega_h$. The value associated with P is denoted by q_P . The collection of all degrees of freedom form the algebraic vector $q_h \in \mathcal{P}_h$,

$$q_h = (q_P)_{P \in \Omega_h}.$$

The dimension of \mathcal{P}_h is equal to the number of polyhedrons in Ω_h .

- The space of discrete flux fields \mathcal{F}_h is defined by attaching a *vector* $\mathbf{v}_{P,f}$ to every element P and every face f of P . The collection of all degrees of freedom form the algebraic vector $\mathbf{v}_h \in \mathcal{F}_h$,

$$\mathbf{v}_h = (\mathbf{v}_{P,f})_{f \in P, P \in \Omega_h}.$$

The dimension of \mathcal{F}_h is equal to three times the number of the boundary faces plus six times the number of internal faces.

For a discrete flux field $\mathbf{v}_h \in \mathcal{F}_h$, we denote by \mathbf{v}_P its restriction to P , i.e. $\mathbf{v}_P = (\mathbf{v}_{P,f})_{f \in P}$. The vectors \mathbf{v}_P form a linear space $\mathcal{F}_{h,P}$, the restriction of \mathcal{F}_h to element P . To build a mimetic scheme, we need to reduce the number of independent flux degrees of freedom by imposing some continuity conditions.

For every element P in Ω_h and every face f of P , we define the vector $\mathbf{n}_{P,f}(\mathbf{x})$ as the unit normal at point \mathbf{x} of f pointing outside of P . Let $\tilde{\mathbf{n}}_{P,f}$ be the average normal vector,

$$\tilde{\mathbf{n}}_{P,f} = \frac{1}{|f|} \int_f \mathbf{n}_{P,f}(\mathbf{x}) dS. \quad (12.20)$$

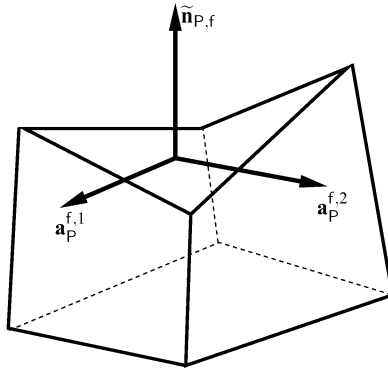


Fig. 12.3. A local coordinate system for the strongly curved face (top face) of a generalized hexahedron

Lemma 12.1 gives the following lower bound:

$$\|\tilde{\mathbf{n}}_{P,f}\| \geq \frac{2\gamma_*}{\tau_*^4}. \quad (12.21)$$

In addition, we assign to each mesh face f a pair of arbitrary unit vectors $\mathbf{a}_P^{f,1}$ and $\mathbf{a}_P^{f,2}$ orthogonal to $\tilde{\mathbf{n}}_{P,f}$ and orthogonal to each other. These three vectors form an orthogonal coordinate system for every face f as shown in Fig. 12.3, where the strongly curved face is the top face of a hexahedron. We set, for convenience of notation,

$$\mathbf{a}_P^{f,3} = \frac{\tilde{\mathbf{n}}_{P,f}}{\|\tilde{\mathbf{n}}_{P,f}\|}.$$

Hereafter, we assume that mesh functions \mathbf{v}_h in space \mathcal{F}_h satisfy the following continuity conditions.

(C1) (*Continuity of discrete fluxes*). For each face f , shared by two polyhedrons P_1 and P_2 , we assume that

$$\mathbf{v}_{P_1,f} \cdot \tilde{\mathbf{n}}_{P_1,f} = -\mathbf{v}_{P_2,f} \cdot \tilde{\mathbf{n}}_{P_2,f}. \quad (12.22)$$

Moreover, for every strongly curved face f , we assume the full continuity of the local flux vector. This means that together with (12.22) we also have

$$\mathbf{v}_{P_1,f} \cdot \mathbf{a}_P^{f,i} = \mathbf{v}_{P_2,f} \cdot \mathbf{a}_P^{f,i}, \quad i = 1, 2. \quad (12.23)$$

The continuity condition **(C1)** reduces the number of independent flux unknowns. On moderately curved faces, only the normal component of $\mathbf{v}_{P,f}$ is continuous, and the other two components can be treated as *internal degrees of freedom*. In a computer program, they are eliminated during the assembly process by the static condensation.

The necessity of using three independent flux unknowns on each strongly curved face is an intrinsic property of a generalized polyhedral mesh and is the possible

reason why nobody succeeded in development of a convergent method with only one flux unknown per mesh face.

Remark 12.2. In the case of discontinuous materials, we will have to replace the full continuity of flux across strongly curved faces by continuity of the normal flux and tangential components of the gradient.

The constant η_* in (12.16) is at our choice. If we choose it too large, then most faces will be classified as moderately curved and the asymptotically optimal convergence rate will be observed only on very fine meshes. Indeed, as we will show later, the constant η_* enters the *a priori* estimates. Hence, in practice, we are likely to face the usual trade-off between the cost of the method and the quality of the solution.

Let us define the projection operators $(\cdot)^I$ from continuum spaces of sufficiently smooth functions to discrete spaces. For a function $q \in L^1(\Omega)$, we define a cell-centered scalar field $q^I \in \mathcal{P}_h$ by

$$q^I = (q_P^I)_{P \in \mathcal{P}}, \quad q_P^I = \frac{1}{|P|} \int_P q dV. \quad (12.24)$$

It is immediate to verify that for any $P \in \Omega_h$ we have

$$\int_P (q_P^I)^2 dV \leq \int_P q^2 dV \quad \forall q \in L^2(P). \quad (12.25)$$

For every vector function $\mathbf{v} \in (H^1(\Omega))^3$, we define a face-centered discrete flux field $\mathbf{v}^I \in \mathcal{F}_h$ as follows:

$$\mathbf{v}^I = (\mathbf{v}_{P,f}^I)_{f \in \mathcal{F}, P \in \mathcal{P}}, \quad (12.26)$$

where

$$\mathbf{v}_{P,f}^I \cdot \mathbf{a}_P^{f,i} = \frac{1}{|f|} \int_f \mathbf{v} \cdot \mathbf{a}_P^{f,i} dS \quad \text{for } i = 1, 2, \quad (12.27)$$

$$\mathbf{v}_{P,f}^I \cdot \mathbf{a}_P^{f,3} = \frac{1}{|f| \|\tilde{\mathbf{n}}_{P,f}\|} \int_f \mathbf{v} \cdot \mathbf{n}_{P,f} dS. \quad (12.28)$$

In Sect. 12.4.1, we will prove that this projection operator is well defined and uniformly bounded. If function \mathbf{v} is continuous across the interior mesh faces, it is easy to see that the resulting 3-D vector $\mathbf{v}_{P,f}^I$ satisfies the continuity property **(C1)**. The projection operator has three important properties. First, for a constant function \mathbf{c} , we obtain from (12.27)–(12.28) that

$$\mathbf{c}_{P,f}^I = \mathbf{c}. \quad (12.29)$$

Second, the definition of the projection operator implies the flux conservation property:

$$\int_f \mathbf{v} \cdot \mathbf{n}_{P,f} dS = \|\tilde{\mathbf{n}}_{P,f}\| |f| \mathbf{v}_{P,f}^I \cdot \mathbf{a}_P^{f,3} = |f| \mathbf{v}_{P,f}^I \cdot \tilde{\mathbf{n}}_{P,f} = \mathbf{v}_{P,f}^I \cdot \int_f \mathbf{n}_{P,f} dS = \int_f \mathbf{v}_{P,f}^I \cdot \tilde{\mathbf{n}}_{P,f} dS. \quad (12.30)$$

Note that in the last integral we consider $\mathbf{v}_{P,f}^I$ as a constant vector field on f . Finally, using estimate (12.21), we obtain the following upper bound:

$$\|\mathbf{v}_{P,f}^I\| \leq \frac{\tau_x^4}{2\gamma_*|f|^{1/2}} \left(\int_f |\mathbf{v}|^2 dS \right)^{1/2}. \quad (12.31)$$

12.3.2 Strong and weak forms of discrete equations

The discrete divergence operator, $\text{div}_h: \mathcal{F}_h \rightarrow \mathcal{P}_h$, arises naturally from the Gauss divergence theorem and (12.30) as

$$\text{div}_P(\mathbf{v}_h) = \frac{1}{|f|} \sum_{f \in \partial P} \mathbf{v}_{P,f} \cdot \tilde{\mathbf{n}}_{P,f} |f| = \frac{1}{|f|} \sum_{f \in \partial P} \int_f \mathbf{v}_{P,f} \cdot \mathbf{n}_{P,f} dS. \quad (12.32)$$

Note that this primary mimetic operator uses only the normal component of the local flux vector. A part of the commuting diagram (see Lemma 2.2) holds true for this operator.

Lemma 12.3. *The projection operators $(\cdot)^I$ commute with the discrete and continuum divergence operators.*

Proof. Let \mathbf{v} be a sufficiently smooth vector-valued function. Using (12.32), (12.20), (12.30), the Gauss divergence theorem, and (12.24), we obtain

$$\begin{aligned} \text{div}_P(\mathbf{v}_P^I) &= \frac{1}{|P|} \sum_{f \in \partial P} \mathbf{v}_{P,f}^I \cdot \tilde{\mathbf{n}}_{P,f} |f| = \frac{1}{|P|} \sum_{f \in \partial P} \int_f \mathbf{v}_{P,f}^I \cdot \mathbf{n}_{P,f} dS \\ &= \frac{1}{|P|} \int_{\partial P} \mathbf{v} \cdot \mathbf{n}_P dS = \frac{1}{|P|} \int_P \text{div } \mathbf{v} dV = (\text{div } \mathbf{v})_P^I \end{aligned} \quad (12.33)$$

for every element P in Ω_h . This proves the assertion of the lemma. □

According to the discrete vector and tensor calculus developed in Chap. 2, the derived mimetic gradient operator, $\tilde{\nabla}_h: \mathcal{P}_h \rightarrow \mathcal{F}_h$, is given by

$$\tilde{\nabla}_h = -M_{\mathcal{F}}^{-1} \text{div}_h^T M_{\mathcal{P}},$$

where matrices $M_{\mathcal{F}}$ and $M_{\mathcal{P}}$ are induced by the inner products in spaces \mathcal{F}_h and \mathcal{P}_h , respectively. In space \mathcal{P}_h , we consider

$$[p_h, q_h]_{\mathcal{P}_h} = \sum_{P \in \Omega_h} p_P q_P |P| \quad \forall p_h, q_h \in \mathcal{P}_h. \quad (12.34)$$

Thus, the matrix $M_{\mathcal{P}}$ is diagonal with volumes $|P|$ on the diagonal. The inner product in space \mathcal{F}_h is more involved and we will define it in the next subsection. Here, we simply state that

$$[\mathbf{u}_h, \mathbf{v}_h]_{\mathcal{F}_h} = \mathbf{u}_h^T M_{\mathcal{F}} \mathbf{v}_h \quad \forall \mathbf{u}_h, \mathbf{v}_h \in \mathcal{F}_h.$$

The matrix $M_{\mathcal{F}}$ is often irreducible, so that its inverse is a dense matrix. Fortunately, in a computer code, this matrix is never calculated explicitly.

Using the discrete flux and divergence operators, the mimetic approximation of equations (12.1)–(12.3) with $g^D = 0$ reads:

Find $(\mathbf{u}_h, p_h) \in \mathcal{F}_h \times \mathcal{P}_h$ such that

$$\begin{aligned} \mathbf{u}_h + \tilde{\nabla}_h p_h &= \mathbf{0}, \\ \operatorname{div}_h \mathbf{u}_h &= b^I, \end{aligned} \quad (12.35)$$

where $b^I \in \mathcal{P}_h$ is the cell-centered field with the mean values of the source function b over elements P .

Now, we are able to present the weak form of the mimetic method. We multiply the first equation in (12.35) by $\mathbf{v}_h^T M_{\mathcal{F}}$ and use the duality of mimetic operators (see (2.27)). Then, we multiply the second equation by $q_h^T M_{\mathcal{P}}$ to obtain

Find $(\mathbf{u}_h, p_h) \in \mathcal{F}_h \times \mathcal{P}_h$ such that

$$\begin{aligned} [\mathbf{u}_h, \mathbf{v}_h]_{\mathcal{F}_h} - [p_h, \operatorname{div}_h \mathbf{v}_h]_{\mathcal{P}_h} &= 0 & \forall \mathbf{v}_h \in \mathcal{F}_h, \\ [\operatorname{div}_h \mathbf{v}_h, q_h]_{\mathcal{P}_h} &= [b^I, q_h]_{\mathcal{P}_h} & \forall q_h \in \mathcal{P}_h. \end{aligned} \quad (12.36)$$

12.3.3 Stability and consistency conditions

In this section, we detail the two fundamental conditions of stability and consistency that lead to a convergent mimetic scheme. Let us write the inner product in space \mathcal{F}_h as a sum of elemental inner products defined for every element P in Ω_h :

$$[\mathbf{u}_h, \mathbf{v}_h]_{\mathcal{F}_h} = \sum_{P \in \Omega_h} [\mathbf{u}_P, \mathbf{v}_P]_{\mathcal{F}_{h,P}} \quad \forall \mathbf{u}_h, \mathbf{v}_h \in \mathcal{F}_h. \quad (12.37)$$

According to the theory developed in Chap. 4, the inner product must satisfy the stability and consistency conditions.

Let K_P be a constant tensor on P such that

$$\sup_{\mathbf{x} \in P} \sup_{1 \leq i, j \leq 3} |(K(\mathbf{x}))_{i,j} - (K_P)_{i,j}| \leq C_K^* h_P, \quad (12.38)$$

where C_K^* is a constant independent of P . In practice, we use either the mean value of K or we set $K_P = K(\mathbf{x}_P)$.

(S1) (Stability condition). There exist two positive constants σ_* and σ^* which are independent of mesh Ω_h and such that

$$\sigma_* |P| \mathbf{v}_P^T \mathbf{v}_P \leq [\mathbf{v}_P, \mathbf{v}_P]_{\mathcal{F}_{h,P}} \leq \sigma^* |P| \mathbf{v}_P^T \mathbf{v}_P \quad \forall \mathbf{v}_P. \quad (12.39)$$

The stability assumption states that the local inner product matrix must be spectrally equivalent to the scalar matrix $|P|I$. In practice, the constants σ_* and σ^* depend only on the skewness of polyhedron P and on the tensor K_P . This assumption ensures stability of a mimetic discretization.

Let us define the following space:

$$S_{h,P} = \{ \mathbf{v} \in (W^{1,s}(P))^3, 6/5 \leq s < 2, \text{ with } \operatorname{div} \mathbf{v} \in \mathbb{P}_0(P), \mathbf{v} \in (\mathbb{P}_0(f))^3 \forall f \in \partial P \}.$$

According to the theory developed in Part I of this book, this space must satisfy three assumptions **(B1)**–**(B3)**. We recall the first two assumptions.

(B1) The local projection operator $(\cdot)_P^I$ from $S_{h,P}$ to $\mathcal{F}_{h,P}$ must be surjective.

(B2) The space $S_{h,P}$ must contain the trial space of constant vector functions:

$$\mathcal{T}_P = \{\mathbf{v} : P \rightarrow \mathbb{R}^d \text{ such that } \mathbf{v} = K_P \nabla q \text{ with } q \in \mathbb{P}_1(P)\}.$$

It is possible to verify that the space $S_{h,P}$ above satisfies both conditions, while the third assumption **(B3)** will be addressed below. In particular, in order to show condition **(B2)**, it is sufficient to solve a local Stokes-like problem as shown in Eq. (12.89).

(S2) (*Consistency condition*). For every function $\mathbf{v} \in S_{h,P}$, any linear polynomial q^1 , and every element P we have

$$[(K_P \nabla q^1)_P^I, \mathbf{v}_P^I]_{\mathcal{F}_{h,P}} = \int_P \nabla q^1 \cdot \mathbf{v} dV. \tag{12.40}$$

Consistency is an exactness property and guarantees the first order of accuracy of the resulting mimetic scheme. By definition, if $\mathbf{v} \in S_{h,P}$ then $\text{div} \mathbf{v}$ is constant on P and from Lemma 12.3 we obtain that $(\text{div} \mathbf{v})|_P = \text{div}_P(\mathbf{v}_P^I)$. Likewise, since for all $f \in \partial P$ it holds that $\mathbf{v}|_f$ is a constant vector field, it is easy to check from definitions (12.27)–(12.28) that

$$\mathbf{v}_{P,f}^I \cdot \mathbf{a}_P^{f,i} = \mathbf{v}|_f \cdot \mathbf{a}_P^{f,i} \quad \forall f \in \partial P, i = 1, 2, 3.$$

Therefore $\mathbf{v}_{P,f}^I = \mathbf{v}|_f$ and we immediately have

$$\int_f q^1 \mathbf{v} \cdot \mathbf{n}_{P,f} dS = \int_f q^1 \mathbf{v}_{P,f}^I \cdot \mathbf{n}_{P,f} dS \quad \forall f \in \partial P.$$

We integrate by parts the right-hand side of (12.40) and use these formulas to obtain

$$[(K_P \nabla q^1)_P^I, \mathbf{v}_P^I]_{\mathcal{F}_{h,P}} = - \int_P q^1 \text{div}_P(\mathbf{v}_P^I) dV + \sum_{f \in \partial P} \int_f q^1 \mathbf{v}_{P,f}^I \cdot \mathbf{n}_{P,f} dS. \tag{12.41}$$

The terms in the right-hand side are explicitly computable and **(B3)** of Chap. 4 is verified for the bilinear form

$$\mathcal{B}_P(\mathbf{v}, \mathbf{u}) = \int_P K_P^{-1} \mathbf{v} \cdot \mathbf{u} dV.$$

More precisely, assumption **(B3)** of Chap. 4, adapted to the current case, reads:

(B3) $\mathcal{B}_P(\mathbf{v}, \mathbf{u})$ with $\mathbf{v} \in S_{h,P}$ and $\mathbf{u} = K_P \nabla q^1$ can be computed *exactly* using only q^1 and the degrees of freedom of \mathbf{v} .

Integration over a curved face f requires an explicit representation of this face. The most simple representation of f is made by its triangulation, which is an acceptable face model for the majority of the internal mesh faces. When a curved face is located on material or domain boundaries, a local parametrization of these boundaries can be used to calculate the integral.

Remark 12.3. The calculation of the boundary face integrals may require numerical quadratures. The impact of the numerical integration error on the accuracy of the mimetic schemes is not analyzed in this book, see [253, 256] and references therein for examples of theoretical and numerical analysis of approximate consistency conditions.

Remark 12.4. Note that we do not require the space $S_{h,P}$ to be finite dimensional and isomorphic to $\mathcal{F}_{h,P}$. Nevertheless nothing forbids us to choose it such that, in addition to the above conditions, we have

$$\dim(S_{h,P}) = \dim(\mathcal{F}_{h,P}). \quad (12.42)$$

12.3.4 Derivation of mimetic inner product

In this section we show in detail the construction of a mimetic inner product in the space \mathcal{F}_h that satisfies assumptions **(S1)** and **(S2)**. We refer to [93] for a complete list of available results. By the definition of the inner product, each contribution in (12.37) can be written in a matrix form:

$$[\mathbf{u}_P, \mathbf{v}_P]_{\mathcal{F}_{h,P}} = \mathbf{u}_P^T M_P \mathbf{v}_P, \quad (12.43)$$

where M_P is a symmetric and positive definite matrix.

Let $N_P^{\mathcal{F}}$ be the number of faces in P , so that the size of vectors \mathbf{u}_P and \mathbf{v}_P is $\ell_P = 3N_P^{\mathcal{F}}$. For every positive integer number $r \leq \ell_P$, we define two unique integer numbers $\alpha(r)$ and $\beta(r)$ such that

$$1 \leq \alpha(r) \leq N_P^{\mathcal{F}} \quad \text{and} \quad 1 \leq \beta(r) \leq 3.$$

We use $\alpha(r)$ and $\beta(r)$ to label the degrees of freedom of \mathbf{v}_P associated with the faces f of ∂P and with the basis vectors $\mathbf{a}_P^{f,i}$ that are defined on each face. In particular, we say that the r -th component of \mathbf{v}_P is associated with face $f_{\alpha(r)}$ of polyhedron P and with the basis vector $\mathbf{a}_P^{f_{\alpha(r)},\beta(r)}$ (this correspondance is practically implemented by taking, for example, $r = 3(\alpha(r) - 1) + \beta(r)$). Hereafter, we shall write $\mathbf{a}_P^{(r)}$ to simplify the notation.

Due to the bilinear structure of the integrals in the right-hand side of (12.41), it is sufficient to consider only four linearly independent functions. Taking $q^1 = 1$, we recover the definition of the discrete divergence operator div_P . This adds no constraints on the inner product matrix. For linear functions orthogonal to a constant, formula (12.41) is simplified as:

$$[(K_P \nabla q^1)_P, \mathbf{v}_P]_{\mathcal{F}_{h,P}} = \sum_{f \in \partial P} \int_f q^1 \mathbf{v}_{P,f}^I \cdot \mathbf{n}_{P,f} dS \quad \forall \mathbf{v} \in S_{h,P}. \quad (12.44)$$

The formula shows the remarkable property of characterizing the inner product using only boundary integrals.

There are three linearly independent linear functions orthogonal to a constant. They are $x_i - x_{P,i}$, $i = 1, 2, 3$, where $\mathbf{x} = (x_1, x_2, x_3)$ is a 3-D position vector and $\mathbf{x}_P =$

$(x_{P,1}, x_{P,2}, x_{P,3})$ is the centroid of P . Inserting these linear functions in (12.44), we obtain

$$[(K_P \nabla x_i)_P, \mathbf{v}_P^I]_{\mathcal{F}_{h,P}} = \sum_{f \in \partial P} \int_f (x_i - x_{P,i}) \mathbf{v}_{P,f}^I \cdot \mathbf{n}_{P,f} dS. \quad (12.45)$$

Let us introduce the matrices R and N , with size $\ell_P \times 3$, which are defined by

$$R_{r,i} = \int_{f_{\alpha(r)}} (x_i - x_{P,i}) \mathbf{a}_P^{(r)} \cdot \mathbf{n}_{P,f_{\alpha(r)}} dS \quad \text{and} \quad N_{r,i} = ((K_P \nabla x_i)_P)_r, \quad (12.46)$$

where $r = 1, 2, \dots, \ell_P$ and $i = 1, 2, 3$. These matrices obviously depend on P but we omit this subscript until the end of this section to ease the notation. Let R_i and N_i denote columns of matrices R and N , respectively. Recalling the definition of the inner product, we obtain

$$(\mathbf{v}_P^I)^T M_P N_i = (\mathbf{v}_P^I)^T R_i \quad \forall \mathbf{v}_P^I, \quad i = 1, 2, 3.$$

Since \mathbf{v}_P^I is an arbitrary vector, the above formulas can be written as the matrix equation:

$$M_P N = R. \quad (12.47)$$

The theory developed in Chap. 4 gives us a parametric family of solutions to this matrix equation. To show that this family contains symmetric and positive definite matrices, we have to prove some of the properties of matrices N and R . The following lemma relates to the general results in Sect. 4.3.

Lemma 12.4. *The matrices N and R satisfy*

$$R^T N = N^T R = |P| K_P. \quad (12.48)$$

Proof. Let us first observe that

$$((K_P \nabla x_i)_P)_r = (K_P \nabla x_i)_P \cdot \mathbf{a}_P^{(r)} = K_P \nabla x_i \cdot \mathbf{a}_P^{(r)},$$

which follows from (12.29) because $K_P \nabla x_i$ is a constant vector and $\mathbf{a}_P^{(r)}$ is an orthogonal set of unit basis functions. Using this relation and the definitions of matrices N and R given in (12.46) we obtain:

$$N_i^T R_j = \sum_r (K_P \nabla x_i) \cdot \mathbf{a}_P^{(r)} \int_{f_{\alpha(r)}} (x_j - x_{P,j}) \mathbf{a}_P^{(r)} \cdot \mathbf{n}_P dS. \quad (12.49)$$

For $1 \leq r \leq \ell_P$, there must exist three distinct values r_1, r_2 and r_3 that identify the same face, i.e., $f_{r_1} = f_{r_2} = f_{r_3}$, and the three basis vectors $\mathbf{a}_P^{(r_1)}$, $\mathbf{a}_P^{(r_2)}$, and $\mathbf{a}_P^{(r_3)}$ associated with that face, i.e., $\beta(r_i) = i$ for $i = 1, 2, 3$. We reformulate the summation in (12.49) as a summation on the faces $f \in \partial P$ by collecting the three contributions from each face that are associated with the basis vectors $\mathbf{a}_P^{(r_i)}$. Noting that $\sum_{i=1}^3 \mathbf{a}_P^{(i)} (\mathbf{a}_P^{(i)})^T = I$ because $\{\mathbf{a}_P^{(i)}\}$ is a complete orthogonal set and using the Gauss-Green formula for

the linear functions x_i and x_j , Eq. (12.49) becomes

$$\mathbf{N}_i^T \mathbf{R}_j = \int_{\partial\mathcal{P}} (\mathbf{K}_\mathcal{P} \nabla x_i) \cdot \mathbf{n}_\mathcal{P} (x_j - x_{\mathcal{P},j}) dS = \int_{\mathcal{P}} \mathbf{K}_\mathcal{P} \nabla x_i \cdot \nabla x_j dV = |\mathcal{P}| (\mathbf{K}_\mathcal{P})_{i,j}. \quad (12.50)$$

Since i and j are arbitrary, this completes the proof. \square

Since $\mathcal{F}_{h,\mathcal{P}}$ is extension of a related space from Chap. 5, we have immediately a few results such as the matrix \mathbf{N} has the full rank. Using Lemma 12.4, we can rephrase Lemma 4.7 as follows.

Lemma 12.5. *Let \mathbf{D} be an $\ell_\mathcal{P} \times (\ell_\mathcal{P} - 3)$ matrix whose $\ell_\mathcal{P} - 3$ columns span the null space of \mathbf{N}^T , so that $\mathbf{N}^T \mathbf{D} = 0$. Then, for every $(\ell_\mathcal{P} - 3) \times (\ell_\mathcal{P} - 3)$ symmetric positive definite matrix \mathbf{U} , the symmetric matrix*

$$\mathbf{M}_\mathcal{P} = \mathbf{M}_\mathcal{P}^{(0)} + \mathbf{D} \mathbf{U} \mathbf{D}^T, \quad \mathbf{M}_\mathcal{P}^{(0)} = \frac{1}{|\mathcal{P}|} \mathbf{R} \mathbf{K}_\mathcal{P}^{-1} \mathbf{R}^T, \quad (12.51)$$

satisfies (12.47) and is positive definite.

Since \mathbf{U} has size $\ell_\mathcal{P} - 3$, a general symmetric positive definite matrix of this size has $(\ell_\mathcal{P} - 2)(\ell_\mathcal{P} - 3)/2$ free parameters, yielding a family of matrices. The liberty of choosing \mathbf{U} within this family can be used to tackle other computational problems, e.g., to enforce the discrete maximum principle (see Chap. 11 for more detail).

One of the efficient ways for solving the diffusion problem in a mixed form is based on the KKT theory of constrained minimization (see e.g. [289, Chap. 16]) where the constraints are given by (12.22) and (12.23). The solution of the KKT system is reduced to the solution of a sparse system for Lagrange multipliers with a symmetric positive definite matrix. In the finite element context this is often called a *hybridization* and is usually attributed to Fraeijns de Veubeke [174] (see also [29], or [88, pp. 178–181]).

The hybridization procedure uses only the inverse of matrix $\mathbf{M}_\mathcal{P}$, while the explicit knowledge of the matrix itself is not required. Let $\mathbf{W}_\mathcal{P}$ denote the inverse of matrix $\mathbf{M}_\mathcal{P}$. Then

$$\mathbf{W}_\mathcal{P} \mathbf{R} = \mathbf{N}. \quad (12.52)$$

This equation differs from (12.47) only by swapping of matrices \mathbf{N} and \mathbf{R} . Thus, we have the result similar to Lemma 12.5.

Lemma 12.6. *Let $\tilde{\mathbf{D}}$ be a $\ell_\mathcal{P} \times (\ell_\mathcal{P} - 3)$ matrix whose $\ell_\mathcal{P} - 3$ columns span the null space of \mathbf{R}^T , so that $\mathbf{R}^T \tilde{\mathbf{D}} = 0$. Then, for every $(\ell_\mathcal{P} - 3) \times (\ell_\mathcal{P} - 3)$ symmetric positive definite matrix $\tilde{\mathbf{U}}$, the following symmetric matrix*

$$\mathbf{W}_\mathcal{P} = \frac{1}{|\mathcal{P}|} \mathbf{N} \mathbf{K}_\mathcal{P}^{-1} \mathbf{N}^T + \tilde{\mathbf{Q}} \tilde{\mathbf{U}} \tilde{\mathbf{Q}}^T \quad (12.53)$$

satisfies (12.52) and is positive definite.

Since, in practice, we are interested only in the matrix M_P^{-1} , we can build W_P and define $M_P^{-1} := W_P$. Moreover, it is not difficult to show that such a matrix M_P can still be written in the form (12.51), where the choice of the matrices U and D obviously depends on the choice of \tilde{U} and \tilde{D} .

Let us look again at the stability assumption (S1) and show that the new mesh shape regularity assumption (GR) leads to mesh independent bounds. We rescale the matrices N and R and prove a technical lemma. Let us define

$$\tilde{N} := N K_P^{-1} \quad \text{and} \quad \tilde{R} := \frac{1}{|P|} R, \tag{12.54}$$

so that

$$\tilde{R}^T \tilde{N} = \tilde{N}^T \tilde{R} = I_3. \tag{12.55}$$

According to (12.46), the r -th row of N is $(\mathbf{a}_P^{(r)})^T K_P$; thus, the r -th row of \tilde{N} is $(\mathbf{a}_P^{(r)})^T$. Let C_i be the 3×3 matrices associated with faces f_i of P and located on the main diagonal of matrix C :

$$C = \text{diag}\{C_1, \dots, C_{N_P^{\mathcal{F}}}\}, \quad C_i^T = \begin{pmatrix} \mathbf{a}_P^{f_i,1} & \mathbf{a}_P^{f_i,2} & \mathbf{a}_P^{f_i,3} \end{pmatrix}.$$

The orthogonality property of vectors \mathbf{a}_P gives,

$$C_i C_i^T = C_i^T C_i = I_3 \quad \text{and} \quad C C^T = C^T C = I_{\ell_P}. \tag{12.56}$$

If we further introduce the $\ell_P \times 3$ matrix R_0 by

$$(R_0)_{r,i} = \int_{f_{\alpha(r)}} \nabla x_{\beta(r)} \cdot \mathbf{n}_{P, f_{\alpha(r)}} (x_i - x_{P,i}) dS,$$

where $r = 1, \dots, \ell_P$ and $i = 1, 2, 3$, then

$$R = C R_0 \quad \text{and} \quad \tilde{N} = \begin{pmatrix} C_1 \\ C_2 \\ \vdots \\ C_{N_P^{\mathcal{F}}} \end{pmatrix}. \tag{12.57}$$

Lemma 12.7. *Let P be a shape-regular generalized polyhedron. Then, for any $\mathbf{w} \in \mathfrak{R}^3$, we have*

$$\|\tilde{N}\mathbf{w}\| = \sqrt{N_P^{\mathcal{F}}}\|\mathbf{w}\| \quad \text{and} \quad \frac{1}{\sqrt{N_P^{\mathcal{F}}}}\|\mathbf{w}\| \leq \|\tilde{R}\mathbf{w}\| \leq \frac{3\tau_*^6}{2\gamma_*\rho_*}\|\mathbf{w}\|. \tag{12.58}$$

Proof. Using (12.56)–(12.57), we obtain

$$\|\tilde{N}\mathbf{w}\|^2 = \mathbf{w}^T \tilde{N}^T \tilde{N} \mathbf{w} = \mathbf{w}^T (C_1^T C_1 + C_2^T C_2 + \dots + C_{N_P^{\mathcal{F}}}^T C_{N_P^{\mathcal{F}}}) \mathbf{w} = N_P^{\mathcal{F}} \mathbf{w}^T \mathbf{w},$$

which proves the equality in (12.58). To estimate the norm of matrix $\tilde{\mathbf{R}}$, we note that

$$|P|^2 \|\tilde{\mathbf{R}}\mathbf{w}\|^2 = \|\mathbf{R}_0\mathbf{w}\|^2 = \sum_{k=1}^{N_P^{\mathcal{F}}} \left\| \int_{f_k} \mathbf{n}_{P,f_k} (\mathbf{w} \cdot (\mathbf{x} - \mathbf{x}_P)) dS \right\|^2. \quad (12.59)$$

Note that $\|\mathbf{x} - \mathbf{x}_P\| \leq h_P$ for any point $\mathbf{x} \in P$. Thus,

$$|P|^2 \|\tilde{\mathbf{R}}\mathbf{w}\|^2 \leq \|\mathbf{w}\|^2 \sum_{k=1}^{N_P^{\mathcal{F}}} |f_k| \int_{f_k} \|\mathbf{x} - \mathbf{x}_P\|^2 dS \leq \|\mathbf{w}\|^2 h_P^2 \sum_{k=1}^{N_P^{\mathcal{F}}} \int_{f_k} dS. \quad (12.60)$$

Now, we consider the pyramids $\hat{\mathbf{Q}}_k$ forming P and having \hat{f}_k as the bases. Using formula (12.19) to bound the height $H_{\hat{\mathbf{Q}}_k}$ of the pyramid $\hat{\mathbf{Q}}_k$, we obtain

$$|P| \geq \frac{1}{\tau_*^3} \sum_{k=1}^{N_P^{\mathcal{F}}} |\hat{\mathbf{Q}}_k| = \frac{1}{3\tau_*^3} \sum_{k=1}^{N_P^{\mathcal{F}}} |\hat{f}_k| H_{\hat{\mathbf{Q}}_k} \geq \frac{2\gamma_* \rho_* h_P}{3\tau_*^4} \sum_{k=1}^{N_P^{\mathcal{F}}} |\hat{f}_k| \geq \frac{2\gamma_* \rho_* h_P}{3\tau_*^6} \sum_{k=1}^{N_P^{\mathcal{F}}} |f_k|.$$

Inserting this in (12.60), gives

$$\|\tilde{\mathbf{R}}\mathbf{w}\|^2 \leq \left(\frac{3\tau_*^6}{2\gamma_* \rho_*} \right)^2 \|\mathbf{w}\|^2, \quad (12.61)$$

which is the upper bound in (12.58). The proof of the lower bound starts with the Gauss-Green formula

$$\sum_{k=1}^{N_P^{\mathcal{F}}} \int_{f_k} n_{P,f_k,i} (\mathbf{w} \cdot (\mathbf{x} - \mathbf{x}_P)) dS = w_i |P|.$$

Applying this result to (12.59), we obtain

$$\begin{aligned} |P|^2 \|\tilde{\mathbf{R}}\mathbf{w}\|^2 &\geq \frac{1}{N_P^{\mathcal{F}}} \sum_{i=1}^3 \left(\sum_{k=1}^{N_P^{\mathcal{F}}} \int_{f_k} n_{P,f_k,i} (\mathbf{w} \cdot (\mathbf{x} - \mathbf{x}_P)) dS \right)^2 \\ &\geq \frac{1}{N_P^{\mathcal{F}}} \sum_{i=1}^3 |P|^2 w_i^2 = \frac{|P|^2}{N_P^{\mathcal{F}}} \|\mathbf{w}\|^2. \end{aligned}$$

This proves the assertion of the lemma. \square

From Lemma 12.7, we may easily obtain estimates for the *unscaled* matrices \mathbf{R} and \mathbf{N} and their products with the tensor \mathbf{K}_P . In particular, using assumption **(H1b)**, we may prove that

$$\frac{1}{(\mathcal{N}^s \kappa^*)^{1/2}} |P| \leq \frac{\|\mathbf{K}_P^{-1/2} \mathbf{R}^T \mathbf{w}\|}{\|\mathbf{w}\|} \leq \frac{3\tau_*^6}{2\kappa_*^{1/2} \gamma_* \rho_*} |P| \quad \forall \mathbf{w} \neq 0. \quad (12.62)$$

Theorem 12.1. *Let the assumptions of Lemmas 12.5 and 12.7 hold. In addition, we assume that there exist two positive constants s_* and s^* , independent of P , such that*

$$s_* |P| \|\mathbf{v}_P\|^2 \leq \|\mathbf{U}^{1/2} \mathbf{D}^T \mathbf{v}_P\|^2 \quad \forall \mathbf{v}_P \in \text{img}(\mathbf{D}) \quad (12.63)$$

and

$$\|U^{1/2}D^T\mathbf{v}_P\|^2 \leq s^*|P|\|\mathbf{v}_P\|^2 \quad \forall \mathbf{v}_P \in \mathcal{F}_{h,P}. \quad (12.64)$$

Then, the matrix M_P in (12.51) satisfies assumption **(S1)**. More precisely, we have

$$\min \left\{ \frac{1}{2}s_*, \alpha_* \right\} |P|\|\mathbf{v}_P\|^2 \leq \mathbf{v}_P^T M_P \mathbf{v}_P \leq \max \{s^*, \alpha^*\} |P|\|\mathbf{v}_P\|^2, \quad (12.65)$$

where

$$\alpha_* = \frac{4\kappa_*\gamma_*^2\rho_*^2 s_*}{N^{\mathcal{F}}\kappa_* (18\tau_*^2 + 4s_*\kappa_*\gamma_*^2\rho_*^2)} \quad \text{and} \quad \alpha^* = \frac{9\tau_*^2}{4\kappa_*\gamma_*^2\rho_*^2}.$$

The proof of this theorem follows closely the proof of Theorem 4.2 (see also Theorem 3.6 in [93]); therefore, it is omitted. The rational is that the matrix $U^{1/2}D^T$ must be scaled properly with respect to material properties and the volume of P .

Remark 12.5. Let us assume that a generalized polyhedron is close to a regular polyhedron but anisotropic, i.e. $\tau_* \approx 1$ and $\gamma_*\rho_* \ll 1$. Then, the condition numbers of matrices $M_P^{(0)}$ and M_P grow as $(\gamma_*\rho_*)^{-2}$ and $(\gamma_*\rho_*)^{-4}$, respectively. This shows that the result of general Theorem 4.2 is optimal with respect to geometry.

Remark 12.6. In numerical computations, we recommend to orthonormalize the columns of matrix D and select $U = u|_{\ell_P}$, where u is the characteristics value of matrix $M_P^{(0)}$, for example, its mean eigenvalue or trace. The same applies to the construction of matrix W_P based on Lemma 12.6.

Let $m_P \neq 0$ be the number of the internal degrees of freedom for the flux, i.e., those degrees of freedom that are associated with the basis vectors $\mathbf{a}_P^{f,1}$ and $\mathbf{a}_P^{f,2}$ for each face f of ∂P . Due to static condensation, only part of matrix W_P has to be computed. Let us show why it is true. After permutation of columns and rows, matrices M_P and W_P may be written in a 2×2 block form:

$$M_P = \begin{pmatrix} M_{11} & M_{12} \\ M_{21} & M_{22} \end{pmatrix} \quad \text{and} \quad W_P = \begin{pmatrix} W_{11} & W_{12} \\ W_{21} & W_{22} \end{pmatrix},$$

where the first diagonal blocks correspond to the internal degrees of freedom. Matrices U and \tilde{U} can be chosen such that $W_P = M_P^{-1}$. The algorithms of static condensation and subsequent hybridization require the inverse of the Schur complement $M_{22} - M_{21} [M_{11}]^{-1} M_{12}$ which is nothing but the matrix W_{22} . The corresponding block of \tilde{D} can be computed with $3(\ell_P - m_P)^2 + O(\ell_P)$ flops. If all faces of element P are moderately curved, we have $m_P = 2N_P^{\mathcal{F}}$ and the above optimization becomes essential.

12.4 Convergence analysis and error estimates

Here, we prove optimal convergence estimates for both primary variables p and \mathbf{u} . Some of the proofs follow the pattern established in Chap. 5 where we proved the optimal convergence estimates for meshes with planar polygonal faces. Therefore, we shall omit some technical details which can be found there and focus more on the careful treatment of curved faces.

For the sake of simplicity, we assume that $p \in H^2(\Omega)$. However, this is not a serious restriction and, with an additional effort, it is possible to use a weaker regularity and to obtain lower-order convergence estimates.

The convergence analysis will be performed in the mesh dependent $L^2(\Omega)$ -type norms:

$$\| \|q_h\| \|_{\mathcal{T}_h}^2 = [q_h, q_h]_{\mathcal{T}_h} \quad \text{and} \quad \| \| \mathbf{v}_h \| \|_{\mathcal{F}_h}^2 = [\mathbf{v}_h, \mathbf{v}_h]_{\mathcal{F}_h}.$$

We will also use the mesh dependent $H(\text{div}, \Omega)$ norm for $\mathbf{v}_h \in \widehat{\mathcal{F}}_h$,

$$\| \| \mathbf{v}_h \| \|_{\text{div}}^2 = \sum_{P \in \Omega_h} \| \| \mathbf{v}_P \| \|_{\text{div}, P}^2, \quad \| \| \mathbf{v}_P \| \|_{\text{div}, P}^2 = [\mathbf{v}_h, \mathbf{v}_h]_{\mathcal{F}_h, P} + h_P^2 \| \text{div}_P \mathbf{v}_P \|_{L^2(P)}^2.$$

and the mesh dependent $H^1(\Omega)$ -type norm for $\mathbf{v} \in H^1(\Omega)$,

$$\| \| \mathbf{v} \| \|_{1, h}^2 = \sum_{P \in \Omega_h} \| \| \mathbf{v} \| \|_{1, h, P}^2, \quad \| \| \mathbf{v} \| \|_{1, h, P}^2 = \| \| \mathbf{v} \| \|_{L^2(P)}^2 + h_P^2 | \mathbf{v} |_{H^1(P)}^2.$$

12.4.1 Stability analysis

We analyze the stability of the mimetic discretization (12.36) following the well-established theory of saddle-point problems [88]. We recall the result which is well known for smooth domains and has been extended to Lipschitz domains by Bramble (see [76] and the references therein).

Lemma 12.8. *Let Ω be a connected bounded Lipschitz domain in \mathfrak{R}^3 . There exists a positive constant $\tilde{\beta} = \tilde{\beta}(\Omega)$ such that: for every $q \in L^2(\Omega)$ with zero mean value in Ω there exists a vector-valued function $\mathbf{v} \in (H_0^1(\Omega))^3$ such that*

$$\text{div } \mathbf{v} = q \quad \text{and} \quad \tilde{\beta} \| \| \mathbf{v} \| \|_{H^1(\Omega)} \leq \| \| q \| \|_{L^2(\Omega)}.$$

From this lemma we obtain almost immediately the following result.

Lemma 12.9. *Let Ω be a connected bounded Lipschitz domain in \mathfrak{R}^3 . There exists a positive constant $\beta = \beta(\Omega)$ such that: for every $q \in L^2(\Omega)$ there exists a vector-valued function $\mathbf{v} \in (H^1(\Omega))^3$ such that*

$$\text{div } \mathbf{v} = q \quad \text{and} \quad \beta \| \| \mathbf{v} \| \|_{H^1(\Omega)} \leq \| \| q \| \|_{L^2(\Omega)}. \quad (12.66)$$

Proof. First, for every $q \in L^2(\Omega)$, we define \bar{q} by

$$\bar{q} = \frac{1}{|\Omega|} \int_{\Omega} q \, dV.$$

Then, we consider the function $v = (x^2 + y^2 + z^2)\bar{q}/6$ and set $\mathbf{v}^1 = \nabla v$. Thus,

$$\operatorname{div} \mathbf{v}^1 = \bar{q} \quad \text{and} \quad c_1(\Omega) \|\mathbf{v}^1\|_{H^1(\Omega)} \leq \|\bar{q}\|_{L^2(\Omega)}$$

for some constant $c_1(\Omega)$ depending only on Ω . Since the mean value of $q - \bar{q}$ is zero, we can use Lemma 12.8 to find a vector-valued function \mathbf{v}^0 such that

$$\operatorname{div} \mathbf{v}^0 = q - \bar{q} \quad \text{and} \quad \tilde{\beta} \|\mathbf{v}^0\|_{H^1(\Omega)} \leq \|q - \bar{q}\|_{L^2(\Omega)}.$$

Let $\mathbf{v} = \mathbf{v}^0 + \mathbf{v}^1$. We have:

$$\begin{aligned} \|\mathbf{v}\|_{H^1(\Omega)}^2 &= \|\mathbf{v}^0 + \mathbf{v}^1\|_{H^1(\Omega)}^2 \leq 2(\|\mathbf{v}^0\|_{H^1(\Omega)}^2 + \|\mathbf{v}^1\|_{H^1(\Omega)}^2) \\ &\leq \frac{2}{\tilde{\beta}} \|\bar{q}\|_{L^2(\Omega)}^2 + \frac{2}{c_1(\Omega)} \|q - \bar{q}\|_{L^2(\Omega)}^2 \\ &\leq 2 \max\left(\frac{1}{\tilde{\beta}}, \frac{1}{c_1(\Omega)}\right) (\|\bar{q}\|_{L^2(\Omega)}^2 + \|q - \bar{q}\|_{L^2(\Omega)}^2). \end{aligned}$$

Using the L^2 -orthogonality of \bar{q} and $q - \bar{q}$, we see that

$$\|\bar{q}\|_{L^2(\Omega)}^2 + \|q - \bar{q}\|_{L^2(\Omega)}^2 = \|q\|_{L^2(\Omega)}^2$$

and we have easily the desired result with $1/\beta = \sqrt{2}(\max\{1/\tilde{\beta}, 1/c_1(\Omega)\})^{1/2}$. \square

Let P be a generalized polyhedron, and f be one of its faces. Definition 12.2 implies that there exists a generalized pyramid Q_f with the base f . Let \hat{Q}_f be the pyramid used in Definition 12.1 (together with the map Φ) to construct the generalized pyramid Q_f , i.e. $Q_f = \Phi(\hat{Q}_f)$ and $f = \Phi(\hat{f})$. In view of Agmon's inequality (see property **(M4)**) applied to pyramid \hat{Q}_f , there exists a constant C^{Agm} , depending only on constant γ_* of Definition 12.1, such that

$$\|\chi\|_{L^2(\hat{f})}^2 \leq C^{Agm} \left(H_{\hat{Q}}^{-1} \|\chi\|_{L^2(\hat{Q})}^2 + H_{\hat{Q}} |\chi|_{H^1(\hat{Q})}^2 \right) \quad \chi \in H^1(\hat{Q}_f) \quad (12.67)$$

Mapping back and forth from Q to \hat{Q} and using (12.5), we can show that there exists a constant C_*^{Agm} , depending only on the shape constants γ_* and τ_* of Assumption **(GR)**, such that

$$\|\chi\|_{L^2(f)}^2 \leq C_*^{Agm} \left(h_P^{-1} \|\chi\|_{L^2(Q_f)}^2 + h_P |\chi|_{H^1(Q_f)}^2 \right) \quad \chi \in H^1(P). \quad (12.68)$$

The following results extends a bound, which is natural for continuum norms, to the mesh dependent norms.

Lemma 12.10. *Let $\mathbf{v} \in (H^1(\Omega))^3$ and $\mathbf{v}^I \in \mathcal{F}_h$ be its projection defined in (12.26). Under assumptions **(H1b)**, **(GR)** and **(S1)**, there exists a positive constant β_s^* independent of the mesh such that*

$$\beta_s^* \|\mathbf{v}^I\|_{div} \leq \|\mathbf{v}\|_{1,h}. \quad (12.69)$$

Proof. Using bound (12.31), applying Agmon's inequality for pyramids (12.68) to each component of \mathbf{v} , and using bound (12.17) we get:

$$\begin{aligned} \|\mathbf{v}_{P,f}^I\| &\leq \frac{\tau_*^4}{2\gamma_* |\mathbf{f}|^{1/2}} \left(\int_f \|\mathbf{v}\|^2 dS \right)^{1/2} \\ &\leq \frac{\tau_*^4}{2\gamma_* |\mathbf{f}|^{1/2}} \left(C_*^{Agm} (h_P^{-1} \|\mathbf{v}\|_{L^2(Q_f)}^2 + h_P |\mathbf{v}|_{H^1(Q_f)}^2) \right)^{1/2} \\ &\leq \frac{\tau_*^4}{2\gamma_*} \frac{C_*^{Agm}}{a_*} \left(h_P^{-3} \|\mathbf{v}\|_{L^2(Q_f)}^2 + h_P^{-1} |\mathbf{v}|_{H^1(Q_f)}^2 \right)^{1/2}. \end{aligned}$$

Recalling assumption **(S1)** and the definition of norm $\|\cdot\|_{1,h,P}$, we have

$$\begin{aligned} [\mathbf{v}_P^I, \mathbf{v}_P^I]_{\mathcal{F}_{h,P}} &\leq \sigma^* \sum_{f \in \partial P} h_P^3 \|\mathbf{v}_{P,f}^I\|^2 \\ &\leq \sigma^* \sum_{f \in \partial P} h_P^3 \frac{\tau_*^8}{4\gamma_*^2} \frac{C_*^{Agm}}{a_*} \left(h_P^{-3} \|\mathbf{v}\|_{L^2(Q_f)}^2 + h_P^{-1} |\mathbf{v}|_{H^1(Q_f)}^2 \right) \\ &\leq \sigma^* \frac{\tau_*^8}{4\gamma_*^2} \frac{C_*^{Agm}}{a_*} \sum_{f \in \partial P} \|\mathbf{v}\|_{1,h,Q_f}^2 \\ &= \frac{\sigma^* \tau_*^8 C_*^{Agm}}{4\gamma_*^2 a_*} \|\mathbf{v}\|_{1,h,P}^2. \end{aligned} \quad (12.70)$$

Furthermore, from (12.33) and (12.25), we obtain

$$\|\operatorname{div}_P(\mathbf{v}_P^I)\|_{L^2(P)}^2 = \|(\operatorname{div} \mathbf{v})_P^I\|_{L^2(P)}^2 \leq \|\operatorname{div} \mathbf{v}\|_{L^2(P)}^2 \leq 3 |\mathbf{v}|_{H^1(P)}^2.$$

Combining the last two estimates, we prove the assertion of the lemma with $1/(\beta_s^*)^2 = \max\{3, \sigma^* \tau_*^8 C_*^{Agm} / (4\gamma_*^2 a_*)\}$. \square

Let W_h be the space of divergence-free discrete flux fields:

$$W_h = \{\mathbf{v}_h \in \mathcal{F}_h : \operatorname{div}_h \mathbf{v}_h = 0\}.$$

We begin the stability analysis by noticing that the inner product (12.37) is continuous. It is also obvious that it satisfies the W_h -ellipticity condition:

$$[\mathbf{v}_h, \mathbf{v}_h]_{\mathcal{F}_h} \geq \|\mathbf{v}_h\|_{div}^2 \quad \forall \mathbf{v}_h \in W_h. \quad (12.71)$$

Lemma 12.11. *Under assumptions of Lemma 12.10, there exists a positive constant β_* independent of q_h , \mathbf{v}_h , and h such that*

$$\inf_{q_h \in \mathcal{P}_h} \sup_{\mathbf{v}_h \in \mathcal{F}_h} [\text{div}_h \mathbf{v}_h, q_h]_{\mathcal{P}_h} \geq \beta_* \|\mathbf{v}_h\|_{\text{div}} \|q_h\|_{\mathcal{P}_h}. \quad (12.72)$$

Proof. Let us consider $q_h = \{q_P\}_{P \in \Omega_h} \in \mathcal{P}_h$, and the piecewise constant function \tilde{q} that takes the value q_P over cell P . Applying Lemma 12.9, we find a function $\mathbf{v} \in H(\text{div}, \Omega)$ such that

$$\text{div } \mathbf{v} = \tilde{q} \quad \text{and} \quad \beta \|\mathbf{v}\|_{H^1(\Omega)} \leq \|\tilde{q}\|_{L^2(\Omega)}.$$

We define a discrete flux field as $\mathbf{v}_h = \mathbf{v}^I$. The commuting property (12.33) implies that $\text{div}_h \mathbf{v}_h = (\text{div } \mathbf{v})^I = q_h$. Combining the last inequality with (12.69) and noting that $\|\mathbf{v}\|_{1,h} \leq \beta \|\mathbf{v}\|_{H^1(\Omega)}$, we obtain

$$\beta_s^* \beta \|\mathbf{v}_h\|_{\text{div}} \leq \beta \|\mathbf{v}\|_{1,h} \leq \beta \|\mathbf{v}\|_{H^1(\Omega)} \leq \|\tilde{q}\|_{L^2(\Omega)} = \|q_h\|_{\mathcal{P}_h}.$$

This gives immediately the *inf-sup* condition (12.72) with $\beta_* = \beta_s^* \beta$. □

12.4.2 Convergence of the vector variable

According to Lemma 12.2, every element P is star-shaped with respect to a sphere of radius $\rho_* h_P$. Hence, the approximation property **(M5)** can be extended to a generalized polyhedron P that satisfies assumption **(GR)**. More precisely, there exists a positive constant C^{lm} , depending only on ρ_* , such that, for every $q \in H^{m+1}(P)$, $m = 0, 1$, there exists a $q_P^{(m)} \in \mathbb{P}_m(P)$ such that

$$\|q - q_P^{(m)}\|_{L^2(P)} + \sum_{k=1}^s h_P^k \|q - q_P^{(m)}\|_{H^1(P)} \leq C^{lm} h_P^{m+1} |q|_{H^{m+1}(P)}. \quad (12.73)$$

The proofs of the two following lemmas can be found in [91]. They are based on standard arguments such as the Cauchy-Schwarz inequality, ellipticity property **(Hb)**, Lemma 12.10, and approximation result (12.73).

Lemma 12.12. *Let $q \in H^2(\Omega)$ and $q_P^{(1)}$ be the linear approximation of q over P satisfying (12.73). Then, there exists a positive constant C_1 independent of q and h such that for every $\mathbf{v}_h \in \mathcal{F}_h$ it holds:*

$$\sum_{P \in \Omega_h} \left[(K \nabla (q - q_P^{(1)}))^I_{P, \mathbf{v}_P} \right]_{\mathcal{F}_{h,P}} \leq C_1 h |q|_{H^2(\Omega)} \|\mathbf{v}_h\|_{\mathcal{F}_h}. \quad (12.74)$$

Lemma 12.13. *There exists a positive constant C_2 independent of h such that for every $\mathbf{v}_h \in \mathcal{F}_h$ and every $q \in H^2(\Omega)$ it holds*

$$\left[((K - \bar{K}) \nabla q)^I, \mathbf{v}_h \right]_{\mathcal{F}_h} \leq C_2 h (|q|_{H^1(\Omega)} + h |q|_{H^2(\Omega)}) \|\mathbf{v}_h\|_{\mathcal{F}_h}, \quad (12.75)$$

where \bar{K} is a suitable piecewise-constant approximation of K on Ω_h .

Lemma 12.14. *Let $q \in H^2(\Omega) \cap H_0^1(\Omega)$ and $q_P^{(1)}$ be the linear approximation of q over P satisfying (12.73). Then, under assumptions **(H1b)** and **(C1)**, there exists a positive constant C_3 independent of q and h such that for every $\mathbf{v}_h \in \mathcal{F}_h$ it holds:*

$$\sum_{P \in \Omega_h} \sum_{f \in \partial P} \int_f q_P^{(1)} \mathbf{v}_{P,f} \cdot \mathbf{n}_{P,f} dS \leq C_3 h \|q\|_{H^2(\Omega)} \|\mathbf{v}_h\|_{\mathcal{F}_h}. \quad (12.76)$$

Proof. In the proof we have to distinguish between boundary faces, strongly curved faces, and moderately curved faces.

First, let f be a boundary face, and P be the only element containing f . Since $q = 0$ on f , the contribution of this face to the sum in (12.76) can be estimated using (12.68) and (12.39):

$$\begin{aligned} \int_f q_P^{(1)} \mathbf{v}_{P,f} \cdot \mathbf{n}_{P,f} dS &= \int_f (q_P^{(1)} - q) \mathbf{v}_{P,f} \cdot \mathbf{n}_{P,f} dS \\ &\leq \|q - q_P^{(1)}\|_{L^2(f)} \|\mathbf{v}_{P,f}\|_{L^2(f)} = \|q - q_P^{(1)}\|_{L^2(f)} \|\mathbf{v}_{P,f}\| |f|^{1/2} \\ &\leq a_*^{-1} (C_*^{A_{gm}})^{1/2} h_P |q|_{H^2(P)} \|\mathbf{v}_{P,f}\| |P|^{1/2} \\ &\leq C_{3,a} h |q|_{H^2(P)} \|\mathbf{v}_P\|_{\mathcal{F}_{h,P}}, \end{aligned}$$

where $C_{3,a} = (C_*^{A_{gm}})^{1/2} (a_* \sigma_*)^{-1}$.

Second, let f be a strongly curved interior face, and P_1 and P_2 be the two elements sharing f . Due to assumption **(C1)**, all three components of \mathbf{v}_h are continuous across f , so that *at every point* of f we have

$$\mathbf{v}_{P_1,f} \cdot \mathbf{n}_{P_1,f} + \mathbf{v}_{P_2,f} \cdot \mathbf{n}_{P_2,f} = 0.$$

Using the continuity of q , we can estimate the contribution of this face to the total sum:

$$\begin{aligned} \sum_{i=1}^2 \int_f q_{P_i}^{(1)} \mathbf{v}_{P_i,f} \cdot \mathbf{n}_{P_i,f} dS &= \sum_{i=1}^2 \int_f (q_{P_i}^{(1)} - q) \mathbf{v}_{P_i,f} \cdot \mathbf{n}_{P_i,f} dS \\ &\leq \sum_{i=1}^2 \|q - q_{P_i}^{(1)}\|_{L^2(f)} \|\mathbf{v}_{P_i,f}\|_{L^2(f)} \\ &\leq \sum_{i=1}^2 a_*^{-1} (C_{face}^*)^{1/2} h_{P_i} |q|_{H^2(P_i)} \|\mathbf{v}_{P_i,f}\| |P_i|^{1/2} \\ &\leq \sum_{i=1}^2 C_{3,b} h |q|_{H^2(P_i)} \|\mathbf{v}_{P_i}\|_{\mathcal{F}_{h,P_i}}. \end{aligned} \quad (12.77)$$

Third, let f be a moderately curved face f shared by two elements P_1 and P_2 . Due to assumption **(C1)**, only the component of \mathbf{v}_h in the direction of $\tilde{\mathbf{n}}_{P,f}$ is continuous

across f . From (12.6) we obtain that

$$\int_f q^{(0)} (\mathbf{n}_{P_i,f} - \tilde{\mathbf{n}}_{P_i,f}) dS = 0 \quad (12.78)$$

for $i = 1, 2$ and every constant $q^{(0)}$. Adding and subtracting the average normal $\tilde{\mathbf{n}}_{P_i,f}$, and then using (12.78) in the first term and the continuity of q and \mathbf{v}_h in the second term, we obtain

$$\begin{aligned} \sum_{i=1}^2 \int_f q_{P_i}^{(1)} \mathbf{v}_{P_i,f} \cdot \mathbf{n}_{P_i,f} dS &= \sum_{i=1}^2 \int_f (q_{P_i}^{(1)} - q_{P_i}^{(0)}) \mathbf{v}_{P_i,f} \cdot (\mathbf{n}_{P_i,f} - \tilde{\mathbf{n}}_{P_i,f}) dS \\ &\quad + \sum_{i=1}^2 \int_f (q_{P_i}^{(1)} - q) \mathbf{v}_{P_i,f} \cdot \tilde{\mathbf{n}}_{P_i,f} dS. \end{aligned} \quad (12.79)$$

The second term in (12.79) can be estimated exactly as in (12.77):

$$\sum_{i=1}^2 \int_f (q_{P_i}^{(1)} - q) \mathbf{v}_{P_i,f} \cdot \tilde{\mathbf{n}}_{P_i,f} dS \leq \sum_{i=1}^2 C_{3,b} h |u|_{H^2(P_i)} \|\mathbf{v}_{P_i}\|_{\mathcal{F}_h, P_i}.$$

To estimate the first term, we finally use the fact that f is a moderately curved face, and in particular inequality (12.16):

$$\begin{aligned} \int_f (q_{P_i}^{(1)} - q_{P_i}^{(0)}) \mathbf{v}_{P_i,f} \cdot (\mathbf{n}_{P_i,f} - \tilde{\mathbf{n}}_{P_i,f}) dS &\leq \eta_* |f|^{1/2} \|q_{P_i}^{(1)} - q_{P_i}^{(0)}\|_{L^2(f)} \|\mathbf{v}_{P_i,f}\|_{L^2(f)} \\ &\leq \eta_* \alpha_*^{-1} C_{**}^{face} h_{P_i} \|u\|_{H^1(P_i)} |\mathbf{v}_{P_i,f}| |P_i|^{1/2} \\ &\leq C_{3,c} h \|q\|_{H^2(P)} \|\mathbf{v}_{P_i}\|_{\mathcal{F}_h, P_i}, \end{aligned}$$

where C_{**}^{face} depends only on C_*^{Int} and C_*^{Agm} while $C_{3,c}$ also depends on the constant α_* appearing in (12.17) and the constant η_* appearing in (12.16).

Collecting all the above estimates and noting that every element appears as many times as the number of its faces, we prove the assertion of the lemma. \square

Theorem 12.2. *Let (p, \mathbf{u}) with $p \in H^2(\Omega)$ be the solution of (12.1)–(12.3) with $g^D = 0$, and $(p_h, \mathbf{u}_h) \in \mathcal{P}_h \times \mathcal{F}_h$ be the solution of (12.36) under assumptions **(H1b)**, **(GR)**, **(S1)**–**(S2)**, and **(C1)**. Moreover, let \mathbf{u}^1 be the interpolant of \mathbf{u} introduced in (12.27)–(12.28). Then,*

$$\|\mathbf{u}^1 - \mathbf{u}_h\|_{\mathcal{F}_h} \leq Ch \|p\|_{H^2(\Omega)}, \quad (12.80)$$

where the constant C is independent of h and p .

Proof. We define the error mesh function as $\varepsilon_h = \mathbf{u}^1 - \mathbf{u}_h$. From (12.2), (12.35), and (12.33) we easily have:

$$\operatorname{div}_h \varepsilon_h = \operatorname{div}_h(\mathbf{u}^1 - \mathbf{u}_h) = b^1 - b^1 = 0. \quad (12.81)$$

The first equation in (12.35) implies that

$$\|\|\|\varepsilon_h\|\|\|_{\mathcal{F}_h}^2 = [(-\mathbb{K}\nabla p)^I, \varepsilon_h]_{\mathcal{F}_h} - [(-\nabla_h p_h), \varepsilon_h]_{\mathcal{F}_h}.$$

From Eq. (12.81) it follows that:

$$[\nabla_h p_h, \varepsilon_h]_{\mathcal{F}_h} = [p_h, \operatorname{div}_h \varepsilon_h]_{\mathcal{F}_h} = 0.$$

Thus, we obtain

$$\|\|\|\varepsilon_h\|\|\|_{\mathcal{F}_h}^2 = [(-\mathbb{K}\nabla p)^I, \varepsilon_h]_{\mathcal{F}_h}.$$

Let $\bar{\mathbb{K}}$ be a piecewise constant tensor with value \mathbb{K}_P in element P . Then, adding and subtracting terms, we break the error into three parts:

$$\begin{aligned} \|\|\|\varepsilon_h\|\|\|_{\mathcal{F}_h}^2 &= [(-\mathbb{K}\nabla p)^I + (\bar{\mathbb{K}}\nabla p)^I, \varepsilon_h]_{\mathcal{F}_h} + \sum_{P \in \Omega_h} [(-\bar{\mathbb{K}}\nabla p + \bar{\mathbb{K}}\nabla p_P^{(1)})^I_P, \varepsilon_P]_{\mathcal{F}_{h,P}} \\ &+ \sum_{P \in \Omega_h} [(-\bar{\mathbb{K}}\nabla p_P^{(1)})^I_P, \varepsilon_P]_{\mathcal{F}_{h,P}} = \mathbf{I}_1 + \mathbf{I}_2 + \mathbf{I}_3. \end{aligned} \quad (12.82)$$

Using (12.41) and (12.81), the third term can be developed as follows:

$$\begin{aligned} \mathbf{I}_3 &= \sum_{P \in \Omega_h} \left\{ \sum_{f \in \partial P} \int_f p_P^{(1)} \varepsilon_{P,f} \cdot \mathbf{n}_{P,f} dS - \int_P p_P^{(1)} \operatorname{div}_P \varepsilon_P dV \right\} \\ &= \sum_{P \in \Omega_h} \sum_{f \in \partial P} \int_f u_P^{(1)} \varepsilon_{P,f} \cdot \mathbf{n}_{P,f} dS. \end{aligned} \quad (12.83)$$

Term \mathbf{I}_1 is bounded by Lemma 12.12. Term \mathbf{I}_2 is bounded by Lemma 12.13. Term \mathbf{I}_3 is bounded by Lemma 12.14. This proves the assertion of the lemma. \square

12.4.3 Convergence of the scalar variable

The first estimate for the scalar variable mimics closely (but not exactly) the corresponding result for polyhedral meshes derived in Chap. 5. The original proof of this estimate given in [91] is based on a duality argument. To get the first-order convergence rate, we assume that Ω is convex; however, a lower order convergence rate could be obtained under less restrictive regularity assumptions.

Theorem 12.3. *Let Ω be a convex domain. Under assumptions of Theorem 12.2, we have*

$$\|\|p_h - p^I\|\|_{\mathcal{F}_h} \leq Ch \left(\|p\|_{H^2(\Omega)} + \|b\|_{H^1(\Omega)} \right), \quad (12.84)$$

where the constant C is independent of h , p and b .

Note that the load term in (12.84) can be also substituted with the more realistic term

$$\left(\sum_{P \in \Omega_h} \|b\|_{H^1(P)}^2 \right)^{1/2}. \quad (12.85)$$

12.5 Exact reconstruction operators

In this section, we prove a superconvergence estimate for the scalar variable under the condition that an *exact* reconstruction operator exists for the mimetic scheme. The exact reconstruction operator allows us to write the mimetic inner product as an L^2 integral for functions in $S_{h,P}$. The space $S_{h,P}$ has been introduced in the consistency condition **(S2)**. It satisfies assumptions **(B1)**–**(B3)** and, for the present section, also the additional dimensionality restriction (12.42).

We stress again that only the existence of an exact reconstruction operator has to be shown, but it is not required for the practical implementation of the method.

12.5.1 Existence of the exact reconstruction operator

We assume that for every element P in Ω_h there exists a reconstruction operator $R_P: \mathcal{F}_{h,P} \rightarrow S_{h,P}$ satisfying the following three properties.

(L1) For every discrete field $\mathbf{v}_P \in \mathcal{F}_{h,P}$, the reconstructed function has constant divergence and preserves boundary data:

$$\begin{aligned} R_P(\mathbf{v}_P)|_f &= \mathbf{v}_{P,f} && \text{on } f \in \partial P, \\ \operatorname{div} R_P(\mathbf{v}_P) &= \operatorname{div}_P \mathbf{v}_P && \text{in } P. \end{aligned} \tag{12.86}$$

(L2) The reconstruction operator is a left inverse of the projection operator on the space \mathcal{T}_P of constant vector functions:

$$R_P(\mathbf{c}_P^1) = \mathbf{c} \quad \forall \mathbf{c} \in (\mathbb{P}_0(P))^3. \tag{12.87}$$

(L3) For a given mimetic inner product, the reconstruction operator reproduces it exactly:

$$[\mathbf{u}_P, \mathbf{v}_P]_{\mathcal{F}_{h,P}} = \int_P K_P^{-1} R_P(\mathbf{u}_P) \cdot R_P(\mathbf{v}_P) dV \quad \forall \mathbf{u}_P, \mathbf{v}_P \in \mathcal{F}_{h,P}. \tag{12.88}$$

These assumptions mimic that in Chap. 5. Hence, a proof of the existence of R_P is almost identical to the proof of Lemma 5.10 with minor modifications related to the definition of a minimum reconstruction operator.

Let us fix a number s such that $6/5 \leq s < 2$ and for every $\mathbf{v}_P \in \mathcal{F}_{h,P}$ consider the Stokes-like problem: Find $\boldsymbol{\beta} \in (W^{1,s}(P))^3$ and $\chi \in L^s(P)$ such that

$$\begin{aligned} -\Delta \boldsymbol{\beta} + \nabla \chi &= \mathbf{0} && \text{in } P, \\ \operatorname{div} \boldsymbol{\beta} &= \operatorname{div}_P \mathbf{v}_P && \text{in } P, \\ \boldsymbol{\beta} &= \mathbf{v}_{P,f} && \text{on } f \in \partial P. \end{aligned} \tag{12.89}$$

We define the minimum reconstruction operator by $\tilde{R}_P(\mathbf{v}_P) := \boldsymbol{\beta}$. We recall that in three dimensions for $s \geq 6/5$, we have $W^{1,s}(P) \subset L^2(P)$. It is clear that this reconstruction operator satisfies properties **(L1)** and **(L2)**. It can be modified to satisfy property **(L3)**.

Let $\tilde{S}_{h,P} = \tilde{R}_P(\mathcal{F}_{h,P})$. We apply a change of basis in $\tilde{S}_{h,P}$, taking the three constant vectors in the first three positions, and we apply the corresponding change of variables in $\mathcal{F}_{h,P}$. Let functions $\mathbf{w}_1, \dots, \mathbf{w}_{\ell_P}$ form the new basis in $\tilde{S}_{h,P}$, where $\mathbf{w}_1 = (1, 0, 0)^T$, $\mathbf{w}_2 = (0, 1, 0)^T$, and $\mathbf{w}_3 = (0, 0, 1)$. Without loss of generality, we assume that the basis functions are orthogonal in the following sense:

$$\int_P K_P^{-1} \mathbf{w}_i \cdot \mathbf{w}_j dV = 0, \quad 1 \leq i \leq 3 < j \leq \ell_P.$$

Thus, the weighted mass matrix G_P for the basis $\{\mathbf{w}_i\}$ has the block diagonal structure:

$$G_P = \begin{pmatrix} |P| K_P^{-1} & 0 \\ 0 & \hat{G}_P \end{pmatrix}, \quad (\hat{G}_P)_{i-3, j-3} = \int_P K_P^{-1} \mathbf{w}_i \cdot \mathbf{w}_j dV \quad i, j > 3 \quad (12.90)$$

The corresponding change of basis in $\mathcal{F}_{h,P}$ results in an equivalency transformation for the mimetic inner product matrix M_P . The transformed matrix, \tilde{M}_P , has the following block-diagonal structure:

$$\tilde{M}_P = \begin{pmatrix} |P| K_P^{-1} & 0 \\ 0 & \hat{M}_P \end{pmatrix}, \quad (12.91)$$

where, of course, \hat{G}_P and \hat{M}_P are generally different. This is due to the fact that the mimetic inner product satisfies the consistency condition, i.e. it is exact when one of the two arguments corresponds to a constant vector function.

Now, we can proceed like in the proof of Lemma 5.10 and modify the last $\ell_P - 3$ basis functions still preserving properties (L1)–(L2). We formulate the final result without a proof, see [91] for more detail.

Lemma 12.15. *Let \tilde{R}_P be the minimal reconstruction operator and M_P be a given mimetic inner product matrix. Furthermore, let matrices \tilde{M}_P and \hat{G}_P be given by formulas (12.91) and (12.90), respectively. If $\tilde{M}_P - \hat{G}_P$ is a symmetric semi-positive definite matrix, then, there exists an exact reconstruction operator R_P satisfying (12.88).*

Corollary 12.1. *Let the conditions of Lemma 12.15 hold. Then, an exact reconstruction operator exists if*

$$\|M_P^{1/2} \mathbf{v}_P\| \geq \|G_P^{1/2} \mathbf{v}_P\| \quad \forall \mathbf{v}_P \in \text{img}(D).$$

The proof of this corollary is based on deriving an explicit form for the equivalency transformation mentioned above.

When the columns of D are orthonormal vector and $U = u \mathbf{1}_{\ell_P}$, the above lemma requires u to be sufficiently large. Indeed, since $\mathbf{v}_P \in \text{img}(D)$, we obtain $DD^T \mathbf{v}_P = \mathbf{v}_P$ since DD^T is the orthogonal projector onto $\text{img}(D)$ and

$$\mathbf{v}_P^T M_P \mathbf{v}_P = \frac{1}{|P|^{1/2}} \|K^{-1/2} R^T \mathbf{v}_P\|^2 + u \|\mathbf{v}_P\|^2 \geq u \|\mathbf{v}_P\|^2. \quad (12.92)$$

On the other hand,

$$\mathbf{v}_P^T G_P \mathbf{v}_P \leq \lambda_{\max}(G_P) \|\mathbf{v}_P\|^2, \quad (12.93)$$

where $\lambda_{\max}(G_P)$ is the maximum eigenvalue of G_P . Thus, it is sufficient to take u larger than $\lambda_{\max}(G_P)$ to satisfy Lemma 12.15 and hence, to guarantee theoretically a superlinear convergence of the related mimetic scheme.

Remark 12.7. Since, the superconvergence is observed for a wider range of parameters u , the existing theory, based on the exact reconstruction operator is not complete.

12.5.2 Superlinear convergence of the scalar variable

Let us assume that we an exact reconstruction operator $R_P(\mathbf{v}_P)$ does exist. Then, a better convergence estimate for the scalar variable can be derived in the mesh dependent L^2 norm.

Note that, from **(S1)** and **(L3)**, we have the following stability property:

$$\|R_P(\mathbf{v}_P)\|_{L^2(P)}^2 \leq \sigma^* |P| \mathbf{v}_P^T \mathbf{v}_P. \quad (12.94)$$

Theorem 12.4. *In addition to the conditions of Theorem 12.3, we assume that for each element P there exists a exact reconstruction operator $R_P(\cdot)$ with the properties **(L1)**–**(L3)**. Furthermore, let K be piecewise constant tensor. Then, it holds*

$$\| \|p_h - p^I\| \|_{\mathcal{F}_h} \leq Ch^2 \left(\|p\|_{H^2(\Omega)} + |b|_{H^1(\Omega)} \right), \quad (12.95)$$

where the constant C is independent of h , u and b .

Proof. Let $\mathbf{v} \in (H^1(P))^3$ be specified later and \mathbf{v}_P^I be its projection to $\mathcal{F}_{h,P}$. Using the continuity condition (12.94) and following closely the proof of Lemma 12.10, especially inequality (12.70), we obtain

$$\|R_P(\mathbf{v}_P)\|_{L^2(P)}^2 \leq \frac{C_R^* \tau_*^8 C_*^{A_{gm}}}{4\gamma_*^2 a_*} \|\mathbf{v}\|_{1,h,P}^2. \quad (12.96)$$

Let \mathbf{v}^0 be the mean value (component-wise) of function \mathbf{v} over P . Using assumption **(L2)**, estimate (12.96) and the approximation result (12.73), we have

$$\begin{aligned} \|R_P(\mathbf{v}_P) - \mathbf{v}\|_{L^2(P)} &\leq \|R_P(\mathbf{v}_P - (\mathbf{v}^0)^I)\|_{L^2(P)} + \|\mathbf{v}^0 - \mathbf{v}\|_{L^2(P)} \\ &\leq \left(\frac{C_R^* \tau_*^8 C_*^{A_{gm}}}{4\gamma_*^2 a_*} \right)^{1/2} \|\mathbf{v} - \mathbf{v}^0\|_{1,h,P} + \|\mathbf{v}^0 - \mathbf{v}\|_{L^2(P)} \\ &\leq Ch_P |\mathbf{v}|_{H^1(P)}. \end{aligned} \quad (12.97)$$

Hereafter all generic constants C are independent of h and P .

Let $\varepsilon_h = p^I - p_h$ be the error mesh function. Let $\tilde{\varepsilon}_h$ be a piecewise constant function with value ε_P over element P . We consider the elliptic problem

$$\begin{aligned} -\operatorname{div}(\mathbf{K}\nabla v) &= \tilde{\varepsilon}_h & \text{in } \Omega, \\ v &= 0 & \text{on } \partial\Omega. \end{aligned} \quad (12.98)$$

The convexity of Ω implies that there exists a constant C_Ω , depending only on Ω , such that

$$\|v\|_{H^2(\Omega)} \leq C_\Omega \|\tilde{\varepsilon}_h\|_{L^2(\Omega)} = C_\Omega \|\varepsilon_h\|_{\mathcal{P}_h}. \quad (12.99)$$

We set $\mathbf{v} = \mathbf{K}\nabla v$. Furthermore, let $R(\mathbf{v}^I)$ be the global exact reconstruction operator such that its restriction to element P is $R_P(\mathbf{v}_P^I)$. Following essentially [143] and using (12.36), then (12.24) with assumption **(L1)**, then integrating by parts, and finally using (12.1) and (12.88), we obtain

$$\begin{aligned} \|\varepsilon_h\|_{\mathcal{P}_h}^2 &= [\operatorname{div}_h \mathbf{v}^I, p_h - p^I]_{\mathcal{P}_h} = [\mathbf{u}_h, \mathbf{v}^I]_{\mathcal{P}_h} - \int_\Omega q \operatorname{div} R(\mathbf{v}^I) dV \\ &= [\mathbf{u}_h, \mathbf{v}^I]_{\mathcal{P}_h} + \int_\Omega (\mathbf{K}^{-1} \mathbf{K}) \nabla q \cdot R(\mathbf{v}^I) dV \\ &= \int_\Omega \mathbf{K}^{-1} (R(\mathbf{u}_h) - \mathbf{u}) R(\mathbf{v}^I) dV. \end{aligned}$$

Adding and subtracting \mathbf{v} , we have

$$\begin{aligned} \|\varepsilon_h\|_{\mathcal{P}_h}^2 &= \int_\Omega \mathbf{K}^{-1} (R(\mathbf{u}_h) - \mathbf{u}) (R(\mathbf{v}^I) - \mathbf{v}) dV + \int_\Omega \mathbf{K}^{-1} (R(\mathbf{u}_h) - \mathbf{u}) \mathbf{v} dV \\ &= \mathbf{J}_1 + \int_\Omega (R(\mathbf{u}_h) - \mathbf{u}) \nabla v dV = \mathbf{J}_1 - \int_\Omega v \operatorname{div} (R(\mathbf{u}_h) - \mathbf{u}) dV \\ &= \mathbf{J}_1 - \int_\Omega (b^I - b) v dV \\ &= \mathbf{J}_1 - \int_\Omega (b^I - b) (v - v^I) dV = \mathbf{J}_1 + \mathbf{J}_2. \end{aligned} \quad (12.100)$$

The terms \mathbf{J}_1 and \mathbf{J}_2 can be easily bounded using the previous estimates and usual arguments. Indeed, the triangle inequality, then assumption **(L3)**, and finally Theorem 12.2 and estimate (12.97) imply that

$$\begin{aligned} \|R(\mathbf{u}_h) - \mathbf{u}\|_{L^2(\Omega)} &\leq \|R(\mathbf{u}_h - \mathbf{u}^I)\|_{L^2(\Omega)} + \|R(\mathbf{u}^I) - \mathbf{u}\|_{L^2(\Omega)} \\ &\leq \|\mathbf{u}_h - \mathbf{u}^I\|_{\mathcal{P}_h} + \|R(\mathbf{u}^I) - \mathbf{u}\|_{L^2(\Omega)} \\ &\leq Ch \|p\|_{H^2(\Omega)}. \end{aligned}$$

Using (12.97) and regularity result (12.99), we obtain

$$\|R(\mathbf{v}^I) - \mathbf{v}\|_{L^2(\Omega)} \leq Ch \|\mathbf{v}\|_{H^1(\Omega)} \leq CC_\Omega^* h \|\varepsilon_h\|_{\mathcal{P}_h}.$$

The approximation property (12.73) gives the following estimates:

$$\|b^I - b\|_{L^2(\Omega)} \leq C^{Int} h |b|_{H^1(\Omega)}$$

and

$$\|v - v^J\|_{L^2(\Omega)} \leq C^{Int} h |v|_{H^1(\Omega)} \leq C^{Int} C_{\Omega}^* h \|\varepsilon_h\|_{\mathcal{D}_h}.$$

Inserting the last estimates into (12.100), we prove the assertion of the theorem. \square

Remark 12.8. Note that also in this case the load term in (12.95) can be easily substituted with the more realistic term

$$\left(\sum_{P \in \Omega_h} |b|_{H^1(P)}^2 \right)^{1/2}. \tag{12.101}$$

Example 12.1. Let us consider a model diffusion problem in the unit cube with the identify tensor K and the smooth solution

$$p(x, y, z) = x^2 y^3 z + 3x \sin(yz).$$

We measure the accuracy of the mimetic solution (p_h, \mathbf{u}_h) in the mesh dependent norms induced by the inner products (12.34) and (12.37). The mesh faces are classified on moderately and strongly curved using $\eta_* = 0.2$.

The convergence rate is calculated numerically using a sequence of generalized hexahedral (see Fig. 12.1) and polyhedral (see Fig. 12.4) meshes. In Fig. 12.1 a part of the unit cube was cut out to show the interior mesh. Each hexahedral mesh is generated from an orthogonal cubic mesh with mesh step h by moving each mesh vertex v into a random position inside a cube $C(v)$ centered at the vertex. The sides of cube $C(v)$ are aligned with the coordinate axes and their length equals to $0.8h$. Each polyhedral mesh is generated in a similar fashion from a Voronoi mesh. For the chosen threshold η_* , 68% of the interior mesh faces are classified as strongly curved.

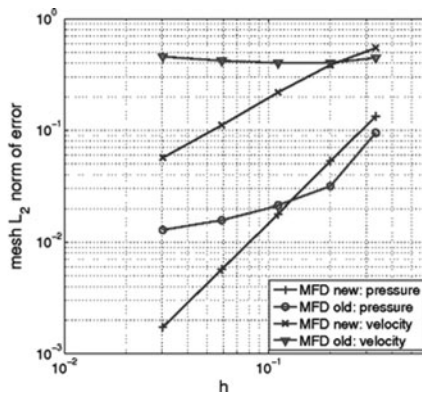
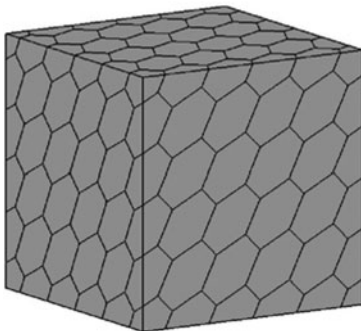


Fig. 12.4. The trace of the generalized polyhedral mesh (left picture) and convergence graphs (right picture) showing the optimal convergence rates for the new MFD method (+ and x) and lack of convergence for the old MFD method (triangles and circles)

The mimetic scheme uses the stability matrix $W_p^{(1)}$ with the orthogonal \tilde{D} and scalar $\tilde{U} = \tilde{u}_p l$, where $\tilde{u}_p = \text{trace}(K_p)/|P|$. The convergence graphs in Fig. 12.1 show the optimal convergence rate for the new mimetic scheme and the lack of convergence for the lowest order Raviart-Thomas finite element method with and the mimetic scheme described in Chap. 5. Note that the last two scheme use *one* degree of freedom per mesh face to approximate the flux on strongly curved faces.

A similar statement can be drawn from Fig. 12.4. The mimetic scheme from Chap. 5 lacks convergence for both primary variables. The new scheme exhibits the first-order convergence rate for the flux and the second-order convergence rate for the scalar variables.

References

1. Aarnes, J.E., Krogstad, S., Lie, K.-A.: Multiscale mixed/mimetic methods on corner-point grids. *Computat. Geosci.* **12**(3), 297–315 (2007)
2. Aavatsmark, I.: An introduction to multipoint flux approximations for quadrilateral grids. *Computat. Geosci.* **6**, 405–432 (2002)
3. Aavatsmark, I., Barkve, T., Bøe, Ø., Mannseth, T.: Discretization on unstructured grids for inhomogeneous, anisotropic media. I. Derivation of the methods. *SIAM J. Sci. Comput.* **19**(5), 1700–1716 (1998)
4. Aavatsmark, I., Barkve, T., Bøe, Ø., Mannseth, T.: Discretization on unstructured grids for inhomogeneous, anisotropic media. II. Discussion and numerical results. *SIAM J. Sci. Comput.* **19**(5), 1717–1736 (1998)
5. Abba, A., Bonaventura, L.: A mimetic finite difference discretization for the incompressible Navier-Stokes equations. *Int. J. Numer. Meth. in Fluids* **56**(8), 1101–1106 (2008)
6. Abramowitz, M., Stegun, I.A.: *Handbook of Mathematical Functions with Formulas, Graphs, and Mathematical Tables*. 9th Dover printing, 10th gpo printing edition. Dover, New York (1964)
7. Agmon, S.: *Lectures on Elliptic Boundary Value Problems*. Van Nostrand (1965)
8. Ainsworth, M., Oden, J.T.: A posteriori error estimation in finite element analysis. *Comput. Meth. Appl. Mech. Engrg.* **142**(1–2), 1–88 (1997)
9. Ainsworth, M., Oden, J.T.: *A posteriori error estimation in finite element analysis*. Pure and Applied Mathematics. Wiley-Interscience [John Wiley & Sons], New York (2000)
10. Alpak, F.O.: A mimetic finite volume discretization method for reservoir simulation. *SPE Journal* **15**(2), 436–453 (2010)
11. Amoruche, C., Bernardi, C., Dauge, M., Girault, V.: Vector potentials in three dimensional non-smooth domains. *Math. Mod. Meth. Appl. Sci.* **21**, 823–864 (1998)
12. Andreianov, B., Bendahmane, M., Karlsen, K.H.: A gradient reconstruction formula for finite volume schemes and discrete duality. In: *Finite Volumes for Complex Applications V*, pp. 161–168. ISTE, London (2008)
13. Andreianov, B., Boyer, F., Hubert, F.: Discrete duality finite volume schemes for Leray-Lions type elliptic problems on general 2D meshes. *Numer. Meth. Partial Diff. Eq.* **23**(1), 145–195 (2007)
14. Antonietti, P.F., Beirão da Veiga, L., Mora, D., Verani, M.: A stream function formulation of the Stokes problem for the virtual element method. Submitted for publication.

15. Antonietti, P.F., Beirão da Veiga, L., Verani, M.: A mimetic discretization of elliptic obstacle problems. Technical report, MOX, Dipartimento di Matematica, Politecnico di Milano (2010). <http://mox.polimi.it/progetti/publicazioni/>
16. Antonietti, P.F., Beirão da Veiga, L., Verani, M.: Hierarchical a posteriori error estimators for the mimetic discretization of elliptic problems. *SIAM J. Numer. Anal.* **51**, 654–675 (2013)
17. Antonietti, P.F., Beirão da Veiga, L., Verani, M.: A mimetic discretization of elliptic obstacle problems. *Math. Comput.* **82**, 1379–1400 (2013)
18. Antonietti, P.F., Beirão da Veiga, L., Verani, M.: Numerical performance of an adaptive mfd method for the obstacle problem. In: *Numerical Mathematics and Advanced Applications. Proceedings of the 9th European Conference on Numerical Mathematics and Advanced Applications*, Springer-Verlag, Berlin Heidelberg (2013)
19. Antonietti, P.F., Bigoni, N., Verani, M.: Mimetic discretizations of elliptic control problems. *J. Sci. Comp.* **56**(1), 14–27 (2013)
20. Antonietti, P.F., Bigoni, N., Verani, M.: Mimetic finite difference approximation of quasi-linear elliptic problems. MOX Technical Report 38/2012, submitted for publication
21. Antonietti, P.F., Verani, M., L, Zikatanov: A two-level method for mimetic finite difference discretizations of elliptic problems (in preparation 2013)
22. Apanovich, Yu.A., Lymkis, E.D.: Difference schemes for the Navier-Stokes equations on a net consisting of Dirichlet cells. *USSR Comput. Math. and Math. Phys.* **28**(2), 57–63 (1988)
23. Arakawa, A.: Computational design for long-term numerical integration of the equations of fluid motion: Two-dimensional incompressible flow. Part I. *J. Comput. Phys.* **1**, 119–143 (1966)
24. Arakawa, A., Lamb, V.R.: A potential enstrophy and energy conserving scheme for the shallow water equations. *Mon. Wea. Rev.* **109**, 18–36 (1981)
25. Ardelyan, N.V.: The convergence of difference schemes for two-dimensional equations of acoustic and Maxwell's equations. *USSR Comput. Math. and Math. Phys.* **23**(5), 93–99 (1983)
26. Ardelyan, N.V.: Method of investigating the convergence of non-linear finite-difference schemes. *Diff. Eq.* **23**(7), 737–745 (1987)
27. Ardelyan, N.V., Chernigovskii, S.V.: Convergence of difference schemes for two-dimensional gas-dynamics equations in acoustic approximations with gravitation taken into account. *Diff. Eq.* **20**(7), 807–813 (1984)
28. Arnold, D.: An interior penalty finite element method with discontinuous elements. *SIAM J. Numer. Anal.* **19**, 742–760 (1982)
29. Arnold, D.N., Brezzi, F.: Mixed and non-conforming finite element methods: implementation, post-processing and error estimates. *Math. Modelling Numer. Anal.* **19**, 7–35 (1985)
30. Arnold, D.N., Brezzi, F., Douglas Jr, J.: PEERS: A new mixed finite element for plane elasticity. *Japan J. Appl. Math.* **1**, 347–367 (1984)
31. Arnold, D.N., Brezzi, F., Fortin, M.: A stable finite element for the Stokes equations. *Calcolo* **21**, 337–344 (1984)
32. Arnold, D.N., Falk, R.S.: Asymptotic analysis of the boundary layer for the Reissner-Mindlin plate problem. *SIAM J. Math. Anal.* **27**(2), 486–514 (1996)
33. Arnold, D.N., Falk, R.S., Winther, R.: Finite element exterior calculus, homological techniques and applications. *Acta Numerica* **15**, 1–155 (2006)
34. Arnold, D.N., Falk, R.S., Winther, R.: Finite element exterior calculus: from Hodge theory to numerical stability. *Bull. Amer. Math. Soc. (N.S.)* **47**(2), 281–354 (2010)

35. Baghai-Wadji, A.: Conservative finite difference method as applied to electromagnetic radiation problems in saw devices. In: Foster, F.S. (ed.) Proceedings of the IEEE Int. Ultrasonics Symposium, 2–6 October, Quebec, Canada (2006)
36. Bakirova, M., Burdiashvili, M., Vo'tenko, D., Ivanov, A., Karpov, V., Kirov, A., Korshiyaya, T., Krukovskii, A., Lubimov, B., Tishkin, V., Favorskii, A., Shashkov, M.: On simulation of a magnetic field in a spiral band reel. Technical Report, Keldysh Inst. of Appl. Math. the USSR Acad. of Sci., in Russian (1981)
37. Bank, R.E.: Hierarchical bases and the finite element method. *Acta Numerica* **5**, 1–43 (1996)
38. Bank, R.E., Weiser, A.: Some a posteriori error estimators for elliptic partial differential equations. *Math. Comput.* **44**(170), 283–301 (1985)
39. Bartolo, C.D., Gambini, R., Pullin, J.: Consistent and mimetic discretizations in general relativity. *J. Math. Phys.* **46**, 032501–01–032501–18 (2005)
40. Bazan, C., Abouali, M., Castillo, J., Blomgren, P.: Mimetic finite difference methods in image processing. *Comput. Appl. Math.* **30**(3), 701–720 (2011)
41. Beirão da Veiga, L.: A residual based error estimator for the mimetic finite difference method. *Numer. Math.* **108**(3), 387–406 (2008)
42. Beirão da Veiga, L.: A mimetic finite difference method for linear elasticity. *M2AN Math. Model. Numer. Anal.* **44**(2), 231–250 (2010)
43. Beirão da Veiga, L., Brezzi, F., Cangiani, A., Manzini, G., Marini, L.D., Russo, A.: Basic principles of virtual element methods. *Math. Models Methods Appl. Sci.* **23**(01), 199–214 (2013)
44. Beirão da Veiga, L., Brezzi, F., Marini, L.D.: Virtual Elements for linear elasticity problems. *SIAM J. Numer. Anal.* **51**, 794–812 (2013)
45. Beirão da Veiga, L., Droniou, J., Manzini, G.: A unified approach to handle convection terms in mixed and hybrid finite volumes and mimetic finite difference methods. *IMA J. Numer. Anal.* **31**, 1357–1401 (2011)
46. Beirão da Veiga, L., Gyrya, V., Lipnikov, K., Manzini, G.: Mimetic finite difference method for the Stokes problem on polygonal meshes. *J. Comput. Phys.* **228**(19), 7215–7232 (2009)
47. Beirão da Veiga, L., Lipnikov, K.: A mimetic discretization of the Stokes problem with selected edge bubbles. *SIAM J. Sci. Comp.* **32**(2), 875–893 (2010)
48. Beirão da Veiga, L., Lipnikov, K., Manzini, G.: Convergence analysis of the high-order mimetic finite difference method. *Numer. Math.* **113**(3), 325–356 (2009)
49. Beirão da Veiga, L., Lipnikov, K., Manzini, G.: Convergence of the mimetic finite difference method for the Stokes problem on polyhedral meshes. *SIAM J. Numer. Anal.* **48**(4), 1419–1443 (2010)
50. Beirão da Veiga, L., Lipnikov, K., Manzini, G.: Arbitrary-order nodal mimetic discretizations of elliptic problems on polygonal meshes. *SIAM J. Numer. Anal.* **49**, 1737–1760 (2011)
51. Beirão da Veiga, L., Lipnikov, L., Manzini, G.: Arbitrary order nodal mimetic discretizations of elliptic problems on polygonal meshes. Technical Report 32PV10/30/0, IMATI-CNR, via Ferrata, 1, 27100 Pavia, Italy (2010)
52. Beirão da Veiga, L., Lovadina, C., Mora, D.: Numerical results for mimetic discretization of Reissner–Mindlin plate problems. *Calcolo* **50**, 209–237 (2013)
53. Beirão da Veiga, L., Manzini, G.: An a posteriori error estimator for the mimetic finite difference approximation of elliptic problems. *Int. J. Numer. Methods Engrg.* **76**(11), 1696–1723 (2008)

54. Beirão da Veiga, L., Manzini, G.: A higher-order formulation of the mimetic finite difference method. *SIAM J. Sci. Comp.* **31**(1), 732–760 (2008)
55. Beirão da Veiga, L., Manzini, G.: Residual a posteriori error estimation for the Virtual Element Method for elliptic problems. Submitted for publication (2012)
56. Beirão da Veiga, L., Manzini, G.: A Virtual Element Method with arbitrary regularity. Technical Report LA-UR-12-22975, Los Alamos National Laboratory, Los Alamos, New Mexico (US). In press, *IMA J. Numer. Anal.* (2012). doi: 10.1093/imanum/drt018
57. Beirão da Veiga, L., Mora, D.: A mimetic discretization of the Reissner–Mindlin plate bending problem. *Numer. Math.* **117**(3), 425–462 (2011)
58. Benson, D.J., Bazilevs, Y., De Luycker, E., Hsu, M.-C., Scott, M., Hughes, T.J.R., Belytschko, T.: A generalized finite element formulation for arbitrary basis functions: From isogeometric analysis to XFEM. *Int. J. Numer. Meth. Eng.* **83**(6), 765–785 (2010)
59. Bercovier, M., Pironneau, O.A.: Error estimates for finite element method solution of the Stokes problem in primitive variables. *Numer. Math.* **33**, 211–224 (1977)
60. Berman, A., Plemmons, R.J.: Nonnegative matrices in the mathematical sciences. *Classics in Applied Mathematics*. SIAM, New York (1994)
61. Berndt, M., Lipnikov, K., Moulton, J.D., Shashkov, M.: Convergence of mimetic finite difference discretizations of the diffusion equation. *East-West J. Numer. Math.* **9**, 253–284 (2001)
62. Berndt, M., Lipnikov, K., Shashkov, M., Wheeler, M.F., Yotov, I.: A mortar mimetic finite difference method on non-matching grids. *Numer. Math.* **102**(2), 203–230 (2005)
63. Berndt, M., Lipnikov, K., Shashkov, M., Wheeler, M.F., Yotov, I.: Superconvergence of the velocity in mimetic finite difference methods on quadrilaterals. *SIAM J. Numer. Anal.* **43**(4), 1728–1749 (2005)
64. Bertolazzi, E., Manzini, G.: A cell-centered second-order accurate finite volume method for convection-diffusion problems on unstructured meshes. *Math. Models Methods Appl. Sci.* **8**, 1235–1260 (2004)
65. Bertolazzi, E., Manzini, G.: A second-order maximum principle preserving finite volume method for steady convection-diffusion problems. *SIAM J. Numer. Anal.* **43**(5), 2172–2199 (2005)
66. Bertolazzi, E., Manzini, G.: On vertex reconstructions for cell-centered finite volume approximations of 2-D anisotropic diffusion problems. *Math. Models Methods Appl. Sci.* **17**(1), 1–32 (2007)
67. Bochev, P., Hyman, J.M.: Principle of mimetic discretizations of differential operators. In: Arnold, D., Bochev, P., Lehoucq, R., Nicolaides, R., Shashkov, M. (eds) *Compatible Spatial Discretizations*. Proceedings of IMA Hot Topics workshop on Compatible Discretizations. IMA vol. 142. Springer, New York (2006)
68. Bochev, P., Shashkov, M.: Constrained interpolation (remap) of divergence-free fields. *Comp. Meth. Appl. Mech. Engrg.* **194**, 511–530 (2005)
69. Boffi, D., Brezzi, F., Demkowicz, L.F., Durán, R.G., Falk, R.S., Fortin, M. (eds.): *Mixed Finite Elements, Compatibility Conditions, and Applications*. Lecture Notes in Mathematics. vol. 1939. Springer-Verlag, Berlin Heidelberg (2008)
70. Bonaventura, L., Ringler, T.: Analysis of discrete shallow-water models on geodesic delaunay grids with c-type staggering. *Monthly Weather Rev.* **133**, 2351–2373 (2005)
71. Bornemann, F.A., Erdmann, B., Kornhuber, R.: A posteriori error estimates for elliptic problems in two and three space dimensions. *SIAM J. Numer. Anal.* **33**(3), 1188–1204 (1996)

72. Bossavit, A.: Mixed finite elements and the complex of Whitney forms. In: *The mathematics of finite elements and applications*, VI (Uxbridge, 1987), pp. 137–144. Academic Press, London (1988)
73. Bossavit, A.: Differential forms and the computation of fields and forces in electromagnetism. *European J. Mech. B Fluids* **10**(5), 474–488 (1991)
74. Bossavit, A.: Mixed methods and the marriage between "mixed" finite elements and boundary elements. *Numer. Meth. PDEs* **7**(4), 347–362 (1991)
75. Bossavit, A.: *Computational electromagnetism: Variational Formulations, Complementarity, Edge Elements*. Academic Press Inc., San Diego, CA (1998)
76. Bramble, J.H.: A proof of the inf-sup condition for the Stokes equations on Lipschitz domains. *Math. Mod. Meth. Appl. Sci.* **3**, 361–371 (2003)
77. Brandts, J.H., Korotov, S., Krizek, M.: The discrete maximum principle for linear simplicial finite element approximations of a reaction-diffusion problem. *Linear Algebra and its Applications* **429**(10), 2344–2357 (2008). Special issue in honor of Richard S. Varga
78. Brenner, S., Scott, L.: *The Mathematical Theory of Finite Element Methods*. Springer-Verlag, Berlin Heidelberg (1994)
79. Brezis, H.: Problèmes unilatéraux. thèse d'Etat. *J. Math. Pures. Appl.* **IX**(72), 1–168 (1971)
80. Brezis, H.: *Functional Analysis, Sobolev Spaces and Partial Differential Equations*. Springer, New York (2010)
81. Brezis, H., Stampacchia, G.: Sur la régularité de la solution d'inéquations elliptiques. *Bull. Soc. Math. France* **96**, 153–180 (1968)
82. Brezzi, F., Boffi, D., Fortin, M.: Reduced symmetry elements in linear elasticity. *Comm. Pure Appl. Anal.* **8**, 95–121 (2009)
83. Brezzi, F., Buffa, A.: Innovative mimetic discretizations for electromagnetic problems. *J. Comput. Appl. Mech.* **234**, 1980–1987 (2010)
84. Brezzi, F., Buffa, A., Lipnikov, K.: Mimetic finite differences for elliptic problems. *M2AN Math. Model. Numer. Anal.* **43**(2), 277–295 (2009)
85. Brezzi, F., Buffa, A., Manzini, G.: Mimetic scalar products for discrete differential forms. To appear in *J. Comput. Phys.* (2014)
86. Brezzi, F., Douglas, J., Marini, L.D.: Two families of mixed finite elements for second order elliptic problems. *Numer. Math.* **47**, 217–235 (1985)
87. Brezzi, F., Douglas Jr., J., Fortin, M., Marini, L.D.: Efficient rectangular mixed finite elements in two and three space variables. *Math. Mod. Numer. Anal.* **21**, 581–604 (1987)
88. Brezzi, F., Fortin, M.: *Mixed and Hybrid Finite Element Methods*. Springer-Verlag, New York (1991)
89. Brezzi, F., Hager, W.W., Raviart, P.A.: Error estimates for the finite element solution of variational inequalities. *Numer. Math.* **28**, 431–443 (1977)
90. Brezzi, F., Lipnikov, K., Shashkov, M.: Convergence of the mimetic finite difference method for diffusion problems on polyhedral meshes. *SIAM J. Numer. Anal.* **43**(5), 1872–1896 (2005)
91. Brezzi, F., Lipnikov, K., Shashkov, M.: Convergence of mimetic finite difference method for diffusion problems on polyhedral meshes with curved faces. *Math. Models Methods Appl. Sci.* **16**(2), 275–297 (2006)
92. Brezzi, F., Lipnikov, K., Shashkov, M., Simoncini, V.: A new discretization methodology for diffusion problems on generalized polyhedral meshes. *Comput. Methods Appl. Mech. Engrg.* **196**(37–40), 3682–3692 (2007)

93. Brezzi, F., Lipnikov, K., Simoncini, V.: A family of mimetic finite difference methods on polygonal and polyhedral meshes. *Math. Models Methods Appl. Sci.* **15**(10), 1533–1551 (2005)
94. Brezzi, F., Marini, L.D.: Virtual element method for plate bending problems. *Comput. Methods Appl. Mech. Engrg.* **253**, 455–462 (2012)
95. Brezzi, F., Pitkäranta, J.: On the stabilization of finite element approximations of the Stokes equations. In: Hackbush, W. (ed) *Efficient Solutions of Elliptic Systems. Notes on Numerical Fluid Mechanics*, vol. 10. Braunschweig, Wiesbaden (1984)
96. Buffa, A.: Remarks on the discretization of some noncoercive operator with applications to heterogeneous maxwell equations. *SIAM J. Numer. Anal.* **43**(1), 1–18 (2006)
97. Buffa, A., Christiansen, S.H.: A dual finite element complex on the barycentric refinement. *Math. Comput.* **76**(260), 1743–1769 (2007)
98. Burdiashvili, M., Vo'tenko, D., Ivanov, A., Kirov, A., Tishkin, V., Favorskii, A., Shashkov, M.; A magnetic field of a toroidal spiral with a screen. Technical report, Keldysh Inst. of Appl. Math., the USSR Acad. of Sci., in Russian (1984)
99. Burman, E., Ern, A.: Discrete maximum principle for galerkin approximations of the laplace operator on arbitrary meshes. *C. R. Math. Acad. Sci. Paris* **338**(8), 641–646 (2004)
100. Burton, D.E.: Consistent finite-volume discretization of hydrodynamic conservation laws for for unstructured grids, Lawrence Livermore National Laboratory, Report UCRL-JC-118788 (1994)
101. Burton, D.E.: Multidimensional discretization of conservation laws for unstructured polyhedral grids. Lawrence Livermore National Laboratory, Report UCRL-JC-118306 (1994)
102. Campbell, J., Hyman, J.M., Shashkov, M.: Mimetic finite difference operators for second-order tensors on unstructured grids. *Comput. Math. Appl.* **44**, 157–173 (2002)
103. Campbell, J., Shashkov, M.: A tensor artificial viscosity using a mimetic finite difference algorithm. *J. Comput. Phys.* **172**(2), 739–765 (2001)
104. Campbell, J.C., Shashkov, M.J.: A compatible Lagrangian hydrodynamics algorithm for unstructured grids. *Selcuk J. Appl. Math.* **4**, 53–70 (2003)
105. Cangiani, A., Gardini, F., Manzini, G.: Convergence of the mimetic finite difference method for eigenvalue problems in mixed form. *Comp. Meth. Appl. Mech. Engrg.* **200**(9–12), 1150–1160 (2011)
106. Cangiani, A., Manzini, G.: Flux reconstruction and pressure post-processing in mimetic finite difference methods. *Comput. Methods Appl. Mech. Engrg.* **197**(9–12), 933–945 (2008)
107. Cangiani, A., Manzini, G., Russo, A.: Convergence analysis of the mimetic finite difference method for elliptic problems. *SIAM J. Numer. Anal.* **47**(4), 2612–2637 (2009)
108. Caramana, E.J., Burton, D.E., Shashkov, J.M., Whalen, P.P.: The construction of compatible hydrodynamics algorithms utilizing conservation of total energy. *J. Comput. Phys.* **146**, 227–262 (1998)
109. Caramana, E.J., Shashkov, M.J.: Elimination of artificial grid distortion and hourglass-type motions by means of Lagrangian subzonal masses and pressures. *J. Comput. Phys.* **142**, 521–561 (1998)
110. Caramana, E.J., Shashkov, M.J., Whalen, P.P.: Formulations of artificial viscosity for multi-dimensional shock wave computations. *J. Comput. Phys.* **144**, 70–97 (1998)
111. Castillo, J.E., Grone, R.D.: A matrix analysis approach to higher-order approximations for divergence and gradients satisfying a global conservation law. *SIAM J. Matrix Anal. Appl.* **25**(1), 128–142 (2003)

112. Castillo, J.E., Hyman, J.M., Shashkov, M.J., Steinberg, S.: High-order mimetic finite difference methods on nonuniform grids. Special Issue of Houston Journal of Mathematics, Ilin, A.V., Scott, L.R. (eds.), 347–361 (1995)
113. Chainais-Hillairet, C., Droniou, J.: Finite volume schemes for non-coercive elliptic problems with Neumann boundary conditions. *IMA J. Numer. Anal.* **31**(1) 61–85 (2011)
114. Chard, J.A., Shapiro, V.: A multivector data structure for differential forms and equations. *Math. Comput. Simulation* **54**(1–3), 33–64 (2000)
115. Ciarlet, P.G.: *The Finite Element Method for Elliptic Problems*. North-Holland, Amsterdam (1978)
116. Ciarlet, P.G.: *Mathematical Elasticity, vol. 1. Three dimensional elasticity*. North-Holland, Amsterdam (1987)
117. Ciarlet, P.G.: *Mathematical Elasticity, vol. 2. Lower-dimensional theories of plates and rods*. North-Holland, Amsterdam (1990)
118. Clemens, M., Weiland, T.: Discrete electromagnetism with the finite integration technique. *Progress in Electromagnetic Research* **32**, 65–87 (2001)
119. Collins, R.: Mathematical modelling of controlled release from implanted drug-impregnated monoliths. *Pharmaceutical Science & Technology Today* **1**(6), 269–276 (1998)
120. Coudière, Y.: *Analyse de schémas volumes finis sur maillages non structurés pour des problèmes linéaires hyperboliques et elliptiques*. PhD Thesis, Université “P. Sabatier” de Toulouse, Toulouse III, Toulouse, France (1999)
121. Coudière, Y., Hubert, F.: A 3D discrete duality finite volume method for nonlinear elliptic equation. *SIAM J. Sci. Comput.* **33**(4), 1739–1764, (2011)
122. Coudière, Y., Pierre, C., Rousseau, O., Turpault, R.: A 2D/3D discrete duality finite volume scheme. Application to ECG simulation. *Int. J. Finite Volumes* **6**(1) (2009)
123. Coudière, Y., Vila, J.-P., Villedieu, P.: Convergence rate of a finite volume scheme for a two-dimensional diffusion convection problem. *Math. Model. Numer. Anal.* **33**(3), 493–516 (1999)
124. Coudière, Y., Villedieu, P.: Convergence of a finite volume scheme for the linear convection-diffusion equation on locally refined meshes. *Math. Model. Numer. Anal.* **34**(6), 1123–1149 (2000)
125. Crouziez, M., Raviart, P.A.: Conforming and non-conforming finite element methods for solving the stationary Stokes equations. *R.A.I.R.O. Anal. Numer.* **7**, 33–76 (1973)
126. Cryer, C.W.: Successive overrelaxation methods for solving linear complementarity problems arising from free boundary problems. In: *Free Boundary Problems, vol. I* (Pavia, 1979), pp. 109–131. *Ist. Naz. Alta Mat. Francesco Severi*, Rome (1980)
127. Cueto, E., Sukumar, N., Calvo, B., Martínez, M., Cegoñino, J., Doblaré, M.: Overview and recent advances in natural neighbour Galerkin methods. *Arch. Comput. Meth. Engrg.* **10**(4), 307–384 (2003). doi 10.1007/BF02736253
128. Dawson, C., Aizinger, V.: Upwind-mixed methods for transport equations. *Comput. Geosci.* **3**, 93–110 (1999)
129. Delcourte, S., Domelevo, K., Omnes, P.: A discrete duality finite volume approach to Hodge decomposition and div-curl problems on almost arbitrary two-dimensional meshes. *SIAM J. Numer. Anal.* **45**(3), 1142–1174 (2007)
130. Demin, A.V., Korobitsyn, V.A., Mazurenko, A.I., Khe, A.I.: Calculation of the flows of a viscous incompressible liquid with a free surface on two dimensional lagrangian nets. *USSR Comput. Math. and Math. Phys.* **28**(6), 81–87 (1988)

131. Denisov, A.A., Koldoba, A.V., Povesgenko, Yu.A.: The convergence to generalized solutions of difference schemes of the reference-operator method for Poisson's equation. *USSR Comput. Math. and Math. Phys.* **29**(2), 32–38 (1989)
132. Desbrun, M., Hirani, A.N., Leok, M., Marsden, J.E.: Discrete exterior calculus. Technical Report arXiv:math/0508341v2, Cornell University Library, Ithaca, New York (2005)
133. Destuynder, P., Salaun, M.: *Mathematical Analysis of Thin Plate Models*. Springer-Verlag, Berlin Heidelberg (1996)
134. Dezin, A.A.: Method of orthogonal expansions. *Siberian Mathematical Journal* **9**(4), 788–797 (1968)
135. Dezin, A.A.: Some models related to the Euler equations. *Diff. Eq.* **6**(1), 12–20 (1970)
136. Dezin, A.A.: Natural differential operators and the separation of variables. *Diff. Eq.* **9**(1), 18–23 (1973)
137. Dezin, A.A.: Combination model of euclidean space and difference operators. *Siberian Mathematical Journal* **16**(4), 536–545 (1975)
138. Dezin, A.A.: *Multidimensional Analysis and Discrete Models*. CRC Press, Boca Raton, Florida (1995)
139. Dmitrieva, M.V., Ivanov, A.A., Tishkin, V.F., Favorskii, A.P.: Construction and investigation of support-operators finite-difference schemes for Maxwell equations in cylindrical geometry. Technical report, Keldysh Inst. of Appl. Math. the USSR Acad. of Sci., in Russian (1985)
140. Dodziuk, J.: Finite-difference approach to the Hodge theory of harmonic forms. *American Journal of Mathematics* **98**(1), 79–104 (1976)
141. Domelevo, K., Omnes, P.: A finite volume method for the Laplace equation on almost arbitrary two-dimensional grids. *Math. Model. Numer. Anal.* **39**(6), 1203–1249 (2005)
142. Douglas, A., Bochev, P., Lehoucq, R., Nicolaides, R., Shashkov, M. (eds.): *Compatible Spatial Discretizations*, vol. 142. Springer, New York (2006)
143. Douglas, J., Roberts, J.E.: Global estimates for mixed methods for second order elliptic equations. *Math. Comput.* **44**, 39–52 (1985)
144. Douglas Jr., J., Roberts, J.E.: Mixed finite element methods for second order elliptic problems. *Math. Apl. Comput* **1**(1), 91–103 (1982)
145. Droniou, J.: Error estimates for the convergence of a finite volume discretization of convection-diffusion equations. *J. Numer. Math.* **11**(1), 1–32 (2003)
146. Droniou, J., Eymard, R.: A mixed finite volume scheme for anisotropic diffusion problem on any grid. *Numer. Math.* **1**(105), 35–71 (2006)
147. Droniou, J., Eymard, R.: Study of the mixed finite volume method for Stokes and Navier-Stokes equations. *Numer. Meth. PDEs.* **25**(1), 137–171 (2009)
148. Droniou, J., Eymard, R., Gallouet, T., Herbin, R.: A unified approach to mimetic finite difference, hybrid finite volume and mixed finite volume method. *Math. Models Methods Appl. Sci.* **20**(2), 1–31 (2010)
149. Dupont, T., Scott, R.: Polynomial approximation of functions in Sobolev spaces. *Math. Comp.* **34**(150), 441–463 (1980)
150. Dusinberre, G.M.: Heat transfer calculations by numerical methods. *Journal of the American Society for Naval Engineers* **67**(4), 991–1002 (1955)
151. Dusinberre, G.M.: *Heat-transfer calculation by finite differences*. International Textbook Company, Scranton, Pennsylvania (1961)
152. Dvorak, P.: New element lops time off CFD simulations. *Machine Design* **78**(169), 154–155 (2006)

153. Solov'eva, E., Shashkov, M.: Application of the basic operator method for difference scheme construction on non-matching grids. Technical report, Keldysh Inst. of Appl. Math. the USSR Acad. of Sci., in Russian (1984)
154. Edwards, M.G.: Unstructured, control-volume distributed, full-tensor finite-volume schemes with flow based grids. *Comput. Geosci.* **6**, 433–452 (2002)
155. Edwards, M.G., Rogers, G.F.: Finite volume discretization with imposed flux continuity for the general tensor pressure equation. *Comput. Geosci.* **2**, 259–290 (1998)
156. Elliott, C.M., Ockendon, J.R.: Weak and variational methods for moving boundary problems. *Research Notes in Mathematics*, vol. 59. Pitman (Advanced Publishing Program), Boston, Massachusetts (1982)
157. Elshebli, M.A.T.: Discrete maximum principle for the finite element solution of linear non-stationary diffusion-reaction problems. *Applied Mathematical Modelling* **32**(8), 1530–1541 (2008). Special issue on Numerical and Computational Issues related to Applied Mathematical Modelling
158. Ely, G.P., Day, S.M., Minster, J.-B.: A support-operator method for viscoelastic wave modelling in 3-d heterogeneous media. *Geophys. J. Int.* **172**(1), 331–344 (2008)
159. Ely, G.P., Day, S.M., Minster, J.-B.: A support-operator method for 3-d rupture dynamics. *Geophys. J. Int.* **177**, 1140–1150 (2009)
160. Eymard, R., Gallouët, T., Herbin, R.: The finite volume method. In: Ciarlet, P., Lions, J.L. (eds.) *Handbook for Numerical Analysis*, pp. 715–1022. North Holland (2000)
161. Eymard, R., Gallouët, T., Herbin, R.: A finite volume for anisotropic diffusion problems. *C. R. Math. Acad. Sci. Paris* **339**(4), 299–302 (2004)
162. Eymard, R., Gallouët, T., Herbin, R.: A new finite volume scheme for anisotropic diffusion problems on general grids: convergence analysis. *C. R. Math. Acad. Sci. Paris* **344**(6), 403–406 (2007)
163. Eymard, R., Gallouët, T., Herbin, R.: Discretization of heterogeneous and anisotropic diffusion problems on general non-conforming meshes. SUSHI: a scheme using stabilization and hybrid interface. *IMA J. Numer. Anal.* **30**(4), 1009–1043 (2008)
164. Eymard, R., Gutnic, M., Hillhorst, D.: The finite volume method for Richards equation. *Comput. Geosci.* **3**, 259–294 (1999)
165. Eymard, R., Henri, G., Herbin, R., Hubert, F., Kloforn, R., Manzini, G.: 3D benchmark on discretizations schemes for anisotropic diffusion problems on general grids. In: Fort, J., Furst, J., Halama, J., Herbin, R., Hubert, F. (eds.) *Finite Volumes for Complex Applications VI, Problems and Perspectives*, vol. 2, pp. 95–130. Springer-Verlag, Berlin Heidelberg (2011)
166. Falk, R.S.: Error estimates for the approximation of a class of variational inequalities. *Math. Comput.* **28**, 963–971 (1974)
167. Favorskii, A., Korshiya, T., M., Shashkov, Tishkin, V.: Variational approach to the construction of finite-difference schemes for the diffusion equations for magnetic field. *Diff. Eq.* **18**(7), 863–872 (1982)
168. Favorskii, A., Korshiya, T., Shashkov, M., Tishkin, V.: A variational approach to the construction of difference schemes on curvilinear meshes for heat-conduction equation. *USSR Comput. Math. and Math. Phys.* **20**, 135–155 (1980)
169. Favorskii, A., Samarskii, A., Tishkin, V., Shashkov, M.: On constructing fully conservative difference schemes for gas dynamic equations in eulerian form by the method of basic operators. Technical report, Keldysh Inst. of Appl. Math. the USSR Acad. of Sci., in Russian (1981)

170. Favorskii, A., Shashkov, M., Tishkin, V.: The usage of topological methods in the discrete models construction. Technical report, Keldysh Institute of Applied Mathematics of the USSR Academy of Sciences, in Russian (1983)
171. Favorskii, A.P.: Variational discrete models of hydrodynamics equations. *Diff. Eq.* **16**(7), 834–845 (1980)
172. Favorskii, A.P., Korshiya, T., Tishkin, V.F., Shashkov, M.: Difference schemes for equations of electro-magnetic field diffusion with anisotropic conductivity coefficients. Technical report, Keldysh Inst. of Appl. Math. the USSR Acad. of Sci., in Russian (1980)
173. Fortin, M.: Utilization de la méthode des éléments finis en mécanique des fluides. *Calcolo* **12**, 405–441 (1975)
174. Fraeijns de Veubeke, B.: Displacement and equilibrium models in the finite element method. In: Zienkiewicz, O.C., Holister, G. (eds.): *Stress Analysis*. John Wiley and Sons, New York (1965)
175. Franca, L.P., Hughes, T.J.R.: Two classes of mixed finite element methods. *Comput. Methods Appl. Mech. Engrg.* **69**, 89–129 (1988)
176. Friedman, A.: *Variational principles and free-boundary problems*. Pure and Applied Mathematics. John Wiley & Sons Inc., New York (1982)
177. Fries, T.-P., Belytschko, T.: The extended/generalized finite element method: An overview of the method and its applications. *Int. J. Numer. Meth. Engrg.* **84**(3), 253–304 (2010)
178. Ganzha, V., Liska, R., Shashkov, M., Zenger, C.: Support operator method for Laplace equation on unstructured triangular grid. *Selcuk J. Appl. Math.* **3**, 21–48 (2002)
179. Gasilov, V., Goloviznin, Kurtmullaev, V., R., Semenov, V., Favorskii, A., Shashkov, M.: The numerical simulation of the quasi spherical metal liner dynamics. In: *Proceedings of Second Int. Conf. on Megagauss Magnetic Field Generation and Related Topics*, Washington D.C., USA, July (1979)
180. Gasilov, V., Goloviznin, V., Kurtmullaev, R., Semenov, V., Sosnin, N., Tishkin, V., Favorskii, A., Shashkov, M.: Numerical simulation of the compression of toroidal plasma by quasi-spherical liner. Technical report, Preprint Keldysh Inst. of Appl. Math. the USSR Acad. of Sci., in Russian (1979)
181. Gasilov, V., Goloviznin, V., Taran, M., Tishkin, V., Favorskii, A., Shashkov, M.: Numerical simulation of the rayleigh-taylor instability for incompressible flows. Technical report, Keldysh Inst. of Appl. Math. the USSR Acad. of Sci., in Russian (1979)
182. Gilbarg, D., Trudinger, N.S.: *Elliptic Partial Differential Equations of Second Order*. *Classics in Mathematics*. Springer-Verlag, Berlin Heidelberg New York (2001)
183. Girault, V.: Theory of a finite difference method on irregular networks. *SIAM J. Numer. Anal.*, **11**(2), 260–282 (1974)
184. Girault, V., Raviart, P.-A.: *Finite Element Methods for Navier-Stokes Equations*. *Springer Series in Computational Mathematics*, vol. 5. Springer-Verlag, Berlin Heidelberg New York Tokyo (1986)
185. Glowinski, R., Lions, J.-L., Trémolières, R.: *Numerical analysis of variational inequalities*. *Studies in Mathematics and its Applications*, vol. 8. North-Holland Publishing Co., Amsterdam (1981)
186. Goloviznin, V.M., Korshunov, V.K., Sabitova, A., Samarskaya, E.A.: Stability of variational-difference schemes in gas-dynamics. *Diff. Eq.* **20**(7), 852–858 (1984)
187. Goloviznin, V.M., Korshunov, V.K., Samaraskii, A.A.: Two-dimensional difference schemes of magneto-hydrodynamics on triangle lagrange meshes. *USSR Comput. Math. and Math. Phys.* **22**(4), 160–178 (1982)

188. Goloviznin, V.M., Samarskii, A.A., Favorskii, A.P.: A variational approach to constructing finite-difference mathematical models in hydrodynamics. *Sov. Phys. Dokl.* **22**(8), 432–434 (1977)
189. Goloviznin, V.M., Samarskii, A.A., Favorskii, A.P.: Use of the principle of least action for constructing discrete mathematical models in magnetohydrodynamics. *Sov. Phys. Dokl.* **24**(6), 441–443 (1979)
190. Grisvard, P.: Elliptic problems in nonsmooth domains. Monograph and Studies in Mathematics, vol. 24. Pitman, Boston (1985)
191. Guevara-Jordan, J.M., Arteaga-Arispe, J.: A second-order mimetic approach for tracer flow in oil reservoirs. Latin American & Caribbean Petroleum Engineering Conference, 15–18 April 2007, Buenos Aires, Argentina, Published by Society of Petroleum Engineers Document ID 107366-MS (2007)
192. Gyrya, V., Lipnikov, K.: High-order mimetic finite difference method for diffusion problems on polygonal meshes. *J. Comput. Phys.* **227**(20), 8841–8854 (2008)
193. Gyrya, V., Lipnikov, K.: M-adaptation method for acoustic wave equation on square meshes. *J. Comp. Acoustics* **20**(4), 1250022-1:23 (2012)
194. Gyrya, V., Lipnikov, K., Aronson, I., Berlyand, L.: Effective shear viscosity and dynamics of suspensions of micro-swimmers at moderate concentrations. *J. Math. Bio.* **65**(5), 707–740 (2011)
195. Herbin, R., Hubert, F.: Benchmark on discretization schemes for anisotropic diffusion problems on general grids. In: Eymard, R., Herard, J.M. (eds.) Proceedings of Finite Volumes for Complex Applications V, Aussois, France. Hermès, Hermès (2008)
196. Hermeline, F.: A finite volume method for the approximation of diffusion operators on distorted meshes. *J. Comput. Phys.* **160**(2), 481–499 (2000)
197. Hermeline, F.: Approximation of diffusion operators with discontinuous tensor coefficients on distorted meshes. *Comput. Methods Appl. Mech. Engrg.* **192**(16–18) 1939–1959 (2003)
198. Hermeline, F.: Approximation of 2-D and 3-D diffusion operators with variable full tensor coefficients on arbitrary meshes. *Comput. Methods Appl. Mech. Engrg.* **196**(21–24), 2497–2526 (2007)
199. F. Hermeline. A finite volume method for approximating 3D diffusion operators on general meshes. *J. Comput. Phys.* **228**(16), 5763–5786 (2009)
200. Hiptmair, R.: Canonical construction of finite elements. *Math. Comput.* **68**(228), 1325–1346 (1999)
201. Hiptmair, R.: Finite elements in computational electromagnetism. *Acta Numerica* **11**, 237–339 (2002)
202. Hirani, A.N.: Discrete exterior calculus. PhD Thesis, California Institute of Technology (2003)
203. Hopf, E.: Elementare Bemerkungen über die Lösungen partieller Differentialgleichungen zweiter Ordnung vom elliptischen Typus. *Sitzungsber. Preuss. Akad. Wiss.*, 19 (1927)
204. Hughes, T.J.R., Allik, H.: Finite elements for compressible and incompressible continua. Proceedings of the Symposium on Civil Engineering, Vanderbilt University (1969)
205. Hyman, J., Morel, J., Shashkov, M., Steinberg, S.: Mimetic finite difference methods for diffusion equations. *Comput. Geosci.* **6**(3-4), 333–352 (2002)
206. Hyman, J., Shashkov, M.: The approximation of boundary conditions for mimetic finite difference methods. *Comput. Math. Appl.* **36**, 79–99 (1998)
207. Hyman, J., Shashkov, M.: Mimetic discretizations for Maxwell’s equations and the equations of magnetic diffusion. *Progress in Electromagnetic Research* **32**, 89–121 (2001)

208. Hyman, J., Shashkov, M., Steinberg, S.: The numerical solution of diffusion problems in strongly heterogeneous non-isotropic materials. *J. Comput. Phys.* **132**(1), 130–148 (1997)
209. Hyman, J.M., Scovel, J.C.: Deriving mimetic difference approximations do differential operators using algebraic topology. Unpublished Report of Los Alamos National Laboratory (1988)
210. Hyman, J.M., Shashkov, M.: Adjoint operators for the natural discretizations of the divergence, gradient and curl on logically rectangular grids. *Appl. Numer. Math.* **25**, 413–442 (1997)
211. Hyman, J.M., Shashkov, M.: Mimetic discretizations for Maxwell's equations. *J. Comput. Phys.* **151**, 881–909 (1999)
212. Hyman, J.M., Shashkov, M.: The orthogonal decomposition theorems for mimetic finite difference methods. *SIAM J. Numer. Anal.* **36**(3), 788–818 (1999)
213. Hyman, J.M., Shashkov, M., Steinberg, S.: The effect of inner products for discrete vector fields on the accuracy of mimetic finite difference methods. *Comput. Math. Appl.* **42**, 1527–1547 (2001)
214. Hyman, J.M., Steinberg, S.: The convergence of mimetic discretization for rough grids. *Int. J. Comput. Math. Appl.* **47**(10–11), 1565–1610 (2004)
215. Hyman, M., Shashkov, J.M.: Natural discretizations for the divergence, gradient and curl on logically rectangular grids. *Comput. Math. Appl.* **33**(4), 81–104 (1997)
216. Isaev, V.N., Sofronov, I.D.: Construction of discrete models for equations of gas dynamics based on transformation of kinetic and internal energy of continuum medium. *VANT – Questions of Atomic Science and Technology* **1**(15), 3–7, in Russian (1984)
217. Ishihara, K.: Strong and weak discrete maximum principles for matrices associated with elliptic problems. *Linear Algebra and its Applications* **88–89**, 431–448 (1987)
218. Jackson, J.D.: *Classical Electrodynamics*, 2nd edn. Wiley (1962)
219. Jaffre, J.: Decentrage et elements finis mixtes pour les equations de diffusion-convection. *Calcolo* **21**, 171–197 (1984)
220. Jaffre, J., Roberts, J.E.: Upstream weighting and mixed finite elements in the simulation of miscible displacements. *RAIRO Model. Math. Anal. Numer.* **19**(3), 443–460 (1985)
221. Jaillet, P., Lamberton, D., Lapeyre, B.: Variational inequalities and the pricing of American options. *Acta Appl. Math.* **21**(3), 263–289 (1990)
222. Kadomtsev, B.B.: *Tokamak Plasma: A Complex Physical System (Plasma Physics)*. Taylor & Francis (1993)
223. Karátson, J., Korotov, S., Krizek, M.: On discrete maximum principles for nonlinear elliptic problems. *Mathematics and Computers in Simulation* **76**(1-3), 99–108 (2007)
224. Kellogg, R.B., Osborn, J.E.: A regularity result for the Stokes problem in a convex polygon. *Funct. Anal.* **21**, 397–431 (1976)
225. Kikuchi, F.: Mixed formulations for finite element analysis of magnetostatic and electrostatic problems. *Japan J. Appl. Math.* **6**, 209–221 (1989)
226. Kinderlehrer, D., Stampacchia, G.: An introduction to variational inequalities and their applications. *Classics in Applied Mathematics*, vol. 31. SIAM, Philadelphia, PA (2000)
227. Kirpichenko, P., Sokolov, V., Tarasov, J., Tishkin, V., Turina, N., Favorskii, A., Shashkov, M.: A numerical simulation of over-compressed detonation wave in a conic canal. Technical report, Keldysh Inst. of Appl. Math. the USSR Acad. of Sci., in Russian (1984),
228. Klausen, R.A., Stephansen, A.F.: Mimetic MPFA. In: *Proc. 11th European Conference on the Mathematics of Oil Recovery*. Bergen, Norway, A12, EAGE (2008)

229. Knoll, D., Morel, D., Margolin, L.G., Shashkov, M.: Physically motivated discretization methods: A strategy for increased predictiveness. *Los Alamos Sci.* **29**, 188–212 (2005)
230. Koldoba, A.V., Poveshenko, Yu.A., Popov, Yu.P.: The approximation of differential operators on non-orthogonal meshes. *Diff. Eq.* **19**(7), 919–927 (1983)
231. Kononov, A.N.: Numerical methods for static problems of elasticity. *Siberian Mathematical Journal* **36**(3), 491–505 (1995)
232. Korobitsin, V.A.: Axisymmetric difference operators in an orthogonal coordinate system. *USSR Comput. Math. and Math. Phys.* **29**(6), 13–21 (1989)
233. Korobitsin, V.A.: Basic operators method for construction of difference schemes in curvilinear orthogonal coordinate system. *Mathematical Modeling* **2**(6), 110–117 (1990)
234. Korotov, S., Krizek, M., Neittaanm aki, P.: Weakened acute type condition for tetrahedral triangulations and the discrete maximum principle. *Math. Comput.* **223**, 107–119 (2001)
235. Korshiya, T.K., Tishkin, V.F., Favorskii, A.P., Shashkov, M.J.: Flow-variational difference schemes for calculating the diffusion of a magnetic field. *Sov. Phys. Dokl.* **25**, 832–836 (1980)
236. Kozhakhmedov, N.B.: Solution of the first boundary-value problem for the Lamé's equation by the application of invariant finite-difference operators. *Diff. Eq.* **6**(5), 694–705 (1970)
237. Krylov, A.L.: Models with finite number of degrees of freedom for class of problems in mathematical physics. (Difference systems with conservation laws). *Sov. Phys. Dokl.* **7**, 18–20 (1962)
238. Krylov, A.L.: Difference approximations to differential operators of mathematical physics. *Soviet Math. Dokl.* **9**(1), 138–142 (1968)
239. Kuznetsov, Y., Lipnikov, K., Shashkov, M.: The mimetic finite difference method on polygonal meshes for diffusion-type problems. *Comput. Geosci.* **8**, 301–324 (2004)
240. Kuznetsov, Y., Repin, S.: New mixed finite element method on polygonal and polyhedral meshes. *Russ. J. Numer. Anal. Math. Modelling* **18**(3), 261–278 (2003)
241. Landau, L.D., Lifshitz, E.M.: *The Classical Theory of Fields*, 1st edn. Addison-Wesley (1951)
242. Le Potier, C.: Schéma volumes finis monotone pour des opérateurs de diffusion fortement anisotropes sur des maillages de triangles non structurés. *C. R. Math. Acad. Sci. Paris* **341**(12), 787–792 (2005)
243. Le Potier, C.: Schéma volumes finis pour des opérateurs de diffusion fortement anisotropes sur des maillages non structurés. *C. R. Math. Acad. Sci. Paris* **340**(12), 921–926 (2005)
244. Lebedev, V.I.: Method of orthogonal projections for finite-difference analog of one system of equations. *Reports of USSR Academy of Sciences* **113**(6), 1206–1209, in Russian (1957)
245. Lebedev, V.I.: Difference analogues of orthogonal decompositions, basic differential operators and some boundary problems of mathematical physics, I. *USSR Comput. Math. and Math. Phys.* **4**(3), 69–92 (1964)
246. Lebedev, V.I.: Difference analogues of orthogonal decompositions, basic differential operators and some boundary problems of mathematical physics, II. *USSR Comput. Math. and Math. Phys.* **4**(4), 36–50 (1964)
247. Lipnikov, K., Manzini, G.: High-order mimetic methods for unstructured polyhedral meshes. Technical Report LA-UR-13-21177. Los Alamos National Laboratory (2013), submitted to *J. Comput. Phys.*

248. Lipnikov, K., Manzini, G., Brezzi, F., Buffa, A.: The mimetic finite difference method for 3D magnetostatics fields problems on polyhedral meshes. *J. Comput. Phys.* **230**(2), 305–328 (2011)
249. Lipnikov, K., Manzini, G., Svyatskiy, D.: Analysis of the monotonicity conditions in the mimetic finite difference method for elliptic problems. *J. Comput. Phys.* **230**(7), 2620–2642 (2011)
250. Lipnikov, K., Manzini, G., Svyatskiy, D.: Monotonicity conditions in the mimetic finite difference method. In: Fort, J., Furst, J., Halama, J., Herbin, R., Hubert, F. (eds.) *Springer Proceedings in Mathematics Finite Volumes for Complex Applications VI Problems & Perspectives*, vol. 1, pp. 653–662. Springer-Verlag, Berlin Heidelberg (2011)
251. Lipnikov, K., Morel, J., Shashkov, M.: Mimetic finite difference methods for diffusion equations on non-orthogonal non-conformal meshes. *J. Comput. Phys.* **199**(2), 589–597 (2004)
252. Lipnikov, K., Moulton, J.D., Svyatskiy, D.: A Multilevel Multiscale Mimetic (M^3) method for two-phase flows in porous media. *J. Comput. Phys.* **227**, 6727–6753 (2008)
253. Lipnikov, K., Nelson, E., Reynolds, J.: Mimetic discretization of two-dimensional magnetic diffusion equations. *J. Comput. Phys.* **247**, 1–16 (2013)
254. Lipnikov, K., Shashkov, M., Svyatskiy, D.: The mimetic finite difference discretization of diffusion problem on unstructured polyhedral meshes. *J. Comput. Phys.* **211**(2), 473–491 (2006)
255. Lipnikov, K., Shashkov, M., Svyatskiy, D., Vassilevski, Yu.: Monotone finite volume schemes for diffusion equations on unstructured triangular and shape-regular polygonal meshes. *J. Comput. Phys.* **227**(1), 492–512 (2007)
256. Lipnikov, K., Shashkov, M., Yotov, I.: Local flux mimetic finite difference methods. *Numer. Math.* **112**(1), 115–152 (2009)
257. Liska, R., Shashkov, M., Ganza, V.: Analysis and optimization of inner products for mimetic finite difference methods on triangular grid. *Mathematics and Computers in Simulation* **67**, 55–66 (2004)
258. Liu, Y., Chew, W.C.: Time domain support operator method on unstructured grids. In: *Proceedings of Antennas and Propagation Society International Symposium 2004. IEEE 20–25 June*, vol. 1, pp. 53–60 (2004)
259. Liu, Y.A., Chew, W.C.: The unstructured support operator method and its application in waveguide problems. *Microwave and Optical Technology Letters* **46**(5), 495–500 (2005)
260. Maikov, A.R., Sveshnikov, A.G., Yakunin, S.A.: Mathematical modeling of microwave plasma generator. *USSR Comput. Math. and Math. Phys.* **25**(3), 149–157 (1985)
261. Manzini, G., Ferraris, S.: Mass-conservative finite volume methods on 2-D unstructured grids for the Richards’ equation. *Adv. Water Resour.* **27**(12), 1199–1215 (2004)
262. Manzini, G., Putti, M.: Mesh locking effects in the finite volume solution of 2-D anisotropic diffusion equations. *J. Comput. Phys.* **220**(2), 751–771 (2007)
263. Manzini, G., Russo, A.: A finite volume method for advection-diffusion problems in convection-dominated regimes. *Comput. Methods Appl. Mech. Engrg.* **197**(13–16), 1242–1261 (2008)
264. Manzini, G., Russo, A.: Monotonicity conditions in the nodal mimetic finite difference method for diffusion problems on quadrilateral meshes. Technical Report LA-UR-13-23476, Los Alamos National Laboratory, Los Alamos, New Mexico (US) (2013)
265. Margolin, L., Shashkov, M.: Using a curvilinear grid to construct symmetry-preserving discretization for Lagrangian gas dynamics. *J. Comput. Phys.* **149**, 389–417 (1999)

266. Margolin, L., Shashkov, M., Smolarkiewicz, P.: A discrete operator calculus for finite difference approximations. *Comput. Methods Appl. Mech. Engrg.* **187**(3–4), 365–383 (2000)
267. Margolin, L.G., Adams, T.F.: Spatial differencing for finite difference codes. Technical report, Los Alamos National Laboratory Report – LA-UR-10249 (1985)
268. Margolin, L.G., Tarwater, A.E.: A diffusion operator for lagrangian meshes. In: Morgan, K., Lewis, R.W., Habashi, W.G. (eds) *Proceedings of the Fifth International Conference on Numerical Methods in Thermal Problems Montreal*, p. 1252. Montreal, Canada (1987). See also Lawrence Livermore National Laboratory Report UCRL – 95652
269. Marrone, M.: Computational aspects of the cell method in electrodynamics. In: Teixeira, F.L. (ed.) *Geometric Methods in Computational Electromagnetics*, PIER 32, pp. 317–356. EMW Publishing, Cambridge, MA (2001)
270. Mattiussi, C.: An analysis of finite volume, finite element, and finite difference methods using some concepts from algebraic topology. *J. Comput. Phys.* **133**(2), 289–309 (1997)
271. Mattsson, K.: Boundary procedures for summation-by-parts operators. *J. Sci. Comput.* **18**(1), 133–153 (2003)
272. Mattsson, K., Nordström, J.: Summation by parts operators for finite difference approximations of second derivatives. *J. Comput. Phys.* **199**(2), 503–540 (2004)
273. Mikhailova, N., Tishkin, V., Turina, N., Favorskii, A., Shashkov, M.: Numerical modeling of two-dimensional gas-dynamic flows on a variable-structure mesh. *USSR Comput. Math. and Math. Phys.* **26**(5), 74–84 (1986)
274. Mills, R., Lu, C., Lichtner, P.C., Hammond, G.: Simulating subsurface flow and transport on ultrascale computers using PFLOTRAN. *J. Phys. Conference Series*, vol. 78 (2007)
275. Mindlin, R.D.: Influence of rotatory inertia and shear on flexural motions of isotropic, elastic plates. *ASME Journal of Applied Mechanics* **18**, 31–38 (1951)
276. Mishev, I.: Nonconforming finite volume methods. *Comput. Geosci.* **6**, 253–268 (2002)
277. Morel, J., Roberts, R., Shashkov, M.: A local support-operators diffusion discretization scheme for quadrilateral $r-z$ meshes. *J. Comput. Phys.* **144**(1), 17–51 (1998)
278. Mousavi, S., Sukumar, N.: Numerical integration of polynomials and discontinuous functions on irregular convex polygons and polyhedrons. *Comput. Mech.* **47**(5), 535–554 (2011)
279. Murphy, J.W., Burrows, A.: BETHE-Hydro: An arbitrary lagrangian-eulerian multidimensional hydrodynamics code for astrophysical simulations. *The Astrophysical Journal Supplement Series* **179**, 209–241 (2008)
280. Myasnikov, V.P., Zaslavsky, M.Yu., Pergament, A.Kh.: Averaging algorithms and the support-operator method for poroelasticity problems. *Doklady Physics* **49**(8), 483–487 (2004)
281. Narasimhan, T.N., Whitherspoon, P.A.: An integrated finite difference method for analyzing fluid flow in porous media. *Water Resource Research* **12**(1), 57–64 (1976)
282. Nedelec, J.C.: Mixed finite elements in \mathbb{R}^3 . *Numer. Math.* **35**, 315–341 (1980)
283. Nedelec, J.C.: A new family of mixed finite elements in \mathbb{R}^3 . *Numer. Math.* **50**, 57–81 (1986)
284. Nicolaides, R.A.: A discrete vector field theory and some applications. In: *Proceedings of IMACS’91 – 13th IMACS World Congress on Computation and Applied Mathematics*, pp. 120–121, Trinity College, Dublin, Ireland (1991)
285. Nicolaides, R.A.: Direct discretization of planar div-curl problems. *SIAM J. Numer. Anal.* **29**(1), 32–56 (1992)

286. Nicolaides, R.A., Trapp, K.A.: Covolume discretizations of differential forms. In: Arnold, D., Bochev, P., Lehoucq, R., Nicolaides, R., Shashkov, M. (eds.) *Compatible discretizations. Proceedings of IMA hot topics workshop on compatible discretizations*, IMA Vol. Math. Appl., pp. 161–172. Springer, New York (2006)
287. Nicolaides, R.A., Wang, D.-Q.: Convergence analysis of a covolume scheme for maxwell's equations in three dimensions. *Math. Comput.* **67**(223), 947–963 (1998)
288. Nicolaides, R.A., Wu, X.: Covolume solutions of three-dimensional div-curl equations. *SIAM J. Numer. Anal.* **34**(6), 2195–2203 (1997)
289. Nocedal, J., Wright, S.: *Numerical Optimization*. Springer-Verlag, Berlin Heidelberg New York (1999)
290. Nochetto, R.H., Siebert, K.G., Veeger, A.: Pointwise a posteriori error control for elliptic obstacle problems. *Numer. Math.* **95**(1), 163–195 (2003)
291. Nordbotten, J.M., Aavatsmark, I., Eigestad, G.T.: Monotonicity of control volume methods. *Numer. Math.* **106**(2), 255–288 (2007)
292. Nuckolls, J., Wood, L., Thiessen, A., Zimmerman, G.: Laser compression of matter to super-high densities: Thermonuclear (CTR) applications. *Nature* **239**, 139–142 (1972)
293. Olsson, P.: Summation by parts, projections, and stability. I. *Math. Comput.* **64**(211), 1035–1065, S23–S26 (1995)
294. Olsson, P.: Summation by parts, projections, and stability. II. *Math. Comput.* **64**(212), 1473–1493 (1995)
295. Palmer, R.S.: Chain models and finite element analysis: an executable CHAINS formulation of plane stress. *Comput. Aided Geom. Design* **12**(7), 733–770 (1995)
296. Palmer, R.S., Shapiro, V.: Chain models of physical behavior for engineering analysis and design. *Research in Engineering Design* **5**, 161–184 (1993)
297. Patterson, N., Thornton, K.: Investigation of mixed cell treatment via the support operator method. In 53rd Annual Meeting of the APS Division of Plasma Physics, November 14–18. American Physical Society (2011)
298. Peric, M., Ferguson, S.: The advantage of polyhedral meshes. Technical report, CD Adapco Group (2005). www.cd-adapco.com/news/24/TetsvPoly.htm
299. Perot, J.B.: Conservation properties of unstructured staggered mesh schemes. *J. Comput. Phys.* **159**, 58–89 (2000)
300. Perot, J.B., Subramanian, V.: Higher-order mimetic methods for unstructured meshes. *J. Comput. Phys.* **219**(1), 68–85 (2006)
301. Perot, J.B., Vidovic, D., Wesseling, P.: Mimetic reconstruction of vectors. In: Arnold, D.N., Bochev, P.B., Lehoucq, R.B., Nicolaides, R.A., Shashkov, M. (eds.) *Compatible Spatial Discretizations. The IMA Volumes in Mathematics and its Applications*, vol. 142. Springer, New York (2006)
302. Pierre, C.: *Modélisation et simulation de l'activité électrique du coeur dans le thorax, analyse numérique et méthodes de volumes finis*. PhD thesis, Université de Nantes, France (2005)
303. Quarteroni, A.: *Numerical Models for Differential Problems*. MS&A, vol. 2. Springer-Verlag Italia, Milan (2009)
304. Quarteroni, A., Valli, A.: *Numerical Approximation of Partial Differential Equations* Springer Series in Computational Mathematics, vol. 23. Springer, Berlin Heidelberg New York (1984)
305. Raviart, P.A., Thomas, J.M.: A mixed finite element method for second order elliptic problems. In: Galligani, I., Magenes, F. (eds.) *Math. Aspects of Finite Element Method*, Lecture Notes in Math., vol. 606. Springer-Verlag, New York (1977)

306. Reisser, E.: The effect of transverse shear deformation on the bending of elastic plates. *ASME Journal of Applied Mechanics* **12**, A68–77 (1945)
307. Ringler, T.D., Randall, D.A.: A potential enstrophy and energy conserving numerical scheme for solution of the shallow-water equations on a geodesic grid. *Monthly Weather Rev.* **130**(5), 1397–1410 (2002)
308. Rodrigues, J.-F.: *Obstacle problems in mathematical physics*. North-Holland Mathematics Studies, vol. 134. North-Holland Publishing Co., Amsterdam (1987)
309. Rose, M.: A numerical scheme to solve $\mathbf{div} \underline{u} = \rho$, $\mathbf{curl} \underline{u} = \zeta$. Technical report, ICASE Report No. 82-8 (1982)
310. Sabitova, A., Samarskaya, E.A.: Stability of variational-difference schemes for the problems of gas-dynamics with heat conduction. *Diff. Eq.* **21**(7), 861–864 (1985)
311. Sadourny, R.: The dynamics of finite-difference models of the Shallow-Water equations. *J. Atmos. Sci.* **32**, 680–689 (1975)
312. Samarskii, A.A., Tishkin, V.F., Favorskii, A.P., Yu, M.: Shashkov. On the representation of finite difference schemes of mathematical physics in operator form. *Sov. Phys. Dokl.* **26**(6), 590–592, American Institute of Physics (1981)
313. Samarskii, A.A.: *Introduction to Theory of Difference Schemes*, in Russian. Nauka (1971)
314. Samarskii, A.A.: *The Theory of Difference Schemes*, in Russian. Nauka (1977)
315. Samarskii, A.A.: *The Theory of Difference Schemes*. Pure and Applied Mathematics. CRC Press (2001)
316. Samarskii, A.A., Favorskii, A.P., Tishkin, V.F., Shashkov, M.Yu.: Operator Variational difference scheme for a mathematical physics equations, in Russian. Tbilisi State University, Tbilisi, Georgia, USSR (1983)
317. Samarskii, A.A., Gulín, A.V.: Stability of Difference Schemes, in Russian, 416. Nauka (1973)
318. Samarskii, A.A., Popov, Yu.P.: Finite difference schemes for gas dynamics. Nauka (1975)
319. Samarskii, A.A., Tishkin, V.F., Favorskii, A.P., Shashkov, M.Yu.: Employment of the reference-operator methods in the construction of finite difference analogs of tensor operations. *Diff. Eq.* **18**(7), 881–885 (1983)
320. Samarskii, A.A., Tishkin, V.F., Favorskii, A.P., Shashkov, M.Yu.: Operational finite-difference schemes. *Diff. Eq.* **17**, 854–862 (1981)
321. Scharfetter, D.L., Gummel, H.K.: Large signal analysis of a silicon read diode. *IEEE Trans. on Elec. Dev.* **16**, 64–77 (1969)
322. Scott, L.R., Zhang, S.: Finite element interpolation of nonsmooth functions satisfying boundary conditions. *Math. Comput.* **54**, 483–493 (1990)
323. Shashkov, M.: *Conservative Finite Difference Methods*. CRC Press, Boca Raton, FL (1996)
324. Shashkov, M., Steinberg, S.: Support-operator finite-difference algorithms for general elliptic problems. *J. Comput. Phys.* **118**, 131–151 (1995)
325. Shashkov, M., Steinberg, S.: Solving diffusion equations with rough coefficients in rough grids. *J. Comput. Phys.* **129**, 383–405 (1996)
326. Silin, D.B., Patzek, T.W.: Support-operators method in the identification of permeability tensor orientation. *SPE Journal*, pp. 385–398, SPE 74709, 2000 SPE/DOE Improved Oil Recovery Symposium, Tulsa, 3–5 April, 2000 (2001)
327. Solovev, A., Shashkov, A.: Finite-difference schemes for solution of heat equation on dirichlet grid. Technical report, All Union Center for Mathematical Modeling, USSR Acad. of Sci., Moscow, in Russian (1991)

328. Solov'ev, A., Shashkov, M.: Difference scheme for the "dirichlet particles" method in cylindrical coordinates, conserving symmetry of gas-dynamical flow. *Diff. Eq.* **24**(7), 817–823 (1988)
329. Solov'ev, A., Solov'eva, E., Tishkin, V., Favorskii, A., Shashkov, M.: Approximation of finite-difference operators on a mesh of Dirichlet cells. *Diff. Eq.* **22**(7), 863–872 (1986)
330. Song, S., Dong, T., Zhou, Y., David, A., Yuen, D.A., Zhonghua, L.: Seismic wave propagation simulation using support operator method on multi-GPU system. Technical Report 34, Minnesota Supercomputing Institute, University of Minnesota (2011)
331. Sorokin, S.B.: The method of step-by-step inversion for numerical solution of the biharmonic equation. *Siberian Mathematical Journal* **36**(3), 569–573 (1995)
332. Stenberg, R.: Analysis of mixed finite element methods for the Stokes problem: a unified approach. *Math. Comput.* **42**, 9–23 (1984)
333. Stenberg, R.: A technique for analyzing finite-element methods for viscous incompressible flow. *Int. J. Numer. Meth. in Fluids* **11**(6), 935–948 (1990)
334. Stenberg, R.: Postprocessing schemes for some mixed finite elements. *Math. Model. Numer. Anal.* **25**, 151–168 (1991)
335. Stratton, J.A.: *Electromagnetic theory*, 1st ed. McGraw-Hill, New York (1941)
336. Sukumar, N., Malsch, E.: Recent advances in the construction of polygonal finite element interpolants. *Archives of Computational Methods in Engineering* **13**(1), 129–163 (2006)
337. Sukumar, N., Tabarraei, A.: Conforming polygonal finite elements. *Int. J. Numer. Meth. Engrg.* **61**(12), 2045–2066 (2004)
338. Svård, M., Mattsson, K., Nordström, J.: Steady-state computations using summation-by-parts operators. *J. Sci. Comput.* **24**(1), 79–95 (2005)
339. Linde, T.J., Plewa, T., Weirs, V.G. (eds.): *Adaptive mesh refinement, theory and applications*. Lecture Notes in Computational Science and Engineering, vol. 41. Springer-Verlag, Berlin Heidelberg (2005)
340. Tabarraei, A., Sukumar, N.: Extended finite element method on polygonal and quadtree meshes. *Comput. Methods Appl. Mech. Engrg.* **197**(5), 425–438 (2008)
341. Taflove, A.: Application of the finite-difference time-domain method to sinusoidal steady state electromagnetic penetration problems. *IEEE T. Electromagn. C.* **22**(3), 191–202 (1980)
342. Taran, M., Tishkin, V., Favorskii, A., Feoktistov, L., Shashkov, M.: On simulation of the collapse of a quasi-spherical target in a hard cone. Technical Report 127, Keldysh Inst. of Appl. Math. the USSR Acad. of Sci., in Russian (1980)
343. Teixeira, F.L.: Time-domain finite-difference and finite-element methods for Maxwell equations in complex media. *IEEE T. Antenn. Propag.* **56**(8), 2150–2166 (2008)
344. Thuburn, J., Cotter, C.J.: A framework for mimetic discretization of the rotating shallow-water equations on arbitrary polygonal grids. *SIAM J. Sci. Comput.* **34**(3), B203–B225 (2012)
345. Tikhonov, A.N., Samarskii, A.A.: Homogeneous difference schemes. *USSR Comput. Math. and Math. Phys.* **1**(1), 5–67 (1962)
346. Tishkin, V.F.: Variational-difference schemes for the dynamical equations for deformable media. *Diff. Eq.* **21**(7), 865–870 (1985)
347. Tishkin, V.F., Favorskii, A.P., Shashkov, M.Yu.: Variational-difference schemes for the heat conduction equation on non-regular grids. *Sov. Phys. Dokl.* **24**(6), 446–450 (1979)
348. Tishkin, V.F., Shashkov, M.Yu.: Numerical modeling of Physical Experiment. Central Institute for Informatics, Technology and Economics Research in Atomic Science and Technology, in Russian (1987)

349. Tonti, E.: Sulla struttura formale delle teorie fisiche. *Rend. Sem. Mat. Fis. Milano* **46**, 163–257 (1976)
350. Tonti, E.: The reason for analogies between physical theories. *Appl. Math. Modelling* **1**(1), 37–50 (1976/77)
351. Tonti, E.: Finite formulation of the electromagnetic field. In: Teixeira, F.L. (ed.) *Geometric Methods in Computational Electromagnetics*, PIER 32, pp. 1–44. EMW Publishing, Cambridge, MA (2001)
352. Trapp, K.A.: Inner products in covolume and mimetic methods. *ESAIM: Math. Mod. Numer. Anal.* **42**, 941–959 (2008)
353. Vejchodsky, T., Korotov, S., Hannukainen, A.: Discrete maximum principle for parabolic problems solved by prismatic finite elements. *Mathematics and Computers in Simulation* **80**(8), 1758–1770 (2010)
354. Velarde, G., Ronen, R.Y., Martinez-Val, J.M.: *Nuclear Fusion by Inertial Confinement: A Comprehensive Treatise*. CRC Press (1992)
355. Verfürth, R.: *A review of a posteriori error estimation and adaptive mesh refinement*. Wiley and Teubner, Stuttgart (1996)
356. Volkova, R., Kruglikova, L., Misheskaya, E., Tishkin, V., Turina, N., Favorskii, A., Shashkov, M.: SAFRA. Functional filling. the program for solving 2-D problems of the controlled laser fusion. Manual. Technical report, Keldysh Inst. of Appl. Math. the USSR Acad. of Sci., in Russian (1985)
357. Wachspress, E.: *A rational Finite Element Basis*. Academic Press (1975)
358. Walters, W.P., Zukas, J.A.: *Fundamentals of Shaped Charges*. John Wiley & Sons Inc. (1989)
359. Weiland, T.: A discretization method for the solution of Maxwell's equations for six-component fields. *Electronics and Communications AEU* **31**(3), 116–120 (1977)
360. Wheeler, M.F., Yotov, I.: A multipoint flux mixed finite element method. *SIAM J. Numer. Anal.* **44**, 2082–2106 (2006)
361. Whitney, H.: *Geometric Integration Theory*. Princeton University Press, Princeton (1957)
362. Williamson, M., Meza, J., Moulton, D., Gorton, I., Freshley, M., Dixon, P., Seitz, R., Steefel, C., Finsterle, S., Hubbard, S., Zhu, M., Gerdes, K., Patterson, R., Collazo, Y.T.: Advanced simulation capability for environmental management (ascem): An overview of initial results. *Technology and Innovation* **13**, 175–199 (2011)
363. Wu, J., Dai, Z., Gao, Z., Yuan, G.: Linearity preserving nine-point schemes for diffusion equation on distorted quadrilateral meshes. *J. Comput. Phys.* **229**(9), 3382–3401 (2010)
364. Yee, K.S.: Numerical solution of initial boundary value problems involving Maxwell's equations in isotropic media. *IEEE T. Antenn. Propag.* **14**(3), 302–307 (1966)
365. Zukas, J.A.: *High velocity impact dynamics*. Wiley (1990)

Index

- advective flux, 290
 - θ scheme, 291
 - Scharfetter-Gummel scheme, 291
 - upwinding, 291
- Agmon inequality, 36
- algebraic consistency condition, 85, 98, 150, 164, 231, 272, 285, 287, 353
- basic laws of electromagnetism, 197
- bilinear form
 - coercive, 28
 - consistency condition, 94, 161, 215, 229, 264, 282, 304
 - matrix formula, 101, 111, 178
 - polygon, 98, 165
 - quadrilateral, 232, 332
 - square, 168
 - stability condition, 96, 109, 161, 215, 229, 282, 303
- commuting property, 51, 119, 149, 226, 268, 280, 349
- discrete space
 - cell-based, 44, 118, 147, 223, 267, 346
 - edge-based, 43, 156, 198, 212, 248, 278
 - face-based, 44, 118, 147, 199, 223, 267, 290, 346
 - vertex-based, 43, 156, 212, 248, 277, 303
- discretization method
 - algebraic topology, 6
 - cell method, 15
 - covolume, 15
 - DDFV, 16
 - diamond scheme, 16
 - FDTD, 7
 - finite volume, 291
 - integrated finite difference, 16
 - local support operator, 12
 - mixed finite element, 8, 17, 130
 - multi-point flux approximation, 17
 - summation by parts, 15
 - support operator, 9
 - virtual element, 14, 155, 265
- elliptic regularity
 - convex domain, 132
- Euler’s polyhedron formula, 65
- formula
 - Clement interpolant, 236
 - Green, 19, 42, 201
 - show-lace, 165
- Helmholtz decomposition, 64, 65
- Hopf’s lemma, 311
- inf-sup condition, 131, 236, 249, 358
- inner product
 - consistency condition, 68, 122, 150, 175, 206, 210, 270, 281, 351
 - inverse matrix formula, 113, 354
 - matrix formula, 89, 124, 273
 - parallelepiped, 327
 - parallelogram, 323
 - pentagon, 329
 - polygon, 124, 211

- mimetic, 8, 91, 270, 280
 - stability condition, 68, 121, 150, 175, 205, 270, 280, 350
 - weighted, 201
- Korn-type inequality, 239
- macroelement, 250
- equivalence class, 250
- matrix
- assembly procedure, 20
 - M-matrix, 312
 - singular M-matrix, 319
- mesh
- face-connected, 57
 - generalized polyhedral, 339
 - generalized pyramid, 341
 - polygonal, 39
 - polyhedral, 34
 - shape-regular, 34, 344
 - simple partition, 35
 - simply-connected, 57
- mimetic operator
- derived, 8
 - derived curl, 54, 201, 213
 - derived divergence, 54, 157, 202
 - vector case, 227
 - derived gradient, 53, 349
 - kernel, 58–60, 62
 - primary, 8
 - primary curl, 48, 199, 213, 280
 - primary divergence, 48, 201, 202, 226, 268, 349
 - primary gradient, 48, 202, 213, 280
 - vector Laplacian, 55, 227
- projection operator
- cell-based, 47, 119, 223, 267, 348
 - edge-based, 46, 199, 213, 249, 279
 - face-based, 47, 119, 199, 224, 268, 348
 - vertex-based, 46, 213, 224, 249, 278, 303
- quadrature rule, 162, 171, 223
- reconstruction operator
- admissible, 71
 - exact, 136, 275, 365
 - minimal, 73
 - properties, 71, 151, 179, 188, 216, 235, 304
- shock-capturing
- exponential boundary layers, 299
 - parabolic boundary layers, 299
- Stokes theorem, 41
- tensor
- elastic moduli, 30, 267, 276
 - strongly elliptic, 24, 161
- Tonti, 7, 14

MS&A – Modeling, Simulation and Applications

Series Editors:

Alfio Quarteroni
École Polytechnique Fédérale
de Lausanne (Switzerland)
and
MOX – Politecnico di Milano (Italy)

Tom Hou
California Institute of Technology
Pasadena, CA (USA)

Claude Le Bris
École des Ponts ParisTech
Paris (France)

Anthony T. Patera
Massachusetts Institute of Technology
Cambridge, MA (USA)

Enrique Zuazua
Basque Center for Applied
Mathematics
Bilbao (Spain)

Editor at Springer:

Francesca Bonadei
francesca.bonadei@springer.com

1. L. Formaggia, A. Quarteroni, A. Veneziani (Eds.)
Cardiovascular Mathematics
2009, XIV+522 pp, ISBN 978-88-470-1151-9
2. A. Quarteroni
Numerical Models for Differential Problems
2009, XVI+602 pp, ISBN 978-88-470-1070-3
3. M. Emmer, A. Quarteroni (Eds.)
MATHKNOW
2009, XII+264 pp, ISBN 978-88-470-1121-2
4. A. Alonso Rodríguez, A. Valli
Eddy Current Approximation of Maxwell Equations
2010, XIV+348 pp, ISBN 978-88-470-1934-8
5. D. Ambrosi, A. Quarteroni, G. Rozza (Eds.)
Modeling of Physiological Flows
2012, X+414 pp, ISBN 978-88-470-1934-8
6. W. Liu
Introduction to Modeling Biological Cellular Control Systems
2012, XII+268 pp, ISBN 978-88-470-2489-2

7. B. Maury
The Respiratory System in Equations
2013, XVIII+276 pp, ISBN 978-88-470-5213-0
8. A. Quarteroni
Numerical Models for Differential Problems, 2nd Edition
2014, XX+656pp, ISBN 978-88-470-5521-6
9. A. Quarteroni, G. Rozza (Eds.)
Reduced Order Methods for modeling and computational reduction
2014, X+332pp, ISBN 978-3-319-02089-1
10. J. Xin, Y. Qi
An Introduction to Mathematical Modeling and Signal Processing in Speech
and Hearing Sciences
2014, XII+208pp, ISBN 978-3-319-03085-2
11. L. Beirão da Veiga, K. Lipnikov, G. Manzini
The Mimetic Finite Difference Method for Elliptic Problems
2014, XVI+392pp, ISBN 978-3-319-02662-6

For further information, please visit the following link:
<http://www.springer.com/series/8377>